VIRGINIA DIVISION OF MINERAL RESOURCES PUBLICATION 132

STUDIES IN EASTERN ENERGY AND THE ENVIRONMENT

AAPG Eastern Section Special Volume
September 19-21, 1993
Williamsburg, Virginia

Edited by
A. P. Schultz and E. K. Rader

COMMONWEALTH OF VIRGINIA
DEPARTMENT OF MINES, MINERALS, AND ENERGY
DIVISION OF MINERAL RESOURCES
Stanley S. Johnson, State Geologist

CHARLOTTESVILLE, VIRGINIA
1994

VIRGINIA DIVISION OF MINERAL RESOURCES PUBLICATION 132

STUDIES IN EASTERN ENERGY AND THE ENVIRONMENT

AAPG Eastern Section Special Volume
September 19-21, 1993
Williamsburg, Virginia

Edited by
A. P. Schultz and E. K. Rader

COMMONWEALTH OF VIRGINIA
DEPARTMENT OF MINES, MINERALS, AND ENERGY
DIVISION OF MINERAL RESOURCES
Stanley S. Johnson, State Geologist

CHARLOTTESVILLE, VIRGINIA
1994

CONTENTS

B. CASE STUDIES

PREFACE

The Eastern Section Meeting of the American Association of Petroleum Geologists brought together an unusually diverse group of geologists, hydrologists, environmental scientists, and earth science educators. The theme of the meeting was "Energy, Environment and Education". Never before has the interplay of these three elements been more critical to the quality of life on Planet Earth.

With the growing increase in public awareness of environmental issues, it has become more difficult to balance our need to exploit energy and mineral resources with our desire for a clean and safe environment. It is imperative for those in the energy and mineral industries to look to their earth science colleagues for the data to make informed decisions that balance these often conflicting agendas. In a similar way, it is important for earth scientists to be more aware of the societal impact of their research, particularly within the framework of our ever growing industrial world. Interdisciplinary cooperation, and the broader based knowledge gained from such cooperation can be a powerful tool enabling earth scientists, both in applied and theoretical research, to control the direction of environmental legislation. Such legislation is in need of an informed view.

Within our global village, news of environmental catastrophe travels fast. In a similar way, public imagination can be quickly and easily over stimulated by "newsy" stories of climate change, the greenhouse effect, and other ecological disasters. As earth scientists in industry, government and academia, we must continue to gather relevant data needed to objectively evaluate mankind's effect on the natural cycles of highly complex earth processes. By combining this data in new, interdisciplinary ways and making it accessible to our political leaders, we have the hope of achieving the balance between energy and the environment.

In the spirit of the 1993 AAPG Eastern Section Meeting, this volume contains selected studies from the various poster and oral presentations. The papers were submitted by the meeting participants and are grouped into specific topics under the two main headings of Energy and Environment. There is much here of interest to anyone involved with the many facets of Earth Science.

The editors thank the many contributors to this volume. Your efforts are most appreciated. Special thanks go to the Virginia Division of Mineral Resources and Stan Johnson, Virginia State Geologist for publication support. Finally, on behalf of the participants of the meeting and the authors of the papers, we thank Richard F. Meyer. His vision to "incorporate the elements of energy, environment and education " was realized within the context of the meeting and this volume. It is my hope that his vision will be a model for continued scientific dialogue and cooperation across the many fields of Energy and Earth Science into the 21st century.

Art Schultz
Reston, Va
11/1/93

HIGH-SULFUR COALS IN THE EASTERN KENTUCKY COAL FIELD

James C. Hower and Ursula M. Graham
University of Kentucky
Center for Applied Energy Research
3572 Iron Works Pike
Lexington, KY 40511
Cortland F. Eble
Kentucky Geological Survey
Lexington, KY 40506

ABSTRACT

The Eastern Kentucky coal field is notable for relatively low-sulfur, "compliance" coals. Virtually all of the major coals in this area do have regions in which higher sulfur lithotypes are common, if not dominant, within the lithologic profile. Three Middle Pennsylvanian coals, each representing a major resource, exemplify this.

The River Gem coal bed is the stratigraphically lowest coal bed mined extensively throughout the coal field. In Whitley County the sulfur content increases from 0.6% at the base to nearly 12% in the top lithotype. Pyrite in the high-sulfur lithotype is a complex mixture of sub- to few-micron syngenetic forms and massive epigenetic growths. In some cases, multiple generations of pyrite growth can be recognized. High sulfur is attributed to post-depositional influx of sulfate-rich waters associated with the overlying marine Betsie shale. A systematic microscopic study of the textural and spatial relationships among individual pyrite types and macerals in the coal was performed as part of this study. Pyrite crystals with distinct morphological characteristics were selected for a detailed SEM study aimed at differentiating growth, overgrowth, and replacement processes during the formation of pyrite in these coals. Trace element analyses in individual pyrite grains from distinct pyrite generations were performed. Among the many types of pyrite in these coals, framboidal pyrite is the least understood although it is abundantly present. Framboids were selected and the spatial relationship among framboids, organic matrix, and other pyrite types was investigated.

The stratigraphically higher Pond Creek coal bed is extensively mined in portions of the coal field. Although generally low in sulfur, in northern Pike and southern Martin counties, the top third can have up to 6% sulfur. Uniformly low sulfur profiles can occur within a few hundred meters of high sulfur coal. Pyrite occurs as 10-50 m euhedra and coarser massive forms. In this case, sulfur distribution may have been controlled by sandstone channels in the overlying sediments.

High-sulfur zones in the lower bench of the Fire Clay coal bed, the stratigraphically highest coal bed considered here, are more problematical. The rider and thin upper benches can be high in sulfur. The lower bench, which is of highly variable thickness and quality, is generally overlain by a kaolinitic flint clay, the consequence of a volcanic ash fall into the peat swamp. In southern Perry and Letcher counties a black, illite-chlorite clay lies between the flint clay and the lower bench. General lack of lateral continuity of lithotypes in the lower bench suggests that the precursor swamp consisted of discontinuous peat-forming environments that were spatially variable and regularly inundated by sediments. Some of the peat-forming areas may have been marsh-like in character.

No single model can account for the pyrite and sulfur emplacement in the eastern Kentucky coals.

INTRODUCTION

High-sulfur coals are generally not associated with the coalfields of the Central Appalachians. Cobb et al. (1982) estimated that 43% of the coal in eastern Kentucky would have less than 1.2 lb SO_2/MBtu (0.54 kg SO_2/MJ). Of the three coals considered in this study, the Pond Creek and the Fire Clay were the top two producing coal beds in eastern Kentucky through the 1976-1991 period. The River Gem and correlatives ranked seventh over the same time span (information from John Hiett, Kentucky Department of Mines and Minerals). The locations of the study areas are shown on Figure 1.

Virtually any major coal bed has regions or lithotypes which are markedly higher in sulfur than the normal range for the commercial coal. In this study we will discuss aspects of the pyrite forms and sulfur trends in three major coal beds in the Eastern Kentucky coalfield. Each of the coals is distinct with respect to the pyrite forms observed and the inferred environment of deposition involved in pyrite formation.

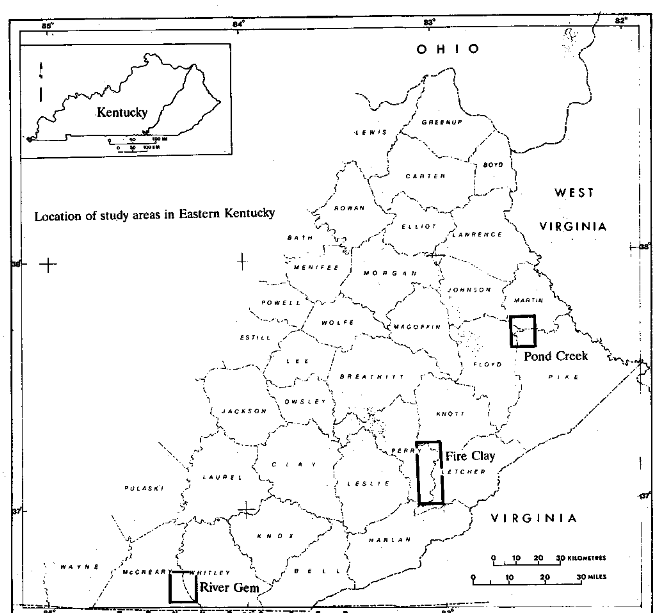

Figure 1. Location of the study areas in eastern Kentucky. The River Gem mine sites are in the Hollyhill quadrangle. The Pond Creek sites are in the Thomas quadrangle. The Fire Clay sites are in the Vicco, Hazard North, and Tilford quadrangles.

PROCEDURE*

The samples were collected by Center for Applied Energy Research and Kentucky Geological Survey geologists at active mine sites. The chemical and petrographic results reported here were compiled at those organizations. Palynographic analysis was performed at the Kentucky Geological Survey using procedures described by Eble et al. (1994).

DISCUSSION

RIVER GEM/CLINTWOOD/ MANCHESTER

The River Gem (correlative with Manchester, Lily, Clintwood, Hance, Zachariah, among others) coal bed in Whitley County exhibits a large variation in sulfur content from the base of the coal to the upper lithotypes. Hower and Pollock (1989) investigated the petrology of the coal bed in that region and portions of the following discussion are adapted from that study. Examples of the pyrite forms are illustrated on Figure 2a and 2b and Figure 3a to 3d.

The deposition of the River Gem was considered to have comprised at least three stages: a lower bench (sampled in three lithotypes), a bone lithotype, and an upper bench/rider. The first series of lithotypes is generally lower sulfur. The bone, with its transition to a parting at one site, has up to 26.6% ash and 7.9% sulfur (total) while the upper bench, generally a bright lithotype, has up to 27% ash and, at a different site, 11.4% sulfur (including 6.3% pyritic sulfur). The generalized palynology of the lithotypes at two of the sites is illustrated on Figure 4. Following the deposition of the higher herbaceous lycopsid (*Densosporites*) lithotype, the coal bed is increasingly dominated by *Lycospora*. The coal bed is overlain by the Betsie Shale Member, which has brackish-water fossils reported from the area (Acquaviva, 1978; D. Chesnut, pers. commun., 1987).

The bone contains more silicate minerals and would have been a relatively high mineral matter lithotype even without the syngenetic and epigenetic pyrite. The pyrite is finer grained than in the upper bench, having an overall appearance of being a more syngenetic assemblage than in the upper bench. A pyrite form common in this lithotype, and also found in the upper bench in varying quantities, was identified as "specular" pyrite. As illustrated on Figure 2a, it is a fine, isolated form most commonly occurring in corpocollinite. Pyrite also occurs as framboids, euhedra, massive overgrowths of the latter forms, and even as second generation overgrowths encompassing the previous overgrowths. Figure 2b illustrates an assemblage of framboidal pyrite with some of the framboids overgrown by secondary pyrite crystallization. The complexity of the pyrite is seen on the SEM images. Figures 3a and 3b are of pyrite framboids within the larger mass on Figure 2b. Note the variety of forms and overgrowths present. The progressive overgrowth of a framboid cluster is particularly well illustrated on Figure 3b. Figures 3c and 3d also illustrate stages of overgrowth. At the rims of the overgrown framboidal clusters the octahedral and pyritohedron habits of individual crystals can be recognized. Further examples of pyrite forms in the River Gem coal bed were provided in the paper by Hower and Pollock (1989).

As noted by Hower and Pollock (1989): "the differentiation between syngenetic and epigenetic pyrite in such high-sulfur coals is certainly difficult as the progression of crystal growth followed by successive generations of pyrite overgrowths was likely to have been an ongoing process, particularly if the peat was under persistent encroachment by marine waters." No other coal in eastern Kentucky studied to date exhibits the complexity of sulfide forms found in the River Gem, although the pyritic sulfur percentage is exceeded in a few isolated cases, and consequently, the diagenetic history of the River Gem coal bed in Whitley County is similarly complex. It is likely that the River Gem swamp was inundated by marine waters during the course of deposition of the uppermost lithotypes as well as following the end of peat deposition and the deposition of the marine Betsie Shale member.

POND CREEK/LOWER ELKHORN

The Pond Creek coal bed, also known as the Lower Elkhorn in the study area, and its correlatives (Blue Gem, Imboden, Path Fork) is generally a low sulfur coal resource. Portions of the coal bed in northern Pike and southern Martin counties are higher in sulfur than the "typical" Pond Creek in the region which has virtually no pyritic sulfur. The following assessment of the Pond Creek is based on studies of the petrology and geochemistry of the coal by Hower and Pollock (1988), Hower and Bland (1989), and Hower et al. (1991). Helfrich and Hower (1991) studied the palynology and petrology of the coal bed in central Pike County and related trends found in that area to the depositional setting. Our study area is isolated from that region and palynological studies of the coals in our study area have not yet been completed.

In the studies cited above, we recognized distinct differences in the lithology of the coal bed relative to its geographic position with respect to the Belfry anticline, a northeast-plunging penecontemporaneous structure crossing Pike County from southwest to northeast. The structure has various styles across the county but is generally seen as either an anticline or an oversteepening of the monoclinic northwest regional dip of the Pond Creek coal bed. The study area is near the Rome Trough, an east-west trending basement trough which was active throughout the Paleozoic.

The coal bed to the northwest of the anticline was found to have a bottom third characterized by a durain/dull clarain with Zr and TiO_2 enrichment. The middle third had brighter lithologies than the base and had an ash geochemistry notable for its CaO enrichment. The top third has the greatest geochemical variation owing to the variation in sulfur content. At one mine site the whole coal has 1.83% S_{total} with a top lithotype containing 5.73% S_{total} while the whole coal just 110 m to the west has 0.56% S_{total} (all sulfur analyses on dry basis). Similar sulfur variations are known from other mines in the region, with the high sulfur areas having sinuous trends reminiscent of channels.

The pyrite forms in the Pond Creek coal bed suggest more of an epigenetic emplacement as opposed to the complex array of forms found in the River Gem coal bed. Some framboidal pyrite is seen in the high sulfur lithotypes but most of the relatively fine pyrite is in the form of isolated, 10-50 m euhedra (Figure 2c). The massive pyrite is in the form of overgrowths of the finer forms (Figure 2d) and as other massive (including cleat) forms. The pyrite observed with the SEM is massive with no pyrite observed (Figure 3e and 3f). Recrystallization around the rims of the pyrite masses was observed. Siderite is also observed in the lithotype below the uppermost lithotype. Large siderite nodules have been observed in the coal bed and siderite is also present in the overlying gray shale and is less prevalent in as lag deposits in the sandstone channels (J. Popp, pers. comm., 1993). Overall, the pyritic sulfur in the Pond Creek is from relatively fewer, coarser pyrite grains than in the River Gem.

The emplacement of the pyrite appears to have been primarily through the epigenetic influx of sulfate-rich waters from overlying channels.

FIRE CLAY/HAZARD NO. 4

The Fire Clay coal bed in Perry and Letcher counties is a low-sulfur resource which is marketed as a metallurgical coal as well as a steam coal. High-sulfur zones were observed in two places within the coal bed: in the rider and uppermost lithotypes and in the lower bench below the flint clay parting characteristic of the Fire Clay coal bed in eastern Kentucky and West Virginia. The following discussion is from studies by Eble and Grady (1990), Eble et al. (1994), and Hower et al. (1994) on the paleoecology and utilization aspects of the coal bed in central Eastern Kentucky.

The high-sulfur lithotypes at the top of the coal bed are found in the northern part of the study area, near the Perry-Knott County line. Total sulfur of up to 10.39% (dry) (7.95% $S_{pyritic}$) was found in a thin rider coal. The uppermost lithotype at a nearby site has 3.14% S_{total} and 1.83% $S_{pyritic}$. The only other lithotypes exceeding 1% S_{total} at the latter site are immediately below partings and no lithotype from the main coal bed exceeds 1% S_{total} at the previous site. The pyrite forms are dominated by massive varieties with overgrowths of earlier framboids (Figure 2e), massive layers, and fusinite-lumen fills prevalent. Framboidal associations within larger masses of individual pyrite crystals are seen (Figure 3g). The alignment of pyrite with respect to the maceral suggests that replacement of organic matter by pyrite was a pyrite emplacement mechanism. It is likely that the high sulfur at the top of the Fire Clay coal bed at these sites was emplaced by a mechanism similar to that of the Pond Creek discussed above, an epigenetic emplacement controlled by post-peat channels, although the resulting forms are different.

The high-sulfur lithotypes below the flint clay parting are more problematical. The flint clay parting itself is a kaolinitized volcanic ash-fall deposit which is found throughout the region (Lyons et al., 1992). In southern Perry and Letcher counties the flint clay is underlain, either directly or with a thin intervening coal, by an illite-chlorite clay. Overall, the basal portion of the coal bed, below the flint clay, does not exhibit the lateral continuity in thickness and quality characteristic of the post-flint clay upper bench. In contrast to the dominance of *Lycospora* in the upper bench, the lower bench is characterized by a mixed palynomorph assemblage consisting of small lycopsid, fern, calamite, and cordaite miospores. The mire was not laterally continuous florally and perhaps not continuous across the region as the lower bench appears to be missing at some sites. This setting for the base of the coal bed is repeated throughout the coalfield. Helfrich and Hower (1991) found the lower lithotypes of the Pond Creek coal bed in central Pike County to exhibit rather poor petrographic and palynologic lateral continuity.

The high-sulfur lithotypes do not attain the extreme levels noted for other settings discussed above. The lithotype below the illitic clay has 2.18 and 2.26% S_{total} at two southern Letcher County sites and a thin coal between the illitic clay and the flint clay has 3.09% S_{total}. The pyrite forms are generally fine framboids and euhedra with some massive overgrowths (Figure 2f and 3h). Considering the lack of lateral continuity of the lithotype character it is possible that the mire was ephemeral and, at times, brackish. The illitic partings have more Fe_2O_3 than the flint clay and were likely the source of iron for the fixation of sulfate in the brackish peat.

CONCLUSIONS

The three coals discussed in this paper each developed relatively high sulfur zones under somewhat different conditions. The River Gem high sulfur lithotypes appear to have formed under the syndepositional and postdepositional influence of marine or brackish waters. The Pond Creek high sulfur zones do not appear to have the lateral continuity of the River Gem zones and may have developed under the influence of postdepositional channels. The uppermost lithotype of the Fire Clay coal bed may have undergone pyrite emplacement in a similar manner to the Pond Creek. The lithotypes underlying the black illitic clay below the flint clay parting in the southern portion of the study area may have been influenced by the input of Fe-rich sediments into the brackish mire. Each setting has a unique character in the environment and in the amount and nature of the pyrite. No single model can account for the pyrite and sulfur emplacement in the eastern Kentucky coals.

ACKNOWLEDGEMENTS

John Popp and Bob Rathbone reviewed the manuscript.

REFERENCES

Acquaviva, D.J., 1978, Stratigraphy and depositional environments of a part of the Lower Breathitt Formation (Penn.) near Williamsburg, Ky.: M.S. thesis, Lexington, The University of Kentucky, 155 p.

Cobb, J.C., Currens, J.C., and Enoch, H.G., 1982, Compliance coal resources in Kentucky: Kentucky Geological Survey, ser. 11, Information Circular 9 52 p.

Eble, C.F., and Grady, W.C., 1990, Paleoecological interpretation of a Middle Pennsylvanian coal bed in the Central Appalachian Basin, U.S.A.: International Journal of Coal Geology, v. 16, p. 255-286.

Eble, C.F., Hower, J.C., and Andrews, W.M., Jr., 1994, Paleoecology of theFire Clay coal bed in a portion of the Eastern Kentucky coal field: Palaeogeography, Palaeoclimatology, Palaeoecology, in press.

Helfrich, C.T., and Hower, J.C., Palynologic and petrographic variation in the Pond Creek coal bed, Pike County, Kentucky: Organic Geochemistry, v. 17, p. 153-159.

Hower, J.C., Andrews, W.M., Jr., Wild, G.D., Eble, C.F., Dulong, F.T., and Salter, T.B., 1994, Quality of the Fire Clay coal bed, southeastern Kentucky: Journal of Coal Quality, in press.

Hower, J.C. and Bland, A.E., 1989, Geochemistry of the Pond Creek Coal Bed, Eastern Kentucky Coalfield: Int. Journal of Coal Geology, v. 11, pp. 205-226.

Hower, J.C., and Pollock, J.D., 1988, Petrology of the Pond Creek coal bed in eastern Kentucky: Organic Geochemistry, v. 12, pp. 297-302.

Hower, J.C. and Pollock, J.D., 1989, Petrology of the River Gem Coal Bed, Whitley County, Kentucky: Int. Journal of Coal Geology, v. 11, pp. 227-245.

Hower, J.C., Pollock, J.D., and Griswold, T.B., 1991, Structural controls on petrology and geochemistry of the Pond Creek coal bed, Pike and Martin Counties, eastern Kentucky, in D.C. Peters, ed., Geology in coal resource utilization: Am. Assoc. of Petroleum Geologists, Energy Minerals Division, p. 413-427.

Lyons, P.C., Outerbridge, W.F., Triplehorn, D.M., Evans, H.T., Jr., Congdon, R.D., Capiro, M., Hess, J.C., and Nash, W.P., 1992, An Appalachian isochron: A kaolinized Carboniferous air-fall volcanic-ash deposit (tonstein): Geological Society of America Bulletin, v. 104, p. 1515-1527.

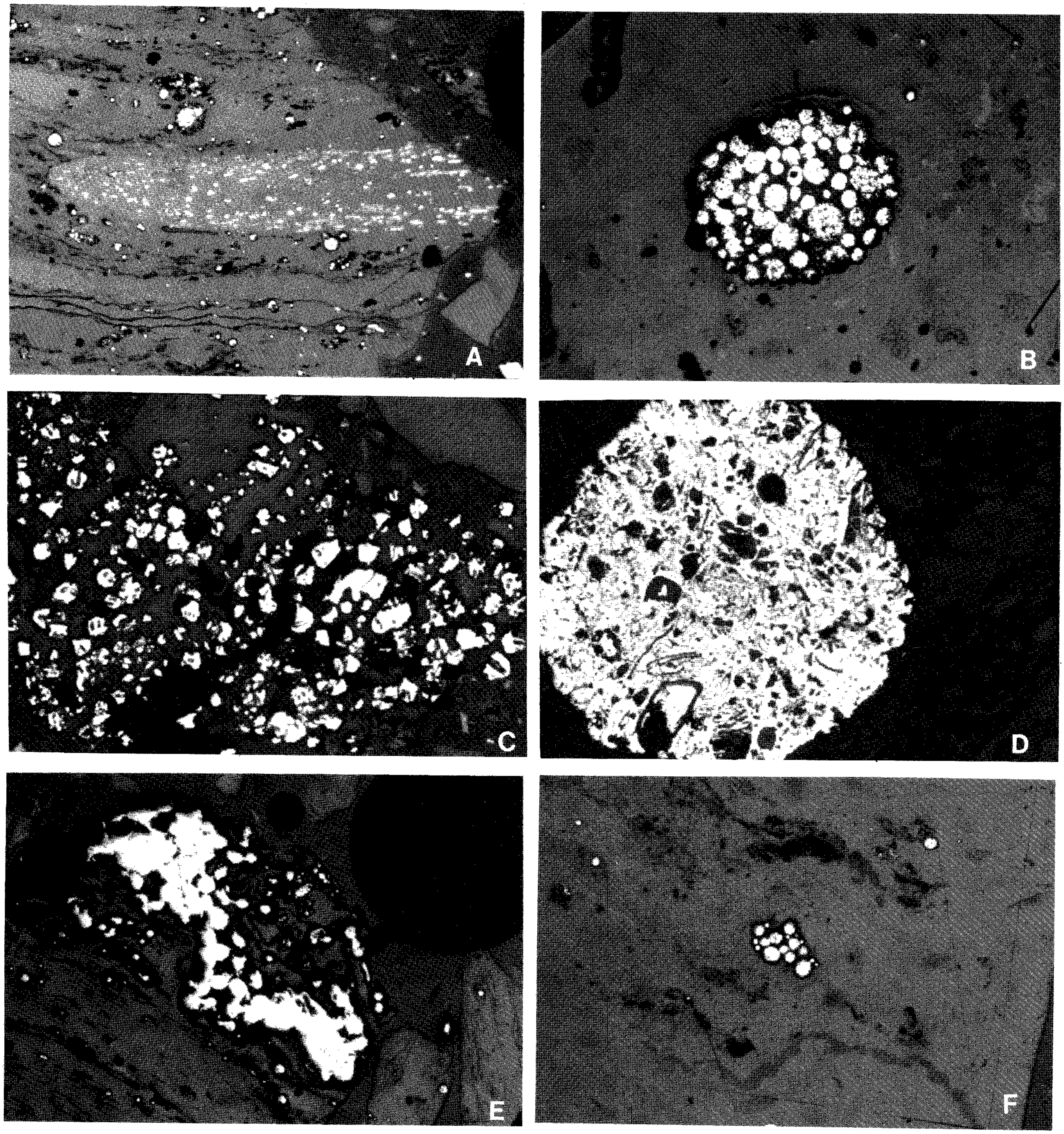

Figure 2. **a.** "Specular" pyrite in corpocollinite, River Gem (KCER-5392) (530 m on long axis); **b.** Framboidal pyrite, River Gem (KCER-5435) (530 m on long axis); **c.** Euhedral pyrite, Pond Creek (KCER-3561) (2.11 mm on long axis); **d.** Massive overgrowth incorporating plant tissue, Pond Creek (KCER-3550) (530 m on long axis); **e.** Massive layer of pyrite including overgrowths of framboids, Fire Clay upper lithotypes (KCER-4651) (1.06 mm on long axis); **f.** Framboidal pyrite, Fire Clay sub-flint clay lithotypes (KCER-4700) (530 m on long axis).

Figure 3. Opposite page. **a.** SEM image of pyrite from KCER-5435 (see Figure 2b); **b.** SEM image of pyrite overgrowth from lower right portion of Figure 3a; **c.** SEM image of "loose" aggregate of pyrite crystals and overgrown framboid (KCER-5392); **d.** SEM image of pyrite overgrowth from KCER-5392; **e.** SEM image of pyrite mass from KCER-3562; **f.** SEM image of pyrite mass from KCER-3550; **g.** SEM image of individual pyrite crystals with included framboidal associations (KCER-4651); **h.** SEM image of individual pyrite crystals with overgrowth of framboidal clusters (KCER-4700).

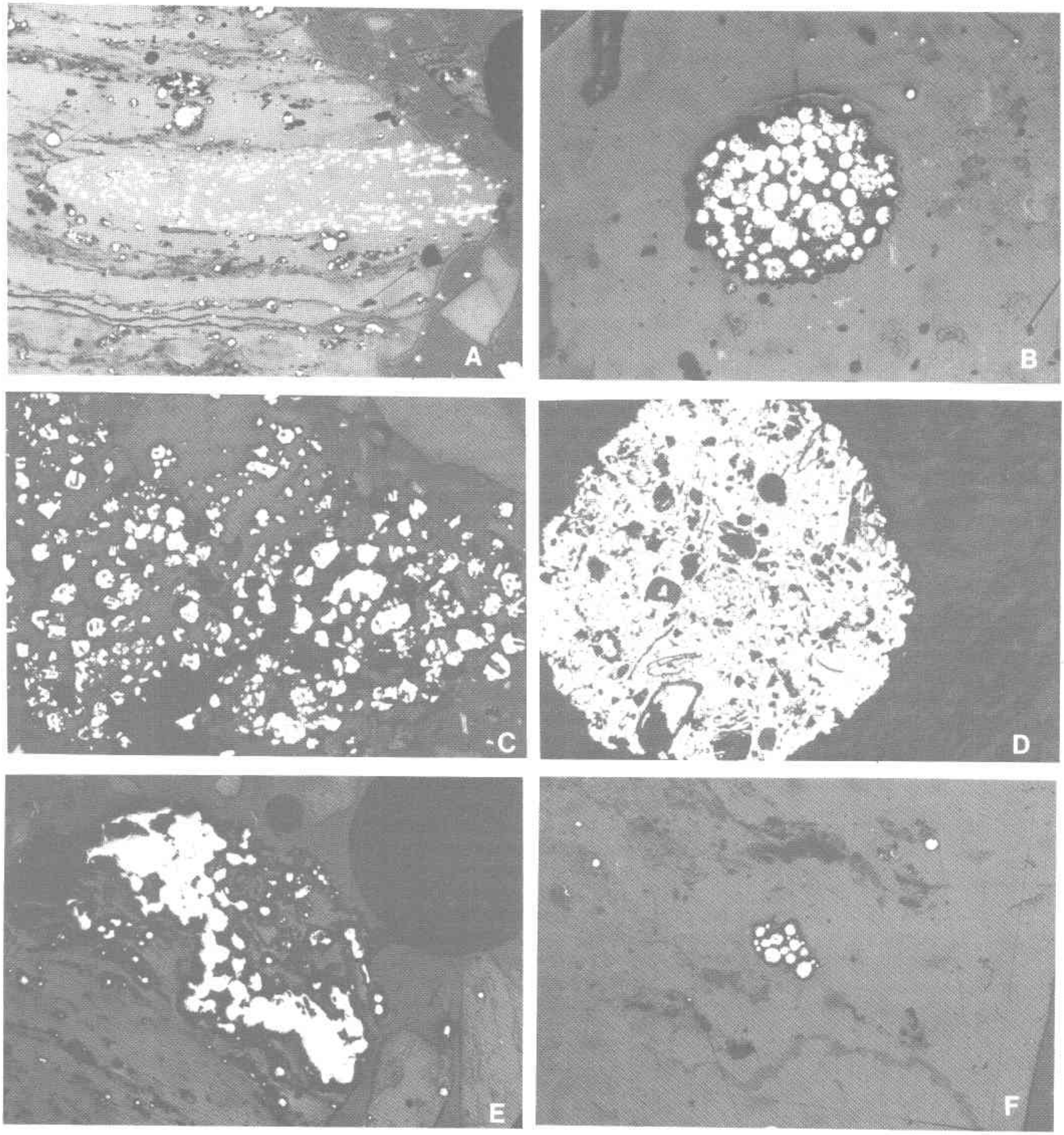

Figure 2. a. "Specular" pyrite in corpocollinite, River Gem (KCER-5392) (530 m on long axis); b. Framboidal pyrite, River Gem (KCER-5435) (530 m on long axis); c. Euhedral pyrite, Pond Creek (KCER-3561) (2.11 mm on long axis); d. Massive overgrowth incorporating plant tissue, Pond Creek (KCER-3550) (530 m on long axis); e. Massive layer of pyrite including overgrowths of framboids, Fire Clay upper lithotypes (KCER-4651) (1.06 mm on long axis); f. Framboidal pyrite, Fire Clay sub-flint clay lithotypes (KCER-4700) (530 m on long axis).

Figure 3. Opposite page. a. SEM image of pyrite from KCER-5435 (see Figure 2b); b. SEM image of pyrite overgrowth from lower right portion of Figure 3a; c. SEM image of "loose" aggregate of pyrite crystals and overgrown framboid (KCER-5392); d. SEM image of pyrite overgrowth from KCER-5392; e. SEM image of pyrite mass from KCER-3562; f. SEM image of pyrite mass from KCER-3550; g. SEM image of individual pyrite crystals with included framboidal associations (KCER-4651); h. SEM image of individual pyrite crystals with overgrowth of framboidal clusters (KCER-4700).

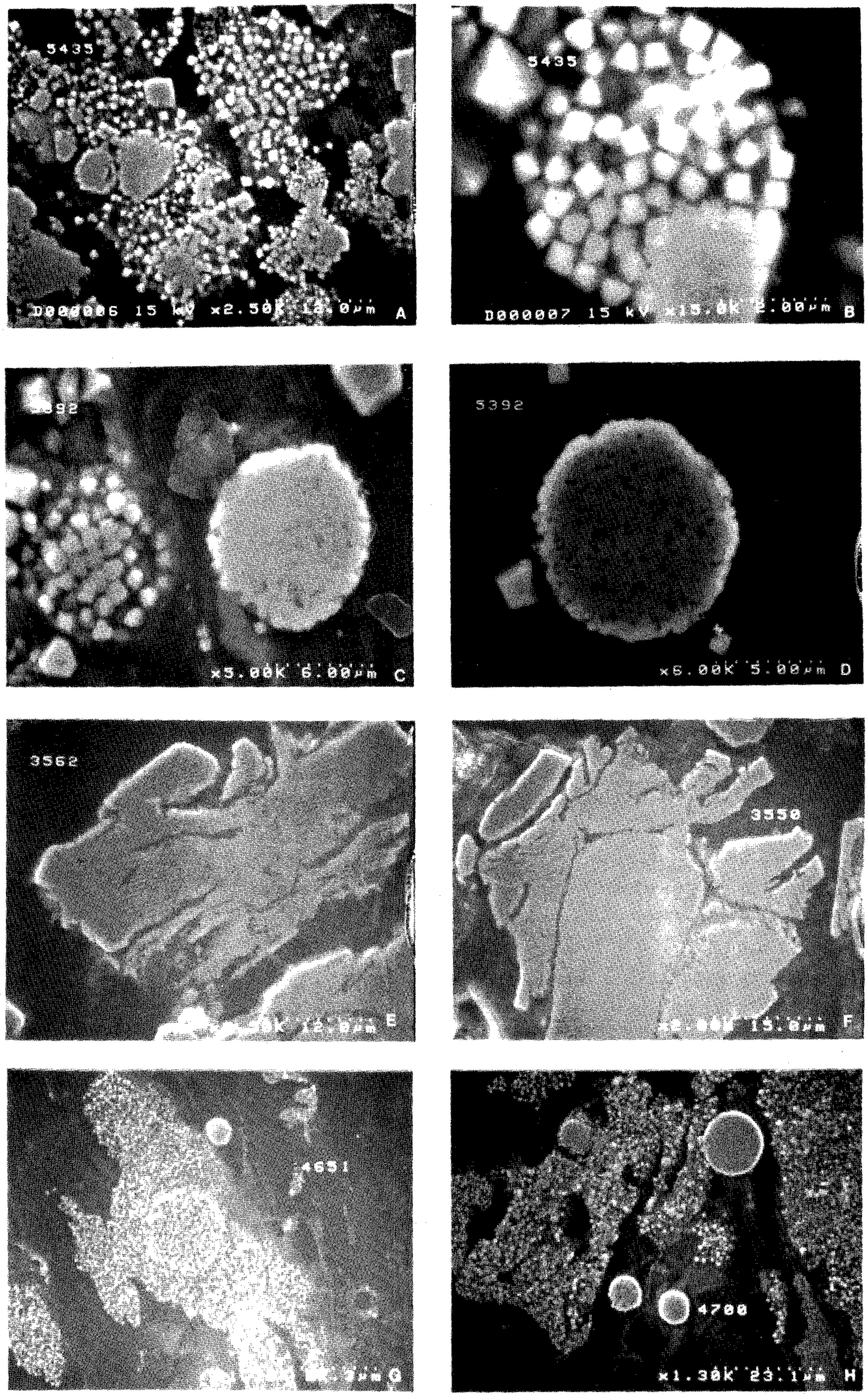
5435
A
5435
B
×5.00K 6.00μm C
5392
×6.00K 5.00μm D
3562
E
3550
F
4651
G
4700
×1.30K 23.1μm H

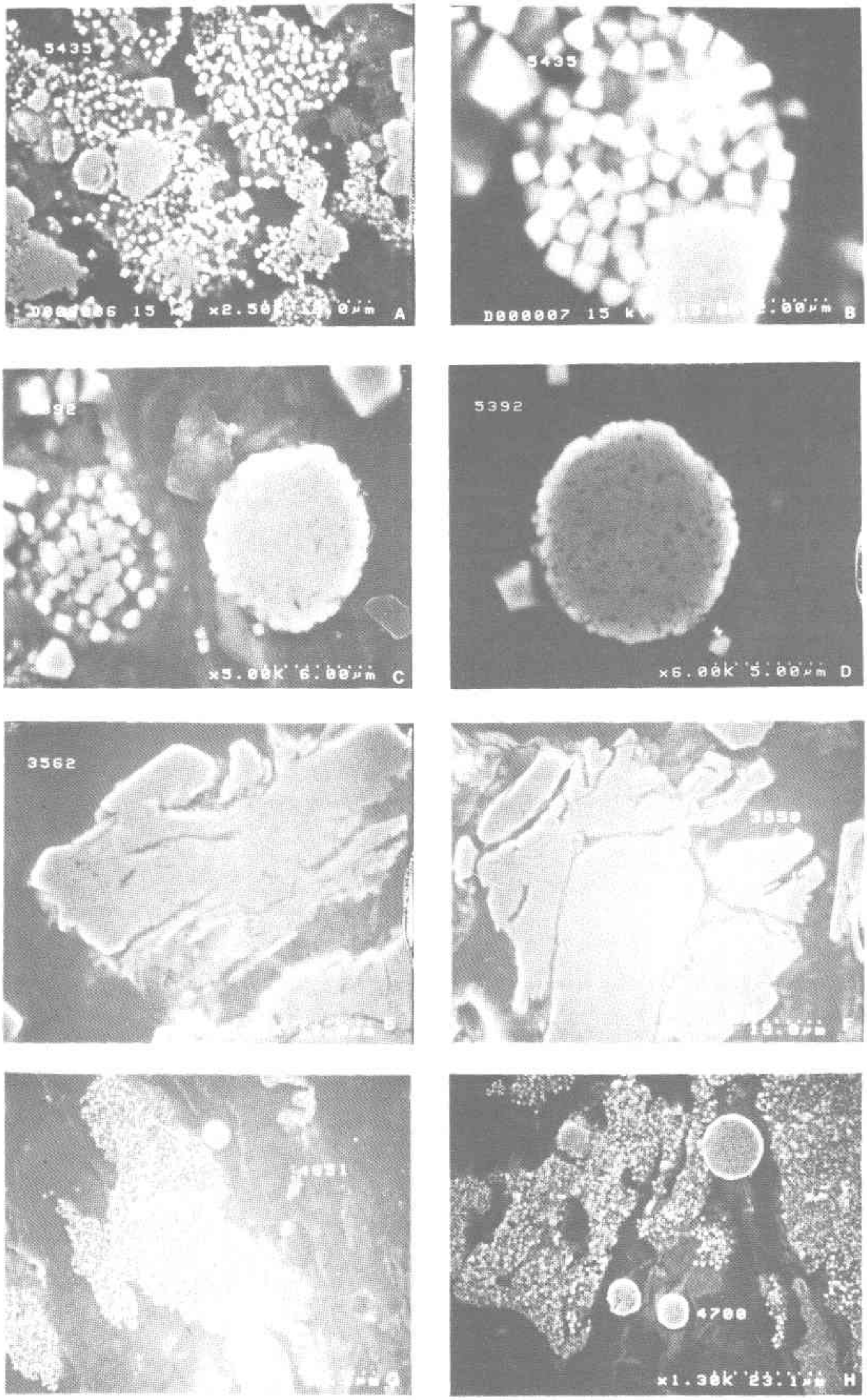
5435
A
5435
D000007 15 kV
B
5392
x5.00k 6.00µm C
5392
x6.00k 5.00µm D
3562
4700
x1.30k 23.1µm H

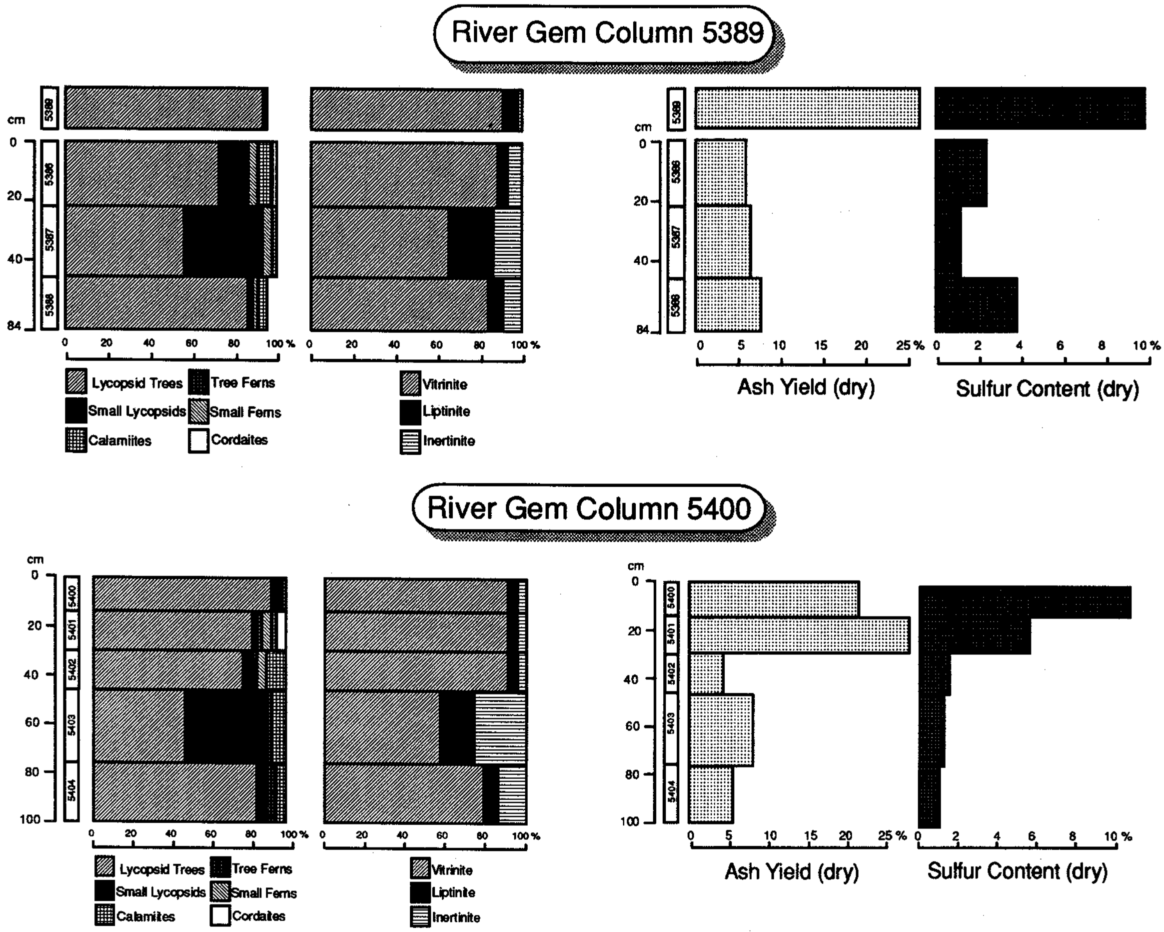

Figure 4. Generalized palynology of the River Gem coal bed at two mine sites.

CONFIRMING A STATISTICALLY DERIVED TOTAL COAL-SULFUR MODEL: SYDNEY COAL BASIN, NOVA SCOTIA (UPPER CARBONIFEROUS, CANADA)

Erwin L. Zodrow
Department of Earth Science,
University College of Cape Breton,
Sydney, Nova Scotia, Canada B1P 6L2

ABSTRACT

Earlier use of oblique factor analysis derived a statistical model of total coal-sulfur formation in the Sydney coal basin. In this paper, I describe initial empirical testing for investigating the applicability of the model to coal-mine planning and the coal-exploration process in the Sydney Coalfield, Nova Scotia. The testing is done through a regression equation, which is deduced from the oblique factor model and it involves 11 coal samples from France, Germany and Nova Scotia (Sydney coal basin). From these samples, total coal-sulfur percentages were obtained both by analytical chemistry and by estimation using the deduced regression as a prediction tool. Resulting discrepancies between the two sets of data are compared. Larger discrepancies lead me to reject the model for the European test samples; smaller discrepancies generally confirm the model for the Sydney samples. By inference, the model is acceptable as basically sound for the Sydney coal basin, although future modifications are suggested. An important conclusion from this study is that in the absence of a general model, each coal basin should be modelled separately.

INTRODUCTION

The Upper Carboniferous (Pennsylvanian) coal basin of Sydney, Nova Scotia, Canada, has been mined continuously since the middle of the 19th century for its volatile "A" bituminous coals. At one time, the coal basin was Canada's only coal producer and helped fuel the industrial revolution. Today, approximately 3 million long tons are mined annually which represent approximately 10% of Canada's annual coal output.

Because of geochemical, sedimentological, and diagenetic conditions in the Sydney coal basin, varying amounts of pyrite are present in the seams— from less than 1 weight percent (wt. %) to over 15 wt. %. However, total coal sulfur (pyritic + organic + sulfatic sulfur), of which the latter two forms are minor contributors, ranges from approximately 0.40 wt. % to over 21 wt. %. The mean and standard deviation of the total coal-sulfur content for the sampled Sydney seams is 4.78±4.31 wt. % (Zodrow, 1991; 1987).

For mine planning, in view of beneficiation and mixing coals for lowered total-sulfur content, and for exploration it would be advantageous to use a scientifically developed coal-sulfur model (Casagrande, 1987). For this purpose, I proposed (Zodrow, 1991) for the first time a statistically-derived model based on total coal-sulfur formation in the rhythmically bedded coals of the Sydney coal basin. The model is based on modern oblique factor-analytical methods (Harman, 1965) which was used for three interrelated reasons:

1. it assumes the hypothetico-deductive methodology of practicing science and a causality scheme consisting of multiple causes and effect relations (see below),

2. the factors represent interpretable chemistry— elemental concentration measurements (Massart and Kauffman, 1983), and

3. the larger data base, consisting of 31 variables and 137 samples (Zodrow, 1991), admits an effective use of factor analysis as a data-reduction tool.

The proposing of a statistical model is in itself not a sufficient reason for accommodating it into coal-mining planning and exploration. Therefore, the present paper is initiating empirical testing to evaluate it for such applications.

TOTAL COAl-SULFUR MODEL BY OBLIQUE FACTOR ANALYSIS: A SUMMARY

Five hypothetical factors (numbered Factor 1, 2 3, 4, and 6) define the total coal-sulfur model (TCSM). They are arranged as a causality scheme of the oblique factor model (Zodrow, 1991) as follows:

$$\text{total coal-sulfur} = 0.39\text{Factor }1 + 0.94\text{Factor }2 + 0.43\text{Factor }3 + 0.32\text{Factor }4 - 0.43\text{Factor }6$$

effect <-------------- **flow of causes**--------------

where the factor coefficients are the statistical correlations between factors and their effect. The factors are interpreted and represent different types of influxes into the developing peat swamps of the Sydney coal basin that control pyrite formation as follows. Thus emphasized are detrital and geochemical processes which played a part in the organic deposition of the coal peats during Upper Carboniferous time:

F1, clayey sediments carrying sulfate and metals, notably iron;
F2, recycled sulfate from solution of Lower Carboniferous (Mississippian) evaporite deposits that are stratigraphically below the Sydney coal formation;
F3, hydrothermal sulfide fluids differentiated from the process in F1; and
F4, Pb-rich fluids restricted to the youngest coals of the Sydney basin.

Factor 6 is interestingly controversial and presently not interpretable in both the TCSM and the conceptual geological scheme of total coal-sulfur occurrence (Zodrow, 1991, Table 7). This is not only because the factor is negative (excepting one correlation) and implies causally that the effect is best defined or explained by the increasing absence of the hypothetical cause, but also because its statistical existence may be dependent on parametric manipulation of the oblique factor solution. This exposes the problem of interpreting and understanding the meaning of negative cause-effect relation in total coal-sulfur formation in the Sydney Coalfield.

Further study is required (Zodrow, 1991, p. 141). As part of the methodology, factor analysis routinely ranks the calculated factors according to decreasing importance (in terms of decreasing explained factor variance). Therefore, the detrital and geochemical processes latent in Factor 1 are relatively the most influential and those of Factor 6 the least.

FACTOR ANALYSIS AND REGRESSION: INITIAL EMPIRICAL EVALUATION OF TCSM

Intuitively, a logical connection exists between the causality scheme and multiple regression prediction. The logic is given by Harman (1965), and Cazes (1970) presents a description of the connection, which by extension applies to factor analysis. The multiple regression equation for the prediction of total coal- sulfur is deduced from the structure matrix (Zodrow, 1991, Table 11, Eq. 5; Zodrow, 1970) and admitted as predictors to the total coal-sulfur regression are those variables that show the comparatively largest explained variance between an oblique factors and a geochemical variable (as in the structure matrix, see details in Zodrow, 1991, Table 11). Since there are only 5 causes in TCSM, only 5 predictor variables are possible for the erection of the multiple regression model. It is intuitive that the deduced regression, based on the causal relationship between the total coal-sulfur effect and its multiple hypothetical causes, is assumed *à priori* to show the comparatively maximum explained regression variance for the oblique factor solution and its parametric assumptions (Zodrow, 1991, p. 132-137. As derived, it is also intuitive that the regression predictors have latent coal-geological interpretability. The geochemical predictors in regression to estimate total coal sulfur wt. % are, according to the stated procedure, Al% (aluminum), Fe% (iron), Se ppm (selinium), Pb ppm (lead), and Ni ppm (nickel), Zodrow, 1991, Eq.4, and are expressed as statistical functionality asfollows:

total coal sulfur = f(Al, Fe, Se, Pb and Ni);
where the predictors are ranked according to decreasing importance in harmony with the causality scheme.

Therefore, the calculated multiple regression equation from which the total coal sulfur wt. % can be estimated is given as follows:

$$\begin{array}{ll} \text{total coal-sulfur} & \\ \text{wt. \%} & = 0.467 + 0.16\text{Al} + 1.08\text{Fe} + 0.098\text{Se} - \\ & \quad 0.002\text{Pb} + 0.02\text{Ni}; \\ (\pm\mathbf{1.71} & \quad \mathbf{0.229} \quad \mathbf{0.17} \quad \mathbf{0.06} \quad \mathbf{0.027} \\ & \quad \mathbf{0.002} \quad \mathbf{0.009}, \text{respectively}); \end{array}$$

explained multiple regression variance is 84.8%; bracketed, bold values indicate the error which can be regarded as standard deviation of regression coefficients; the value ±1.71 under 'total coal sulfur' is called the error of the total coal-sulfur estimate.

As derived, the calculated coal-sulfur regression equation is a tool that can be used to empirically test TCSM. The first step in the procedure is to obtain a set of test samples, independent of the data set that served as input for the oblique factor analysis. By analytical chemistry, total coal-sulfur wt. % is obtained from the test samples, as well as concentrations of Al, Fe, Se, Pb and Ni which are used for estimating total coal sulfur wt. %. From the results, discrepancies between estimated and analytically obtained total coal-sulfur wt. % are calculated and used as an inductive argument for confirming (or not) the hypothesis.

THE TEST SAMPLES

For the testing, 11 coal samples were used: one from Germany (early Permian age), one from the French Massif Centrale (Stephanian, late Upper Carboniferous age), and 9 from the Sydney coal basin (Westphalian C to Stephanian age), Table 1. These are not part of the input data for the factor analysis (Zodrow,1987). In particular, the samples from the Lower Lloyd Cove, Bouthillier, Emery and Gardiner Seams (Sydney coal basin), and the samples from the European coal seams had no sample representation in the input data (Zodrow, 1987). The remaining test samples from the Sydney coal basin were collected from localities at coal seams others than those from which the original samples were collected and in some cases several kilometers away to approximate as much as possible random sampling conditions. The sample from France and one sample from the Lower Lloyd Cove Seam are grab samples (Table 1) and do not conform to the required 15-cm incremental samples from whole-seam channel samples as specified by the sampling methodology (Zodrow, 1987). To maintain variable and sample methodological consistency between the input data (Zodrow, 1987) and the testing samples, coal samples were obtained and prepared by the author, and samples were chemically analyzed in accordance with the analytical procedures established for the studies (Zodrow 1987, 1991).

TESTING RESULTS

Results of the testing are summarized and the ash content is shows for information in Table 1. Observed ('observ.') refers to total coal-sulfur wt. % that was analytically determined for each of the test samples; estimated ('est.') refers to the total coal-sulfur wt. % that was obtained by the deduced regression equation using the Al, Fe, Se, Pb, and Ni data in Table 1. Discrepancies, bold bracketed values in Table 1, are in reference to 'obser.'. They range from approximately zero (Lower Lloyd Cove and Emery Seam test samples) to slightly more than double the observed total coal-sulfur wt. % (Phalen Seam and German test samples). In terms of percentage error, this ranges from zero to over 100%. It is, however, important to observe that the discrepant values (or 'regression residuals') are well within the ±1.71 error range of the total coal-sulfur estimate associated with the deduced multiple regression model. This, in effect, inspires geological confidence in the model.

However, the Sydney test samples on average show the smallest discrepancies. Also, the number of overestimation, (7) is not symmetrical with the number of underestimation (4). Furthermore, there is a tendency for medium total coal-sulfur wt. % to be associated with underestimation.

DISCUSSION

Some shortcomings of the applicability of the regression model are clearly indicated by the large discrepant estimates from three of the test samples (Phalen Seam and European samples).

The failure of the Phalen-Seam sample to confirm the regression model stems from the influence Factor 1 has in the derivation of the regression coefficients. Geologically, it is probably caused by the introduction into the Sydney Coalfield of anhydrite sulfur as contributing to the detrital mineral part. This helps explain why Al, which is strongly identified with the clay minerals, is indeed a detrital variable. Therefore, in the absence of contributing detrital minerals, ash content, Fe and Al contributions are expected to be low with a resulting low total-sulfur content. This is precisely the data that the Phalen sample shows at the sample location (Table 1) and the inference is that total sulfur is probably organic in derivation (Newman, 1935) and not of pyritic origin as assumed in the TCSM.

Secondly, the near 100% discrepancy in the German sample illustrates yet a different situation for the regression failure. The sample shows very low total coal sulfur, extremely low Al and Fe content, combined with an extremely high ash content (more than 7 times the average of the input data, Zodrow, 1991, Table 2). The inference is that although similar to the Phalen Sample, total coal sulfur is probably organic. The high ash content, however, points to palaeoenvironmental conditions and contributing mineral parts that are different from those that prevailed in the Sydney Coalfield.

Thirdly, the causes of the high total coal-sulfur overestimate for the French sample is difficult to pinpoint at this stage of the empirical investigation particularly as concentration levels are similar to those in the Sydney Samples, excepting ash and Pb, and those of the Phalen seam. The latter is approximately 3.5 times and the former 6 times the averages of the input data (Zodrow, 1991, Table 2). Therefore, it is difficult to reason exactly what the peat-formation process or other organic depositional conditions were in the French Upper Carboniferous Period.

The regression model can further be used for simulating total coal-sulfur predictions under various hypothetical palaeoenvironmental conditions. For example, the effect on the change of the multiple regression estimate ±1.71 wt. % of total coal sulfur was tested, given that the organic-sulfur variable be numerically simulated under these two mutually exclusive hypotheses: if the total coal-sulfur in one of the 137 samples of the input data (Zodrow, 1987) were:

1. larger than 2 wt. % (designated high-sulfur coal), organic sulfur is assumed proportionately less than 1%, or
2. below 2 wt. % (designated low-sulfur coal), no pyritic sulfur is assumed present, only organic sulfur.

The result indicates that a reduction from ±1.71 to ±1.61 wt. % in the estimate was possible. This may not represent the optimal situation, as the boundary between the presence/absence of organic sulfur is not known but was subjectively chosen at an average of 2 wt. % total coal sulfur. However, the simulated reduction is interpreted as being additionally supportive for including an organic sulfur variable in future TCSM models of the Sydney Coalfield. The variable was not included in the input data set as it was thought unimportant at that time because of minor occurrence generally in coal samples (for example see Beaton, 1986). Obviously the assumption requires rethinking for future work.

By the assumptions of oblique factor analysis, it could be shown that some factors are correlated (oblique) and others are not (orthogonal), Zodrow, 1991, Table 10. If this can be confirmed, then some of the Al, Fe, Se, Pb and Ni regression predictors are probably not all independent of each other as required by one of the assumptions about regression. Consequently, estimates (Table 1) are probably biased and the degree and direction of which are difficult to ascertain at this juncture.

CONCLUSION

Consequences of the statistically derived TCSM were empirically tested by a deduced quintic regression equation. Judging from a limited of number of test samples, it appears that the regression model is restrictive as it failed under test-sample conditions of:

1. lower total coal-sulfur content, or
2. higher or lower ash content, or
3. lower metal content particularly Fe and Al, or
4. a combination of all of the above.

This applies to the European test cases and suggests that the samples were probably drawn from coal seams with palaeoenvironmental, sedimentological and geochemical conditions different from those of the Sydney coals. It is interesting to note that these conditions were probably closest to those that prevailed in the Phalen Seam of the Sydney Coalfield.

It is therefore concluded at this time that a coal-sulfur model different from TCSM is required for the European cases and that Carboniferous coal basins be modelled separately until a synthetic model evolved with general applicability to total coal- sulfur distribution in the Carboniferous Period.

However, the model does work reasonably well for most of the test samples from the Sydney coal basin. This is evident in the face of:

1. using only a smaller sample set (n=137) from 9 out of possibly 24 thicker coal beds (>25 cm thick) in the Sydney basin (Bell, 1938), and
2. frequent coal-facies changes which means that composition of coal beds are laterally very variable as already described by Hawley's (1955) pioneering work on trace elements in the Sydney Coalfield and confirmed since (Zodrow, 1987; Mukhopadhyay, 1992).

These, together with the geological arguments why the regression model failed certain sample test samples, certainly provide some connective insight into the applicability and the limitations of TCSM.

For refinement of TCSM, future work would include three aspects. First, additional samples are needed not only from coal beds previously not sampled but also to better represent lateral geochemical variation in Sydney's coals in the data set (see some results by Hawley, 1955). Required are furthermore organic and sulfatic variables. This may have the desired effects of clarifying Factor 6 as to meaning and identification.

Secondly, for the exploration applicability of TCSM with concomitant economic and environmental consideration arising from coal utilization, a thorough study of the nature of organic sulfur is required (see Casagrande, 1987). Since sulfur bonded to carbon and ester sulfur is far more difficult to remove from the coal than inorganic sulfur in the form of cleat pyrite, the knowledge of their proportionate contributions to the total coal sulfur is crucial. Particularly as it appears that the organic sulfur content should be multiplied by a factor of 3-4 for comparison with coal only containing inorganic sulfur (Moore and Moore, 1976, p. 96-97). Results from such a study would furnish additional variables for the model.

Thirdly, the coefficients of the refined future TCSM and the deduced multiple regression model require rigorous statistical testing as outlined in chapters 16 and 17 (Harman, 1965): Measurements of Factors and Statistical Tests of Hypotheses in Factor Analysis, respectively. Additional regression-coefficient testing, as outlined by Lebart *et al.* (1979), is also suggested to further test if derived coefficients are statistically equivalent to those derived from testing data. This testing procedure will also involve investigations of confidence limits, errors of the estimate of multiple regression, and of scatter diagrams of multiple-regression residuals to test for bias (Zodrow *et al.*, 1982).

In conclusion, TCSM is regarded by inference as a working hypothesis for use in the Sydney coal basin.

ACKNOWLEDGMENTS

This study was supported by funds from the National Science and Engineering Research Council of Canada, for which I am very grateful. I am very grateful to Marcel R. Labonté, Institute of Sedimentary and Petroleum Geology, Geological Survey of Canada, for invaluable constructive comments and suggestions to improve the MS.

REFERENCES CITED

Bell, W.A., 1938. Fossil flora of Sydney Coalfield, Nova Scotia. Memoir 215, Geological Survey of Canada.

Casagrande, D.J., 1987. Sulphur in peat and coal. *in* Coal and Coal-bearing Strata: Recent Advances, A.C. Scott, editor, p.87- 105.

Cazes, P., 1970. Application de l'analyze des données au traitement de problèmes géologiques. Thèse du 3e cycle, C.N.R.S. Bibliotheque du centre de documention, Paris, France.

Harman, H.H., 1965. Modern factor analysis. Fourth impression. The University of Chicago Press.

Hawley, J.E., 1955. Spectrographic study of some Nova Scotia coals. Canadian Institute of Mining and Metallurgy, Transactions, 58: p. 412-426.

Lebart, L., Morineau, A. and Fénélon, J.P., 1979. Traitement des données Statistiques, Méthodes et Programmes. Dunod, Editeurs, Paris.

Massart, D.L., and Kauffman, L., 1983. The interpretation of analytical chemical data by the use of cluster analysis. A series of Monographs on Analytical Chemistry and its Applications. Edited by P. J. Elving, J.D. Winefordner and I.M. Kolthoff. John Wiley and Sons.

Moore, J.W. and Moore, E.A., 1976. Environmental chemistry. Academic Press, New York.

Mukhopadhyay, P. K., 1992. Research Report, elemental (metals and nonmetals) and petrographic characterization of Carboniferous coals from Nova Scotia, Canada: Parameters impacting on resource use and possible new potential. The Energy Resources Division, Nova Scotia Department of Natural Resources, Halifax, p. 51 plus tables, figures and appendices.

Newman, W.R., 1935. Microscopic features of the Phalen Seam, Sydney Coalfield, N.S. Canadian Journal of Research, 12: p.533- 553.

Zodrow, E.L., 1970. Factor analyses and magnetite formation and distribution in the Smallwood Mine. Society of Mining Engineers, AIME, Transactions, 247: p. 61-69.

Zodrow, E.L., Shaw, W. and Forgeron, S., 1982. Feasibility of volumetric coal estimation by trend-surfaces: Harbour Seam of Sydney Coalfield, Cape Breton Island, Nova Scotia, Canada. Mining Engineering, Transactions of AIME, 272: p. 1821-1826.

Zodrow, E.L., 1987. Geochemical trends in whole-seam coal channel samples from the Sydney Coalfield (Upper Carboniferous), Nova Scotia, Canada. Maritime Sediments and Atlantic Geology. 23: p. 141-150.

Zodrow, E.L., 1991. A coal-sulfur model for Sydney Coalfield (Upper Carboniferous), Nova Scotia, Canada. Atlantic Geology, 27: p. 127-142.

Table 1. Total coal-sulfur values by analytical chemistry and by estimation.

weightpercent			ppm			wt.% total coal sulfur	
Ash	Al	Fe	Se	Pb	Ni	observ.	est.
Sydney Coalfield, Nova Scotia (youngest to oldest seam)							
Unnamed Seam, 20-cm thick; 15 cm sampled							
20.2	1.32	8.16	0.20	187.9	78.9	9.27	10.71 **(1.44)**
•Lower Lloyd Cove Seam, 100-cm thick;grab sample near top of seam							
28.3	0.38	15.93	2.54	161.3	44.1	17.60	18.54 **(0.94)**
4 km from above location, 420-cm thick; 0 -15 cm* sampled							
22.6	0.97	10.26	1.58	52.2	11.9	11.90	11.99 **(0.09)**
Stubbart Seam, Prince Mine, 215-cm thick; 0 to 18 cm sampled							
11.2	1.42	1.79	0.11	11.6	35.2	2.96	3.32 **(0.36)**
•Bouthillier Seam, 200-cm thick; 45 cm to 60 cm sampled							
13.3	0.61	5.75	1.19	26.3	6.3	7.31	6.96 **(-0.35)**
Phalen Seam, 158-cm thick; 15 cm sampled, position not known							
2.8	0.23	0.76	0.67	7.2	3.9	0.70	1.45 **(0.75)**
•Emery Seam, 168-cm thick; 30 cm to 45 cm sampled							
5.1	0.58	1.18	0.05	4.3	10.4	2.09	2.04**(-0.05)**
•Gardiner Seam, 75-cm thick; 25 cm to 37 cm sampled							
12.0	1.04	2.53	0.09	13.1	13.9	4.06	3.63**(-0.43)**
Mc Aulay Seam, 35-cm thick, 6 cm to 15 cm sampled							
10.8	0.23	4.00	0.65	36.7	7.3	5.46	4.96**(-0.50)**
European coals							
•France, St. Helene, thickness not recorded, grab sample							
34.2	1.36	3.52	0.34	270.2	22.6	3.30	4.43 **(1.13)**
•Germany, Manebach, 20-cm thick; entirely sampled							
73.4	0.03	0.06	0.20	15.4	4.2	0.32	0.61 **(0.29)**

•= Seam not included in the original input data base (Zodrow, 1987, p.141, Table 2). Bracketed bold value is discrepancy.

* = Measurement from top towards bottom of the seam.

PETROLOGY OF JURASSIC (KIMMERIDGIAN) COALS, ATLANTIC CONTINENTAL SLOPE, NEW JERSEY

James C. Hower and Garry D. Wild
University of Kentucky
Center for Applied Energy Research
3572 Iron Works Pike
Lexington, KY 40511

ABSTRACT

Ten Jurassic coals and one Cretaceous lignite were studied from the COST B-3 well on the Atlantic continental slope off New Jersey. The reflectance of the lignite is 0.32% R_{max} and the Jurassic coals fall primarily in the high volatile A bituminous 0.71-0.78% R_{max} range. The coals exhibit a variety of maceral compositions, dominated by massive and resinite-impregnated vitrinite varieties.

INTRODUCTION

The COST B-3 borehole was drilled by Chevron for an 11-member consortium in 1978 and 1979 on the U.S. Atlantic continental slope 150 km southeast of Atlantic City, New Jersey (38° 55' 0.655" N/ 72° 46' 22.578" W) (Figure 1). The well penetrated 3.99 km of Tertiary through Jurassic sediments below the ocean floor to a total depth of 4.822 km. The geology and organic geochemistry of COST B-3 rocks are summarized in the volume edited by Scholle (1980a). Poppe and others (1990) examined Neocomian and Aptian/Barremian coals from the Gulf 718-1 well, also offshore New Jersey, as well as Mesozoic coals in two Georges Bank wells (Poppe and others, 1992a,b).

Two portions of the core are of interest in this study. A single Cretaceous (Albian) coal was recovered at 2.076 km below the sediment-water interface. Ten Jurassic coals were recovered from the 3.485-3.926 km interval. Steinkraus (1979) and Valentine (1980) assigned this entire coal-bearing interval to the Upper Jurassic (Kimmeridgian according to Steinkraus). Poag (1980), based on foraminifera, placed the section (including samples KCER-8039 and -8040; see Table 1) below our sample KCER-8038 in the Callovian (Middle Jurassic).

The Albian section of sandy shales, mudstones, and thin sandstones was interpreted by Poag (1980) to represent inner shelf to marginal marine environments. The Callovian (?) to early Kimmeridgian (3.99-3.589 km depth) section of gray shales, limestones, and thin sandstones interbedded with thin coals represent shallow-marine to coastal-marsh deposits with shallow-marine to coastal-marsh deposits with shallow-marine back-reef limestones. The younger Kimmeridgian strata in this core contains more limestones with fewer coals.

PROCEDURE

Samples were acquired from William MacQuowan, University of Kentucky (by way of Chevron USA, Inc.). Chips from the intervals of interest were recovered by float-sink separation at 1.8 specific gravity. Partings and mineral-rich lithotypes were thus lost in processing. The small quantity of coal recovered precluded chemical analysis.

The coal particles were mixed with epoxy and examined on a polished surface using white light, oil immersion microscopy. Further petrographic examination of the pellets followed etching of the polished surface after procedures published by Stanton and Moore (1991).

DISCUSSION

The results of the petrographic examination of the coals is presented on Tables 1 and 2.

The vitrinite maximum reflectance of the single Albian sample is 0.32% R_{max}. This is in good agreement with the reflectance profile reported by Miller et al. (1980; data from Core Labs). The Jurassic coals, however, all have reported R_{max} values significantly higher than the 0.47-0.57% R_o range found in the cuttings. Miller and others (1980) and Scholle (1980b) acknowledge that the R_o values represent a minimum estimate of the maturation. A coal at 3.917 km (not recovered in this study) had R_o values in the 0.83-1.13% range (Scholle, 1980b), suggesting an R_{max} in excess of 0.90%, higher than any coal in this study. The reflectance gradient through the Jurassic section is not particularly well defined. Only three coals are outside of the 0.71-0.78% R_{max} range. This is consistent with a low (23° C/km) geothermal gradient (Scholle, 1980b). The Jurassic gradient would have been higher owing to the proximity to the Mesozoic Atlantic spreading center but the coals would have been at a considerably shallower depth.

The petrography of the coals will be described in ascending order with identification by the laboratory number and the depth to the base of the coal bed from the sea floor. Most of the Jurassic coals show well preserved vitrinite forms, with telinite dominating. Gelocollinite is an important constituent in most coals but it only approaches or exceeds 50% of the telinite-collinite-gelocollinite (the dominant vitrinite varieties) group in a few cases to be noted below. The thicker coals, up to ca. 1.5 m, are in the KCER-8031 to -8034 and KCER-8038 to -8040 intervals.

KCER-8040 (3.926 km)

This coal sample consists of vitrinite with included resinite (Figure 2a) with some of the "vitrinite" being totally impregnated with resinite. With the exception of the massive vitrinite-resinite clarite, much of the microlithotype composition is detrital inertinite-liptinite-vitrinite assemblages. The vitrinite in the later microlithotype is dominated by gelocollinite with lesser amounts of vitrodetrinite. Massive vitrinertite was noted (Figure 2b), some with fine pyrite (Figure 2c). Liptinite-alginite laminae occur in the coal.

As noted above, KCER-8040 and KCER-8039 may be Callovian age. Based on the recovery of drill chips, admittedly a rather inexact assessment technique, those two coals are among the thicker of the Jurassic coals.

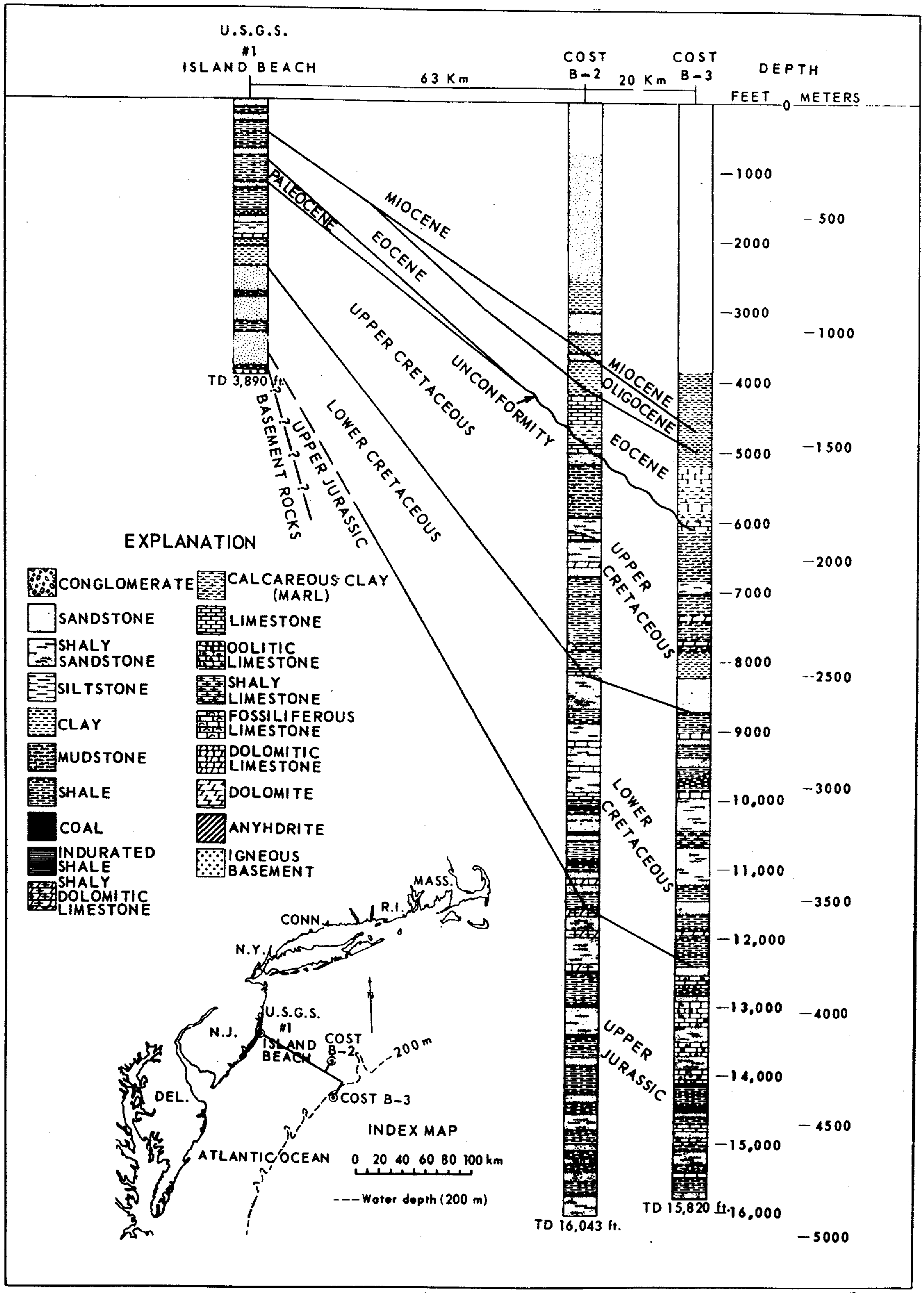

Figure 1. Location and generalized stratigraphy for COST B-3 and vicinity (from Mattick and Bayer, 1980).

TABLE 1. MACERAL COMPOSITION, MAXIMUM REFLECTANCE, AND MEAN (RANDOM) REFLECTANCE OF MESOZOIC COALS FROM COST B-3 (NOTE: PVIT - PSEUDOVITRINITE, SEMIFUS - SEMIFUSINITE)

Sample	Vitrinite	Pvit	Fusinite	Semifus	Micrinite	Macrinite	Exinite	Resinite	R_{max}	st. dev.	R_{mean}	st. dev.
8030	64.4	4.6	7.2	5.0	5.6	0.0	1.4	11.8	0.32	0.09		
8031	73.3	8.4	1.6	1.7	2.8	0.1	8.8	3.3	0.74	0.04	0.70	0.05
8032	72.5	7.4	3.0	3.0	3.0	0.4	5.5	5.2	0.74	0.04	0.67	0.05
8033	68.1	7.7	1.9	5.9	7.8	0.0	3.3	5.2	0.72	0.04	0.69	0.05
8034	67.6	6.4	7.7	7.0	6.5	0.0	3.1	1.7	0.67	0.04	0.65	0.04
8035	69.1	12.9	0.4	6.0	2.8	0.1	1.5	7.2	0.76	0.07	0.72	0.07
8036	64.4	1.2	1.2	19.8	3.6	0.4	0.6	8.8	0.74	0.06	0.70	0.06
8037	92.8	3.4	0.6	1.4	0.0	0.2	0.2	1.6	0.71	0.05	0.68	0.06
8038	40.6	10.1	18.6	12.8	4.4	0.2	5.6	7.8	0.82	0.07	0.78	0.08
8039	61.2	3.2	10.3	12.8	0.9	0.0	6.4	5.0	0.78	0.06	0.76	0.06
8040	53.2	10.1	8.4	18.4	2.9	0.0	3.2	3.8	0.83	0.07	0.75	0.10

KCER-8039 (3.876 km)

This coal sample has abundant massive vitrinite with included resinite (Figure 2d) and framboidal pyrite. Some semifusinite overlaps the vitrinite reflectance range. The fusinite occurs as sub-micron grains to large, virtually unstructured particles. Detrital microlithotypes, with sub-micron to few-micron grains were observed. Liptinite rich (bituminite?) cannel microlithotypes occur (Figure 2e).

KCER-8038 (3.862 km)

Vitrinite occurs in massive forms, as fine telinite with resinite, and as vitrodetrinite with inertodetrinite and, in some assemblages, clay. This coal has one of the higher gelocollinite percentages. Framboidal and euhedral pyrite occurs in the vitrinite. Note that this coal bed has the highest inertinite content and one of the highest resinite contents of the Jurassic coals.

This coal marks the base of the Kimmeridgian in Poag's assessment of the foraminifera assemblages.

KCER-8037 (3.809 km)

This thin coal sample is dominated by massive fine-textured telinite (Figure 2f) which may be resinized. The composition of the vitrinite is about 99% telinite plus corpocollinite as viewed on etched surfaces. The uniformity of the vitrinite leaves the impression of a nearly monospecific source. The rare fusinite occurs as massive pieces. Massive and, to a lesser degree, framboidal pyrite occurs in the vitrinite.

KCER-8036 (3.642 km)

The distinctive features of this coal sample are microlithotypes dominated by detrital macerals. The assemblages include mixtures of detrital and larger inertinites, detrital clarite, and inertodetrinite in a micrinite-vitrodetrinite groundmass. The massive telinite/telocollinite observed in the underlying coals was not found although the colloresinite-telinite assemblage is common. Pyrite occurs in massive forms.

KCER-8035 (3.642 km)

Vitrinite occurs in massive (telinite/telocollinite) forms, as telinite with colloresinite, and as a banded telocollinite (although in etched forms these bands appear to be dominated by a fine telinite). Layers of formless inertinite macerals, either semifusinite (as counted in the analysis) or macrinite, occur within the vitrinite bands. Vitrinite also occurs in intertongueing bands with inertodetrinite and clays (Figure 2g). Other mineral matter is framboidal and euhedral pyrite in vitrinite and a TiO_2 mineral with inertodetrinite.

KCER-8034 (3.58 km)

Vitrinite occurs as the colloresinite-telinite assemblage and in telocollinite bands with complex mixtures of inertinite and detrital macerals such as the inertodetrinite shown on Figure 2h. Overall, the banding is more common and better developed than any previously seen in the underlying coals. Marcasite, not observed in the underlying coals, occurs with pyrite, in places as massive overgrowths of pyrite. The coal is one of the thickest in the series of Jurassic coals.

KCER-8033 (3.498 km)

This coal sample is dominated by detrital maceral-mineral assemblages. This coal, as well as the overlying Jurassic coals, has a higher percentage of gelocollinite as observed in etched section than most of the other coals. Some vitrinite occurs in bands and associated with resinite. The three highest Jurassic coals appear to be intermediate in thickness relative to 8034, 8039, and 8040.

KCER-8032 (3.490 km)

This coal sample is dominated by finely laminated bands of detrital macerals. Massive vitrinite, some with resinite and some with framboidal pyrite, was observed.

KCER-8031 (3.485 km)

Overall, the coal is similar to the latter two coals Vitrinite occurs with resinite (Figures 2i and 2j) and as a telocollinite/

TABLE 2. VITRINITE TYPES ON ETCHED PELLETS

Sample	Telinite	Corpocollinite	Gelocollinite	Vitrodetrinite	Gelinite
8031	44	9	44	2	0
8032	42	14	40	4	t
8033	38	16	40	6	0
8034	56	7	35	2	0
8035	59	15	16	10	0
8036	58	6	36	0	0
8037	86	14	t	0	0
8038	49	4	42	5	0
8039	53	6	34	6	0
8040	59	11	25	5	0

desmocollinite mix (Figure 2k).

KCER-8030 (2.076 km)

The lone Albian coal is distinguished both by it's age and it's lignite rank. The huminite fraction is dominated by ulminite and texto-ulminite (Figure 2l). Massive resinite was observed.

PETROGRAPHIC SUMMARY

The rank gradient over the 439 m coal-bearing portion of the Jurassic is not particularly well-defined, but, combined with the Cretaceous lignite 1.4 km above the uppermost Jurassic coal, it does suggest coalification at relatively low paleogeothermal gradients. This is not surprising given the relatively passive tectonic setting of the coals. As the coals were buried deeper, they were also increasingly removed from the mid-ocean ridge, the primary locus of metamorphism in the expanding ocean. The latter situation is in distinct contrast to similar rank coals in the Appalachians which were proximal to the orogenic belt, therefore attaining high volatile A bituminous rank at shallower depths and higher geothermal gradients.

Without further evidence from palynologic studies it is difficult to fully assess the petrographic data. The abundance of resinite in many of the coals suggests that gymnosperms may have been an important element in the flora. The high inertinite content of four of the five lower coals suggests that there may have been a change in the vegetation following the deposition of KCER-8036. The lack of any information on Jurassic coals from the vicinity further limits the scope of the study, virtually eliminating the possibility of assessing these coals with respect to their depositional setting.

ACKNOWLEDGEMENTS

William MacQuowan, University of Kentucky, provided the samples. Cortland Eble and Robert Rathbone reviewed the manuscript.

REFERENCES

Mattick, R.E., and Bayer, K.C., 1980, Geologic setting and hydrocarbon activity, in Scholle, P.A.,(ed.), Geological Studies of the COST No. B-3 Well, United States Mid-Atlantic Continental Slope Area: U.S. Geological Survey Circular 833, p. 4-12.

Miller, R.E., Schultz, D.M., Claypool, G.E., Smith, M.A., Lerch, H.E., Ligon, D., Owings, D.K., and Gary, C., 1980, Organic geochemistry, in Scholle, P.A.,(ed.), Geological Studies of the COST No. B-3 Well, United States Mid-Atlantic Continental Slope Area: U.S. Geological Survey Circular 833, p. 85-104.

Poag, C.W., 1980, Foraminiferal stratigraphy, paleoenvironments, and depositional cycles in the Outer Baltimore Canyon Trough, in Scholle, P.A., (ed.), Geological Studies of the COST No. B-3 Well, United States Mid-Atlantic Continental Slope Area: U.S. Geological Survey Circular 833, p. 44-65.

Poppe, L.J., Hall, R.E., Cousminer, H.L., Stanton, and Steinkraus, W.E., 1990, Biostratigraphy, lithofacies and paleoenvironments of the Gulf 718-1 well, U.S. Mid-Atlantic Outer Continental Shelf: Marine Geology, v. 92, p. 27-50.

Poppe, L.J., Poag, C.W., and Stanton, R.W., 1992a, Lithology, stratigraphy, and paleoenvironments of the Mobil 312-1 well, Georges Bank Basin, U.S. North Atlantic Outer Continental Shelf: Northeastern Geology, v. 14, p. 156-170.

Poppe, L.J., Poag, C.W., and Stanton, R.W., 1992b, Mid-Mesozoic (Mid-Jurassic to Early Cretaceous) evolution of the Georges Bank Basin, U.S. North Atlantic outer continental shelf: sedimentology of the Conoco 145-1 well: Sedimentary Geology, v. 75, p. 171-192.

Scholle, P.A., ed., 1980a, Geological Studies of the COST No. B-3 Well, United States Mid-Atlantic Continental Slope Area: U.S. Geological Survey Circular 833, 132 p.

Scholle, P.A., 1980b, Data summary and petroleum potential, in Scholle, P.A.,(ed.), Geological Studies of the COST No. B-3 Well, United States Mid-Atlantic Continental Slope Area: U.S. Geological Survey Circular 833, p. 13-19.

Stanton, R.W, and Moore, T. A., 1991, Types of vitrinite macerals I; The

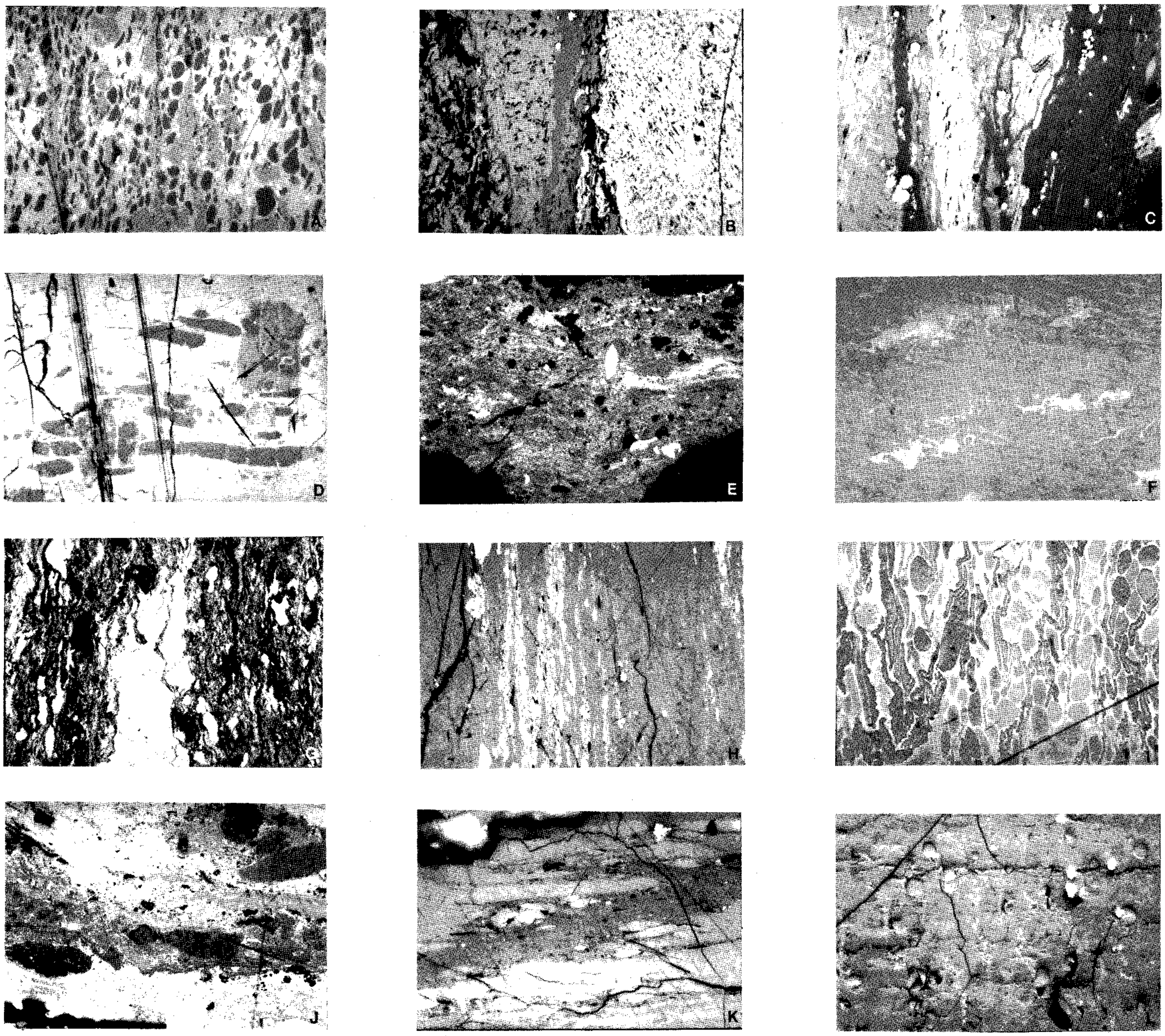

Figure 2. Selected microphotographs of Mesozoic coals. All photos 330 m on long axis. **a**. vitrinite/resinite assemblage (KCER-8040); **b**. semifusinite/fusinite/vitrinite (KCER-8040); **c**. massive semifusinite with vitrinite and fusinite (KCER-8040); **d**. resinite/vitrinite assemblage (KCER-8039); **d**. canneloid microlithotype with bituminite (?) (KCER-8039); **f**. resinite in vitrinite (KCER-8037); **g**. vitrinite band in detrital matrix (KCER-8035); **h**. vitrinite with inertodetrinite (KCER-8034); **i**. resinite (KCER-8031); **j**. resinite in vitrinite (KCER-8031); **k**. telocollinite/desmocollinite assemblage (KCER-8031); **l**. ulminite with corpohuminite (KCER-8030).

necessity for etching: The Society for Organic Petrology Newsletter, v. 8, n. 1, p. 8-10.

Steinkraus, W.E., 1979, Biostratigraphy, in Amato, R.V., and Simonis, E.K.,(ed.), Geological and operational summary, COST No. B-3 well, Baltimore Canyon Trough area, Mid-Atlantic OCS: U.S. Geological Survey, Open-File Report 79-1159, p. 21-31.

Valentine, P.C., 1980, Calcareous nannofossil biostratigraphy, paleoenvironments, and post-Jurassic continental margin development, in Scholle, P.A.,(ed.), Geological Studies of the COST No. B-3 Well, United States Mid-Atlantic Continental Slope Area: U.S. Geological Survey Circular 833, p. 67- 83.

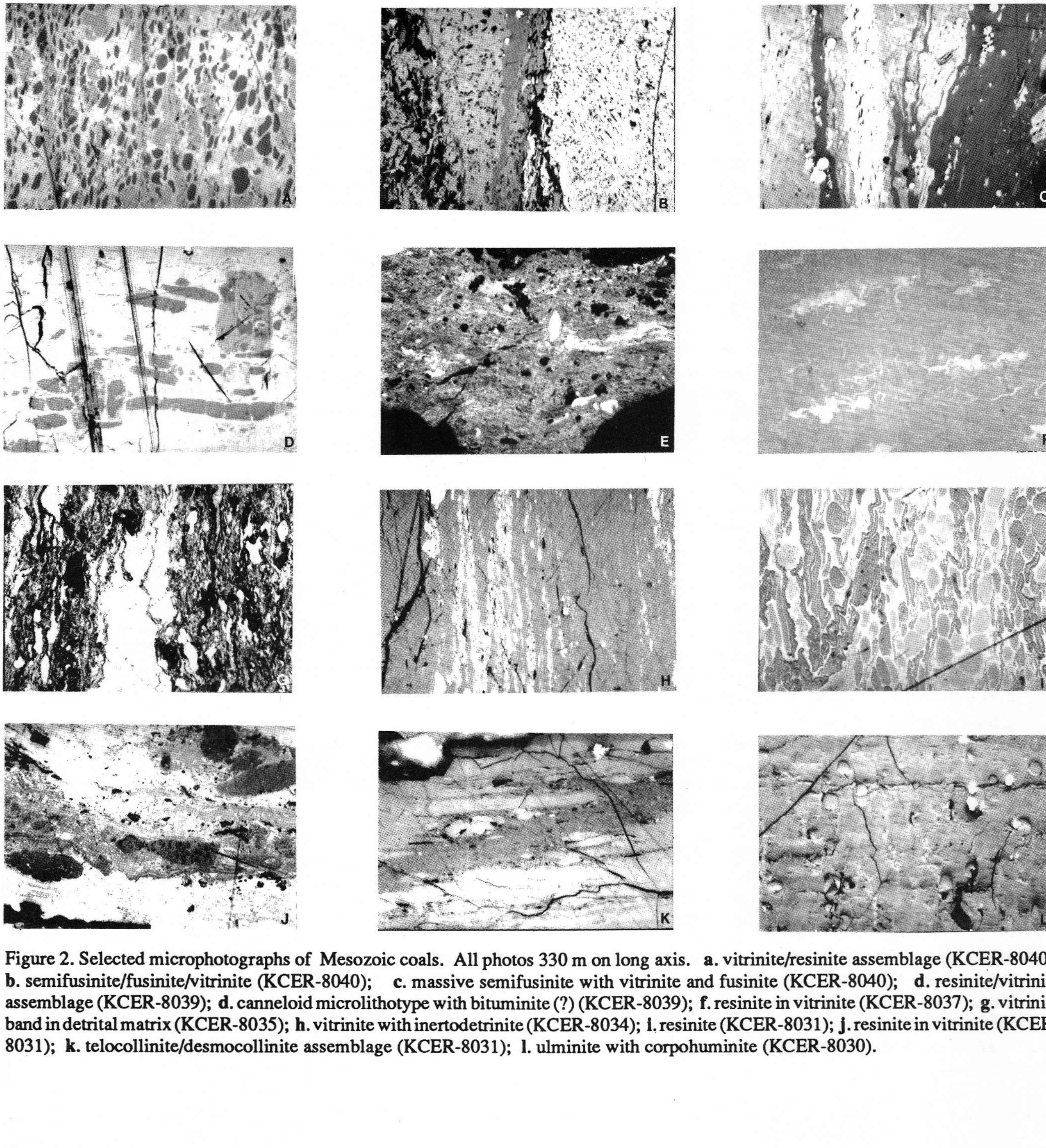

Figure 2. Selected microphotographs of Mesozoic coals. All photos 330 m on long axis. **a.** vitrinite/resinite assemblage (KCER-8040); **b.** semifusinite/fusinite/vitrinite (KCER-8040); **c.** massive semifusinite with vitrinite and fusinite (KCER-8040); **d.** resinite/vitrinite assemblage (KCER-8039); **d.** canneloid microlithotype with bituminite (?) (KCER-8039); **f.** resinite in vitrinite (KCER-8037); **g.** vitrinite band in detrital matrix (KCER-8035); **h.** vitrinite with inertodetrinite (KCER-8034); **i.** resinite (KCER-8031); **j.** resinite in vitrinite (KCER-8031); **k.** telocollinite/desmocollinite assemblage (KCER-8031); **l.** ulminite with corpohuminite (KCER-8030).

necessity for etching: The Society for Organic Petrology Newsletter, v. 8, n. 1, p. 8-10.

Steinkraus, W.E., 1979, Biostratigraphy, in Amato, R.V., and Simonis, E.K.,(ed.), Geological and operational summary, COST No. B-3 well, Baltimore Canyon Trough area, Mid-Atlantic OCS: U.S. Geological Survey, Open-File Report 79-1159, p. 21-31.

Valentine, P.C., 1980, Calcareous nannofossil biostratigraphy, paleoenvironments, and post-Jurassic continental margin development, in Scholle, P.A.,(ed.), Geological Studies of the COST No. B-3 Well, United States Mid-Atlantic Continental Slope Area: U.S. Geological Survey Circular 833, p. 67- 83.

AN INTEGRATED APPROACH TO RESERVOIR MODELING - GRANNY CREEK FIELD, WEST VIRGINIA

Kurt A. Donaldson
Department of Geology and Geography,
West Virginia University, Morgantown, WV 26505

ABSTRACT

The usefulness of the following methods was evaluated in the investigation of heterogeneity within the Mississippian Big Injun sandstone of Granny Creek oil field, West Virginia: (1) database, (2) cross-sections, (3) two-dimensional maps, (4) three-dimensional block models, (5) geographic information system (GIS), (6) rule-based expert system, and (7) basin history models. Each method had its strengths and weaknesses depending on which parameters were being evaluated. A database was designed to provide an effective means for maintaining, manipulating, and integrating the vast amount of well data. The Big Injun Cross-section program was created to correlate depositional environments, porosity, permeability, stratigraphic, and petrographic data. The flexible design allows for additional subsurface property values. Many two-dimensional maps of various properties were created by hand or computer. The most useful maps in our analysis were exported to a geographic information system software package for further spatial analysis. Dynamic Graphics' Interactive Volume Modeling software was used to display porosity and permeability data that vary continuously in three-dimensional space. A primarily raster-based geographic information system was utilized to extend the capabilities of a traditional database query by performing analyses based on geographical position. Over one hundred raster images and numerous vector overlay files were created to accelerate the analysis and presentation of two-dimensional spatial data. An expert system was designed to give expert advice regarding reservoir heterogeneity at any current or proposed well in Granny Creek. The Granny Creek Expert System captured the logical reasoning of geoscientists and engineers regarding heterogeneity of the Big Injun reservoir, and then made that expert knowledge available to less experienced personnel. Four mathematical models were created to reconstruct Granny Creek's "basin" history. The basin history models provided insight into the basin-forming mechanisms and hydrocarbon generation at Granny Creek field. Finally, an evaluation of the above methods and their usefulness in the analysis of quantitative, logical, and spatial data should prove valuable for future projects.

INTRODUCTION

The 2500 acre Granny Creek oil field in Clay and Roane Counties, West Virginia (Figure 1), was discovered in 1925. Since its discovery, the oil field has produced an estimated 9.1 million barrels of oil from both primary and secondary production (Haught, 1964; Swales, 1988). More than 600 wells have been drilled in the field, with most of the wells spaced between 400 to 600 feet apart.

The Big Injun Sandstone, a lower Mississippian member of the Price formation, is the primary oil producing reservoir for Granny Creek field. The Big Injun's depths range from 1950 to 2250 feet and has an average pay thickness of 20 feet. Variability in production indicates that structural, stratigraphic, and diagenetic heterogeneities exist in the Big Injun that control production trends (Donaldson et al., 1992).

Research geologists, geophysicists, petroleum engineers, and geostatisticians have investigated whether heterogeneities exist in the Big Injun reservoir (Donaldson et al., 1992). During the past three years scientists and engineers of the study have compiled a vast amount of data documenting reservoir heterogeneity. Integrating and analyzing the reservoir data was assisted by the application of spatial, logical, and quantitative methods. Each method was rated by (1) how quickly and easily the method integrated various types of data; (2) how beneficial the technique was in delineating reservoir heterogeneity; and (3) how cost-benefiting the particular method was in completing jobs satisfactorily within a short period. Evaluated was the usefulness of the following methods: database, cross-sections, contour maps, three-dimensional block models, geographical information system (GIS), expert system, and basin history models.

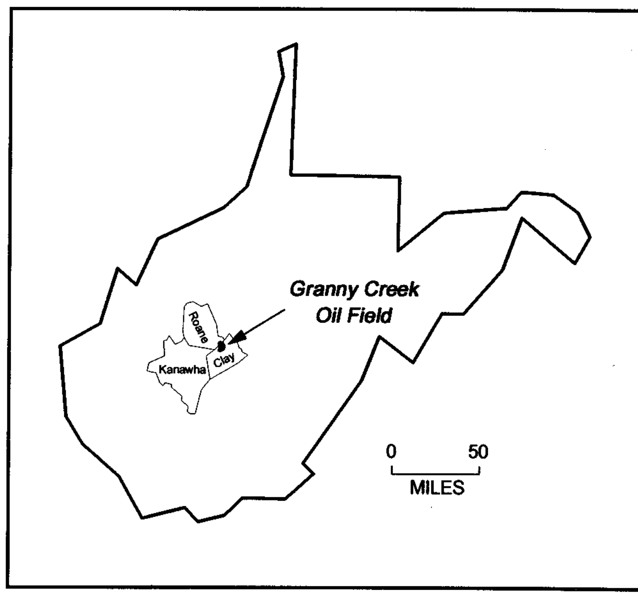

Figure 1: Location map of Granny Creek oil field, West Virginia.

DATABASE

A database was created to integrate effectively the vast amount of well data generated from the study of Granny Creek oil field. The Granny Creek database also provided a foundation for retrieving information, drawing conclusions and making critical decisions much faster than if the data were stored in a text file. Scientists using the Granny Creek database were able to (1) maintain and update well information, (2) locate and retrieve well data that meets a given set of specifications, (3) sort and rearrange data into a predetermined order, (4) integrate or link well data files together, and (5) produce statistical reports for quantitative analysis. Spatial databases, which add a spatial dimension to traditional databases, are commonly part of geologic studies such as that undertaken here.

SPATIAL METHODS

In geology, many critical relationships are discovered by spatial analysis. A variety of techniques, including cross-sections, contour maps, 3D block models, and geographical information system displays, were used to analyze spatially-referenced geologic and production data. Each method gives the individual doing the research a specialized tool for investigating spatial patterns of importance. For Granny Creek field, cross-sections and block models were beneficial in delineating stratigraphic and depositional subsurface intervals, whereas contour maps and GIS helped in examining two-dimensional subsurface data for the entire field. GIS also made easier the integration, analyses and presentation of vast amounts of spatial data.

2D CROSS-SECTIONS

A Big Injun Cross-Section (BICS) program was created by the author to compare stratigraphic, engineering, petrographic, and depositional data. Because cross-sections could be rapidly produced at any scale, they could be readily compared with other cross-section variables. Thus BICS was an effective method for comparing different types of 3D subsurface data for spatial analysis. Completed cross-sections of Granny Creek were also helpful in investigating the different stratigraphic and depositional intervals within the reservoir. The cross-sections were limited, however, in that they neither provided 3D visualization nor displayed continuous data for the entire field. In addition, no volume calculations, such as oil in place, could be made.

2D MAPS

Maps of various properties were created by hand or computer. Most of the computer generated maps were made using two commercial software contouring packages, Surface III and Mapping Contouring System (MCS). The mapping software rendered fast, helpful information on the distribution of rock properties in two dimensions. Employing both contouring packages provided the user with a suite of interpolation schemes, from inverse distance and krigging to triangulation.

A disadvantage of 2D maps was that they did not provide 3D visualization of subsurface properties. Another limitation was in integrating vast amounts of spatial data. Converging data from many different maps was best accommodated by a GIS application that simplified and enhanced the analysis of multivariate spatial data. Consequently, grids of the most important contour maps were exported to a 2D geographic information system (GIS) package for further spatial analysis.

3D BLOCK MODELS

Dynamic Graphic' Interactive Volume Modeling (IVM) software was used to model, visualize, and analyze porosity and permeability data that varied continuously in 3D space. This new technology allowed for true 3D modeling so that geologists or non-geologists could better visualize different subsurface intervals. A permeability/porosity block model of Granny Creek field was rotated, sliced, and peeled to display important stratigraphic and depositional zones. Unlike cross-sections, block models allowed for visualization of the entire Granny Creek field in three-dimensional space. The 3D software was limited, though, in its ability to model multiple geological and engineering properties.

2D GIS

A geographic information system (GIS) is a computer-assisted system that acquires, stores, processes and displays spatial data. GIS extends the capabilities of a traditional database query by performing analyses based on geographic position. To accelerate the analysis and presentation of 2D spatial data for Granny Creek oil field, a primarily raster-based GIS was used.

Once the base images, such as reservoir thickness and mean porosity, were created, various GIS operations were applied to better characterize the reservoir. To determine locations of optimal oil production, for example, a spatial query of six geologic and engineering variables was made utilizing the RECLASS and OVERLAY operations (Figure 2). Valuable GIS operations not usually found in other spatial analysis software are vector overlay, image enhancement, image cross-classification, draped images onto perspective displays, and spatial statistics. These and other GIS operations facilitate the integration, analyses and presentation of two-dimensional spatial data.

LOGICAL REASONING METHOD: EXPERT SYSTEM

Logical reasoning was also employed extensively in the expert system developed for Granny Creek. Expert systems are computer systems that use logical reasoning to solve problems that are normally handled by human experts. The Granny Creek Expert System (GCES) was designed to give expert advice regarding reservoir heterogeneity at any current or proposed well. A person using GCES is queried by the computer for pertinent data about the reservoir. When the expert system acquires enough information, it displays conducive knowledge about potential oil production and heterogeneity for that well.

The design of the expert system demanded that experts, in this case geologists, geophysicists, and engineers, record their reasoning or any intuitions about reservoir heterogeneity into concise, organized decision trees, along with probability statistics to estimate the likelihood of certain events occurring. Experts used *IF premise-1 and premise-2 and . . . THEN conclusion* statements to define important relationships discovered during their investigation of reservoir heterogeneity. Every decision or rule tree was then encoded into a knowledge base. Four knowledge bases: stratigraphy, structure, engineering, and petrology, were developed to integrate all types of reservoir data.

The success of the expert system will depend on the experts' ability to establish a comprehensive knowledge base for their research area. If certain geologic or engineering variables that influence reservoir heterogeneity are unknown or not readily delimited, then the expert system cannot be trusted.

QUANTITATIVE METHODS

Quantitative analysis was an integral part of evaluating Granny Creek data because a vast amount of data had been collected to investigate the characteristics of the Big Injun reservoir. Many statistical and modeling methods exist to help investigators better understand a reservoir's geological and engineering properties. Such statistical techniques include descriptive or multivariate statistics, while certain reservoir properties can be portrayed with stochastic, deterministic, or reservoir simulation models. Although quantitative methods are ideal for discovering or confirming rela-

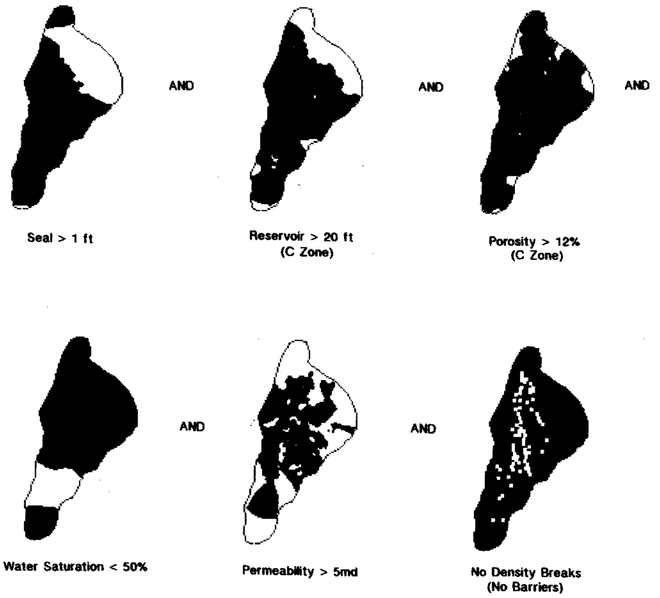

Figure 2: Spatial query of six geologic and engineering variables to determine locations of optimal oil production. Solid black areas denote true conditions.

tionships among unique properties, like the other methods, they have their limitations. With quantitative methods it is often difficult to explain mathematically how every geological variable affects the reservoir.

STATISTICS

There are many types of elementary statistics that can be employed to investigate relationships among various geological and engineering variables. As for Granny Creek, database reports provided beneficial summary statistics about integrated reservoir data. The integrated data was grouped by different variables, like stratigraphy and deposition, to search out trends that may be helpful in understanding the reservoir. Besides database reports, descriptive statistics of density logs were computed for detailed porosity analyses. Probability statistics also were computed for the Granny Creek Expert System to establish belief and occurrence probabilities for each knowledge base

. Multivariate statistics are important for examining multiple variables, especially when so many subsurface variables exist as is true for Granny Creek field. These methods use computers to evaluate the many geological and engineering variables that may influence reservoir heterogeneity, and then group or cluster variables together that have similar properties. For Granny Creek field ,multivariate statistics could be used to evaluate core data; specifically permeability, porosity, and petrographic properties. Factor analysis, principal component analysis, and cluster analysis are some of the techniques that could be employed.

BASIN HISTORY MODELS

Four mathematical models were created to reconstruct Granny Creek's "basin" history: (1) decompaction, (2) backstripping, (3) thermal, and (4) geohistory. These mathematical models provided insight into the basin-forming mechanisms and hydrocarbon generation at the Granny Creek field. The decompaction and backstripping models show the subsidence history of Granny Creek field, while the thermal model portrays the unroofing history of the field. By coupling the decompaction and thermal models together, a geohistory model was created to illustrate the complete history of the basin.

SYSTEM DESIGN

Figure 3 shows an organized, systematic approach for integrating well data of Granny Creek. The system design depicts the methods employed in the analyses of quantitative, logical, and spatial well data. In this design, the top-down flow of data begins at the database, where raw data is first entered before executing any of the other analytical applications such as block models or GIS. Typically, all the methods in this diagram (Figure 3) rely on scattered well data. From the database the user can quickly extract data for other methods. For instance, if an investigator wants to perform statistical analyses on well data of a specific depositional zone, then that data can be retrieved quickly from the database.

The expert system and GIS are located at the bottom of the flow diagram because they depend on input from integrated database reports, statistics, contour maps, cross-sections, and block models. GIS merges a vast amount of spatial data while the expert system encompasses every experts' logical reasoning. Because reservoir information often is exchanged between the expert system and GIS, the data flow is two-way. Knowing which geological variables to evaluate in a spatial query, for instance, is an example of essential information passed from the expert system to GIS. GIS, in turn, from its spatial analyses of numerous images, provides knowledge to the expert system. During the spatial analyses of Granny Creek, for example, the Geographical Information System cross-classified two stratigraphic images (mouth bars and seal) to form a new image showing the combinations of the categories of the original images. Spatial statistics next were applied to the cross-classified image to compute probabilities of certain geologic variables for each new region. This helpful information was then used to update the expert system.

Also, basin history models were evaluated. These models are shown in another schematic (Figure 4) because the models contain data that are not easily compatible with well data. Seismic data, for instance, is generated along a transect and is thus not very compatible with a scattered well data format like the Granny Creek well database. Another problem is that the seismic data usually requires large storage devices. Consequently, huge seismic data sets are commonly stored on tapes or CD-ROM media. However, all this does not mean that seismic data cannot be integrated with well data. After the raw seismic data is processed, isochron, isotime or fault interpretation maps can easily be assimilated with the other methods described above.

CONCLUSIONS

Seven methods were evaluated on how successfully and quickly they integrated reservoir data to help understand heterogeneity within the Big Injun sandstone. It was found that each method had its strengths and weaknesses depending on which parameters were being evaluated. Various spatial techniques, including cross-sections, contour maps, block models, and GIS, were helpful in discovering spatial patterns of importance. Cross-sections and block models were beneficial in delineating stratigraphic and depositional subsurface intervals, whereas contour maps and GIS helped in examining two-dimensional subsurface data for the entire field. GIS also contributed greatly to the integration, analyses and presentation of large amounts of spatial data. Besides the spatial methods, the logical reasoning of each expert was stored in the Granny Creek Expert System (GCES) to give expert advice regarding reservoir heterogeneity at any current or proposed well. Importantly, it was the only method that emulated the decision-making of the Granny Creek experts. As for quantitative analyses, methods essential to discovering and confirming geological processes within the reservoir included database statistical reports, basin history models, and multivariate statistics. The advantages and disadvantages of each technique are summarized in Table 1. To apply all of these methods to other projects, though, may not always be feasible due to time or cost constraints, resources available, and knowledge and experience of the operator. Therefore, it may be necessary to determine which of these factors are important so that the techniques that are most productive to the project can be used.

At Granny Creek, comprehensive data analyses occurred only if all seven spatial, logical, and quantitative techniques were employed in a systematic manner. Since there was an enormous amount of data to examine, choosing the appropriate method was essential. Knowing the capabilities and limitations of each technique expedited the processing and analyses of Granny Creek data and thus allowed for more time to do other vital work. Also important was knowing how to transfer data quickly between different applications. Understanding data processing from the first step of entering raw data in a database to producing completed maps, for example, can be extremely helpful.

Table 1 Evaluation of methods

TYPE OF ANALYSIS	TECHNIQUE	BEST FOR	LIMITATIONS
Spatial	2D Cross-Sections	Subsurface Analysis	3D Visualization
		Multiple Property Analysis	Volume Calculations
	2D Maps	Interpolation Schemes	3D Visualization
	2D GIS	Powerful Analysis Tools	3D Visualization
		Multiple Property Analysis	Interpolation Schemes
	3D Block Diagrams	3D Visualization	Multiple Property Analysis
Logical	Expert System	Logical Reasoning	Propositional Logic (True/False)
Quantitative	Basin History Models	Insight into Basin History	Many Assumptions
	Statistics	Discover/confirm Relationships	Quantifying Relationships

Although many experts in geology and engineering have studied Granny Creek, it is likely that all the complex geological processes that influence oil production are not completely understood. Thus it is imperative that compiled data and analysis regarding the reservoir be available for those interested in reexamining the oil field in the future. For Granny Creek much of the collected data and analyses are organized so that others can easily access it by using any personal computer and by operating the customized applications, that is: Granny Creek database, Big Injun Cross-Section (BICS), Granny Creek Expert System (GCES), and a software interface to view over 130 raster images and vector files. Lastly, though this was an oil and gas project, many methods applied here could easily be used in other scientific disciplines like hydrogeology and forestry.

REFERENCES CITED

Donaldson, A.C., R. Shumaker, C. Laughrey, K. Aminian, M. Hohn, 1992, Measuring and predicting reservoir heterogeneity in complex deposystems, Annual Fiscal Report for Year 1991; Department of Energy Contract Number DE-AC22-90BC14657, 62 p.

Haught, O.L., 1964, Oil and gas report on Braxton and Clay County, West Virginia; West Virginia Geological Survey Bulletin 29, 19 p.

Swales, D.L., 1988, Petrology of sedimentation of the Big Injun and Squaw Sandstones, Granny's Creek Field, West Virginia; Unpublished Masters Thesis, West Virginia University, Morgantown, West Virginia, 116 p.

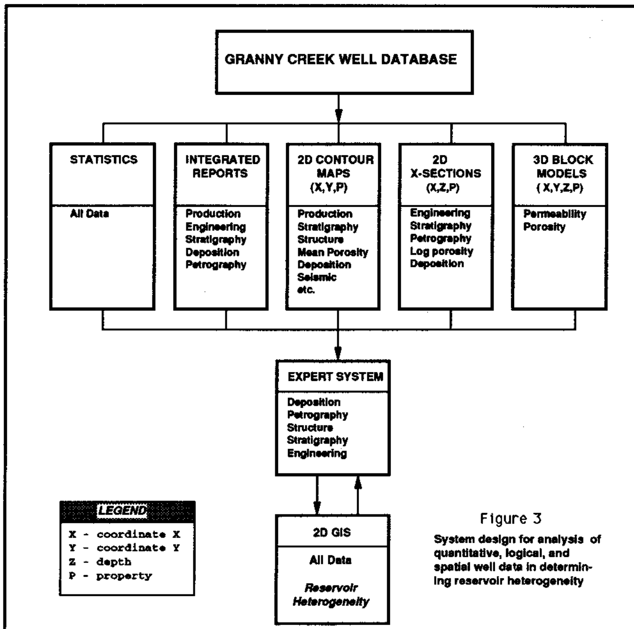

Figure 3
System design for analysis of quantitative, logical, and spatial well data in determining reservoir heterogeneity

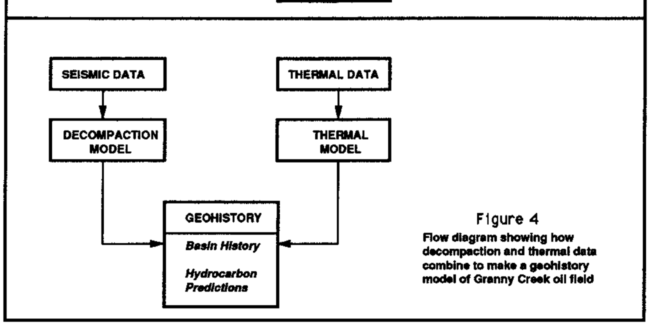

Figure 4
Flow diagram showing how decompaction and thermal data combine to make a geohistory model of Granny Creek oil field

SEQUENTIAL DEVELOPMENT OF STRUCTURAL HETEROGENEITY AND ITS RELATIONSHIP TO OIL PRODUCTION: GRANNY CREEK, WEST VIRGINIA

Wilson, Thomas H., Robert C. Shumaker, and Li Zheng
Department of Geology and Geography, West Virginia University, Morgantown, WV

ABSTRACT

Analysis of Vibroseis and weight-drop seismic data over the Granny Creek oil field in the Appalachian foreland of West Virginia indicates that the field's development has been affected by episodic reactivation during the Paleozoic of fault blocks rooted in the pre-Cambrian crystalline basement. The imprint of basement structures along the margin of the Rome Trough penetrates the overlying Paleozoic sedimentary cover. Reactivation histories of individual fault blocks (inferred from dip-slip components) vary considerably throughout the Paleozoic. In general, the relative displacement of these basement fault blocks decreases rapidly following Iaptian rifting during the Lower-to-Middle Cambrian. Fault displacements during the Ordovician to Pennsylvanian are generally minor but reveal periods of increased tectonic activity often marked by rotational inversion of some fault blocks.

The distribution of late stage detached structures during Alleghenian orogenesis also appears in part to be controlled by mechanical anisotropy within the detached section coincident with deeper reactivated basement structures. The net effect is a complex time-variable pattern of structures that in part controls the location of the reservoir and heterogeneity within the geometrical framework of the reservoir. Variations of production within the field appear to be related in part to small detached structures and reactivated basement faults.

BACKGROUND

The Granny Creek field is located in the central Appalachians Plateau above the margin of a failed rift known as the Rome Trough. Oil production at Granny Creek is from the lower fine grained C member of the Big Injun sandstone. Highest production within this member appears to be further restricted primarily to the C2, marine influenced proximal mouth-bar facies between the C1 and C2 facies (Zou and Donaldson, 1992; Zou et al., 1993; Donaldson et al., 1993). Depositional shales up to 2 feet in thickness separate the different facies in the lower Big Injun and act as permeability barriers (Zou and Donaldson, 1992; Donaldson et al., 1993). The correlation of high production from the field within the C2 fairway is good in the northern part of the field. The southern part of the field is less productive as a whole, even within the C2 fairway.

Zou et al. (1993) also note that local areas of poor production often occur in areas where anomalous high density zones are encountered in the Big Injun C member. These zones, which have a diagenetic origin, are interpreted to form low angle permeability barriers. Similarities in the distributions of production and the Big Injun B-sand suggest that the B-sand may serve as the reservoir seal (Zou and Donaldson, 1992; Donaldson et al., 1993). The B sand is a courser grain fluvial channel sand deposit in which low permeabilities are attributed to secondary quartz cementation (Britton and Heald, 1993).

High permeability pathways between wells in the waterflood program at Granny Creek have been reported by operators of the Granny Creek field. These wells have been identified by rapid breakthrough, pressure, and pumping and tracer tests (Shumaker et al., 1993a). Zheng et al. (1993) report the presence of seismic amplitude anomalies and time-offsets in the vicinity of these pathways (also referred to as thief zones). Direct communication between wells reduces the efficiency of the waterflood recovery operation. Relocation of the injection wells is often necessary. TV logs in some of these problem wells reveal that communication pathways are through fractures in the overlying brittle Greenbrier Limestone (Morrison, 1993, personal communication). With few exceptions these interwell, high permeability zones, trend northeast-southwest, generally falling between N15E and N25E. These zones do not appear to affect primary production from the Big Injun.

Analysis of oriented core from a communicating well along one of these high permeability zones (Dowell/Schlumberger, 1986) suggested that the northeast-trending communication was probably through low-angle, slickensided fractures (small reverse faults) in the Greenbrier Limestone (Shumaker et al., 1993a). The faults have northeast strikes similar to those of small detached structures mapped in the Pennsylvanian coals at the surface (Shumaker et al., 1993a). Once waterflooding of the reservoir was initiated, these more highly fractured areas are interpreted to be areas where the pressure build up was large enough that breakthrough between the reservoir and fracture systems in the overlying Greenbrier Limestone could occur.

SEISMIC STUDIES

Reflection seismic studies were also conducted at Granny Creek with the intent of defining subsurface features within or associated with the reservoir that might account for primary production heterogeneity encountered in the field. Locations of reflection seismic lines used in this study are shown in Figure 1. Initially 14 miles of Vibroseis data were collected at Granny Creek. 110 foot group intervals and a 20-to-110 Hz sweep was used in the acquisition of Vibroseis data. 14 additional miles of Vibroseis data were provided for interpretation by Columbia Natural Resources. Later in the study, 14 miles of high-resolution weight-drop data were collected primarily in the northern more highly productive part of the field. The high-res lines were collected using 45 foot and 25 foot group intervals.

Correlation of prominent reflection events with Paleozoic stratigraphic intervals was based on a synthetic seismograms constructed from density and sonic logs of the VSP well and others from outside the field. The reflection from the Big Injun sandstone lies in a composite reflection event formed by the Big Injun and overlying Big and Little Lime intervals. The Big Injun reflection event and several reflectors down to and including the basement are easily followed throughout the field. The basement reflector drops northwest into the Rome Trough across two faults in the central and northern part of the field, however, time-structural variability within shallow reflection events is generally subtle to unnoticeable

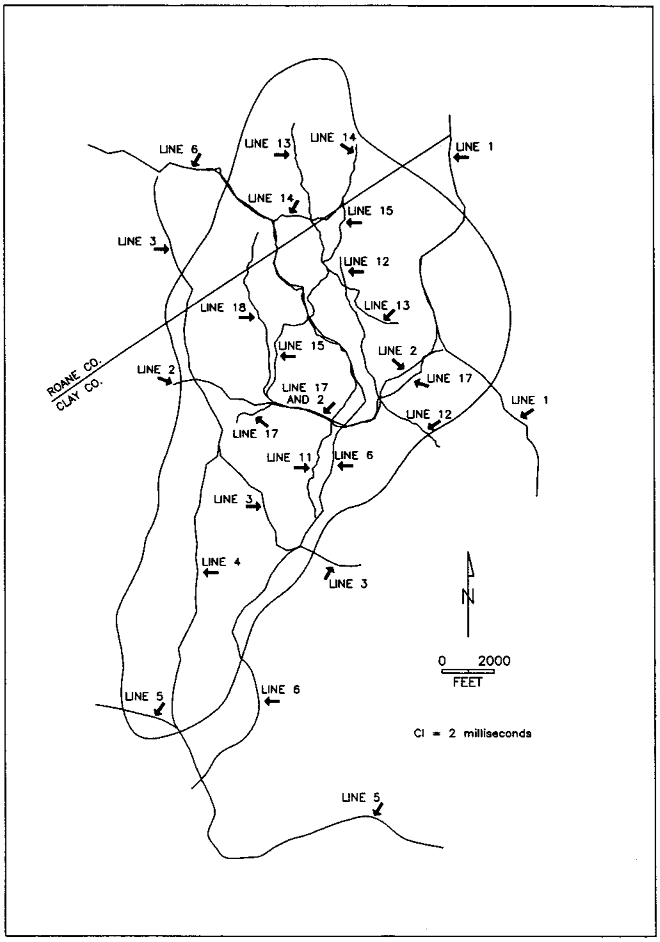

Figure 1: The outline of the Granny Creek field and the locations of seismic lines across the area are shown. Lines 1 through 6 are Vibroseis lines and the remainder are high resolution weight-drop lines.

OBJECTIVES

Because of limited resolution, a detailed seismic stratigraphic evaluation of the Big Injun sandstone was not possible, however, seismic analysis does reveal interrelationships between heterogeneity within the structural framework of the reservoir and oil production. Continuous seismic profiling along lines, with an average spacing of a thousand feet or so, provides the opportunity to identify and evaluate possible structural interrelationships to production. The Vibroseis lines provide an image of the entire Paleozoic section so it is also possible to unravel the development of individual structures in a historical context. Our ultimate interest is to determine if the structural development of the field has some influence on oil production from the Big Injun reservoir.

METHODOLOGY

Structures within the reservoir interval are generally small. Maximum structural relief of 160 feet occurs in the northern part of the field over a total distance of 2 miles. Structures within the field itself generally have amplitudes of only 10 to 20 feet and are visible on seismic sections only when plotted at an expanded time-scale. To enhance time-structures and facilitate their comparison, major reflection events were digitized and plotted relative to each other at an exaggerated time scale. These plots reveal systematic variation unnoticed in the original seismic displays. The existence of traveltime differences are also difficult to observe in the standard seismic display. Differences may be subtle but significant. Traveltime differences plotted at an expanded time scale provide growth history information including periods of stability, fault-block rotation, fault offset (dip-slip component only), and offset inversion.

The expanded time-scale plots of relative arrival time and time-difference (represented schematically in Figure 2) are the basic data used to determine the tectonic history of the field. Further analysis of the data was undertaken by constructing single-fault and multi-block reactivation history diagrams (RHD) (Figure 2). Single-fault RHD's depict fault dip-slip offset as a function of time and also describe accompanying footwall and hanging wall block rotation. Multi-block RHD's describe displacements of two or more fault blocks along a seismic profile as a function of time. The multi-block RHD provides a kinematic representation of the entire line, based on subdivisions of the line into individual semi-independently moving blocks. Plotted dip-slip displacements represent the average displacement of the top of each block relative to a common reference point. In this study, the reference point is always the east or southeast end of a seismic line. The process of constructing single- and multi-block RHD's is summarized schematically in Figure 2.

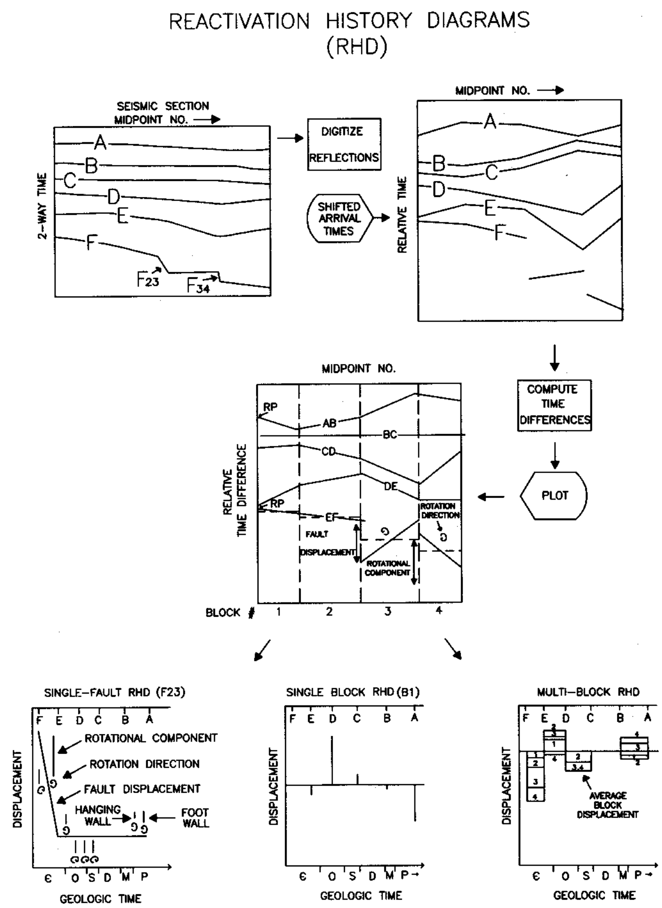

Figure 2: The construction of different types of Reactivation History Diagrams (RHD) is illustrated schematically.

TIME-STRUCTURAL CHARACTERISTICS OF THE RESERVOIR INTERVAL

Vibroseis lines reveal that the Big Injun and surrounding intervals form a syncline with minor internal structural variability. Cumulative oil production from the field is confined to the syncline and is highest in the northern part of the field. These abrupt increases of production occur in the vicinity of folds within the syncline. There is an absence of closure on these folds, which exist as plunging noses on a gently dipping flank. Differences between the time structure and well-log structure are present, and generally attributed to errors in well-log depth, coarseness of well spacing compared to seismic midpoint spacing, long-wavelength static anomalies, and errors picking the top of the Big Injun due to noise and the composite nature of the Big Injun reflection event. Long-wavelength static anomalies are the most significant source of error in the data base as a whole. Velocity anomalies are not believed to produce relationships observed in the data (Wilson et al., 1993). Based on well-log derived velocities, superimposed structural inter-relationships cannot be explained as velocity anomalies.

Correlation coefficients between cumulative production and structural relief along lines crossing the heart of the field are 0.6 to 0.65. Although the highs in production are often associated with local flexures, there is little correlation between the amplitude of a structure and cumulative production associated with it. Also, to the west, increased structural relief is associated with the fall of production at the edge of the field, and the gas/oil contact lies at a roughly constant elevation along the east limb of the Warfield anticline (Shumaker et al., 1993a). Hence, internal structures may enhance local cumulative production, whereas, the large structural relief to the west elevates the reservoir into the gas cap (Shumaker et al., 1993b).

We are undoubtedly dealing with multivariate influences on production from the reservoir as noted by Zou et al. (1992), Zheng et al. (1993), and K. Donaldson (1993). Donaldson, in particular, puts the variety of influences in perspective for us. Our main aim in the remainder of this paper is to document the development of structural heterogeneity within the field associated not only with the reservoir interval, but throughout much of the Paleozoic time interval; and to determine in what way structural characteristics of the reservoir influence oil production.

SEQUENTIAL DEVELOPMENT

As noted above, the area is underlain by major faults (Figure 3) associated with the southeastern margin of the Rome Trough. Fault trends beneath Granny Creek are interpreted from the basement time-contour map (Figure 3). Traveltimes through the succession of stratigraphic intervals extending from the Early Cambrian to Middle Pennsylvanian reveal the presence of a common pattern. Their effect on the Paleozoic sedimentary cover diminishes rapidly after deposition of the Lower Cambrian Rome shales, but, through periodic reactivation, they remain a persistent influence on the depositional patterns of later intervals. Overlying intervals tend to thicken along a NNE-SSW trend in the northern half of the field. The intervals tend to thin across depositional hinges which cut across the central part of the field. Maximum subsidence and hinge-line trends illustrate the penetrative influence of the basement faults. The behavior of the basement block lying along the western margin of the field is unclear in isochron maps, because of limited seismic coverage. The Big Injun isochron and structure map (Shumaker et al. 1993a) reveal a north-northeast trending flank along the west margin of the field parallel to these faults, which suggests that the flank may be the result of relative uplift of the block to the west sometime following deposition of the Big Injun.

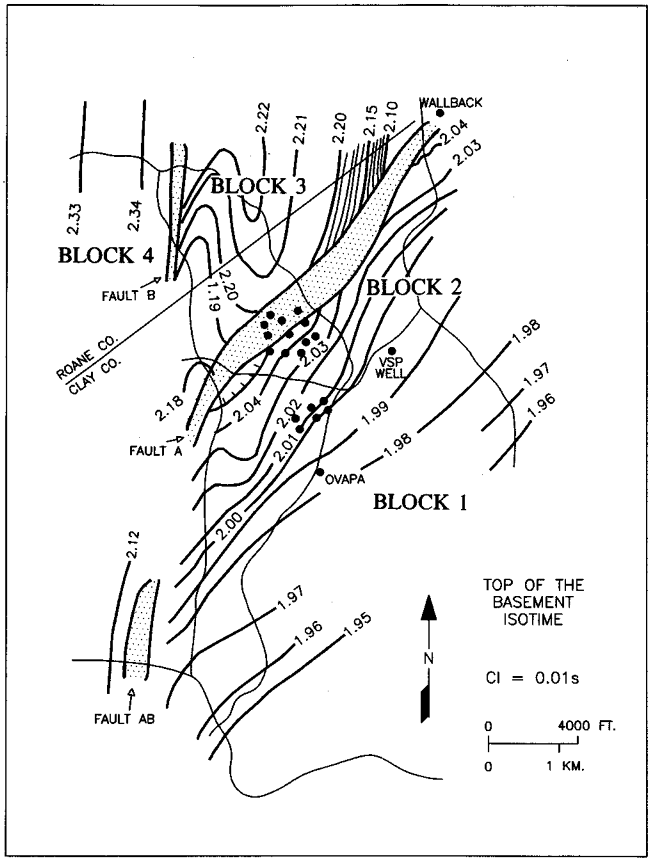

Figure 3: The locations of basement faults beneath the field are shown along with the locations of the Vibroseis lines. Individual fault blocks identified on multi-fault reactivation history diagrams labeled.

A detailed description of the motion of these fault blocks is provided by the multi-block reactivation history diagram (Figure 4). This and similar diagrams were constructed for each of the seismic lines across the field. Relative displacements are normalized to meters per million years. The seismic line from which this diagram was constructed extends the entire length of the field and crosses the highest producing areas in the northern part of the field. Numbers 1 through 4 refer to structural subdivisions of the field observed along the seismic profile. Blocks 1 through 4 are also noted on the basement isotime map (Figure 3). Blocks 1 and 2 lie within the less productive areas in the southern part of the field and trend NE-SW through the area. Block 3 underlies the high producing area in the northern part of the field and is bounded on each side by major basement faults. Block 4 is separated from block 3 by a basement fault, and lies along the western margin of the field.

Average block displacements (see Figure 2) are measured with respect to the southeastern end of the line. The diagram indicates that during the Early and Middle Cambrian, fault blocks in the northern part of the field (3 and 4) dropped rapidly into the Rome Trough (at rates of 10 and 20 meters/million years respectively). Relative to the southern edge of the field, Blocks 1 and 2 have relatively small displacement or rotation. During the Late Cambrian and Early Ordovician, block displacements decrease abruptly to 1.5 meters/million years and less. Blocks 3 and 4 drop together more-or-less as a single block.

A slight increase in average block displacement occurs during the Middle Ordovician. Average block displacements are still less than 2 meters/million years. Block 1 has been uplifted relative to the south end of the line by a small amount. This period of time coincides roughly with the Taconic orogeny. Block displacements decrease again during the Upper Ordovician and Silurian. Block displacements cease altogether during the Upper Silurian to Middle Devonian, spanning most of the Acadian orogeny.

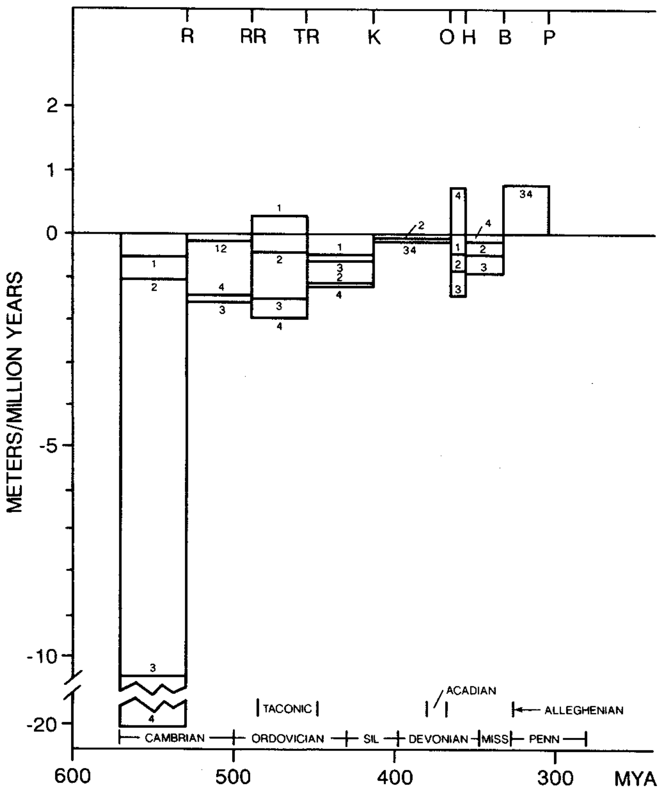

Figure 4: Multi-block reactivation history diagram is shown for Vibroseis line 6.

Increased basement-block reactivation is implied during the Middle Devonian by the thickening and thinning of the section during this time period. Thinning over the block along the western border of the field suggests relative inversion of this block during the Upper Devonian. Thickening over the remainder of the field suggests reactivation of the deeper basement structures. Some overlap with the Acadian time-period suggests that this activity may be related to the Acadian orogeny.

Additional reactivation occurs in the Upper Devonian to Middle Mississippian interval. However, thickening observed during this time period is associated in part with small folds observed in the Big Injun and shallower section and may be due to detachment of the section along a decollement in the Huron shales. Structural relief of these folds does not account for all section thickening so that significant relative subsidence of Block 3 is inferred to have occurred during this time period. Interpretations of the shallow Upper Mississippian and Pennsylvanian section imaged in the seismic reveal inversion of blocks 3 and 4. These blocks appear to have moved upward together, relative to the southern half of the field.

Multi-block reactivation history diagrams constructed for the other lines across the field reveal a similar history of deformation within Granny Creek field. Large displacements are generally confined to the Early and Middle Cambrian, although south and west of the field substantial displacements (5 to 6 meters/million years) continue into the early Ordovician. Relative inversions of basement blocks to the north and west occur consistently during periods of time associated with orogenic activity (Taconic and Acadian). The structural rise occurring along the western margin of the field is larger than that accounted for by the cumulative inversions observable in the seismic data. This suggests that inversion, post-dating the Middle Pennsylvanian, must have occurred. Within the context of the earlier Paleozoic record, this latest inversion is assumed to have occurred during the Alleghenian orogeny. The earliest phases of that orogenic event may be indicated by the inversions observed during the Late Mississippian and Early Pennsylvanian.

STRUCTURAL HISTORY AND OIL PRODUCTION

The preceding discussion highlights the importance of both basement and detachment tectonics in the structural evolution of the field. High oil production is noted not only for areas underlain by active basement structures, but also for areas interrupted by small folds. The small folds are detached as inferred from correlation of folds with thickening of the Upper Devonian Huron shale to Mississippian Big Injun section. Thickening of the section is generally much greater than fold relief so that growth over underlying basement structures is inferred. The absence of increased traveltime beneath time-structures in other areas, and computer model studies indicate that these lows are not the result of velocity anomalies. The coincidence of growth and detached structure leads to speculation that reactivation of basement structures weakened the overlying section and precipitated fold development.

The correlation of high cumulative oil production with small structural features in the field led to the acquisition of additional data concentrated primarily in the northern highly productive half of the field so that structural interrelationships could be examined in greater detail. The additional seismic data was collected using a weight-drop source. Resolution in the shallow part of the section was very good, but events below the Onondaga could not be observed. Also, the reflection from the Huron shales was too incoherent to be used for interval transit time comparisons. The new data combined with previously collected Vibroseis data provided a more detailed image of the reservoir and surrounding intervals in the northern part of the field.

The isochron map of the Onondaga-to-Big Injun interval (Lower Devonian to Middle Mississippian) (Figure 5) compiled from both data sets reveals two areas of increased traveltime in the northern half of the field. Increased traveltime through this section reaches more than 20 milliseconds and corresponds to thickness increases of more than 140 feet. The coincidence of high production with thickening of the Onondaga to Big Injun interval is quite good. The shaded regions correspond to areas where 10-year cumulative production is greater than 20,000 barrels (Hohn et al., 1993). Structural relief inferred from seismic data in this area is less than section thickening and implies that thickening is in large part controlled by syndepositional subsidence. Structural features observed on an isotime map of the Big Injun reflection event suggest that the thickened area coincides with a monoclinal flexure along the west flank of the field. A slight monoclinal flexure is also observed in the structure contour map of the top of the Big Injun (Shumaker et al., 1993a).

Anomalous thickening of the Big Injun-to-Onondaga interval is confined to an area smaller than the basement block (Block 3) over which it occurs. The observations suggest that section thickening results from a combination of syndepositional subsidence, and detachment and folding. The detached folds were later rotated back to the east forming monclinal flexures.

Analysis of a regional seismic line which spans the Rome Trough to the south of Granny Creek suggests that the entire Rome Trough region began to rise sometime during the Devonian Onondaga to Mississippian Greenbrier time period. The data from Granny Creek indicate that this rise may not have been uniform and that some blocks (such as Block 3) continued to drop during this period of time. Continued rise of the Rome Trough following the Middle Mississippian is also inferred from the higher resolution seismic lines across Granny Creek. These observations suggest that the region overlying the Rome Trough experienced minor but persistent uplift during the late Paleozoic. The full force of Alleghenian orogenesis brought minor detached structures across the region. With the development of these detached structures, orogenic stresses and loading of the plate margin may also have produced significant inversion along individual basement faults in the Rome Trough and along its margins.

As Shumaker et al. (1993a and 1993b) note, Big Injun oil fields are found in synclines and on the flanks of anticlines bounded by basement structures. The persistent occurrence of inversion structures within the Rome Trough during the late Paleozoic could form the regional scale hydrocarbon trap, which Shumaker et al. (1993b) suggest once existed. Subsequent detachment followed by, or coeval with, late-stage inversion along individual fault blocks partitioned the region into the numerous oil and gas bearing fields observed across the Rome Trough and along its border.

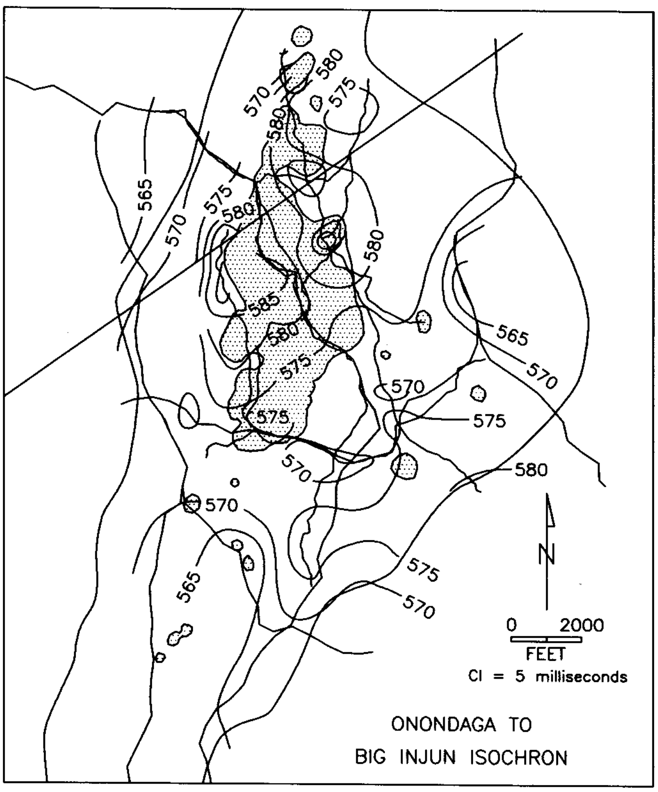

Figure 5: Isochron map of the Devonian Onondaga to Mississippian Big Injun Interval is compared to areas of high cumulative production within the field. Shaded regions correspond to areas where 10-year cumulative oil production is greater than 20,000 barrel

CONCLUSIONS

Seismic studies at Granny Creek reveal interrelationships between the distribution of oil production and basement and detached structure. Active subsidence prior to deposition of the reservoir interval may produce mechanical heterogeneity leading to late-stage localization of detached structures over the deeper basement structures. The western margin of the field is interpreted to have formed by uplift of basement blocks following or during the development of detached structures. The chronology of structural events believed to enhance production from the reservoir interval is interpreted as follows: 1) basement growth during the Middle and Late Devonian, 2) detached structures formed during the Alleghenian, and were accompanied or followed by 3) uplift of basement blocks along the west margin of field. The reservoir is interpreted to be better in the northern half of the field through occurrence of increased structural closure within the more porous C2 facies of the Big Injun at the time of oil migration into the area. This requires migration of oil into already existing detached structures in the northern part of the field, prior to the development of the west flank of the field by basement fault inversion. The absence of present-day closure in high producing areas implies that diagenetic barriers must have formed before the detached structures were rotated into their current configuration by basement uplift along the western margin of the field.

ACKNOWLEDGEMENTS

This research was funded by the U. S. Department of Energy under contract number DE-AC22-90BC14657 titled Measuring and Predicting Reservoir Heterogeneity in Complex Deposystems. Columbia Natural Resources and Pennzoil provided production data and additional geophysical data over the field. Assistance and discussions with Gouqi He, Joe Lemon, Greg Morrison, and Richard Beardsley where helpful and greatly appreciated. Thanks also to Debbie Benson and Alison Hanham for drafting the figures.

REFERENCES CITED

Britton, James Q., and Heald, Milton T., 1993, Porosity and Permeability Relationships as Observed within a Heterogeneous Sand, Granny Creek Field, Clay and Roane Counties, West Virginia: in Proceedings of the 23rd Appalachian Petroleum Geology Symposium, Publication no. 5, p. 6-7.

Donaldson, Kurt, 1993, An integrated Approach to Reservoir Modeling: American Association of Petroleum Geologists, vol. 77/8, p. 1467.

Donaldson, Alan C., Zou, Xiangdong, and Donaldson, Kurt, 1993, Stratigraphic Controls: in DOE Final Report Measuring and Predicting Reservoir Heterogeneity in Complex Deposystems, 161 p, plus figures and Appendices.

Dowell Schlumberger, 1986, Formation evaluation of the J. B. Casto 133 and J. B. Casto 134 wells: Dowel, Schlumberger Formation Analysis Laboratory (report to Pennzoil), p. 1-8, 64-65, 85-88.

Hohn, Michael, McDowell, Ron, and Vargo, Ana, 1993, Spatial Trends in Oil Production: in DOE Final Report Measuring and Predicting Reservoir Heterogeneity in Complex Deposystems, 161 p, plus figures and Appendices.

Shumaker, Robert C., Wilson, Thomas H., and Zheng, Li, 1993a, Structural Controls: in DOE Final Report Measuring and Predicting Reservoir Heterogeneity in Complex Deposystems, 161 p, plus figures and Appendices.

Shumaker, Robert C., Donaldson, Alan C., Wilson, Thomas H., Zheng, Li, and

Zou, Xiangdong, 1993b, Big Injun Oil Explained: DOE Quarterly Report, 12p.

Wilson, Thomas H., Shumaker, Robert C., Zheng, Li, He, Guoqui, and Hunter, Dave, 1993, Seismic Studis, *in* DOE Final Report Measuring and Predicting Reservoir Heterogeneity in Complex Deposystems, 161 p, plus figures and Appendices.

Zheng, Li, Wilson, Thomas H., and Shumaker, Robert C., 1993, Small-Scale Structural Heterogeneity and Well-Communication Problems in the Granny Creek Oil Field of West Virginia: American Association of Petroleum Geologists, vol. 77/8, p.1478.

Zou, Xiangdong, and Donaldson, Alan C., 1992, Reservoir Sedimentology of the Big Injun Sandstone in Granny Creek Field, West Virginia: in Proceedings of the 23rd Appalachian Petroleum Geology Symposium.

Zou, Xiangdong, Donaldson, Alan C., and Donaldson, Kurt, 1993, Reservoir Heterogeneity of the Big Injun Sandstone in West Virginia: Stratigraphic (Including Diagenesis) Controls on Oil Production in Granny Creek: in Proceedings of the 23rd Appalachian Petroleum Geology Symposium, Publication no. 5, pp. 127-129.

STRATIGRAPHIC COMPARISON OF SIX OIL FIELDS (WV) PRODUCING FROM BIG INJUN SANDSTONES

Zou, Xiangdong and Donaldson, Alan C., Department of Geology and Geography, West Virginia University, Morgantown, WV 26506-6300

ABSTRACT

Clustered within western West Virginia, a part of the central Appalachian basin, are six oil fields which produce from the Early Mississippian Big Injun sandstones and three oil fields that produce either from the underlying Squaw or Weir sandstones. Shales separate these sandstones which occur stratigraphically between the Sunbury Shale (maximum flooding surface) and the pre-Greenbrier unconformity (maximum regressive erosional surface) and they represent highstand regressive deposits associated with the post-orogenic phase of foreland basin accumulation. Stratigraphic studies show two Big Injuns: an upper sandstone called Maccrady Big Injun separated from lower Price/Pocono Big Injun sandstone by red shales. Both Big Injun sandstones consist of fine-grained river-mouth bars capped by coarse-grained river channel deposits. Although the six fields are within three adjacent counties, Maccrady Big Injun sandstones of Blue Creek (Kanawha) and Rock Creek (Roane) fields are younger and were deposited by a different fluvial-deltaic system than Price/Pocono Big Injun sandstones of Granny Creek (Clay), Tariff (Roane), Clendenin (Clay) and Pond Fork (Kanawha) fields. Upper Weir sandstones are thick, narrow north-trending belts underlying Pond Fork and Blue Creek fields with properties suggesting wave-dominated shoreline deposits. Allocycles spanning separate drainage systems indicate eustasy. Post-orogenic flexural adjustments probably explain stacked sandstone belts with superposed paleovalleys of overlying unconformities (pre-Greenbrier, pre-Pennsylvanian), particularly where aligned along or parallel basement structures of the Rome trough or West Virginia dome. Differential subsidence or uplift during sedimentation influenced the position, geometry, trend and distribution patterns of these reservoir sandstones rather then their preservation during erosion of pre-Greenbrier unconformity.

INTRODUCTION

Big Injun sandstones have served as major oil and gas reservoirs in western West Virginia for almost a century. Big Injun is a driller's term, referring to the first sandstone penetrated during drilling beneath the Greenbrier Limestone (Big Lime) of Late Mississippian age. The usage has caused erroneous correlations of different sandstones and confusion about the lithologic variation reported in the literature (Overbey, Tucker, and Ruly, 1963; Overbey, 1967; and Ruly, 1970). The problem occurs because of 1) existence of the pre-Greenbrier unconformity beneath the Greenbrier Limestone, which indicates that erosion has removed different amounts of Price/Pocono strata so that different-age Price/Pocono sandstones "pinch out" against the overlying Greenbrier Limestone across the basin (Figure 2 and 3); 2) the basal Greenbrier exhibits considerable quartz and dolomite, mistaken by drillers for Pocono/Price siliciclastics; and 3) facies changes of sandstone to shale which record the discontinuous nature of Early Mississippian sandstones. This reflects their fluvial-deltaic origin and complex structural controls (Figure 4). An objective of this study is to clarify the correlations and to compare "Big Injun" reservoirs in different oil fields both stratigraphically and depositionally.

Six oil fields producing from "Big Injun" sandstones, including Rock Creek, Tariff, Blue Creek, Granny Creek, Clendenin and Pond Fork fields, in Roane, Kanawha and Clay Counties of West Virginia (Figure 1) were selected for this stratigraphic comparison and are distributed within a 20 x 30 mile area. Within these fields, the reservoir heterogeneity of the Granny Creek field is best understood.

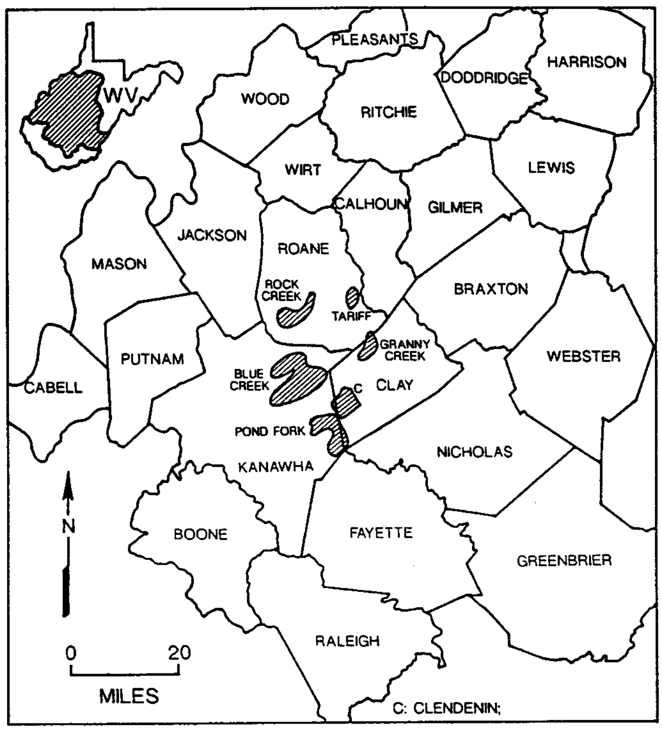

Figure 1. Location map of six oil fields producing from Big Injun sandstones in western West Virginia.

CORRELATION

The uppermost Sunbury Shale of Early Mississippian age represents the maximum flooding surface of a sequence that is bounded by the pre-Berea unconformity at its base and the pre-Greenbrier unconformity at its top. This highly radioactive shale is laterally extensive and was used as the datum in the regional study of 23 counties in western West Virginia. Where this shale loses its radioactivity, in the eastern part of the area (Riddlesburg Shale, Bjerstedt, 1986; Boswell, Donaldson, and Lewis, 1987), multilateral sandstones that overlie this shale at a uniform interval also serve as a secondary datum and confirmation of the correlation. The Maccrady Formation, a red shale with sandstone interbeds between the Price/Pocono and Greenbrier Formations in the outcrop of southeastern West Virginia, is recognized in the subsurface in

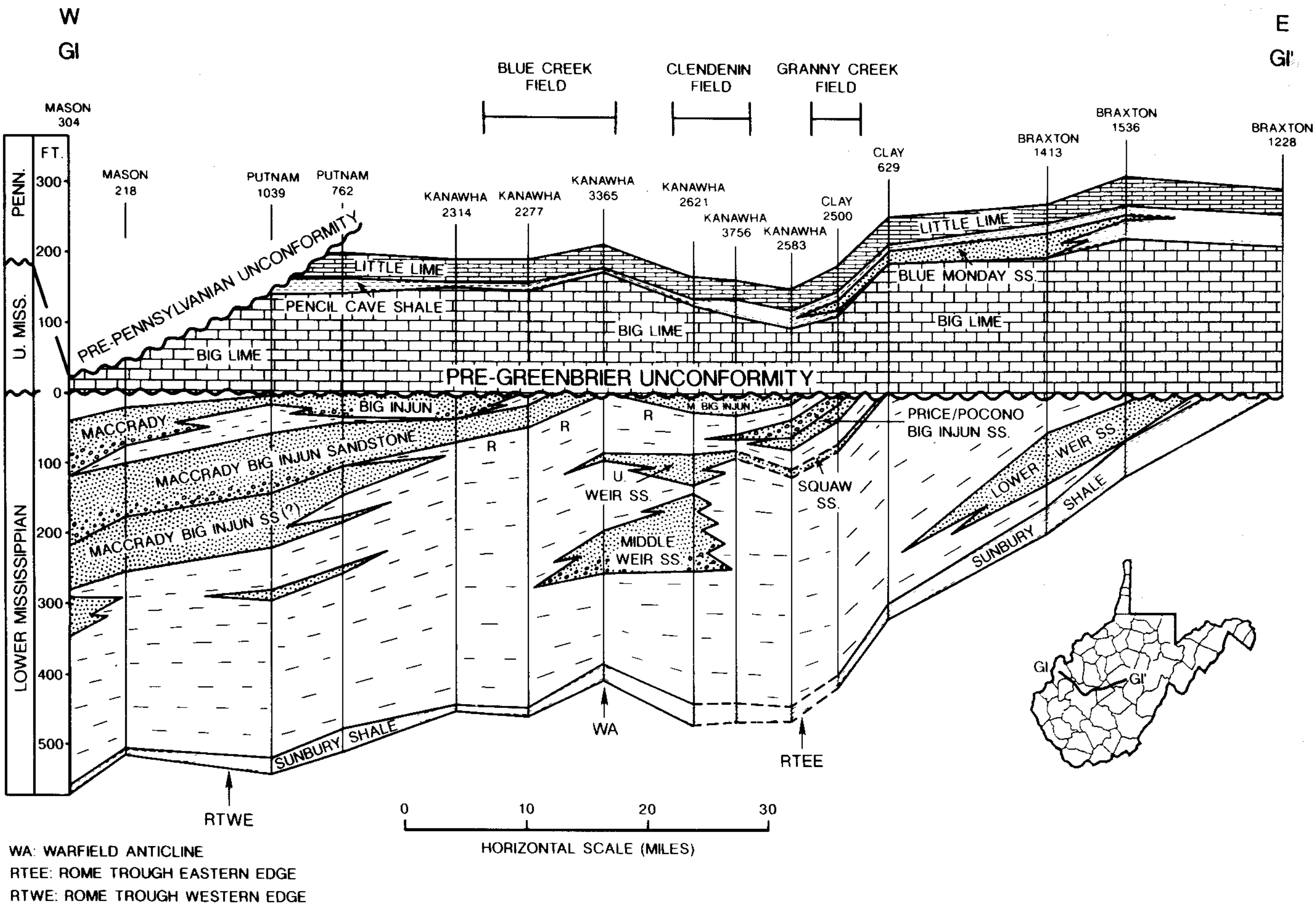

Figure 2. Generalized stratigraphic profile (GI-GI') in western West Virginia. Pre-Greenbrier unconformity (datum) shows increased eastward erosion of the Lower Mississippian rocks, resulting in angular contacts with different reservoir sandstones along the profile (modified from Zou and Donaldson, 1991).

southwestern West Virginia and its presence separates the "Big Injun" into the Price/Pocono Big Injun below and the Maccrady "Big Injun" above these redbeds. This distinction supports the correlations based on interval thickness above the Sunbury Shale in the six selected oil fields.

As shown on figure 2, from west to east, different sandstones in the Lower Mississippian "pinch out" against the pre-Greenbrier unconformity. Along this generalized GI-GI' cross-section, Blue Creek, Clendenin and Granny Creek fields mainly produce oil from the first sandstones named "Big Injun" underneath the unconformity. As indicated earlier, recognition of redbeds from sample logs permits the distinction between Price/Pocono Big Injun and Maccrady Big Injun sandstones.

The distinction of Weir sandstones from overlying "Big Injun" sandstones is based on three criteria: 1) interval thickness between Sunbury Shale and various overlying sandstones; 2) log signatures representing the sandstone; and 3) recognition of regression-transgression cycles within and above the Weir interval. The interval thickness between Sunbury Shale and overlying sandstones seems to remain relatively uniform within the study area. Commonly, the intervals between the following sandstones and the Sunbury Shale are: the lower Weir sandstones, 150 feet; the middle Weir sandstones, 100 to 250 feet; the upper Weir sandstones, 250 to 400 feet; and the Big Injun sandstones, 350 to 450 feet. Occasionally, geophysical wireline signatures are useful in identifying a particular sandstone unit. In eastern Kanawha County, where the correlation of sandstones is most difficult, the middle Weir sandstones have a unique bell- shaped (fining-upward) log signature, the upper Weir sandstones have a "blocky" cylindrical log signature or a thick funnel-shaped (coarsening-upward) log signature, whereas the Big Injun sandstones almost always have a thin funnel-shaped (coarsening-upward) log signature. The third important criterion used to distinguish different sandstones within the Lower Mississippian is the recognition of regression-transgression cycles within the rocks of the highstand systems tract. These regression-transgression cycles consist of couplets of the major sandstone units overlain by shale intervals. Correlation of these cycles on the gamma-ray log readily adapts to the various Weir (lower, middle and upper) and Big Injun (Price/Pocono and Maccrady) sandstones.

In the Rock Creek field, the major oil reservoir is the Maccrady Big Injun sandstone, whereas minor production is from the overlying basal oolitic unit of Greenbrier Limestone. The Tariff field consists only of a reservoir in the Price/Pocono Big Injun sandstones. In the Blue Creek field, the major reservoirs are the Maccrady Big Injun, upper Weir and middle Weir sandstones, whereas the basal unit of the Greenbrier Limestone is its minor reservoir. In the Granny Creek field, the major reservoir is the Price/Pocono Big Injun sandstones, and its minor reservoir is the Squaw sandstone, which is time-equivalent to the upper Weir sandstone. In the Clendenin and Pond Fork fields, the major reservoirs include the Maccrady Big Injun, Price/Pocono Big Injun, upper Weir and the middle Weir sandstones.

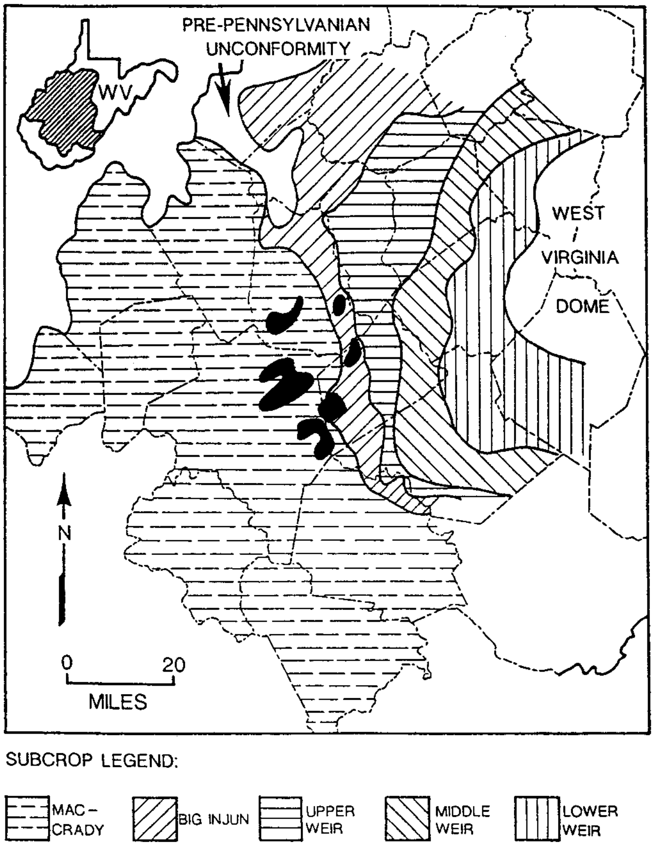

Figure 3. Subcrop map of pre-Greenbrier unconformity, the boundary between the Lower and the Upper Mississippian strata in western West Virginia. Location of the six oil fields on map also indicates whether Big Injun reservoir is Maccrady and/or Price/ Pocono sandstones.

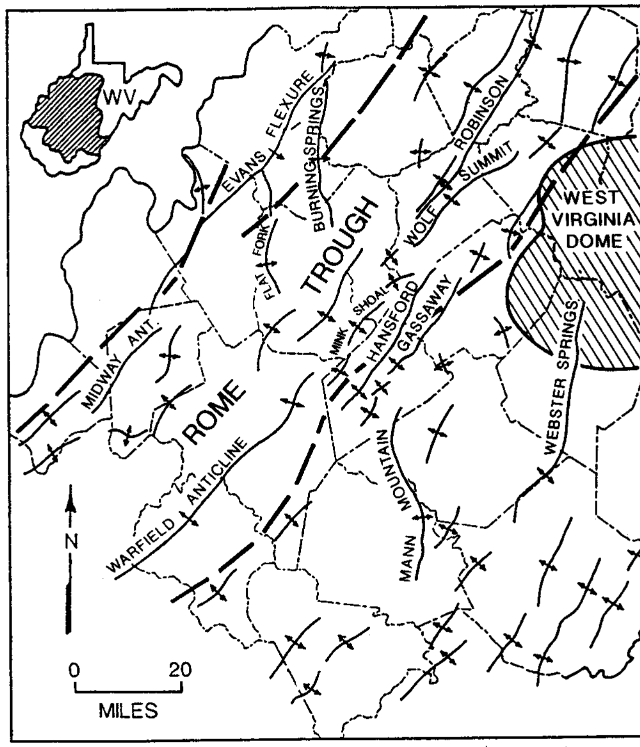

Figure 4. Structural map of western West Virginia (Modified from Shumaker, 1991).

POSITION, GEOMETRY, TREND, FACIES, AND DISTRIBUTION PATTERN OF BIG INJUN AND WEIR SANDSTONES

The thickness map of the Pocono Big Injun (Fig. 5) shows it rimming the West Virginia dome in a narrow belt with its eastern edge truncated by the pre-Greenbrier unconformity. In the regional study area, this narrow belt of sandstone is 5 to 18 miles wide from Fayette to Roane counties, at least 20 feet thick, oriented N10W, which is also the trend of its eroded edge, and exhibits a facies change to shale along its western margin. This facies change to shale occurs between the Granny Creek and Rock Creek fields. Maximum sandstone thickness of about 60 feet occurs in two separate pods along this belt, one in Fayette County and the other in Clay County (associated with Granny Creek field). Core and geophysical log data from the Granny Creek field indicate this sandstone was deposited as distributary-mouth bars and channel fill of a bed-load fluvial delta. The thick sandstone accumulations along this narrow belt probably represent two locations where ancient rivers of separate drainage basins deposited their deltaic sediments at the shoreline. Probably, lateral switching of delta lobes (fire-hose effect) of these two river systems, other small streams, and littoral drift account for the sandstone thicknesses along other segments of this narrow belt.

Pocono Big Injun sandstones occur in Wirt and Richie counties in a southwest-northeast trending belt, which is about 20 to 30 miles wide, with eroded margins as a result of the pre-Greenbrier unconformity to the east and the pre-Pottsville unconformity along the southern (Wirt and Wood counties) and western (Wood and Pleasants counties) margins. This belt of sandstone in the study area mostly is 60 to 120 feet thick, thickening northward, bifurcating southwestward, and exhibiting a facies change to shale to the south in Roane County where it merges with the previously mentioned northwest-trending belt of Pocono Big Injun. This thicker belt of sandstone is interpreted to represent southwesterly prograded fluvial-deltaic deposits in the study area probably supplied by an ancient river from the eastern orogenic mountains that flowed around the northern part of the West Virginia dome.

A thickness map of the Maccrady Big Injun sandstones (Fig. 6) shows a concentration in the study area in southwestern West Virginia. The sandstones are thickest in Mason and Cabell counties and continue as a thick trend northward into Ohio. These sandstones thin into West Virginia and show lobes mainly to the east and south where facies change to shales occurs. One such lobe extends into the Rock Creek field, where truncation by the pre-Greenbrier unconformity also affects the thinning of the sandstones. The Maccrady Big Injun sandstones are concentrated along the western edge of the Rome trough and spread within the trough with thinning along the axis of the Warfield anticline.

Thickness maps of the middle Weir (Fig. 7) and upper Weir (Fig. 8) sandstones are similar in their distribution patterns. These two Weir sandstones are vertically stacked along the eastern edge of the Rome trough. Both sandstones occur in a northeast-trending belt. Three thick sandstone lobes are located along this belt for both sandstones. The middle Weir sandstones are very thick; narrowly

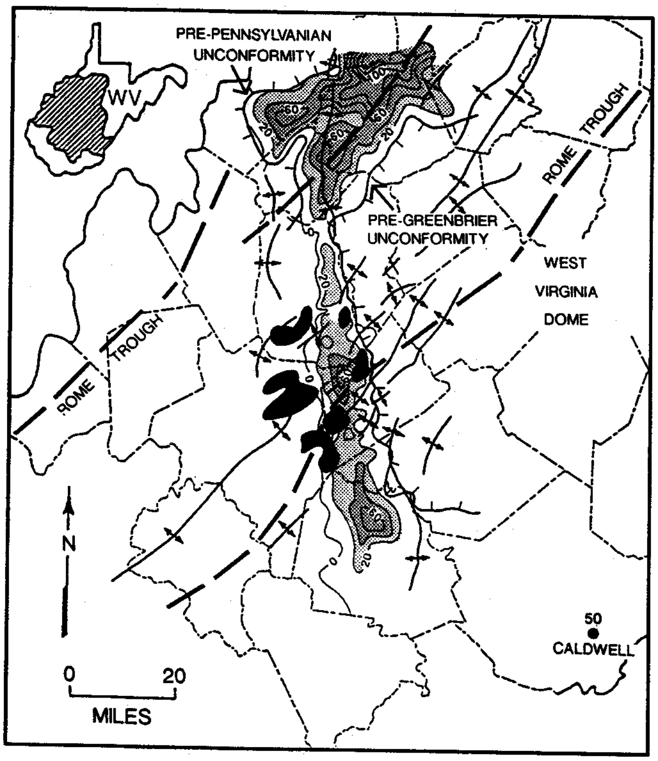

Figure 5. Isolith map of the Price/Pocono Big Injun sandstones, superimposed with some major structures, in western West Virginia (modified from Zou and Donaldson, 1991).

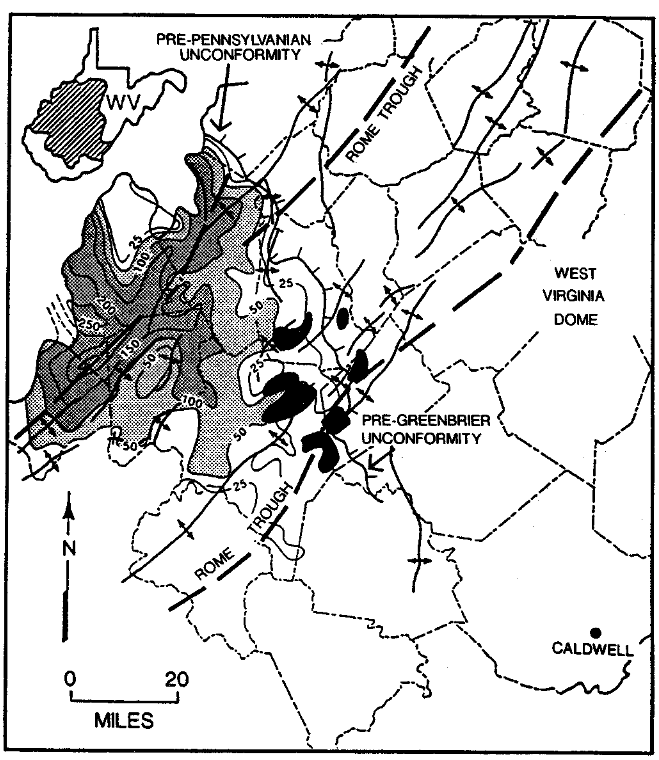

Figure 6. Isolith map of the Maccrady Big Injun sandstones, superimposed with some major structures, in western West Virginia (modified from Zou and Donaldson, 1991).

distributed and lobe-shaped; usually exhibit fining upward textures or remain essentially uniform in grain size ("blocky") vertically; and show flaser bedding, intraclasts, large-scale cross beds, and bioturbation (Zou, 1993). The interpreted depositional environments for the middle Weir sandstones are transgressing barrier islands and estuarine channel systems. The rate of deposition was about equal to the rate of subsidence. This resulted in a still-stand shoreline (Zou, 1993). On the other hand, the upper Weir sandstones are either "blocky" or coarsening upward texturally. The upper Weir sandstones contain abundant monocrystalline quartz, have a lack of original matrix of argillaceous and mica minerals, and have good porosity. The upper Weir sandstones are interpreted to have been deposited in a wave-dominated delta of wave reworked bars (Jewell, 1988; Zou, 1993).

HETEROGENEITY BETWEEN OIL FIELDS

The stratigraphic heterogeneities between oil fields seem to be related to the control of basement structures on sedimentation of the Big Injun sandstone, or conversely, its erosion as a result of uplift of the West Virginia dome. A comparison of the distribution of large basement blocks, which differentially subsided during the Paleozoic, with the sandstone isolith maps (Fig. 5 to 8) shows thinning or absence where the Cambridge arch and its faulted southward extension occur in West Virginia under the Burning Springs anticline. The West Virginia dome caused the extrabasinal rivers that emanated from the orogenic mountain belt to the east to flow around it during the deposition time of the Price/Pocono Big Injun of Early Mississippian. The bedload-type stream that deposited the sandstones and conglomerates in Granny Creek field probably was intrabasinal, with its headwaters within the dome area. This braid delta and its feeder braided stream flowed from the ancient dome westward across the eastern edge of the Rome trough. The confirmation of the minor size of the drainage basin traversing the Granny Creek area is reflected in the relatively small extent of the braid delta from the center of the West Virginia dome. The extrabasinal river flowing around the northern periphery, paralleled the northwestern edge of the dome in Richie and Wirt counties and straddles the western margin of the Rome trough. The Maccrady Big Injun sandstones occupy the Rome trough as fluvial-deltaic lobes, which are extensions of the interpreted paleovalley fill deposits (depoaxis in Mason and Cabell counties) located in and cutting across the upthrown block of the western margin of the Rome trough. The Pocono Big Injun sandstones are thickest within the eastern margin of the Rome trough in the vicinity of the Granny Creek field. The resulting thick southwest trend of the Pocono Big Injun thins and ends in the area of the Pottsville unconformity west of the Burning Springs structure. Multistory (vertically stacked) Mississippian sandstone reservoirs identified as Weir and Big Injun occur along the axis of the Rome trough in West Virginia, as well as along a parallel sag in Ohio between the Waverly arch and the Cambridge arch. Where the Cambridge arch turns toward West Virginia and the Burning Springs anticline, this thick trend of Big Injun extends southward along the western flank of these positive structures into Mason, Cabell, Putnam and Kanawha counties. This thickness trend also is approximately parallel to the pinch-out trend of the Big Injun, which occurs along the south-oriented margin of the pre-Greenbrier unconformity. Both Pocono and Maccrady Big Injun sandstones are recognized in the thick sandstone trend of southeastern Ohio that extends into southwest West Virginia south of the Burning Springs anticline. These Big Injun sandstones are interpreted to represent fluvial-deltaic deposits of a very large river system that developed with the merging of orogenically derived rivers from the east with cratonic-derived rivers from the north and northwest (ancient Ontario River drainage system). The large

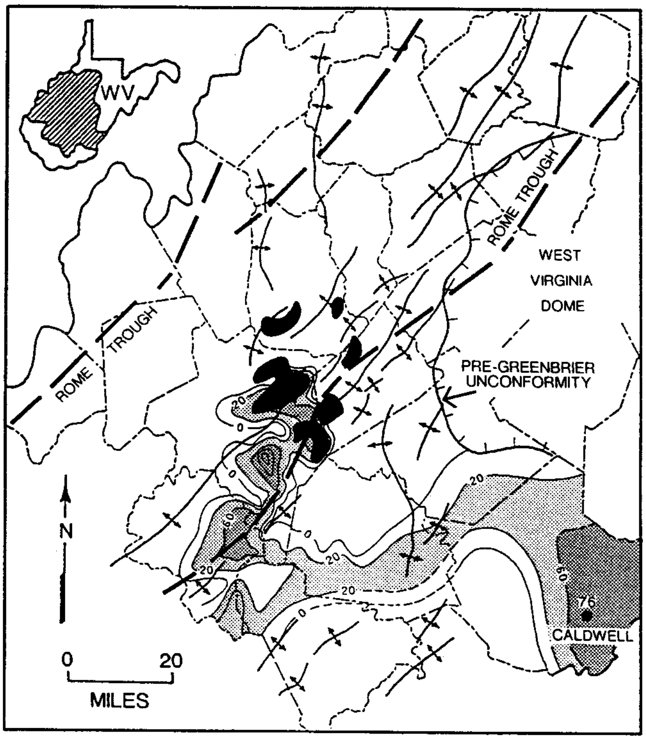

Figure 7. Isolith map of the middle Weir sandstones, superimposed with some major structures, in western West Virginia (modified from Zou and Donaldson, 1991).

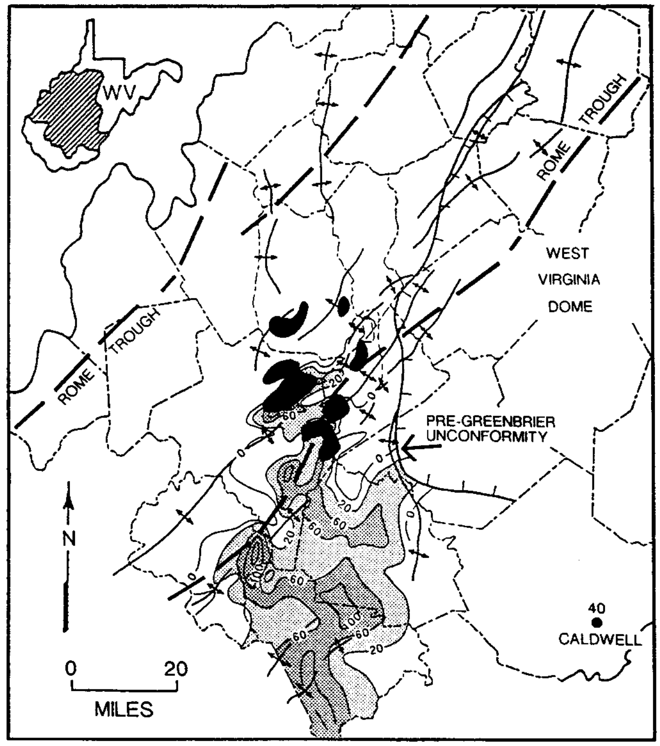

Figure 8. Isolith map of the upper Weir sandstones, superimposed with some major structures, in western West Virginia (modified from Zou and Donaldson, 1991).

drainage basin was structurally controlled (Zou and Donaldson, 1992).

Basement structures apparently controlled the paleoflow directions of Big Injun rivers as well as the distribution patterns of erosion associated with the West Virginia dome. This relationship is evident at the regional scale between oil fields, and the local scale within fields such as the Granny Creek field. Lateral discontinuities are located where basement structures were active during Early Mississippian sedimentation and erosion.

The subcrop map of the pre-Greenbrier Limestone (Fig. 3) shows the different Lower Mississippian sandstones immediately underlying the Greenbrier Limestone in the regional study area. Oil fields producing from the first sandstone beneath the Greenbrier Limestone can be correctly identified stratigraphically by using this map. The map indicates that the reservoir rock immediately underlying the Greenbrier Limestone is 1) Price/Pocono Big Injun for Granny Creek and Tariff fields, 2) Maccrady Big Injun for Rock Creek and Blue Creek fields, and 3) Maccrady and/or Price/Pocono Big Injun for Clendenin and Pond Fork fields.

CONCLUSION

1) "Big Injun" sandstone reservoirs in six selected oil fields in western West Virginia consist of four different sandstones, middle Weir, upper Weir, Price/Pocono Big Injun and Maccrady Big Injun sandstones, of Early Mississippian age.

2) The Lower Mississippian strata in western West Virginia were deposited in a post-orogenic phase of the middle Appalachian basin, and their deposition was strongly controlled by some syndepositional structures.

3) The Lower Mississippian in western West Virginia can be viewed as a sequence bounded by two regional unconformities, and all four reservoir sandstones are highstand systems tract products.

4) The middle Weir sandstones are transgressing barrier-island and estuarine channel deposits, the upper Weir sandstones wave-dominate deltaic and wave-reworked bar deposits, the Price/Pocono Big Injun sandstones fluvial-deltaic deposits, and the Maccrady Big Injun sandstones valley-fill and fluvial-deltaic deposits.

REFERENCES CITED

Bjerstedt, Thomas W., 1986, Stratigraphy and Deltaic Depositional Systems of the Price Formation (Upper Devonian-Lower Mississippian) in West Virginia: unpublished PhD dissertation, West Virginia University, Morgantown, WV 26506, p. 86-92.

Boswell, Ray, Donaldson, Alan C., and Lewis, J.S., 1987, Subsurface stratigraphy of the Upper Devonian and Lower Mississippian of northern West Virginia: Southeastern Geology, v. 28, no. 2, p.105-131.

Calvert, Gary, 1983, Subsurface structure of the Burning Springs Anticline, West Virginia - Evidence for a two-stage structural development, in Shumaker, Robert C.,(ed.), Appalachian Basin Industrial Associates, 1983, p. 147-162.

Donaldson, Alan C. and Shumaker, Robert C., 1981, Late Paleozoic Molasse of Central Appalachian, in Miall, Andrew D.,(ed.), Sedimentation and Tectonics in Alluvial Basins: Geological Association of Canada Special Paper 23, p. 108.

Donaldson, Alan C. and Zou, Xiangdong, 1991, Relationship of the Pocono Big Injun sandstones to the Pre-Greenbrier unconformity in West Virginia: regional stratigraphic considerations for reservoir heterogeneity: The Twenty-Second Annual Appalachian Petroleum Geology Symposium: "Exploration Strategies in the Appalachian Basin", poster.

Faill, Rodger T., 1985, The Acadian orogeny and the Catskill Delta, in Woodrow, Donald L. and Sevon, William D.,(eds.), The Catskill Delta: The Geological Society of American Special Paper 201, p. 15.

Jewell, Gregory A., 1988, Stratigraphy and depositional environments of Upper Devonian and Lower Mississippian sandstones of southeastern West Virginia: unpublished master thesis, West Virginia University, Morgantown, WV 26506, p. 83-95.

Overbey, W.K.Jr., Tucker, R.C. and Ruley, E.E., 1963, Recent developments in the Big Injun Horizon in West Virginia: Producers' Monthly, v. 27, no. 7, p. 18-22.

Overbey, W.K.Jr., 1967, Lithologies, environments and reservoirs of the Middle Mississippian Greenbrier Group in West Virginia: Producers' Monthly, v. 31, n. 2, p. 25-32.

Reinson, Gerald E., 1992, Transgressive barrier island and estuarine system, in Walker, Roger G., and James, Noel P.,(eds.), Facies model: Response to sea level change: Geological Association of Canada, p. 180 and 183.

Van Wagoner, J.C., Mitchum, R.M., Campion, K.M. and Rahmanian, V.D., 1990, Siliciclastic sequence stratigraphy in well logs, cores, and outcrops: Concepts for high-resolution correlation of time and facies: American Association of Petroleum Geologists Methods in Exploration Series, n. 7, p. 43-47.

Zou, Xiangdong and Donaldson, Alan C., 1991, Regional stratigraphic analysis of the Big Injun sandstones (Mississippian) of West Virginia: American Association of Petroleum Geologists Bulletin, v. 75, n. 8, p. 1391 abst.

Zou, Xiangdong and Donaldson, Alan C., 1992, Regional Big Injun (Price/Pocono) subsurface stratigraphy of West Virginia: Geological Society of America Abstracts with Programs, v. 24, n. 7, sept. 1992.

Zou, Xiangdong and Donaldson, Alan C., 1993, Reservoir heterogeneity of Big Injun sandstone in West Virginia: Stratigraphic (including diagenesis) controls on oil production in Granny Creek field: American Association of Petroleum Geologists 1993 Annual Convention Program, p. 207.

THE GEOCHEMISTRY OF THE UTICA SHALE (ORDOVICIAN) OF NEW YORK STATE AND QUEBEC

R.E. Hannigan
University of Rochester, Department of
Geological Sciences, Rochester, NY 14627
and
C.E. Mitchell
State University of New York at Buffalo,
Department of Geology, Amherst, NY 14260

ABSTRACT

During the past decade there has been considerable discussion concerning the depositional setting of organic rich sediments and sedimentary rocks. The Ordovician Utica Shale of Central New York State and the St. Lawrence Lowland of Quebec is an over-mature, black shale. Samples were collected at 0.3 meter intervals from the lower *Corynoides americanus* Zone (basal Utica Shale) to the mid *Geniculograptus pygmaeus* Zone (upper Utica Shale) and were analyzed for organic carbon, sulfur, and iron content. The organic carbon values are high for a black shale of Ordovician age. Elemental sulfur, acid volatile sulfur, and pyritic sulfur values indicate that the sediments were not sulfidic. This suggests that most of the free reactive sulfur was bound by pyrite prior deposition or immediately following deposition within the first few centimeters of sediment. Organic sulfur values, which are low for a truly anoxic depositional regime, support this interpretation. Reactive iron values obtained through acid digestion are low as well. Accordingly, the iron available to react with free sulfides probably did so in the water column or along the sediment water interface. The degree of pyritization (DOP) throughout the section is high. DOP values fluctuate between 0.5 and 0.8, indicating that depositional conditions were fully anoxic with short-lived periods of dysaerobic conditions.

INTRODUCTION

The study of black shale low temperature geochemistry has recently become a field of strong interest for petroleum research, biogeochemical, and organic geochemical study. Techniques developed within the past two decades allow researchers to identify the conditions under which black shale was deposited. The occurrence of black shale no longer automatically implies an anoxic environment inhospitable to bottom dwelling organisms (Huyck, 1990). Black shale can be deposited under fresh water to marine, and oxic to fully anaerobic conditions. Low temperature geochemical techniques allow researchers to glimpse conditions within the water column and at the water-sediment interface prior to and during diagenesis. We here apply these techniques to gain an better understanding of the depositional conditions of the upper Mohawkian and lower Cincinnatian (Ordovician) Utica Shale.

The Utica Shale is graptoliferous, non-metalliferous, and organically over-mature ($R_o<1$). The Utica Shale crops out in central New York State and the St. Lawrence Lowland of Quebec (Fig. 1), where it is exposed in numerous long, continuous sections that are easily accessible by foot (Figure 2). This pyritic black shale was deposited as basin fill in the Taconic Foreland Basin. It typically exhibits shallow dips and little tectonic disturbance. A detailed biostratigraphic framework confines the Utica Shale in time (Ruedemann, 1912, 1925; Riva, 1969 a, b and 1974). An integrated chronostratigraphy incorporating graptolite, conodont, and K-bentonite correlation provides additional time constraint (Goldman et al., in press) within which sediment composition and other features can be compared among sites. Thus, the Utica Shale offers an excellent opportunity to examine temporal and regional patterns of black shale deposition.

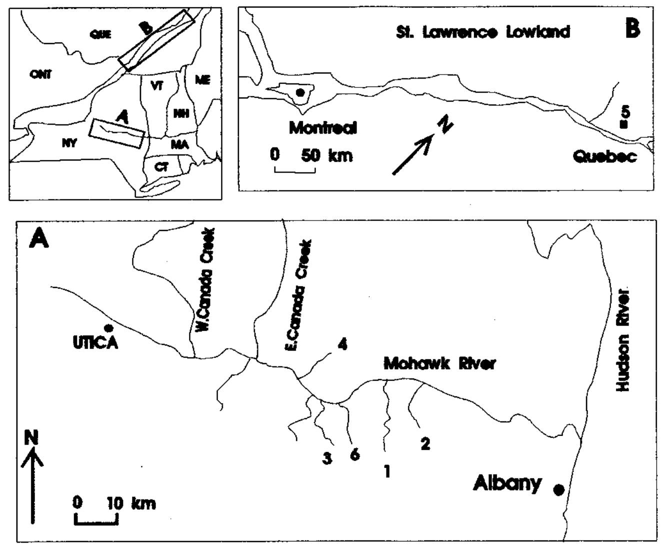

Figure 1. Sites used in this study: A-1: Canajoharie Creek, A-2: Flat Creek, A-3: Nowadaga Creek, A-4: Caroga Creek, A-6: Yatesville Creek; B-5: Neuville Creek.

Ulrich, in 1911, and Ruedemann in 1912 and 1925 remarked that the Utica Shale formed as the result of mud carried out to sea past the littoral zone and laid down in quiet water. According to Ulrich, this deposition took place under "varying conditions of depth and degrees of enclosure" (Ulrich, 1911, p.358). Ruedemann (1925) noted that the Utica Shale contains an appreciable amount of organic matter, which he attributed to the decomposition of plant material and graptolite detritus. He later concluded that the deposition of the Utica Shale was related to limited circulation within a barred basin and separate troughs (Ruedemann, 1935).

Hay and Cisne (1989) analyzed the depositional regime of the Utica Shale based on samples taken at 1.5 meter intervals along several sections in central New York State through the use of X-ray diffraction techniques and analysis of organic carbon concentration. They found that weight percent organic carbon in their samples varied from 1.0 to 3.5%, about a mean value of 1.75 %. Based on these and other data, Hay and Cisne suggested that the Taconic Foreland Basin was density stratified and that bottom water conditions fluctuated between dysaerobic and anoxic in cycles of between 50,000 and 100,000 years duration. The length of the cycles is based

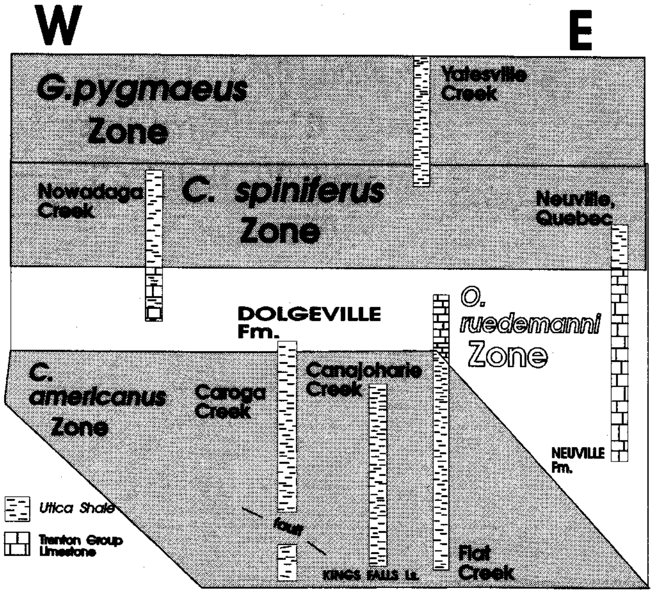

Figure 2. Relative stratigraphic position of the sites used in this study.

on their assumption that the sedimentation rate of the Utica Shale was 50-100 m/m.y, however, Hay and Cisne did not explain how they obtained this estimate of sedimentation rate. Railsback et al. (1990) employed oxygen isotopic data obtained from brachiopod shells preserved within the Utica Shale and the coeval Trenton Group carbonates to further refine the depositional conditions of this basin. Based on changes in oxygen isotopic values along a down-slope transect, they proposed that the deposition of the Utica Shale occurred under low oxygen conditions (dysaerobic) in warm, saline deep water. Railsback and his co-workers remarked that these conditions, while rare in modern oceans, were common in the Lower Paleozoic. It is important to note, however, that both the inference of deposition under cyclical anoxia and under warm saline bottom water depend critically on precise temporal correlation between the carbonate shelf and deep basin — correlations that now appear likely to be incorrect (Goldman et al., in press). The application of carbon-sulfur-iron systematics to the Utica Shale further tests these interpretations and shows that conditions within the Taconic Foreland Basin during this interval of Earth history were complex.

ANALYTICAL METHODS

Samples of the Utica Shale were taken from its base in the *C. americanus* Zone to its top in the *G. pygmaeus* Zone at approximately 0.3 meter intervals along six sections (Fig.1). The samples were collected by trenching the section to avoid collecting weathered material; severely weathered intervals were excluded. Samples were then ground to 60 mesh. Total organic and inorganic carbon concentrations were determined using a LECO carbon analyzer before and after ashing at 450°C. Carbonate mineral concentrations were calculated from the inorganic carbon values assuming $CaCO_3$ stoichiometry. Total reduced inorganic sulfur was measured using the chromium reduction method of Zhabina and Volkov (1978) and Canfield et al. (1986). Both the carbon and sulfur analyses resulted in a reproducibility of ±2.1% or better. Reactive iron values were obtained through acid digestion. Pyritic iron values were derived from the sulfur values obtained through chromium reduction.

To describe the carbon-sulfur-iron systematics of the Utica Shale, degree of pyritization (DOP) values were determined. DOP = Pyritic Iron (Pyritic Iron + Reactive Iron). The values of DOP reflect the degree to which the depositional system was iron, organic carbon or sulfur limited. The study of the relationships between carbon, sulfur, iron, and DOP allow for the characterization of the conditions under which the Utica Shale was deposited:

Aerobic conditions- DOP< 0.42; dissolved O_2 >0.22 Ml/L
Restricted (dysaerobic) conditions- DOP 0.46<DOP<0.75; dissolved O_2 between 0.1 Ml/L and 0.22 Ml/L
Inhospitable (anaerobic) conditions- DOP 0.75<DOP<1.0; dissolved O_2 <0.1 Ml/L

RESULTS AND INTERPRETATION

Table 1 presents average values within each graptolite biozone for the carbon, sulfur, and iron species examined in this study. The organic carbon and carbonate carbon values are similar to those obtained in earlier studies. To test Hay and Cisne's (1989), conclusion that the organic carbon content of the Utica Shale exhibits periodic variation, we performed spectral analysis of the stratigraphically more closely spaced data obtained in this study. Spectral analysis is a multivariate statistical technique that partitions variation in a time series into components according to the duration of the intervals and assumes ergodicity within the data (Davis, 1986). The spectral analysis of the Utica Shale data used height in section as the time series variable and each geochemical value as the dependent variable (Table 2). The values of organic carbon, inorganic carbon and carbonate carbon showed no periodicity within the sampling interval of 0.3 meters.

CARBON-SULFUR-IRON SYSTEMATICS

The bacterial reduction of organic matter under anaerobic conditions results in the production of free sulfide (H_2S). The presence of this sulfur fraction is detected as total inorganic sulfur. Total inorganic sulfur is that portion of the free sulfide that is no longer reactive and includes pyritic sulfur, acid volatile sulfur and elemental sulfur. Separation of these sulfur species is possible but was not attempted in this study. The Utica Shale has undergone at least some catagenesis, and consequently, the acid volatile fraction of the total inorganic sulfur is probably minimal (Lisa Pratt, pers. comm., 1992). Table 1 shows the average values of sulfur for the Utica Shale. Aside from the relationship between sulfur and carbon, iron and sulfur also have an intricate relationship. Sulfur will bind to reactive iron either within the water column or along the sediment water interface to form pyrite. Whether or not the pyrite formed within the water column provides information about the conditions of the water column and sediment because pyrite forms best under dysaerobic sulfidic conditions. Average values of reactive iron obtained through acid solubilization are presented in Table 1.

Electron transfer reactions catalyzed by sulfate reducing bacteria in aerobic marine sediments play an important role in determining the abundance and speciation of preserved sulfur and carbon prior to and after burial. The organic matter (TOC) present within a sample acts as a host for elements such as sulfur. Therefore, the pathway by which sulfur is incorporated into a sediment is dependent on the reactivity of the organic matter present (Zaback and Pratt, 1992). The relationship of total organic carbon to total inorganic sulfur throughout a black shale unit provides a detailed description of the conditions of deposition. Sediment carbon-sulfur relationships can be summarized schematically in a plot of weight percent organic carbon versus weight percent total inorganic sulfur (Fig.3). Sulfidic conditions occur when sulfur is depleted in the

Table 1. Average geochemical values.

Graptolite Biozone	Organic Carbon	Inorganic Carbon	Carbonate Carbon	Pyritic Sulfur	Reactive Iron	Pyritic Iron	DOP
C. americanus	2.19	8.33	79.07	1.42	0.45	1.23	0.73
O. ruedemanni	2.21	7.60	77.40	1.57	0.45	1.36	0.71
C. spiniferus	1.94	5.10	62.61	1.30	0.47	1.33	0.74
G. pygmaeus	2.53	2.41	46.05	1.62	0.53	1.41	0.72

Table 2. Spectral density contrast values.

Graptolite Biozone	t_ψ data	t_ψ table (* trend)
C. americanus	-1.72	-2.11
O. ruedemanni	-1.55	-2.11
C. spiniferus	-1.61	-2.06
G. pygmaeus	-1.96	-2.11

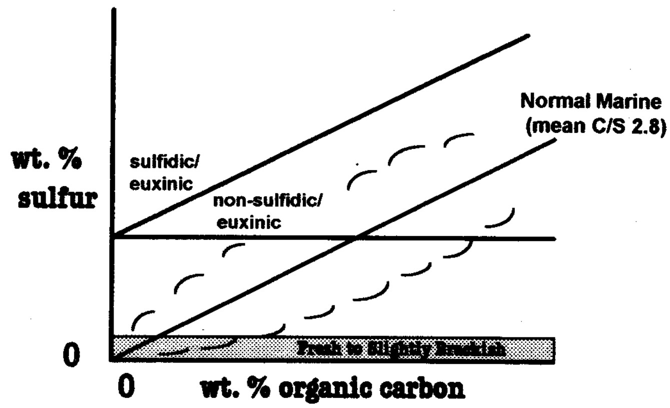

Figure 3. Schematic representation of the relationship between organic carbon and sulfur (after Lyons and Berner, 1992).

water column by reactive carbon matter or within the first few centimeters of sediment by sulfur reducing bacteria. Depletion of sulfur by organic matter can occur in fresh to brackish water conditions, and sediment from these environments plot in a low sulfur region over a broad range of organic carbon values. Organic carbon and sulfur are coupled under aerobic marine conditions and plot along the "normal marine" regression (derived from data collected from Holocene marine regions; Lyons, 1992). Sediments deposited under anoxic (euxinic) conditions may plot in one of two regions. These two regions are defined by the amount of sulfur present within a sample and can be either sulfidic or non-sulfidic. The presence or absence of measurable dissolved sulfide (TIS) is used as an environmental indicator of sulfidic and non-sulfidic anoxic environments (Berner, 1981). In a sulfidic environment, there may or may not be dissolved oxygen within the pore water spaces. A non-sulfidic environment is one in which there is no free sulfide available within the sediment, productivity approximates zero and there is no pore water dissolved oxygen (Chester, 1990).

Figure 4a-d illustrates the relationship between carbon and sulfur in each of the Utica Shale graptolite biozones. Interpretation of these plots, on the first order, can be done by comparing them to Figure 3. The normal marine regression line is used as a point of reference as is the line of best fit. The line of best fit is derived from the reduced major axis of weight percent organic carbon against weight percent sulfur. In all four biozones the line of best fit approximates the euxinic line of Figure 3. There is little variation in the relationship between carbon and sulfur from site to site. Conditions similar to these occur in many euxinic/anoxic environments such as the Black Sea (Lyons and Berner, 1992).

The position of the line of best fit not only describes the relative availability of oxygen but also describes limiting conditions in the formation of pyrite. Oxygen availability is reflected by the total inorganic sulfur formed through anaerobic metabolization of particulate organic matter. High values of total inorganic sulfur indicate anaerobic conditions. A slope value of less than 0.2, in modern environments, indicates restricted, inhospitable bottom water conditions, whereas a slope greater than 0.2, in modern environments,indicates restricted to oxic bottom water conditions (Minster et al., 1992). A slope of approximately 0.2, as seen in the Utica Shale, suggests carbon limited pyrite formation occurring within the sediment. Besides the slope portion of the line equation, the Y-intercept value also provides information. A positive Y-

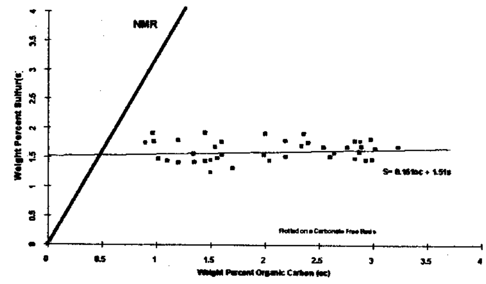

Figure 4a

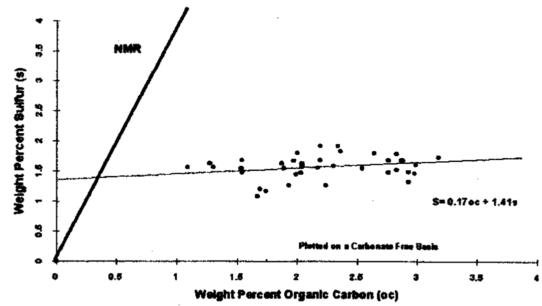

Figure 4b

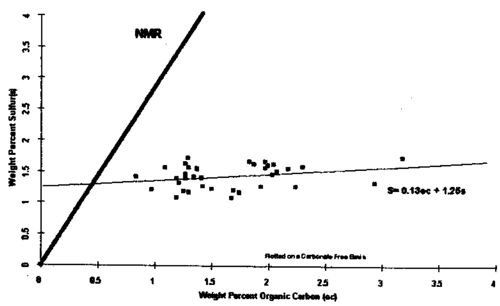

Figure 4c

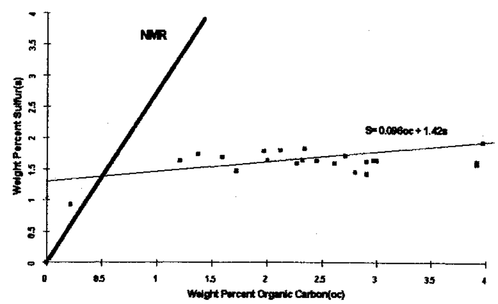

Figure 4d

Figure 4a - d. Carbon-Sulfur relationships of the Utica Shale.

intercept reflects pyrite formation within the water column independent of local organic matter reactivity and therefore was iron limited (Lyons and Berner, 1992). The lines of best fit for the four biozones of the Utica Shale indicate that the conditions of the bottom water and sediment water interface were anoxic. Pyrite formation occurred within the water column in consequence of anoxic water column conditions. Pyrite formation was not organic carbon limited at this time. The decoupling of sulfur and organic carbon shows that conditions within the water column were dysaerobic, that oxygen availability decreased through the thermocline, and conditions were anoxic / sulfidic at the sediment water interface.

DEGREE OF PYRITIZATION

Pyrite is a common authigenic constituent of black shales and is usually found in association with organic matter. This association is a consequence of bacterial metabolization of organic matter under reducing conditions. Pyrite is a product of bacterial sulfate reduction, which yields dissolved sulfide, reaction of the H_2S with iron minerals to form iron monosulfides, and the reaction of iron monosulfides with elemental sulfur to form pyrite (Berner, 1970). Thus, the formation of authigenic pyrite occurs best under low oxygen, sulfidic conditions where the availability of dissolved sulfides and reactive iron is high. The degree of pyritization (DOP) is a measure of the extent to which the original total reactive iron has been transformed to pyrite. This transformation is a function of the relative rate of supply of reactive iron and H_2S. DOP values are used to assess the role of iron limitation in the formation of pyrite.

The average values of DOP are given in Table 1. DOP values between 0.46 and 0.75 are suggestive of fully dysaerobic conditions and DOP values above 0.75 suggest anoxic conditions (Raiswell et al., 1988). These high DOP values, like the insignificant correlation between organic carbon and total inorganic sulfur shown in Fig. 4, suggest strong reactive iron limited conditions both within the water column and along the sediment water interface. Pyrite formation can occur either in the water column (syngenetic) or within the first few centimeters of sediment (diagenetic). Pyrite formation is affected by both the amount of organic matter available for bacterial metabolization, which limits the H_2S supply, and the amount of available reactive iron. As mentioned previously, sulfur and organic carbon have an integral relationship. The carbon-sulfur plots not only reflect the relationship between the two but also show whether pyrite was formed syngenetically or diagenetically. Syngenetic pyrite formation occurs within the water column near or at the nitrate zero (base of the denitrification zone), is reactive iron limited, and produces anhedral rather than euhedral or framboidal crystal shapes. Diagenetic pyrite formation occurs within the zone of bioturbation, is carbon limited and yields framboidal or subhedral-euhedral pyrite crystals. It is important to distinguish between the two types of pyrite because if the pyrite found within a sample is entirely diagenetic the water column was probably well oxygenated, whereas, syngenetic pyrite indicates low oxygen water column conditions. Therefore, the presence of pyrite does not reflect the conditions within the water column unless there is a distinction made between the two pyrite types. Figure 5 shows a scanning electron micrograph of a sample of the Utica Shale from within the *C. americanus* Zone at Flat Creek. The pyrite is anhedral (bean-shaped). The rarity of framboidal pyrite in this and other samples examined lends support to the observation that a substantial portion of the pyrite present in the Utica Shale formed within the water column (Robert Folk, pers. comm., 1992).

Figure 5. Scanning Electron micrograph 20,000X (courtesy of Robert Folk, Texas A & M University).

DISCUSSION

Hay and Cisne (1989) and Railsback, et al. (1990) suggested that the Utica Shale was deposited under dysaerobic to slightly anoxic conditions (DO_2 0.5-0.0 Ml/L). Our analysis of carbon-sulfur-iron systematics in the Utica Shale are in general agreement with these earlier findings but suggest a somewhat more complex situation. The water column was primarily anoxic (dissolved oxygen less than 1.0) but the sediment water interface was anoxic/ sulfidic (dissolved oxygen below 0.1 Ml/L). The carbon to sulfur ratios within the Utica Shale are low (below the normal marine value of 2.8). Low carbon/sulfur ratios are characteristic of anoxic depositional conditions (Lyons and Berner, 1992). The organic carbon values are mid-range for a black shale (Huyck, 1990). When organic carbon values are high, the availability of reactive iron becomes the dominant factor in the production of euxinic carbon/ sulfur ratios.

The relationship between carbon and sulfur in the Utica Shale sections (Fig. 4a-d) from central New York State show that pyrite formation occurred within the water column augmented by a contribution from carbon-limited (diagenetic) pyrite formation within the first few centimeters of sediment. While remobilization of free sulfide and reactive organic matter occurs within the first few centimeters of sediment prior to lithification, its effects were probably negligible in this instance since most of the pyrite preserved in the Utica Shale formed within the water column.

CONCLUSIONS

Black shale carbon-sulfur-iron systematics provide a detailed description of paleoenvironmental depositional conditions. The type and amount of organic matter present allow researchers to understand the diagenetic history of a sedimentary rock and also better explain the absence or presence of economically valuable metals or petroleum products as both are affected by the amount and thermal maturity of the organic matter. Total inorganic sulfur and its relationship to organic carbon depict conditions of deposition relative to normal marine Holocene conditions. Their relationship also explains the degree of metal enrichment many black shales demonstrate since both sulfur and organic carbon behave as host phases for such metals as iron. Iron, consequently, can be evaluated in the context of the presence of a reactive phase to yield even more information about depositional conditions and also reveal information about water column conditions. These three factors, when studied together, allow researchers to characterize black shales in a way that best defines a given unit's depositional conditions and diagenetic history.

The paleoenvironmental depositional conditions of the Utica Shale were identified through the analysis of carbon-sulfur-iron systematics. The Utica Shale falls within the formal definition given by Huyck (1991) of a black shale. The shale is dark in color, fine grained, laminated, and contains appreciable organic carbon (1.5 to 3.0 weight percent, i.e., considerably greater than the 0.5% minimum required by definition). The carbon-sulfur-iron systematics indicate that the Utica Shale was deposited under anoxic conditions that exhibited some heterogeneity over time and space in the Mohawk Valley region. The observed extent of pyritization reflects anoxic bottom water conditions within the basin. The occurrence of syngenetic pyrite formation within the water column suggests that water above the sea bed was anoxic/ sulfidic.

Hay and Cisne in 1989 proposed that the distribution of the organic carbon was cyclical and that the Utica Shale was deposited under primarily dysaerobic conditions. This study shows that there is no statistically significant periodicity in the chemical properties and that the environment of deposition for the Utica Shale was primarily anoxic (sulfidic) at the sediment water interface. The high organic carbon values and iron-limited (syngenetic) pyrite formation all argue for high organic productivity within the water column given the high sediment influx (the *C. americanus* and *O ruedemanni* zones within the Utica Shale are 3 to 4 times thicker than the corresponding Trenton Group carbonates on the western margin of the study area). There was a steady detrital contribution to the supply of reactive iron. Organic productivity outstripped sulfate reduction and pyrite formation rates. These results agree with modern analog environments such as the Timor Trough, Black Sea and Santa Barbara Basin.

ACKNOWLEDGEMENTS

We would like to thank Dr. Robert Berner of Yale University and Dr. Tim Lyons of the University of Michigan for their help in learning the DOP technique and allowing us the use of the laboratory at Yale University. This research was supported, in part, by a grant for graduate student study from the Geological Society of America and a Mark Diamond Grant from the State University of New York at Buffalo.

REFERENCES CITED

BERNER, R.A. 1970. Sedimentary Pyrite Formation: American Journal of Science, v.267, p.19-42.

BERNER, R.A. 1981. A new geochemical classification of sedimentary environments: Journal of Sedimentary Petrology, v.51, p. 359-365.

CANFIELD, D.E., R. RAISWELL, J.T. WESTRICH, C.M. REAVES AND R.A. BERNER. 1986. The use of chromium reduction in the analysis of reduced inorganic sulfur in sediments and shales: Chemical Geology, v. 54, p. 149-155.

CHESTER, R. 1990. Marine Geochemistry. Unwin Hyman Publishers, London, 698 pp.

DAVIS, J.C. 1986. Statistics and Data Analysis in Geology. 2nd Edition. John Wiley and Sons, New York. 646 pp.

GOLDMAN, D., MITCHELL, C.E., BERGSTRÖM, S.M., DELANO, J.W. and TICE, S. In press. K-bentonites and graptolite biostratigraphy of in the

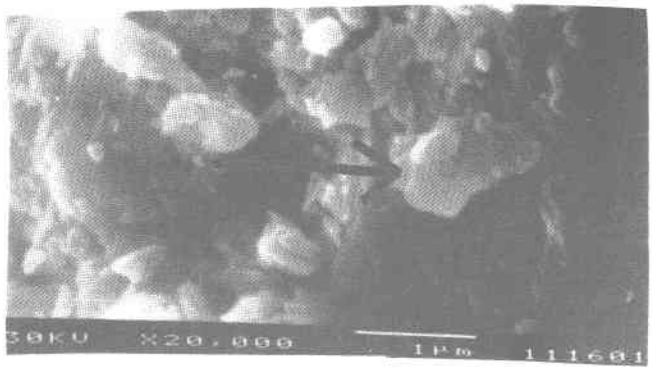

Figure 5. Scanning Electron micrograph 20,000X (courtesy of Robert Folk, Texas A & M University).

DISCUSSION

Hay and Cisne (1989) and Railsback, et al. (1990) suggested that the Utica Shale was deposited under dysaerobic to slightly anoxic conditions (DO_2 0.5-0.0 Ml/L). Our analysis of carbon-sulfur-iron systematics in the Utica Shale are in general agreement with these earlier findings but suggest a somewhat more complex situation. The water column was primarily anoxic (dissolved oxygen less than 1.0) but the sediment water interface was anoxic/ sulfidic (dissolved oxygen below 0.1 Ml/L). The carbon to sulfur ratios within the Utica Shale are low (below the normal marine value of 2.8). Low carbon/sulfur ratios are characteristic of anoxic depositional conditions (Lyons and Berner, 1992). The organic carbon values are mid-range for a black shale (Huyck, 1990). When organic carbon values are high, the availability of reactive iron becomes the dominant factor in the production of euxinic carbon/ sulfur ratios.

The relationship between carbon and sulfur in the Utica Shale sections (Fig. 4a-d) from central New York State show that pyrite formation occurred within the water column augmented by a contribution from carbon-limited (diagenetic) pyrite formation within the first few centimeters of sediment. While remobilization of free sulfide and reactive organic matter occurs within the first few centimeters of sediment prior to lithification, its effects were probably negligible in this instance since most of the pyrite preserved in the Utica Shale formed within the water column.

CONCLUSIONS

Black shale carbon-sulfur-iron systematics provide a detailed description of paleoenvironmental depositional conditions. The type and amount of organic matter present allow researchers to understand the diagenetic history of a sedimentary rock and also better explain the absence or presence of economically valuable metals or petroleum products as both are affected by the amount and thermal maturity of the organic matter. Total inorganic sulfur and its relationship to organic carbon depict conditions of deposition relative to normal marine Holocene conditions. Their relationship also explains the degree of metal enrichment many black shales demonstrate since both sulfur and organic carbon behave as host phases for such metals as iron. Iron, consequently, can be evaluated in the context of the presence of a reactive phase to yield even more information about depositional conditions and also reveal information about water column conditions. These three factors, when studied together, allow researchers to characterize black shales in a way that best defines a given unit's depositional conditions and diagenetic history.

The paleoenvironmental depositional conditions of the Utica Shale were identified through the analysis of carbon-sulfur-iron systematics. The Utica Shale falls within the formal definition given by Huyck (1991) of a black shale. The shale is dark in color, fine grained, laminated, and contains appreciable organic carbon (1.5 to 3.0 weight percent, i.e., considerably greater than the 0.5% minimum required by definition). The carbon-sulfur-iron systematics indicate that the Utica Shale was deposited under anoxic conditions that exhibited some heterogeneity over time and space in the Mohawk Valley region. The observed extent of pyritization reflects anoxic bottom water conditions within the basin. The occurrence of syngenetic pyrite formation within the water column suggests that water above the sea bed was anoxic/ sulfidic.

Hay and Cisne in 1989 proposed that the distribution of the organic carbon was cyclical and that the Utica Shale was deposited under primarily dysaerobic conditions. This study shows that there is no statistically significant periodicity in the chemical properties and that the environment of deposition for the Utica Shale was primarily anoxic (sulfidic) at the sediment water interface. The high organic carbon values and iron-limited (syngenetic) pyrite formation all argue for high organic productivity within the water column given the high sediment influx (the *C. americanus* and *O ruedemanni* zones within the Utica Shale are 3 to 4 times thicker than the corresponding Trenton Group carbonates on the western margin of the study area). There was a steady detrital contribution to the supply of reactive iron. Organic productivity outstripped sulfate reduction and pyrite formation rates. These results agree with modern analog environments such as the Timor Trough, Black Sea and Santa Barbara Basin.

ACKNOWLEDGEMENTS

We would like to thank Dr. Robert Berner of Yale University and Dr. Tim Lyons of the University of Michigan for their help in learning the DOP technique and allowing us the use of the laboratory at Yale University. This research was supported, in part, by a grant for graduate student study from the Geological Society of America and a Mark Diamond Grant from the State University of New York at Buffalo.

REFERENCES CITED

BERNER, R.A. 1970. Sedimentary Pyrite Formation: American Journal of Science, v.267, p.19-42.

BERNER, R.A. 1981. A new geochemical classification of sedimentary environments: Journal of Sedimentary Petrology, v.51, p. 359-365.

CANFIELD, D.E., R. RAISWELL, J.T. WESTRICH, C.M. REAVES AND R.A. BERNER. 1986. The use of chromium reduction in the analysis of reduced inorganic sulfur in sediments and shales: Chemical Geology, v. 54, p. 149-155.

CHESTER, R. 1990. Marine Geochemistry. Unwin Hyman Publishers, London, 698 pp.

DAVIS, J.C. 1986. Statistics and Data Analysis in Geology. 2nd Edition. John Wiley and Sons, New York. 646 pp.

GOLDMAN, D., MITCHELL, C.E., BERGSTRÖM, S.M., DELANO, J.W. and TICE, S. In press. K-bentonites and graptolite biostratigraphy of in the

Middle Ordovician of New York State and Quebec: A new chronostratigraphic model. Palaios, v. 9(1).

HAY, B.J., and CISNE, J.L. 1989. Deposition in the Oxygen-deficient Taconic Foreland Basin, late Middle Ordovician. *In* B.D. KEITH (ed.),The Trenton Group (Upper Ordovician Series) of eastern North America: Deposition,diagenesis, and petroleum: American Association of Petroleum Geologists, Studies in Geology No. 29, Tulsa, Oklahoma, p. 113-134.

HUYCK, H.L.O. 1990. When is a metalliferrous black shale not a black shale? *In*, Metalliferrous Black Shales and Related Ore Deposits-Proceedings, 1989 United States Working Group Meeting, International Geological Correlation Program Project 254, U.S.G.S.Circular 1058 (H.L.O. Huyck and R.I. Grauch, eds.), p. 42- 56.

HUYCK, H.L.O. 1991. Black Shales: An economic geologists perspective: *In*, J. Stivers, ed. 1990 Eastern Oil Shale Symposium, Institute for Mining and Minerals Research, University of Kentucky, p.207-217.

LYONS, T.W. 1992. Comparative study of Holocene Black Sea sediments from oxic to anoxic sites of deposition: geochemical and sedimentological criteria: Ph.D. dissertation, Yale University, New Haven Connecticut, 377 pp

LYONS, T.W. and BERNER, R.A. 1992. Carbon-sulfur-iron systematics of the uppermost deep-water sediments
of the Black Sea: Chemical Geology, v.99, p.1-27.

MINSTER, T., NATHAN, Y., and RAVEH, A. 1992. Carbon and sulfur relationships in marine Senonian organic-rich, iron-poor sediments from Israel- a case study: Chemical Geology, v. 97, p. 145-161.

MITCHELL, C.E., GOLDMAN, D., BERGSTRÖM. S.G., DELANO, J.,SAMSON, S.D. 1991. Chronostratigraphy of the Trenton Group and Utica Shale, Pt.1: Preliminary revision of lithofacies and age relationships. G.S.A. Abstracts with Programs, v. 23(1), p. 196.

RAILSBACK, L.B., ACKERLY, S.A., ANDERSON, T.F., and CISNE, J.L. 1990. Palaeontological and isotope evidence for warm saline deep waters in Ordovician oceans: Nature, v. 343, p. 156-159.

RAISWELL, R., BUCKLEY, R., BERNER, R.A., and ANDERSON, T.F. 1988. Degree of pyritization of iron as
a paleoenvironmental indicator of bottom-water oxygenation: Journal of Sedimentary Petrology, v. 58, p. 812-819.

RIVA, J., 1969a, Middle and Upper Ordovician graptolite faunas of St. Lawrence Lowland of Quebec, and of Anticosti Island: American Association of Petroleum Geologists, Memoir 112, p. 579-595.

RIVA, J., 1969b, Utica and Canajoharie shales in the Mohawk Valley. *In* J. M. BIRD (ed.), New England Intercollegiate Geological Conference, 61st Annual Meeting, State University of New York at Albany, p. 13.1-13.7.

RIVA, J., 1974, A revision of some Ordovician graptolites of eastern North America: Palaeontology, v. 17, p. 1-40.

RUEDEMANN, R. 1912. The Lower Siluric shales of the Mohawk Valley. New York State Museum Bulletin, v. 162, 151 p.

RUEDEMANN, R., 1925. The Utica and Lorraine formations of New York,Part 1, Stratigraphy: New York State Museum Bulletin, v. 258, 174 p.

RUEDEMANN, R. 1935. The ecology of black mud shales of New York: Journal of Paleontology., v.9. p. 79-91.

ULRICH, E.O. 1911. Revision of the Paleozoic Systems: Geological Society of America v.22(3), 179pp.

ZABACK, D.A. and PRATT, L.M. 1992. Isotopic composition and speciation of sulfur in the Miocene Monterey Formation: Re-evaluation of sulfur reactions during early diagenesis in marine environments: Geochimica et Cosmochimica Acta, v.56, p. 763-774.

ZHABINA, N.N and VOLKOV, I.I. 1978. A method of determination of various sulfur compounds in sea sediments and rocks: *In*, W.E. Krumbein, ed., Environmental Biogeochemistry and Geochemistry, v.3, Methods, Metals, and Assessment, Ann Arbor, Michagan, pp. 735-746.

GEOLOGY OF THE CUMBERLAND GAP AREA, KENTUCKY, TENNESSEE, AND VIRGINIA

Kenneth J. Englund, Roger E. Thomas, and John B. Roen
U.S. Geological Survey, Reston, VA 22092

ABSTRACT

Cumberland Gap, in the tristate area of Kentucky, Tennessee, and Virginia, is the construction site of a highway tunnel that has provided new data on the controversial contact relation between the Pennington and Lee Formations. The correlation of a section of Upper Mississippian and Lower Pennsylvanian rocks traversed by the pilot bore of the highway tunnel, particularly the correlation with counterparts on the northeast side of the gap, is hampered by left-lateral displacement on the intervening Rocky Face fault. Strike-slip movement of nearly 2 miles has placed contrasting stratigraphic sections in juxtaposition. For example, the Little Stone Gap Member of the Hinton Formation, a widely recognized marine bed in the central Appalachians, and part of the underlying Stony Gap Sandstone Member of the Hinton (or lower member of the Pennington Formation) are truncated erosionally at the base of the Pinnacle Overlook Member of the Lee Formation on the northeast side of the gap. In the pilot bore section, however, both members of the Hinton are present, but the Stony Gap Sandstone Member, mostly well-sorted and ripple-bedded quartzose sandstone, about 154 feet thick, has been identified as the Pinnacle Overlook Member in some recent reports. The conglomeratic Pinnacle Overlook Member actually occurs above the Little Stone Gap Member (also known as the Avis Limestone of Reger, 1926) and is split into two conglomeratic sandstone units, a common feature of the Pinnacle Overlook Member. The succeeding Bluestone Formation (or upper member of the Pennington Formation) is readily recognized by the presence of varicolored shale, a characteristic feature that distinguishes the Bluestone or Pennington from the Lee Formation. However, in the pilot bore section, the Bluestone Formation (or the upper part of the upper member of the Pennington) with its greenish-gray and grayish-red shale has been identified as the Dark Ridge Member of the Lee Formation in some recent reports. Also, the Bluestone in the pilot bore section contains marine fossils that were reported to be of Early Pennsylvanian age, although specific fossil names were not listed. Regionally, the Bluestone is classified as Mississippian and Pennsylvanian in age on the basis of Mississippian marine fossils in the lower and middle parts and Pennsylvanian plant-impression fossils, notable *Neuropteris pocahontas*, found in upper beds of the formation in West Virginia. Strata overlying the Bluestone in the pilot bore section are in the Lee Formation and include the (1) Chadwell Member, mostly conglomeratic sandstone about 130 feet thick, (2) Dark Ridge Member, dark-gray shale and ripple-bedded sandstone about 40 feet thick, (3) Middlesboro Member, mostly conglomeratic sandstone about 410 feet thick, and (4) lower part of the Hensley Member.

INTRODUCTION

Cumberland Gap (fig. 1), in the tristate area of Kentucky, Tennessee, and Virginia, is known historically for the access it provided during the westward trek of early settlers. Located in the central part of the Cumberland overthrust sheet, the geology of this area is known for its many contributions to an understanding of the stratigraphy and structure of the central Appalachian basin. A recent contribution is a section of upper Paleozoic rocks that was measured by Vanover (1989) in the pilot bore of a highway tunnel under construction near Cumberland Gap. The pilot bore is approximately 0.4 mile southwest of the gap and extends southeastward through Pennsylvanian, Mississippian, Devonian, and Silurian strata that dip from about 35 to 40 degrees northwestward. This paper is focused on the stratigraphy and correlation of Upper Mississippian and Lower Pennsylvanian formations in the pilot bore section and on the relation of these strata to the geology of the Cumberland Gap area.

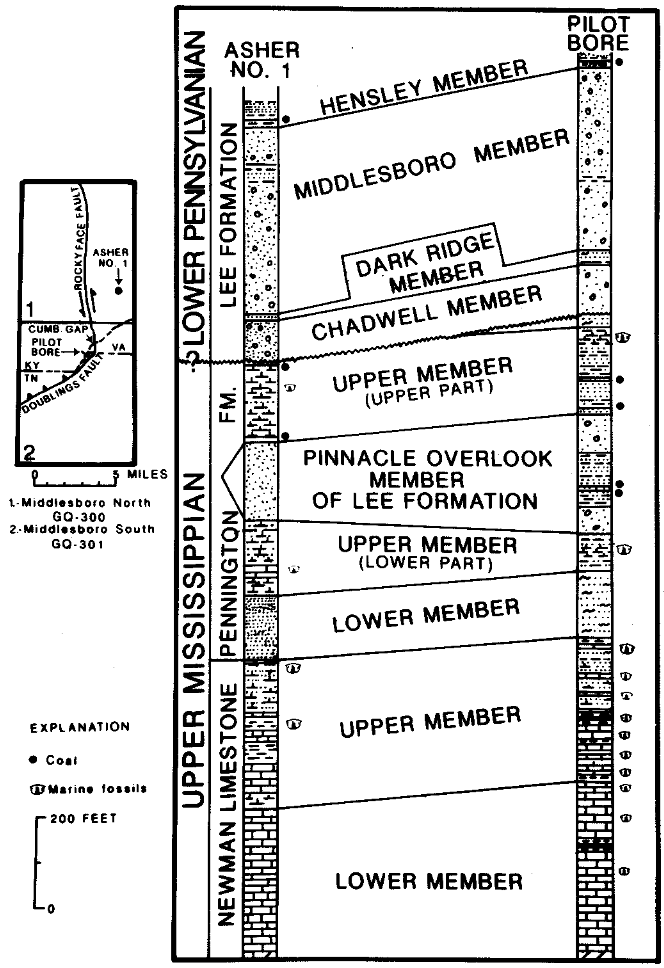

Figure 1.-Correlation (this report) of Upper Mississippian and Lower Pennsylvanian strata in the Asher No. 1 test hole (described by K.J. Englund in 1959) and in the pilot bore (described by J.D. Vanover in 1988 (Vanover, 1989)).

STRATIGRAPHIC SUMMARY

Rocks of Late Mississippian and Early Pennsylvanian ages in the Cumberland Gap area consist of as much as 2,500 feet of intercalated limestone, shale, and sandstone with minor amounts of siltstone, claystone, and coal. Initially, these strata were assigned to, in ascending order, the Newman Limestone, Pennington Shale, and Lee Formation (Ashley and Glenn, 1906). The lithology of these units and their correlatives or alternatively used nomenclature in the central Appalachian basin are as follows: The lower member of the Newman represents the thickest and most widespread marine incursion in the sequence. It is also known as the Greenbrier Limestone in the Appalachian basin and consists mostly of medium-gray, thick-bedded, very finely to coarsely crystalline limestone, a few beds of which are oolitic, cherty, or argillaceous. Marine conditions prevailed also during the deposition of the upper member of the Newman, but the upper member is a relatively nonresistant unit of mostly varicolored shale interbedded with limestone, argillaceous limestone, siltstone, and sandstone. In areas northeast of Cumberland Gap, this upper part of the Newman, known also as the Bluefield Formation, contains a few thin coal beds and associated rooted underclay that mark the beginning of an intermittent regressive trend in Late Mississippian time. The Pennington Shale, later changed to Formation, is mostly shale and sandstone with a few beds of fossiliferous marine limestone, coal, and claystone, all representative of transgressive or regressive deposition. It is approximately equivalent to the Hinton and Bluestone Formations. The lower member of the Pennington, known also as the Stony Gap Sandstone Member of the Hinton Formation, is a resistant well-sorted ripple-bedded orthoquartzite that has been traced in the central and southern Appalachians from West Virginia to Georgia (Englund and others, 1989). Coal beds as much as 30 inches thick, rooted underclay and plant-bearing shale indicate regressive trends in easternmost outcrops of the Hinton. The upper member of the Pennington Formation consists mostly of varicolored shale interbedded with thin beds of fossiliferous marine limestone or shale, nonresistant ripple-bedded sandstone, coal, and underclay. The Lee Formation consists mostly of massive beds of conglomeratic orthoquartzite and orthoquartzite separated by lesser amounts of nonresistant sandstone, shale, siltstone, coal, and claystone that are mainly nearshore-barrier and back-barrier beds. It was subdivided into the Pinnacle Overlook, Chadwell, Dark Ridge, Middlesboro, and Hensley Members, and Bee Rock Sandstone Member (Englund, 1964b). Of these members, the Pinnacle Overlook and lower part of the Chadwell are known to intertongue with the Pennington or Bluestone and, because of this relation, were considered to be Mississippian in age (Englund, 1964b, p. B33). Factors that have influenced the identification and correlation of Upper Mississippian and Lower Pennsylvanian units in the Cumberland Gap area are (1) naming of formations, (2) definition of a formation, (3) nature of the Pennington-Lee contact, and (4) displacement on the Rocky Face fault.

NAMING OF FORMATIONS

Lacking a modern stratigraphic code, Campbell (1893) named the Newman Limestone, Pennington Formation, and Lee Formation for Newman Ridge in Tennessee and Pennington Gap and Lee County in Virginia, respectively, and described "best exposed" or "well exposed" sections of each formation at Big Stone Gap in Virginia, beyond the type areas. To a certain extent, this lack of specific type sections led to different interpretations of the formation names. For example, in places, the name "Newman" has been restricted to the limestone sequence or lower member, and strata in the upper member have been recognized as, or included in, the Pennington Formation. Likewise, the Lee has included in it or excluded from it strata of the Pocahontas Formation in various reports. Because of these different applications, this report will attempt to focus on the most common usage of the formation name supplemented by other formation and member names used in the central Appalachians. Of the three principal formation names, perhaps Lee is the most controversial. The formation was named by Campbell (1893) who stated "the name Lee is applied to it here, from Lee county, Virginia, as it constitutes the northwestern line of that county from near Pennington gap to Cumberland gap, a distance of 35 miles." Since then, geologic reports and maps of the Cumberland Gap area have included in the Lee Formation the sandstone at the crest of Cumberland Mountain along the northwestern Lee County line (Ashley and Glenn, 1906; Butts, 1940; Hauser and others, 1957; Englund and Harris, 1961; Englund, 1964a). In conforming to this definition and use of the name Lee Formation, the sandstone unit of the Lee at the crest of Cumberland Mountain on the northeast side of Cumberland Gap was named Pinnacle Overlook Member of the Lee Formation (Englund, 1964b). The Pinnacle Overlook Member consists of conglomeratic orthoquartzite, a lithology that is typical of the Lee. This lithic similarity was recognized by Dean and others (1989, fig. 27); however, in contrast to previous usage, they chose to place the Pinnacle Overlook Member in the Pennington Formation.

DEFINITION OF A FORMATION

According to the North American Stratigraphic Code (1983), "A formation is a body of rock identified by lithic characteristics and stratigraphic position." The lithic characteristics of the Lee Formation have been described in early reports as (1) "Conglomerates, shales, and coals" by Campbell (1893), (2) "massive sandstone" by Ashley and Glenn (1906), (3) "Coals, plant-bearing shales, underclays, and sandstones with scattered quartz pebbles characterize the lower Lee" by Wanless (1946), and (4) "massive conglomeratic sandstone and nonresistant intervals of thin-bedded sandstone, siltstone, shale, coal, and underclay" by Englund (1964b). Of these lithic features, only the massive sandstone and conglomeratic sandstone (orthoquartzite and conglomeratic orthoquartzite) are unique to the Lee Formation because the other rock types also occur in subjacent and suprajacent formations. In contrast, the lithology of the Pennington Formation has been characterized in early reports as (1) "shale" by Campbell (1893) and by Ashley and Glenn (1906), (2) "Variegated red and olive-green shales, olive-gray siltstones, thin buff generally unfossiliferous limestone or shale" by Wanless (1946), and (3) "red, purple, and green clay shale, pink, red, green and brown (normally calcareous) sandstone, and yellow shaly or silty fossiliferous limestone" by Rodgers (1953). Consequently, the Lee Formation is recognized lithically by massive conglomeratic orthoquartzite and the Pennington by the presence of varicolored (greenish-gray and grayish-red) shale.

NATURE OF THE PENNINGTON-LEE CONTACT

The contact between the Pennington and Lee Formations in the Cumberland Gap area was treated initially as an unconformity betwe- en Late Mississippian varicolored shale, marine limestone, and nonresistant sandstone and a coal-bearing sequence of Early Pennsylvanian age characterized by conglomeratic orthoquartzite, a relation that had been observed in other parts of the Appalachian basin. This practice was prevalent in the central Appalachian basin even though several authors pointed out problems or inconsistencies in the placement of the systemic boundary. Wanless (1946, p. 11) noted that in southwestern Virginia "there appears to be a conformable transition from Mississippian sediments to the Early Pennsylvanian." Rodgers (1953, p. 111) reported that in eastern Tennessee "the contact thus records the change from marine to nonmarine deposition, but it may not be drawn at the same level everywhere and possibly some beds included in the Pennington formation northeast of the Jacksboro fault are equivalent to some included in the Pennsylvanian farther southwest." The solution to this contact problem was proposed by Englund and Smith (1960), who mapped an intertonguing relation between upper beds of the Pennington (varicolored shale and fossiliferous marine limestone) and lower beds of the Lee (conglomeratic orthoquartzite and orthoquartzite), as later depicted by Englund and Harris (1961, fig. 5). The position of the systemic boundary in this intertonguing sequence was unknown at that time, but because sufficient data indicated that the Pennington elsewhere was Mississippian in age, the parts of the Lee that intertongued with the Pennington in the Cumberland Gap area-namely the Pinnacle Overlook Member and the lower part of the Chadwell Member-were considered also to be Mississippian in age (Englund, 1964b, p. B33). In subsequent reports, the systemic boundary was placed anywhere from the Chadwell Member to the base of the Middlesboro Member. Data from extensive geologic mapping and core drilling in southwestern Virginia confirmed that the Pennington Formation was older than the basal Pennsylvanian Pocahontas Formation. Therefore, the Pennington Formation as well as that part of the Lee that intertongues with it are Mississippian in age. Regionally, the Pocahontas is truncated erosionally at the Lower Pennsylvanian unconformity and is absent at Cumberland Gap. A possible correlative of the Pocahontas, indicated by flora, is the Dark Ridge Member of the Lee Formation (Englund and DeLaney, 1966), which most likely is younger than the Pocahontas Formation, because the flora that typifies the Pocahontas is now known to range higher upsection in the New River Formation (Gillespie and Pfefferkorn, 1979). The Bluestone Formation, a correlative of the upper part of the Pennington, does contain Pennsylvanian plant fossils, including Neuropteris pocahontas, in its upper shale member that intertongues with the basal sandstone member of the Pocahontas in southern West Virginia and adjacent areas of Virginia (Englund, 1968). However, this upper shale member of the Bluestone is not recognized in the Cumberland Gap area. Accordingly, the Lower Pennsylvanian unconformity, also commonly referred to as the Mississippian-Pennsylvanian unconformity, is probably at the base of the upper part of the Chadwell Member and is represented by a sharp contact near the middle of the member in its type section (Englund, 1964b, p. B34).

DISPLACEMENT OF THE ROCKY FACE FAULT

Paleozoic strata of the Appalachian basin including the Cumberland Gap area increase in thickness southeastward; thus, left-lateral displacement on the Rocky Face fault has placed contrasting stratigraphic sections in juxtaposition across the fault. This relation obscures the correlation of units not only on the basis of thickness, but also more importantly, of lateral changes in lithic features. Because of strike-slip movement of nearly 2 miles along the Rocky Face fault (Englund, 1961), a stratigraphic section similar to that of the pilot bore should occur on the opposite side of the fault about 2 miles to the north. The closest available section to that point is in the Asher No. 1 test hole; it is located across the fault about 3 miles to the north in the Middlesboro North quadrangle; hence, it has a somewhat thinner section than that in the pilot bore (fig. 1). As an example, the interval from the base of the Newman Limestone to the top of the Middlesboro Member of the Lee is 2,017 feet in the pilot bore and 1,880 feet in the Asher No. 1. However, the Asher No. 1 does exhibit a stratigraphic section with lithic features that are useful for a comparison or correlation with the pilot bore section (fig. 1). The Asher No. 1 section is based on a description of drill cuttings, so that conglomerate or pebbles were not always recognizable in the slowly drilled and highly pulverized orthoquartzites. Similarly, ripple bedding was obscured. In contrast, the shale was more easily drilled, and some of its chips were large enough to contain recognizable fragments of marine fossils. The generalized section for the Middlesboro North quadrangle (Englund and others, 1964), based largely on outcrop data, does show that the Pinnacle Overlook Member or lower tongue of the Lee is partly conglomeratic, the Stony Gap Member of lower member of the Pennington is ripple bedded, and marine fossils were found at the same stratigraphic positions as those in the pilot bore section.

CORRELATION OF THE PILOT BORE SECTION

The correlation of the pilot bore section, as presented herein, involves strata for the base of the Newman Limestone to the top of the Middlesboro Member of the Lee Formation (fig. 2). The base of the lower member of the Newman Limestone is well delineated in the central Appalachian basin and also in the subject area by a thin bed of dolomite or dolomitic limestone. The contact between the lower and upper members of the Newman, corresponding to the Greenbrier-Bluefield contact, is gradational and is placed to separate the dominantly limestone sequence, about 385 feet thick, from as overlying nonresistant shaly sequence. The upper member of the Newman is about 335 feet thick and includes, in its upper part, a sequence of calcareous and greenish-gray, nonresistant ripple-bedded sandstone with interbedded fossiliferous limestone and shale. This sequence is lithically similar to the upper part of the Newman in the original description (Campbell, 1893), as well as to the equivalent Bluefield Formation in recent usage. This part of the upper member of the Newman, about 154 feet thick, was identified as the lower member of the Pennington by Vanover and others (1989) and by Vanover (1989). Although the Newman-Pennington contact is gradational and therefore may not always be placed at the same position everywhere, the basal bed of the Pennington as well as that of the Hinton Formation is the resistant quartzose ripple-bedded Stony Gap Member that is also known as the lower member of the Pennington Formation in the Cumberland Gap area. It is about 154 feet thick in the pilot bore section where it was identified as the Pinnacle Overlook Member of the Lee Formation by Vanover and others (1989), Vanover (1989), and Watson and Ettensohn (1991). A key to this correlation is the Little Stone Gap Member of the Hinton, a calcareous siltstone containing marine fossils, which is also at the base of the upper member of the Pennington. This fossil bed, also known as the Avis Limestone of Reger (1926), was traced southeastward across southwestern Virginia to the vicinity of Cumberland Gap (Englund and DeLaney, 1966). On the northeast side of Cumberland Gap, the Little Stone Gap Member and part of the underlying Stony Gap Sandstone Member are truncated at the base of the overlying Pinnacle Overlook Member of the Lee. This relationship was depicted in the generalized section of the Middlesboro South quadrangle (Englund, 1964a) and in several cross sections (Englund and DeLaney, 1966; Englund and others, 1989), Therefore, the Pinnacle Overlook Member is above rather than below the Little Stone Gap Member in the pilot bore section and consists of two conglomeratic quartzose sandstone units, a common feature of the member especially where it is decreasing in thickness (Englund and DeLaney, 1966, fig. 2). These conglomeratic sandstones were included in the Chadwell Member by Vanover and others (1989) and Vanover (1989). The succeeding upper part of the upper member of the Pennington or Bluestone Formation in the pilot bore section, readily recognized by the presence of varicolored shale, was identified as the Dark Ridge Member of the Lee Formation by Vanover and others (1989) and Vanover (1989) (fig. 2). It also contains marine fossils of reported Pennsylvanian age (Vanover and others, 1989) in a thin bed that was not recognized in outcrops on the northeast side of the gap. There, Englund (1964b, p. B34) reported "Along most of the outcrop belt the top of the member (Pinnacle Overlook) grades abruptly into greenish-gray or reddish-gray shale in an upper tongue of the Pennington Formation which immediately northwest of the outcrop area contains a thin bed of fossiliferous limestone." The presence of this fossil bed was not reported in the Middlesboro South quadrangle but was reported in the adjacent Middlesboro North quadrangle (Englund and others, 1964) and in nearby areas. Throughout the central Appalachian basin, only two marine fossil beds have been recognized in the Bluestone Formation; one is in the Pride Shale Member, and the other is in the Bramwell Member. Both are in strata correlated with Foraminiferal Zone 19 of the Mississippian and contain much of the same molluscan fauna (Hoare, 1993). The Bramwell Member has been traced southwestward across southwestern Virginia to Pennington Gap, where it is last recognized (Englund and others, 1989). The Pride Shale Member having marine fossils has been recognized in Virginia and southward in Tennessee and Georgia. Therefore, regional relations indicate that the marine fossil bed in the upper part of the upper member of the Pennington is most likely the same as that in the Pride Shale Member of the Bluestone. The identification of the succeeding Chadwell, Dark Ridge, and Middlesboro Members of the Lee Formation is based on their characteristic lithology, thickness, and stratigraphic position (fig. 2).

CONCLUSIONS

Regardless of the correlations or nomenclature used, conglomeratic sandstone and terrestrial coal beds are intercalated with varicolored shale and fossiliferous marine beds in the pilot bore section. This relation is interpreted as a continuation of regression and transgression between terrestrial and marine deposition that began in the Appalachian basin as early as Late Devonian (Englund and Thomas, 1990, fig. 2) and, consequently, is not related to the Mississippian-Pennsylvanian boundary.

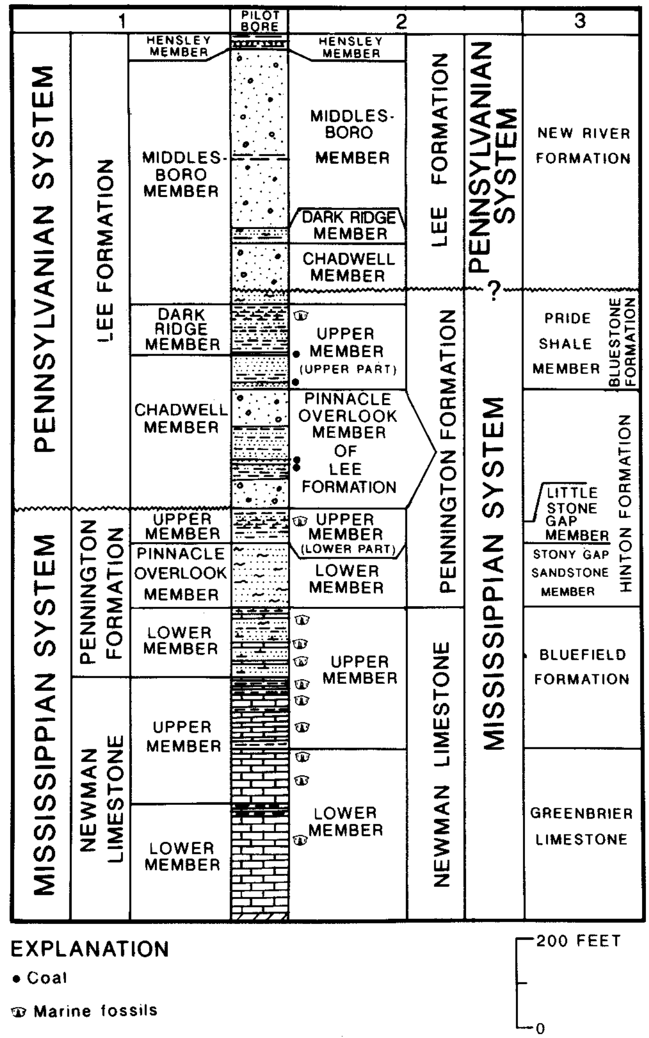

Figure 2.-Correlation of Upper Mississippian and Lower Pennsylvanian strata in the pilot bore section at Cumberland Gap (1) Vanover and others; 1989, and Vanover, 1989; (2) this report; and (3) other nomenclature used in the central Appalachian basin.

REFERENCES CITED

Ashley, George H., and Glenn, Leonidas C., 1906, Geology and mineral resources of part of the Cumberland Gap coal field, Kentucky: United States Geological Survey Professional Paper 49, 239 p.

Butts, Charles, 1940, Geology of the Appalachian Valley in Virginia: Virginia Geological Survey Bulletin 52, Part 1, Geologic Text and Illustrations, 568 p.

Campbell, Marius R., 1893, Geology of the Big Stone Gap coal field of Virginia and Kentucky: United States Geological Survey Bulletin 111, 106 p.

Dean, Claude S., Vanover, John D., and Perkins, Robert B., 1989, Itinerary: Day 1: Friday, September 22, 1989: *in* Dean, Claude S., and Moshier, Stephen O., (editors), Cumberland Mountain: The inside story, Geological Society of Kentucky Field Trip Guidebook, p. 9-23.

Englund, Kenneth J., 1961, Rotational block of the Cumberland overthrust sheet in southeastern Kentucky and northeastern Tennessee: United States Geological Survey Professional Paper 424-C, p. C74-C76.

Englund, Kenneth J., 1964a, Geology of the Middlesboro South quadrangle, Tennessee-Kentucky-Virginia: United States Geological Survey Geologic Quadrangle Map GQ-301.

Englund, Kenneth J., 1964b, In the Cumberlands of southeastern Kentucky, stratigraphy of the Lee Formation: United States Geological Survey Professional Paper 501-B, p. B30-B38.

Englund, Kenneth J., 1968, Geologic map of the Bramwell quadrangle, West Virginia-Virginia: United States Geological Survey Geologic Quadrangle Map GQ-745.

Englund, Kenneth J., and DeLaney, A. Otis, 1966, Intertonguing relation of the Lee Formation in southwestern Virginia: United States Geological Survey Professional Paper 550-D, p. D47-D52.

Englund, Kenneth J., Gillespie, William H., Cecil, C. Blaine, Crawford, Thomas J., Windolph, John F., Jr., Blake, Basoombe M., Jr., and Fedorko, Nick, 1989, Field guide to Mississippian and Lower Pennsylvanian coal-bearing rocks in the Appalachian basin: *in* Englund, Kenneth J., (editor), Characteristics of the mid-Carboniferous boundary and associated coal-bearing rocks in the central and southern Appalachian basin, 28th International Geological Congress Field Trip Guidebook T352B, p. 73-118.

Englund, Kenneth J., and Harris, Leonard D., 1961, Itinerary-Geologic features of the Cumberland Gap area, Kentucky, Tennessee, and Virginia: Geological Society of Kentucky Field Trip Guidebook, 30 p.

Englund, Kenneth J., Roen, John B., and DeLaney, A. Otis, 1964, Geology of the Middlesboro North quadrangle, Kentucky: United States Geological Survey Geologic Quadrangle Map GQ-300.

Englund, Kenneth J., and Smith, Henry L., 1960, Intertonguing and lateral gradation between Pennington and Lee Formations in the tri-state area of Kentucky, Tennessee, and Virginia [abstract]: Geological Society of America Bulletin v. 71, n. 12, part 2, p. 2015.

Englund, Kenneth J., and Thomas, Roger E., 1990, Late Paleozoic depositional trends in the central Appalachian basin: United States Geological Survey Bulletin 1839-F, p. F1-F19.

Gillespie, William H., and Pfefferkorn, Hermann W., 1979, Distribution of commonly occurring plant megafossils in the proposed Pennsylvanian System stratotype; *in* Englund, Kenneth J., Arndt, Harold H., and Henry, Thomas W. (editors), Proposed Pennsylvanian System stratotype, Virginia and West Virginia, Ninth International Congress of Carboniferous Stratigraphy Meeting Field Trip 1 Guidebook, Washington, D.C., American Geological Institute, p. 87-96.

Hauser, Robert E., Walker, Frank H., and Nelson, Vincent E., 1957, Itinerary: Some stratigraphic and structural features of the Middlesboro basin: Geological Society of Kentucky and Appalachian Geological Society Field Trip Guidebook, 35 p.

Hoare, Richard D., 1993, Mississippian (Chesterian) bivalves from the Pennsylvanian stratotype area in West Virginia and Virginia: Journal of Paleontology, v. 67, n. 3, p. 374-396.

North American Commission on Stratigraphic Nomenclature, 1983, North American stratigraphic code: American Association of Petroleum Geologists Bulletin, v. 67, n. 5, p. 841-875.

Reger, David B., 1926, Mercer, Monroe, and Summers Counties: West Virginia Geological Survey [County Report], 963 p.

Rodgers, John, 1953, Geologic map of east Tennessee with explanatory text: Tennessee Division of Geology Bulletin 58, 167 p.

Vanover, John D., 1989, Pilot tunnel stratigraphy: in Dean, Claude S., and Moshier, Stephen O. (editors), Cumberland Mountain: The inside story, Geological Society of Kentucky Field Trip Guidebook, p. 39-43.

Vanover, John D., Dean, Claude S., and Perkins, Robert B., 1989, Itinerary: Day 2-Pilot bore traverse: *in* Dean, Claude S., and Moshier, Stephen O. (editors), Cumberland Mountain: The inside story, Geological Society of Kentucky Field Trip Guidebook, p. 24-30.

Wanless, Harold R., 1946, Pennsylvanian geology of a part of the southern Appalachian coal field: Geological Society of America Memoir 13, 162 p.

Watson, Anna E., and Ettensohn, Frank R., 1991, Nature and origin of the Mississippian-Pennsylvanian unconformity in the Cumberland Gap area [abstract]: Geological Society of America Northeast-Southeast Sections Joint Meeting Abstracts with Programs, March 1991, p. 146.

UPPER DEVONIAN OUTCROP STRATIGRAPHY ALONG THE APPALACHIAN BASIN MARGIN IN SOUTHEASTERN WEST VIRGINIA AND SOUTHWESTERN VIRGINIA AND IMPLICATIONS FOR HYDROCARBON EXPLORATION

John M. Dennison
University of North Carolina at Chapel Hill
Chapel Hill, North Carolina
Jonathan K. Filer
College of William and Mary
Williamsburg, Virginia
Thomas J. Rossbach
University of North Carolina at Wilmington
Wilmington, North Carolina

ABSTRACT

A stratigraphic section of the Devonian Catskill Delta complex connects 22 stratigraphic columns extending 263 miles from Norton, Virginia, to Ketterman Knob near Riverton, West Virginia, roughly parallel to the structural strike of the Allegheny Front. Sixteen of these columns were plane-tabled for the first time for this study. Devonian delta strata reach a maximum thickness of 6,900 feet at the Durbin-Hightown combined column in the Augusta Lobe deltaic deposit. They thin somewhat northeastward toward Devonian Grant Bay. There is progressive fining southwestward toward Norton, where the Devonian portion of the Delta consists of 756 feet of prodelta dark muds. Nonmarine beds of the Hampshire Formation pass through a series of facies changes to shallow marine, turbidite, and prodelta dark shales.

Portions of the deltaic beds, upturned in outcrop, are locally concealed by faults, most notably by the St. Clair fault from near Bluefield to near Gap Mills. A smaller fault, near Lindside and Glen Lyn, cuts out uppermost Devonian and lower Pocono strata.

Hydrocarbon potential is poor to moderate in the Devonian of southeastern West Virginia. Most promising for production is the Gordon sand and its silty equivalents in Greenbrier, Monroe, and Mercer counties, and the siltstone equivalents in Greenbrier County of Pound (= Benson) and Briery Gap (= Alexander) Sandstones. These beds may have exploration potential as true sands in the easternmost Appalachian Plateau in Pocahontas County. In extreme southwestern Virginia, the organic black shales are already being developed for Devonian Shale gas production.

INTRODUCTION

This paper presents a new stratigraphic cross section with member-level detail of the Middle and Upper Devonian formations exposed along the general trend of the Allegheny Front from Norton, Virginia to Ketterman Knob near Riverton, West Virginia (Figure 1). The sections vary from gently dipping (at Durbin) to steeply dipping, vertical, and even more extreme with overturned dips averaging 30° (at Lindside). Individual sections are mostly unfaulted, but three significant faults which cut out portions of Devonian strata are shown.

PREVIOUS WORK

The area was first mapped into stratigraphic formations in the period 1920-1940, with 1:62,500 scale geologic maps in West Virginia county reports, and in Virginia at 1:250,000 scale (Butts, 1933, 1940). A few measured sections were included in those reports. Woodward (1943) summarized the Devonian stratigraphy and prepared a stratigraphic cross section (his Plate D, stratigraphic cross section J-J'), with one generalized data column per county, roughly along the path of our cross section. His discussion recognized the general nature of Catskill Delta facies, but his cross section showed very little facies information. Dennison (1985) presented schematic cross sections of facies patterns and age relationships along the general trend of our more detailed present cross section. The best general stratigraphic nomenclature summary for the Middle and Upper Devonian of the Appalachian basin is by Woodrow and others (1988).

Sections 17-22 (Hightown to Ketterman Knob) were included in the previously published stratigraphic cross section along Allegheny Front which extended from Route 250 (called Hightown in our Figure 1) northeast for 96 miles to Corriganville, Maryland (Dennison, 1970, 1971). Paleontology of these northern sections was described by McGhee (1976), stemming from his thesis at University of North Carolina at Chapel Hill. Petrology of the northern sandstones was described by Kirchgessner (1973). Other studies, many originating from theses and dissertations, whose data entered into Figure 1 are Dennison (1961), Dennison and Hasson (1979), Avary and Dennison (1980), McDonnell (1981), White (1984), Lyke (1986), Dennison, Beuthin, and Hasson (1986), Hasson and Dennison (1988), Filer (1992), and Rossbach (1992). The data at Caldwell are partly from Kammer and Bjerstedt (1986).

Figure 1 follows the strike trend of Allegheny Front. Another stratigraphic cross section by Dennison, Barrell, and Warne (1988) is perpendicular to the trend of Figure 1, with the two cross sections intersecting at the Briery Gap Run stratigraphic column.

ACKNOWLEDGEMENTS

Portions of the field work were supported by University of North Carolina Research Council Grant 43800, and by Appalachian Basin Industrial Associates. Study of the section near Norton was supported by an *ad hoc* consortium of these companies: Ashland Exploration, Cabot Oil and Gas, Coastal Oil and Gas, Equitable Resources Exploration, and Penn Virginia Resources. Field assistance with plane-table measurements of sections by Heikki Bauert, Priscilla Dennison, Ruben Giral , and Thomas Wynn is much appreciated. Heikki Bauert executed the computer drafting of Figure 1. We thank Andrew G. Warne and Kenneth O. Hasson for manuscript reviews.

PROCEDURES

Sixteen new sections of Devonian Catskill Delta strata were measured from Norton, Virginia to Durbin, West Virginia. These were combined with six sections previously measured by Dennison (1970) to form a stratigraphic section extending 263 miles from Norton northeast to Ketterman Knob near Riverton, West Virginia. The total section was based on 41 miles of traverses with plane table and alidade mapping at 1:2,400 scale of stratigraphic details, followed by trigonometric calculations of thicknesses of exposed and covered intervals. Lithologic descriptions and faunal content were used to zone the strata into formations and members, extending stratigraphic nomenclature developed along the Allegheny Front of the Eastern Panhandle of West Virginia southwestward to the facies change from coarser strata to shale/siltstone turbidites (Brallier Formation) and finally to dark shales of the Chattanooga Shale. The original stratigraphic cross section was compiled at 1:3,600 thickness scale and at 1:250,000 horizontal distance scale. Figure 1 was reduced from that larger compilation and simplified somewhat.

STRATIGRAPHIC SUMMARY

Figure 1 summarizes our findings, in a diagram indeed equivalent to thousands of words. Available space in the stratigraphic cross section limits us to abbreviation of stratigraphic nomenclatural detail, spelled out more fully in the legend for that figure.

LITHOSTRATIGRAPHIC NOMENCLATURE

No new stratigraphic names are proposed in this paper. Original sources for nearly all of the names used are described in the literature previously cited, and they are all part of the formal stratigraphic nomenclature used in the Appalachian basin (Woodrow and others, 1988).

The classic Catskill Delta lithologic succession is shown at the northeast end of Figure 1, with the delta beginning with a sharp contact of Needmore Shale resting on Oriskany Sandstone. The Needmore black shale to calcitic shale and limestone is followed upward by the black Millboro Shale with prominent limestone-bearing markers of the Purcell and Tully Members. Upward coarsening into turbidite siltstones and shales marks the base of the Brallier Formation. One conspicuous turbidite bundle in the lower Brallier is called the Back Creek Siltstone Member. The Brallier Formation is in turn overlain by sandstone turbidites and shoaling marine sandy strata of the Greenland Gap Group, which is divided into two formations. The lower Scherr Formation has some sandstones, mostly turbidite bundles, with one prominent bundle known as the Minnehaha Springs Member. The Foreknobs Formation is named for a row of knobs held up by medium- to thick-bedded sandstone admixed with mostly siltstones. The Foreknobs contains five marine members. The basal Mallow Member contains turbidites to shoaling marine sandstone near the top. The Briery Gap Sandstone Member represents a sea-level drop with sand rapidly prograding westward into the Appalachian basin (= Alexander sand of drillers). Sea level rise brought an exceptionally diverse marine shelf fauna into the Blizzard Member. Another sea-level drop produced the Pound Sandstone Member, which swept westward from shoaling waters into turbidite fans (= Benson sand of drillers).

Open-marine shelf conditions again returned with pronounced sea-level rise, as indicated by abundant marine fossils in the Red Lick Member, and then the basin was slowly filled until nonmarine, mostly bright red strata of the Hampshire Formation created the subaerial part of the Catskill Delta. Transgression by a rising sea level produced an important marker of black Sunbury Shale, which marks the base of the Mississippian; thereafter significant red coloration is lacking in the Pocono Formation, also called the Price Formation in both West Virginia and Virginia by Kammer and Bjerstedt (1986) and Bjerstedt and Kammer (1988). This color change may be a climatostratigraphic marker.

Faint reddish coloration (brownish gray, mostly marine redbeds) occurs at several horizons in the Foreknobs Formation and within the Scherr Formation (and at an equivalent position in the Brallier Formation). These may represent sea-level drops which brought more shoreward facies farther out into the basin, or they may be climatostratigraphic markers which formed when climatic conditions created redder soils in the provenance area of the marine deposits.

The strata generally become finer toward the southwest, eventually passing into black shale facies. The Scherr Formation loses its sandstones and passes into the upper Brallier Formation. Two siltstone bundles in the Brallier of the southwest are basinward extensions from the sandstones of the Briery Gap and Pound Members. Nonmarine redbeds of the Hampshire Formation thin to the southwest, so that they disappear at the edge of Devonian land between Alleghany and White Sulphur Springs, with the possible exception of some bright red strata tens of feet beneath the Pocono (Cloyd-Berea conglomerate) at Gap Mills. Devonian sandstone (even conglomeratic) persists at the approximate Gordon sand horizon as far southwest as Gap Mills. At Bluefield some dark shale intertongues occur in the Brallier Formation, extending northeast from the various members of the Chattanooga Shale. A segment extending 33 miles along the Allegheny Front in Tazewell County, Virginia, has the Middle and part of the Upper Devonian omitted and concealed in outcrop by thrust faults. Therefore, Figure 1 has a control column at Asberrys in the Clinch Mountain outcrop belt, with a more easterly and coarser facies pattern in Figure 1 than actually occurs in wells in the Appalachian Plateau closest to Tazewell. We show more detailed divisions within the Chattanooga Shale near Norton than previously indicated. Our divisions there are based on careful outcrop description accompanied by an outcrop gamma-ray log made with a hand-held scintillometer. These fine divisions of Chattanooga Shale can be traced by borehole gamma-ray logs to their type areas in Ohio and New York.

Our work suggests one error in published geologic mapping at the West Virginia-Virginia boundary near the Mountain Grove section. Previous mapping shows a syncline of Pocono strata there. Thickness data from our stratigraphic column suggests that the pebbly quartz sandstone at the mountain summit is probably the Gordon sand (or slightly older), rather than Berea (Cloyd) or Pocono beds.

The stratigraphic cross section of Figure 1 cuts obliquely across the true facies changes. Regional isopachs (Figure 1) of the Appalachian Upper Devonian trend approximately due north. The stratigraphic cross section actually extends about N30°E to the right of Gap Mills and about S60°W to the left of Gap Mills in Figure 1. Thus the rates of facies changes in a stratigraphic cross section perpendicular to depositional strike would be greater than they appear on Figure 1.

ARBITRARY STRATIGRAPHIC CUTOFFS

Dashed vertical lines in Figure 1 indicate arbitrary stratigraphic cutoffs, where some formational diagnostic characteristic is lost by facies change. The Scherr Formation ends at the West Virginia-Virginia boundary (between the Dry Run and Route 642 columnar sections), because the Scherr Formation becomes finer grained and the last sandstone disappears. Thus the Scherr passes laterally into the Brallier Formation. The Minnehaha Springs

Member turbidite bundle loses its sand southwestward, but a siltstone bundle can still be identified as the Minnehaha Springs Member within the Brallier Formation as far southwest as White Sulphur Springs.

The Mallow Member generally coarsens upward, and also becomes finer grained toward the southwest. This results in arbitrary cutoffs of the base of the Mallow Member (and of the base of the Foreknobs Formation) between Alleghany and White Sulphur Springs. Loss of all sandstone in the Mallow, Briery Gap, Blizzard, and Pound Members southwest of White Sulphur Springs results in an arbitrary cutoff of the base of the Foreknobs, jumping up to the upper Red Lick position near Gap Mills. The Red Lick loses all of its sandstone between Gap Mills and Bluefield, so that Gap Mills is the farthest southwest that the term Foreknobs Formation is used in our stratigraphic cross section.

ASH BEDS

Volcanic ashes provide important time surfaces in the Devonian of the Appalachian basin. The Tioga Ash occurs at the boundary between the Needmore and Millboro Shales at the northeast end of Figure 1. From just southwest of Frost to Asberrys, the Tioga occurs at the contact of the Huntersville Chert and Millboro Shale. Farther southwest toward Norton the base-of-Chattanooga unconformity cuts out the Tioga Ash, so that at Norton Upper Devonian Rhinestreet Shale rests on lower Onondaga-equivalent beds at the top of the Wildcat Valley Sandstone Formation. The Tioga volcano was situated near present-day Fredericksburg, Virginia, with roots now hidden beneath the metamorphic overthrusts of the Piedmont (Dennison and Textoris, 1987). The name Tioga Ash comes from the first discovery of this marker bed in the gas fields of Tioga County, Pennsylvania.

The Belpre Ash is named from wells near Belpre, Ohio. It is known in the Valley and Ridge Province in scattered outcrops between Norton, Virginia, and Clinch Mountain near Rogersville, Tennessee.

The Center Hill Ash forms an important marker within the Chattanooga Shale in central Tennessee, near the Center Hill Reservoir. It occurs in the gray shale of the lower Java Member at Norton, Virginia, and also it has been found at White Sulphur Springs 20 feet above the top of the siltstone bundle which is a basinward extension from the Briery Gap Sandstone.

All three of these ash beds are well known in the Appalachian basin subsurface, in cores and gamma ray logs.

PALEONTOLOGIC DATA

Marine faunas were listed but not illustrated in the older literature concerning the area of Figure 1. McGhee (1976) gave faunal details concerning the right end of Figure 1, from the Hightown section northeastward. Rossbach (1992) was the first to illustrate photographically the fauna of the Foreknobs Formation farther to the south, including detailed faunal zonation of the Minnehaha Springs and Rucker Gap columnar sections shown in Figure 1. Rossbach places the Frasnian-Famennian boundary within the lower Red Lick Member at Rucker Gap, perhaps only tens of feet above the top of the Pound Sandstone Member, but possibly as high as hundreds of feet up in the Red Lick there. No definite Famennian taxa were found to mark the boundary precisely in the Rucker Gap section.

The botanical marker of *Foerstia* occurs in the middle gray shale portion of the Huron Shale at Norton.

FACIES CHANGES

Several facies changes have already been described in the comments on stratigraphic nomenclature. Other facies patterns will be mentioned briefly.

Huntersville Chert is a facies equivalent of Needmore Shale. Some lower Brallier Formation probably passes laterally into Millboro Shale. Eventually the entire Brallier passes into dominantly dark shale of the Chattanooga Shale, except for the somewhat silty Three Lick Bed at Norton. The Three Lick Bed seems to be an extension from the Gordon sand position, which in turn projects southwestward from the base of the Hampshire Formation near Rucker Gap. This probably represents a time of abrupt sea-level drop corresponding to the Cattaraugus Redbeds of New York. There are occasional quartz pebbles in the Pound Sandstone as far southwest as Frost, and in the younger Gordon sandstone as far southwest as Gap Mills. Figure 1 shows the oldest quartz pebbly beds in the Devonian deltaic strata, and it is evident that the base of quartz pebbly beds climbs stratigraphically higher toward the southwest. At the end of Devonian-beginning of Mississippian a coarse sandstone unit (Berea) is usually present, but locally it is a quartz-pebble conglomerate (Cloyd). The Cannon Hill and Rowlesburg Members of the Hampshire Formation were named by Boswell, Donaldson, and Lewis (1987). The Rowlesburg is the familiar bright red-dominated portion of the Hampshire Formation nonmarine beds with more mudstone than sandstone. The Cannon Hill Member is nonmarine also, but dominantly yellowish gray to light olive gray sandstone with subordinate beds of red shale. The Cannon Hill Member, as we show it, is probably diachronous.

The position of the highest marine fossils in the Red Lick Member is shown in Figure 1, generally a couple hundred feet below the lowest nonmarine redbeds.

The general positions of Grant Bay and Augusta Lobe in the Catskill Delta complex are marked by both facies changes and thickness changes. Brownish gray dull redbeds within the marine Upper Devonian are more abundant near the Augusta Lobe, which represents the delta of a major Devonian river. The Back Creek Siltstone seems to be associated only with the Augusta Lobe, perhaps as a result of rapid uplift and erosion of the provenance area.

UNCONFORMITIES

Two extensive and two minor unconformities affect the area of Figure 1. The most widespread is the Wallbridge Discontinuity, which occurs at the base of the Huntersville Chert-Needmore Shale. This unconformity was caused by one of the major Paleozoic sea-level drops which exposed the North American craton.

Another unconformity occurs at the base of the Chattanooga Shale at Norton, projects into the Millboro Shale at Bluefield (Dennison and others, 1992), and probably dies out in the Millboro Shale at roughly the Tully Limestone position between White Sulphur Springs and Frost. This unconformity has been mapped in the subsurface within the Devonian Shales of West Virginia, but only now are we able to identify and approximately trace it within the Millboro Shale of the Valley and Ridge outcrops. This unconformity within the Devonian Shales is interpreted as a tectonic unconformity expanding westward toward a peripheral bulge.

The base of Wildcat Valley Sandstone is unconformable on Hancock Limestone at Norton, as a third unconformity which marks the base of the Devonian. Also, a very localized unconformity occurs within the Wildcat Valley Sandstone in the Norton area, where Onondaga-age strata rest unconformably on late Helderberg strata, with omission of Oriskany-age beds.

Mappers in the 1920's interpreted the southward disappearance of non-marine strata of the Hampshire Formation as a pre-Pocono unconformity. Woodward (1943) recognized this phenomenon as a facies change of the nonmarine Hampshire into uppermost marine strata which he assigned to the Chemung Formation (which Dennison in 1970 replaced with the name Foreknobs Formation in the area of Figure 1). Our cross section documents facies tongues of brownish gray, marine redbeds in the otherwise non-red and marine Red Lick Member (Foreknobs Formation), occurring as extensions from the nonmarine, bright redbeds of the Rowlesburg Member (Hampshire Formation). The Cannon Hill Member is mostly non-red, but nonmarine, deposited in reducing conditions at or near sea level where the water table was too high for oxidized sandy redbeds to develop.

TIME LINES

The time lines formed by the Tioga, Belpre, and Center Hill Ash beds represent the best time surfaces in Figure 1. The abrupt transgression marked by the Pound Sandstone overlain by the more silty strata of the Red Lick Member (and its position farther southwest marked by a siltstone bundle in the Brallier Formation overlain by the blackish Dunkirk shale tongue, and even farther southwest by gray Java Shale overlain by black Huron Shale) is a prominent time surface. This widespread surface indicating abrupt deepening of the sea was used as the primary datum for drawing Figure 1. The coarse clastic pulses marked by the Back Creek Siltstone Member, Minnehaha Springs Member, and the Briery Gap Sandstone (and its equivalent siltstone bundle in the Brallier Formation) are probably time bands on the stratigraphic cross section, with the last two related to sea-level drops. Within the Foreknobs Formation brownish gray dull redbeds form extensive bands which parallel these other time lines, so the "mid-Blizzard red" and other color markers can probably be used as approximate time lines in Figure 1. The limestone with shale zones labeled as Tully and as Purcell within the Millboro Shale are important time surfaces, extending from the northeast portion of Figure 1 northward to New York as the Tully Limestone and Cherry Valley Limestone, respectively.

STRUCTURAL COMPLICATIONS

A small fault occurs at Dry Run, with Oriskany Sandstone thrust over Millboro Shale, omitting the Needmore Shale. Thinned Brallier Formation at Ketterman Knob may result from shearing in a generalized zone, without any specific fault plane.

The largest fault on Figure 1 is localized between Gap Mills and Bluefield, in an interval where Ordovician carbonates are thrust by the St. Clair fault to conceal much of the Millboro and lower Brallier Formations. Furthermore, the stratigraphic section near Lindside has a thinned sequence from Tioga Ash, through Millboro Shale, and lower Brallier strata, resulting from general shearing attenuation of a markedly overturned Devonian section overridden by the St. Clair fault. At Glen Lyn and Rich Creek on opposite sides of New River, the St. Clair fault places Ordovician Beekmantown Dolomite in direct contact with Brallier Formation. In Figure 1 beneath the St. Clair fault pattern a succession of straight strata inclined about 45° to the right shows the expected rate of stratigraphic thickening of lower Brallier Formation without the complications of faulting near Glen Lyn, Rich Creek, and Lindside.

We also show a newly discovered fault near Lindside, Rich Creek, and Glen Lyn which omits much of the upper Brallier and much of the Pocono (Price) Formation. This last fault is evidenced by well records a few miles to the north in Monroe and Summers counties, where Devonian delta thicknesses in wells are similar to the much greater thicknesses which would be indicated by projecting between only the Gap Mills and Bluefield columnar sections.

The exceptionally thick upper Red Lick column at Durbin results from calculations using an averaged dip of 21° for a large concealed interval. A structural terrace in that concealed area in the town of Durbin could result in a reduced Red Lick thickness more like the sections at Dry Run, Hightown, and Rucker Gap.

HYDROCARBON EXPLORATION IMPLICATIONS

Southeastern West Virginia has essentially no methane production from the Devonian, but southwestern Virginia has important gas and some oil production from the Devonian Shales (Chattanooga Shale of Figure 1). One goal for the present study was to evaluate hydrocarbon possibilities for southeastern West Virginia.

Dark, organic shales at Norton are best developed in the Rhinestreet, lower and upper Huron, and Sunbury positions. Unfortunately the organic shales of the Chattanooga do not extend very far northeast in Figure 1. Details of the Brallier Formation at Bluefield show a few feet of blackish shale interbeds at several places in the stratigraphic column, but none worthy as drilling targets. One very dark gray shale bed occupies a few feet of the Blizzard-equivalent position at White Sulphur Springs. Thus, none of these dark shales are reasonable drilling targets, although they could have served as source beds for gas or oil generation. Probably the strata have been heated too hot through burial and orogeny to contain Devonian oil northeast of Bluefield in the vicinity of Figure 1.

The numerous siltstones are too argillaceous to make good reservoirs in today's economy. These include siltstone bundles in the Brallier Formation such as the Back Creek, Minnehaha Springs, and siltstone projections equivalent to the Briery Gap, Pound, and even Gordon sandy beds shown in Figure 1. The Elk sand of drillers corresponds to coarser zones in the Mallow Member, but these Mallow sands become finer rapidly toward the southwest, with true sandstone in the Mallow reaching only as far southwest as White Sulphur Springs. Argillaceous sandstone facies of the Briery Gap and Pound may occur in northwestern and central Greenbrier County. The Gordon is somewhat cleaner, but still a siltstone, in the column at White Sulphur Springs, and it has the best possibility for gas in the Upper Devonian of Greenbrier County. It is interesting that the Gordon is more winnowed, and even pebbly, but thin at Gap Mills. This suggests that the Gordon could have spotty production in northern Monroe County or eastern Summers County. Some of the sandstone labeled as Gordon to the southwest in Figure 1 may actually be as young as the Gordon stray or Fifty Foot sands, which generally extend as far west as or even slightly farther than the Gordon in the subsurface of northern West Virginia.

It is also noteworthy that the Red Lick Formation has been concealed by faulting at Lindside, Rich Creek, and Glen Lyn, so that the Devonian deltaic section appears deceptively shaly in those exposures. The uppermost Devonian is indicated as somewhat sandy in nearby oil and gas well records in Monroe and Summers Counties. Perhaps Berea tests in those counties should continue down a few hundred feet into the Devonian.

In the eastern Appalachian basin to the west of the northeast portion of Figure 1, gas production may be possible from the Gordon, Benson, and Alexander sands in Pocahontas County, extending established production south from southwestern Randolph County.

The Gordon sand shown in the Upper Devonian at Asberrys is deceptive. It is important to remember that the Asberrys column is situated in a more southeasterly outcrop belt than any other columnar section in Figure 1, so the Asberrys column represents a nearer shore facies development than would be expected beneath the edge of the Appalachian Plateau at that longitude. Thus, production possibilities from the Gordon-equivalent or true Gordon are probably limited to east of Bluefield, in eastern Mercer County and eastward.

REFERENCES CITED

Avary, K L., and Dennison, J. M., 1980, Back Creek Siltstone Member of Devonian Brallier Formation in Virginia and West Virginia: Southeastern Geology, v. 21, p. 121-153.

Bjerstedt, T. W. and Kammer, T. W., 1988, Genetic stratigraphy and depositional systems of the Upper Devonian-Lower Mississippian Price-Rockwell deltaic complex in the central Appalachians, U.S.A.: Sedimentary Geology, v. 54, p. 265-301.

Boswell, R. M., Donaldson, A., C., and Lewis, J. S., 1987, Subsurface stratigraphy of the Acadian clastic wedge of northern West Virginia: Southeastern Geology, v. 28, p. 105-131.

Butts, C., 1933, Geologic map of the Appalachian Valley of Virginia with explanatory text: Virginia Geological Survey, Bulletin 42, 56 p. + map.

Butts, C., 1940, Geology of the Appalachian Valley in Virginia: Virginia Geological Survey Bulletin 52, Part I, 560 p.

Dennison, J. M., 1961, Stratigraphy of Onesquethaw Stage of Devonian in West Virginia and bordering states: West Virginia Geological Survey Bulletin 22, 87 p.

Dennison, J. M., 1970, Stratigraphic divisions of Upper Devonian Greenland Gap Group ("Chemung Formation") along Allegheny Front in West Virginia, Maryland, and Highland County, Virginia: Southeastern Geology, v. 12, p. 53-82.

Dennison, J. M., 1971, Petroleum related to Middle and Upper Devonian deltaic facies in central Appalachians: American Association of Petroleum Geologists Bulletin, v. 55, p. 1179-1193.

Dennison, J. M., 1985, Catskill delta shallow marine strata, *in* Woodrow, D. M., and Sevon, W. A., editors, Catskill Delta Symposium, Geological Society of America Special Paper 201, p. 91-206.

Dennison, J. M., Bambach, R. K., Dorobek, S. L., Filer, J. K., and Shell, J. A., 1992, Silurian and Devonian unconformities in southwestern Virginia, *in* Dennison, J. M. and Stewart, K. G., editors, Geologic Field Guides to North Carolina and Vicinity: Chapel Hill, North Carolina, Department of Geology University of North Carolina at Chapel Hill, Geologic Guidebook No. 1, p. 79-105.

Dennison, J. M., Barrell, S. M., and Warne, A. G., 1988, Northwest-southeast cross section of Devonian Catskill Delta in east-central West Virginia and adjacent Virginia, *in* Dennison, J. M., editor, Geologic Field Guide, - Devonian Delta of East-Central West Virginia and Adjacent Virginia: Appalachian Geological Society, p. 12-35.

Dennison, J. M., Beuthin, J. D., and Hasson, K. O., 1986, Latest Devonian-earliest Carboniferous marine transgressions--central and southern Appalachians, USA: Annals de la Société géologique de Belgique, T. 109--1986, p. 123-129 (Special Volume "Aachen 1986", Late Devonian events around the Old Red Continent).

Dennison, J. M. and Hasson, K. O., 1979, Stratigraphic cross section of Devonian shales along the Allegheny Front from Maryland to Highland County, Virginia: Proceedings West Virginia Academy of Science, v. 49, p. 104-110.

Dennison, J. M. and Textoris, D. A., 1987, Paleowind and depositional tectonics interpreted from Devonian Tioga Ash Bed: Appalachian Basin Industrial Associates, Program - Spring Meeting, May 7-8, 1987, Knoxville, Tennessee, v. 12, p.107-132.

Filer, J. K., 1992, Sedimentation cycles near the Frasnian-Famennian boundary in the Appalachian basin and their implications: Ph. D. dissertation, University of North Carolina at Chapel Hill, 286 p.

Hasson, K. O. and Dennison, J. M., 1988, Devonian shale lithostratigraphy, central Appalachians, U. S. A., *in* McMillan, N. J., Embry, A. F., and Glass, D. J., editors, Devonian of the World: Canadian Society of Petroleum Geologists Memoir 14, v. 2, p. 157-177 (Proceedings Second International Symposium on the Devonian System, Calgary, Alberta, Canada, August 1987).

Kammer, T. W. and Bjerstedt, T. W., Stratigraphic framework of the Price Formation (Upper Devonian-Lower Mississippian) in West Virginia: Southeastern Geology, v. 27, p. 13-33.

Kirchgessner, D. A., 1973, Sedimentology and petrology of Upper Devonian Greenland Gap Group along the Allegheny Front, Virginia, West Virginia, and Maryland: Ph. D. dissertation, University of North Carolina at Chapel Hill, 93 p.

Lyke, W. L., 1986, The stratigraphy, paleogeography, depositional environment, faunal communities, and general petrology of the Minnehaha Springs Member of the Scherr Formation, an Upper Devonian turbidite sequence, central Appalachians: Southeastern Geology, v. 26, p. 173-192.

McDonnell, D. E., 1981, Limits of the Devonian Hampshire Formation in parts of Virginia and West Virginia: M. S. thesis, University of North Carolina at Chapel Hill, 128 p.

McGhee, G. R., Jr., 1976, Late Devonian benthic marine communities of the central Appalachian Allegheny Front: Lethaia, v. 9, 111-136.

Rossbach, T. J., 1992, Biostratigraphy of the Upper Devonian Greenland Gap Group in West Virginia and Virginia: Ph. D. dissertation, University of North Carolina at Chapel Hill, 176 p.

White, E. , 1984, Upper Devonian Chemung and Brallier Formations in outcrop and subsurface of southeastern West Virginia and adjacent Virginia: M. S. thesis, University of North Carolina at Chapel Hill, 59 p.

Woodrow, D. L., Dennison, J. M., Ettensohn, F. R., Sevon, W. T., and Kirchgasser, W. T., 1988, Middle and Upper Devonian stratigraphy and paleogeography of the central and southern Appalachians and eastern Midcontinent, *in* McMillan, N. J., Embry, A. F., and Glass, D. J., editors, Devonian of the World: Canadian Society of Petroleum Geologists Memoir 14, v. 1, p. 277-301 (Proceedings Second International Symposium on the Devonian System, Calgary, Alberta, Canada, August 1987).

Woodward, H. P., 1943, Devonian System of West Virginia: West Virginia Geological Survey, v. 15, 655 p.

LEGEND FOR FIGURE 1

ABBREVIATIONS AND STRATIGRAPHIC NAMES

ASM	Angola Shale Member of Chattanooga Shale Formation
BA	Belpre Ash
BCSM	Back Creek Siltstone Member of Brallier Formation (= Sycamore sand of subsurface)
BF	Brallier Formation
bgr	brownish gray redbeds (usually marine)
BGSM	Briery Gap Sandstone Member of Foreknobs Formation (= Alexander sand of subsurface)
BM	Blizzard Member of Foreknobs Formation
br	bright redbeds (mostly moderate red and usually nonmarine)
BSGSM	Big Stone Gap Shale Member of Chattanooga Shale Formation
BSM	Berea (Cloyd) Sandstone Member of Pocono (Price) Formation
CCM	Cloyd Conglomerate Member of Price Formation
CHA	Center Hill Ash
CHM	Cannon Hill Member of Hampshire Formation (dominated by light olive gray sandstone)
	Chattanooga Shale Formation (no abbreviation)
CSM	Cleveland Shale Member of Chattanooga Shale Formation
DST	Dunkirk Shale Tongue from Huron Shale Member of Chattanooga Shale
FF	Foreknobs Formation of Greenland Gap Group
	Greenland Gap Group (no abbreviation)
Gs	Gordon sand (of subsurface exposed on outcrop)
Gse	Gordon sand (of subsurface) equivalent sandstone
HCF	Huntersville Chert Formation
HF	Hampshire Formation
HG	Helderberg Group
HLF	Hancock Limestone Formation
hmf	highest marine fossils in Catskill Delta complex
HSM	Huron Shale Member black shale of Chattanooga Shale Formation (with Dunkirk Shale, basal tongue of dark shale)
JSM	Java Shale Member gray shale of Chattanooga Shale Formation
lbsm	lower black shale member of Chattanooga Shale Formation
lqc	lowest quartz pebble conglomeratic beds in Catskill delta section
mgsm	middle gray shale member of Chattanooga Shale Formation
MM	Mallow Member of Foreknobs Formation
MSF	Millboro Shale Formation
MSM	Minnehaha Springs Member (of Scherr and Brallier Formations)
NSF	Needmore Shale Formation
OFe	Oswayo Formation equivalent: shaly to silty strata caused by Cleveland transgression
OSF	Oriskany (Ridgeley) Sandstone Formation
PF	Price Formation
PM	Purcell Member limestone and shale in Millboro Shale Formation
P(P)F	Pocono (Price) Formation
PSM	Pound Sandstone Member of Foreknobs Formation (= Benson sand of subsurface)
RLM	Red Lick Member of Foreknobs Formation
RM	Rowlesburg Member (dominantly bright red, nonmarine) of Hampshire Formation
RSM	Rhinestreet Shale Member black shale of Chattanooga Shale Formation
sbeBGSM	siltstone bundle in Brallier Formation equivalent to Briery Gap Sandstone Member of Foreknobs Formation
sbePSM	siltstone bundle in Brallier Formation equivalent to Pound Sandstone Member of Foreknobs Formation
	Scherr Formation of Greenland Gap Group (no abbreviation)
SSM	Sunbury Shale Member of Price Formation, Pocono Formation, or Chattanooga Shale Formation
TA	Tioga Ash
TLB	Three Lick Bed gray shale and siltstone in Chattanooga Shale

LINES AND MARKS

│	location of exposed portion of measured section
¦	cutoff of named stratigraphic units
....	fault
━━━	formation boundary
───	boundary of member or lithologic subdivision
xxxxxx	ash bed
-----	redbed zones in mostly marine strata
+	highest marine fossils
●	quartz pebbles (pebbly sandstone or conglomerate)

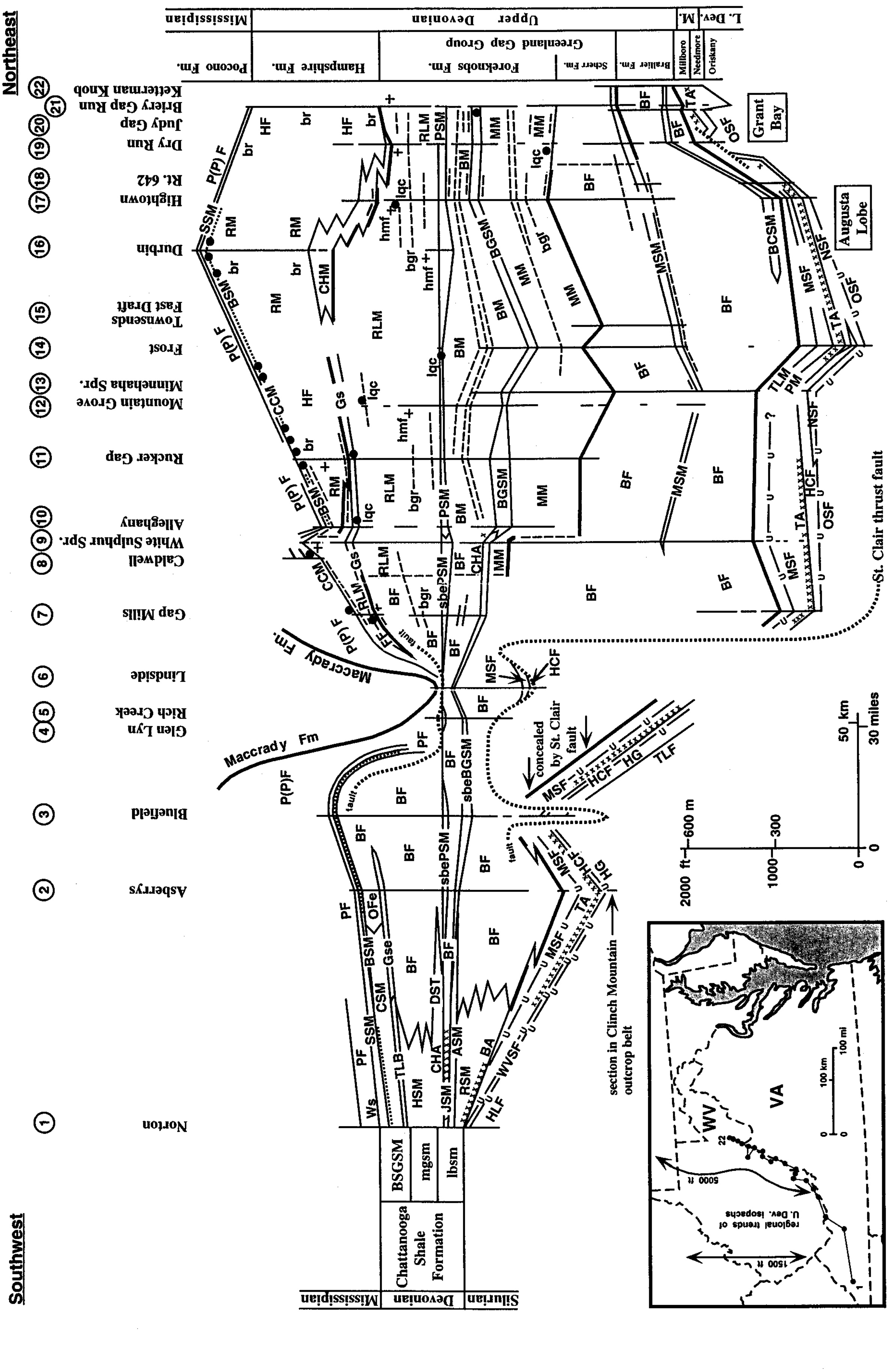

Figure 1. Northeast-southwest stratigraphic cross section of Middle and Upper Devonian strata near the Virginia-West Virginia boundary.

UPPER CRETACEOUS AND TERTIARY STRATIGRAPHY OF CORE-HOLE KEN-BF 180 CLARIFIES AQUIFER NOMENCLATURE IN KENT COUNTY, MARYLAND

Harry J. Hansen and David D. Drummond
Maryland Geological Survey, Baltimore, MD. 21218

ABSTRACT

Aquifers underlying the upper Delmarva Peninsula in Maryland were initially identified by correlation with lithostratigraphic units. These include the Paleocene Aquia aquifer and the Upper Cretaceous Monmouth, Magothy, and Raritan(?) aquifers. Although both formations and aquifers are mappable rock bodies, their boundary discontinuities (contacts) are different. A dual nomenclatural system may be ambiguous because geologically significant contacts often are not defining boundaries in a hydraulic sense.

For example, six lithostratigraphic units comprise the three major aquifers cored in Ken-Bf 180 (a 480-ft. boring drilled near Chesterville, Md.):

AQUIA AQUIFER:

- Middle to Upper Oligocene Old Church(?) Formation (5 ft. thick): Fine to medium, glauconitic (<25%)sand.
- Upper Paleocene Aquia Formation (86 ft. thick): A 23-ft., clayey, medium to fine, glauconitic (15-60%)sand, grading upward into a medium to coarse, intensely weathered, glauconitic sand.
- Lower Paleocene Hornerstown Formation (95 ft. thick): A fine to medium (occasionally coarse), glauconitic(15-40%) sand with patchy sideritic cement.

MONMOUTH AQUIFER:

- Upper Cretaceous (Maestrichtian) Mount Laurel Formation (78 ft. thick): A 22-ft., clayey, glauconitic (<35%), very fine to fine sand (with patchy, calcareous cement), grading upward into a medium to fine, glauconitic (<15%), silty sand.

MAGOTHY-RARITAN(?)-UPPER PATAPSCO AQUIFER SYSTEM:

- Upper Cretaceous (Santonian to Campanian) Magothy Formation (18 ft. thick): Gray to blackish, lignitic clay (not an aquifer at site).
- Upper Cretaceous (Middle Cenomanian) Raritan(?) Formation (54 ft. thick): A 12-ft., mottled brownish gray, silty clay to very fine sandy silt underlain by two lignitic, brownish gray, pebbly sands; a 4-ft. clay separates the upper sand (22 ft.) from the less feldspathic lower (16 ft.) sand.

INTRODUCTION

A 480-ft core-hole (Ken-Bf 180) was drilled near Chesterville, Maryland (39°17'06" N lat., 75°54'52" W long.) to obtain stratigraphic information needed for a cooperative hydrogeologic study of Kent County undertaken by the Maryland Geological Survey and the U.S. Geological Survey (figure 1).

Kent County is located on the eastern shore of Chesapeake Bay on the upper Delmarva Peninsula. Coastal Plain units in the county dip southeasterly at less than one degree.

Ken-Bf 180 was located at a site in northeastern Kent County where the upper Paleocene to upper Cretaceous section could be cored at relatively shallow depths. This section includes the Aquia, Monmouth, Magothy, and Raritan(?) aquifers (figure 1). The cores from Ken-Bf 180 were analyzed to resolve stratigraphic ambiguities resulting from a dual nomenclatural system that used lithostratigraphic names (Miller, 1926) to identify hydrogeologic units (Overbeck and Slaughter, 1958).

ACKNOWLEDGMENTS

Core-hole Ken-Bf 180 was drilled by the U.S. Geological Survey in June 1991. Preliminary results of the core study were published in Maryland Geological Survey Open-File Report No. 93-02-7 (Hansen, 1992). This paper is largely an abridged version of the report. In addition to the authors, contributors to Maryland Geological Survey Open-File Report No. 93-02-7 include: Gregory Gohn (U.S. Geological Survey) who prepared a summary of the lithologic log of Ken-Bf 180 using field descriptions by Gohn, Thomas Gibson (U.S. Geological Survey), and David Drummond; Gilbert Brenner (State University of New York at New Paltz) (palynomorphs), Richard Olsson (Rutgers University) (foraminifera), and Gregory Gohn (ostracodes) who performed biostratigraphic studies of selected samples; and Richard April (Colgate University) who undertook grain-size analyses, heavy-mineral point counts, and x-ray diffraction analyses of selected samples.

STRATIGRAPHY OF CORE HOLE KEN-BF 180

The stratigraphy of core hole Ken-Bf 180 is described in ascending order from oldest unit to youngest unit. The test site is about 55 feet above sea level. Depths are given in feet below land surface.

LOWER CRETACEOUS ELK NECK BEDS OF THE PATAPSCO FORMATION (476.3 FT TO 480 FT TOTAL DEPTH)

Mottled (red and gray), silty clay and lignitic wood were cored in the bottom 4 feet of Ken-Bf 180 (Appendix A, *in* Hansen, 1992). A core from 478 ft contains a terrestrial palynomorph assemblage that Brenner (Appendix C *in* Hansen, 1992) considers to be late Albian (Zone IIC). Wolfe and Pakiser (1971) have assigned palynomorphic Zone IIC and Zone III (lower Cenomanian) to the Elk Neck beds of the Patapsco Formation.

UPPER CRETACEOUS ELK NECK BEDS OF THE PATAPSCO FORMATION(?) AND/OR UPPER CRETACEOUS RARITAN FORMATION(?) (422.3 FT TO 476.3 FT)

The interval logged between 422.3 ft and 476.3 ft is mainly comprised of two pebbly sands of fluvial origin separated by a 4.2-ft micaceous, light-gray to yellowish-gray, silty clay. The basal contact of the lower sand (460 ft to 476.3 ft) is sharp and pebbly. The quartz sand is pinkish to brownish gray and ranges in texture from

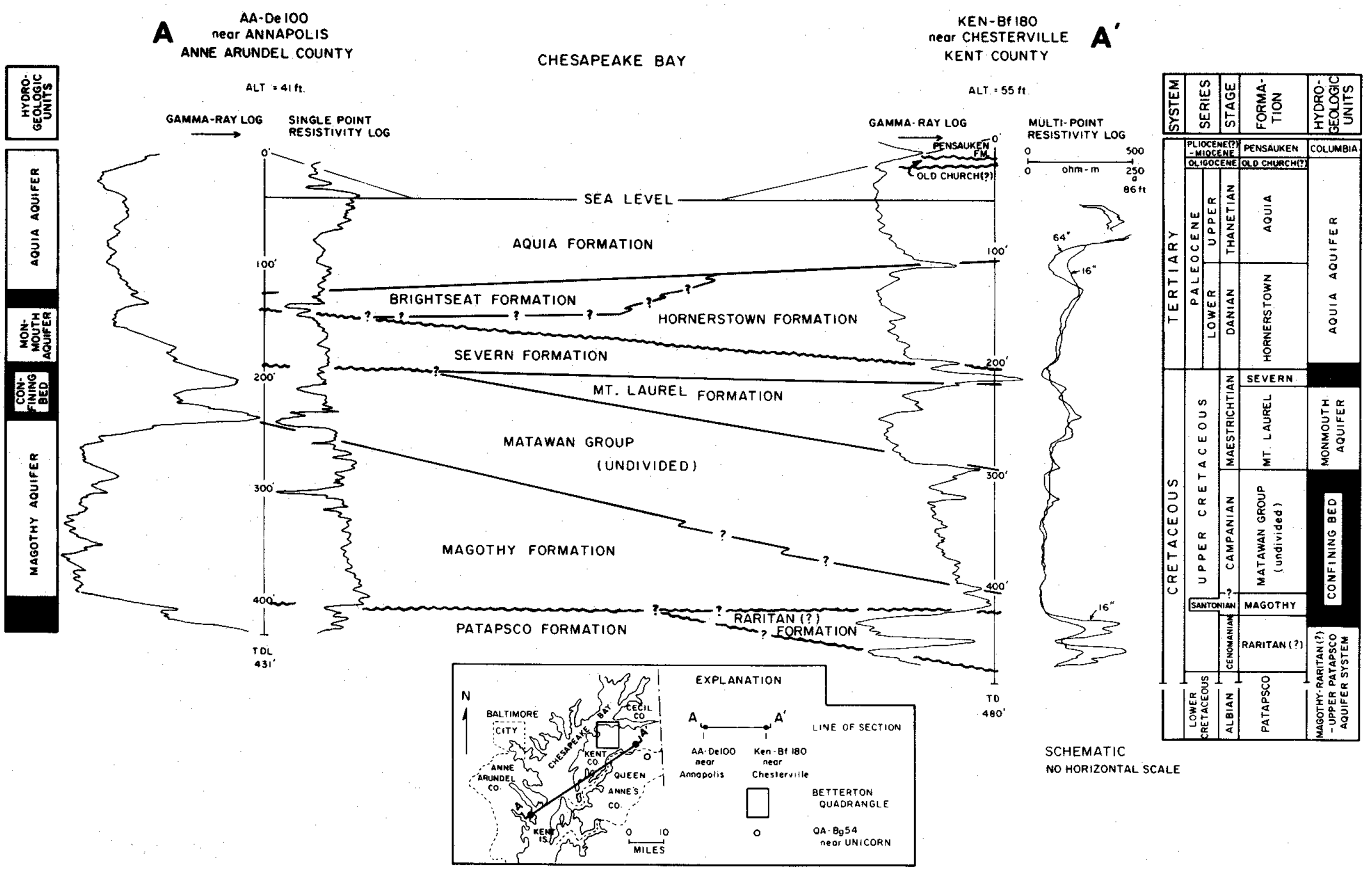

Figure 1. Cross-section A-A', extending from Annapolis, Md. to near Chesterville, Md., showing correlation of Paleocene and Upper Cretaceous units and location of core-hole Ken-Bf 180.

fine to very coarse with granules and small pebbles. The upper 6 feet of the lower sandy interval is a very fine to fine, micaceous quartz sand. The upper unit (434 ft - 455.8 ft) includes interbedded sands, pebbly sands, and gravels that fine upward into a fine to coarse sand. It consists chiefly of quartz and feldspar with some lignite and associated pyrite and is light gray to brownish gray in color. Heavy minerals from 455 ft are dominated by the SSK (sillimanite, staurolite, kyanite) suite, chiefly staurolite (59 percent). From 422.3 ft to 434 ft (and in sharp contact with the overlying Magothy Formation) is a micaceous, silty clay to very fine sandy silt. Scattered lignitic wood is present; it is mottled irregularly light gray to brownish gray.

A core sample from 461 ft contains specimens of *Complexipollis* sp. K of Christopher (1979), which according to Brenner (Appendix C *in* Hansen, 1992) is restricted to the middle Cenomanian *Atlantopollis-Complexipollis* Zone (Zone IV). It appears, therefore, that pre-Magothy beds younger than the Elk Neck Beds of the Patapsco Formation may be present in core hole Ken-Bf 180. Zone IV beds in the Middle Atlantic area are generally assigned to the Raritan Formation. The presence of Zone IV beds and the apparent absence of lower Cenomanian Zone III-Elk Neck beds are surprising. Zone III beds have been identified palynologically in both northern Delaware (Doyle and Robbins, 1977) and in adjacent Cecil County, Maryland (James Doyle *in* Edwards and Hansen, 1979), whereas Zone IV beds are generally restricted to the deeper portions of the Salisbury Embayment (Owens and Gohn, 1985). The reported occurrence of *Complexipollis* in Ken-Bf 180 suggests, however, that the "Raritan problem" in northeast Maryland remains unresolved. In Kent County middle (or upper) Cenomanian beds may occur, perhaps as fluvial paleochannel deposits entrenched into the underlying Patapsco Formation. On the other hand, the palynomorph ranges used to zone the Elk Neck beds and Raritan Formation in Maryland may reflect in some cases local ecological factors, rather than chronostratigraphic correlation.

UPPER CRETACEOUS MAGOTHY FORMATION (404 FT - 422.3 FT)

The Magothy Formation in Ken-Bf 180 is notable for the absence of a sandy facies. The unit is a waxy, gray to blackish clay with common occurrences of lignitic wood and pyrite. The Magothy is bounded by sharp upper and lower contacts with about 1-inch relief. At the test site the Magothy is represented by relatively thin (19 ft), marsh or back-bay sediments, a lithofacies reported in northern Delaware by Spoljaric (1972) to interfinger with nearshore fluvio-deltaic sands. In the Betterton quadrangle of northwest Kent County, Minard (1974) mapped 30 to 35 ft of Magothy. He reported that it is predominantly a yellow-brown (weathered) to light gray lignitic, quartz sand with discontinuous layers of silt and clay (varying in thickness from a few inches to 15 ft). Minard (1974) assigned an earliest Campanian age to the Magothy Formation. Two Magothy samples from Ken-Bf 180 studied by Brenner (Appendix C *in* Hansen, 1992) contained normapollen types, which he considers Santonian to early Campanian.

At Annapolis, Maryland (AA-De 100; fig. 1) the Magothy is approximately 150 feet thick and, according to Glaser (*in* Mack, 1974), consists of a fluvial facies overlain by 20 to 30 feet of sediments representing a shore-line complex. During Magothy deposition this area was proximal to a locally significant source of fluvial sediments. The build-up of Magothy sands at Annapolis diminish northeastwards toward Kent County, where thinner, redistributed strand zone deposits accumulated and the on-set of shelfal sedimentation occurred earlier (figure 1).

UPPER CRETACEOUS MATAWAN GROUP (UNDIVIDED) (295 FT - 404 FT)

The Matawan Group is a sequence of glauconitic, dark-gray to olive-gray silty clays and very fine to find sands. It has an overall regressive (shoaling) aspect with some medium-grained sands logged in the upper part (295 ft to 320 ft). Sand-size glauconite ranges up to about 60 percent; the pellets are usually "fresh," dark green, polylobate types showing little alteration. Mica (muscovite) is a common accessory (<5 percent). The HEGAT suite (hornblende, epidote, garnet, actinolite, and tremolite) comprises 45 percent of the non-opaque, detrital heavy minerals (at 319 feet). Bedding is often massive with some mottling and burrows, suggesting bioturbated sediments. The Matawan Group below about 320 ft is generally noncalcareous, resulting in meager microfossil assemblages of calcareous forms such as foraminifera.

Gohn (Appendix A *in* Hansen, 1992) assigned the sandy beds between 295 ft and 320 ft to the Marshalltown Formation. He also logged two "pre-Marshalltown cycles" in the Matawan Group, each bounded by sharp, flat contacts. In the Betterton quadrangle Minard (1974) subdivided the Matawan Group into three formations, from oldest to youngest, the Merchantville (20-40 ft), the Englishtown (15-18 ft), and the Marshalltown (20-40 ft). The same tripartite nomenclature has been used in Delaware by Houlik, Olsson, and Aurisano (1983) to describe sediments outcropping along the Chesapeake and Delaware Canal and by Benson, Jordan, and Spoljaric (1985) to subdivide the Matawan Group in a well at Dover.

Biostratigraphic data for the Matawan Group in Ken-Bf 180 is sparse, but suggests a Campanian age. Gohn (Appendix B *in* Hansen, 1992) observed (at 360 ft) the long-ranging ostracode species *Curfsina communis*, which indicates an age no older than Campanian. The more diagnostic *Planileberis*? *costatana*, which has a first appearance in the late middle or late Campanian, occurs at 311 ft. Olsson (Appendix D *in* Hansen, 1992) considered foraminifera recovered from 301 ft to be a typical Campanian marine shelf assemblage (±150-meter paleodepth); identified species included *Archeoglobigerina blowi*, *A. cretacea*, and *Globotruncana rosetta*.

In Kent County shelfal sediments of the Matawan Group thicken both down-dip and northeastward along strike (Hansen, 1992, plate 2), achieving a maximum thickness of about 160 feet. The Matawan thins southwestward toward Annapolis where the onset of shelfal deposition was delayed as fluvio-deltaic lithofacies, more typical of the Magothy Formation, continued to accumulate into the early Campanian (figure 1).

UPPER CRETACEOUS MOUNT LAUREL FORMATION (217.9 FT TO 295 FT)

Two formations of the Monmouth Group occur in Ken-Bf 180, the Mount Laurel Formation and the Severn Formation. The upper beds of the Matawan Group grade into the Mount Laurel Formation. The Mount Laurel Formation is a coarsening-upward sand sequence. The lower 22 feet of the unit is a medium gray, clayey, very fine to fine sand; the sand is glauconitic (up to 35 percent) with dark-green polylobate grains dominant. The lower sand of the Mount Laurel is calcareous with weakly cemented zones (calcite) and local concentrations of large pelecypods. Burrowing is common.

The upper 56 feet of the Mount Laurel Formation is a light-olive-gray, medium to fine, silty sand with the coarser beds in the upper 20 feet of the unit. The sand grains commonly have clayey coatings. The upper beds of the Mount Laurel are less glauconitic (15 percent) than the lower beds. The glauconites are predominantly dark-green polylobate types, but unlike the underlying sands, show appreciable brownish, iron-staining. Earthy grains and polished brown pellets (perhaps goethite) are a noticeable accessory. The sand is dominantly quartzose with grains commonly iron-stained. The upper sands of the Mount Laurel Formation are calcareous with irregular calcite-cemented zones and sparse shell fragments. HEGAT minerals (46 percent) characterize the heavy mineral suite at 242 feet. Bioturbation and clay-lined burrows are evident.

Biostratigraphic information from the core suggests that the Mount Laurel Formation is Maestrichtian. The cephalopod *Belemnitella americana* (small, juvenile form) was logged at 271 ft. It is an index fossil for the Mount Laurel Formation (Owens, Minard, Sohl, and Mello, 1970). Gohn (Appendix B *in* Hansen, 1992) reported that two stratigraphically important ostracode species occur in a Mount Laurel sample from 285 ft. He points out that the joint occurrence of *Planileberis*? *costatana* and *Escharacytheridea pinochii* is suggestive of the early Maestrichtian. Olsson (Appendix D *in* Hansen, 1992) reported foraminifera from 239 ft that included *Globotruncana arca*, *G. tricarinata*, *Rugoglobigerina milamensis*, and a benthonic assemblage more typically Maestrichtian than Campanian.

The Mount Laurel Formation occurs throughout the subsurface of Kent County, but is apparently absent (figure 1) at Annapolis (AA-De 100) where strata assigned to the Severn Formation overlie the Matawan Group (undivided) (Minard, 1980). In Kent County the Mount Laurel Formation ranges in thickness from about 25 ft to 80 ft. Minard (1974) mapped what now appears to be an anomalously thick (up to 130 ft) section of Mount Laurel Formation in the Betterton quadrangle.

UPPER CRETACEOUS SEVERN FORMATION (204.2 FT - 217.9 FT)

In core hole Ken-Bf 180, about 14 feet of Maestrichtian strata overlie the Mount Laurel Formation. These beds are assigned to the Severn Formation of Minard, Sohl, and Owens (1977). It is a glauconitic, dark-gray, clayey, very fine to fine sand. The unit is massive, texturally mottled, and contains common shell fragments. The basal foot is in sharp contact with the underlying Mount Laurel Formation and consists of quartz granules, phosphate pebbles, and shell fragments. The prominent gamma-ray log peak near the base of the Severn Formation may reflect the occurrence of phosphate and/or the relatively high concentration of glauconite (65%) in the lower part of the formation. The glauconite grains are dark-green and relatively unaltered. Quartz grains are appreciably less iron-stained than found in the underlying Mount Laurel Formation.

A core sample from 214 feet yielded Maestrichtian foraminiferal and palynomorph species. Olsson reported the presence of *Guembelitria cretacea* in a middle shelf (paleodepth, >100 meters) foraminiferal assemblage (Appendix D *in* Hansen, 1992). Brenner (Appendix C *in* Hansen, 1992) found dinoflagellates assigned by Benson (1976) to the Severn Formation and pollen species that Waanders (1974) reported from the Monmouth Group. Gohn found ostracode species at 210 feet, which range from late Campanian to Maestrichtian (Appendix B *in* Hansen, 1992). The Cretaceous (Severn Formation)/Tertiary (Hornerstown Formation) boundary occurs at 204.2 feet; it is a sharp contact with 0.5 inch of relief.

Because the Severn Formation is relatively thin and not easily distinguished using cutting descriptions and geophysical logs, its distribution in Kent County is problematic. The strong gamma-ray log spike characteristic of the Severn at core-hole site Ken-Bf 180 is often subdued or absent elsewhere. This gamma-ray spike, which appears to be facies dependent, is useful for local correlations, but does not have regional synchroneity. In Kent County both the Severn Formation and the underlying Mount Laurel Formation appear to be present, but subdivision of the Monmouth Group is tentative without biostratigraphic data. According to Minard (1980), the Monmouth Group in the Annapolis area consists solely of the Severn Formation (figure 1).

LOWER PALEOCENE HORNERSTOWN FORMATION (109.1 FT - 204.2 FT)

The Hornerstown Formation is a massive, fine to medium, locally coarse, glauconitic sand. It is usually olive brown (upper part) to grayish olive (lower part) and has a "salt and pepper" aspect. The sands of the Hornerstown Formation are better sorted and less clayey than the underlying Mount Laurel Formation. Generally speaking, the Hornerstown is a regressive sand that coarsens upwards. Glauconite grains are generally polylobate, dark green, and show only minor alteration to limonite. Glauconite percentages in the Hornerstown Formation decrease upward from 30-40 percent in the lower part to 15-25 percent in the upper part. Glauconite grains sampled from both above (104 ft) and below (116.5 ft) the Aquia-Hornerstown contact (109.1 ft) are light green in contrast to the dark green and blackish grains generally observed elsewhere in the core. Iron-stained quartz grains are common throughout the Hornerstown Formation with the more intense staining characteristic of the coarser-grained sands. The Hornerstown is locally semi-indurated and incipiently cemented, chiefly by siderite which forms a matrix of very fine crystals in places. Non-opaque heavy mineral separates from 178 feet and 125 feet are dominated by labile HEGAT minerals, chiefly garnet (27 percent) (April *in* Appendix F, Hansen, 1992).

A gamma-ray deflection occurs near the base of the Hornerstown Formation reflecting higher glauconite content and, perhaps, minor occurrences of phosphate. The K/T boundary occurs between this spike and the larger gamma-ray peak that characterizes the Severn Formation. Another gamma-ray log deflection occurs in the upper part of the Hornerstown Formation near the Aquia contact and is associated with a glauconite-rich, clayey sand. These gamma-ray log signatures are useful for local correlation (figure 1).

The Hornerstown Formation in Ken-Bf 180 is considered largely, if not entirely, early Paleocene (Danian) in age, although only one sample (155.5 ft) has been biostratigraphically assigned. Olsson (Appendix D *in* Hansen, 1992) reported finding several diagnostic foraminiferal species (*Eoglobigerina* sp., *Guembelitria cretacea*, and *Pararotalia perclara*) indicative of the early Paleocene, which he tentatively placed in Zone P1a (Berggren and Miller, 1988). The age of the Hornerstown is bracketed by the last occurrence of Cretaceous (Maestrichtian) ostracodes at 204.2 ft and the first occurrence of *Oleneothyris harlani* (brachiopod) at about 109 feet. *O. harlani* is a widely dispersed index fossil that occurs near the base of the upper Paleocene (Thanetian) Aquia Formation in Kent County (Hansen, 1977). Also a basal late Paleocene foraminiferal assemblage (Zone P3) that included the nominate taxon *Morozovella angulata* was reported from 110.5 ft by Olsson (Appendix D *in* Hansen, 1992). Gibson (per. comm., 1989) assigns the lower Paleocene Brightseat Formation occurring west of the Chesapeake

Bay to foraminiferal Zone P1c. The presence of coeval beds in Ken-Bf 180 is unconfirmed biostratigraphically. If present, these strata must occur between 110 ft and 153 ft, which correlates with the upper part of the Hornerstown Formation. The Brightseat facies, which represents a transgressive marine oscillation separating two regressive sand sequences, could be represented by the gamma-ray log deflection near the top of the Hornerstown (fig. 1).

The Hornerstown Formation is widely distributed in central and eastern Kent County and can be correlated using geophysical logs southward to Kent Island (in adjacent Queen Anne's County) where Zone P1b foraminiferal assemblages have been observed (Olsson *in* Table 10b, Drummond, 1988). A thin, early Paleocene (Zone P1c) section, traditionally assigned to the Brightseat Formation, occurs in the Annapolis area. The early Paleocene (Zones P1a, P1b) Hornerstown Formation of Kent County is missing, although the Brightseat Formation could conceivably be a facies of its uppermost beds (figure 1).

In easternmost Kent County the Hornerstown Formation is thinner and more clayey than elsewhere in the county. This downdip facies change has also been observed in a core-hole (QA-Bg 54) near Unicorn, Md. (Hansen, 1977) and at Dover, Delaware (Benson, Jordan, and Spoljaric, 1985).

UPPER PALEOCENE AQUIA FORMATION (23.5 FT - 109.1 FT)

The Aquia Formation is a regressive (shoaling) sand unit that coarsens upward. In the basal 23 ft of the formation the clayey, medium to fine-grained sands are calcareous; the glauconite (15 to 60 percent) is relatively fresh, but the quartz grains are commonly iron-stained giving the olive-brown to grayish-olive sand a "salt and pepper" aspect. The glauconite grains in general are more ovoid-shaped and lighter green in the lower Aquia beds than observed in the units above or below. Mollusk and brachiopod fragments are commonly observed in the lower beds of the Aquia, particularly below 99 feet. A sharp, flat contact with the underlying Hornerstown Formation is reported at 109.1 ft.

The upper 63 ft of the Aquia Formation in Ken-Bf 180 is coarser grained (coarse to medium), less clayey, and better sorted than the lower part of the formation. The upper part is weathered, particularly the top 20 feet. The quartz grains are intensely iron-stained and often have clayey cutans suggestive of a weathering profile. The glauconites are partially altered to limonite. Brownish earthy grains and polished pellets are also present. The sands have a brownish to yellow-brown, "salt and pepper" aspect. The weathered nature of the Aquia Formation is reflected in non-opaque heavy mineral assemblages from 26 feet and 86 feet (Soller and Owens, 1991). The labile HEGAT minerals decrease to 15 percent and 31 percent respectively, chiefly due to the absence of garnet. The more resistive SSK suite is comparably more dominant, chiefly due to higher percentages of staurolite (April *in* Appendix F, Hansen, 1992).

The upper Aquia is noncalcareous and lacks fossils or shell fragments. Sparse reddish siderite(?) nodules and cemented layers were observed, most commonly below 69 feet. A sharp, flat contact with overlying middle to upper Oligocene beds was observed at 23.5 feet. The presence of shallow Oligocene beds with relatively fresh glauconites, fine pyrite clusters, and only minor iron-staining raises a question concerning the age of the Aquia weathering profile. A large contrast in weathering intensity across the contact suggests that it is largely pre-Oligocene (Hansen, 1974).

Much of the Aquia Formation is leached of fossil material. In Ken-Bf 180 late Paleocene (Thanetian) foraminifera (Zone P3) and the brachiopod *Oleneothyris harlani* were observed in the calcareous sediments near the base of the formation. Similarly, Thanetian forams were reported by Olsson (*in* Appendix B, Hansen, 1977) from the unweathered basal part of the Aquia Formation in a core-hole (QA-Bg 54) located in adjacent Queen Anne's County, Md.

(figure 1). The only megafossils Minard (1974) found in the Aquia in the Betterton quadrangle were also restricted to the basal few feet and consisted mostly of *O. harlani* and a pelecypod, *Gryphaea dissimilaris*. Thanetian microfossils have been reported from the Aquia Formation in the Annapolis area (Gilbert Brenner, per. comm., 1990).

The Aquia Formation occurs in the shallow subsurface of eastern Kent County where its subcrop is truncated by surficial sediments. In some previous studies (e.g., Hansen, 1972) the glauconitic sands now assigned to the lower Paleocene Hornerstown Formation were included in the Aquia, which broadened its apparent subcrop area (Clark, 1915). In its subcrop belt the highly weathered Aquia is overlain by pebbly Pensauken Formation of late Miocene(?) to early Pliocene(?) age. In Kent County, the Aquia Formation has experienced several episodes of erosion and weathering, as suggested by the different ages of the overlying units. Downdip, in eastern Kent County, the Aquia is apparently overlain by both Oligocene and lower Miocene beds (Hansen, 1977; 1992); in southwestern Kent County and adjacent Kent Island (Drummond, 1988), the Nanjemoy Formation (early Eocene) appears to overlie the Aquia Formation.

MIDDLE TO UPPER OLIGOCENE OLD CHURCH(?) FORMATION (18.5 FT TO 23.5 FT)

Overlying the Aquia Formation in core-hole Ken-Bf 180 is five feet of clayey, glauconitic (up to 25 percent), fine to medium, quartz sand. It is dusky brown to light gray and has a "salt and pepper" aspect. It is noncalcareous with no observed megafossils. It is moderately iron-stained, but the glauconites are relatively unweathered. The glauconite grains are generally ovoid-shaped and medium green. The morphology, color, and weathering characteristics of the glauconites are distinctively different from the Aquia Formation. The sands between 18.5 ft and 23.5 ft are relatively "unweathered" compared to the underlying Aquia Formation, which is intensively weathered and iron-stained. April (Appendix F *in* Hansen, 1992) reports that garnet (32 percent) is a prominent part of the non-opaque heavy minerals, although the SSK suite (chiefly staurolite) is slightly more abundant than the HEGAT minerals (45 percent and 38 percent respectively).

Olsson (Appendix D *in* Hansen, 1992) found a middle to late Oligocene foraminiferal assemblage in a core sample from 19 feet. Key species include *Guembelitria triseriata*, *Globorotalia minutissima*, and *Chiloguembelina ototara*. The glauconitic sand in core-hole Ken-Bf 180 between 18.5 ft and 23.5 ft is tentatively assigned to the Old Church(?) Formation, a name Ward (1985) has given to upper Oligocene beds elsewhere in Maryland. In Delaware, unnamed upper Oligocene beds have been reported from a well site located near Dover (Benson, Jordan, and Spoljaric, 1985).

UPPER MIOCENE(?) TO LOWER PLIOCENE(?) PENSAUKEN FORMATION (0 FT TO 18.5 FT)

Only two feet of core from the Pensauken Formation was recovered in Ken-Bf 180. Dark yellowish-orange, poorly sorted, sandy, silty, and clayey gravel was partially recovered in cores from 13 to 18.5 ft. Rounded quartz, feldspar, quartzite, and chert pebbles up to 2 inches were observed. A clay diffractogram of a sample cored at about 15 feet has strong peaks for kaolinite + halloysite(?), illite, and illite/smectite; labile, non-opaque heavy minerals (HEGAT suite) constitute 46 percent of the sample (April *in* Appendixes F and G, Hansen, 1992).

The name Pensauken Formation was assigned to surficial pebbly sands and gravels in Kent County by Owens and Denny (1979), who considered the deposits largely late Miocene in age. Earlier, Overbeck and Slaughter (1958) and Jordan (1964) had assigned equivalent strata to the Pleistocene(?) Wicomico Formation and Columbia Formation respectively. Paleochannels may occur at the base of the Pensauken Formation accounting for the local variability in the unit's thickness.

HYDROSTRATIGRAPHY OF CORE-HOLE KEN-BF 180

A hydrostratigraphic unit is "a mappable body of rock that is defined and identified on the basis of the nature, extent, and magnitude of its hydraulic conductivity and its boundary discontinuities" (Committee on Hydrostratigraphic Units, 1983). Because hydraulic continuity is a defining attribute, aquifers may consist of more than one geologic formation (Laney and Davidson, 1986). It would be preferable to have separate nomenclatures for aquifers and formations, but the old names are widely used and have legal status in Maryland's ground-water appropriation regulations. More than likely, dual nomenclatures will continue to exist. The stratigraphy of Ken-Bf 180 illustrates the need for hydrogeologists and stratigraphers to define their mapping units carefully so that misunderstandings can be minimized.

The Columbia aquifer consists chiefly of the surficial Pensauken Formation in Kent County (Bachman and Wilson, 1984). The Pensauken in core hole Ken-Bf 180 is thin (18.5 feet) with limited saturated thickness. A relatively thick, unconfined (water-table) aquifer occurs at the site, however, because the subcropping Aquia aquifer (Overbeck and Slaughter, 1958) is hydraulically connected with the Pensauken. The Aquia aquifer consists of the Old Church(?) Formation, the Aquia Formation, and the Hornerstown Formation. Although geologically distinct, the units of the Aquia aquifer are hydraulically connected across sand-on-sand contacts; discrete confining beds are lacking. In core-hole Ken Bf-180 the Aquia aquifer is underlain by a confining unit (between 198 and 218 feet) that includes basal beds of the Hornerstown Formation and the Severn Formation. This confining bed hydraulically separates the Aquia aquifer from the underlying Monmouth aquifer (Overbeck and Slaughter, 1958). In Kent County the Monmouth aquifer coincides with the Mount Laurel Formation. Recently (Vroblesky and Fleck, 1991) the name "Severn aquifer" has been substituted for Overbeck and Slaughter's Monmouth aquifer; however, inasmuch as the aquifer correlates with the Mount Laurel Formation (not the Severn Formation), the old nomenclature should probably be retained in Kent County.

In core-hole Ken-Bf 180 the Matawan Group (292 ft to 404 ft) forms a major confining unit. Although several clayey, very fine sands occur in the upper part of the Matawan Group, they lack the textural characteristics of an aquifer and are not a significant source of ground water.

The Magothy Formation (404 ft to 422 ft) in core-hole Ken-Bf 180 is represented by a clayey facies so that it functions hydrologically as part of the Matawan confining bed. Elsewhere in Kent County, in areas where it occurs as a sandy facies, the Magothy Formation functions as an aquifer. The base of the Magothy Formation is a major unconformity. Because sand beds also occur in the underlying Raritan(?) and upper Patapsco Formations, there is a complex stratigraphy across the unconformity. In some places a sandy facies of the Magothy Formation directly overlies an older sand forming a composite aquifer. In Kent County the term Magothy aquifer has been misleadingly applied to both the sandy facies of the Magothy Formation and the composite aquifer created where the

Magothy and underlying Raritan(?) or upper Patapsco are in sand-on-sand contact or separated by a leaky confining bed. In recognition of its composite nature it should more properly be referred to as the Magothy-Raritan(?)-Upper Patapsco aquifer system. In Ken-Bf 180 the Raritan(?) sands logged between 434 ft and 478 feet are assigned to this aquifer system (figure 1).

CONCLUSIONS

In Maryland aquifers were historically correlated with lithostratigraphic units (formations and groups). These include the Paleocene Aquia aquifer and the Upper Cretaceous Monmouth aquifer, Magothy aquifer and Raritan (?) aquifer. Long-term usage has entrenched these names in the literature and given them legal status through the State's regulation of ground-water pumpage. Although both formations and aquifers are by definition mappable rock bodies, their boundary discontinuities (contacts) are different; the former is defined by lithic contrast and the latter by hydraulic discontinuity. A dual nomenclatural system can be misleading because it implies an exact correlation that often does not exist insofar as contacts of geologic importance may not be defining boundaries in a hydraulic sense (e.g., sand-on-sand contacts). Nomenclatures should be carefully compared to avoid ambiguity, particularly when the scale of investigation covers several counties.

Stratigraphic data from core-hole Ken-Bf 180 provided an opportunity to compare the nomenclatural schemes identifying aquifers and formations in Kent County, Md., and to correlate them with similarly named units in the Annapolis, Md. area (AA-De 100) (figure 1).

1.In Ken-Bf 180 the Aquia aquifer consists of the middle to upper Oligocene Old Church(?) Formation, the upper Paleocene Aquia Formation, and the lower Paleocene Hornerstown Formation. In core-hole AA-De 100 at Annapolis the Aquia aquifer consists solely of the Aquia Formation. It is underlain by the lower Paleocene Brightseat Formation, a leaky confining bed. Correlation of the Hornerstown and Brightseat Formations is uncertain, although the units may be coeval facies in part.

2.The Monmouth aquifer in Ken-Bf 180 correlates with the Upper Cretaceous (Maestrichtian) Mount Laurel Formation. It is overlain by younger Maestrichtian confining beds assigned to the Severn Formation. In the Annapolis area (AA-De 100), however, the Monmouth aquifer correlates with a sandy facies of the Severn Formation. West of Chesapeake Bay the Mount Laurel Formation is missing from the stratigraphic section.

3.In Kent County, Md. the relatively thin Magothy Formation includes clayey facies that lack aquifer characteristics. Consequently, the "Magothy" aquifer in places may actually consist of subcropping Raritan(?) or upper Patapsco sands. It is nomenclaturally more accurate to refer to this complex hydrogeologic unit as the Magothy-Raritan(?)-upper Patapsco aquifer system. On the other hand, in the Annapolis area the Magothy Formation is relatively thick and dominantly sandy. Here the Magothy aquifer is largely equivalent to the Magothy Formation, although it too may include subcropping sands of the upper Patapsco Formation in places.

REFERENCES CITED

Bachman, L. J., and Wilson, J. M., 1984, The Columbia aquifer of the Eastern Shore of Maryland: Maryland Geological Survey Report of Investigations 40, 144 p.

Benson, D. G., 1976, Dinoflagellate taxonomy and biostratigraphy at the Cretaceous-Tertiary boundary, Round Bay, Maryland: Tulane Studies in Paleontology, v. 12, n. 4, p. 169-233.

Benson, R. N., Jordan, R. R., and Spoljaric, N., 1985, Geological studies of Cretaceous and Tertiary section, test well Je 32-04, central Delaware: Delaware Geological Survey Bulletin n. 17, 69 p.

Berggren, W. A., and Miller, K. G., 1988, Paleogene tropical planktonic foraminiferal biostratigraphy and magnetobiochronology: Micropaleontology, v. 34, n. 4, p. 362-380.

Christopher, R. A., 1979, Normapolles and triporate pollen assemblages from the Raritan and Magothy Formations (Upper Cretaceous) of New Jersey: Palynology, v. 3, p. 73-121.

Clark, W. B., 1915, Map of Kent County showing the geological formations: Maryland Geological Survey, scale 1:62,500.

Committee on Hydrostratigraphic Units, 1983, Committee activities *in* The Hydrogeologist — Newsletter of the Hydrogeologic Division of the Geological Society of America, July 1983, p. 3.

Doyle, J. A., and Robbins, E. I., 1977, Angiosperm pollen zonation of the continental Cretaceous of the Atlantic Coastal Plain and its application to deep wells in the Salisbury embayment: Palynology, v. I, p. 43-78.

Drummond, D. D., 1988, Hydrogeology, brackish-water occurrence, and simulation of flow and brackish-water movement in the Aquia aquifer in the Kent Island area, Maryland: Maryland Geological Survey Report of Investigations 51, 131 p.

Edwards, J., and Hansen, H. J., 1979, New data bearing on the structural significance of the upper Chesapeake Bay magnetic anomaly: Maryland Geological Survey Report of Investigations 30, 44 p.

Hansen, H. J., 1972, A user's guide for the artesian aquifers of the Maryland Coastal Plain: Part II: Aquifer characteristics: Maryland Geological Survey Open File Report 72-02-1, 123 p.

Hansen, H. J., 1974, Sedimentary facies of the Aquia Formation in the subsurface of the Maryland Coastal Plain: Maryland Geological Survey Report of Investigations 21, 47 p.

Hansen, H. J., 1977, Geologic and hydrologic data for two core holes drilled through the Aquia Formation . . . in Prince George's and Queen Anne's Counties, Maryland: Maryland Geological Survey Open-File Report 77-02-1, 77 p.

Hansen, H. J., 1992, Stratigraphy of Upper Cretaceous and Tertiary sediments in a core-hole drilled near Chesterville, Kent County, Maryland: Maryland Geological Survey Open-File Report 93-02-7, 38 p.

Houlik, C. W, Olsson, R. K., and Aurisano, R. W., 1983, Upper Cretaceous (Campanian-Maestrichtian) marine strata in the subsurface of northern Delaware: Southeastern Geology, v. 24, n. 2, p. 57-65.

Jordan, R. R., 1964, Columbia (Pleistocene) sediments of Delaware: Delaware Geological Survey Bulletin 12, 59 p.

Laney, R. L., and Davidson, C. B., 1986, Aquifer-nomenclature guidelines: U.S. Geological Survey Open-File Report 86-534, 46 p.

Mack, F. K., 1974, An evaluation of the Magothy aquifer in the Annapolis area, Maryland: Maryland Geological Survey Report of Investigations 22, 75 p.

Miller, B. L., 1926, The geology of Kent County in Kent County: Maryland Geological Survey, p. 57-95.

Minard, J. P., 1974, Geology of the Betterton quadrangle, Kent County, Maryland, and a discussion of the regional stratigraphy: U.S. Geological Survey Professional Paper 816, 27 p.

Minard, J. P., 1980, Geology of the Round Bay quadrangle, Anne Arundel County, Maryland: U.S. Geological Survey Professional Paper 1109, 30 p.

Minard, J. P., Sohl, N. F., and Owens, J. P., 1977, Re-introduction of the Severn Formation (Upper Cretaceous) to replace the Monmouth Formation in Maryland, *in* Sohl, N. F., and Wright, W. B., editors, Changes in stratigraphic nomenclature by the U.S. Geological Survey, 1976: U.S. Geological Survey Bulletin 1435-A, p. 132-133.

Overbeck, R.. M., and Slaughter, T. H., 1958, The water resources of Cecil, Kent and Queen Annes Counties: Maryland Department of Geology, Mines and Water Resources Bulletin 21, 478 p.

Owens, J. P., Minard, J. P., Sohl, N. F., and Mello, J. E., 1970, Stratigraphy of the outcropping post-Magothy Upper Cretaceous formations in southern New Jersey and northern Delmarva Peninsula, Delaware and Maryland: U.S. Geological Survey Professional Paper 674, 60 p.

Owens, J. P., and Denny, C. S., 1979, Upper Cenozoic deposits of the central Delmarva Peninsula Maryland and Delaware: U.S. Geological Survey Professional Paper 1067-A, A28 p.

Owens, J. P., and Gohn, G. S., 1985, Depositional history of the Cretaceous Series in the U.S. Atlantic coastal plain — stratigraphy, paleo-environments, and tectonic controls of sedimentation *in* Poag, C. W., editor, Geologic evolution of the United States Atlantic margin: New York, Van Nostrand Reinhold, p. 25-86.

Soller, D. R., and Owens, J. P., 1991, The use of mineralogic techniques as relative age indicators for weathering profiles on the Atlantic Coastal Plain, USA, *in* M. J. Pavich, editor, Weathering and soils: Geoderma, v. 51, n. 1-4, p. 111-131.

Spoljaric, N., 1972, Upper Cretaceous marine transgression in northern Delaware: Southeastern Geology, v. 14, n. 1, p. 25-37.

Vroblesky, D., and Fleck, W. B., 1991, Hydrogeologic framework of the Coastal Plain of Maryland, Delaware, and the District of Columbia: U.S. Geological Survey Professional Paper 1404-E, E45 p.

Waanders, G. L., 1974, Palynology of the Monmouth Group: (Maastrichtian) from Monmouth Co., New Jersey, U.S.A.:Ph.D. thesis, Department of Botany, Michigan State University.

Ward, L., 1985, Stratigraphy and characteristic mollusks of the Pamunkey Group (lower Tertiary) and Old Church Formation of the Chesapeake Group — Virginia coastal plain: U.S. Geological Survey Professional Paper 1346, 78 p.

Wolfe, J. A., and Pakiser, H. M., 1971, Stratigraphic interpretations of some Cretaceous microfossil floras of the Middle Atlantic States: U.S. Geological Survey Professional Paper 750-B, p. B35-B47.

REGRESSIVE TO TRANSGRESSIVE QUATERNARY DEPOSITS IN A DELMARVA COASTAL LAGOON, HOG ISLAND BAY, VIRGINIA

OERTEL, George F.[1], WOO, Han J.[2], KEARNEY, Michael S.[3], and FOYLE, Anthony M.[1]

ABSTRACT

Shallow sediments in coastal barrier lagoons of the southern Delmarva Peninsula contain sandy mud sequences 3-8 meters thick. The sequences were originally believed to be the result of lagoonal fill during the late Holocene, however, it is now believed that the sequences were, in part, produced during regression, transgressive-reworking and transgression. Textural distinction alone is not possible because sandy muds and muddy sands of the regressive coastal deposits are textually similar to Holocene transgressive deposits.

During the late Wisconsinan regression, strand plain deposits (of the Wachapreague Formation) were deposited seaward of the Mappsburg shoreline. Sandy ridges contain several prominent basal gravel layers and are closely spaced immediately south of the "highstand" mouth of the ancestral Machipongo River near Fowling Point, Virginia. During regression, the swales between ridges were partially filled with mud containing modest amounts of the pollen of spruce (26%) and birch (2-6%). As the late Wisconsinan sea receded across the shelf, the Machipongo River mouth and regressive strand plain deposits migrated eastward over the Mappsburg shoreface.

During the late Wisconsinan and early Holocene, the strand plain ridges and swales were subaerially exposed and stood high above sea level. During the middle to late Holocene, the ancestral Machipongo valley was inundated by rising sea level forming an estuary with muddy fringe marshes along its margins. The topographically higher and adjacent portions of the relict strand plain became a brackish swamp, where the pollen of hickory, pondweed, cat-tail and other grasses accumulated with organic muds. As rising water in the estuary spilled over the banks of the Machipongo River, it formed a marsh lagoon above the relict stand plain surface, and between the mainland and the outer barriers. The formation of the lagoon appears to be relatively recent, because sediments rich in ragweed pollen (4-9%) were found immediately above Wachapreague sands or muds containing modest amounts of spruce and birch.

INTRODUCTION

The southern Delmarva Peninsula is a series of highstand coastal spits formed during the Pleistocene (Fig. 1). During the last highstand (oxygen-isotope stage 5e), a shoreface scarp (the Mappsburg Scarp) was left along the seaward margin of the Accomack and Nassawadox spits, that formed the axis of the peninsula (Mixon, 1985). Following the highstand, regressive deposits (Wachapreague Formation, Mixon, 1985) were left seaward of the spits, as the sea receded across the shelf. The present Holocene highstand has submerged much of the Wachapreague Formation under the floor of the modern coastal barrier lagoon. Thus, the modern lagoon deposits are juxtaposed above the sandy muds and muddy sands of the Wachapreague Formation. Lithofacies distinction between the two similar facies are often tenuous. Mixon (1985) described a cool climate pollen flora associated with Wachapreague beds that would be clearly distinct from the pollen of the modern warm-climate flora. However, the problem of correlation of beds is still difficult because of the intense dissection of the landscape during lowstand exposure.

A variety of stratigraphic studies in the area has increased our knowledge of the sedimentary sequences below Virginia's coastal lagoons. Newman and Rusnak (1965) and Newman and Munsart (1968) made stratigraphic interpretations of portions of the middle Virginia barrier island/ lagoons based on lithofacies analysis of vibracores. They described muds between the barrier islands and the mainland which generally thickened in a seaward direction but appeared to thin beneath several barrier islands. Samples of peat between -2 and -6 meters yielded radiocarbon dates of 2,500 to 5,000 BP.

Shideler and others (1984) worked in the southern most portion of the barrier island/lagoon complex and described Holocene deposits generally between 5 to 10 m thick. They published 6 radiocarbon dates. Five dates were Holocene, ranging from 650 to 3,800 BP. The youngest date came from a sample at -7.7 m, and illustrates the existence of pronounced relief on the lagoon floor, and the high potential for the accumulation of organic-rich material in areas that are not associated with sea level. The four other Holocene dates ranged from 1,400 to 3,800 BP and were determined from samples retrieved between -0.4 and -1.5 m (msl-datum). A peaty sample from -3.8 m yielded a date which was too old for reliable age determination.

Finkelstein and Ferland (1987) illustrated a variety of Holocene facies below the lagoons which thickened in the seaward direction. Their diagrams indicated that the lagoonal fill facies often achieved thicknesses from 7 to >10 m below the modern barrier islands. Their radiocarbon dates were generally less than 3,500 years BP from samples less than 5m deep. Data in Finkelstein and Ferland (1987) table 2, illustrates significant variance from the expected relationship between depth and age.

Byrnes (1988) conducted a detailed study of a lagoon in the northern part of the Virginia barrier island/lagoon complex. Byrnes (1988) constructed 3 lithofacies sections across the Metompkin lagoon based on the analysis of 12 vibracores. His findings were similar to those of previous workers. The lagoonal sediments thickened in a seaward direction to depths greater than 8-9 meters beneath Metompkin Island.

Oertel and others (1989a) first challenged the concept of 7-10m thick Holocene lagoonal fills. Their study in the lagoon system behind Cobb Island was assisted by the analysis of pollen in the finegrained sediments. Pollen assemblages containing >5% spruce and > 1-2% fir led the authors to suggest much of the mud beneath the lagoon floor was pre-Holocene. Only the upper beds of cores from the outer part of the lagoon contained strictly warm climate Holocene pollen suites. Oertel and others (1992) suggested that the coastal lagoons were not basins slowly filling with sediment, but

[1]. Department of Oceanography, Old Dominion University, Norfolk, VA
[2]. Korea Ocean Research and Development Institute, Seoul, Korea
[3] Department of Geography, University of Maryland, College Park, MD

were depressions being inundated by rising sea level.

The purpose of this paper is to describe the relationship between the regressive Wachapreague deposits and transgressive Holocene deposits in the barrier lagoon behind Hog Island, Virginia. Hog Island Bay is an open-water section of the Virginian coastal barrier lagoon complex (Fig. 1). This section of the lagoon is about 10 km wide and has an open-water area about 6.5 km wide. The lateral margins of Hog Island Bay are delineated by a band of marsh islands that extend from the mainland to Hog Island. The Hog Island Bay lagoon is connected to the Atlantic Ocean through the tide-dominated Machipongo Inlet. The narrow inlet throat (0.5 km) has a deep gorge (with a scour pit approximately 30m deep) and a relatively large ebb delta which extends 5 km onto the continental shelf.

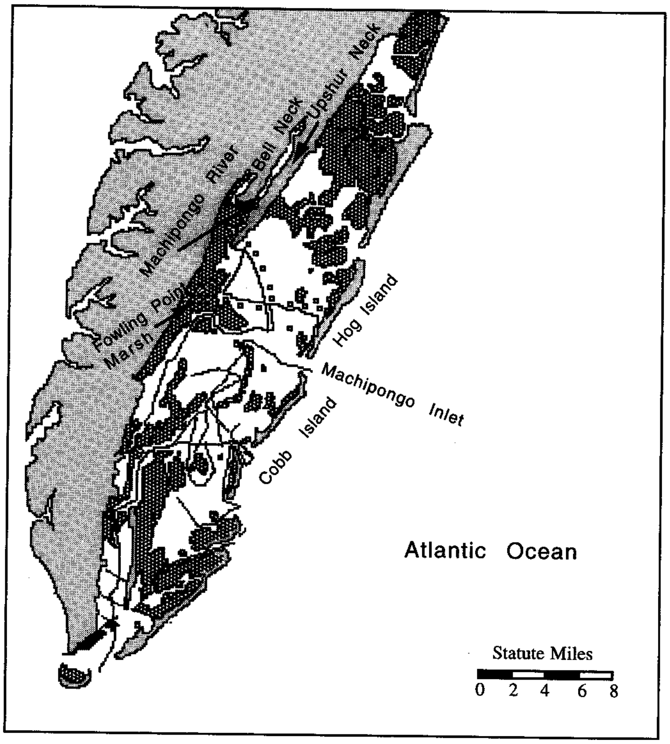

Figure 1. Location map of the study area showing vibracore sample stations and seismic cruise track.

METHODS

Twenty vibracores and 30km of shallow seismic reflection data were used to determine the boundary between Holocene and Pleistocene units in the Hog Island Bay lagoon. Cores were taken in hammocks on the west side of the lagoon, in the lagoon, and in the backbarrier of Hog Island. Each core was split, photographed, logged, and subsampled for textural analysis, microfossil analysis, and dating. Selected sections of the core were X-ray radiographed for microstructural analyses.

Textural analyses were conducted following standard techniques, and facies descriptions were based on percentage of sand, silt, and clay following Folk (1980). The distribution of biogenic and physical sedimentary structures was determined from visual analysis of cores and X-ray radiographs. Pollen analyses were conducted following the standard KOH-acetylation procedure (Faegri and Iversen, 1975). Concentration of palynomorphs was achieved using the Napyrophosphate procedure of Bates and others (1978). Assemblages were based on a minimum of 200 grains/ sample. Six pre-defined groups of potential biofacies were established from the expected mixing of sediments from three ecological groups (1. warm-climate floral, 2. fresh aquatic flora, and 3. cold climate flora). Canonical variate analysis was used to discriminate assemblages of 23 different pollen, and classify 41 samples from the coastal lagoon into the 6 a priori groups. Radiocarbon dates of organic material were determined by Beat Analytic Inc., Miami, Florida.

High resolution seismic reflection was conducted using a Geopulse® boomer system run at 175 J, fired at 0.25s, and band-pass filtered between 750 and 2000 Hz. Loran C was used for navigation and open-water areas. Landscape and navigation marker reference was used for location in the marsh and tidal channels, respectively. Adjacent to the mainland, reflectors were correlated with the surface of the Wachapreague Formation and the surface of the Mappsburg Scarp. Under the lagoon, reflectors were correlated with known facies horizons in core logs.

REGRESSIVE LANDSCAPE

Along the landward margin of the lagoon behind Hog Island, the Wachapreague Formation has the topographic expression of a typical strand plain. Just south of where the Machipongo River enters into the lagoon, the Wachapreague Formation appears as sets of hammocks that are parallel to subparallel with the Mappsburg Scarp (a paleo-shoreface). The hammocks are relict strand plain ridges with crests that decrease in elevation under the lagoon.

North of the Machipongo River mouth, the Wachpreague Formation occurs as two prominent ridges (Upshur Neck and Bell Neck) between the Mappsburg Scarp and the lagoon. The axis of the Bell Neck ridge ranges from 1.5 to 2 km east of the Mappsburg Scarp. The Upshur Neck ridge is located seaward of the Bell Neck spit, approximately 4 km east of the Mappsburg Scarp and is almost 20 km long. The two ridges are late Pleistocene spits that formed as the stage 5e sea receded, the two spits prograded from newly exposed headlands to the north.

South of the Machipongo River mouth, the ridges are smaller, more closely spaced and extend a greater distance from the Mappsburg Scarp. There are at least 12 ridges discernible between the Mappsburg Scarp and the edge of the lagoon. Most of the ridges are about 0.5 km apart, although some are about 0.25 km apart. The crests of the ridges are highest in elevation closest to the Mappsburg Scarp and get progressively lower toward the margin of the lagoon. Drainage and tidal exchange between the ridges is in a trellised pattern with a pronounced shore-parallel orientation of low-order streams. This series of ridges is believed to be a deltaic strand plain complex associated with the Machipongo River. Many of the tidal streams along the outer part of the strand plain have been totally submerged by the recent sea-level rise or partially filled by marsh sedimentation.

Much of the relict drainage of the late Pleistocene Machipongo watershed is still present on floor of the Hog Island Bay lagoon. The main thalweg of the channel forms a relatively deep scar on the lagoon floor between the mouth of the river and the tidal re-entrant with the sea. The tributaries of the Machipongo River are dendritic, and partially delineate the area of the Machipongo watershed submerged on the lagoon floor.

FACIES ANALYSIS

Vibracores were primarily obtained from the submerged interfluve areas between the tributaries of the Machipongo River. Two cores were obtained from the margins of buried tributaries on the margins of the Machipongo River. Cores from the interfluve areas had distinct lithofacies patterns. Core logs from the shallow tidal flats illustrated relatively coarse upper sections which fined downward and then coarsened to a sandy basal unit (Fig. 2). The changes in mean grain size primarily reflected the variations in the percentage of sand. The basal sands were generally encountered at depths ranging from -4.8 m to the surface of the lagoon floor. The average depth of the basal sand unit was about 2.5 m below mean low water. The average depth of the nodal point of fines between the upper and lower sandy units was -1.7 m (mlw-datum). In a core (FM9) located 2.5 km east of Fowling Point Marsh, the lower sand unit was encountered at -4.65 m (mlwdatum). An organic-rich layer about -4.2 m was dated at 3,870 ± 150 BP, and suggests a 0.9 mm/yr sedimentation rate for the 3.5 m of sediment that accumulated over that horizon. This is consistent with the Pb-210 sedimentation rates determined by Oertel and others (1989b) for a fringe marsh in another part of the coastal lagoon complex. Assuming that the organic material was a high-marsh peat formed during initial inundation of the area, then the rate of sea-level rise to the modern high peats has been about 1.5 mm/yr. While this is about half the rate of sea-level rise predicted by Braatz and Aubrey (1989), it is 60% higher than the 0.9 mm/yr sedimentation rate. Thus, during the late Holocene, the rate of sedimentation was not able to keep ahead of sea-level rise, and marshes and tidal flats were slowly submerged forming shallow bays.

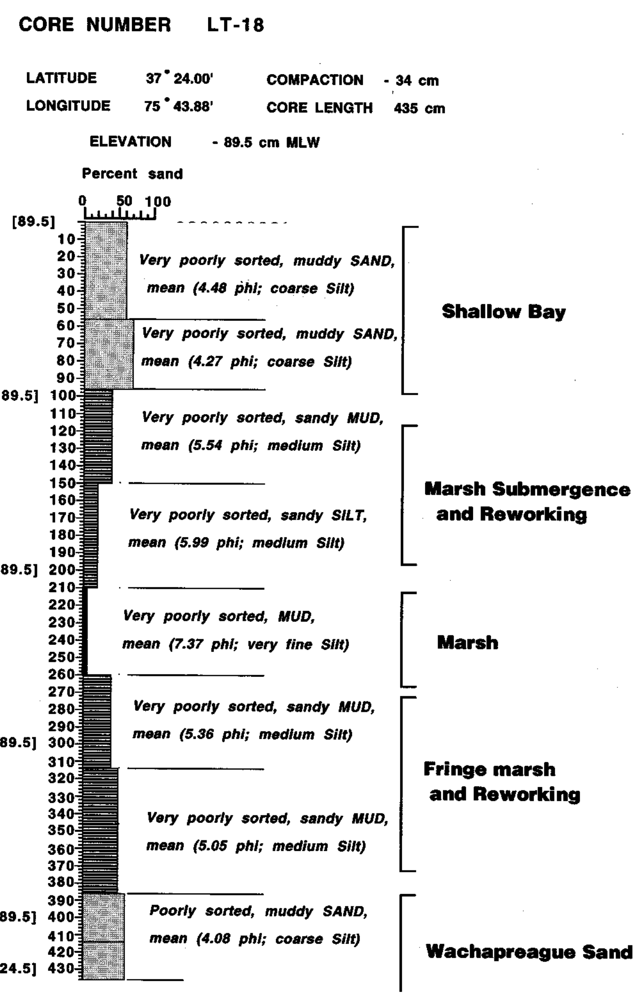

Figure 2. Vibracore log illustrating the fining up, and fining down textural cycle caused by increasing lagoonal water depth.

The transition from the regressive muddy sands of the Wachapreague Formation to the modern bay sands is recorded in the fine sediments separating the two units. The local floral and climatic history of the area is reflected in the pollen that accumulated with these fine sediments. Mixon (1985) found that up to 22 percent of the arboreal pollen in the upper units of the Wachapreague Formation was spruce. The pine grains were generally small, and the oak and hickory were sparse. Several samples from our vibracores also had significant amounts of spruce (6%) and birch (6%), as well as modest amounts of hemlock.

Warm climate pollen contained pollen of gum and ragweed. The late Holocene marsh facies (cores HI-17, HI-21, and LT-20) on the seaward side of the Hog Island Bay lagoon contained totally warm climate pollen suites. The warm pollen facies in core HI-17 was at about +1m (mlw-datum) which is approximately equal to -0.5 mhw-datum. A peaty horizon at about mlw in this core was dated at 1,320 ± BP. Thus, warm pollen suite represents, at least, the past 1,000-2,000 years of mud and pollen sedimentation. The only warm-pollen suite that was not associated with a marsh was on the landward side of the lagoon. The upper part (< 20cm) of core GM-1 (located 0.75km from the landward side of the lagoon) had pollen of flora which were only present during warm climatic conditions.

Initially, it was thought that 3 a priori groups of pollen assemblages should be present in the fine-grained sediment sequences; (1) the cool climate Wachapreague pollen, (2) the modern warm climate pollen, and (3) a transition zone where the cool and warm climate pollen were mixed. However, pollen identification indicated that pollen associated with fresh marshes, ponds and streams were also prevalent in many samples. While the third group is not strongly climate dependent, it does suggest a very water-laden landscape. The addition of the third "floral landscape" state suggested that a complete sedimentary sequence could involve 6 pollen groups between the Wachapreague and the present; (1) the cool climate Wachapreague pollen, (2) a transition zone where the cool and aquatic pollen were mixed (3) the aquatic pollen, (4) a transition zone where aquatic pollen and warm climate pollen were mixed, and (5) the modern, warm-climate pollen. A 6th floral facies could result from erosional removal of intermediate facies and direct mixing of a cool and warm climate pollen.

Forty-one samples were analyzed for pollen in 20 cores taken in the Hog Island Bay lagoon. Twenty-three pollen types were tested with the 6-group scenario using a canonical variate analysis. All of the samples (n=41) were classified into the 6 a priori groups based on the absence or presence of the 23 different pollen types. Approximately 5.5% of the samples indicated a totally warm-climate facies, 22% of the samples indicated a totally aquatic-pollen facies, and 11% of the samples indicated a totally cool climate facies. A mixing of aquatic and warm-climate facies was indicated in 5% of the samples, whereas a mixing of aquatic and cool climate pollen facies was indicated in 43% of the samples, and 13.5% of the samples indicated a warm-cool pollen mixture. No core illustrated a complete sequence with all of the end member pollen groups and all of the mixed pollen groups. Cool/warm mixtures generally occurred at thin (< 3m) muddy units near antecedent highs in topography. Pollen associated with aquatics were present in thicker muddy units, and occurred at elevations between -3 and -6m (mlw-datum).

SEISMIC ANALYSIS

Shallow seismic reflection was used to determine the thickness and character of the Holocene and Wachapreague sediments in the Hog Island Bay lagoon. Transects running across the tidal flat east of the Fowling Point marsh were particularly useful. The top of the Wachapreague Formation is near sea level along the western side of the lagoon near Fowling Point, and served as a reference point from which the top of the Wachapreague was assumed to dip under the lagoon. Adjacent to Fowling Point, a shore-normal seismic section illustrated an undulating surface which decreased in elevation from about mlw to -7.4 m (mlw-datum) near the outer edge of the tidal flat. Vibracores FM-8, FM-9, and FM-10 all encountered a sandy layer between 0 and -7.9 m (mlw-datum) which corresponded to this surface. Although the regional slope of the reflector is considerably less than 1 degree, the surface has three highs indicative of buried ridges. The buried ridges are about 0.5km apart and have a relief of 2-2.5 m. Inclined reflectors below the ridge crest dip in a landward direction. The thickness of the lagoonal sediments above the reflector varies from less than 1 m to about 4.5 m.

Another relatively continuous reflector below the "Wachapreague reflector" is relatively flat, and slopes from about -8 m adjacent to Fowling Point to about -12 m at a point 1.7 km east of Fowling Point. This reflector is believed to be the ravinement of the highstand Mappsburg shoreline, which marks the base of the Wachapreague Formation. Reflectors within the Wachapreague Formation were landward dipping.

PALEO-ENVIRONMENTS

Following the stage 5e highstand, regressive deposits accumulated seaward of the Mappsburg shoreline. The lowering of sea level rejuvenated headlands 20 km north of the modern Machipongo River causing a spit (Bell Neck Ridge) to engulf a portion of the Mappsburg shoreface and about 5 small watersheds forming the ancestral Parting Creek drainage basin. En echelon development of a larger and more seaward spit (Upshur Neck Ridge) captured the Parting Creek system and added three more watersheds to the composite drainage basin that formed the primordial Machipongo River. The Machipongo River had a strong influence on the subsequent deposition of fluviodeltaic sediments during continued regression. Immediately south of the river entrance a deltaic strand plain produced a downdrift offset in the position of the shoreline. The strand plain is discernible about 7-10 km south of the Machipongo/Upshur Neck river entrance from relict landscape features. Its seaward development has been recognized in vibracores and high resolution seismic profile records, and extends across 75% of the modern lagoon. Thus, during the early stages of regression, the landscape was strongly influenced by accretional features. Spits and spit platforms spread sandy deposits over the Mappsburg shoreface north of the Machipongo entrance, while strand plain deposits were regressing seaward, and south of the Machipongo River entrance.

During the stage 4-2 regression, erosional incision and subaerial evolution of the Machipongo River drainage basin were more important processes sculpturing the landscape than the accretional features of the early regression. During the stage 2 lowstand, this area became the head of the Machipongo valley which was elevated far above base level, and tributaries in the watershed cut through portions of the thinner and less resistant strand plain sediments. Downward scour along the thalweg for thousands of years produced a deep scar in the landscape with local relief greater than 15 m.

When the Holocene transgression reached the Hog Island Bay area, the valley floor of the Machipongo River was the first surface to be inundated. Initial inundation took place about 7,000 BP when sea level was about 15m below present level, and the shoreline was approximately 15km east of the modern shoreline. The margins of the newly formed estuary had terrestrial landscapes about 9m above the estuary floor. Initially, the estuary probably had a narrow tidal stream bordered by broad wetlands. As sea level rose, the tidal stream deepened and the wetlands "climbed" up the gentle valley slopes. About 3,500 to 4,000 BP the estuarine waters began spilling over the edges of the valley onto the interfluve areas. South of the Machipongo River estuary, the interfluve surface was characterized by the ridge and swale topography of the regressive Wachapreague strand plain. As sea level approached this surface, it produced a "near base level" lowland that was shielded from marine exposure by a shoreline 4 km to the east. The suite of aquatic pollen in the sediments suggests that the surface was relatively wet, and probably contained closely spaced small streams, ponds, swamps, and wetlands. Thus, the aquatic pollen suite associated with plants in these environments was initially mixed with the "cool" climate pollen in the swales of the Wachapreague strand plain. When the rising sea caused the surface to fall between the upper part of the tidal zone and mean sea level, the strand plain surface was eventually colonized by tidal wetlands. The fine-grained marsh facies of the wetlands mixed with the both the basal sands of Wachapreague ridges and the thin regressive muds in the swales between the ridges. In general, the mixing produced a fining upward sequence as sea level rose, and accumulating muds were distanced vertically from the basal sands.

The presence of a broad salt marsh over the surface was apparently relatively short lived since the rate of sea-level rise was about 60% greater than the marsh sedimentation rate. Based on the relative rates of sea-level rise and sedimentation, it is estimated that much of the broad salt-marsh platform was submerged about 1,500-2,000 BP. The relatively modern open-water lagoonal environment has induced a physical reworking of the submerged fine-grained marsh facies. The reworking process winnowed fines for transport to fringe marshes leaving a progressively coarser lag of sand over the shallow lagoon floor.

ACKNOWLEDGMENTS

This project was partially supported from funding from the National Science Foundation (BSR8702333-06), and the Barrier Island Program at Old Dominion University. Mr. R.C. Kidd (Marine Technician, Department of Oceanography, Old Dominion University, Norfolk, Virginia, U.S.A.) provided technical assistance in field investigations and the operation of the seismic system.

REFERENCES CITED

Bates, C.D., Coxon, P. and Gibbard, P.L., 1978. A new method for preparation of clay-rich sediment samples for palynological investigation. New Phytologist v. 81; p. 459-463.

Braatz, B.V. and Aubrey, D.G. 1987. Recent relative sea-level change in eastern North America. In: Nummedal D., Pilkey, O. H., Howard, J. D. (editors), Sea level rise and coastal evolution. Society of Economic Paleontologists and Mineralolgists , Tulsa, OK, Special Publication n. 41; p. 29-48.

Byrnes, M.R. 1988. Holocene Geology and Migration of a low-profile barrier island system, Metompkin Island, Virginia. Ph D Thesis, Department of Oceanography, Old Dominion University, Norfolk, VA, 302 pp.

Faegri, K. and Iversen, J., 1975. Textbook of pollen analysis. Blackwell, Oxford, 295 pp.

Finkelstein, K. and Ferland, M.A. 1987. Back-barrier response to sea-level rise, eastern shore of Virginia. In: Nummedal D., Pilkey, O. H., Howard, J. D. (editors), Sea level rise and coastal evolution. Society of Economic Paleontologists and Mineralolgists, Tulsa, OK, Special Publication, n. 41; p. 145-155.

Folk, R.L., 1980. Petrology of sedimentary rocks, Hemphill, Austin, Texas, 184 pp.

Mixon, R.B. 1985. Stratigraphic and geomorphic framework of the uppermost Cenozoic deposits in the southern Delmarva Peninsula, Virginia and Maryland. United States Geological Survey, Reston, VA, Professional Paper 1067-G; 53 pp.

Newman, W.S. and Munsart, C. A. 1968. Holocene geology of the Wachapreague lagoon, eastern shore Peninsula. Marine Geology, v. 6; p. 81-105.

Newman, W.S. and Rusnak, G.N. 1965. Holocene submergence of the eastern shore of Virginia. Science, v. 148; p. 1464-1466.

Oertel, G.F., Kearney, M.S., Leatherman, S. P. and Woo, H.J. 1989a. Anatomy of a barrier island platform: outer barrier lagoon, southern Delmarva Peninsula, Virginia. Marine Geology, v. 88; p. 303-318.

Oertel, G.F., Wong, G.T.F. and Conway, J.D., 1989b. Sediment accumulation at a fringe marsh during transgression, Oyster, Virginia. Estuaries, v. 12; p. 18-26.

Oertel, G.F., Kraft, J.C., Kearney, M.S. and Woo, H.J., 1992. A Rational Theory for Barrier Lagoon Development. In: Fletcher, C.H. and Wehmiller, J.F. (editors), Quaternary Coasts of the United States: Marine and Lacustrine Systems. Society of Economic Paleontologists and Mineralolgists, Tulsa, OK, Special Publication, n. 48.; p. 77-87.

Shideler, G.L., Ludwick, J.C., Oertel, G.F., and Finkelstein, K., 1984. Quaternary stratigraphic evolution of the southern Delmarva Peninsula, coastal zone, Cape Charles, Virginia. Geological Society of America Bulletin, v. 95; p. 489-502

INNER CONTINENTAL SHELF AND NEARSHORE PROCESSES: A BRIEF STATUS REPORT

L.D. Wright
School of Marine Science
Virginia Institute of Marine Science
College of William and Mary
Gloucester Point, Virginia 23062

ABSTRACT

Anticipating and planning for the societal impacts of coastal change requires that we be able to model large scale, long-term changes in shoreline position, coastal configuration, and nearshore energy regime. This problem must be treated on the scale of the entire inner region of the continental shelf; it is not simply a beach problem. Popular models of inner shelf and nearshore equilibrium are generally too simplistic and take no account of the reality of inner shelf sediment transport phenomena of which wind-driven across-shelf flows are of first order importance. Other important flows include those related to asymmetric wave orbital velocities, infragravity oscillations, internal waves, and buoyant plumes (positive and negative). Inner shelf micromorphology is also among the fundamental determinants of across-shelf sediment transport: the presence or absence of ripples can determine whether sand moves shoreward or seaward.

THE SIGNIFICANCE OF THE INNER CONTINENTAL SHELF

Coastal responses to short-lived events such as storms are typically attributed to surf zone and runup processes that operate in the immediate vicinity of the shore. Probably the most obvious coastal changes involve redistributions of sediment on time scales of a year or less. Classical models describe these changes in terms of onshore - offshore exchanges of sand between the intertidal beach and the outer regions of the surf zone. However, the surf zone - beach realm is rarely a closed system even on annual time scales; it is not at all closed on time scales of decades or longer (Wright, 1987). If one is interested in predicting or explaining large-scale, long term coastal changes such as the shoreline transgressions and regressions of the late Quaternary or projected responses to potential future changes in climate or sea level, the problem assumes the dimensions of the entire continental shelf (Figure 1). The shelf is most often the sink, and in many cases the immediate source of coastal sediments; it also conditions the physical oceanographic processes that drive coastal behavior.

The inner shelf links the land margin to the mid and outer shelf and to the deep sea. Not only does it serve as a conduit for across-margin particulate transport but it also modulates the hydrodynamic forces that drive surf zone and estuarine processes (e.g. Nittrouer and Wright, in press; Wright, 1993). Sediment transport processes on the inner shelf are more intense than over the mid and outer shelf, in part, because the shallow depths place the bed within the reach of even fairweather waves. Additionally, however, the inner shelf is friction dominated and surface and bottom boundary layers overlap and frequently occupy the entire water column. This means, quite simply, that, under most circumstances, the frictional effects of winds blowing over the sea surface are transmitted directly to the sea bed. It also means that the drag effects imparted on the flow by the micromorphology of the bed can extend all the way to the sea surface and thereby influence the flows that exist throughout the water column (Mitchum and Clarke, 1986).

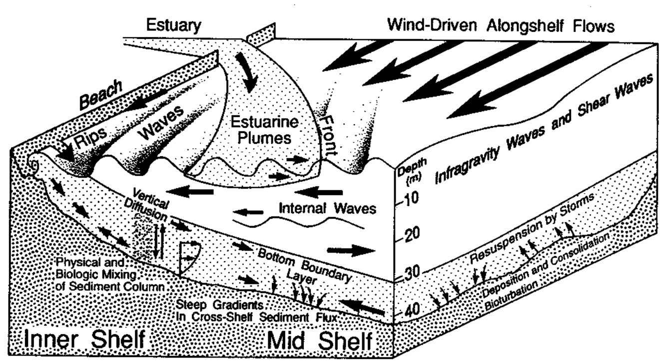

Figure 1. Conceptual diagram illustrating some of the physical processes responsible for across-shelf sediment transport (from Nittrouer and Wright, in press).

THE EQUILIBRIUM PROFILE: CLASSICAL CONCEPTS

Bruun proposed in 1954 that the profile of equilibrium of beaches and the inner shelf (or "shoreface") should be considered the shape that permits the long-term rate of dissipation of wave energy flux to remain equal everywhere across the profile. Inside the surf zone the rate of dissipation depends on turbulence caused by breaking as well as bottom friction; outside the surf zone it depends only on bottom friction. Dean (1977; 1991) and Dean and Maurmeyer (1983) have carried the development of Bruun's notion further and promoted the model for a concave upward profile of the form:

$$h = ax^m$$

where h is local water depth, x is distance seaward from shore and a and m are constants. Dean concluded from an analysis of 503 profiles from the U.S. Atlantic and Gulf Coasts that m = 2/3 which implies equal dissipation of wave energy flux per unit volume of water column. However, Inman and others (1993) found that m = 2/5 which is consistent with the more understandable model of equal dissipation per unit area of bed. Implicit in Dean's model is the assumption that across-shelf sediment transport is caused solely by waves and that, when disequilibrium occurs, sediment is diffused from regions of intense dissipation to adjacent regions of less intense dissipation.

The equilibrium models of Bruun (1954) and Dean (1977) have been criticized by Pilkey and others (1993) among others because of the simplistic assumptions underlying those models and because the models take no explicit account of convective and advective transport processes such as mean currents, gravity, and wave asymmetries. Nevertheless, those models, even if they are incorrect, offer qualitative insights into how profiles might evolve with changes in sea level or changes in net sediment input or removal. Following his 1954 hypothesis on the nearshore profile of equilibrium, Bruun (1962) proposed that this profile shape should be maintained as sea level rose. Modern applications of this so called "Bruun Rule" include numerical models for large scale shoreline response. One such model developed by Cowell and others (1991) gives results that are qualitatively consistent with observed shelf stratigraphies.

TRANSPORT PHENOMENA IN THE SURF ZONE AND ON THE INNER SHELF

Most coastal scientists and engineers associate beach behavior with wave activity. This is, of course, because it is primarily the bed shear stresses induced by wave orbital motions that agitate and resuspend beach and nearshore sands. However, coastal erosion or accretion occurs as a consequence of sediment experiencing net seaward, alongshore, or onshore transport. The flows that cause these net transports involve much more than the waves themselves even though many of the important surf zone flows are secondary products of wave dissipation. Outside the surf zone, wind driven, vertically segregated flows probably dominate the transport of sediment across the inner shelf (Wright and others, 1991; Nittrouer and Wright, in press). In recent years, many advances have been made in understanding and modeling these complex flows. Figure 1 illustrates some of the important transport mechanisms.

Within the surf zone, circulation is almost entirely driven by forces that result from the dissipation of breaking waves (e.g. Battjes and others, 1990; Massel, 1989). Alongshore currents and rip currents that frequently attain speeds of over 1 m s^{-1} are examples (e.g. Massel, 1989). Also important are the vertically segregated onshore-offshore flows typified by the well documented near bed "undertow" that transports particles seaward (e.g. Wright and others, 1982; Svendsen, 1984; Roelvink and Stive, 1988). Most of these intense flows are confined to the region between the breakpoint and the beach but large storm generated rips can extend well out over the inner shelf (Cowell, 1986).

It has become well understood over the past two decades that the dissipation of wave energy across the surf zone is accompanied by growth of low frequency infragravity oscillations with periods in the range of 30 to 300 seconds. These oscillations consist of both trapped mode edge waves and leaky mode standing waves (Guza and Thornton, 1985a). Field observations in storm-driven surf zones show that suspended sediment transport associated with infragravity motions can be 3 to 4 times larger than that associated with incident waves (Beach and Sternberg, 1988). Furthermore, it has been shown that infragravity flows cause predominantly seaward transport (Osborne and Greenwood, 1992 a, b). In addition to the trapped and leaky mode infragravity waves, low frequency (far infragravity; frequency < 0.01 Hz) oscillations have recently been observed and attributed to shear instabilities in the alongshore current (Dodd and others, 1992).

The longer term loss or gain of sediment from or to the nearshore zone depends on across-shelf flows over the inner shelf. The regime of the inner shelf differs from that of the surf zone in that circulation is not primarily driven by wave breaking. It differs from that of the outer shelf in that Coriolis force is subdued over the inner shelf but friction there is of major importance with surface and bottom boundary layers overlapping and often occupying the entire water column (Mitchum and Clarke, 1986; Huyer, 1990). Field observations over a wide range of conditions indicate that net water transport and suspended sediment fluxes over the inner shelf are dominated by near-bottom flow responses to surface wind stresses (Wright and others, 1991; Madsen and others, in press). Important secondary roles are also played by internal waves (Pineda, 1991), infragravity oscillations (Wright and others, 1991) and asymmetric wave orbital motions (Niedoroda and others, 1984; Guza and Thornton, 1985b).

Field measurements of near-bottom transports were made on the inner shelf of the Middle Atlantic Bight during the severe and prolonged "Halloween Storm" of October 1991 (Madsen and others, in press; Wright, 1993; Wright and others, in review). The storm persisted for five days and generated waves with heights and periods of up to 6 m and 22 s. Although the instrumentation was destroyed, current profile and suspended sediment concentration profile data were recovered from a site on the 13 m isobath. Wind-driven mean along-shelf currents at 1.24 m above the bed attained speeds of nearly 0.5 m s^{-1}; across-shelf flows, primarily seaward-directed, had speeds varying from 0.05 to 0.15 m s^{-1}. These seaward flows intensified in association with groups of high waves. Total, mean current, and skin friction bed shear stresses were increased, relative to moderate energy values, by more than an order of magnitude. Notably, the highest shear stresses occurred in association with high, long period swell during the late phase of the storm after winds had turned offshore creating shoreward mean flows near the bed.

The dispersal of estuarine and river-borne sediments over the inner shelf is effected, at least initially, by buoyant plumes. These may be either positively or negatively buoyant; the former contribute to surface transports, the latter to near-bottom transports (Wright and Nittrouer, in press). Both plume types tend to be bounded offshore by sharp fronts (Simpson and James, 1986; Garvine, 1987). In many cases, such as off the mouth of the Amazon, sediment-laden positively buoyant surface plumes may reach no farther seaward than the inner shelf before being turned alongshore (e.g. Geyer and others, 1991). Seaward of the mouths of rivers with very high concentrations of suspended sediment, negatively-buoyant plumes may carry sediment short distances across the inner shelf before experiencing early extinction and depositing the sediment (e.g. Huanghe of China; Wright and others, 1990).

MICROMORPHODYNAMICS OF THE INNER SHELF

The importance of net mean across-shelf flows such as those just described to suspended sediment transport is fairly obvious and relatively easy to measure. Less obvious and more difficult to document, however, are the processes that cause bed load transport and suspended load transport very close to the bed where concentrations are highest. The processes that operate within a few centimeters of the bed are highly complex and often subtle. They involve the interaction of combined wave-current boundary layers with ripples and other bed micromorphologies (e.g. Grant and Madsen, 1986; Drake and Cacchione, 1992; Wright, 1993). These interactions are non-linear and of relatively high order. The effects on sediment transport, however, can be of first order: the appearance or disappearance of wave-induced ripples can cause reversals in the direction of across-shelf transport (e.g. Nielsen, 1979; 1992). For example, at times of high bed stress (e.g. during storms) ripples are washed out and sand will move in the direction of net bed stress, which, in the case of asymmetric orbital velocities will be shoreward. Under fairweather conditions, ripples cause a phase lag between maximum bed stress and maximum suspended sediment concentration and orbital asymmetries can cause net offshore transport.

Modern models of wave-current boundary layers take account of the effects of ripples and other features on hydraulic roughness and the partitioning of stress between form drag and skin friction (e.g. Grant and Madsen, 1986; Glenn and Grant, 1987). Models also exist for predicting ripple geometries in terms of bed stress and sand size (Grant and Madsen, 1982; Nielsen, 1981; 1988). Applications of these models to natural inner continental shelf regimes show that ripple roughness, and presumably the direction of sediment transport, varies dramatically with wave conditions and with depth across the shelf (e.g. Wright, 1993). Among the sediment transport models that take explicit account of ripple effects is the "grab and dump" model proposed by Nielsen (1988).

FUTURE DIRECTIONS

The dynamics of the inner continental shelf have, until recently, been seriously neglected. For this reason there remain many questions to be addressed before we can forecast large scale coastal changes with confidence. A few of these questions are summarized below.

1. Significant geological inheritance from antecedent regimes remains present on most shelves. The last postglacial sea level transgression took place only a short while ago in geological terms and, over some shelves, it is ongoing. Therefore it is common for inner continental shelves to exhibit relict features and patterns of sediment distribution that were produced by earlier events. Examinations of across-shelf morphology, shallow stratigraphy and sediment distribution must preface any serious study of contemporary morphodynamic processes. The preserved features initialize the stage for subsequent processes and, to varying degrees, direct the course of continued evolution.

2. Much more empirical and theoretical work needs to be focused on the question of what processes determine the balance of onshore and offshore transports that define equilibrium and, most importantly, disequilibrium. A first step is to understand the physical oceanography of the inner shelf as it exists over different shelf configurations.

3. Special attention must be focused on the across-shelf components of the flows. Even though those flows are usually weak in comparison with the alongshelf flows, they are responsible for across-shelf transport of particles (e.g. Nittrouer and Wright, in press) and for molding the inner shelf profile.

4. Understanding the hydrodynamics of combined wave-current bottom boundary layers and the closely coupled micromorphodynamics of the bed itself are crucial to understanding the entrainment and transport of shelf sediments.

5. Changes in the morphology of depositional landforms such as the inner continental shelf result from spatial gradients in sediment transport. Therefore, to model changes in profile configuration or shoreline movements, we must model not only the absolute rates of sediment transport but also the transport divergence (horizontal gradients in total flux).

6. The inner shelf is not an abiotic realm. Benthic organisms play fundamental roles in binding or disturbing sediment particles and thereby altering the difficulty or ease with which particles can be entrained. Organisms also may alter the average particle size by creating larger aggregates from fines (e.g. as fecal pellets); they may mix the sediment column; and they may influence -or dominate- hydraulic roughness. We need to focus much more attention on the coupling of physical and biogeochemical processes.

ACKNOWLEDGEMENT

My ongoing studies of inner shelf processes are supported by the National Science Foundation, Grants OCE-9017828 and OCE-9123513.

REFERENCES CITED

Battjes, J.A., 1988. Surf-zone dynamics. Ann. Rev. Fluid Mech. 20:257-293.

Battjes, J.A., R.J. Sobey, and M.J.F. Stive, 1990. Nearshore circulation. *in*: Ocean Engineering Science, B. LeMehaute and D.M. Hanes (eds.), pp. 467-494, John Wiley & Sons, Inc., New York.

Beach, R.A. and R.W. Sternberg, 1988. Suspended sediment transport in the surf zone: Response to cross-shore infragravity motion. Mar. Geol. 80:61-79.

Bruun, P., 1954. Coastal erosion and development of beach profiles. U.S. Army Beach Erosion Board Technical Memorandum No. 44, U.S. Army Corps of Engineers, Waterways Experiment Station, Vicksburg, MS.

Bruun, P., 1962. Sea-level rise as a cause of shore erosion. Proc. Am. Soc. Civil Eng., J. Waterways and Harbors Div., 88(WWI):117-130.

Cowell, P.J., 1986. Australian "megarip" study. EOS 67:449.

Cowell, P.J., P.S. Roy, and R.A. Jones, 1990. Shoreface translation model: Application to management of coastal erosion. *in* Applied Quaternary Studies, G. Brierley and J. Chappell (eds.), Workshop Proc., Canberra, Australia, pp. 57-73.

Dean, R.G., 1977. Equilibrium beach profiles: U.S. Atlantic and Gulf coasts. Department of Civil Engineering, Technical Report No. 12, University of Delaware, Newark, DE.

Dean, R.G., 1991. Equilibrium beach profiles: Characteristics and applications. J. Coastal Res. 7(1):53-84.

Dean, R.G. and E.M. Maurmeyer, 1983. Models for beach profile response. *in*: Handbook of Coastal Processes and Erosion, S.B. Komar (ed.), pp. 151-166, CRC Press.

Dodd, N., J. Oltman-Shay, and E.B. Thorton, 1992. Shear instabilities in the longshore current: A comparison of observation and theory. J. Phys. Oceanogr. 22:62-82.

Drake, D.E. and D.A. Cacchione, 1992. Wave-current interaction in the bottom boundary layer during storm and non-storm conditions: Observations and model predictions. Cont. Shelf Res. 12:1331-1352.

Garvine, R.W., 1987. Estuarine plumes and fronts in shelf waters: A layer model. J. Phys. Oceanogr. 17:1877-1896.

Geyer, W. Rockwell, R.C. Beardsley, J. Candela, B.M. Castro, R.V. Legeckis, S.J. Lentz, R. Limeburner, L.B. Miranda, and J.H. Trowbridge, 1991. The physical oceanography of the Amazon outflow. Oceanogr. 4:8-14.

Glenn, S.M. and W.D. Grant, 1987. A suspended sediment stratification correction for combined wave and current flows. J. Geophys. Res. 92:8244-8264.

Grant, W.D. and O.S. Madsen, 1982. Movable bed roughness in oscillatory flow. J. Geophys. Res. 87:469-481.

Grant, W.D. and O.S. Madsen, 1986. The continental shelf bottom boundary layer. Ann. Rev. Fluid Mech. 18:265-305.

Guza, R.T. and E.B. Thornton, 1985a. Observations of surf beat. J. Geophys.

Res. 90:3161-3172.

Guza, R.T. and E.B. Thornton, 1985b. Velocity moments in the nearshore. ASCE J. Waterways, Port, Coastal Ocean Eng. 111:235-256.

Huyer, A., 1990. Shelf circulation. *in*: Ocean Engineering Science, B. Mehaute and D.M. Hanes (eds.), pp. 423-466, John Wiley & Sons, Inc., New York.

Inman, D.L., M.H.S. Elwany, and S.A. Jenkins, 1993. Shorerise and bar berm profiles on ocean beaches. J.Geophys. Res. 98:(in press).

Madsen, O.S., L.D. Wright, J.D. Boon, and T.A. Chisholm, in press. Wind stress, bed roughness, and sediment suspension on the inner shelf during an extreme storm event. Cont. Shelf Res.

Massel, S.R., 1989. Hydrodynamics of Coastal Zones. Elsevier Science Publishers B.V., New York.

Mitchum, G.T. and A.J. Clarke, 1986. The frictional nearshore response to forcing by synoptic scale winds. J. Phys. Oceanogr. 16:934-946.

Niedoroda, A.W., D.J.P. Swift, T.S. Hopkins, and C.M. Ma, 1984. Shoreface morphodynamics on wave-
dominated coasts. Mar. Geol. 60:331-354.

Nielsen, P., 1979. Some basic concepts of wave sediment transport. ISVA, Tech. Univ. Denmark, Ser. Pap. 20.

Nielsen, P., 1981. Dynamics and geometry of wave generated ripples. J. Geophys. Res. 86:6467-6472.

Nielsen, P., 1988. Three simple models of wave sediment transport. Coastal Eng. 12:43-62.

Nielsen, P., 1992. Coastal Bottom Boundary Layers and Sediment Transport. 324 p., World Scientific, New Jersey.

Nittrouer, C.A. and L.D. Wright, in press. Transport of particles across continental shelves. Rev. Geophys.

Osborne, P.D. and B. Greenwood, 1992a. Frequency dependent cross-shore suspended sediment transport.1. A non-barred shoreface. Mar. Geol. 106:1-24.

Osborne, P.D. and B. Greenwood, 1992b. Frequency dependent cross-shore suspended sediment transport.2 A barred shoreface. Mar. Geol. 106:25-52.

Pilkey, O.H., R.S. Young, S.R. Riggs, A.W. Sam Smith, H. Wu, and W.D. Pilkey, 1993. The concept of shoreface profile of equilibrium: A critical review. J. Coastal Res. 9:255-278.

Pineda, J., 1991. Predictable upwelling and the shoreward transport of planktonic larvae by internal tidal bores. Science 253:548-551.

Roelvink, J.A. and M.J. Stive, 1988. Bar-generating cross-shore flow mechanisms on a beach. J. Geophys. Res. 94:4785-4800.

Simpson, J.H. and I.D. James, 1986. Coastal and estuarine fronts. In: Baroclinic Processes on ContinentalShelves, C.N.K. Mooers (ed.), AGU, 63-93.

Svendsen, I.A., 1984. Mass flux and undertow in a surf zone. Coastal Eng. 8:347-365.

Wright, L.D., 1987. Shelf-surf zone coupling: diabathic shoreface transport. Proc., Coastal Sediments '87,pp. 25-40, New Orleans.

Wright, L.D., 1993. Micromorphodynamics of the inner continental shelf: A Middle Atlantic Bight case study. J. Coastal Res., Special Issue Number 15, pp. 93-124.

Wright, L.D., J.D. Boon, S.C. Kim, and J.H. List, 1991. Modes of cross-shore sediment transport on the shoreface of the Middle Atlantic Bight. Mar. Geol. 96:19-51.

Wright, L.D., R.T. Guza, and A.D. Short, 1982. Dynamics of a high energy dissipative surf zone. Mar. Geol. 45:41-62.

Wright, L.D. and C.A. Nittrouer, in press. Dispersal of river sediments in coastal seas: six contrasting cases. Estuaries.

Wright, L.D., W.J. Wiseman, Z.-S. Yang, B.D. Bornhold, G.H. Keller, D.B. Prior, and J.N. Suhayda, 1990. Processes of marine dispersal and deposition of suspended silts off the modern mouth of the Huanghe (Yellow River). Cont. Shelf Res. 10:1-40.

Wright, L.D., J.P. Xu, and O.S. Madsen, in review. Across-shelf benthic transports on the inner shelf of the Middle Atlantic Bight during the Halloween storm of 1991. Submitted to Mar. Geol.

SEA LEVEL VARIABILITY ALONG THE EAST COAST OF THE UNITED STATES

Bruce B. Parker
Office of Ocean and Earth Sciences
National Ocean Service, NOAA
Silver Spring, MD 20910

ABSTRACT

This paper reviews the various causes of sea level variability and provides statistics on the size of these variations for selected stations along the Atlantic Coast of the United States. Although the term "sea level" is generally used for longer-term water level variability, i.e. seasonal, interannual-to-decadal, and long-term trends, for the purposes of this paper we also include tidal variations and subtidal storm surge. While long-term sea level rise would lead to increased coastal erosion, the rate of rise is extremely small in comparison to the heights reached (periodically) by the higher frequency sea level variations. The highest water levels usually occur during storm events, which also produce the largest waves and thus the greatest erosion. For seasonal and interannual sea level variations the duration of the higher water level will be on the order of months to years and so will be long enough to have significant effects on coastal erosion, inundation, wetlands, and saltwater intrusion into groundwater.

INTRODUCTION

The height of sea level can have an important effect on various hazardous coastal processes including coastal erosion, inundation, loss of wetlands, and saltwater intrusion into groundwater (National Research Council, 1987; Gornitz, 1991; Emery and Aubrey, 1991). Concern over a possible accelerated sea level rise caused by global warming due to the accumulation of greenhouse gases has led to numerous studies to assess the impact of this sea level rise on the coast. For example, Gornitz (1991) has developed a Coastal Vulnerability Index and applied it to the U.S. East Coast in order to identify high risk coastal regions.

Although average global sea level rise over the last century has been on the order of 2mm per year (with higher rates in areas with greater land subsidence), various researchers have predicted an acceleration of this rate. These predictions are not based on the analysis of tide gauge data; they are based on models of thermohaline circulation of the ocean (to predict future thermal expansion) and models of ice melting from glaciers and ice sheets on Greenland and Antarctica, run for predicted future global air temperatures. An acceleration in sea level rise has not shown up yet in the world's tide gauge records, nor has a global warming signal been definitively identified separate from natural variability, although there are possible reasons why these effects have not shown up yet.

More than a long-term trend in sea level is necessary to assess possible impacts on the coast. The entire sea level spectrum plays a role. For example, the greatest coastal erosion takes place during storms, because of the much higher levels resulting from the storm surge and the higher waves (which actually cause the erosion). If future global warming does occur it will affect climate, causing changes in storm frequency and intensity and thus the frequency and height of storm surges and waves. The occurrence of storms at the times of highest tides increases their impact. Seasonal variation in sea level at many locations has a magnitude greater than the long-term sea level rise over the past hundred years. Interannual sea level variation is also large enough to have an impact on the coast.

This paper reviews the various causes of sea level variability, including tidal variation, daily-to-weekly changes (including storm surges), seasonal changes, interannua-to-decadal changes, and long-term sea level trends. It also provides statistics on the size of these changes for selected stations along the Atlantic Coast of the United States (including the Florida Gulf Coast, because of the similarity with the Atlantic on some time scales).

WATER LEVEL AND SEA LEVEL: A CLARIFICATION OF TERMS

Water level is the distance of the water's surface above some reference point (referred to as a *datum*). The device that measures water level has generally been called a *tide* gauge because at most locations the astronomical tide is the largest part of the water level variation and the resulting data were usually obtained in order to make tide predictions. (The word *tide* has been used by some in the same fashion as we use the term *water level*, with the distinction then made between the astronomical tide and what was referred to as the *meteorological* tide.) The term water level does not include wind waves, and in fact, the water level is thought of as the surface on which the wind waves propagate. Tide gauges have been designed to eliminate the effects of waves either by damping them out through the use of a stilling well that surrounds the float or through averaging a number of rapidly taken samples as is done by the new acoustic gauges now being used by the National Ocean Service (NOS).

The term *sea level* or *mean sea level* (MSL) is used to indicate that the water level observations have been averaged over some period of time (usually at least a month), so that the shorter period variations (mainly the tide) have been averaged out and in fact can be viewed as oscillating about this *mean sea level*. *Sea level* is only a mean for a particular time period, and it varies over longer time periods, e.g. on a monthly, interannual, and longer basis. This variation in sea level is measured relative to the land. If the land sinks, it will appear that sea level is rising, and likewise if the land rises it will look like sea level is falling. Thus we refer to this as *relative sea level*. A known relationship to the land is maintained by attaching *benchmarks* to permanent features on the land and by geodetic leveling from these benchmarks to a tide staff; frequent simultaneous observations at the tide staff and the tide gauge then allow the tide gauge measurements to be related to the benchmarks. In the newer acoustic gauges used by NOS the leveling is done directly from benchmark to gauge, eliminating the need for the staff.

This whole process of benchmark maintenance and leveling has been very important in some countries like the U.S., because marine boundaries are determined by mean low water datum (separation between state and Federal jurisdiction) and mean high water datum (separation between state and private ownership). When offshore oil was discovered these marine boundaries became even more critical. All this was to the benefit of those researchers who would use the data from these gauges for sea level rise studies.

The most important requirement for these data is datum continuity, i.e. the maintenance of a direct relationship of the measurement to the benchmarks over the years.

CAUSES OF WATER LEVEL VARIATION

The water level measured at a tide gauge is affected by a number of oceanographic and meteorological phenomena, including the astronomical tide, changes in atmospheric pressure, wind, river discharge, ocean circulation, changes in water density, and added water volume due to the melting of ice. The *astronomical tide* is caused by the gravitational effects of the moon and sun, creating very long waves in the ocean which propagate over the continental shelf and into shallow bays, where amplifications, frictional damping, and nonlinear distortions take place. Increased *atmospheric pressure* decreases water level, and vice versa, in what is commonly called the inverted barometer effect. In shallow areas the *onshore-offshore wind component* can directly push water toward the shore (wind setup) or away from it (setdown). The usually more dominant effect is caused further offshore by the *longshore wind component*, which can raise or lower the water level because the Coriolis force causes transport to the right of the wind direction. Along certain coasts the wind also causes upwelling, which affects the temperature and density of the water column. *Steric sea level changes*, i.e. water level changes due to density changes, are caused by either temperature changes in the water column (and the resulting thermal expansion or contraction) or salinity changes (with the fresher water taking up more volume than the same weight of the more dense saline water). Changes in ocean circulation, especially at the western boundaries of oceans (e.g. the Gulf Stream) affect sea level through changes in density and through geostrophic adjustments (i.e. through maintenance of a balance between Coriolis and the cross-stream pressure gradient). *River discharge* can raise water level at a station in the river due to a frictional effect, or to a lesser extent at nearby stations by the addition of less dense fresh water. Some of the river runoff may have been stored in the form of snow or ice for months of each year, or for several years. Additional freshwater volume (that has been in the form of ice for centuries) can be added by the *melting of glaciers or the ice sheets on Greenland and Antarctica*. More information on these effects on water level and sea level can be found in the paper by Chelton and Enfield (1986), in which they provide examples from the Pacific.

TIME SCALES OF VARIATION

The various effects on water level and sea level cover a range of time scales, the largest variations occurring at the higher frequencies. The largest signal is the *astronomical tide*, with most energy in the semidiurnal and diurnal frequency bands, although in shallow-water areas nonlinear effects can cause higher harmonics. The range of tidal variations in many locations is on the order of meters (and on the order of 10 m at a few locations like the Bay of Fundy).

Water level variations on the order two days or longer are usually caused by changes in wind speed and direction and to a lesser extent by changes in atmospheric pressure. These subtidal storm surges are on the order of centimeters to meters, the largest values occurring during hurricanes and extratropical storms (esp. "northeasters"). In shallow water, nonlinear interaction between storm surge and the tide modifies both (Parker, 1991a), in some cases decreasing their combined effect. Variations in river discharge can also occur on these time scales especially near spring freshets, with increases in water level on the order of meters. At these times there is usually a nonlinear interaction with the tide, so that as the water level is rising due to the increased discharge, the tidal range is decreased by the frictional effect of the increased flow.

There is also a seasonal variation in sea level over the year which can be caused by seasonal changes in water temperature, river runoff, or the wind. These seasonal variations in sea level can be on the order of 40 cm, or higher in special locations.

Sea level also varies from year to year, on the order of 10 to 20 cm, due to interannual variations in wind and temperature that generally involve climate variations over large regions of the globe. In the tropical Pacific, for example, the most important interannual sea level variations are a result of El Niño Southern Oscillation (ENSO). But interannual sea level variations at other locations around the globe also reflect the climatic interaction between ocean and atmosphere. At islands the interannual sea level variation tends to correlate well with changes in water density particularly due to water temperature changes. Along continental coasts it tends to correlate well with changes in longshore wind stress and changes in ocean currents (especially along continental east coasts). Internannual sea level variations must be considered in conjunction with the seasonal variations, since the key factors affecting the interannual signal often have a preferential season for their greatest effect.

Sea level also changes very slowly over long time periods, i.e. over decades, centuries, and even millennia. Most recent studies have found an average global rise sea level over the last century on the order of 1 to 2 mm/year. Man-induced global warming resulting from the accumulation of greenhouse gases has received the most attention as a possible cause, but so far these studies have found no strong evidence for the increase in the rate of sea level rise in recent decades that one would expect if this were the cause. Also, there are many other possible reasons for this upward trend in sea level. (See Parker, 1991b, 1992, and Emery and Aubrey, 1991, for discussions of the problems in determining a reliable global sea level trend and in predicting future sea level rise, and for references which summarize the results of these studies.)

Over such long time periods land movement can be a major cause of relative sea level change. The most obvious examples are places where there is significant glacial rebound, such as Juneau, Alaska, where the rising land makes the relative sea level look like it is falling at a rate of 11.5 mm per year. But in other parts of the world, beyond the furthest extension of the glaciers during the last ice age, glacial rebound is downward, making relative sea level look like it's rising. There are a variety of other causes of vertical land movement that may look like sea level rise, including tectonic movement at convergent plate boundaries and subsidence due to sediment compaction and the extraction of water or oil from the ground.

Regional oceanographic or meteorological phenomena may have very-low-frequency components that could affect the calculated trends at particular stations, for example low-frequency changes in wind speed or direction, atmospheric pressure, or ocean circulation. Slowly changing wind speed or direction over several decades could have a low-frequency effect on sea level along coasts where the longshore component has the dominant effect on sea level. Or it could modify the ocean circulation which in turn would affect the water density which would affect the sea level at certain islands. Sturges (1990) and Douglas (1991) both show sea level signals at periods of 40 to 50 years which are visually coherent large regions of the globe.

Sea level has been rising since the last ice age 18,000 years ago, when it was approximately 135 m lower than it is today. During the time the glaciers retreated from covering Europe, Canada, and the northern U.S. (between 15,000 and 7,000 yrBP) sea level rose at 5 to 6 times the present rate. Since approximately 7000 yrBP glacial rebound appears to have been responsible for the last 10 to 20m rise in sea level in the mid and lower latitude (and a 20-30m *fall* in sea level in the northern latitudes).

A rise in *global* sea level due to global warming would primarily be the result of two effects: (1) thermal expansion of the upper layers of the ocean; and (2) the addition of water volume due to the melting of mountain glaciers and ice sheets on Greenland and Antarctica (assuming the global warming did not also cause an increase in snow precipitation over the ice sheets). However, global warming should also produce regional changes in climate, and thus changes in wind patterns, ocean circulation, and other phenomena that affect sea level. Thus, some parts of the world could actually experience lower sea level due to global warming.

TIDAL VARIATION ALONG THE EAST COAST OF THE U.S.

The largest water level variation along the East Coast of the U.S. is usually due to the tide. The mean tide range (the difference between mean high water and mean low water) for selected locations are given in Table 1. For stations on the Atlantic Coast (or just inside entrances to a bay) the tide range increases from about 2 feet (61 cm) at Woods Hole to around 4 feet (122 cm) from Sandy Hook south to Wilmington, increases to approximately 6 feet (183 cm) at Fernandina Beach and then decreases to almost 1 foot at Key West. The range stays quite small throughout the Gulf of Mexico.

Higher tidal ranges occur near the heads of bays of particular lengths and depths, due to amplification resulting from the reflection of the tidal wave. For example, in Delaware Bay we see an 8.1-foot mean range at Trenton versus 4.2 feet (128 cm) at Lewes. In Long Island Sound, Willets Points has a mean range of 7.1 feet (216 ft) versus 2.1 feet (64 cm) at Montauk. The most dramatic amplification, of course, is the 38-ft (11.6 m) mean range in the Bay of Fundy. (compared with the 1.9-ft (58-cm) mean range at Woods Hole, not far from the entrance to the Gulf of Maine); the 18.4-foot range at Eastport illustrates the amplification mid way up the Gulf. In some bays the tide range can be smaller near the head, for example, at Baltimore (1.1 ft; 34 cm) in Chesapeake Bay, which is shallow (so that friction damps the tidal wave) and long enough for an entire tidal wavelength to fit, not the optimum situation for amplification.

The tide along the Atlantic Coast is generally *semidiurnal*, i.e. there are two pairs of high and low waters per day. The heights of two consecutive high waters (or consecutive low waters) will not be the same because there is also a diurnal tidal signal at every location that will make every other high water (or every other low water) of a different height than the previous one. When the difference between successive high waters (or low waters) reaches a certain value the tides become classified as *mixed*. In the Gulf of Mexico the tides have a stronger diurnal signal, so that in some locations (e.g. St. Petersburg in Tampa Bay) there will only be one high water and one low water near times of maximum north or south declination of the moon (once every 13.6 days). This is the time when the Earth axis is at an angle to the tide-producing forces of the moon so that stronger force is felt every other 12.42-hour tidal cycle. The hydrodynamics of the Gulf of Mexico causes the diurnal component to increase in size (relative to the semidiurnal component) as one moves north along Florida Gulf Coast, until at Pensacola it is totally dominant and the tide is diurnal at all times.

The amplitude of the high waters varies throughout the month and throughout the year. The tide range tends to be largest a little after new and full moon, when the moon- and sun-generated tidal forces are working with each other ("spring tides"), instead of against each other during first and last quarter ("neap tide"). Spring tide ranges are also given in Table 1. The tide range also tends to be larger a little after the moon is in perigee, that is when the moon is closest to the earth (the earth-moon orbit being elliptical in shape). Along the entire Atlantic Coast this is actually a larger effect than the spring tide, although it occurs less frequently (once every 27.5 days versus once every 14.8 days for spring tides). The highest tides of any year occur when a new or full moon occurs near the time of perigee, the so-called "perigean spring tides". Boston, for example, which has a mean range of 9.6 ft (2.9 m) and a mean spring range of 11.0 ft (3.4m), can have a range on the order of 14.5 ft (4.4 m) during perigean spring tide.

In areas with diurnal tides, the tide range will be largest near times of maximum north or south declination of the moon (once every 13.6 days). In areas with mixed tides that have a diurnal component that is larger than the spring tide or perigean effects, the largest tidal ranges may also occur near maximum north and south declination. The great diurnal range for all stations is also given in Table 1; this is the height difference between mean higher high water and mean lower low water. The great diurnal range is generally less than the spring range along the entire East Coast until one reaches Key West, at which point it becomes larger. There are a few exceptions in the bays connected to the Atlantic, where hydrodynamics causes more of an amplification of the diurnal tidal wave than the semidiurnal wave. This is the case, for example, in the upper half of Chesapeake Bay (see Baltimore, Annapolis in Table 1) and the upper end of tidal part of the Potomac River (Washington, D.C.), where the tide is classified as *mixed, mainly semidiurnal.*

There is also an 18.6-year variation in tidal range due to the slow variation of the plane of the earth-moon orbit with respect to the equator of the earth. This slow changing of the distance that the moon (overhead) travels north and south of the equator affects the semidiurnal and diurnal tidal constituents differently. In areas with semidiurnal tides, maximum tide ranges should occur in 1996 and 1997; but it should be remembered that this is only a 4 per cent increase in range (above the 18.6-year average) and, since this is a slowly changing effect, there is no dramatic change from year to year. In areas with diurnal tides (e.g. Pensacola) the maximum tide ranges occurred in 1987 and 1988 and amounted to an 11 per cent increase in range (above the 18.6-year average).

DAILY-TO-WEEKLY CHANGES IN WATER LEVEL ALONG THE U.S. EAST COAST

Changes in water level on a daily-to-weekly time scale can be caused by changes in wind, atmospheric pressure, river runoff, and water temperature, although wind-generated storm surge always is the dominant effect (with the exception of increased water levels during heavy river runoff in an estuary). The highest water levels obviously occur during extratropical storms (especially "northeasters") and hurricanes, the same time when the largest wind waves occur for maximum erosion capability. These effects cannot be summarized in as easy a fashion as the tidal effect, because they depend on the weather and especially the frequency of storms. The columns 5-8 in Table 1 show the highest and lowest water levels observed at the tide stations listed. The "highest value" shown in Table 1 is the height above the mean higher high water, and the "lowest value" is the distance below the mean lower low water. (In some cases the larger water level values given in Table 1 are found at the stations that have been operating the longest, so that there was more time for a large storm or hurricane to have occurred.)

These nontidal changes in water level generated by the wind

Table 1. Tidal and short-term meteorological (mainly wind) induced water level variability for selected locations along the Atlantic Coast and Florida Gulf Coast. Columns 2, 3, and 4 give the mean, spring, and diurnal tidal ranges. Columns 5, 6, 7, and 8 give the highest and lowest water levels observed at the tide gauges since they were installed. Columns 9 - 14 give recent examples of the magnitude of surges from large storms or hurricanes; the maximum difference between the measured water level and the predicted tide is shown for each location for each storm. All values are in feet; values are also given in cm in the text. (DDDD indicates that the gauge was destroyed in that storm.)

	TIDAL RANGES			HISTORICAL MAX. & MIN. OBS. LEVELS					RECENT MAX. STORM SURGES (OBS-PRED)					
STATION NAME	Mean Range	Sprng Range	Great Diur. Range	Date Gage Inst	Highest Above MHHW	Date Observed	Lowest Below MLLW	Date Observed	Hurr. Bob 8/91	Extra trop. 10/91	Coast Storm 1/92	Hurr. Andrw 8/922	North eastr 12/92	Extra trop. 3/93
EASTPORT, ME	18.36	20.9	19.32	1929	4.80	06-Apr-77	-4.67	09-Aug-72		2.69			1.19	2.96
BAR HARBOR, ME	10.62	12.2	11.44	1947	3.61	29-Dec-59	-3.35	30-Dec-63					1.44	3.32
PORTLAND, ME	9.11	10.4	9.91	1912	4.26	07-Feb-78	-3.41	30-Nov-55	2.48	3.52			1.77	3.24
BOSTON, MA	9.55	11.0	10.33	1921	4.92	07-Feb-78	-3.57	25-Jan-28	3.63	5.11			3.31	4.22
WOODS HOLE, MA	1.83	2.3	2.25	1933	8.14	31-Aug-54	-3.06	02-Feb-76	5.78	4.35			2.56	3.56
NANTUCKET, MA	3.06	3.6	3.60	1965	4.51	30-Oct-91	-1.90	12-Feb-81	2.01	4.60			3.39	3.42
NEWPORT, RI	3.52	4.4	3.92	1930	9.61	21-Sep-38	-2.87	25-Jan-36	5.51	4.02			3.21	3.98
PROVIDENCE, RI	4.52	5.6	4.96	1938	12.75	21-Sep-38	-3.39	05-Jan-59	6.57	3.41			3.03	4.35
MONTAUK, NY	2.13	2.6	2.59	1947	6.09	31-Aug-54	-3.54	02-Feb-76		4.44			4.10	4.36
WILLETS POINT, NY	7.14	8.4	7.78	1931	9.12	21-Sep-38	-4.15	10-Jan-78	6.71	5.09			7.52	6.22
NEW YORK CITY, NY	4.56	5.5	5.12	1856	5.11	12-Sep-60	-4.07	02-Feb-76	1.77	4.94	3.47		6.05	5.15
SANDY HOOK, NJ	4.66	5.6	5.20	1933	5.25	11-Dec-92	-4.47	02-Feb-76	2.34	4.94	3.70		7.03	5.67
ATLANTIC CITY, NJ	4.09	5.0	4.68	1911	4.52	14-Sep-44	-4.11	10-Jan-78	1.69	4.65	3.36		4.68	4.87
TRENTON, NJ	8.06		8.64	1977	4.76	31-May-84	-5.37	21-Nov-89						
PHILADELPHIA, PA	6.15	6.5	6.75	1900	4.04	25-Nov-50	-6.51	31-Dec-62		4.06	2.69		4.87	4.88
LEWES, DE	4.15	4.9	4.73	1921	4.76	06-Mar-62	-3.94	10-Jan-78	1.29	3.90	4.57		3.96	3.89
OCEAN CITY, MD	3.42	4.1	3.96	1975	3.58	27-Sep-85	-2.89	16-Mar-80	1.22	3.80	DDDD			
BALTIMORE, MD	1.11	1.3	1.66	1902	6.27	23-Aug-33	-4.87	24-Jan-08		2.76	2.30		2.72	1.88
ANNAPOLIS, MD	0.93	1.1	1.43	1929	4.97	23-Aug-33	-3.70	31-Dec-62		2.64	2.25		2.55	2.19
WASHINGTON, DC	2.77	3.0	3.18	1915	8.11	17-Oct-42	-4.81	26-Feb-67		2.76			3.67	2.63
HAMPTON ROADS, VA	2.47	2.9	2.80	1927	5.59	23-Aug-33	-3.21	31-Jan-66		2.93	3.49		2.76	2.21
WILMINGTON, NC	4.12	4.5	4.52	1936	3.71	15-Nov-54	-1.78	12-Feb-81		2.42				5.25
CHARLESTON, SC	5.27	6.1	5.80	1921	7.00	21-Sep-89	-3.49	30-Nov-63	1.01					3.33
SAVANNAH, GA	6.88	8.0	7.47	1935	3.68	15-Oct-47	-4.35	20-Mar-36						2.97
FERNANDINA BCH, FL	6.06	7.0	6.60	1897	7.17	20-Oct-98	-3.83	24-Jan-40						1.41
MAYPORT, FL	4.51	5.3	4.92	1928	2.62	09-Sep-64	-3.16	24-Jan-40						1.16
MIAMI BEACH, FL	2.51	3.0	2.76	1931	3.64	08-Sep-65	-1.60	24-Mar-36						
KEY WEST, FL	1.31	1.6	1.84	1913	2.13	08-Sep-65	-1.43	19-Feb-28						
NAPLES, FL	2.09	2.8	2.94	1965	3.20	21-Dec-72	-2.32	15-Mar-88				1.25		4.09
FORT MEYERS, FL	0.87	1.2	1.19	1965	3.64	23-Nov-88	-2.04	16-Jan-72				0.58		3.47
ST. PETERSBURG, FL	1.57	2.3	2.24	1947	4.22	31-Aug-85	-2.27	08-Sep-65				1.66		4.39
CEDAR KEY, FL	2.78	3.5	3.76	1915	5.30	13-Mar-93	-4.07	18-Sep-47				2.15		5.22
APALACHICOLA, FL	1.11		1.66	1967	5.79	21-Nov-85	-1.69	18-Jan-81				1.83		2.53
PENSACOLA, FL	1.19		1.27	1923	7.55	20-Sep-26	-2.28	06-Jan-24				1.29		0.66
HALIFAX, CANADA	4.4	5.3		1920										
BERMUDA	2.45	3.0	2.78	1932	2.33	01-Dec-67	-1.89	15-Mar-45						

over the continental shelf propagate into and up the bays and estuaries. In some bays that may be the dominant nontidal cause of water level change, except during times of high river runoff (typically in the spring). However, some bays are large enough that direct wind action on the bay is important. Chesapeake Bay is the classic example; because of its particular length and depth the wind sets up a 2-day seiche which has a significant effect on water levels within the bay (and combined with the remote wind-induced water level signal) can dominate the tide.

As mentioned above the Gulf of Mexico has generally small tides so that water level changes can be completely dominated by the wind-induced changes. The diurnal variation in water level in the northeastern Gulf of Mexico has at times completely disappeared with the water level staying (e.g.) low for days due to the winds.

In Table 1 the six columns on the right provide some recent examples of the magnitude of storm surges produced by hurricanes or extratropical storms. The maximum difference between the measured water level and the predicted tide is shown for each location for each storm that affected it.

SEASONAL CHANGES IN SEA LEVEL ALONG THE U.S. EAST COAST

Figure 1 shows the mean annual sea level cycle at 14 stations from Halifax, Canada along the Atlantic Coast and around into the Gulf of Mexico up to Pensacola. For comparison purposes the annual cycles were determined for the same time period at all stations (1948 through the end of 1984, which is two 18.6-year cycles). The range of this seasonal sea level variation (i.e. the difference between the month with the highest mean sea level and the month with the lowest) is the smallest in the north, with Portland (in the Gulf of Maine) showing a range of 0.20 foot and Halifax on the Atlantic Coast of Nova Scotia a little larger at 0.30 foot. The range of seasonal variation increases as one moves south, more than doubling by the time one reaches New York City (0.51), and then doubling again at Fernandina Beach (with a range of 0.99 foot; Mayport, not shown in the plot, a little south of Fernandina Beach has a seasonal range of 1.01 foot). The range then decreases as one goes further south to Miami Beach (0.67) and Key West (0.67) and doesn't increase as one moves north along the Florida Gulf Coast until Cedar Key (0.77 ft, 23 cm; not shown on the plot) and Pensacola (0.79 ft; 24 cm). One will also notice in Figure 1 a bimodal feature in the annual cycles from Hampton Roads to Miami Beach; it is most strongly seen between Charleston and Fernandina Beach.

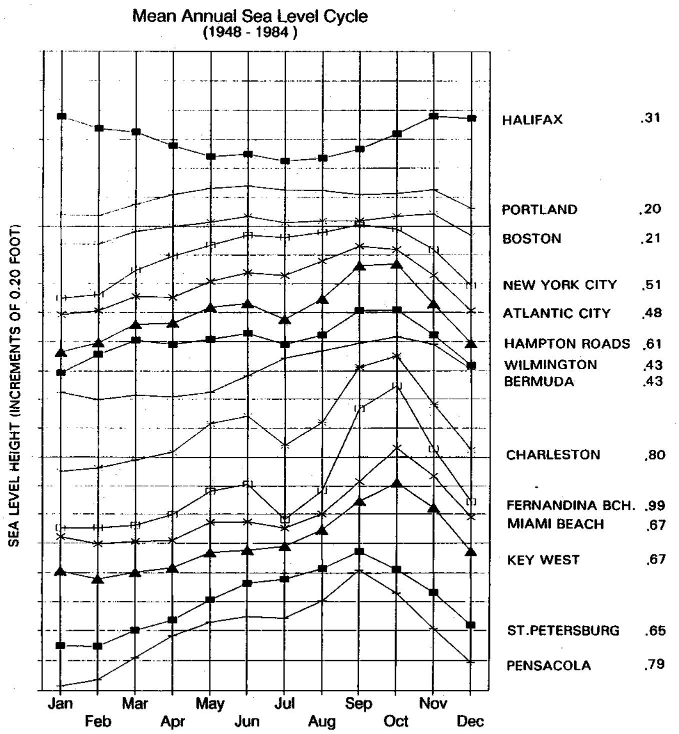

Figure 1.The mean annual sea level cycle at 14 stations from Halifax, Canada along the Atlantic Coast and around into the Gulf of Mexico up to Pensacola (for the period 1948 -1984). Numbers to the right of the station name give the range of the seasonal cycle. (All values in feet; increments along the veritcal axis are 0.2 foot; values are also given in cm in the text.)

These are average cycles (for 1948-1984); individual cycles can vary considerably from year to year. Figure 2 shows how the seasonal sea level range varies from 1935 to 1992 at four of these stations; there are similarities at many stations along the East Coast in how the seasonal cycle change from year to year. For example, many stations had small seasonal ranges in 1980 and large ranges in 1958. At Fernandina Beach the seasonal range was 0.54 ft (16 cm) in 1980, but 1.92 ft (59 cm) in 1958 (compared with the 0.99-ft (30 cm) range for the mean cycle). In fact, the average of the seasonal ranges shown in Figure 2 is 1.27 ft (39 cm) for Fernandina Beach, also larger than the range of the average seasonal cycle.

The causes of these seasonal changes in sea level include seasonal changes in water temperature, wind speed and direction, coastal circulation, and, for estuarine stations, freshwater river discharge. Away from the coast, at Bermuda, the seasonal sea level matches up well with seasonal changes in water temperature. Along the coast seasonal wind patterns also have an important effect. Noble and Gelfenbaum (1992) have demonstrated that seasonal changes in Gulf Stream transport also have a significant effect on seasonal sea level; a decrease in Gulf Stream transport causes an increase in sea level, and vice versa. The largest transports occur in July-August and the lowest occur in October, which matches up well with the minimum sea level in July and the second, higher sea level peak in October that appears in all the curves in Figure 1 from Miami Beach to Hampton Roads.

INTERANNUAL TO-DECADAL CHANGES IN SEA LEVEL ALONG THE U.S. EAST COAST

Figure 3 shows the mean yearly sea levels at 10 stations along the East Coast of the U.S., including Halifax (Canada), Bermuda, and the Florida Gulf Coast up to Pensacola. One notices a great deal of similarity in these plots, with significant peaks seen along large stretches of the coast. For example, a peak yearly sea level in 1948 can be seen clearly visible from Pensacola in the northern Gulf of Mexico all to way to New York City.

Recent maximums and minimums in yearly sea level records from stations along the East Coast of the U.S. appear to coincide with ENSO events in the Pacific. Even more pronounced are the peaks seen in mean sea level for the winter months (December through February) after subtracting out the mean annual sea level cycle (Parker, 1991b). The strong 1982-83 El Niño led to a warm winter in the northeastern U.S., while the 1976-77 event led to a cold winter, but the primary cause of the sea level maximum coinciding with the former and the sea level minimum coinciding with the latter appears to be variation in the longshore wind, which also shows similar maximums and minimums coinciding with El Niños. These peaks appear to be the result of an atmospheric teleconnection related to the westerlies over the U.S.

LONG-TERM SEA LEVEL RISE ALONG THE EAST COAST

Examination of the yearly sea level curves in Figure 3 clearly shows that sea level along the East Coast of the U.S. has been rising for the last century. Table 2 lists the calculated trends for selected stations, both for the entire length of each data series and for the 1923-1992 period to allow intercomparison. The average sea level rise for the East Coast (approximately 2.93 mm/year based on these nine 1923-1992 records) is slightly larger than calculated global averages (e.g. Douglas, 1991, calculated a global average of approximately 1.8 mm/year). The larger East Coast relative sea level rise is likely due to land subsidence. This subsidence may be due to glacial rebound (in this case sinking) of the bulge beyond the edge of the most southerly extent of the ice age glacier, or due to sediment compaction, or possibly due to decline in head in confined aquifers related to municipal and industrial water pumpage (See Emery and Aubrey, 1991; Davis, 1987; Douglas, 1991).

Station Name	1923-1992 ft/yr	1923-1992 mm/yr	series length ft/yr	series length mm/yr	series length dates
Halifax, Canada	.01129	3.44	.01233	3.76	1920-1984
Portland, ME	.00738	2.25	.00640	1.98	1912-1992
Boston, MA	.00866	2.64	.00869	2.65	1921-1992
New York City, NY	.00991	3.02	.00909	2.77	1893-1992
Atlantic City, NJ	.01306	3.98	.01263	3.85	1912-1992
Baltimore, MD	.01043	3.18	.01007	3.07	1903-1992
Charleston, SC	.01076	3.28			1923-1992
Key West, FL	.00784	2.39	.00745	2.27	1913-1992
Pensacola, FL	.00722	2.20			1924-1992

Table 2.Long-term sea level trends at nine stations along the U.S. East Coast for the period 1923-1992 and for the full data series, if greater than 70 years. (New York record begins before 1893, but has large gaps.) All values are in feet; values are also given in cm in the text.

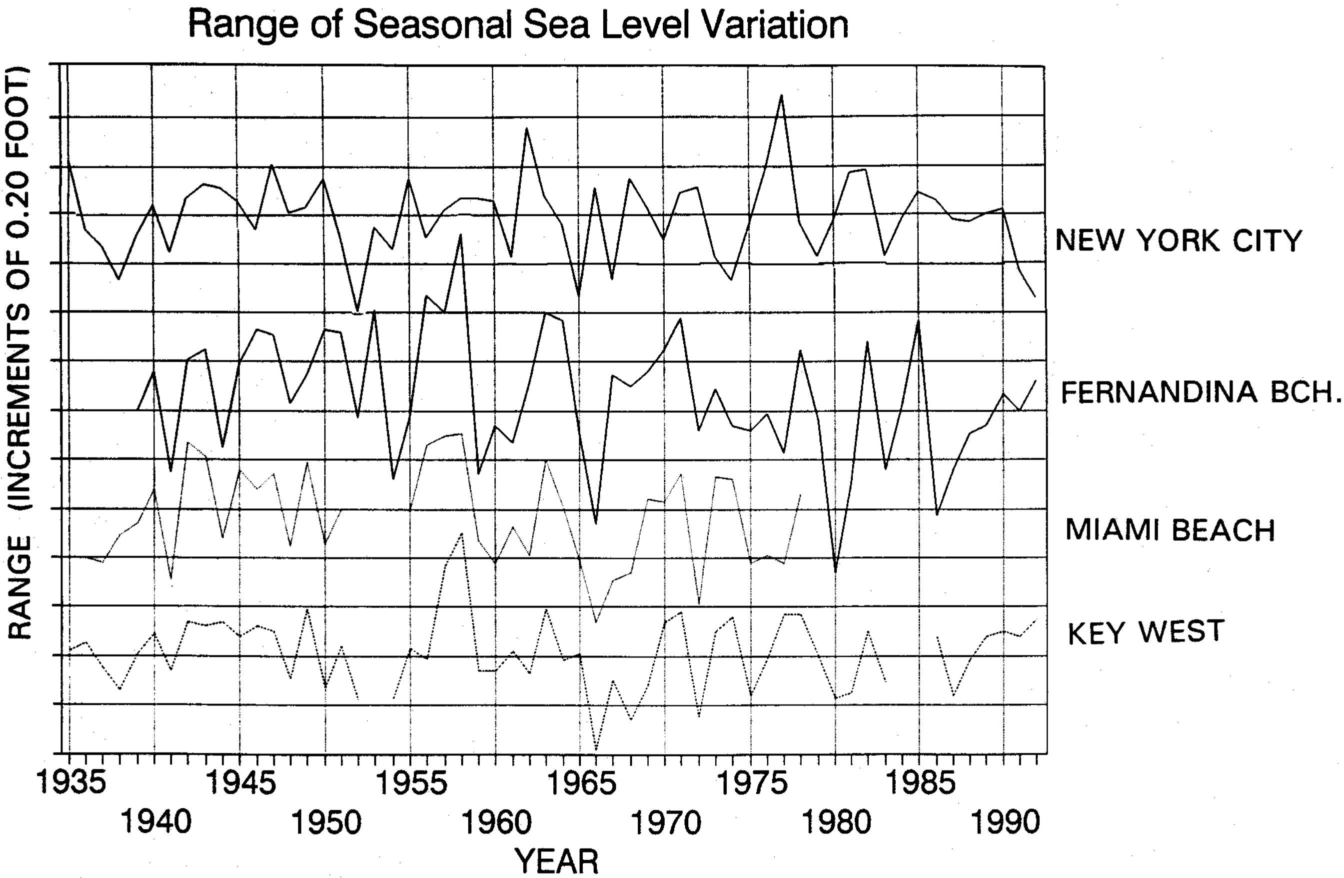

Figure 2.The yearly variation in the seasonal sea level range from 1935 to 1992 at four stations along the East Coast. (Increments along the veritcal axis are 0.2 foot; values are also given in cm in the text.)

CONCLUSIONS

Relative sea level rise along the East Coast has risen from 22 to 40 cm (0.72 to 1.31 ft) over the last hundred years, much of this rise due to land subsidence. The interannual variation in sea level has been as large as 10 to 15 cm (0.3 to 0.5 ft) over a one to five year period. The range of the average seasonal cycle varies from 6 cm (0.20 ft) at Portland, Maine to 31 cm (1.01 ft) at Mayport, Florida. However, the range of the seasonal cycle for an individual year can be double these values. Mean tidal ranges vary from 36 cm (1.19 ft) at Pensacola, Florida to 5.6 m (18.36 ft) at Eastport, Maine; the largest tidal ranges occur a few times a year during perigean spring tides. The largest ranges occur near the heads of bays with the right length and depth to cause amplification of the tide entering from the coast (Eastport is midway up the Gulf of Maine/Bay of Fundy, at the head of which there are 11.6 m-cm (38-ft) mean tidal ranges.). The highest observed water levels have occurred during storms and hurricanes, which can add several feet to the tidal high water.

In trying to assess the impact of these different sea level phenomena on the coast one must also consider the duration of maximum conditions and the intensity of accompanying phenomena, such as waves. The long-term trend in sea level is much smaller than other sea level signals, but these other signals do oscillate and only reach there maximums for finite time periods. During hurricanes and extratropical storms the highest water levels are much greater than those expected for centuries of sea level rise, but their effects may last only for a several days and include only a few tidal high waters. However, it is during these storms that one sees the greatest wave action and the combination of high water levels and the larger waves usually leads to the greatest coastal erosion. This would lead one to believe that the effect of global warming on the frequency and intensity of storms should be just as important as its effect on sea level (although probably even more difficult to predict). For seasonal and interannual sea level variations the duration of the higher water level will be on the order of months to years and so will be long enough to have significant effects on coastal erosion, inundation, wetlands, and saltwater intrusion into groundwater.

ACKNOWLEDGEMENT

The author wishes to thank Stephen Gill and the members of the Tidal Analysis Branch of the Office of Ocean and Earth Sciences in the National Ocean Service, NOAA, (who processed and quality controlled the water level data analyzed for this paper) and especially Leonard Hickman, who maintains the NOS monthly mean sea level database.

REFERENCES CITED

Davis, G.H., 1987, Land subsidence and sea level rise on the Atlantic coastal plain of the United States: Environ. Geol. Water Sci., Vol. 10, No. 2, pp 67-80.

Emery, K.O. and David G. Aubrey, 1991, Sea Levels, Land Levels, and Tide gauges: Springer-Verlag, New York, 237 pp.

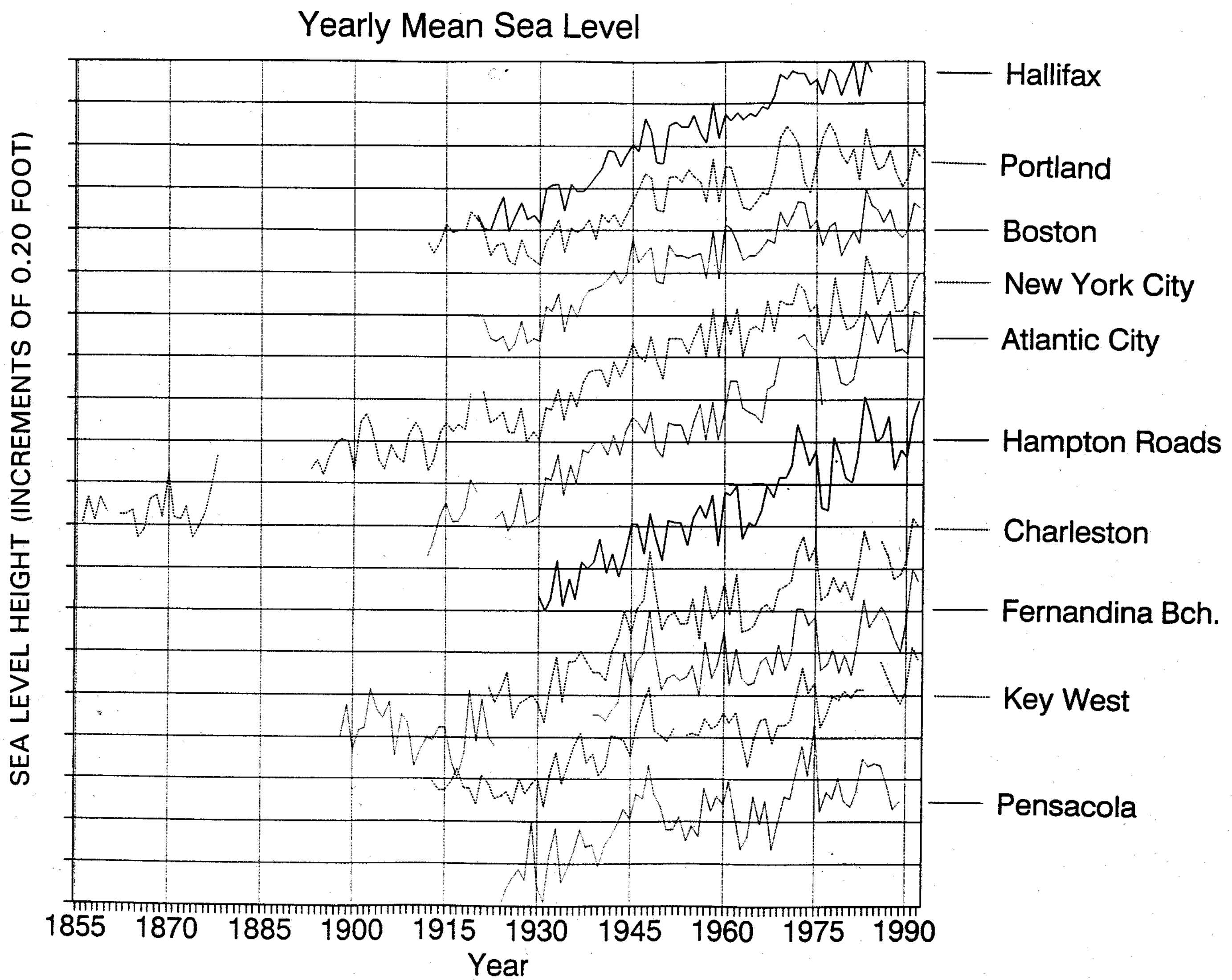

Figure 3.The variation in mean yearly sea levels at 10 stations along the East Coast of the U.S., including Halifax (Canada), Bermuda, and the Florida Gulf Coast up to Pensacola for the time period of their installation. (Increments along the veritcal axis are 0.2 foot; values are also given in cm in the text.)

Chelton, Dudley B. and David B. Enfield, 1986, Ocean Signals in tide gauge records: Journal of Geophysical Research, vol. 91, No. B9, pp. 9081-9098.

Douglas, Bruce C., 1991, Global sea level rise: Journal of Geophysical Research, vol. 96, No. C4, pp. 6981-6992.

Gornitz, Vivien, 1991, Global coastal hazards from future sea level rise: Paleogeography, paleoclimatology, paleoecology (Global Planetary Change Section), Vol. 89, pp 379-398.

National Research Council, 1987, Responding to Changes in Sea Level: Committee on Engineering Implications of Changes in Relative Mean Sea Level, National Academy Press, Washington, D.C., 148 pp.

Noble, Marlene A. and Guy R. Gelfenbaum, 1992, Seasonal fluctuations in sea level on the South Carolina shelf and their relationship to the Gulf Stream: Journal of Geophysical Research, vol. 97, No. C6, pp. 9521-9529.

Parker, Bruce B., 1991, The relative importance of the various nonlinear mechanisms in a wide range of tidal interactions, In: Tidal Hydrodynamics, Bruce B. Parker (Ed.), John Wiley & Sons, Inc., New York, pp 237-268.

Parker, Bruce B., 1991, Sea level as an indicator of climate and global change: The MTS Journal, Vol. 25, No. 4, pp 13-24.

Parker, Bruce B., 1992, The use of long historical sea level records in the study of climate and global change: Proceedings, MTS'92: Global Ocean Partnership, Vol. II, pp 498-506, Washington, D.C., October 19-21, 1992.

Sturges, Wilton, 1990, Large-scale coherence of sea level at very low frequencies, In: Sea Level Change. Geophysics Study Committee of the National Research Council, National Academy Press, Washington, D.C., pp 63-72.

STATE-OF-THE-SCIENCE: STORM CLIMATOLOGY

Robert E. Davis
Department of Environmental Sciences
University of Virginia
Charlottesville, Virginia 22903

ABSTRACT

While hurricanes have garnered a substantial amount of scientific attention because of their destructive potential, winter extratropical storms, or nor'easters, may have a greater impact on the coastline. A climatology of nor'easters is developed by identifying each storm from 1942-1991 that produced at least 1.5 m deep-water waves at Cape Hatteras, North Carolina. A five-category classification is produced based upon a wave power index for each storm. Though overall storm frequencies were below average in the 1980s, the number of strong storms (Classes IV and V) was very high. Most nor'easters that produce the highest waves form over Florida or north of the Bahamas, travel northward, and are blocked by a high pressure system over the Atlantic.

INTRODUCTION

Coastal storms are a primary contributor to changes along the Atlantic coastline. Though most storms have little impact other than minor beach erosion, single extreme events, including strong hurricanes and powerful nor'easters, can deliver more wave energy to a coast than the average accumulated energy over the course of eight months (Dolan et al., 1990). These powerful storm systems often produce extreme erosion, overwash, and structural damage, and are occasionally responsible for the formation of new inlets and channels.

HURRICANES AND NOR'EASTERS

Because of their high wind speeds and the accompanying storm surge, hurricanes have a substantial impact near the point of landfall. However, winter extratropical storms, referred to as nor'easters along the east coast of the United States, are often responsible for significant coastal change along a much longer portion of the coastline. Nor'easter winds are almost always weaker than those of minimal hurricanes, but because of their large size and potential for long durations, high waves from a single nor'easter can occasionally affect several thousand kilometers of coast.

Apart from their potential to cause coastal change, tropical cyclones (both tropical storms and hurricanes) and nor'easters are markedly different types of systems. Tropical cyclones are smaller, meso-scale low pressure systems about 500 km in diameter while most nor'easters are synoptic-scale cyclones that can be as large as several thousand kilometers. Windspeeds in a minimal hurricane are at least 32 ms-1 while sustained nor'easter winds rarely exceed 25 ms-1. Tropical cyclones are "warm-core" systems which derive their energy from latent heat of evaporation from the warm ocean surface, which is converted into sensible heat energy through condensation in deep, cumulus clouds that surround the eye of the storm. Because of their dependence upon warm ocean temperatures for formation and sustenance, tropical cyclones are most common in August and September when the subtropical Atlantic is warmest. Tropical storms and hurricanes form over the open ocean, and typically travel in the northeast trades toward North America before curving toward the northeast as they become embedded in the mid-latitude westerlies. Conversely, nor'easters are "cold-core" cyclones that increase in intensity with height. The strongest nor'easters form in conjunction with a well-developed jet stream which removes air from above the low, thus causing the surface pressure to decline and increasing the surface winds. Unlike tropical cyclones, nor'easters do not necessarily form over water, although many storms form in the Gulf of Mexico or off the U.S. east coast. However, some nor'easters begin their life cycle as mid-latitude cyclones that originate to the lee of the Rockies in Colorado or Alberta. Because nor'easter formation is dependent upon the jet stream, these storms are most common in winter when the jet is strongest and is positioned farthest south over North America.

Owing to their destructive potential, a great deal of scientific research has been devoted to hurricanes and their impacts. Substantially less is known about nor'easters, however. The purpose of this paper is to briefly summarize the climatology of nor'easters.

DEVELOPMENT OF A NOR'EASTER CLIMATOLOGY

The lack of consistent buoy measurements of wave heights and periods for a long time period makes the development of a nor'easter climatology a formidable task. Fortunately, it is possible to extract wave information from surface wind fields, which can be derived from historical surface pressure maps. Using the Sverdrup, Munk, and Bretschneider wave hindcasting method (Leenknect et al., 1992), the significant wave height (H1/3) and duration were computed for each nor'easter from July, 1942 through June, 1992 for Cape Hatteras, North Carolina. A total of 1564 storms were identified over this time period. A nor'easter was classified if its significant wave height reached at least 1.5 m, since field evidence indicates that deep-water waves less than 1.5 m have no impact upon mid-Atlantic barrier islands (Dolan et al., 1988). Thus, the duration of each storm was determined by the period of time in which at least 1.5 m deep-water waves were present at Cape Hatteras. Tropical cyclones were excluded from the data set, but high pressure systems were included if they produced high enough waves.

A combination of factors are necessary for the generation of high waves. One critical ingredient is the storm's fetch--the distance of open ocean over which the winds are blowing. Thus, stationary or slow-moving storms with moderate wind speeds generate much higher waves than fast-moving storms with stronger winds, since in the latter case the fetch is changing rapidly. Therefore, the storm's track is very important in determining the fetch and, ultimately, the wave heights.

THE DOLAN-DAVIS NOR'EASTER INTENSITY SCALE

The windspeed-based Saffir-Simpson Scale has been commonly-used to describe the intensity of hurricanes since the 1970s (Simpson, 1971; Saffir, 1977). While a few similar scales do exist for nor'easters, they are based on windspeed, a variable that is not always closely coupled with the height of waves reaching the coastline. Using information from the nor'easter data base, Dolan and Davis (1992) developed a Nor'easter Intensity Scale based upon a wave power index, which was calculated for each storm by multiplying the square of the significant wave height by the duration. Each storm was classified into one of five categories based upon its power index (Table 1). On the Dolan-Davis Scale, 75 percent of all storms are in Classes I and II, which have significant wave heights < 3 m and durations < 30 hours. The more powerful Class IV and V storms comprise only 3 percent of the data set, and only eight Class V storms occurred over the 50-year period of record. Based upon preliminary research, a table has been developed relating likely coastal impacts to the Dolan-Davis index (Table 2). Impacts from an individual storm will vary substantially locally depending upon bathymetric characteristics and astronomical tides, however. Class I nor'easters have little impact beyond minor beach erosion, while Class V nor'easters cause extensive loss of structures at the community scale and significant alterations in the physical characteristics of the coastline (Dolan and Davis, 1992).

Table 1. Wave characteristics of the five nor'easter classes in the Dolan-Davis intensity scale. The power index (P) is defined as the significant wave height squared times the duration. The mean and standard deviation are represented by $\overline{X}$ and s, respectively.

Storm Class		Frequency N	Frequency %	Sig. Wave Height (m) $\overline{X}$	Sig. Wave Height (m) s	Duration (hr) $\overline{X}$	Duration (hr) s
I	Weak	786	50.3	2.0	0.3	8	4.4
II	Moderate	393	25.1	2.5	0.5	19	7
III	Significant	338	21.6	3.2	0.7	35	17
IV	Severe	39	2.5	5.0	0.9	62	25
V	Extreme	8	0.5	6.8	1.3	97	44

Storm Class		Power Index (m^2hr) $\overline{X}$	Power Index (m^2hr) s	Range (m^2hr)	Range (ft^2hr)
I	Weak	32	20	P≤71.63	P≤771
II	Moderate	107	26	71.63<P≤163.51	771<P≤1760
III	Significant	384	179	163.51<P≤929.03	1760<P≤10,000
IV	Severe	1420	372	929.03<P≤2322.58	10,000<P≤25,000
V	Extreme	4332	2278	P>2322.58	P>25,000

Table 2. Hypothesized relationships between the Dolan-Davis storm class and coastal damage.

Storm Class	Beach Erosion	Dune Erosion	Overwash	Property Damage	Mean Wave Ht. (m)	Mean Duration (hr)
Class I (weak)	Minor changes	None	No	No	2.0	8
Class II (moderate)	Modest: mostly to beach	Minor	No	No	2.5	18
Class III (significant)	Erosion extending across beach	Significant	No	Modest	3.2	35
Class IV (severe)	Severe beach erosion and recession	Severe dune erosion or destruction	On low profile beaches	Loss of structures at community scale	5.0	62
Class V (extreme)	Extreme beach erosion	Dunes destroyed over extensive areas	Massive in sheets and channels	Extensive regional scale losses in millions of dollars	6.8	97

50-YEAR TRENDS IN STORM FREQUENCY

The 50-year time series of nor'easters exhibits several significant changes in storm frequencies (Figure 1). Nor'easters were most common in the 1950s and early 1960s but declined precipitously from 1965 to 1975. Over the last 15 years, the number of storms has increased slightly, but not to 1950s levels. The time series for Class IV and V nor'easters is poorly correlated with the overall time series, however (r=0.11). During the late 1960s, when overall storm frequencies declined, the number of major nor'easters reached the 50-year maximum. During the decade beginning in the 1963-64 storm year (July, 1963 through June, 1964), at least one Class IV or V storm occurred in nine of the ten years. Of the eight Class V storms in the record, seven occurred since 1960. Furthermore, we are currently experiencing a period of strong storms that is comparable to the late 1960s peak. In recent years, major nor'easters included a March 1989 storm noteworthy for its exceptionally long duration (115 hours) (Dolan et al., 1990), an October, 1990 event that drove a ship into the Bonner Bridge, effectively isolating Hatteras Island from the mainland, and the 1991 Halloween Storm that had an extremely large fetch and caused extensive damage along the entire east coast of the United States (Davis and Dolan, 1992). One of the most powerful storms in history occurred in December, 1992, but it has not yet been incorporated into our data set.

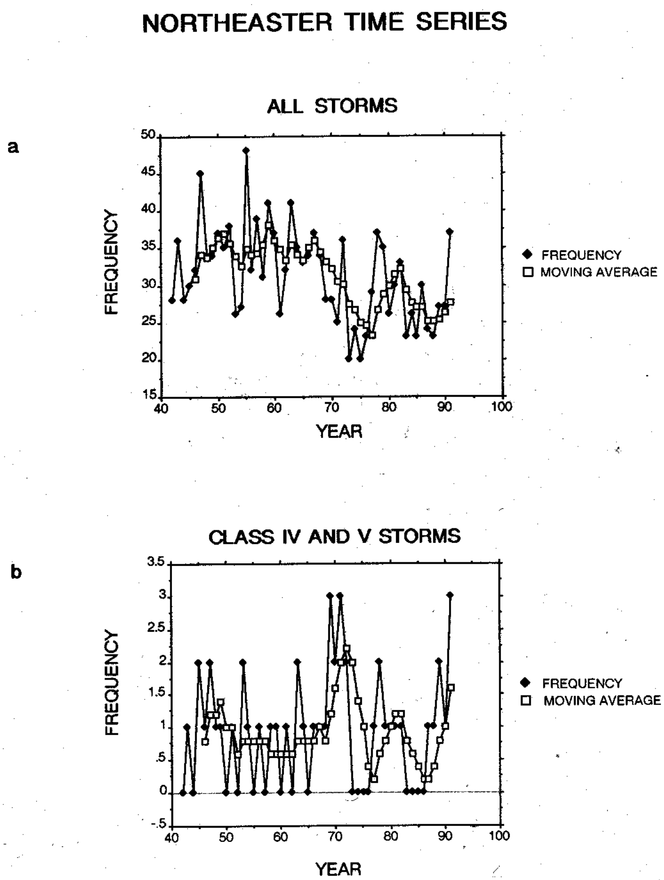

Figure 1. Time series of northeaster frequencies at Cape Hatteras, North Carolina for each storm year (July through June) from 1942-1991. A five-year moving average is superimposed and each datum is aligned with the last year in the five-year period. These graphs depict the time series for all nor'easters (a) and for Class IV and V storms only (b).

STORM TRACKS AND WAVE CLIMATES

To further investigate the relationship between storm tracks and their associated wave heights and coastal impacts, a synoptic climatology of nor'easters was developed (Davis et al., 1993). This involved classifying each storm into one of eight categories based upon its point of origin and track. The eight classes, ordered from highest to lowest wave height, are:

Bahamas Lows--storms which form over the open ocean north of the Bahamas and track northward;

Florida Lows--systems which form over Florida or off Florida+s east coast and track to the north;

Gulf Lows--storms which develop in the Gulf of Mexico, often along a stationary front, and move to the northeast, often through Georgia, and re-intensify over the Gulf Stream;

Coastal Plains Cyclogenesis--a rare class of storms that form over the piedmont or coastal plain and quickly move out to sea toward the east or northeast;

Hatteras Lows--these nor'easters form as secondary cyclones off the Atlantic coast in the vicinity of Cape Hatteras, which is a common spawning ground for winter storms;

Continental Lows--major storm systems which form over Colorado or Alberta and travel east. High waves occur after the trailing cold front passes through Cape Hatteras and the low becomes stalled over the open ocean (e.g., the Halloween Storm of 1991);

Coastal Front--lows which form along a stationary front usually oriented parallel to the East Coast; and

Anticyclones--slow-moving high pressure systems located over the northwest Atlantic with winds strong enough to produce high waves at Cape Hatteras.

Bahamas and Florida Lows have the highest average wave heights of the eight groups (Table 3). The northward movement of these cyclones is often blocked by a high pressure system to the north, either over New England and southeastern Canada or the open Atlantic. As the storm approaches the high pressure system, the pressure gradient increases and the cyclone slows, causing wind speeds to increase and the fetch region to remain stable. Of the eight Class V storms that occurred over the last 50 years, six were classified as Bahamas or Florida Lows.

Table 3. Characteristics of the eight storm types. The mean, standard deviation, and sample size are represented by $\overline{X}$, s, and N, respectively.

Storm Type	Frequency		Sig. Wave Height (m)		Duration (hr)		Power (m^2hr)	
	N	%	$\overline{X}$	s	$\overline{X}$	s	$\overline{X}$	s
Bahamas Low	69	4.4	3.1	1.3	35.6	29.4	530.3	854.1
Florida Low	153	9.8	3.1	1.2	29.6	26.8	450.5	953.3
Gulf Low	220	14.1	2.8	1.0	16.0	12.3	175.0	271.2
Coastal Plain Cyclo.	77	4.9	2.4	0.7	14.6	12.1	121.3	221.9
Hatteras Low	259	16.6	2.4	0.8	14.8	13.1	138.4	305.2
Continental Low	192	12.3	2.4	0.7	13.7	13.6	108.1	239.3
Coastal Front	317	20.3	2.3	0.6	16.0	13.7	115.2	163.4
Anticyclone	277	17.8	2.1	0.5	18.7	15.8	103.4	125.9

CONCLUSIONS

Although this research has added to the existing knowledge base of nor'easters, a substantial amount of work remains. A top priority is the development of similar data bases for various coastal locations. While preliminary research indicates that this climatology is applicable throughout the mid-Atlantic region for the stronger storms (Classes III, IV, and V), a comprehensive data base for several sites in New England and the mid-Atlantic coast would be invaluable in assessing historical changes in coastline position and climatic variability. Furthermore, additional research is needed to link nor'easter frequencies to changes in mid-latitude circulation and jet stream characteristics, as well as the development of a nor'easter watch/warning system by coupling climatological data with output of numerical weather forecast models.

REFERENCES CITED

Davis, R.E., Dolan, R. and G. Demme, 1993: Synoptic climatology of Atlantic coast north-easters. International Journal of Climatology, v. 13, p. 171-189.

Davis, R.E. and R. Dolan, 1992: The -All Hallows+ Eve+ coastal storm--October 1991. Journal of Coastal Research, v. 8, p. 978-983.

Dolan, R. and R.E. Davis, 1992, An intensity scale for Atlantic coast northeast storms: Journal of Coastal Research, v. 8, p. 840-853.

Dolan, R., Inman, D.L. and B.P. Hayden, 1990, The Atlantic coast storm of March 1989: Journal of Coastal Research, v. 6, p. 721-725.

Dolan, R., Lins, H. and B.P. Hayden, 1988, Mid-Atlantic coastal storms: Journal of Coastal Research, v. 4, p. 417-433.

Leenknect, D.A., Szuwalski, A., Sherlock, A.R., and M.E. George, 1992, Automated Coastal Engineering System (ACES): U.S. Army Corps of Engineers, Coastal Engineering Research Center.

Saffir, H.S., 1977, Design and construction requirements for hurricane resistant construction: American Society of Civil Engineers, Preprint Number 2830, p. 20.

Simpson, R.H., 1971, A proposed scale for ranking hurricanes by intensity: Minutes of the Eighth NOAA, NWS Hurricane Conference, Miami, Florida.

STOCHASTIC HYDROLOGY FOR ENGINEERS

Saleh M. Bille
King Saud University
Riyadh, Saudi Arabia

ABSTRACT

A set of varves considered over a certain period of time is called a time series. Chemical varve time-series provide an excellent record of climatic variation with time. They reflect seasonal changes in temperature and precipitation rates. Two examples, one from the Delaware Basin in Texas and New Mexico, and the other from the Greenland icecap revealed a climatic history of meteorological time-series sensitive to temperature and precipitation factors. The laminations constitute a natural "time clock" for studying thickness and compositional variations in these varve time-series. They also facilitate sampling and analysis on a quantity per unit-time basis in order to determine the rates of precipitation and shifts in the rate of deposition of chemical and clastic components, trace elements, organic matter, isotopic changes, water budget, and a host of related processes operating within and outside the water-varve system. Dating of each ice or salt layer (like growth rings on a tree), and analysis of oxygen-isotope ratio, trace element content, and other analyses enabled us to chart yearly variations in weather. Testing of the varving process in relation to seasonal evaporation, periodic storms or precipitation enabled us to reconstruct the sedimentary environments and ancient ecosystems of a climatic history dating back 100,000 years on the Greenland icecap, 265,000 years in southeastern New Mexico, and almost 200 million years ago in west Texas.

INTRODUCTION

Stochastic hydrology plays an important role during decision-making in response to changes in critical operating variables such as temperature and precipitation. Planning a stochastic control scheme over future months and years involves anticipating, or forecasting, the future levels of these and other variables. Interpreting the changes in variables that influence hydrologic processes - such as climatic effects or other environmental relationships - can be significant in this planning process. For mathematical convenience, a time series is assumed to extend to infinity in both past and future time; therefore it may be express in the form:. . . , x_{-2}, x_{-1}, x_0, x_1, x_2,. . . If it is positive, the subscript on any x signifies the number of time units in the future; if it is negative, it signifies the number of time units in the past. A set of random variables such as this is called a stochastic process. Thus, a numerical function of time X(t) measured at discrete time $t = 0, \pm1, \pm2, \ldots$ is called a time series. Stochastic hydrology creates a time series which is treated as a set of random variables that possess certain probability properties.

This paper explores global trends in temperature and precipitation as related to the evolution of the atmosphere and hydrosphere. The purpose is to select or visualize how climatic cycles in varved sediments and features of sedimentary rocks may provide clues to future weather prediction.

VARVE TIME-SERIES

A varve is a pair of contrasting laminae produced by seasonal climatic changes. Typically, they are a summer (light) and winter (dark) band within a single year, resulting in sequence of seasonal cycles. The thickness of varves as a function of time measured at yearly intervals for N years may be expressed as observations X(1), X(2), . . ., X(N) from a hypothetical time series of varve thicknesses extending regressively into the infinite past and progressively into the infinite future. For such a series, the quantity or (the total power),

$$\sigma^2 = \lim_{T \to \infty} \frac{1}{2T} \sum_{t=-T}^{T} X^2(t)$$

when it exists, represents the mean square amplitude or power of the series (Anderson and Koopmans, 1963).

Varves are found in different environmental settings, and the climatic parameters can be derived from them in different ways. Temperature sensitive varves (glacial and evaporite) have the strongest long-term thickness. Evaporite varves appear to be the most sensitive to changes in temperature and the best modulated to quantitative analysis. Their seasonal organic lamina, in the form of sapropel or bituminous material, alternating with other constituents of the varve (calcite, anhydrite, halite) imply that the hydrologic processes controlling the depositional cycles are intimately related to climate. Climatic oscillations are droughts, floods, advance or retreat of glaciers, and other changes in various geophysical phenomena. These changes may have a cyclic pattern of varying amplitude. These range from short-term time spans such as decades or centuries, to long-term trends, such as millennia or hundreds of millions of years. The climate of the earth has varied from warm and hot tropical regimes to ice ages with various degrees of changes between these extremes (Fig. 1). Models of climatic cycles of different wave-lengths and amplitudes, exhibiting both deterministic trends and stochastic or random oscillations, have contributed much in developing solutions to engineering and water resources problems.

GEOPHYSICAL EXPLORATION

Correlations of gamma ray and sonic logs, which measure variations in acoustical and various radioactive properties of the formations penetrated by the bore-hole, were made on the Castile Formation within the Delaware Basin. These can now be correlated with the master core and the strata between boreholes (Fig. 2).

CHEMICAL VARVES

A varve time series for the entire Castile Formation (Upper Permian) in the Delaware Basin of Texas and New Mexico has been defined as the standard section. It has been subdivided into eight subsurface members by correlation between gamma ray and sonic logs of Union-University well (Fig. 2). A prominent oscillation of about a 2000-year cycle of wet and dry seasons is preserved in the Permian Basin for a 265,000 year period, almost 200 million years ago. The standard time-series for the Castile Formation usually have been in the form of bed thickness versus depth, stratigraphic interval, or time in years for varved sequences (Fig. 2). Correlation of cores from different localities with the "master" or "type" time series for the basin is done by direct visual comparisons of laminations. Where a correlation is known to exist but cannot be located visually, the sliding method will extend the range of correlation by decoding the same number of laminae in each series. Correlation coefficients between stratigraphic sequences in different localities are programmed in a computer in order to determine the type of association between the time series in various sequences in the basin.

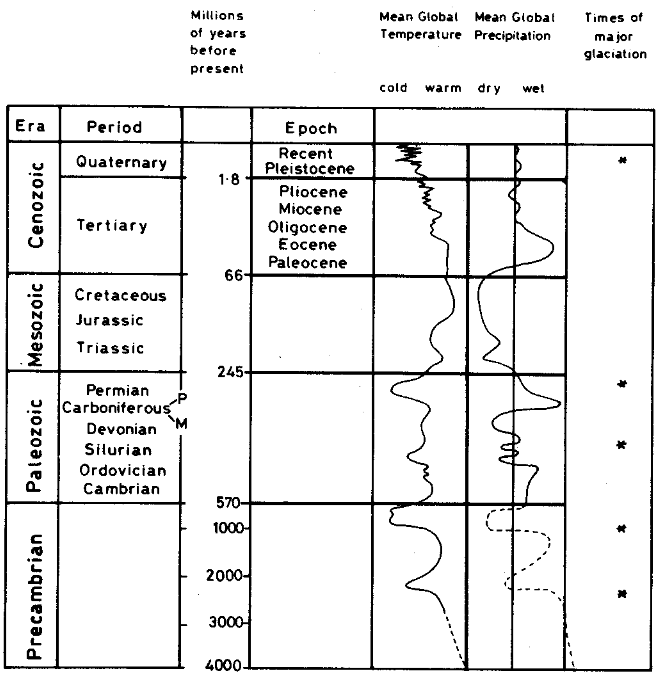

Figure 1. Geologic time chart showing trends in mean global temperatures and precipitation.

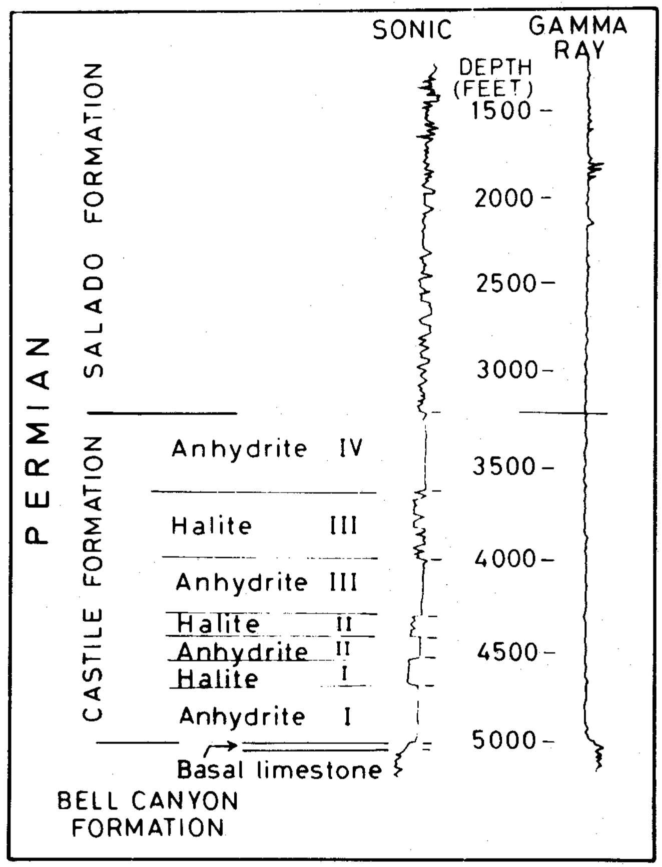

Figure 2. Gamma ray and somic logs of Union-University well depicting members of the Castile Formation.

VARVES FROM GREENLAND ICE CORES

Measurement of seasonal oscillations in O^{18} content within the annual layers of ice in Greenland showed long-term variations in the isotopic composition of the ice. This reflects the climatic changes during the last glaciation with oscillation periods of 120, 940, and 13,000 years. Recent dating and studies of marine sediments have indicated that four major glaciations in the Pleistocene have strong cyclic patterns of glacial/interglacial events, and that each cycle persists for about 100,000 years. Paleo-temperatures in the Camp Century ice core as documented by O^{18} give us an accurate account of Greenland's weather (Dansgaard and others, 1969). Abundant oxygen 18 in a sample indicates a warmer climate. Relatively lower quantity means a colder climate. It was found that 900,000 years ago Greenland was warming, and that a cooling trend less than a century old has resulted in the present severely cold weather. It apparently took a thousand years for the earth to return to warm weather as indicated by the oxygen 18 level. The level has been diminishing in Greenland's ice since 1930. Projecting the established weather pattern, it is predicted that temperatures in the Northern Hemisphere will continue to drop for 25 years before a warming trend sets in.

CYCLE STRATIGRAPHY

The intricate connection between the earth's environments, their solar energy inputs, and the evolving climate is of great interest to practicing water resources hydrologists and engineers. Analyses of data from marine sediments and ice cores using combined deterministic-stochastic models may serve as a useful means in predicting climatic trends and cycles on earth (Bille, 1982). Cycles found in the rock record generally are related to eustasy or climatic effects or both and to tectonics (Borer and Harris, 1991). The presence of climate driven cycles in the laminated marine evaporites of the Castile Formation of Texas and New Mexico is due to short-term stochastic processes and a long-term deterministic response to orbital effects (Bille, 1986). Information compiled on the average period of cyclic bedding indicates that bedding cycles commonly fall within the Milankovitch range (Anderson, 1986). Changes in seasonality, mainly through albedo effects, may explain the apparent correlation between Milankovitch cycles and glaciation. Astronomic cycles cause various hydrological series to be periodic, merely as diurnal and annual cycles. At certain northern latitudes, the Milankovitch effect suggests that ice ages are expected when the total solar radiation for the half-year that contains spring and summer is at a minimum. Young ocean sediments have cycles of 23,000, 42,000, and 100,000 years, similar to Milankovitch cycles. Probably, the Milankovitch mechanism has operated throughout geological time, although glaciations did not appear in the past at regular intervals predicted by Milankovitch. For example, no glaciation has been found during the Mesozoic, one of the warmer eras. This implies that the Milankovitch effect does not cause ice ages but can set off cyclic glacial and interglacial activity if other factors have resulted in a cooling trend over much of the globe.

APPLIED HYDROLOGY

Weather is the state of the atmosphere at a given time and place, described by temperature, moisture, cloudiness, wind velocity, and pressure. Climate is the history of the prevailing or average weather conditions of a region, as determined by temperature and meteorological changes over a period of years. Weather is a tangible event, climate is statistical and consists of numerical data from weather records over a long period of time. Climatic regions result from the interaction of energy and moisture patterns of the water cycle (Bille, 1993). Climate at any locality is controlled by its latitude, physiographic features such as oceans and continents, general atmospheric circulation, and local geographic features such as large lakes and altitude.

GLOBAL CLIMATES AND WATER RESOURCES

Statistical properties of hydrologic time series should be appraised from much longer records than are presently accessible for hydrologic exploration and research. The control scheme on the time series generally projects climatic cycles approaching 10, 50, 100, 1000, and even 10,000 years in response to deterministic stratagems. A variety of evidence shows at least five periods of major global glaciation. These ice ages appeared at intervals of approximately 300 million years and each ice age lasting for several million years. The first and second of these major ice ages occurred some 600 million years ago, and some 250 to 300 million years ago, in the Proterozoic, and Permo-Carboniferous Periods respectively. The third major ice age began about 2 million years ago in the Tertiary Period and has continued to the present. Exponential trends in mean global temperature and precipitation through geological time demonstrate that the times of major glaciation coincide with low temperatures and with precipitations either close to that of the present or drier (Frakes, 1979). The time scale of millions of years shows a series with a consistent moderate upward trend and a very notable and regular seasonal pattern demonstrating that much of the last 200 million years has been relatively warm.

CONCLUSIONS

The entire earth climate system is dependant on energy from the sun as it powers the water cycle. The pattern resulting from the unequal distribution of energy and moisture over the earth's surface produces a climatic region. Climate is never constant but changes daily, seasonally and yearly. The time-series of climatic cycles oscillate at approximately short-term stochastic or random frequencies and long-term deterministic trends of different wavelengths and amplitudes. According to the Milankovitch astronomic theory, cyclical climatic changes that brought on the great ice age are due to the periodic differences in the position of the earth relative to the sun. Climatic cycles found in deep-sea cores extending back for about 0.5 million years show striking correlation with Milankovitch cycles. Also, the varve time-series from the Permian Castile Formation and the Camp Century Pleistocene ice core generally document climatic oscillations of approximately 120, 940, and 13,000 years, comparable with climatic changes in other parts of the world. The optimal control on future change consists of a call for deterministic planning and a stochastic stabilization approach when using our climate-sensitive water resources.

ACKNOWLEDGMENTS

The presentation of this paper at the AAPG 1993 Eastern Section Meeting was subsidized by King Saud University, Riyadh, Saudi Arabia.

REFERENCES CITED

Anderson, R.Y., 1986, The varve microcosm: propagator of cyclic bedding, Paleooceanography, v.1, no. 4, p. 373-382.

Anderson, R.Y., and Koopmans, L.H., 1963, Harmonic analysis of varve time series, Journal Geophysical Research, 68, 877-893.

Bille, S.M., 1982, Hydrologic and weather record from chemical varve time-series, theme 6: Low temperature geochemistry, IAS abstracts of papers, 11th International Congress on Sedimentology, McMaster Univ., Hamilton, Ontario, Canada, p. 15.

Bille, S.M., 1986, Chemoclines in the Castile Formation, Delaware Basin, Texas and New Mexico, Transactions, Annual Conference Southwestern Section American Association of Petroleum Geologists, New Mexico Bureau of Mines and Mineral Resources.

Bille, S.M., 1993, Hydrogeology of the Arabian Peninsula, Contributed paper (poster sessions), AAAS, abstracts of papers, ann. meeting, 11-16 February, Boston, Mass., USA.

Borer, J.M., and Harris, P.M., 1991, Lithofacies and cyclicity of the Yates Formation, Permian Basin: implications for reservoir heterogeneity, American Association of Petroleum Geologists Bulletin, v. 75/4 p. 726-779.

Danagaard, W., Johnson, S.J., Meller, J., 1969, One thousand centuries of climatic record from Camp Century in the Greenland ice sheet, Science, v. 166, 17 October, p. 377-381.

Frakes, L.A., 1979, Climates throughout geologic time: Amsterdam, Elsevier, 310 p.

SHORELINE MANAGEMENT AND POLICY: THE INFLUENCE OF SCIENCE AND SCIENTISTS ON COASTAL EROSION POLICY INNOVATION

Mark Meo, Robert E. Deyle* and Thomas E. James
Science and Public Policy Program
University of Oklahoma
*Department of Urban and Regional Planning
Florida State University

ABSTRACT

Shoreline management and policy are beset by conflicting arguments over the most socially responsible course of action for government to take. Among the central features of this debate are the roles of scientific knowledge in shaping policy alternatives and in influencing the policy change process. This paper explores the dimensions of coastal erosion policy change through case studies of how scientific and technical information was acquired and used by policy entrepreneurs in key policy innovations in Florida, Massachusetts, and North Carolina over the last three decades. The research focus is on the role of science and scientists in the long term policy shift away from the use of fixed structures to stabilize the coast toward nonstructural alternatives and retreat (e.g. setback) strategies. The findings suggest that the states have had to make a substantial commitment to acquiring and utilizing coastal science in order to develop and maintain a proactive posture toward erosion policy reform. As part of that process, scientific knowledge has been used instrumentally (in decision making), conceptually (for enlightenment), and symbolically (to legitimize existing decisions). Additionally, the research lends support to the view that policy entrepreneurs, in tandem with credible scientists, are critical to motivate innovations in erosion policy, and that acute geophysical phenomena such as hurricanes and coastal storms are important strategically for opening policy "windows" through which innovations can be mobilized. Beyond shoreline management, these findings have implications for global change science and policy more broadly.

INTRODUCTION

Coastal erosion of settled shorelines has long confronted planners and managers responsible for rational resource conservation with a public policy dilemma. While the coast, especially the ribbon of sedimentary barriers lying along the Atlantic and Gulf margins, generally has been perceived as undergoing continuous reworking and shaping by wind and waves, scientific understanding or appreciation of the fundamental processes in motion often has been neglected or poorly integrated with land use practices. Rather, the constantly changing shoreline has been subjected to a history of human action marked by ambitious attempts to control the ocean's influence on the coast. It was not until the 1960s, when the intensity of coastal development escalated substantially, that recognition of unanticipated environmental impacts, amplified by notable failures in erosion control technologies, led to a reappraisal of coastal erosion management strategies that is still ongoing (National Academy of Science 1990).

Scientific understanding of coastal processes and the effect of structures built on the shoreline has become important to decision makers for a variety of reasons, including: (1) the incomplete understanding of fundamental erosion processes; (2) the need to accommodate growing coastal development and concomitant demands for protecting private property against hazards; and (3) the growing discontent with federal, state, and local government approaches to state coastal erosion management (Nordstrum 1987; Godschalk et al. 1989; Pilkey and Neal 1992). So intense is the current debate between advocates of the primacy of property rights and those advocating less risky shoreline development policies, however, that the specific pathways by which technical information has been utilized by policy entrepreneurs to effectuate substantive change over the last few decades have become less clear. Some critics, such as Platt et al. (1992), have argued persuasively that progress in shoreline management has become bogged down in a maze of ineffective or conflicting regulations, counterproductive incentives, and political myopia. Thus, a retrospective assessment of the process of shoreline policy change may provide useful insights into how strategic policy innovations that overcome existing impediments and inertia can be designed and carried out.

Though long term policy changes may evolve over one or more decades, discrete changes often are catalyzed in the short term by events that provide a "window" through which entrepreneurial change agents can mobilize innovations (Kingdon 1984). Some innovations may occur relatively quickly with little time for analysis (acute innovations), while others may require substantially more time to bring to fruition. These latter innovations are "incubated" in the sense that new ideas and issues are subjected to greater analysis and refinement until more favorable political circumstances arise (Kingdon 1984; Polsby 1984). In coastal policy, climatic events such as coastal storms and hurricanes, in addition to social and political phenomena, frequently have provided policy entrepreneurs with strategic opportunities to initiate innovative changes in erosion management (Deyle et al. 1994). Even though Congress failed to enact reforms to the National Flood Insurance Program last year, renewed efforts are expected to benefit from such events as the arrival of a Democratic president, taxpayers' growing weariness with fiscal inefficiency, and the destructive storms that swept over the East Coast in late 1992 and early 1993 (Millemann 1993). Hence, understanding how coastal science has been effectively woven into policy innovations over the last several decades should prove useful for designing more effective shoreline management strategies in the future.

In this paper we explore several aspects of coastal erosion policy that address the relationship of scientific understanding of coastal processes to strategic policy innovations in shoreline management in Florida, Massachusetts, and North Carolina. This discussion draws upon the formal and informal linkages between the federal and state governments through which scientific and technical information (STI) has been acquired and used by policy entrepreneurs to reorient coastal erosion policy from dependence on structural stabilization techniques toward greater reliance on nonstructural approaches and retreat (e.g. setback) strategies. In the last few decades, each of the three states discussed here has pioneered innovative approaches in coastal erosion policy with explicit attention afforded to STI. Through case studies of their experiences with coastal erosion, one can better answer such questions as: What is the nature of the coastal policy change process and the policy entrepreneurs who shape it? How important was STI for shoreline policy change? Where did it come from? Who provided it? Was it used instrumentally (for making decisions), conceptually (for enlightenment purposes), or symbolically (to legitimize existing decisions) (Beyer and Trice 1982)? What organizational structures facilitated the application of STI in strategic policy innovations?

STATE COASTAL EROSION POLICY INNOVATIONS

FLORIDA

The basis for state government authority over the coast of Florida is the Swamp Land Act of 1850 (Act of Sept. 28, 1850, ch. 84, 9 Stat. 519, codified at 43 U.S.C.A. § 982-984, West 1986). This Act, written when the peninsula of Florida was still almost uninhabitable, transferred more than 20 million acres from the federal government to the state. The Florida Board of Trustees received the title to the land to reclaim and develop it, along with "limited public trust responsibilities" (Ansbacher and Knetsch 1989, 337). The Governor and Cabinet act as the Board of Trustees and the collegial head of the Department of Natural Resources (DNR). The Board votes on permits for all coastal erosion projects, including groins, jetties, beach nourishment, and armoring (Devereaux 1991). Two other agencies with duties related to coastal barrier island erosion are the Departments of Environmental Regulation (responsible for the state's Coastal Zone Management Program and coordinating with federal activities) and Community Affairs responsible for activities landward of the Coastal Construction Control Lines.

The effects of acute events (storms and hurricanes) and the leadership of key individuals inside and outside of government were major driving forces behind the development of coastal erosion policy in Florida. However, the use of STI and the influence of individuals from the scientific and engineering communities also were very important components of the policymaking process. As an example, this section will focus, for the most part, on the development of working relationships between individuals and units at the University of Florida and Florida State University and state government (primarily the Division of Beaches and Shores in the Department of Natural Resources and its predecessor organizations). STI has served instrumental, conceptual, and symbolic functions in Florida since the mid-1930s (Much of the early history of the influence of the scientific and engineering communities is summarized from James Balsillie's(n.d.) unpublished manuscript). Early studies into the mid-1950s were conducted by several groups, including the Federal Beach Erosion Board, the Division of Water Survey and Research of the State Board of Conservation, the Florida Geological Society, the University of Florida, and the U.S. Army Corps of Engineers. Topics included beach erosion, sand movement, the geology and physiography of the coastal environment, inlets, shore protection and preservation, and storm impacts. Most of these reports were descriptive rather than quantitative in their technical content.

The direct use and influence of STI began in the mid-1950s. In 1955, the Florida Legislature, through Senate Bill 631, provided a biennial budget of $25,000 to the Engineering and Industrial Experiment Station of the Department of Engineering Mechanics at the University of Florida to conduct a study and provide recommendations on the control of beach erosion. That same year, Per Bruun arrived at the University of Florida from Denmark. Bruun had experience with erosion problems in the "low countries" of Europe, and was an authority on coastal processes and model laboratory study procedures. He became the Director of the Coastal Engineering Laboratory (although it was not officially established until July, 1958). In 1957, the group issued its report, "Studies and Recommendations for the Control of Beach Erosion in Florida" (Bruun et al. 1957).

Bruun's interest and influence went beyond simply issuing the study report. In January, 1957, Bruun organized a meeting of representatives from government, academia, and the private sector to determine if there was sufficient interest to create an organization fashioned after the American Shore and Beach Preservation Association. Dean Joseph Weil, Director of the Engineering and Industrial Experiment Station at the University of Florida, and David Smith, also from the University of Florida and who served as Director of the state's Water Resources Control Commission and as a member of the Governor's Water Resources Study Commission, also were active participants. As a result of this effort, the Florida Shore and Beach Preservation Association (FSBPA) was established and held its first meeting on March 1, 1957.

A significant action as a result of the Association's first meeting was preparation of a bill to amend Chapter 253 of the Florida Statutes to create a state department charged with protecting beaches and shores from erosion and conducting research studies for this purpose. Also recommended was the establishment of a modern coastal engineering laboratory along with the required facilities and equipment to be located at the University of Florida (Florida Shore and Beach Preservation Association 1957 in Balsillie n.d., 6). In 1957, the legislature amended Chapter 253 and authorized the Governor and the Cabinet, as the Board of Trustees, to establish and maintain a Department of Beach and Shore Erosion. Although no department was established at that time, it became the conceptual ancestor to the current Division of Beaches and Shores.

In September of 1957, the Trustees provided $20,000 to the University of Florida, and in December a new 130-foot wind tunnel wave tank was dedicated. On July 1, 1958, the facility was officially dedicated as the Coastal Engineering Laboratory (shortly thereafter it became a separate department under the College of Engineering). These actions were the direct result of the efforts of the FSBPA which, in turn, was the result of Per Bruun's concern with Florida's beach erosion problem and his efforts to organize interests around this problem (Balsillie n.d., 6).

From 1958 to 1964, the Board of Trustees acted as final permit approval authority for construction of shore and coastal protection structures. The Coastal Engineering Laboratory (CEL) provided the technical erosion expertise and was the principal source of recommendations concerning erosion prevention alternatives and coastal construction regulation. During this time, the Trustees approved 73 permits with each permit application requiring a study and design recommendation(s) by the CEL. (Balsillie n.d., 7).

In 1963, the Legislature amended Chapter 370 to create the Division of Beaches and Shores (under the Board of Conservation). The legislation also provided for a funding mechanism, the Erosion Control Account, to be administered by the Division and used to conduct research and restoration projects. It also provided for continued technical consulting services to be provided by engineers at the CEL, including Bruun, Dr. James H. Purpura, and Dr. T.Y. Chiu. In the following years, the CEL continued to conduct studies funded by legislative appropriation to the Erosion Control Account. For example, with funding from the 1967-69 appropriation, research conducted by the Laboratory for the Division included an extensive hydrographic and sand tracing study along the Florida lower east coast (Carlton 1971). Thus, the CEL at the University of

Florida became the Department of Natural Resource's main supplier of scientific data on beach dynamics (Stephenson 1986, 6).

In 1970, the state of Florida began to enact a series of provisions which continue to evolve to this day, aimed at protecting the coastal environment and regulating the activities that can take place within it. STI has played a role in the development of these policies to varying degrees. In 1970, the legislature amended Chapter 161, F.S., to include section 161.052 establishing the "50-foot Setback Line." The amendment stipulated that no excavation or construction could occur within 50 feet of the mean high water line without a waiver or variance authorized by the DNR. Although it was not intended to be a prohibitive line, the 50-foot Setback Line was unpopular with Florida citizens who were reluctant to let the government--in the form of the Board of Trustees and the DNR--"take" their land (Bean 1991). The DNR was unhappy with the line as well; it was considered to be inadequate, inaccurately drawn across seasons, arbitrary with no scientific justification, and to be politically set in certain instances (Bean 1991; Chiu 1991; Devereaux 1991; Duden 1991). The Governor and Cabinet and DNR officials found themselves churning out variances by the hundreds each year (Stephenson 1986, 14). This was a policy that was politically acceptable (i.e., it could make it through the policymaking process) but did not consider input from the scientific community to any significant degree.

The 50-foot Setback Line was considered a stop-gap measure until a better technique for establishing the line could be developed (Duden 1991). James Purpura and William Carlton, Director of Beaches and Shores, lobbied to develop a more specific and scientifically-derived line (Balsillie n.d., 9). In 1971, the Legislature enacted Section 161.053, which called for the establishment of the Coastal Construction Setback Line (CCSL) to replace the 50-foot setback line. The line was to define an area within which variance had to be obtained for most construction activities, with the objectives of protecting beachfront property from storm damage and the beach and dune system from excessive erosion (Shows 1978). Rather than being a fixed distance from the mean high water line, for counties with sandy shorelines, the CCSL was to be determined from historical storm and hurricane tides, maximum wave uprush, shoreline morphology, erosion trends, and existing upland development. The lines only were to be established after comprehensive engineering study and topographic survey (Chapter 71-280, Laws of Florida, Chapter 161, Florida Statutes).

James Purpura and T.Y. Chiu of the University of Florida's Coastal and Oceanographic Engineering Department were contracted to provide recommendations as to the location of CCSLs. They worked closely with Carlton and William Sensabaugh at the Bureau of Beaches and Shores. The first line, for Martin County, was approved by the Governor and Cabinet in May, 1972, nine months after the effective date of the legislation, and the process continued until end of 1978. At that point, CCSLs had been established for 22 of the 24 counties involved in the program. Only Broward and Dade counties did not have CCSLs established before the program changed direction in 1978.

Although Beaches and Shores continued to work closely with engineers at the University of Florida to develop the CCSLs throughout this time period, in 1976 action was taken to institutionalize expertise within state government. The Bureau of Beaches and Shores, Setback Line Operation Section, was created and located in Gainesville (the home of the University of Florida). The personnel in the Section formerly were a non-professorial support group at the University of Florida in the Coastal and Oceanographic Engineering Laboratory. The new section was directed by William Sensabaugh with a charge to provide field data, analysis, and administrative support for CCSL establishment. Purpura and Chiu continued to make the final recommendations as to the location of CCSLs, and ninety-eight percent were accepted without changes (Chiu 1991).

In 1978 the legislature renamed the CCSL the Coastal Construction Control Lines (CCCLs) in order to eliminate the negative connotations of the word "setback," which land-owners interpreted as a restriction of their property rights. The statute stated that this line was not intended to "define a seaward limit for upland construction" and also changed the variance provision to an explicit permitting process (Section 5, Chapter 78-257, Laws of Florida). All the CCSLs drawn prior to 1980 were to be redrawn as CCCLS, and lines were to be established for Broward and Dade counties (which did not have CCSLs).

A more standardized and improved methodology for drawing the CCCLs generally is attributed to Chiu and Robert Dean, a highly respected coastal engineer in the Department of Coastal and Oceanographic Engineering at the University of Florida (see Chiu and Dean 1984). With the more sophisticated model, the new CCCLs have been located up to several hundred feet landward of the original lines (Schmahl and Heatwole 1989, 198). The legitimacy of the CCCL was challenged in the 1986 *Island Harbor Beach Club, Ltd. v. Department of Natural Resources* (495 So.2d 209), commonly referred to as the Charlotte County case. Prior to this decision, there was a 21-day waiting period after the CCCL hearing process, which left the record open for local government hearing officers to modify the scientific recommendations before they reached the Board of Trustees. The Florida Court of Appeals decision upheld the DNR scientific methodology for setting CCCLs, thus eliminating the legal option for local protests over placement of the control line. It is possible, however, to contest whether a permit for construction should be granted. The already close ties between the Department of Natural Resources and some members of the academic coastal engineering community were further enhanced in 1982. DNR Executive Director Elton Gissendanner convinced T.Y. Chiu to leave the University of Florida, move to Florida State University in Tallahassee, and set up his operation in the Institute for Science and Public Affairs. Gissendanner was anxious to have Chiu's operation close to DNR headquarters, home of a \$1.7 million computer bought specifically for the computer-intensive control line work (Stephenson 1986, 14).

The above discussion is not meant to imply that the use of STI to address issues of coastal erosion in Florida is a perfect situation. In some instances the STI-producing communities are not consulted, their advice is ignored, they are not sure what recommendations to make, or there is a lack of consensus on the state-of-the-art of the science. James Purpura and T. Y. Chiu began pushing the legislature for guidelines to regulate construction on the beaches in the late 1950s. However, it was not until a storm with unusually high tides hit Panama City and damaged buildings on the beach that the legislature saw the need and began the setback line process in 1970 (Chiu 1991).

In some cases, STI is sought in order to support implementation of a policy, but the science community does not have the information, data, or models to respond. In 1985, the 30-year erosion zone program was established through the Florida Omnibus Growth Management Act (Chapter 163, Part II, Florida Statutes). This provision prohibits permits for major structures proposed in a location which, based on erosion projections, will be seaward of the seasonal high water line within 30 years. The 30-year period reflects the average life of a mortgage for a single-family dwelling. The science community was against the 30-year line, because current data and models were not appropriate or adequate for determining the location of the line. The science and engineering communities expressed concern about the effects on permitting (Balsille 1991;

Flack 1991).

On the other hand, lack of support from the science and engineering communities can contribute to the difficulties associated with getting an innovative policy adopted. In 1985, Debbie Flack, Director of the Division of Beaches and Shores, put forth a "no armoring" proposal as the direction the state should be taking to protect the beaches. Neither the scientists nor engineers came forward with recommendations or support for her policy, and she was not able to convince the Cabinet that a no armoring stance was the best way to proceed. She resigned over this issue (Flack 1991).

After Flack's resignation, the Division argued against armoring permits on a case-by-case basis. In December of 1990, the Governor and Cabinet passed an armoring policy that set vulnerability requirements that must be met before a hardened structure can be permitted. No specific report led to their decision. Rather, it was the result of an on-going education process supported by general STI and pictures (Green 1991). Flack's proposal six years earlier heightened awareness, promoted discussion of the issue, and facilitated the education process--an example of conceptual utilization.

Even if STI exists, there may not be agreement on the conclusions to be drawn from available science. For example, within the various units of the DNR and among representatives of the scientific and engineering communities, a consensus is not apparent with respect to the effects of hardened structures on erosion. Some have indicated that these structures made the problem worse, others believe they are beneficial if constructed properly and under the right conditions, while others do not believe enough research and science exists to make a judgement.

Some disagreement or tension also exists between the science and engineering communities about the use of STI to support the policy process. Among the scientists, there appears to be substantial agreement that a lack of coordination exists between the two communities that would normally lead to the development of engineering responses with a better scientific basis. There is the perception among some that engineers (especially the U.S. Army Corps of Engineers) still want to build without paying sufficient attention to research. They would rather spend millions of dollars to build than thousands to model the problem and propose solutions first (Chiu 1991).

Walt Schmidt of the Florida Geological Survey (1991) does not believe that coastal science has played a key role in the development of Florida's policies. The Division of Beaches and Shores is solution-oriented, and engineers have dominated because they fix rather than study, sometimes without sufficient data to guide the development of a solution. There are only a few coastal sedimentologists or coastal geologists in the state, but there are many engineers. The DNR rarely asks geologists at the Florida Geological Survey for assistance. No scientists from the Survey were involved in the CCCL or 30-year erosion line process. Part of the problem may be perceptual; geologists are sometimes viewed by engineers "as elitists who want to look at rocks and be left alone" (Scott 1991). At the same time, for scientists to be involved, they must want to participate, have information useful to inform engineering solutions or policy decisions, and provide that information in a timely manner. These conditions are not always met (Schmidt 1991; Scott 1991).

Regardless of the source of the STI, that source must be credible and a conduit must exist to transfer the information from the knowledge producers (or those who can access and synthesize information) to the knowledge users. Bruun, Purpura, Chiu, Dean and others had an impact because they (and the universities with which they were associated) were viewed as highly credible sources of information. For example, Dean conducted a study of navigation inlets and concluded that 80 percent of the erosion on Florida's east coast was due to these inlets. This eventually resulted in a provision in the Omnibus Growth Management Act of 1985 that required all navigation districts develop a plan to bypass 100 percent of the sand blocking each inlet. One coastal geologist noted that Dean's conclusions are not necessarily the view of many in the science community, but "his words have the force of God and law" (Davis 1991).

Although the legislature does not understand the science or engineering behind the recommendations, it relies on reputation and credibility. The STI is filtered through the DNR which is viewed as professional and non-political. The FSBPA also plays an important transfer role through its annual conferences and as an on-going source of information for policymakers. Many of the individuals from the academic community that are sources of STI have been active members of the FSBPA (Balsille 1991; Duden 1991; Flack 1991; Tait 1991).

The contractual arrangement between the DNR and individuals and units in the state university system provides access to the most recent research. In some cases, the transfer of STI to the policymaking community and key individuals is even more direct. James Purpura often was characterized as Governor Askew's right hand with respect to coastal issues. Robert Dean left the University of Florida and served as Director of the Division of Beaches and Shores for two years following the resignation of Debbie Flack (Duden 1991).

DNR use of federal sources of STI is mixed. Florida's perception of federal initiatives for coastal management in general has not been very positive. For the most part, the state's policies and programs are viewed as being better than the federal initiatives, and little is to be gained from federal programs. The state does, however, take federal money to support its coastal zone management program and provide the resources to support its other activities. Reports and recommendations from the Corps of Engineers are sometimes viewed with skepticism because of questions about the scientific foundation or whether the most recent STI has been consulted (Bean 1991; Balsillie 1991; Scott 1991). However, the Coastal Erosion Research Center at Vicksburg is often perceived as a very important source for structure design, surveys, and information to understand the morphology of the coast (Devereaux 1991; Terry 1991). It is a major source of the science behind beach nourishment.

The participation and activities of the science and engineering communities and their success in informing public policy with high quality, timely STI has been significant in some areas of coastal erosion policy and a failure in others. It would be unreasonable to expect a perfect system. In many cases, regulation drives the research and is needed to solve problems, confirm ideas, or justify current policies and regulations already in place (Green 1991). To a large degree, coastal engineering and regulation in Florida have developed in tandem for the last 20 years (Grayson 1991).

MASSACHUSETTS

In 1978, when Massachusetts won approval from the National Oceanic and Atmospheric Administration (NOAA) for its state coastal zone management program, it became the first state to adopt a formal networking arrangement that shared regulatory and management responsibilities among state and local agencies. In light of the state's tradition of strong home rule and weak regional government, the primary responsibilities for the acquisition and use of STI relevant to coastal erosion were divided between the regulatory and technical assistance functions provided by the state and developers whose proposed actions could damage the integrity of the shoreline. Regulatory enforcement is provided by the Department of Environmental Protection (formerly the Department of Environmental Quality Engineering), with local government permit review functions implemented through a network of town conservation commissions made up of publicly elected members. The lead responsibility for providing technical advice resides with the Office of Coastal Zone Management (MCZM), a unit within the Office of the Secretary of Environmental Affairs, a cabinet level agency.

In this organizational setting, STI has been used instrumentally to set regulatory standards specified in the state Wetlands Protection Act (WPA) and assist decision making by conservation commissions through their permit review authority. Under this law, activities affecting coastal beaches, dunes, barrier beaches, or coastal banks are subject to regulatory review. When the need arises to revise or redefine specific criteria in the WPA, interagency reviews are conducted, both with public hearings and the assistance of issue-specific technical or scientific advisory committees convened on an *ad hoc* basis.

Consequently, Massachusetts does not maintain an active research staff or sponsor continuing research on geomorphological processes and the effect of built structures on the coast, but relies instead on expertise available in state agencies, area universities, consulting firms, public interest groups, coastal research centers, and consultants from other states. While such a polycentric approach has merit in that it provides MCZM staff an opportunity to explore emerging issues and find common agreement on controversial issues of a scientific or technical nature, it is partly deficient in that it lacks a proactive approach to STI acquisition and dissemination. Moreover, in regions where environmental quality issues affect a common geographic resource, such as Cape Cod, local home rule has been infused into a regional form of government (Cape Cod Commission) that has greater technical capacity to provide STI (Carbonell and Hamilton 1992).

Prior to enactment of the Coastal Zone Management Act (CZMA), Massachusetts had almost 350 years of experience with its shoreline and the critical role that coastal barriers played in buffering storm surge. When the Pilgrims settled Provincetown on Cape Cod in the 1600s, for example, they prohibited activities that would destabilize the large mobile dunes that formed along the tip of the Outer Cape. Succeeding generations were destined to relearn that wisdom over again.

As scientific understanding of erosional processes on the Cape matured, conceptual understanding by the public about the effects that engineered structures could have on the sand budget of coastal barriers expanded. Many coastal inhabitants saw the effects of privately built jetties on downdrift sediment supply. Summer visitors routinely trucked in sand to replenish their beachfront property after winter storms had eroded it away. In addition, a growing number of people, including school teachers and their classes, visited the National Seashore to learn about the dynamic and changing shoreline. By the late 1960s, conceptual STI about coastal erosion was widely disseminated. By 1973, the National Park Service, in its role as custodian of the Cape Cod National Seashore, announced that it would no longer attempt to control shoreline processes anywhere along the coastline within its jurisdiction. After a detailed study of the costs necessary to control erosion along the Cape's easterly shore, the U.S. Army Corps of Engineers reached a similar conclusion (Giese and Giese 1974).

Following the enactment of the federal CZMA in 1972, Massachusetts initiated coastal planning studies, and in 1976 hired Lester Smith as the first MCZM scientist (Smith 1991). Erosion and related issues had been given some attention before then in the WPA, but the policies and regulations in the act were too general. Other laws were equally vague. The Coastal Wetlands Restriction Act, for example, mapped coastal areas, placed deed restrictions on property owners' land, protected walkover dunes, and regulated certain activities. It also contained a state building code, but didn't restrict construction in coastal areas.

As chief scientist, Smith set out to promulgate performance standards for coastal structures, such as groins and jetties, in cooperation with technical staff from the DEP. Due to the nontechnical composition of local conservation commission membership, Smith began an aggressive campaign to educate the commissioners through the Massachusetts Association of Conservation Commissions (MACC), schools, and public educators. He generated a number of documents, including a guidebook. Dave Stanley, the head of DEP, was supportive of Smith's campaign and provided help where he could. Federal CZM funding at the time also enabled Smith to hire several staff scientists for MCZM, which made a significant difference in the agency's ability to review STI (Smith 1991). At this time, Smith hired Jeff Benoit, a geologist and current MCZM director.

Smith met Graham Giese in his capacity as Truro representative to the Barnstable County CZM advisory group. Giese, who also served as scientific advisor to the Association for the Preservation of Cape Cod (APCC), had written a well-received nontechnical report on chronic erosion processes on Cape Cod that summarized the key issues confronting coastal managers (Giese and Giese 1974). Shortly thereafter, Smith involved Giese in the process of devising new regulatory standards for inclusion in the WPA.

Giese was especially well prepared by professional background and temperament to participate in this activity. As an undergraduate student, Giese had conducted research on Cape Cod Bay with John Zeigler of the Woods Hole Oceanographic Institution (WHOI), and did his masters research on the coastal orientations of the Bay at the University of Rhode Island (Giese 1991). After completing his doctorate at the University of Chicago on swash zone dynamics and working in Puerto Rico, he joined the Provincetown Center for Coastal Studies in 1972. He conducted erosion research for the National Park Service and the towns near the Cape Cod National Seashore, and soon earned a reputation as a credible and unbiased source of STI for the local towns and their conservation commission members.

Through a long series of meetings held with DEP staff in which all STI used to justify protection criteria was reviewed thoroughly, Smith and Giese developed a set of performance standards for protecting coastal beaches, coastal dunes, and coastal banks that revolve around the fundamental geomorphological importance of maintaining sediment transport processes to protect the integrity of the shoreline (Smith et al. 1978; Giese 1991). In 1978 the WPA was amended with the regulations in force which were justified by STI drawn from textbooks, journal articles, and published research reports. All structures on or within a 100-foot buffer of coastal dunes were prohibited if they: (1) affected the ability of waves to remove sand from the dune; (2) disturbed the vegetative cover so as to destabilize the dune; (3) increased the potential for storm or flood damage; (4) interfered with the lateral or landward movement of the dune; (5) caused sand to be artificially removed; or (6) interfered with bird nesting habitat.

Engineered structures are permissible on coastal beaches only if they are found to be the minimum size necessary to maintain beach form and sand volume based on supporting coastal engineering, oceanographic, or geological STI. They also have to remain filled to entrapment capacity and must contain a sand by-pass system to transfer downdrift sediment. Barrier beaches are defined as low-lying strips of land that generally consist of coastal beaches and coastal dunes, so the above restrictions apply to them. Finally, coastal banks are protected from engineered structures by regulations based on whether the bank is a source of sediment or a buffer for storm waves. In the case of the former, no construction is allowed unless protection from storm damage is paramount for buildings existing prior to 1978, and consistent with other restrictions if built more recently. Interference with wave action and sediment transport from the bank to the beach cannot occur within a 100-foot buffer landward from the top of the bank. If the bank serves primarily for wave protection, a structure within the 100-foot buffer cannot diminish bank stability, and is permitted only if the bank is found to be significant for storm damage prevention or flood control. Habitat restrictions also apply.

An expanded and more detailed effort to organize STI for coastal erosion management took place in the wake of a record-breaking winter blizzard that severely damaged several coastal towns in 1978. Two years later, Governor King issued Executive Order No. 181 for Barrier Beaches, which sought to break the increasingly costly cycle of investing additional money into storm-vulnerable coastal barriers. Among other directives, EO 181: (1) prohibited use of state funds or federal grants to support development in hazard prone areas; (2) prohibited development in velocity zones (V zones) or primary dune areas of barrier beaches; and (3) permitted construction of structures to maintain navigation channels only if down drift areas are adequately supplied with sediment (King 1980).

As directed by EO 181, MCZM conducted a survey to identify and delineate on topographic maps all of the state's barrier beaches to provide a baseline for management purposes. This undertaking was directed by Les Smith, who left MCZM in 1980 and joined the Provincetown Center for Coastal Studies. In addition to Gary Clayton and Jeff Benoit of the MCZM staff, technical assistance was provided by the Department of Environmental Management (which provided maps for the restricted wetlands program) and the Department of Environmental Protection. The report was reviewed for accuracy by Stephen Leatherman and geologists from Boston College (B. Brenninkmeyer), Boston University (D. Fitzgerald), and Northeastern University (P. Rosen) (Massachusetts Coastal Zone Management 1982).

As a result of the time consuming, consensus-building process by which WPA regulatory criteria are developed, changes come slowly. Gaps in STI are filled when recognized, but at a pace that may be out of synch with the immediate needs of affected property owners. This problem is well illustrated by the events that followed a break in Nauset-Monomoy Barrier Beach system that protected Chatham's harbor and waterfront dwellings. Although the town leadership had a full technical understanding of the instability of the barrier system from a detailed report prepared for it by Giese in 1978, the townspeople had grown complacent about a hazardous event because the barrier system appeared to operate over a 140-year cycle (Fantozzi 1989; Wood 1990).

On January 2, 1987, a severe Northeaster occurred during a perigean spring tide, and ruptured the Nauset-Monomoy barrier system directly east of the Chatham Lighthouse. Immediate reaction to the break was delayed, but by late fall of 1987, public demands were high for state and federal action to curb the rapid rate of erosion taking place along the now vulnerable shoreline. The federal response was quick and related to STI acquisition and dissemination. Giese and David Aubrey, Director of the Coastal Research Center at WHOI, conducted a scientific study of the breach in cooperation with the U.S. Army Corps Coastal Engineering Research Center. Additional information was disseminated by Congressman Studds' office and the Federal Emergency Management Administration, which informed homeowners about the applicability of the National Flood Insurance Program.

The local regulatory response was receptive to taking action, but, for a number of reasons, the affected local property owners failed to file a Notice of Intent with the town conservation commission as required by the WPA. After additional delay, the public agencies held fast to a strict interpretation of the WPA requirements that nonstructural remedies to erosion be attempted prior to consideration of structural solutions. A point of scientific contention was that the homes poised to fall into the eroding shoreline were built upon a coastal dune where all structures are prohibited, and not on a coastal bank (Wood 1990). Due to time and financial constraints, local homeowners failed to obtain any immediate relief, and several ultimately lost their homes to the sea. To clarify this point, an interagency task force assembled by MCZM staff has addressed the issue of defining more precisely the terms "coastal bank," "top of coastal bank," and "land subject to coastal storm flowage" (O'Connell 1991). Participants include staff from the DEP, DEM, MACC, Giese, Smith, Humphries, and Brett Burdick, a consulting geologist.

Over time, the range of individuals called upon to provide and verify coastal STI has remained limited. Staff at MCZM are familiar with the expertise of scientists at area universities, and frequently call upon them. Other professional colleagues can be contacted or visited personally since Boston is the regional headquarters for a number of federal agencies. An important constraint, however, for MCZM staff is the different value academic researchers place on contributing their time and knowledge to assist state agencies. Richard Delaney, former MCZM Director, noted the fact that few scientists from WHOI, MIT, or Harvard were willing to provide assistance to the agency unless a funded research project was involved (Delaney 1991).

In addition to the application of STI for setting regulatory criteria, MCZM staff have continued to use STI in a conceptual manner. Advances in technology, particularly computerized geographic information systems, have facilitated this. A recent example is the completion of the Massachusetts Shoreline Change Project, which utilized Leatherman's innovative metric mapping approach to measure changes in the shoreline over time (Benoit 1989). In addition to publishing and disseminating a written document, MCZM has published an easily understood map of the state which documents vividly the rate of shoreline change experienced at different locations on the coast (Massachusetts Coastal Zone Management 1989).

Based on the state's experience to date, the primary sources of STI have been drawn from existing studies complemented by sponsored research that addresses specific uncertainties. A key factor in the state's program has been the successful role of scientists as policy entrepreneurs, such as Lester Smith, and science advocates, such as Graham Giese, who have used general awareness about the coast to promote a more receptive attitude for coastal protection. To a large degree, the state's prior history with coastal erosion and the existence of public organizations such as the APCC, which attracted a large number of retired scientists and naturalists who resided on the Cape, were very helpful. Also, the active research program carried out by the National Park Service supported scientists such as Stephen Leatherman and Paul Godfrey, whose research findings were useful. STI provided by the U.S. Army Corps of Engineers, the Provincetown Center for Coastal Studies, WHOI, and the universities in the state, such as the University of Massachusetts, which had a multi-year cooperative research program with the NPS at the Cape Cod National Seashore, made the MCZM networking approach to STI function as well as it does.

Although the presence of federal research programs does not appear to play a central role in state STI usage, the work products from these programs have provided useful data and background information for individual scientists to use. In addition, the release of funds to the state by NOAA to organize a state CZM program played a critical role in building expertise. Where environmental issues remain problematic, as they are on Cape Cod, a regional form of government has assumed a greater technical role in order to compensate for the recognized deficiencies of Conservation Commissions--lack of professional training, high turnover, and inflexible time requirements for processing permits.

NORTH CAROLINA

Scientific experts played an active part in the formulation of North Carolina's Coastal Area Management Act (CAMA) in 1974 and in its subsequent implementation. Many were resident experts within state government and the institutional system established to manage the coastal environment. Others were members of the academic community in several of the state's universities and the state's Sea Grant Program. Academic experts from outside the state were primarily accessed by STI gatekeepers within the state coastal management institutional system. The influence of federal agencies and experts in providing relevant STI to state policymakers, including the Corps of Engineers and the National Park Service, was relatively small, despite their presence in the state at the Cape Hatteras and Cape Lookout National Seashores and the Corps's District Office in Wilmington.

Under CAMA, primary administrative and policy making powers for the state's coastal management program were delegated to an appointed citizen commission, the Coastal Resources Commission (CRC). Two members of the CRC are required by statute to be experts in the fields of marine ecology and coastal engineering. One of the CRC's primary responsibilities is the designation of Areas of Environmental Concern (AECs) within which it has authority to regulate development activities through a permitting process administered jointly with local governments.

The CRC is staffed by the Division of Coastal Management (DCM) within what is now called the State Department of Environment, Health, and Natural Resources. Until recently, the DCM included among its staff a technical services coordinator who was the principal STI gatekeeper and boundary spanner for the agency. The CRC also is advised by the Coastal Resources Advisory Council (CRAC), a group of 47 citizens appointed by local governments within the state's 20-county coastal zone. Three members of the CRAC are required by CAMA to be "marine scientists or technologists."

STI played a significant role in several major erosion policy decisions taken by the CRC. The identification and definition of Ocean Erodible and Inlet Hazard AECs required analysis and understanding of scientific knowledge about coastal geomorphologic processes and the development of methodologies for documenting storm-induced and long-term erosion rates. Specific development regulations for these AECs were based on STI concerning coastal erosion processes and geomorphology, coastal engineering, and the chronic erosion rate measurement methodology. Among the important development regulation policies adopted by the CRC were: (1) regulating the destruction, construction, and stabilization of sand dunes; (2) the initiation of a setback requirement for coastal construction based on long-term, chronic erosion rates; and (3) the imposition of severe constraints on the use of hard-engineered erosion control structures such as groins, seawalls, and jetties.

To illustrate the acquisition and use of STI by the CRC in North Carolina's coastal erosion policy, two related decisions will be described in detail: (1) designation of the Ocean Erodible AEC; and (2) imposition of the coastal construction setback requirement. The CRC initially designated Interim AECs (IAECs) in 1976. A review of CRC archives indicates that the Commission and its staff were considering possible regulatory mechanisms at the same time they were assessing how to define appropriate AECs. Thus, the decision to designate an Ocean Erodible IAEC was linked to the idea of imposing some form of construction setback within the designated area (Sullivan 1976).

Initially, the principal focus of the Ocean Erodible AEC appears to have been on protecting sand dunes. A dune protection law has been in place since 1957, but implementation had been delegated to the counties and was considered to have been ineffective (Owens 1991). The principal rationale behind the 1957 law appears to have been the potential of dunes to reduce storm surge and flood damage and the importance of vegetation in stabilizing dunes (Stick 1959). Public opinion at the time was no doubt influenced by dune building projects initiated by the National Park Service in the Cape Hatteras National Seashore in 1936 and again in the late 1950s (Dolan 1972). However, there is no evidence of any formal efforts to acquire or analyze STI about dune stabilization before the law was enacted.

When the Ocean Erodible IAEC was designated, the principal emphasis still appears to have been on protecting the storm buffering value of dunes. There was, however, some sentiment that favored protecting dunes for their ecologic and aesthetic values (Owens 1985) and some recognition of their role as a component of the ocean shore sediment-sharing system. This latter aspect of coastal erosion STI was communicated to the CRC by its technical staff in a memorandum summarizing the scientific literature on coastal geomorphologic processes (Bell 1976).

The 1976 staff memorandum also acknowledges the role of a setback in accommodating the dynamic processes of erosion and accretion. Bell cites a 1972 paper by CRC member Arthur Cooper (Cooper and Linton 1972) that called for oceanfront setbacks to protect structures from "erosion and shoreline change." Cooper, who was an ecologist on the faculty at North Carolina State University (NCSU), may have been influenced by contemporaneous work by Robert Dolan and Paul Godfrey on the value of dunes within the Cape Hatteras National Seashore. Dolan had recommended fixed setbacks in a National Park Service report published that same year (Dolan 1972).

DCM staff and CRC members made a clear distinction between acute, storm-related erosion and flooding, and the phenomenon of long-term cumulative erosion along the oceanfront. They engaged in an aggressive search for a technically sound and legally defensible method of documenting the area influenced by storm flooding and erosion as the basis for both defining the landward boundary of the Ocean Erodible AEC and for setting a construction setback standard. Despite staff reservations about the adequacy of available data (Sullivan 1976), the landward boundary of the Ocean Erodible IAEC was defined by the 25-year storm erosion line that had been developed in a study by researchers at NCSU (North Carolina Coastal Resources Commission 1976). The study (Knowles, Langfelder, and McDonald 1973) divided the state's 320 miles of oceanfront coastline into only seven segments with erosion lines rounded to the nearest ten feet.

Final AECs and applicable development regulations were adopted by the CRC in 1977. The landward boundary of the Ocean Erodible AEC remained defined by the 25-year storm erosion line as estimated by Knowles, Langfelder, and McDonald (United States Department of Commerce c.1978). One of the principal development regulations imposed within the AEC was the requirement that all construction be located behind the landward toe of the frontal dune (Owens 1981). This was the CRC's initial setback requirement.

The 1977 AEC designations and development regulations, which went into effect in early 1978, were viewed by the CRC as a first cut with the full expectation of making revisions after some implementation experience was gained (Owens 1991). In fact, the CRC embarked on a review almost immediately, in August 1978. DCM staff had encountered problems implementing the setback based on the frontal dune (Benton 1991). Permit officers had difficulty in determining exactly where the frontal dunes were, and in some areas, no dunes were present. This problem, plus a sense that a fixed setback was inequitable due to large variations in local long-term erosion rates, led the CRC to seek a basis for defining an erosion-rate based setback, according to David Owens (1992), who served in various capacities with the DCM, including director, from 1979 through 1988. Ultimately, the CRC decided to use long-term erosion rates for defining the landward boundary of the Ocean Erodible AEC as well.

Initially, the DCM staff attempted to identify methods of measuring both the extent of short-term, storm-induced erosion and long-term, chronic erosion (Owens 1984). Earlier studies of long-term erosion conducted by researchers at NCSU using air photo interpretation (Stafford 1968; Wahls 1973) convinced the DCM staff that a defensible method could be developed for defining average annual chronic erosion rates. A study was commissioned with Aziz Tayfun, Jay Langfelder, and Spencer Rogers at NCSU and the state Sea Grant Program, to develop projections of erosion from a 100-year storm as well as long-term shoreline changes (Tayfun, Rogers, and Langfelder 1979). The breakthrough on documenting long-term erosion rates was the discovery of the erosion data and air photo analytic technique developed by Robert Dolan of the University of Virginia (Dolan, Hayden, and Heywood, 1978). DCM staff geologist Stephen Benton and North Carolina Sea Grant agent Spencer Rogers heard a presentation by Dolan at a meeting of the Assateague Shelf and Shore Workshop in Manteo, North Carolina, in April 1979 (Benton 1983a). Dolan gave his data for the northern North Carolina coast to Rogers, who incorporated it in the analysis he was doing with Tayfun and Langfelder.

The method used by Tayfun, Rogers, and Langfelder for measuring storm-induced erosion was adopted from Vallianos of the Corps of Engineers (1974) and Knowles, Langfelder, and McDonald (1973). It subsequently was judged to be too imprecise to serve as a basis for a setback regulation, but it was used in a revised definition of the Ocean Erodible AEC adopted by the CRC in 1979 (Owens 1984). The analysis of long-term erosion rates also was used by the CRC in crafting the new AEC definition and in establishing a setback regulation based on 30 times the average annual erosion rate that was adopted at the same time. The CRC subsequently contracted with Dolan in 1980 to generate raw shoreline change data for the entire coast from aerial photographs taken between 1938 and 1980. These data were then adjusted by a mathematical process developed by Benton and Rogers (Benton 1983a). This process has been used periodically to update the CRC's erosion rate data base and setback lines.

Thus, the 1979 AEC definition incorporated measures of both acute and chronic erosion (North Carolina Coastal Resources Commission 1979):

Ocean Erodible Area: The seaward boundary of this area is the mean low-water line. The landward extent of this area is determined as follows: (A) A distance landward from the first line of stable natural vegetation to the recession line that would be established by multiplying the present long-term annual erosion rate times 30, provided that where there has been no long-term erosion or the rate is less than two feet per year, this distance shall be set at 60 feet landward from the first line of stable natural vegetation; and (B) A distance landward from the recession line established in subparagraph (A) of this paragraph to the recession line that would be generated by a storm having a one percent chance of being equalled or exceeded in any given year [a "100-year storm"].

The accompanying setback regulation also incorporated both measures of erosion. The short-term erosion rate was used to define the "primary dune." The regulation currently stipulates that residential structures of four units or less must be set back from the first line of stable vegetation a distance of 30 times the average annual erosion rate, or a minimum of 60 feet where the rate is less than 2 feet per year. All structures also are required to be located behind the crest of the primary dune (the first dune with an elevation equal to the 100-year storm level plus 6 feet), and/or behind the landward toe of the frontal dune (the first dune behind the vegetation line). Larger structures (any building with more than four residential units or 5,000 square feet of total floor area) must be set back a distance of 60 times the average annual erosion rate or a minimum of 120 feet from the vegetation line, except in areas where the annual erosion rate exceeds 3.5 feet per year. In those cases the setback for large structures is 30 times the average annual erosion rate plus 105 feet.

These examples demonstrate instrumental use of STI by the North Carolina CRC in devising coastal erosion policies. There was a linked process of conceptual use as well, however. The CRC engaged in an ongoing process of self-education about STI relevant to the coastal management issues with which it dealt. Experts were asked to make presentations to the CRC on various occasions, generally in the context of a particular policy issue. Most were researchers from universities within the state (Stanley Riggs of East Carolina State, Jay Langfelder of NCSU, Orrin Pilkey of Duke) or from nearby universities (Robert Dolan of the University of Virginia, Stephen Leatherman of the University of Maryland) or experts in other state agencies. Neil Frank, of the National Hurricane Center in Miami, addressed the CRC at a conference convened in 1982 to discuss the need for additional measures to combat coastal erosion. The staff also prepared periodic technical reports to advise the CRC. Some essentially were literature reviews, such as Bell's 1976 memorandum and a later review of coastal erosion STI prepared by Stephen Benton (Benton 1983b). Others presented the results of technical analyses conducted by the staff or consultants hired by the Commission (see for instance Benton 1983a; Lynch and Benton 1985).

Frequently, these initiatives went beyond the scope of making specific decisions (instrumental use of STI) and served to influence the "conventional wisdom" of the citizens who constituted the policymaking body (conceptual use). Owens (1984) suggests, for instance, that coastal residents did not require formal knowledge of coastal geomorphologic processes to appreciate the phenomenon of chronic erosion. They had first-hand knowledge of the long-term dimension of erosion, since they had witnessed the need to move roads and buildings in the face of a progressively receding shoreline. Owens suggests that educating CRC members about such phenomena as sea level rise served more to validate their observations than to stimulate policy initiatives. Owens (1991) has maintained, however, that the staff's efforts to educate CRC members was not done in a tutorial manner or in an effort to rationalize a specific policy proposal (symbolic use of STI).

For the most part, the STI used in formulating coastal erosion policies in North Carolina was obtained from decentralized sources (in-house and in-state experts, regional universities, published scientific literature, professional conferences), with the exception of publications of the U.S. Army Corps of Engineers Coastal Engineering Research Center (for example, Belly 1963; Caldwell 1967; United States Army Corps of Engineers 1971; LeMehaute 1980; Zaremba and Leatherman 1982), which were evidently known to DCM's technical staff (Benton 1983b). Site-specific erosion studies prepared by the Corps' District office in Wilmington, North Carolina (for example, United States Army Corps of Engineers 1978, 1981), are more properly characterized as decentralized sources of STI.

The major role that can be attributed to the federal government in supporting the acquisition and use of STI in North Carolina's case is financial support. Planning and implementation grants provided to the state through the federal Coastal Zone Management Program enabled the DCM to support its technical staff and to contract with such university-based scientists such as Dolan, Tayfun, and Langfelder. The federally-supported Sea Grant Program made available the expertise of Spencer Rogers, a coastal engineer. Rogers was not a member of the CRC or CRAC, but he frequently attended commission meetings and provided detailed technical comments on proposed commission rules. He served as a member of the commission's 1984 Outer Banks Erosion Task Force and was frequently consulted by the DCM staff for input in the developmental stages of new policies or regulations (Owens 1991).

Despite its physical presence in the state, the National Park Service had little direct influence in providing STI to the North Carolina coastal program, other than through its sponsorship of research by Dolan and Godfrey in the early 1970s (Godfrey 1970; Dolan 1972; Dolan and Godfrey 1972; Godfrey and Godfrey 1976). Staff of the Cape Hatteras National Seashore did serve on the Coastal Resources Advisory Council, and superintendents made periodic presentations to the CRC, but their interchange with the Commission was very limited according to former CRC chair Parker Chesson (1991) and staff geologist Stephen Benton (1991).

Beyond staff use of its technical reports, the influence of the Corps of Engineers on North Carolina's erosion management policies appears to have been principally the result of individual participation. Paul Denison, who participated in the initial drafting of CAMA and served as one of the technical members of the CRAC for about 15 years, retired from the Corps in 1971 before CAMA was enacted, and subsequently worked for an engineering consulting firm in Wilmington. Nonetheless, he was perceived as a representative of the Corps (Cantral 1991). The CRC's interaction with active Corps personnel was largely limited to review of specific permitting cases. However, individuals such as Tom Jarrett, chief of coastal engineering for the Wilmington District, made periodic presentations to the CRC or its committees. Jarrett made a presentation to the Commission's Outer Banks Erosion Task Force in 1984 about different types of erosion control structures (Jarrett 1991).

Because virtually all coastal management decisions in North Carolina are made by the lay Coastal Resources Commission, the technical staff of the Division of Coastal Management have served as the key link between policymakers and STI relevant to coastal erosion issues. Staff geologists Stephen Benton and Melissa McCullough served as the principal STI gatekeepers within the state's coastal management institutional system during the late 1970s and early 1980s, when the CRC developed most of its erosion management policies. Spencer Rogers of the state Sea Grant program was probably the other most influential STI gatekeeper. His role was largely self-initiated and was facilitated by the open decision making process followed by the Commission. STI from centralized sources, principally the U.S. Army Corps of Engineers Coastal Engineering Research Center, appears to have been used largely in a conceptual role rather than an instrumental role. Instrumental STI was chiefly obtained from literature reviews conducted by the staff and from technical studies performed for the CRC by the staff or consultants who were primarily drawn from instate and regional universities.

DISCUSSION

The experiences of Florida, Massachusetts, and North Carolina with the acquisition and use of STI in coastal erosion policy underscore the variability of regional land use issues and the enduring ability of the federal system to motivate innovative approaches to state environmental management. Each of the three states developed strikingly different institutional arrangements for guiding coastal erosion policy and used STI in equally different ways. The case studies illustrate the important role the federal government played in elevating the scientific importance of coastal erosion and providing states with the critical financial resources to address it in a more systematic manner. Beyond the cumulative knowledge about coastal erosion that federal studies generated, the states appeared to use federal STI less often in a direct, instrumental way, and more often in a conceptual and symbolic way. Federal support for coastal scientists also was important. Federal support made possible the existence of credible experts who could provide testimony and research findings, set regulatory criteria and develop management methods, and review state documents for accuracy.

For their part, the states varied greatly in the degree to which STI was used in erosion policy. All of the states pioneered innovations in coastal erosion management that drew upon STI, and which were adopted or modified subsequently by other users, including the federal government. The arrangements developed to link scientists with coastal managers were reflective of the level of STI that was needed on a continuing basis. In this respect, Massachusetts, with its informal network of coastal expertise, lies at one end of the organizational scale and Florida, with its ongoing modeling effort, lies at the other. An important aspect of the scientific community is its relatively small size; most of the key advances in coastal science were well known among coastal scientists, and they were able to keep managers abreast of the state of the art. Advances made by Robert Dolan and Stephen Leatherman in mapping coastal erosion, for example, became widely known relatively quickly among the technical staff in Massachusetts and North Carolina.

For the future of coastal erosion management and of global change processes more generally, the case studies provide some insight into how the federal government might be better organized to acquire and provide STI that can be more readily utilized by the states. Current proposals to reorganize the federal mission agencies in order to improve their competence in environmental research and development (Carnegie Commission 1992) underscore the fragmented and uneven nature of coastal research support within the federal system. State scientists, who often were sponsored by federal funding to carry out narrowly focused research, became critical players in translating their knowledge and expertise into broader policy options. Moreover, while acute events frequently were exploited by policy entrepreneurs to motivate state and federal actions to address coastal erosion, public familiarity with the issues appeared to have been key for sustaining political support. Available experts, entrepreneurial resource planners, and support for documenting the importance of the issue for regional and local decision makers are all likely to be important aspects of improving coastal erosion policy in the near term and linking global change policy to regional planning in the future.

ACKNOWLEDGEMENTS

This paper is based on work supported by the National Science Foundation under Grant No. SES 90-12445. We thank David Aubrey, Woods Hole Oceanographic Institution, and the many informative individuals in Florida, Massachusetts, and North Carolina for their assistance.

REFERENCES CITED

Ansbacher, S.F., and Knetsch, Joe, 1989, The Public Trust Doctrine and Sovereignty Lands in Florida: A Legal and Historical Analysis: Journal of Land Use and Environmental Law, 4:337-75.

Balsillie, J.H.(n.d.), Florida's History of Beach and Coast Preservation, Unpublished in-house document: Bureau of Coastal Data Acquisition, Division of Beaches and Shores, Florida Department of Natural Resources.

Balsillie, J.H., 1991, Bureau of Coastal Data Acquisition, Division of Beaches and Shores, Florida Department of Natural Resources, personal interview, June 10.

Bean, Hal, 1991, Bureau of Coastal Data Acquisition, Division of Beaches and Shores, Florida Department of Natural Resources, personal interview, June 10.

Bell, Elizabeth, 1976, Memorandum to Environmental Committee of the North Carolina Coastal Resources Commission, December 14.

Belly, P.V. 1963, Sand Movement by Wind: Coastal Engineering Research Center Tech. Memo No. 1, U.S. Army Corps of Engineers, Washington, DC.

Benoit, J. R. (ed.), 1989, Massachusetts Shoreline Change Project: Coastal Zone Management Office, Executive Office of Environmental Affairs, Boston, MA.

Benton, S.B., 1983a, Average Annual Long Term Erosion Rate Update Draft Methods Report, North Carolina Division of Coastal Management, Raleigh, NC.

Benton, S.B., 1983b,. Selected Bibliography Ocean Beach and Barrier Island, North Carolina Division of Coastal Management, Raleigh, NC.

Benton, S.B., 1991, North Carolina Department of Environment, Health and Natural Resources, Division of Coastal Management, personal interview, June 17.

Beyer, J. M. and Trice, H. M., 1982, The Utilization Process: A Conceptual Framework and Synthesis of Empirical Findings: Administrative Science Quarterly 27, p. 591-622.

Bruun, P. et al. 1957, Studies and Recommendations for the Control of Beach Erosion in Florida: Florida Engineering and Industrial Experiment Station, College of Engineering, University of Florida, Gaines ville, FL.

Caldwell, J. M., 1967, Coastal Processes and Beach Erosion: Coastal Engineering Research Center Reprint No. 1-67, Washington, DC: U.S. Army Corps of Engineers.

Cantral, Ralph, 1991, North Carolina Department of Economic and Community Development, Division of Community Assistance, personal interview, June 20.

Carbonell, A.J. and Hamilton, Dan, 1992, Creating a Regional Constituency on Cape Cod, In Porter, D.R., (ed.), State and Regional Initiatives for Managing Development, Urban Land Institute, Washington, DC, p. 147-156.

Carlton, W.T., 1971, Department of Natural Resources, State of Florida, Bureau of Beaches and Shores, In Aase, G.(ed.), Association and Governmental Efforts in Beach Erosion Matters, Florida Shore and Beach Preservation Association, Tallahassee FL, p.16-28.

Carnegie Commission, 1992, Environmental Research and Development: Strengthening the Federal Infrastructure, The Commission, New York, NY.

Chesson, Parker(President), 1991, College of the Albemarle, personal interview, June 19.

Chiu, T. Y., 1991, Beaches and Shores Research Center: Florida State University, personal interview, June 11.

Chiu, T. Y. and Dean, R.G., 1984, Methodology on Coastal Construction Control Line Establishment: Department of Natural Resources, Beaches Shores Technical and Design Memorandum No. 8-46. Tallahassee, Florida. (Cited in Schmahl and Heatwole (1989).

Cooper, A.W. and Linton, T.L., 1972, Environmental Characteristics of the Southeastern Atlantic Coastal Zone, In Proceedings of Seminar on Planning and Engineering in the Coastal Zone, Seminar Series No. 2. Coastal Plains Center for Marine Development Science.

Davis, Richard, 1991, Department of Geology, University of South Florida, personal interview, June 14.

Delaney, Richard, 1991, Urban Harbors Institute, University of Massachusetts, personal Interview. June 7.

Devereaux, Al(Chief), 1991, Bureau of Coastal Engineering Regulation, Division of Beaches and Shores, Florida Department of Natural Resources, personal interview, June 10.

Deyle, R.E., Meo, Mark, and James, T.E., 1994, State Policy Innovation and Climate Change: A Coastal Erosion Analog, In Feldman, David and Mann, Dean, (eds.), Global Climate Change and Public Policy: Nelson Hall Publishers, Chicago, IL, in press.

Dolan, Robert, 1972, Beach Erosion and Beach Nourishment: Dune Stabilization Study, Natural Resource Report No. 4: U.S. Dept. of Interior, National Park Service, Office of Natural Science, Washington, DC.

Dolan, Robert and Godfrey, Paul, 1972, Dune Stabilization Study, Natural Resource Report No. 5: U.S. Department of Interior, National Park Service, Office of Natural Science, Washington, DC.

Dolan, Robert, Hayden, Bruce, and Heywood, J.E., 1978, A New Photogrammetric Method for Determining Shoreline Erosion: Coastal Engineering 2, p. 21-39.

Duden, Don,(Assistant Executive Director),1991, Florida Department of Natural Resources, Florida, personal interview, June 10.

Fantozzi, Peggy, 1989, Agency Regulatory Response: Let the Houses Fall in Chatham, Massachusetts: A Case Study: Conference on the State of Our Coastal and Ocean Resources, Sponsored by the New York Department of State, Division of Coastal Resources and Waterfront Revitalization.

Flack, Debbie,(Director of Government Affairs),1991, Florida Shores and Beaches Preservation Association, personal interview, June 11.

Giese, G.S. and Giese, R.B., 1974,. The Eroding Shores of Outer Cape Cod: Informational Bulletin No. 5, Association for the Preservation of Cape Cod, Orleans, MA.

Giese, G.S., 1991, Woods Hole Oceanographic Institution, Woods Hole, MA. personal interview, June 5.

Godfrey, Paul J. 1970. Oceanic Overwash and Its Ecological Implications on the Outer Banks of North Carolina. Washington, DC: U.S. Department of Interior, National Park Service, Office of Natural Science Studies.

Godfrey, Paul J. and M.M. Godfrey. 1976. Barrier Island Ecology of Cape Lookout National Seashore and Vicinity, North Carolina. National Park Service Monograph Series, No. 9. Washington, DC: U.S. Department of Interior, National Park Service.

Godschalk, David R., David J. Brower, and Timothy Beatley. 1989. Catastrophic Coastal Storms: Hazard Mitigation and Development Management. Durham, NC: Duke University Press.

Grayson, Andrew, Assistant Director, Division of Beaches and Shores, Florida Department of Natural Resources. 1991. Personal interview. June 11.

Green, Kirby, Director, Division of Beaches and Shores, Florida Department of Natural Resources. 1991. Personal interview, June 11.

Jarrett, Thomas, U.S. Army Corps of Engineers, Wilmington District. 1991.

Personal interview, June 18.

King, Edward J. 1980. "Executive Order No. 181, Barrier Beaches." August 8, Boston, MA.

Kingdon, John W. 1984. Agendas, Alternatives, and Public Policies. Boston, MA: Little, Brown.

Knowles, C. E., Jay Langfelder, and Richard McDonald. 1973. A Preliminary Study of Storm-Induced Beach Erosion for North Carolina, Report No. 73-5. Raleigh, NC: North Carolina State University, Department of Marine Science and Engineering.

LeMehaute, B. 1980. A Numerical Model for Predicting Shoreline Changes. Coastal Engineering Research Center Misc. Rpt. #80-6. Washington, DC: U.S. Army Corps of Engineers.

Lynch, Lisa L., and Stephen B. Benton. 1985. Potential Inlet Zones on the North Carolina Coast from Virginia to Cape Hatteras. Raleigh, NC: North Carolina Division of Coastal Management.

Massachusetts Coastal Zone Management. 1989. The Massachusetts Shoreline Change Maps. Boston, MA.

Millemann, Beth 1993. "The National Flood Insurance Program." Oceanus 36(1): 6.

National Academy of Sciences. 1990. Managing Coastal Erosion. Washington, DC: National Academy Press.

Nordstrom, Karl F. 1987. "Shoreline Changes on Developed Coastal Barriers," in Rutherford H. Platt, Sheila Pelczarski, and Barbara K. R. Burbank (eds.), Cities on the Beach: Management Issues of Developed Coastal Barriers, Research Paper No. 224. Chicago, IL: University of Chicago, Department of Geography.

North Carolina Coastal Resources Commission. 1976. Chapter 7 Coastal Resources Commission; Subchapter F - Interim Areas of Environmental Concern. Raleigh, NC: The Commission.

North Carolina Coastal Resources Commission. 1979. NRCD - Coastal Resources 7H .0200 Subchapter 7H - State Guidelines for Areas of Environmental Concern. Raleigh, NC: The Commission.

O'Connell, James, Office of Coastal Zone Management, Boston, MA. 1991. Personal interview, June 3.

Owens, David W. 1981. "The Management of Oceanfront Development in North Carolina," In Achievements of the '70s Prospects for the '80s: Proceedings Seventh Annual Conference. Bethesda, MD: The Coastal Society.

Owens, David W. 1984. "Erosion Rates and Hazard Mapping in Coastal Resource Management," In Managing High Risk Flood Areas 1985 and Beyond, Proceedings of the Eighth Annual Conference of the Association of State Floodplain Managers, Portland, Maine, June 11-14. Boulder, CO: Natural Hazards Research and Applications Information Center.

Owens, David W. 1985. "Coastal Management in North Carolina: Building a Regional Consensus." Journal of the American Planning Association 51: 322-329.

Owens, David W., University of North Carolina, Institute of Government. 1991. Personal interview, June 21.

Owens, David W., University of North Carolina, Institute of Government. 1992. Telephone interview, June 11.

Pilkey, Orrin H. and William J. Neal. 1992. "Save Beaches, Not Buildings." Issues in Science and Technology 8(3): 36-41.

Platt, Rutherford H., H. Crane Miller, Timothy Beatley, Jennifer Melville, and Brenda G. Mathenia. 1992. Coastal Erosion: Has Retreat Sounded? Boulder, CO: University of Colorado, Institute of Behavioral Science.

Polsby, Nathan A. 1984. Political Innovation in America: The Politics of Policy Innovation. Berkeley, CA: University of California Press.

Schmahl, George P. and Douglas W. Heatwole. 1989. "Coastal Barrier Island Management in Florida." In Donald K. Stauble (ed.), Barrier Islands: Process and Management. New York: American Society of Civil Engineers, 197-207.

Schmidt, Walter, Florida Geological Survey. 1991. Telephone interview, May 31.

Scott, Thomas M., Senior Geologist/Administrator, Florida Geological Survey. 1991. Personal interview, June 12.

Shows, E. W. 1978. Florida's Coastal Setback Line - An Effort to Regulate Beachfront Development. Coastal Zone Management Journal 4: 151-164.

Smith, Lester B., Gary Clayton, Charles A. Mayo, and Graham S. Giese. 1978. "Testimony Presented to the Department of Environmental Quality Engineering Concerning the Proposed Additions and Amendments to the Existing Regulations Promulgated under the Wetlands Protection Act." June 9.

Smith, Lester B., Daylor Consulting Group, Boston, MA. 1991. Personal interview, June 6.

Stafford, Donald B. 1968. Development and Evaluation of a Procedure for Using Aerial Photographs to Conduct a Survey of Coastal Erosion. PhD Thesis, Raleigh, NC: North Carolina State University.

Stephenson, Frank. 1986. "Beach Erosion: The Front-Line Defense." Florida State University Bulletin Research in Review. 80(3/4):3-23.

Stick, David. 1959. Handbook for Erosion Control. Raleigh, NC: North Carolina Hurricane Rehabilitation Program.

Sullivan, Mark B. 1976. Memorandum to the AEC Subcommittee of the North Carolina Coastal Resources Commission, March 2.

Tait, Stan, Executive Director, Florida Shore and Beach Preservation Association. 1991. Personal interview, June 11.

Tayfun, M. Aziz, Spencer M. Rogers, and Jay Langfelder. 1979. A Methodology Report on Delineation of an Ocean Hazard Zone for North Carolina. Raleigh, NC: North Carolina State University, Department of Marine Science and Engineering.

Terry, Jim, Pinellas County Public Works. 1991. Personal interview. June 13.

United States Army Corps of Engineers. 1971. Report on the National Shoreline Study. Washington, DC: The Corps.

United States Army Corps of Engineers 1978. Plan of Study, Wrightsville Beach, North Carolina. Wilmington, NC: Wilmington District Office.

United States Army Corps of Engineers. 1981. Beach Erosion Control and Hurricane Wave Protection: Carolina Beach and Vicinity, New Hanover County, NC, Final EIS. Wilmington, NC: Wilmington District Office.

United States Department of Commerce. 1978. Final Environmental Impact Statement, Proposed Coastal Zone Management Program for the State of North Carolina. Washington, DC: National Oceanic and Atmospheric Administration, Office of Coastal Zone Management.

Vallianos, L. 1974. "Beach Fill Planning - Brunswick County, N.C." In Proceedings 14th Conference on Coastal Engineering. New York, NY: American Society of Civil Engineers.

Wahls, Harvey E. 1973. A Survey of North Carolina Beach Erosion by Air Photo Methods. Raleigh, NC: North Carolina State University, Center for

Marine and Coastal Studies.

Wood, Timothy J. 1990. Breakthrough: The Story of Chatham's North Beach. Chatham, MA: Hyora Publications, Inc.

Zaremba, R. and S. Leatherman. 1982. Overwash Processes and Foredune Ecology, Nauset Spit, Massachusetts. Coastal Engineering Research Center, Technical Report. Washington, DC: U.S. Army Corps of Engineers.

SAND AND GRAVEL RESOURCES OFFSHORE OF BOSTON HARBOR

J. Bailey Smith
U.S. Army Engineer Waterways Experiment Station, Coastal Engineering Research Center,
3909 Halls Ferry Road, Vicksburg, MS 39180
and
Duncan M. FitzGerald
Boston University, Department of Geology, Boston, MA 02215

ABSTRACT

The shallow sub-bottom geologic character for a 800-square kilometer region offshore of Boston Harbor has been studied to describe sedimentary units and identify deposits of sand and gravel for construction and beach nourishment needs.

Sedimentary units offshore of Boston Harbor include: 1) drumlin highlands composed of mostly till deposits, 2) glacio-marine, fine-grained facies (Boston Blue Clay) consisting of clay and some silt that were deposited during the marine submergence phase of deglaciation and, 3) sand and gravel deposits associated with glacial outwash and possibly submarine fan deposition. Numerous bedrock outcrops associated with the late Precambrian Boston Basin rocks (e.g. Strawberry and Harding Ledges) protrude through much of the offshore sand and gravel deposits.

Economic sand and gravel resources in the offshore are estimated to be at least 13.0 x 10^6 m^3 and are restricted to three sites. Site 1, which is located 2.5 km seaward of Nantasket Beach, ranges between 4.0 and 6.0 m in thickness and contains an estimated 9.9 x 10^6 m^3 of sediment. Site 2 is located immediately seaward of Deer Island and Point Shirley. The deposit has an average thickness of 5.0 m and contains approximately 1.8 x 10^6 m^3 of sand. Site 3 is located at the entrance of Boston Harbor between President Roads and Nantasket Roads channels and contains 1.5 x 10^6 m^3 of sediment.

Sediment removal from Sites 1 and 2 would most likely steepen the nearshore profile, thus creating an offshore sediment sink. In addition, wave refraction patterns would be changed, thus altering erosion-deposition trends along the landward shoreline.

INTRODUCTION

The New England region has had a need for minable sand and gravel deposits dating back to the filling of Back Bay in Boston in the 1800s. A construction boom, that began in Boston during the 1960s and spread quickly to other metropolitan centers in eastern Massachusetts, has exhausted all large accessible aggregate resources in this region. To meet current construction needs, sand and gravel are being transported to Boston from as far away as southern Maine and central New Hampshire.

In addition to the ongoing requirements of the construction industry, the highly erosional nature of much of the area shoreline will necessitate extensive sand nourishment in the near future to preserve many of Massachusetts' highly frequented public beaches. The most readily apparent source of sand to nourish beaches in New England are glacio-fluvial deposits which are normally of poor quality because of the presence of silt, clay and/or gravel. The remaining sources of sand for beach nourishment are wave and tidally reworked glacial deposits on the continental shelf composed of well-sorted sands with a high quartz content.

While there exists a great need for new sand and gravel deposits, industry cannot be expected to begin mining aggregate resources on the continental shelf until the commodity is proven to exist in economic quantities. Also, industry must have the necessary knowledge to explore and produce the resource. This project was designed to assess the location and extent of sand and gravel resources offshore of Boston Harbor, and the effect of mining these deposits on the landward beaches.

METHODS

Surveys were limited to a region extending seaward from Winthrop south, to and including Nantasket Beach, to the 15-m depth contour. This is a distance of approximately 4 km offshore (Figure 1). Field investigations to define sand and gravel resources of the study area included: 100 km of both high resolution seismic profiling and side-scan sonar; 11 vibracores ranging in penetration from 2.2 - 8.8 m (average penetration = 6.0 m); 23 sediment grab samples; and 4 km of ground penetrating radar records.

STRATIGRAPHY

The stratigraphy of the region offshore of Boston Harbor is summarized in the stratigraphic cross section in Figure 2 (Sverdrup, 1990). Basement rocks, a complex of Late Precambrian granitic rocks, underlie much of the region and occasionally crop out above the surface as offshore bathymetric highs (e.g. Strawberry, Harding, Ultonia and Boston Ledges). Overlying the basement rocks are three sedimentary units associated with the Pleistocene Glaciation. Till, ranging in thickness from 3 to 28 m. and deposited during the glacial advance (maximum extent of glaciation was 21,500 yrs. BP (Pratt and Schlee, 1969)) occurs in the study area both in the form of drumlins, and as a mostly thin veneer blanketing the bedrock. The second unit is a glacio-marine, fine-grained clay and silt facies (locally known as the Boston Blue Clay) that was deposited during the marine submergence phase of deglaciation. The deposits thickness is dependent upon paleotopography of the study area and ranges from 0 to 50 m thick. The third sedimentary unit in the Massachusetts Bay Region consists of mud, sand and gravel derived from the reworking of various glacial and glaciofluvial sediments. These deposits are up to 6 m thick. The present day bathymetry of Inner Massachusetts Bay is a product of the paleotopography, sediment deposits, and tidal channel systems.

RESULTS

ECONOMIC SAND AND GRAVEL DEPOSITS

A total of 26.0 x 10^6 m^3 of sand and gravel is estimated to exist in the study area in the form of mostly thin, pervasive deposits. Of these deposits, three sites of sand and gravel accumulation, having a total volume of 13.0 x 10^6 m^3, have been identified as potential economic resources (Figure 3).

Site 1

This site is a triangular-shaped deposit located 2.5 km seaward of Nantasket Beach which parallels the shoreline for 2.4 km. The deposit lies between the 6 and 15 m contours and is confined by Strawberry and Harding Ledges to the northwest and boulder areas to the southeast. The deposit ranges between 4.0 and 6.0 m in thickness, has an areal extent of 1,986,000 m^2, and contains an estimated 9.9 x 10^6 m^3 of sediment.

Three pieces of evidence support the viability of the economic deposit at Site 1. Side-scan sonar records and grab samples indicate that the surface of the deposit consists of sand and minor amounts of gravel (Figures 4 and 5). Note the large region consisting primarily of sand, and sand with bedforms at Site 1 as recorded by side-scan sonar records and grab samples (sample numbers 7-12, and 21)(Figure 5). Gravel deposits associated with erosion of offshore, submerged drumlins are found to the north and south of Site 1.

The subsurface sediments of Site 1 are revealed in vibracores 1 and 2 (Figure 6). Vibracore 1 bottoms in an olive green to blue clay from (3.8-6.2 m) and is overlain by fine to medium sand with layers of coarse sand and pebble-sized gravel and shells throughout (0.0-3.8 m). Vibracore 2 penetrates tan to green clay with abundant silty and sandy layers from 6.0-8.8 m, overlain by fine to medium sand with pebble and shell layers (0.0-6.0 m). Seismic profile data suggest that vibracore 2 is positioned in a paleochannel (Figure 7, 8) and part of a drainage system which trends west-southwest to east-northeast with channels ranging in width between 300 and 900 m. The drainage system is believed to be Pleistocene or older in age and the thickest Quaternary deposits coincide with the deepest paleochannels (thickness of up to 40 m) (Figure 9).

The origin of sand and gravel deposits at Site 1 is related to the evolution of Nantasket Beach. Similarities in sedimentologic and physical setting suggest that sediment accumulations along the inner Massachusetts Bay may follow a similar evolutionary scheme as presented by Boyd et al. (1987) for the eastern Nova Scotia Shore. In this model, barrier islands are described as quasi-stable forms which are stable until the glacial sediment source is depleted. At that point, the barrier becomes transgressive and its sands are moved shoreward to new pinning points where barriers are reestablished. In this depositional transgression, a sand sheet is left behind. The clean, fine-grained nature of the Site 1 sand is a result of the reworking of sediments during this landward migration of the barrier island. It is these sand and gravel deposits are believed to be part of the sand sheet left offshore during the development of Nantasket Beach. Nantasket Beach appears to be a regressive barrier as suggested by seaward-dipping accretionary wedges that were recorded in ground penetrating radar records.

Site 2

The second sand and gravel resource site (Figure 3) is located 700 to 800 m seaward of Deer Island and parallels the shoreline for 500 m. The deposit has an areal extent of 389,000 m^2, an average thickness of 5.0 m containing approximately 1.8 x 10^6 m^3 of sand. The origin of Site 2 sediments are believed to be associated with the ebb-tidal delta shoals of former Shirley Gut, a tidal inlet which closed just 50 years ago.

The sediments of the Site 2 region (including the landward shorelines of Deer Island, and Winthrop and Revere Beaches) are coarser-grained and more poorly sorted than the sediments of Nantasket Beach. The difference in sediment characteristics of the two areas is perhaps explained by the sediment sources and amount of reworking. It appears that the glacial sources of Nantasket Beach and the offshore region contained a greater amount of sand-sized sediments than the predominant drumlin sediment source of the Winthrop Beach area.

Side-scan sonar records of this area indicate that surficial sediments of Site 2 are considerably more gravelly than those of Site 1 offshore of Nantasket Beach (Figure 4). The subsurface composition of the sediments at Site 2 is revealed in vibracore 9 (Figure 6) and their extent in seismic profiles of this region. Vibracore 9, 3.9 m in length, exhibits a coarsening-upward trend from fine to medium sand with some silty sand layers, to medium-coarse sand with abundant gravel at the top. This coarsening upward sequence may represent a decrease in the abundance of sand to this region and reworking of these deposits following the closure of the inlet.

Figure 7 indicates that Site 2 is located in the vicinity of a paleodrainage channel. Isopach data (Figure 9) suggest that the thickness of Quaternary sediments that have filled this paleochannel is up to 20 m.

Seismic data indicate that Site 2 is positioned at the edge of an accretionary wedge of seaward dipping beds which thicken landward. This accretionary signature is consistent with the development of the Shirley Gut ebb-tidal delta.

Site 3

Site 3 is located at the entrance of Boston Harbor between President Roads and Nantasket Roads channels. This deposit is essentially a mid-channel shoal between two strong tidal current systems. This site, which has an areal extent of 330,000 m^2, and a thickness of approximately 5.0 m, contains 1.5 x 10^6 m^3 of sediment.

Side-scan sonar data indicate that the surficial deposits of this site are composed of sand and gravel (Figure 4). Subsurface deposits, as defined by vibracore 11 (Figure 6), indicate that the deposit is composed of sandy-silty clay with isolated pebbles from 5.1-5.3 m, overlain by fine to coarse gravelly sand with several silty layers from 2.5-5.1 m. The upper 2.5 m of the core was lost during retrieval but is believed to be composed of fine to coarse gravelly sand as suggested by core penetration characteristics. Seismic records indicate that the presence of nearby paleodrainage channels (Figure 7) and Quaternary sediments in this region (thickness of 25 m) (Figure 9).

DISCUSSION

The total volume of 13 x 10^6 m^3 of sand and gravel resources in the region immediately offshore of Boston Harbor represents a significant quantity of material for beach nourishment purposes in the vicinity of the Boston Harbor Entrance. This volume would have been more than adequate to supply an ongoing beachfill at Revere Beach by the U.S. Army Corps of Engineers which requires approximately 700,000 m^3 of sediment for a three year event (Smith et al., 1993). A suggested beach nourishment project at Nantasket Beach would require approximately 600,000 m^3 of material (5 km length, 50 m width, and 2 m depth). This sand could be mined from Site 1.

However, the removal of sand from Sites 1 and 2 would have a detrimental effect on the landward Nantasket and Winthrop shorelines, respectively. Because both of these sites are close to the shore, the mining of sand from these locations would steepen the nearshore profile, thus creating an offshore sediment sink. This would cause a migration of sediment to this sink which would probably include a loss of sand from the onshore beaches resulting in erosion. In addition to these problems, a change in the wave refraction patterns along these shorelines would be expected. Since the refraction of waves is governed by the bottom contours, a change in offshore depths will result in a change in the dispersal of wave energy along the beach. Sand removal from Site 3 would have less of an impact on the shoreline as this site is located further offshore than the other two resource areas and is located in a bathymetrically low region.

SUMMARY

1) Determination of the depth and lateral extent of sand and gravel resources offshore of Boston Harbor are based on an extensive data base covering 800 km^2 including 100 km of both seismic profiling data and side-scan sonar data, 11 vibracores, 23 grab samples, and 4 km of ground penetrating radar.

2) Four geologic units in the study area include: 1) Paleozoic or older bedrock outcrops; 2) till including drumlins and ground moraine; 3) glacio-marine clays and; 4) Holocene mud, sand, and gravel deposits.

3) Three regions of economic sand and gravel deposits exist offshore of Boston Harbor out to the 15 m contour. The total of these sand and gravel deposits is 13 x 10^3 m^2. Site 1, which represents a former position of Nantasket Beach, is located offshore of Nantasket Beach and contains an estimated 9.9 x 10^6 m^3 of sediment. Site 2, which is likely the ebb-tidal shoals of the former Shirley Gut tidal inlet, is located seaward of Deer Island in 6-8 m of water and contains an estimated 1.8 x 10^6 m^3 of sand and gravel. Site 3, which is a present day mid-channel shoal located at the entrance of Boston Harbor between President Roads and Nantasket Roads channels, contains 1.5 x 10^6 m^3 of sediment.

4) Removal of sediment from Sites 1 and 2 would be detrimental to the landward beaches and most likely result in their erosion. Mining of the sediment at Site 3 would not adversely effect the coastal areas or navigation.

ACKNOWLEDGEMENTS

Funding for this project comes from a contract with the Massachusetts Coastal Zone Management Office with monies from the U.S. Department of the Interior Minerals Management Service. Permission was granted by the Chief of Engineers to publish this information.

REFERENCES CITED

Boyd, R., Bowen, A.J., and Hall, R.K., 1987. An evolutionary model for transgressive sedimentation on the eastern Shore of Nova Scotia in: FitzGerald, D.M. and Rosen, P.S. (editors), Glaciated Coasts, Academic Press, Incorporated, New York, 364 p.

Pratt, R.M. and Schlee, J.S., 1969. Glaciation on the continental margin off New England: Geological Society of America Bulletin, v. 80, p. 2335-2342.

Smith, W.G., Rosati, J.D. and Lemire, A., 1993. Revere Beach and Point of Pines, Massachusetts shorefront Study: Beach Nourishment Management and Considerations Volume, Proceedings of Coastal Zone '93, New Orleans, Louisiana.

Sverdrup Corporation, 1990. Subsurface exploration report for inter-island tunnel: Deer Island, Boston, Massachusetts: Massachusetts Water Resources Authority Contract Number 5494.

Willett, C.F., 1972. Raytheon final report of Massachusetts Coastal Mineral Inventory Survey for the Division of Mineral Resources, Commonwealth of Massachusetts.

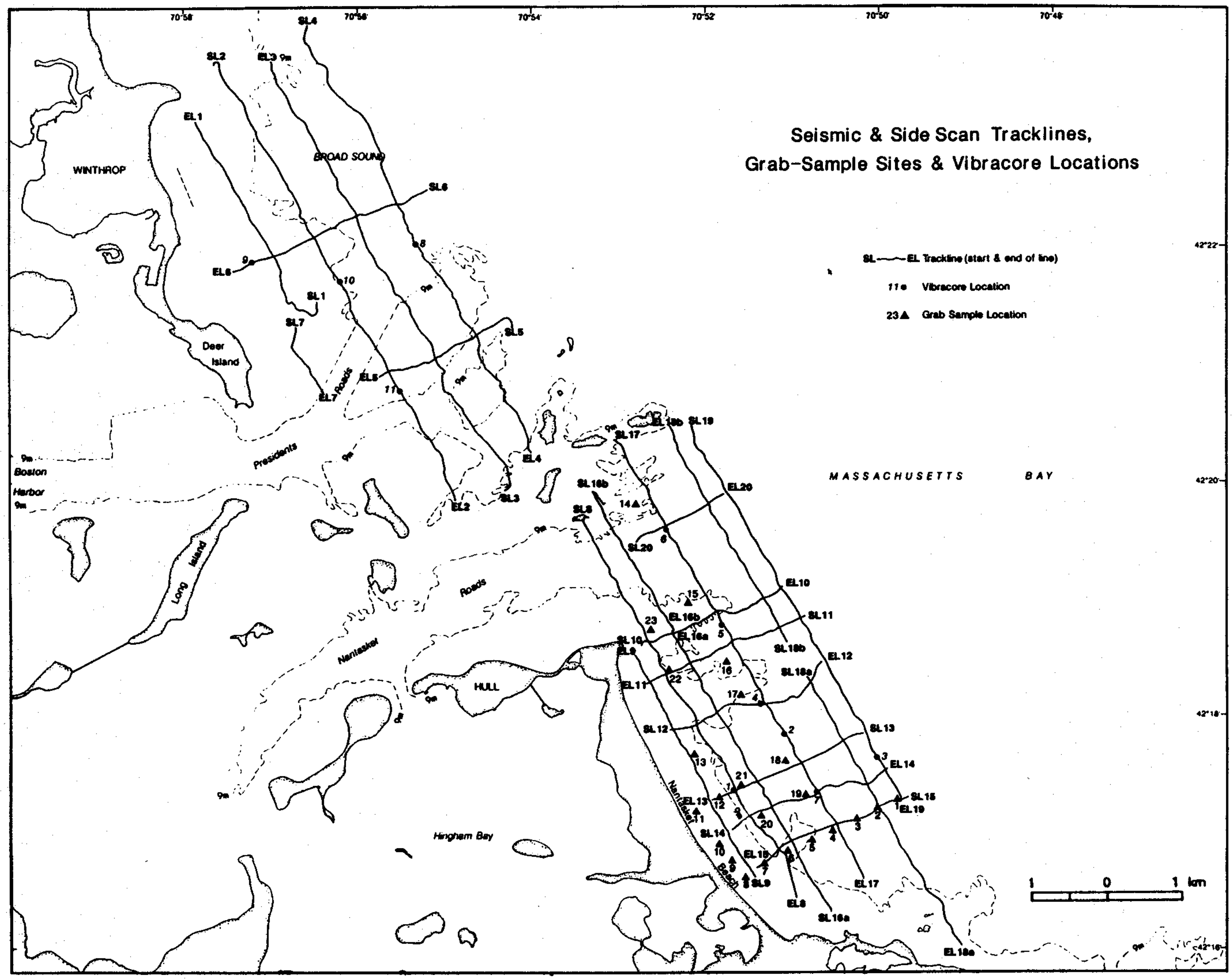

Figure 1. Field investigation study area.

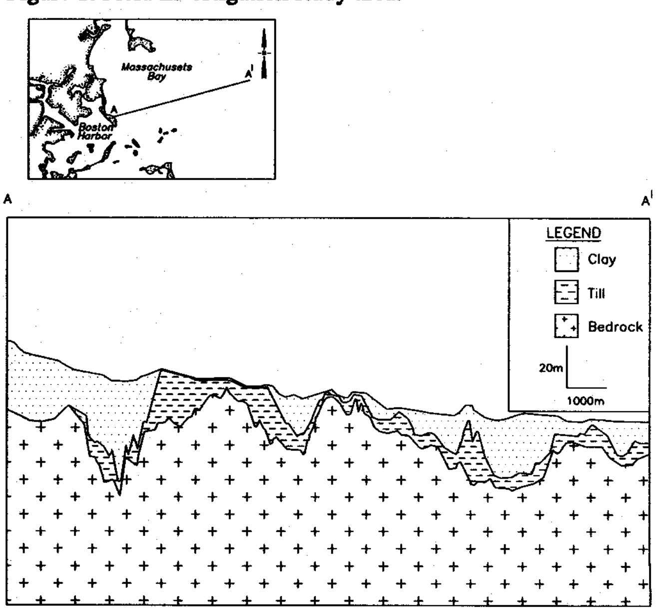

Figure 2. Stratigraphic cross section of the region seaward of Deer Island (after Sverdrup, 1990).

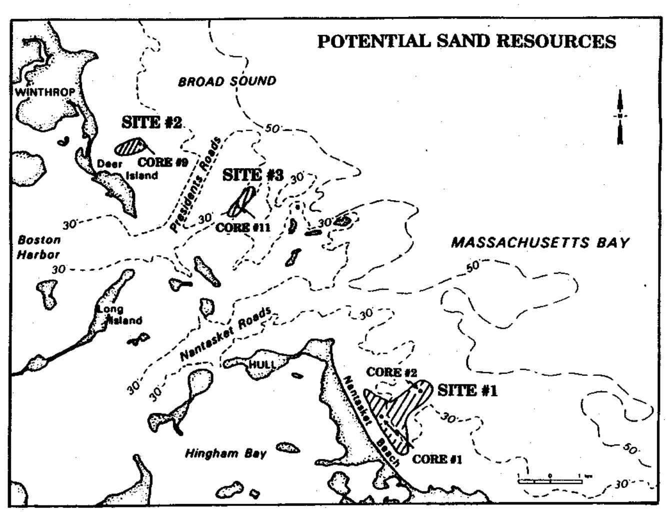

Figure 3. Potential sand with gravel resources within the study area.

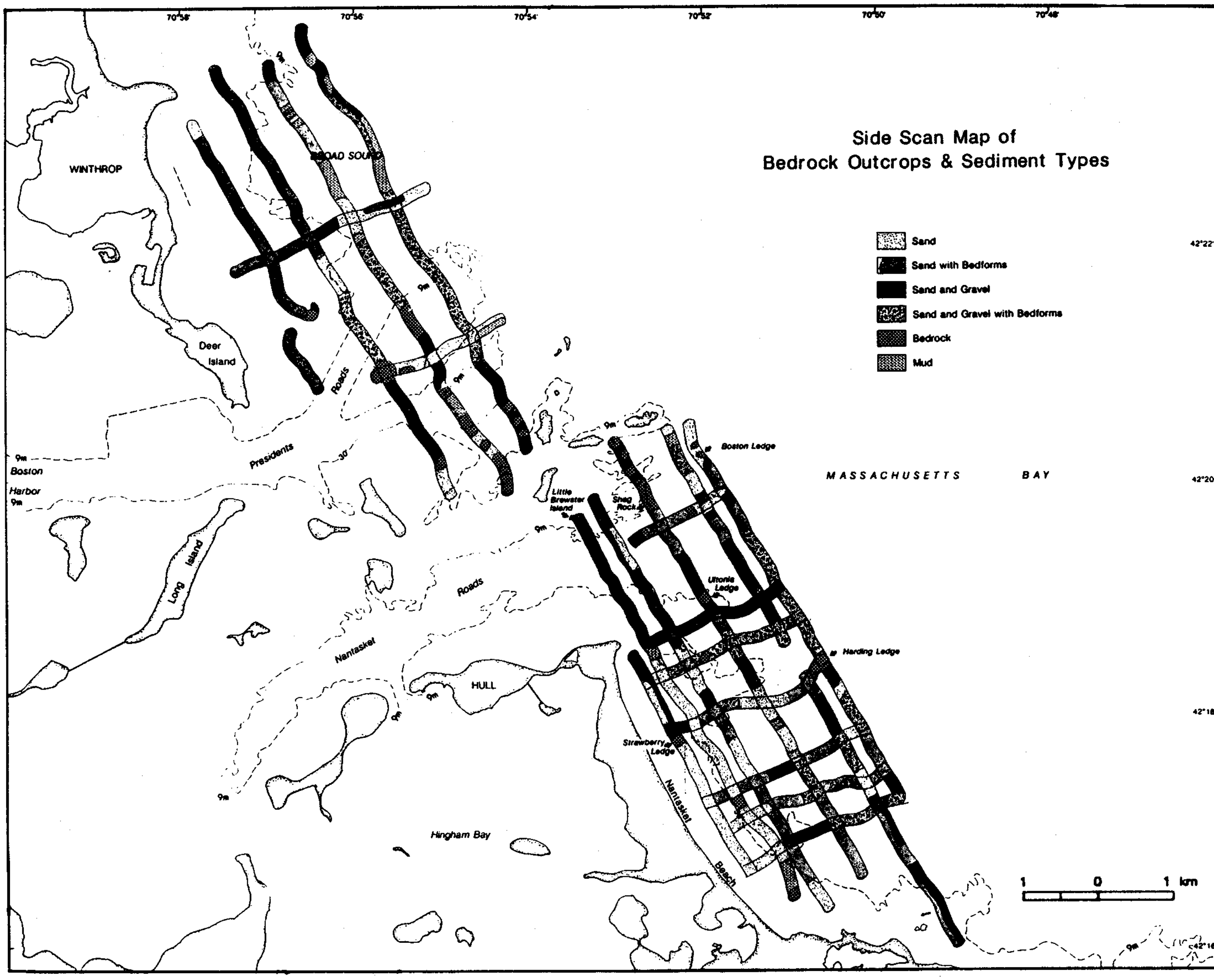

Figure 4. Side-scan sonar map of sediment types.

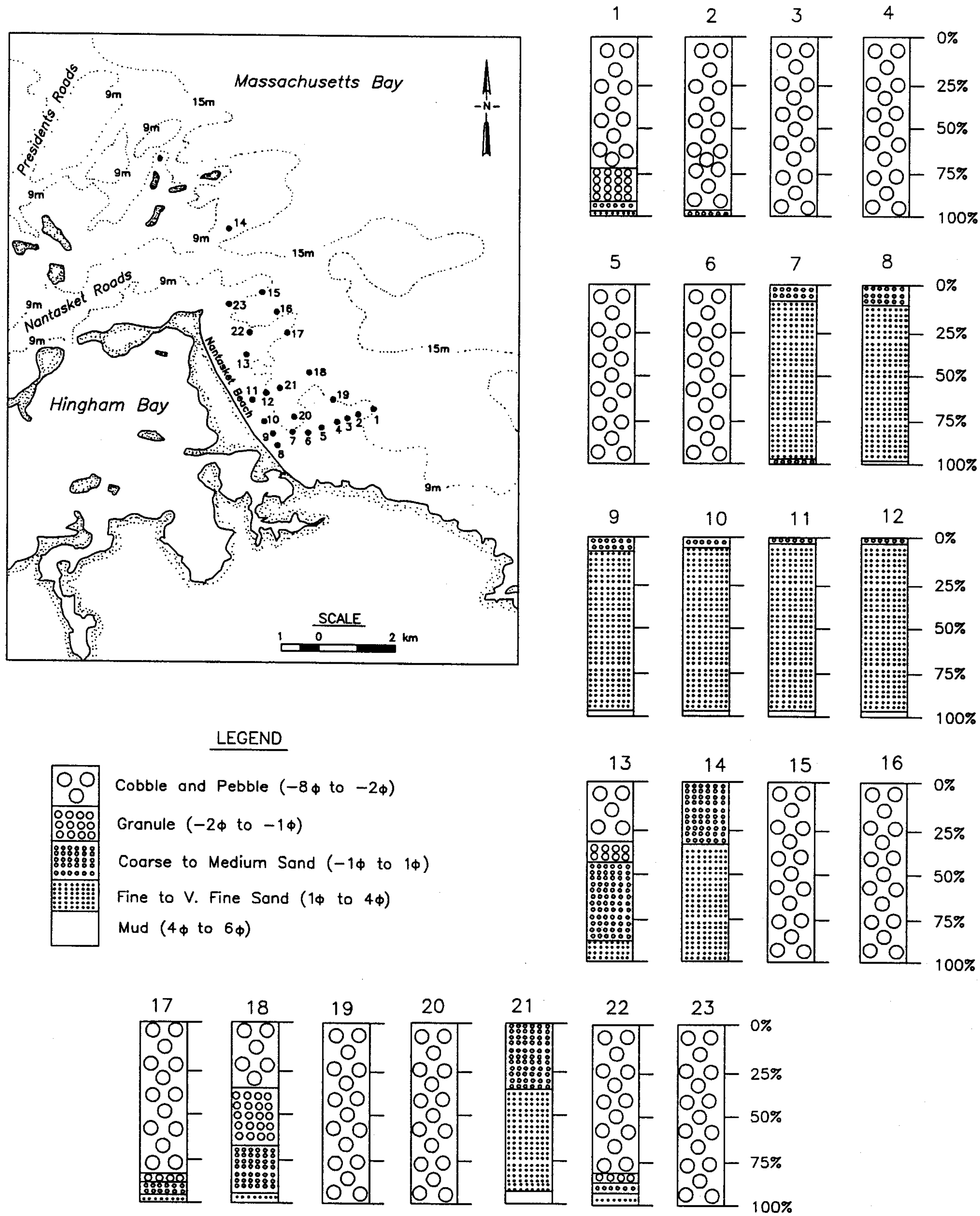

Figure 5. Location and size description of grab samples offshore of Nantasket Beach.

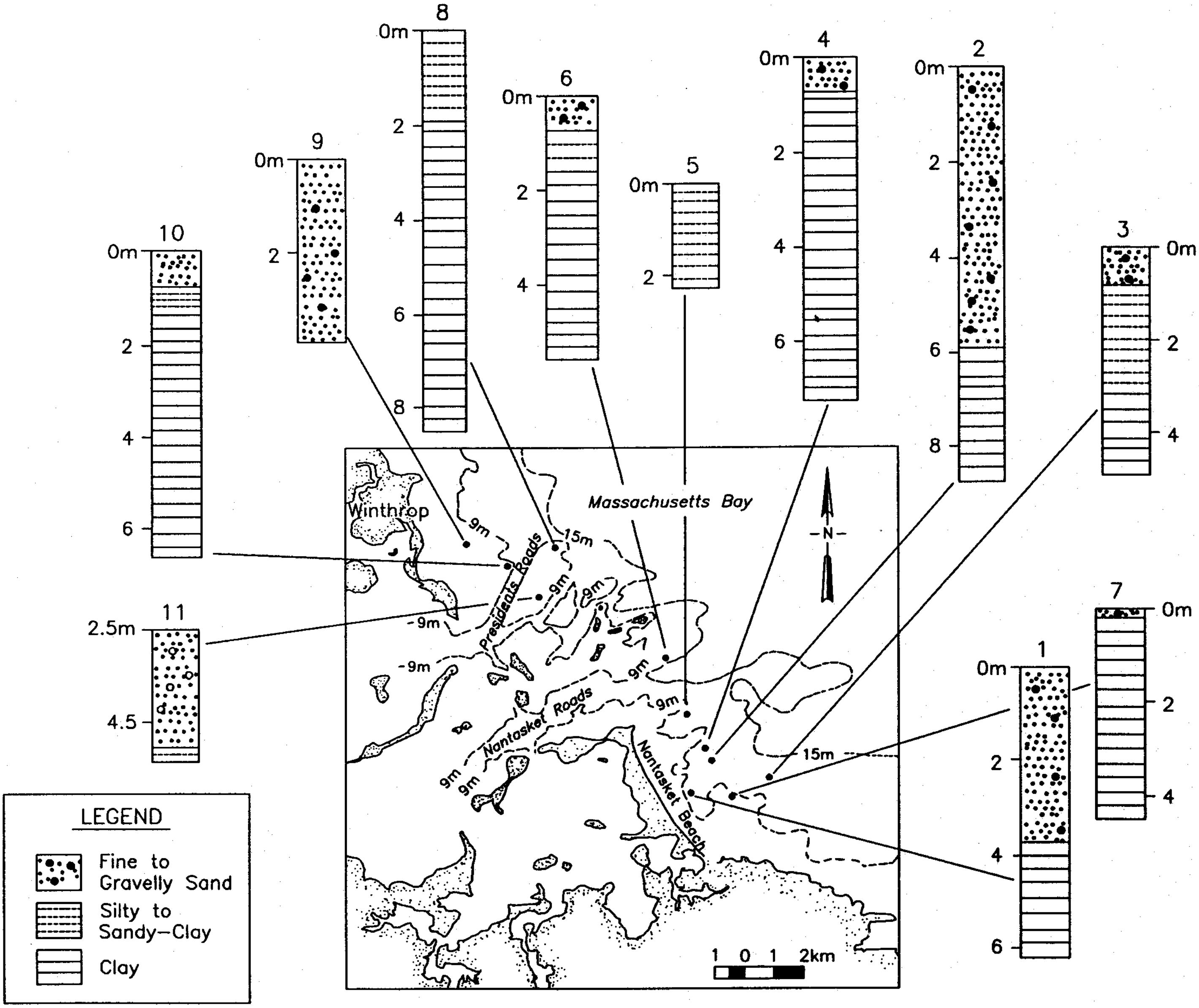

Figure 6. Location and generalized description of vibracores.

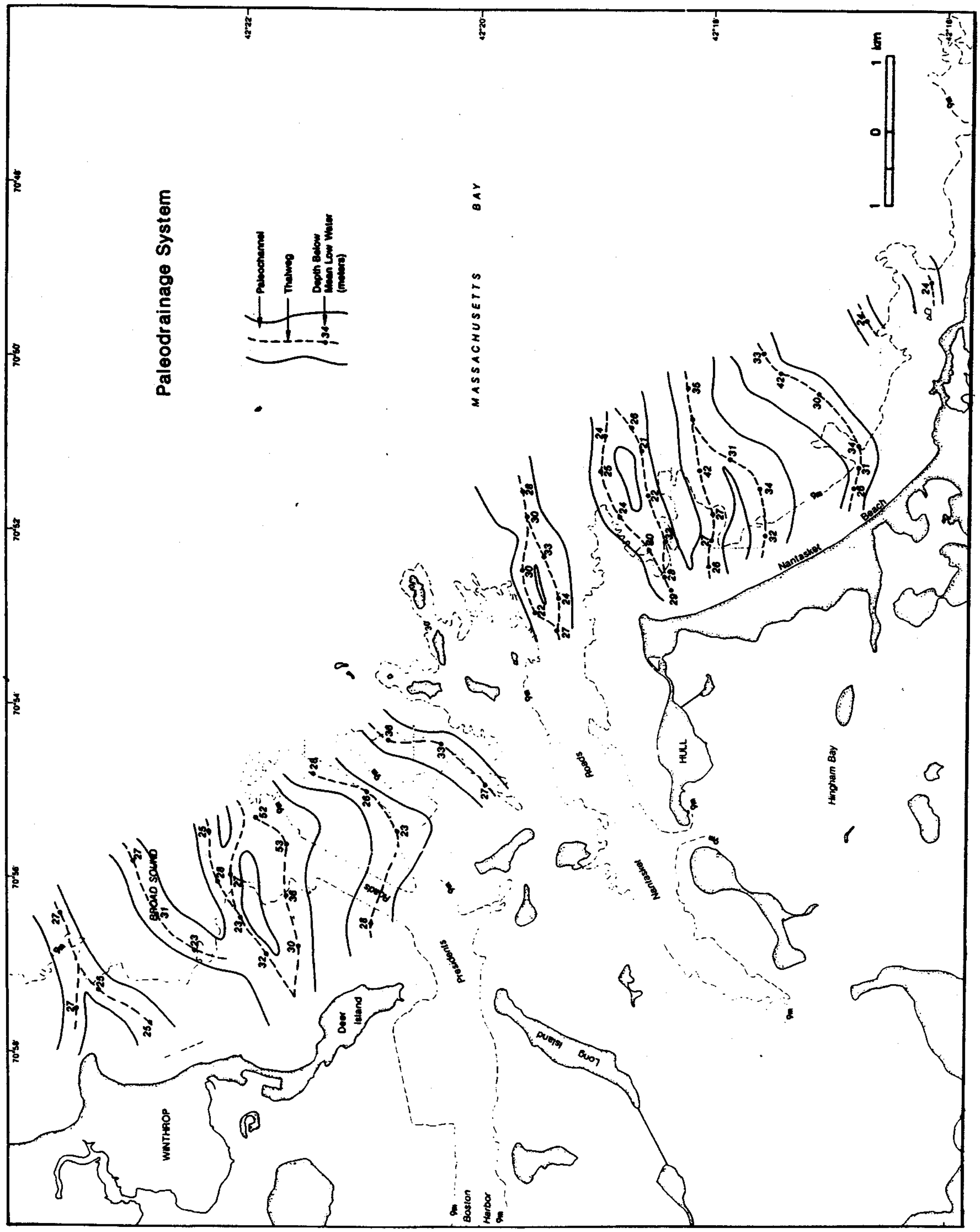

Figure 7. Paleodrainage system of channels for the study area.

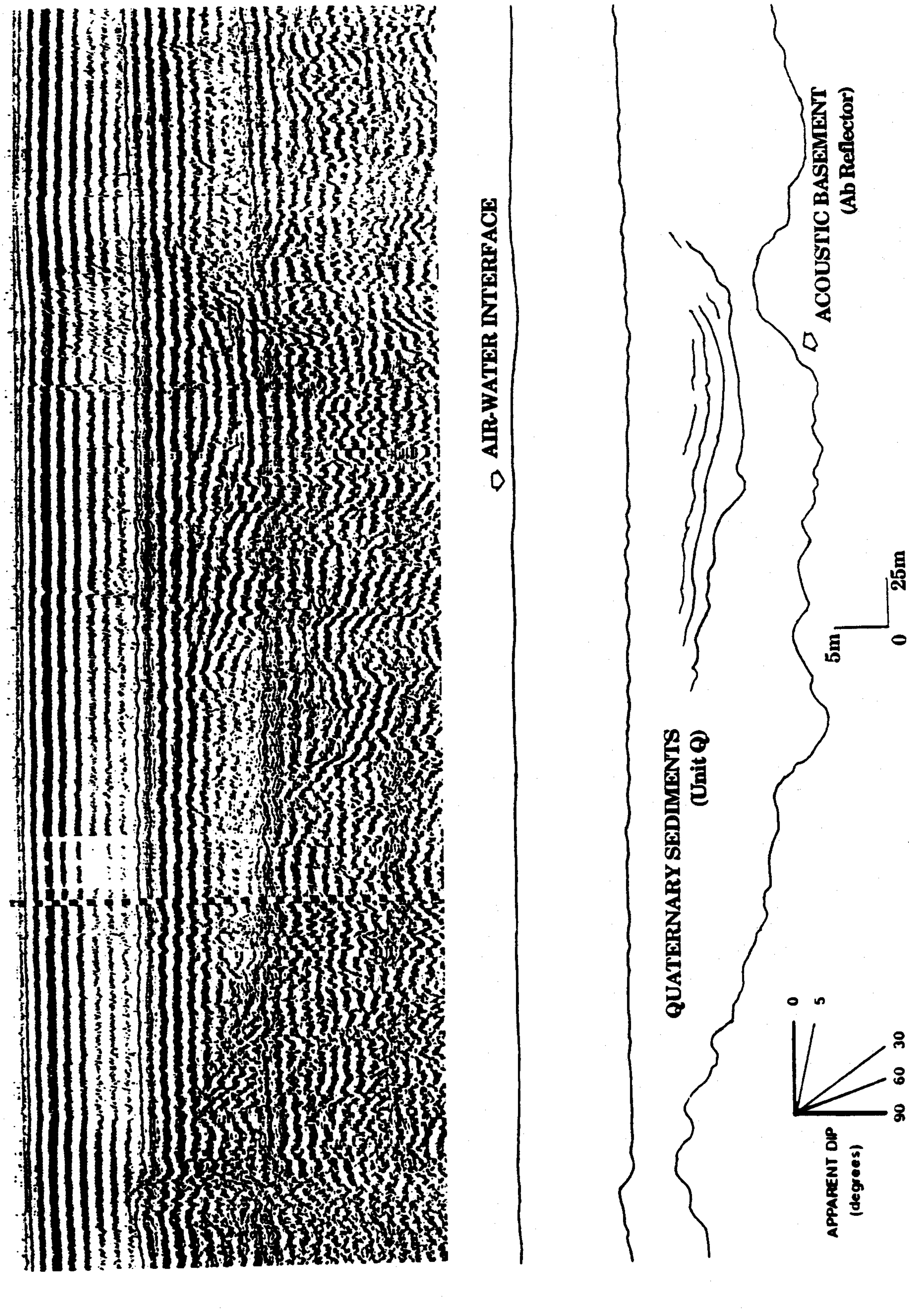

Figure 8. Seismic profile line running northwest-southeast in vicinity of Site 1.

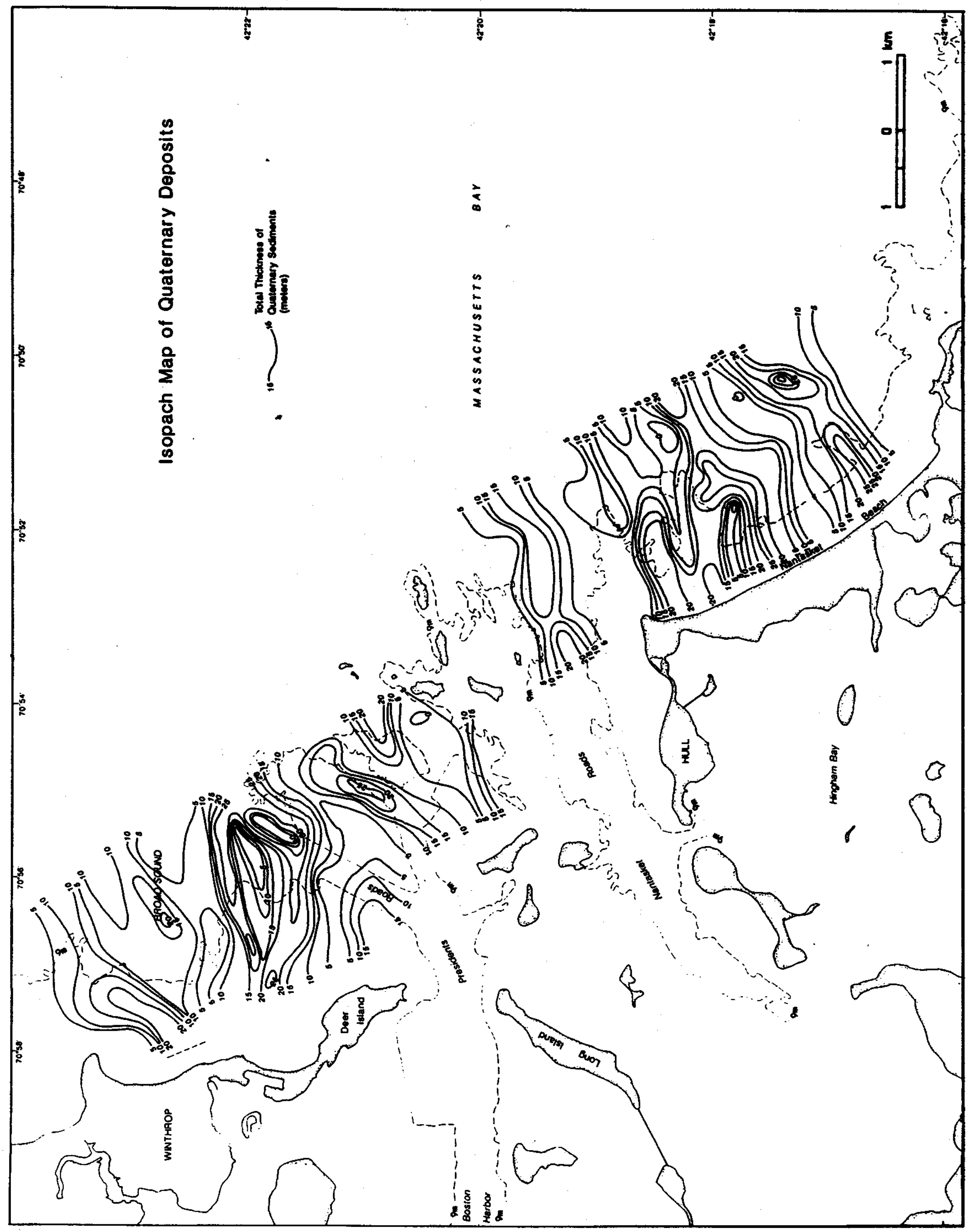

Figure 9. Isopach map of Quaternary deposits for the study area.

BIOREMEDIATION OF PETROLEUM-CONTAMINATED SOILS: THE ENVIRONMENTAL RESTORATION OF A FORMER RAILYARD

Dana S. Jackson and Paul Scovazzo
Kemron Environmental Services, Inc., McLean, VA

Abstract

Petroleum contamination is a pervasive environmental problem. The common remedial solution has been to excavate and landfill the contaminated soils, which is hampered by high costs and space limitations at traditional disposal facilities. Bioremediation is a more attractive soil remediation alternative. It is winning favor primarily because the soil can be treated on site, and the bioremediation systems can function without interfering with existing facilities. Although the concept of bioremediation has existed for many years, its acceptance as a cost effective approach to remediation is only now being realized.

There are several problems to address when considering bioremediation. These are: porosity and permeability of soil, indigenous or off-the-shelf microbes, availability of water, and distribution of nutrients to the microbes. This paper will answer how some of these questions were addressed at one site near Baltimore, Maryland.

The site, a retired railyard and port facility, had maintained a 40,000 gallon diesel locomotive refueling station. The levels of contamination of Total Petroleum Hydrocarbons (TPH) ranged from 100 parts per million (ppm) to greater than 25,000 ppm. The total volume of soil which required treatment was estimated to be more than 70,000 cubic yards. At the Baltimore site, KEMRON chose to utilize indigenous bacteria to affect the remediation. Groundwater was extracted, augmented with nutrients and oxygen through mobile treatment trailers, and returned to the soil for infiltration. This created an environment where the bacteria could naturally degrade the petroleum hydrocarbons to acceptable levels. Once these levels have been achieved, the redevelopment of prime real estate can begin.

INTRODUCTION

CSX Transportation (CSXT), owner of an over 100-year-old railyard and port facility located within the City of Baltimore, wished to redevelop the property to a mixed light industry, commercial, and possibly residential use. The railyard had long since reached the end of its useful life; many service areas such as the roundhouse, the locomotive repair facility and associated turntable had not been in operation for over 20 years. The driving force behind this site's redevelopment is its proximity to waterfront acreage and the Inner Harbor, the heart of downtown Baltimore, with easy access to major highways (Figure 1). The former railyard and associated facilities covered approximately 139 acres surrounded on three sides by the Patapsco River. Most of the former operational units included the Locomotive Repair Facility, which had its own forge, and the Round House and other storage and maintenance buildings which had been built during the early part of this century. Most had fallen into disuse as newer repair facilities were built, because the facility had been designed to service coal-powered steam locomotives. The first step in retiring the yard permanently was to conduct the initial environmental audit of the facility. Several environmental flags were raised, mainly because of former materials handling practices and its age, and the type of work which had been conducted on site through former leasing of unused buildings. As a result of discovering these environmental issues, it was determined that a more formal remedial investigation should be conducted.

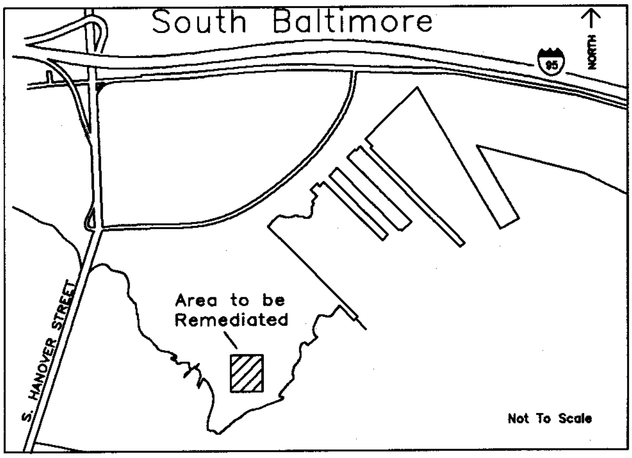

Figure 1. Site Location Baltimore, Maryland.

The most obvious environmental issue was the storage and handling of petroleum products. Of particular concern were diesel and gasoline use at the facility. The potential for petroleum contamination was high because of several reasons; the large number of above- and below-ground fuel storage tanks associated with old facility buildings, intermodal operations, and locomotive refueling located throughout the site. Fifty-nine buildings and structures were searched for petroleum storage tanks, as were historic refueling facilities seen in areal photographs and as-builts. More than 50 petroleum storage tanks were recovered, cleaned and disposed of in accordance with federal, state and local regulations. Tanks ranged in size from less than 350 gallons to 20,000 gallons.

With regard to the small above- and underground storage tanks, a few areas were found to have minor petroleum contaminated soils, most of which required limited remedial action. However, one area was found in need of extensive remediation, the former locomotive refueling station which had two 20,000 gallon above-ground storage tanks supplying fuel to two refueling islands. These refueling islands had been in operation from at least the early 1950's (based on aerial photographs) to the late 1960's, when the repair facility of the yard was abandoned. Results from a limited surface soil investigation for petroleum hydrocarbons indicated that a more detailed subsurface investigation was necessary. The results of this investigation determined that as much as 70,000 cubic yards of soil required remediation. The focus of this paper is the methodologies used to delineate the contamination, the decision process used to choose a remedial solution, and the problems which had to be addressed to implement that solution.

REMEDIAL INVESTIGATION

During the Phase I Site Investigation, we found that several areas adjacent to the refueling station showed evidence of soil stains from possible intermittent fuel spillage. This visual signal, plus the knowledge that refueling stations are historically notorious for soil and groundwater contamination, led to a random sampling of obviously stained areas to determine the levels of surface soil contamination. The results were positive, which indicated there was the potential for heavy contamination of subsurface soils and possibly groundwater.

An early confirmation of contaminated soils resulted from the demolition activities of the former fueling structures. Fuel lines were exposed and being recovered for scrap metal, and excavated soils were found to have high levels of petroleum contamination that generally followed the fuel lines to the refueling. The condition of the fuel lines and the stained soils adjacent to the fueling nozzles confirmed that these were the source. This information reinforced the potential for extensive subsurface soil and groundwater contamination. The focus of the subsurface investigation was then used to confirm our suspicions and delineate the vertical and lateral extent of the potentially contaminated soil.

SUBSURFACE INVESTIGATION

A remedial investigation (RI) was conducted to determine the vertical and lateral extent of known or suspected contaminants. The purpose was to determine the impact on both soil and groundwater. To do this, 23 soil borings were conducted and nine groundwater wells were installed. Each soil boring was sampled continuously using two-foot split spoons to a depth of 30 feet. Seven of these boreholes were converted to 4-inch monitoring wells, and two were converted to 2-inch piezometers to determine groundwater flow direction, aquifer characteristics and impacts on groundwater. Diesel contamination of the soil was found to be extensive, ranging from less than 100 to 25,000 parts per million (ppm). State law uses a regulatory trigger of 100 ppm to require remedial investigations. Fortunately, during our investigation no free product was encountered, and the groundwater showed it had only low levels of dissolved hydrocarbons.

What made this site particularly challenging was the distribution of the contamination in the subsurface soils. Contour maps of contamination levels were made for each two-foot sampled interval. This data showed that it originated from the general area of the former refueling station. Also, the data indicated a non-linear distribution. From this information, we concluded that there was no discrete plume migration in the subsurface. The data indicated that the hydrocarbons had migrated into the subsurface following different preferential pathways of porosity and permeability. These were dependent on where the petroleum infiltrated thus forming laterally discontinuous fans radiating from the general source of area. This distribution was determined to be a result of the porosity and permeability variation within different fill materials used to build the land.

All this information significantly affected the remedial technology decision making process. A historical investigation found that the site had been in use from colonial times. The original shoreline was much different and most of the present land was under water. The current elevation of the site is between 12 to 14 feet above mean sea level. The site had been farmed, and later at the turn of the century, was a source for clay used in the manufacture of bricks. Excavated areas were filled with a variety of different materials including: spoils, construction debris, night soil, and charred debris from the Great Fire of Baltimore of 1905. Aerial photographs indicated that the shoreline had remained relatively unchanged until the early 1960's. Then the southeast shoreline was extended by the construction of two landfill areas. Landfill construction was completed by the late 1970's. In addition, the known historic shoreline had been altered prior to the turn of the century on the eastern side, possibly adding a third more land to pre-1970 shoreline. One additional factor had to be taken into consideration. As the railyard facility grew, old yard patterns were covered with new yard patterns. All these factors were to influence the migration of the hydrocarbons into the subsurface.

The affected area surrounding the refueling island was delineated using standard investigative techniques as mentioned earlier. The final area that required remediation covered a surface of approximately 105,000 square feet with depths of up to 20 feet, for a total volume of soil greater than 70,000 cubic yards. We then needed to choose a technology that would be the most cost effective for the client.

SELECTING A REMEDIAL TECHNOLOGY

Based on the extent of the subsurface contamination, several remedial options were considered. The general approach used to select a remedial technology is a combination of cost, regulatory constraints, and time. For the majority of sites where real estate transactions are involved, the third variable is generally the one which controls the technology chosen. Often, the time frame may already be set and have to be met regardless of cost to keep multimillion dollars deals on schedule; this usually causes less expensive remedial technologies to be excluded. "How clean is clean" depends on the contaminant in question and on the proposed final site usage, such as commercial versus residential. All of these factors influence the remedial technology chosen. In our case, the client asked for the full spectrum of remedial technologies to be presented, based on long term development goals of this property. Four remedial technologies were considered: landfill disposal, soil stabilization, incineration, and bioremediation.

The first remedial technology reviewed was landfill disposal. This was rejected for several reasons. The first and most important reason was the potential for future liability issues; as a generator you never truly relinquish ownership until the material is destroyed. The second reason was the determined expense of excavating all the material, and the fact that much of the contamination would be near the groundwater table. This would present several construction problems. The excavation would require double and possible triple handling of the soil. This is so, because of dewatering and soil erosion control issues, which would drive labor costs high. Not dewatering the soil adds to the disposal costs because volume increases and landfilled soil has to pass a "slump factor" requiring the addition of fill. Another difficulty is that as the groundwater table is approached, the ability to segregate clean from contaminated soil becomes impossible, again increasing disposal costs. The final problem is that all the groundwater pumped to dewater the excavation would require treatment.

The second remedial technology reviewed was soil stabilization. Soil in combination with portland cement is used to create road bed material. The main drawback to this approach is the low limits of the petroleum contamination that have to be acceptable and the large soil volume which has to be treated. The cost estimate for this was $60 per ton.

The third remedial technology considered was soil incineration, either on- or offsite. This technology was rejected because of cost, chiefly because of the potential high moisture content of the soil, the volume to be treated, and the issues related to groundwater treatment during excavation. In addition, because of the high moisture content and the low BTU values of the soil, a large quantity of fuel would be required to complete the remediation. The cost estimate at the time was more than $100 per ton.

The fourth remedial technology considered was bioremediation. The first type of biotechnology reviewed was ex-situ, however, this was rejected for similar transportation-related problems discussed above and because the cost of building a cell large enough to hold all the soil to be treated was prohibitive.

The remedial alternative finally selected was in-situ bioremediation. Our bottom line was based on cost and ability to treat the distribution of contamination in the subsurface. Based on current operation and project projections, the final cost to remediate the soil was projected to be approximately $20 per cubic yard.

BIOREMEDIATION

There are many reasons why bioremediation is an attractive remedial technology. The principal reason is cost, which may be as little as $18 dollars per cubic yard. Bioremediation is applicable to many situations. Determination of its applicability to a particular site depends on three factors: the contaminant to be remediated, time, and whether a long-term facility would disrupt normal business activities at the site. Most light hydrocarbons may be remediated fairly easily and quickly. Heavy tars and oils are much more difficult to break down by microbes, although bioremediation generally is considered a practical approach at this time. Bioremediation may clean a site in as little as three months or up to three years, so a client has to have a very good idea of future land use. The best part about bioremediation is that, in the majority of cases, the construction phase is relatively short, with minimum disruption to the facilities' normal activities. There are two other reasons why bioremediation is gaining more acceptance besides its proven track record, and those are long-term budget control and waste minimization. Environmental compliance officers can control their long-term budget projections and amortize the cost over of a project over several years, rather than having one large expenditure for disposal and treatment all in one lump sum. With landfill space becoming more scarce, the less contaminated material one has to ship offsite the better, so waste minimization is an important consideration.

TREATABILITY STUDY

Before the final decision was made to use bioremediation it had to be determined whether or not the soil in fact would be remediated using this technology. In our case, it took three treatability studies before we could commit to this technology. Generally, only one such test is required.

Treatability studies, in general, are laboratory studies conducted under controlled conditions to determine the appropriateness of a selected remedial technique. At the railyard, soil samples were collected for analysis from test pits at different areas of known contamination. The average concentration of contamination was 9000 ppm. The soil samples were incubated and monitored using an electronic respirometer. One sample was used as a control with no addition of oxygen or nutrients, a second sample was treated with nitrogen and phosphorous (nutrients) and a third was inoculated with "off-the-shelf" bacteria and nutrients. The latter refers to bacteria which have been segregated in the laboratory from strains collected in the field. These soil samples were monitored for several parameters including oxygen uptake, Ph, microbial counts and Total Petroleum Hydrocarbons at the beginning and end of the test. The first test was terminated at 25 days due to interference, the second test at 66 days and the third test at 42 days. During the first experiment respiration levels fell off dramatically, indicating a toxic event had occurred. The soil was analyzed for possible bad actors, and heavy metals were determined to be the cause of the die-off of the off-the-shelf bacteria.

This brings up the question of utilizing indigenous species versus off-the-shelf microbes. The main reason to use indigenous microbial populations is that they have already acclimated to any material present which might be a stress in their environment. The second reason is that they are cost free; all you have to do is feed them. That is not to say that one would never add cultured bacteria, since one may want to inoculate soil with what are perceived as "the better bugs". The populations will then compete, and the best of both populations will survive in the soil. It is rare to have sterile soils. The number of bacteria present in soils is about 10^6 per gram. Factors which control bacteria populations are Ph, temperature, nutrient levels, moisture levels, and dissolved oxygen level. Soil Ph should be close to neutral, soil temperature should be above 40° Fahrenheit to optimize aerobic activity, and nitrogen and phosphorous should be available in sufficient quantities to the microbes to metabolize the hydrocarbons as a food source. However, the most important component of this equation is the availability of oxygen for the microbes to attack the hydrocarbons, without which the microbes attack on the petroleum would be less attractive efficient. The results of our final study, which lasted six weeks using indigenous bacteria and the addition of oxygen and nutrients, indicated a 90 percent reduction of the contaminants in the soil. Having established the technology works, the next step was to build a system that provided the proper levels of nutrients and oxygen to the bacteria.

CONCEPTION AND CONSTRUCTION OF THE BIOREMEDIATION TRAILERS

KEMRON worked closely with the client to determine the best system for their needs, both at this site and possible future sites. Since petroleum contamination is a common problem at many older rail facilities it was determined that we would construct a state-of-the-art mobile bioremediation system with a design life of 20 years. Our experience up to this time were site specific with limited flexibility. Flexibility was a key requirement for our new system. The system was to be designed around the most current water treatment technologies which could be contained on a mobile platform and which would require minimal maintenance due to the remoteness of some of the client's facilities.

As a result of KEMRON's efforts to utilize current wastewater treatment technology and through the skills of CSK Technical, Inc. of Tonowanda, New York, two mobile water treatment trailers were designed and built. Each trailer was equipped with an integrated oil water/water separator, sand filters, air stripper, nutrient tank, a backwash settling tank with external sludge storage, and a multi-function water storage tanks. All the systems functions are controlled by Programmable Logic Controls (PLC) which record such information as dissolved oxygen, Ph, tank volumes, and water levels in the monitoring and extraction wells. All information is monitored offsite via modem. While the trailers were being fabricated, the installation of the groundwater extraction system was completed. The minimum amount of water production which was necessary was a combined flow of 20 gallons per minute.

EXTRACTION WELLS AND RELATED PROBLEMS

Eight extraction wells were installed to an average depth of 20 feet. The extraction pumps used were variable speed, positive displacement pumps, which utilize a helical screw assembly to displace fluid. This type of pump was chosen to minimize the potential for the emulsion of any free product which might be encountered during the remediation. The use of variable speed pumps also allowed for the maximum volume of water to be extracted from the aquifer at each location across the site. Each well was connected to the PLC and the number of times each pump turned on and off due to volume changes was recorded. These detected events are reviewed to determine if the pump is turning on and off too much and should be pumping at a lower rate, conversely if a pump did not turn off at all maybe more water might be extracted at this location. This modulation of each pump is performed remotely until all of the wells are in equilibrium, and withdrawing the maximum number of gallons of water available. The maximum volume of water which can be treated in a 24-hour period is 43,000 gallons, or approximately 15 million gallons a year. Once the system reaches saturation it will become a closed treatment system; for all intent and purposes, the same water will be recycled over and over, bringing nutrients and oxygen to feed the growing bacteria population in the soil. What happens to the bacterial "bloom" when all the petroleum is gone? The bacterial population will die back to levels that can exist consuming the more difficult organic material present in the soils.

One of the modifications which was required prior to continuous operation of the system was the installation of a water pretreatment system for iron. When the system was designed, levels of iron in the water were found to be in the 5 to 15 ppm range. This level is considered high in the water treatment industry and was engineered to be removed using green sand filters. The green sand filters chosen would reduce the level of dissolved iron from as high as 30 ppm to zero. However, after three months of shakedown operation, the levels of dissolved iron had increased from 15 to as high as 100 ppm. The system was only able to remove the iron to a level of 6 ppm, causing considerable fouling of the oil water separator, green sand filters, and air stripper where the iron oxidized. Had this condition been allowed to continue, the whole system would have become completely fouled. As it was, an extensive amount of unscheduled maintenance, including the replacement of the green sands which had become poisoned, had to be conducted to bring the system back to fully operational levels. This increase in the dissolved iron was totally unexpected and required a field modification of the equipment to allow for maximum removal of the dissolved iron from the influent water before entering the treatment trailers. We used an external tank system which employs a bubbler to add oxygen to the water going in to oxidize the iron, and a polymer to force the now suspended iron oxide to flocculate and drop out of suspension. The resolution to this problem cost approximately $30,000, but maintenance costs without it would have been far more expensive over a two-year of period of operation and would have reduced the life of the treatment systems. Another successful step was completed: The trailers were built and we had water. Next we considered how to get the treated water back to the where it was needed.

FIELD DISTRIBUTION SYSTEM

Several problems had to be overcome to make sure that the treated water reached the microbes in the soil. Two specific problems which had to be overcome were the heavy compaction of the upper three feet of soil, and the distribution of contaminants in the soil.

This first problem was due to the multiple yard configurations which had been built over time and the heavy rail traffic in the yard. Initial perk tests indicated that the soil would conduct water to the subsurface; we wanted to ensure that all of the water would enter the field where we wanted it to. The first step to solving this problem was to use a root rake tractor to scarify the site after all the demolition activities had been completed. Several hundred cross ties were recovered from depth, along with demolition debris. This was a good beginning, but we were not comfortable that we had disrupted the upper soil as much as necessary for good infiltration. After the scarification, the site was roughly leveled, and a D-9 size bulldozer with a 6-foot ripping shank was used to rip the soil to depth running parallel to the proposed infiltration galleries. This operation assured that there was a maximum disruption of the upper soils and that the maximum amount of treated water would find its way along the original pathways to the contaminated areas in the subsurface.

The second problem was in designing a system which would treat all the contaminated soil. Since the distribution of the contaminants was present in the surface soils over much of the affected area it was not possible to built traditional infiltration galleries which are constructed below grade. The traditional infiltration gallery would require excavation of three to ten feet and laying distribution pipe on gravel. The problem with this was that the surface soil would not be treated. Secondly, the distance between galleries would have to be very close to ensure that contaminated soils between galleries were treated. A third problem was how to treat the excavated soil from all the trenches. It was obvious that a innovative approach was required.

Our solution was to borrow current civil engineering technology from the storm water management area. The infiltrating system selected could distribute water through a precast plastic half shell, which was placed directly on top of the ground. This product (produced by Infiltrator Systems Inc.) solved our problem of how to direct water to the majority of the surface. This system could be installed directly on the surface with distribution piping attached to the roof of the shell. Holes in the distribution piping directed the treated water upward under pressure. The water then ran down the sides and exited through slits in the side walls of the shell directly to the ground beneath. Even though this distribution system enclosed the contaminated area, we wanted to assurance that the nutrient bearing water reached all the surface soils between each distribution line (Figure 2). The last part of the construction phase before the gallery was installed was the installation of an artificial reservoir. This was done by laying an 8-inch gravel layer across the affected area. Once the system reached equilibrium the gravel bed provided a continuous recharge to all affected soils (Figure 3). After the infiltration gallery was constructed on top of the gravel, It was hydrostatically balanced and then covered with a geo-textile fabric. The fabric allowed rain water to pass through, but not sediment, preventing the clogging of pore space in the gravel. Finally, to allow for all season operation, the system was covered with three feet of soil to prevent the pipes from freezing during the winter months.

CONCLUSIONS

As one can see from this case study, the problems of installing a comprehensive bioremediation system are not something that can be learned from a textbook. It takes a lot of people working together to solve all the different problems which arise. In our study we had four problems:

- Sufficient water flow to treatment trailers
- Dissolved iron in the groundwater
- Porosity and permeability problems of the soil
- Distribution of the contaminant in the soil.

Each of these had to be overcome to assure the success of the system.

The bacteria were there, all we had to do was make sure that they got the nutrients and oxygen that they need to reduce the hydrocarbons bound to the soil. The success of this system demonstrates how we were able to overcome our site specific problems. Each site will pose unique problems; it takes teamwork and multiple disciplines to solve them. Chemical and civil engineers, geologists, hydrogeologists and microbiologists made the remediation of this site possible.

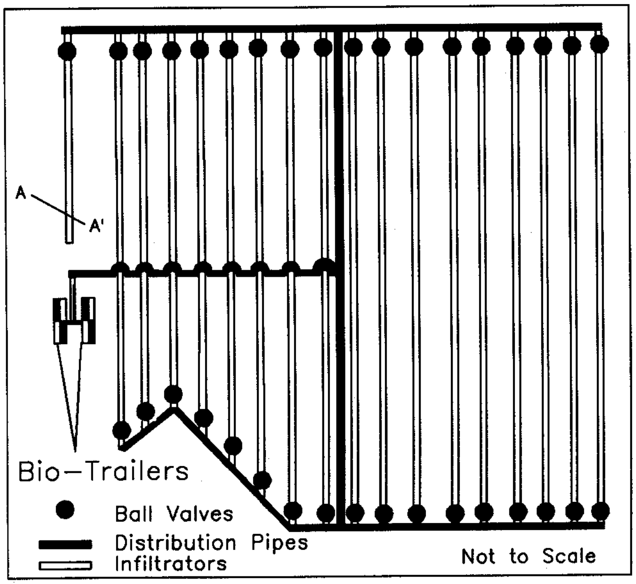

Figure 2. Site Plan of Bio-Trailers and Distribution Gallery.

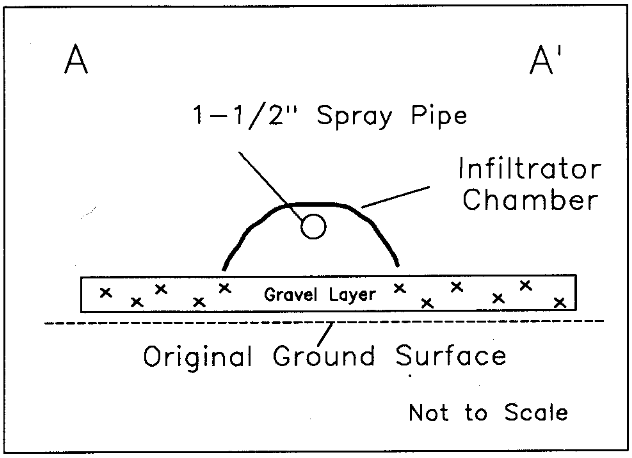

Figure 3. Cross Section of Infiltrator on Gravel Reservoir.

ASSESSING REGIONAL ENVIRONMENTAL FACTORS IN WEST VIRGINIA FROM TEMPORAL SATELLITE DATA AND STREAMFLOW DATA

M. Dennis Krohn, Robert C. Clark, and Charles W. Tremper
U.S. Geological Survey
Reston, VA 22092

ABSTRACT

Two new data sets published on CD-ROM that measure yearly changes in the landscape were examined as a basis for a regional analysis of environmental factors of West Virginia. Changes in a vegetation index were measured from Advanced Very High Resolution Radiometer (AVHRR) satellite images on a biweekly basis at 1-km resolution. The vegetation changes were compared to changes in streamflow for selected drainage basins defined in the Hydro-Climatic Data Network (HCDN) data set. A forest unit depicted on the AVHRR images in the southwestern part of the State serves as a test area for a regional assessment. The forest unit, underlain by the Pennsylvanian age coal-bearing formations, is best expressed in the vegetation data during the spring. This area is bordered to the east by a pair of north-south trending linear features that extend into the northern part of the State. Atmospheric effects in the biweekly composites are presently hindering multi-temporal analysis of the satellite data. Anomalies in the biweekly AVHRR composites related to rainfall can be gauged by comparing modern streamflow records to historic records compiled from the HCDN. Vegetation responses defined from looking at single images at critical times of the year, however, show coherent regional patterns suitable for a regional environmental assessment.

INTRODUCTION

A regional approach to environmental analysis is needed to balance the current site-specific approach of environmental investigations. The regulatory aspects of environmental monitoring focus investigations on assessing damages for liabilities and determining remedies at an individual site. Environmental incidents can be viewed as a narrow fluctuation within an broad spectrum of a dynamic landscape equilibrium. Natural variations of a landscape and its effects on an environmental incident are rarely assessed. Natural landscape cycles, like other cyclical patterns, may diminish or enhance a particular environmental incident. For environmental analysis, we need to look at variations on an annual to multi-year cycle.

We are proposing a regional environmental analysis to look at fluctuations of the landscape, particularly vegetation and hydrology, as a background upon which to conduct specific environmental investigations. We are examining two new temporal data sets published on CD-ROM (Compact disc, read-only memory) to test whether regional features can be discerned that have utility for environmental analyses. The data sets are from the Advanced Very High Resolution Radiometer (AVHRR) and the Hydro-Climatic Data Network (HCDN). The AVHRR is a weather satellite used to make biweekly image mosaics of a continental sized area. The Hydro-Climatic Data Network (HCDN) is a compilation of water records from gauging stations, specifically selected because they represent minimum cultural effects on streamflow. West Virginia was chosen because it is heavily forested with deciduous trees, has a wide range of elevations and slopes, and is the subject of a recent statewide mineral assessment (Cannon and others, in press). This paper is based on data from 1990. The motivation behind this work is to develop procedures for conducting regional environmental assessments, based on procedures developed for regional mineral or hydrocarbon assessments, whereby areas of high- and low-potential environmental hazards can be demarcated on a regional basis.

DATA SETS

AVHRR

The AVHRR is a sensor located on-board a series of polar-orbiting NOAA satellites. Initially launched in 1978, the AVHRR has either a 4 or 5-channel sensor configuration that covers the visible, near-infrared, and thermal-infrared wavelengths (Kidwell, 1991) at a resolution of 1 km. The EROS Data Center in Sioux Falls, South Dakota began producing biweekly image composites of the conterminous U.S. and Alaska in 1990 from the NOAA-11 satellite data. In addition to the five channels, an index of vegetation reflectance is included as the Normalized Difference Vegetation Index (NDVI). The NDVI is based on a marked increase in vegetation reflectance in the near-infrared wavelengths and is calculated as:

$$\text{NDVI} = \frac{\text{Near-IR (Band 2) - Visible (Band 1)}}{\text{Near-IR (Band 2) + Visible (Band 1)}}$$

The index produces values from -1.0 to 1.0, which are linearly scaled from 0 to 200 on the data set.

The images are composited on the basis of the highest NDVI value for a given set of scenes. Clouds, snow, water, and nonvegetated surfaces generally have negative NDVI values and are eliminated. However, clouds located over water bodies may be retained using this method. In addition to the 5 channels and NDVI data, the date of acquisition, and 3 channels of satellite/solar geometry also are included on the CD-ROM. The 19 biweekly composites in 1990 provide continuous coverage from March to October and discontinuous coverage through December.

The AVHRR images and ancillary data for West Virginia are extracted from the 1990 U.S. data set on CD-ROM. All 19 images are mosaicked at 1/5 resolution in the form of a calendar such that two biweekly images are stacked to provide a month of data. Individual images are then enhanced by histogram equalization to emphasize spatial features within an image, but at the loss of the relative relation to the yearly vegetative cycle. Lakes and water bodies are masked. State boundaries are added.

HCDN

The HCDN is a compilation of streamflow records from 1874 to 1978 initially designed for research in global change. Initially, a summary of the data was published (Slack and Landwehr, 1992) and was followed by a CD-ROM of the data in July, 1993. Streamflow records from 1659 sites across the U.S. were determined to be relatively free of "anthropogenic influences" to represent hydrologic conditions under past meteorologic conditions. A key criterion for the selection of contributing stations is the existence of unimpaired basin conditions.

Seventeen streamflow gauging stations in West Virginia (Fig. 1) meet the criteria for the HCDN data set (Table 1). Fifteen stations are still operational and are used in the analysis. Current streamflow records were extracted for 1990 from the State Water Data Reports (Alt, 1992) and compared to the HCDN stations.

Data for the HCDN sites (Table 1) are extracted in two ways. Monthly historic averages from the HCDN CD-ROM are compiled as quartile plots to show the yearly range of flow fluctuation from different drainage basins. Secondly, the daily stream gauge records are extracted from the 1990 USGS water data annual yearbook (Ward and others, 1990) and clustered into the same date ranges as the biweekly AVHRR composites.

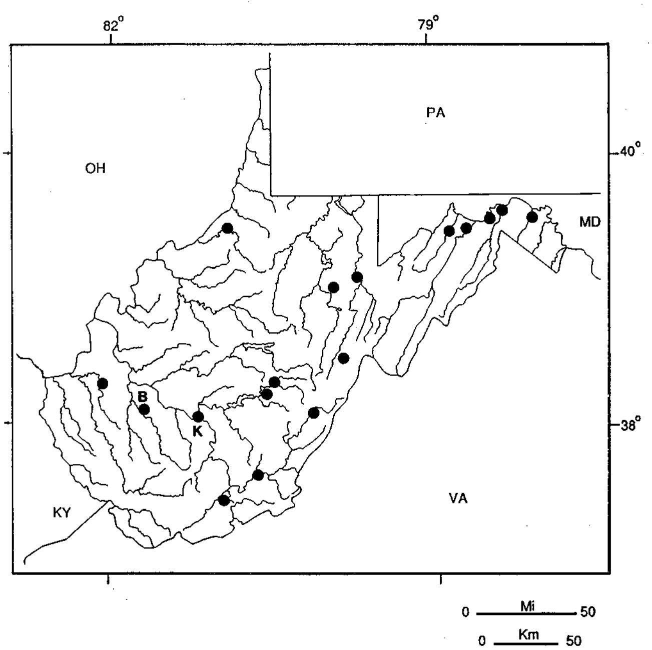

Figure 1 - Locations of Hydro-Climatic Data Network (HCDN) gauging stations on major drainage systems of West Virginia (see Table 1). B= Big Coal River at Ashford; K = Kanawha River at Kanawha Falls

GEOLOGIC BACKGROUND

West Virginia spans three major physiographic provinces, the Blue Ridge, the Valley and Ridge, and the Allegheny Plateau (Fig. 2). The divide between the Valley and Ridge and the Allegheny Plateau is called the Allegheny Front and has some of the highest elevations in the state. The small wedge of Blue Ridge is composed of Upper Pre-Cambrian greenstone and Lower Cambrian quartzite (Pc, Fig. 2). Bedrock underlying the Valley and Ridge is lower Paleozoic carbonate and clastic deep-water to shallow-water sedimentary rocks that have been thrust-faulted into a series of faults and folds. The Allegheny Plateau is underlain by Mississippian, Pennsylvanian and Permian rocks (Cardwell and others, 1968) (M,P, IP, Fig. 2) deposited in transgressive and regressive cycles of marine and nonmarine facies, including shallow-water, siliceous sedimentary rocks, coals, and minor amounts of deeper water clastic and carbonate rocks. Structures are broad open folds with highly incised drainage.

IMAGE ANALYSIS

CALENDAR IMAGE

The calendar image (Fig. 3) and a plot of the mean NDVI values (Fig. 4) shows the vegetative cycle of the hardwood deciduous forests of West Virginia. Forests cover 79% of the land area in West Virginia; of these, 77% are deciduous oak/hickory forests (DiGiovani, 1990). Images from intervals 1 through 4 show the less foliated areas extending south from Lake Erie into the highland areas of the Allegheny Plateau. Vegetation in the Valley and Ridge province leafs out earlier in the spring and arcs around the West Virginia mountains to the southwest. Once vegetation in the highland areas of West Virginia starts to change, it does so rapidly. The sharpest rise in NDVI values is 25 DN (digital numbers) between interval 4 and 5, late April to mid-May (Fig. 4a). Vegetation in the central portion of the Allegheny Plateau exhibits some of the lowest NDVI values in late April to some of the highest NDVI values in early June (Fig. 3). The central highlands retain these high NDVI values for 6 weeks until interval 10, mid-July and then show a gradual decline to interval 17. Interval 18 is the only sample of the transitional decrease in NDVI in the fall, and by early December, interval 19, the NDVI values return to the early spring numbers near 125 DN.

The mean NDVI values (Fig. 4a) show considerable variability not related to a seasonal pattern. Increase of 5 DN values for interval 2 does not appear to have a specific biologic origin on the images. The relatively flat, midsummer portion of the curve shows an alternation between larger and smaller standard deviations (Fig. 4a), which is emphasized by coefficient of variation (CV) (Fig. 4b). The CV, the standard deviation divided by the mean (Fig. 4b), is a measure of the width or scatter of the distribution. The high CV values in the summer months tend to correlate to the lower mean NDVI values. The alternating nature of the NDVI distributions is clearly observed in the intervals of the summer vegetative canopy (Fig. 4b).

INDIVIDUAL IMAGES

Individually enhanced images were analyzed to determine if spatial patterns related to the biologic phenology could be observed. A vegetation unit with lower NDVI response is observed in interval 4 (Figs. 5 and A, Fig. 2); it can be seen in other spring and fall images as well. The unit covers most of SW West Virginia, the plateau section of SW Virginia, and NE Kentucky. The region is bordered on the east by two north-south trending linear drainages (P and N, Fig. 2) in southernmost West Virginia and a broad north-south divide in the northern part of the state. The vegetation unit is also observed in intervals 2, 3, 17 and perhaps interval 8 (Fig. 3). A national classification of NDVI values (Loveland and others, 1991) shows a similar vegetation unit, which is defined by the length of the growing season.

The area of the forest unit mentioned above includes some of the principal coal-mining regions of West Virginia. The underlying Pennsylvanian bedrock (P_L, Fig. 2) is composed of the New River and Kanawha Formations of the Pottsville Group (Cardwell and others, 1968). The primary outcrop lithology in this area is sandstone with some shale. The northern third of the area (P_{MU}, Fig. 2) is underlain by the Pennsylvanian Conemaugh Formation, which has a larger proportion of nonmarine red and grey shales. Major coal measures in these sections include the Kittaning, Freeport, Clarion, Pittsburgh and Pocahontas coal beds. Most of the mining is deep mining, but approximately a quarter of the mines are strip mines that would affect the surface reflectance (Skelly and Loy Consultants, 1979).

Several other features correspond to the vegetation area of interval 4. A major subdivision of soils, Land Resources Area (LRA) 125, is mapped in SW West Virginia by the U.S. Department of Agriculture (1980). The major soils in this area are the Clymer, Gilpin, and Dekalb soils, which are commonly forested. In 1989, forests in the southern unit of West Virginia, which overlaps most of the low NDVI area, were made up of 84% oak/hickory forest group. Only 4.5% of the forest cover consists of pines (DiGiovani, 1990). The combination of siliceous or relatively dry host rock and, intensive land use of the area, and predominantly deciduous forests, are probably some of the reasons the area is distinctive on the AVHRR image.

The northeastern border of the area is marked by the Kanawha River near the HCDN station (K, Fig. 1). The Pennsylvanian New River and Kanawha Formations and the coal mines continue to the northeast (P_{MU}, Fig. 2); some indication of lower NDVI response is present in that area. The southeastern border of the area is defined by two north-south trending linear features (Fig. 5). The eastern linear feature is defined by the drainage of the New River (N, Fig. 2). The western feature follows a portion of Piney Creek (P, Fig. 2) and demarcates the eastern border of the low NDVI area (A, Fig. 2). Neither the New River nor the Piney Creek drainage was included on a statewide compilation of linear features from Landsat radar, or subsurface data (Reynolds, 1979; Pohn, in press).

An interesting aspect of the eastern border is the extension to the north (Fig. 5 and B, Fig. 2). The western Piney Creek linear feature (P, Fig. 2) can be continued 100 km to the north and marks the western edge of a second low NDVI area in the northern half of the State that can be traced to just over the Ohio line (Fig. 5). The eastern New River feature possibly correlates to the eastern edge of the northern low NDVI area (B, Fig. 2), but the border curves to the east as it meets the Pennsylvania State line. The second forest unit cannot be seen in the other biweekly intervals. It does cut across the two Pennsylvanian formations (P_L, P_{MU}, Fig. 2); however, the western edge of the Permian rocks (IP, Fig. 2) does correspond to the western edge of the second candidate vegetation unit and aligns with the linear feature along Piney Creek (P, Fig. 2).

Weather-Related Phenomena

A problem for looking at temporal data is that transient phenomena related to weather may interfere with image interpretation. An example of a weather-related image response is observed on the interval 13 image in late August (Fig. 6) The image shows a large arcuate swath stretching across the center of the state that trails off into southern Ohio. The average NDVI values for the dark swath are 139 ± 2.6 DN, which is lower than the average 151 ± 7.4 DN for the state. The multiple dates of image acquisition in the composite provides an explanation. The more distinct northern boundary of the swath marks the border between the 8/28 acquisition and the 8/30 acquisition. The southern part of the dark area gradually blends with the data set and is part of the 8/28 acquisition.

The HCDN data can provide a means to analyze for transient phenomena. The historic HCDN record for the gauging station at Big Coal River at Ashford and at Kanawha River at Kanawha Falls (B and K, Fig. 1, Table 1) were compared to the 1990 flow records of the stations (Fig. 7, a and b). The historic record shows an extreme range of flow conditions. At Big Coal River, the maximum flow measured at the station is in March at 2866 ft^3/s; the minimum flow is in October at 1.11 ft^3/s. Evaluation of the means and standard deviations show that the high volume floods skewed the data. Rather than a measure of central tendency, the quartile points of the distribution were chosen to determine the bounds of a normal reading for comparison to modern streamflow records (Holmes, 1987).

The historic flow plotted as quartile points of both stations indicates the rise of the spring runoff and the fall low-water periods (Fig. 7, a and b). The curves have similar shapes in spite of the large difference in flow volumes and drainage areas. The variability of the stream as measured by the CV is low in the earlier part of the year but increases toward the low-water periods in the late summer and fall, indicating the most extreme changes in flow due to transient weather phenomena. Smaller drainages have higher values in the fall, indicative of more flash flooding conditions.

The 1990 daily records for the Big Coal River and Kanawha River stations (Alt, 1992) were compiled in 2-week intervals for comparison with the AVHRR data. Like the historic data, the yearly records are skewed toward the larger events. The mean biweekly values were plotted, as well as the minima for the intervals (Fig. 7, c and d). The rationale for this choice is that the low-water conditions represent the closest approximation to ground water conditions that may affect the entire drainage basin. In interval 13, the mean is close to the low-flow for the Big Coal River station (Fig. 7c), but the relative position of the mean is considerably higher for the Kanawha River station (Fig. 7d). Examination of the daily record shows a maximum flow of 15,800 ft^3/sec on August 25, 3 days before the image was acquired. This value is considerably above the historic quartile flow record and would indicate some type of heavy precipitation, which affects the response of the NDVI image. It is interesting to note that the similar high flows were not detected on the Big Coal River station.

Streamflow and NDVI Response

A second means of integrating streamflow data from the HCDN into the satellite vegetation data base is to use the moisture information to help understand the vegetation response. Changes in rainfall during the year are an important factor, although not the only factor, influencing the forest health as is reflected in the different spacings of tree rings (Yanosky and others, 1987). The question is whether temporal NDVI data is able to spatially distinguish vegetation responses related to moisture and relate that to the yearly streamflow reading in comparison to the historic record.

Two noteworthy observations can be gleaned from the 1990 biweekly low-flow records (Fig. 7, c and d). From the Big Coal River station, the high mean stream flow is in interval 4. This is the interval during the vegetation cycle that shows the maximum gain in NDVI from the change in foliation and exhibits some of the best differentiation for regional vegetative units in SW West Virginia. The flows in the fall are low, but are within the range of the quartile low flows from the HCDN record, so they should not provide any unusual moisture stress on the forests during senescence.

The Kanawha River station biweekly records (Fig. 7d) show a different pattern than the Big Coal River station, even though the overall historic patterns from the HCDN data are similar in shape. The Kanawha River station shows 3 maxima, two of which are above the quartile flow records. The maxima in interval 17 is particularly noteworthy because it occurs at a historic time of low flow. NDVI images for interval 17 (fig. 3) show some of the Upper Pennsylvanian rocks in north-central West Virginia, but the vegetative units in SW West Virginia are not distinctive. Even though the Kanawha and Big Coal rivers feed into the same drainage, the dissimilar nature of their 1990 flow curves suggests independence in that year between the two linked drainage basins, suggesting that further differentiation of vegetation communities based on the hydrologic response may be feasible as well.

DISCUSSION

Vegetative patterns can be seen on the NDVI images that are related to geology. The SW West Virginia coal-mining areas are the type of terrain that is likely to be mapped as a distinctive unit in a regional environmental assessment. In a nationwide classification of vegetation units from the NDVI data, Loveland and others (1991) map the unit in SW West Virginia but include it within an area of the Valley and Ridge part of the State. The difference in land use between these two areas suggests that the national classification is too broad.

Integration of HCDN data to AVHRR mosaics is still preliminary, but the initial results are promising. The HCDN data at present can best be used as a background to gauge weather-related effects on the images. The anomalous patterns from interval 13 (08/17-08/30) show the importance and difficulty of understanding these effects. These variations in the data make time-series analysis of the data difficult. The rapid changes in NDVI values in spring and fall suggest focusing on analysis at selected portions of the growing season. Unfortunately, the rapid senescence of leaves in the fall is not completely sampled by the current schedule of biweekly intervals for the AVHRR mosaics. The interval between interval 17 and 18 in late October and early November (Fig. 3) is the interval of rapid decrease in NDVI values. Including this interval in future mosaics would be beneficial for this type of analysis.

SUMMARY

Two new data sets published on CD-ROM, AVHRR and HCDN, are an important resource for mapping yearly changes in landscape and applying them to a regional environmental analysis. A mosaic of images of the deciduous forests of West Virginia clearly displays the annual vegetative cycle. The southwestern part of the state, underlain by the coal-bearing formations, maps as a distinctive forest unit that is partially bordered by a pair of north-south trending linear features. Atmospheric effects related to the mosaicking of the biweekly AVHRR composites are observed and can be gauged by comparing the modern streamflow records using the HCDN data as a background. The time series potential of combining these data sets is hindered by the atmospheric effects present in the mosaicking processing, but individual snapshots at critical times of the year can be used to effectively map regional vegetation units.

REFERENCES CITED

Alt, Darwin, 1992, State water-data reports, hydrologic records of the United States, water years 1990 and 1991: U.S. Geological Survey Open-File Report 92-478, 1 CD-ROM.

Cannon, W.F., Clark, S.H.B., Lesure, F.G., Hinckle, M.E., Paylor, R.L., King, H.M., Simard, C.M., Ashton, K.C., and Kite, J.S., in press, Mineral resources of West Virginia: U.S. Geological Survey, Miscellaneous Investigation Series Map I-2364-A, scale: 1:500,000.

Cardwell, D.H., Erwin, R.B., and Woodward, H.P., 1968, Geologic map of West Virginia: West Virginia Geological and Economic Survey, scale 1:250,000, 2 sheets.

DiGiovani, D.M., 1990, Forest statistics for West Virginia--1975 and 1989: U.S. Department of Agriculture, Forest Service, Northeast Forest Experiment Station, Research Bulletin NE-114, 168 p.

Holmes, Sandra, 1987, Monthly streamflow and groundwater conditions in the United States and Canada, water years 1945-85: U.S. Geological Survey Water-Supply Paper 2314, p. 4.

Kidwell, K.B., 1991, NOAA polar orbiter data users guide: National Oceanic and Atmospheric Administration, National Environmental Satellite Data and Information Service, National Climatic Data Center, 275 p.

Loveland, T.R., Merchant, J.W., Ohlen, D.O., and Brown, J.D., 1991, Development of a land-cover characteristics data base for the conterminous U.S.: Photogrammetric Engineering and Remote Sensing, v. 57, n. 11, p. 1453 - 1463.

Pohn, H.A., in press, Geologic structure and mineral occurrences in eastern West Virginia: U.S. Geological Survey Miscellaneous Series Investigations Map I-2364-J.

Reynolds, J.H., 1979, Landsat linear features of West Virginia: West Virginia Geological and Economic Survey, Publication WV-7A, scale 1:250,000, 2 sheets.

Skelly and Loy Consultants, 1979, West Virginia and Maryland coal mine activity map: McGraw Hill Mining Informational Services, scale approximately 1:750,000.

Slack, J.R., and Landwehr, J.M., 1992, Hydro-climatic data network (HCDN): A U.S. Geological Survey streamflow data set for the United States for the study of climate variations, 1874-1988: U.S. Geological Survey Open-File Report 92-129, 193 p.

U.S. Department of Agriculture, 1980, General soil map of West Virginia: U.S. Department of Agriculture, scale 1:750,000.

Ward, S.M., Hobbs, W.A., Jr., Taylor, F.M., and Waldron, M.C., 1990, Water resources data West Virginia, water year 1990: U.S. Geological Survey Water-Data Report WV90-1, 182 p.

Yanosky, T.M., Robinove, C.J., and Clark, R.G., 1987, Progress in the image analysis of tree rings, *in* Jacoby, G.C. Jr., and Hombeck, J.W., Proceedings of the International Symposium on Ecological Aspects of Tree-Ring Analysis: U.S. Department of Energy, August 17-21, 1986, Tarrytown, New York, CONF-8608144, p. 658-665.

Table 1. Characteristics of HCDN Stream Gauge Stations [from Ward and others, 1990; Slack and Landwehr, 1992]

Name of Station	ID # / County	Location Lat (N) Long (W)	Description	Drainage Area (km²) Forest cover	Mean Flow (ft³/s) Max Flow/Date
Patterson Cr. near Headsville	01604500 Mineral Co.	39°26'35" 78°49'20"	Right bank, 100 ft dwnstrm from Hazel Run	567 74%	168 16,000 8/19/55
South Branch Potomac R. Springfield	01608500 Hampshire Co.	39°26'49" 78°39'16"	Left bank, highway bridge, 2.0 mi E Springfield	3810 74%	1315 240,000 11/5/85
Potomac R. at Paw Paw	01610000 Hampshire Co.	39°32'13" 78°27'28"	Left bank, 250 ft upstrm from highway 51 bridge	8052 76%	3296 235,000 11/5/85
Capon R. near Great Cacapon	01611500 Morgan Co.	39°34'43" 78°18'34"	Left bank at Rock Ford, 3.0 mi SW Great Cacapon	1753 75%	584 87,600 3/18/36
Back Cr near Jones Spring	01614000 Berkeley Co.	39°30'49" 78°02'15"	No longer monitored	629 70%	
Tygart Valley R. at Belington	03051000 Barbour Co.	39°01'45" 79°56'10"	Left bank, opposite Mill Cr.	1057 80%	819 29,500 11/5/85
Cheat R. near Parsons	03069500 Tucker Co.	39°07'20" 79°40'50"	Left bank 2.0 mi N of Parsons	1860 85%	1709 51,300 7/10/1888
Middle Island Cr. at Little	03114500 Tyler Co.	39°28'30" 80°59'50"	Right bank, dwnstrm from highway bridge	1256 60%	641 25,000 6/26/50
Bluestone R. near Pipestem	03179000 Summers Co.	37°32'38" 81°00'38"	Left bank, 1.2 dwnstrm from Mountain Cr.	1020 60%	468 19,300 5/5/77
Greenbrier at Durbin	03180500 Pocahontas Co.	38°32'37" 79°50'00"	Left bank, at Durbin	344 80%	261 37,100 11/5/85
Greenbrier R. at Buckeye	03182500 Pocahontas Co.	38°11'09" 80°07'51"	Right bank, 1000 ft upstrm from Swago Cr.	1399 80%	879 82,000 11/5/85
Greenbrier R. at Alderson	03183500 Monroe Co.	37°43'27" 80°38'30"	Left bank, 400 ft upstrm from highway bridge	3533 80%	1996 90,600 11/5/85
Williams R. at Dyer	03186500 Webster Co.	38°22'44" 80°29'03"	Left bank, at Dyer, 0.2 mi dwnstrm from Craig Run	332 99%	334 22,000 4/4/12
Cranberry R. near Richwood	03187500 Nicholas Co.	38°17'43" 80°31'36"	Left bank, 0.6 mi upstrm Barrenshe Run	208 99%	238 11,200 8/21/89
Kanawha R. at Kanawha Falls	03193000 Fayette Co.	38°08'17" 81°12'52"	Right bank, 2.0 mi dwnstrm from New & Gauley R.	21681 65%	12,533 320,000 9/14/1878
Big Coal R. at Ashford	03198500 Boone Co.	38°10'47" 81°42'42"	Left bank, 300 ft, upstrm from Lick Cr.	1013 95%	518 35,800 9/19/16
Mud R. near Milton	03204500 Cabell Co.	38°23'15" 82°06'46"	No longer monitored	663 80%	

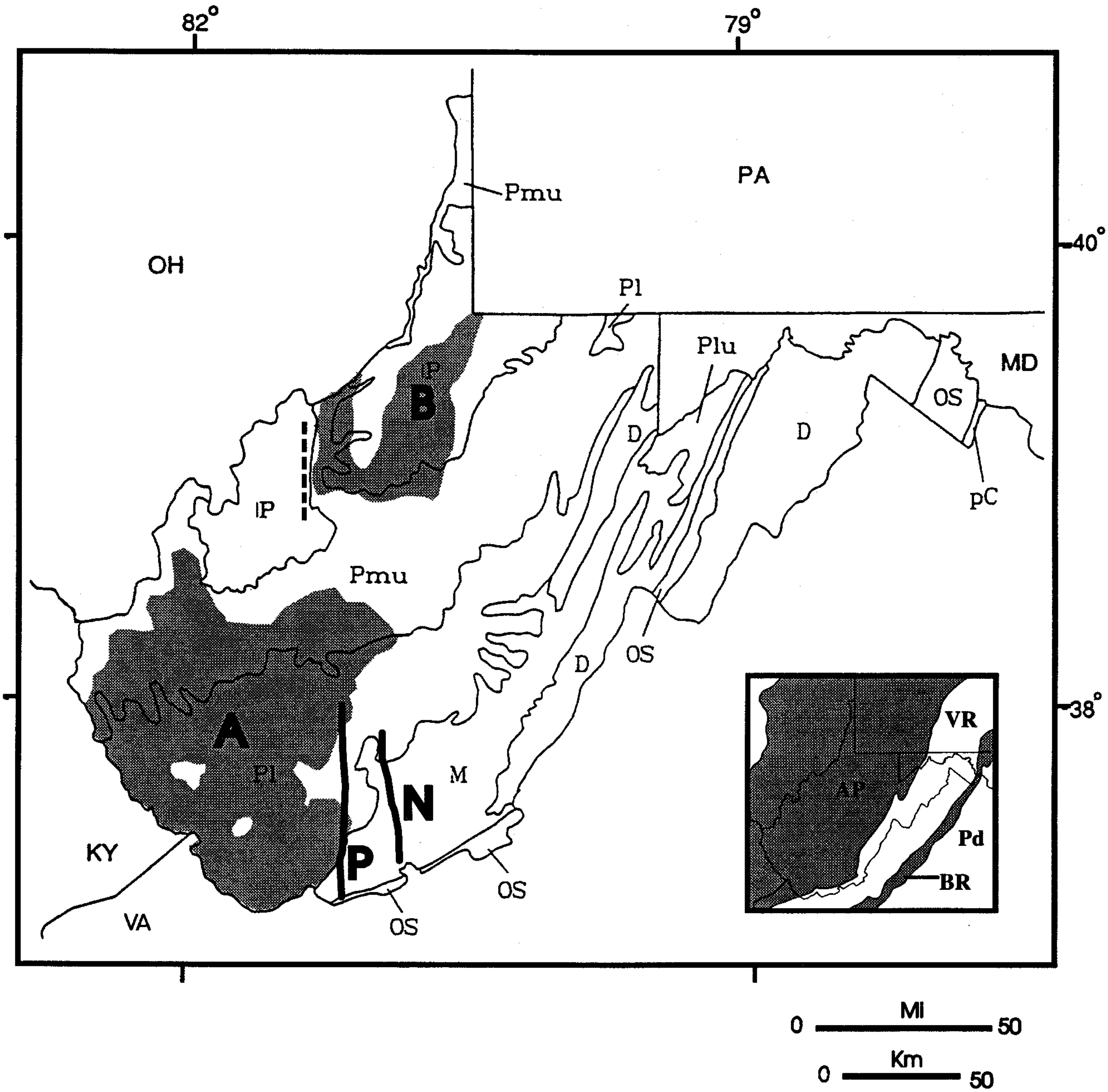

Figure 2 - Map of physiographic provinces and generalized geology of West Virginia (modified from Cardwell and others, 1968) with features interpreted from AVHRR images.

Physiographic Index Map

Pd = Piedmont
BR = Blue Ridge
VR = Valley and Ridge
AP = Allegheny Plateau

Geologic Map

pC = Pre-Cambrian and Cambrian
OS = Ordovician and Silurian
D = Devonian
M = Mississippian
P_L = Lower Pennsylvanian (Kanawha, New River and Pocahontas Formations / Pottsville Group)
P_{LU}= Lower through Upper Pennsylvanian
P_{MU}= Middle and Upper Pennsylvanian (Conemaugh and Allegheny Formations)
IP = Permian and Upper Pennsylvanian (includes Dunkard Formation)

AVHRR Image Interpretations

A = low NDVI forest unit (shaded area)
B= northern extended forest unit (shaded area)
P = Piney Creek linear feature
N = New River linear feature; dashed lines = linear feature extended to northern area.

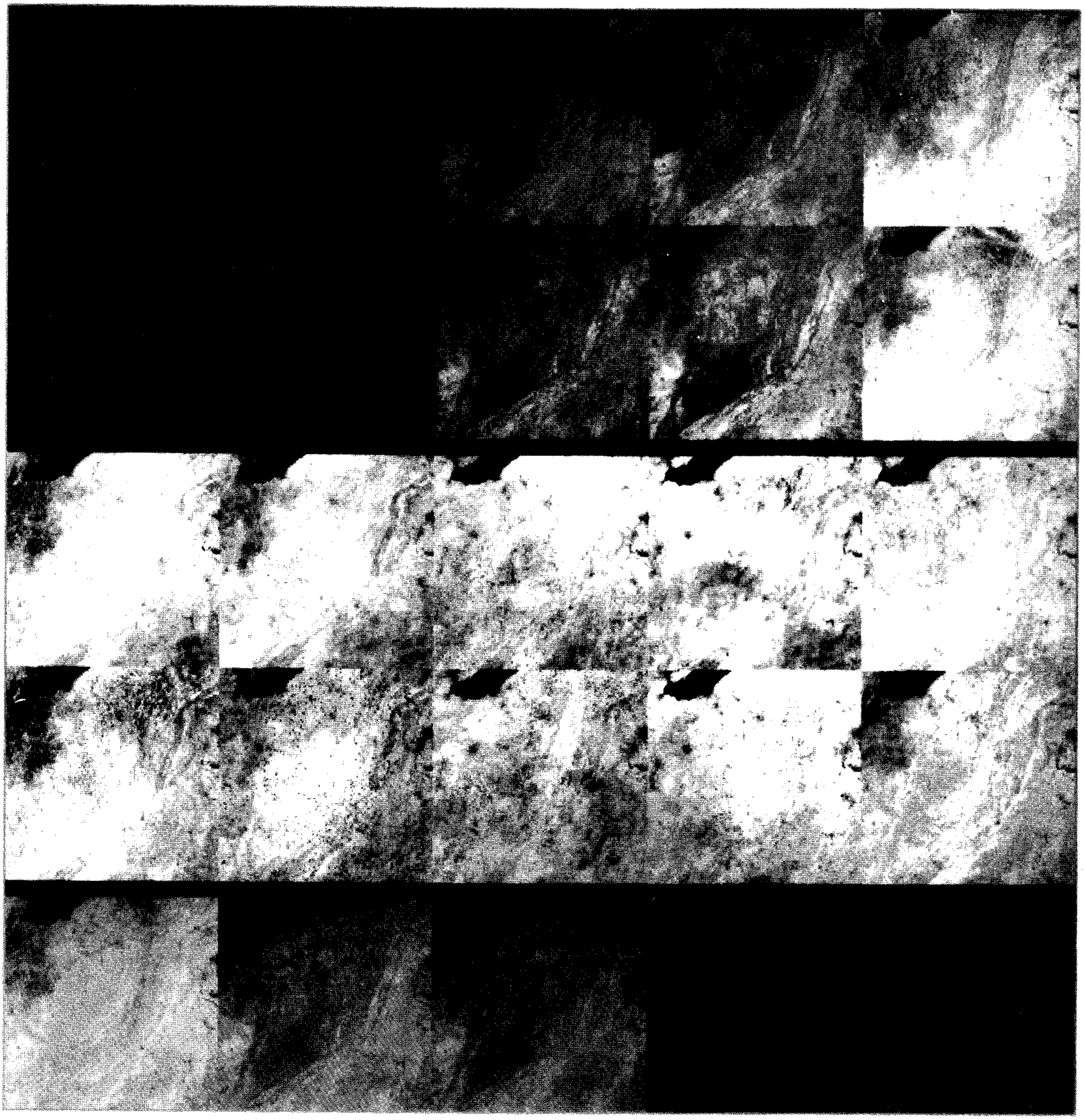

Figure 3. Mosaic of 19 AVHRR biweekly interval images for 1990 into a calendar mosaic NDVI image. Dark areas are low vegetation reflectance; light areas are high vegetation reflectance. Dates and placement of the images are shown below.

		1. March 02 March 15	3. March 30 April 12	5. April 27 May 10
		2. March 16 March 29	4. April 13 April 26	6. May 11 May 24
7. May 25 June 07	9. June 22 July 05	11.July 20 Aug. 02	13.Aug. 17 Aug. 30	15.Sept. 14 Sept. 27
8. June 08 June 21	10.July 06 July 19	12.Aug. 03 Aug. 16	14.Aug. 31 Sept. 13	16.Sept. 28 Oct. 11
17.Oct. 12 Oct. 25	18.Nov. 09 Nov. 22	19.Dec. 07 Dec. 20		

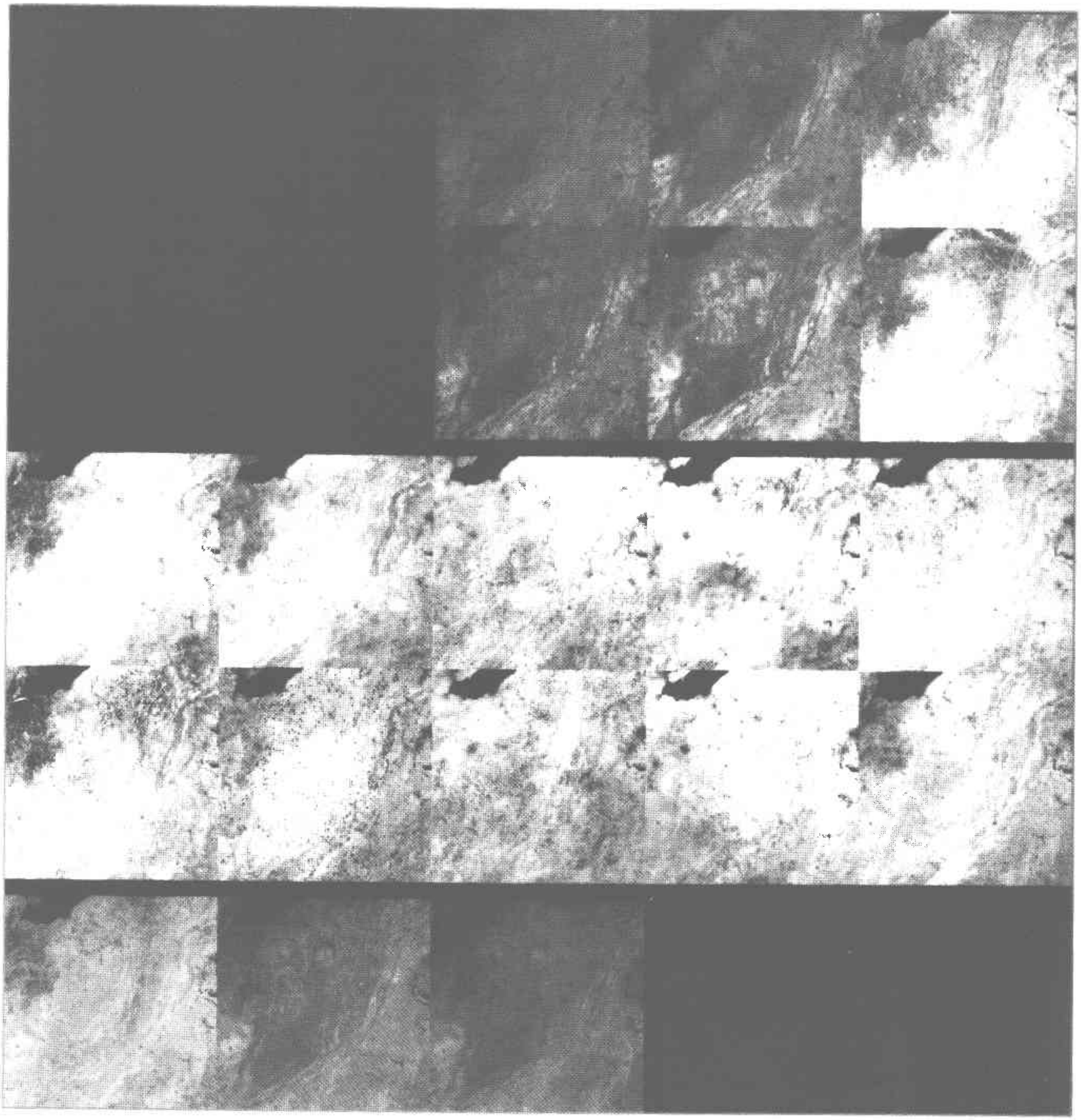

Figure 3. Mosaic of 19 AVHRR biweekly interval images for 1990 into a calendar mosaic NDVI image. Dark areas are low vegetation reflectance; light areas are high vegetation reflectance. Dates and placement of the images are shown below.

		1. March 02 March 15	3. March 30 April 12	5. April 27 May 10
		2. March 16 March 29	4. April 13 April 26	6. May 11 May 24
7. May 25 June 07	9. June 22 July 05	11.July 20 Aug. 02	13.Aug. 17 Aug. 30	15.Sept. 14 Sept. 27
8. June 08 June 21	10.July 06 July 19	12.Aug. 03 Aug. 16	14.Aug. 31 Sept. 13	16.Sept. 28 Oct. 11
17.Oct. 12 Oct. 25	18.Nov. 09 Nov. 22	19.Dec. 07 Dec. 20		

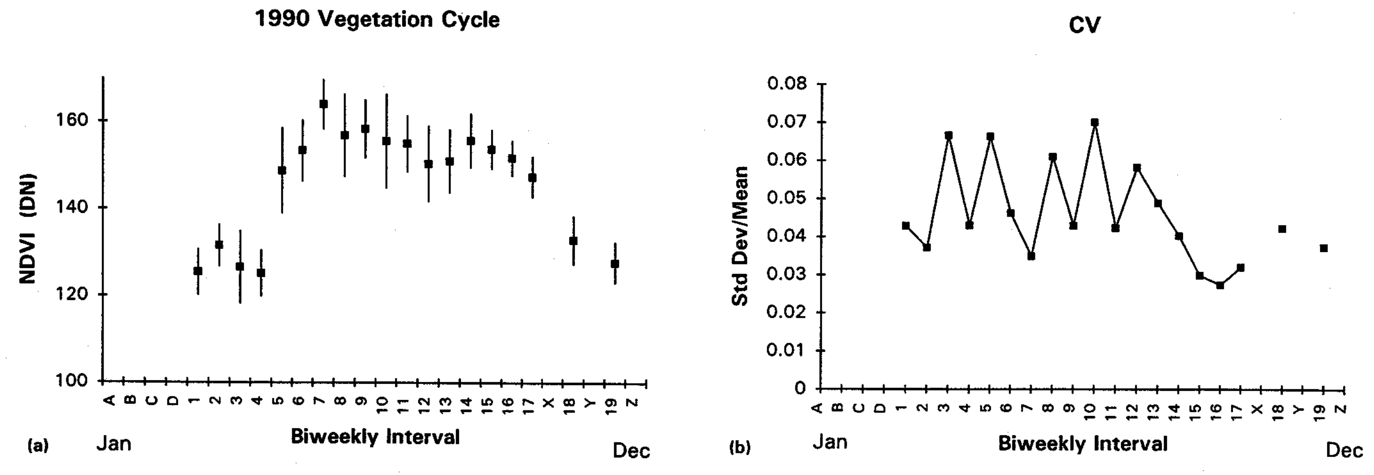

Figure 4. (a) Mean Normalized Difference Vegetation Index (NDVI) values (boxes) and 1 standard deviation variance error bars for West Virginia plotted against biweekly intervals for 1990 season. Biweekly intervals are numbered; letters denote biweekly intervals not sampled in the satellite data. (b) Coefficient of variance (CV) for NDVI values for West Virginia plotted against biweekly intervals for 1990 season.

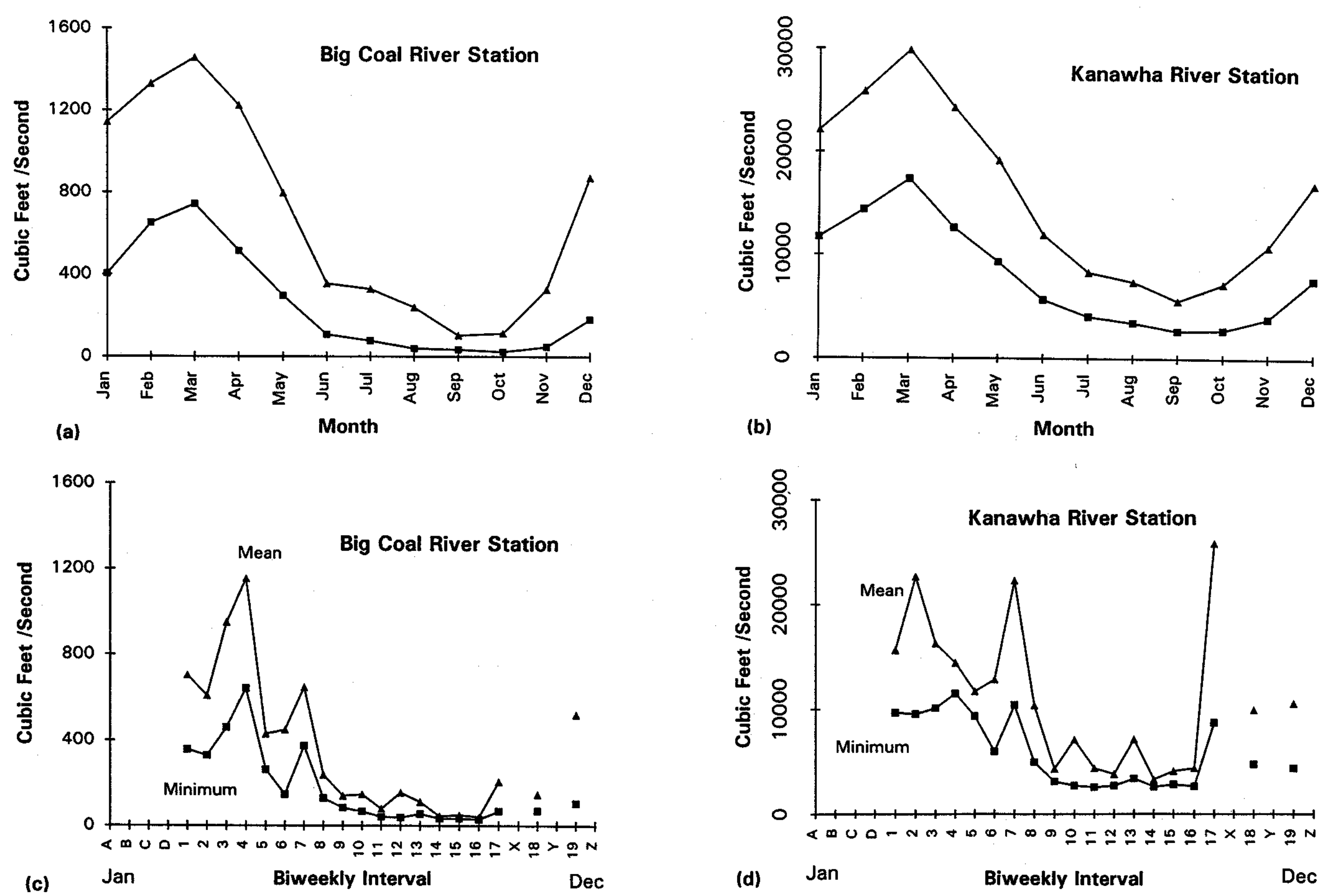

Figure 7. Quartile flow statistics from the HCDN data set for Big Coal River gauging station (a) at Ashford (03198500) and Kanawha River gauging station (b) at Kanawha Falls (03193000) compared to the 1990 biweekly mean and low flow values for Big Coal River (c) and Kanawha River (d) gauging stations.

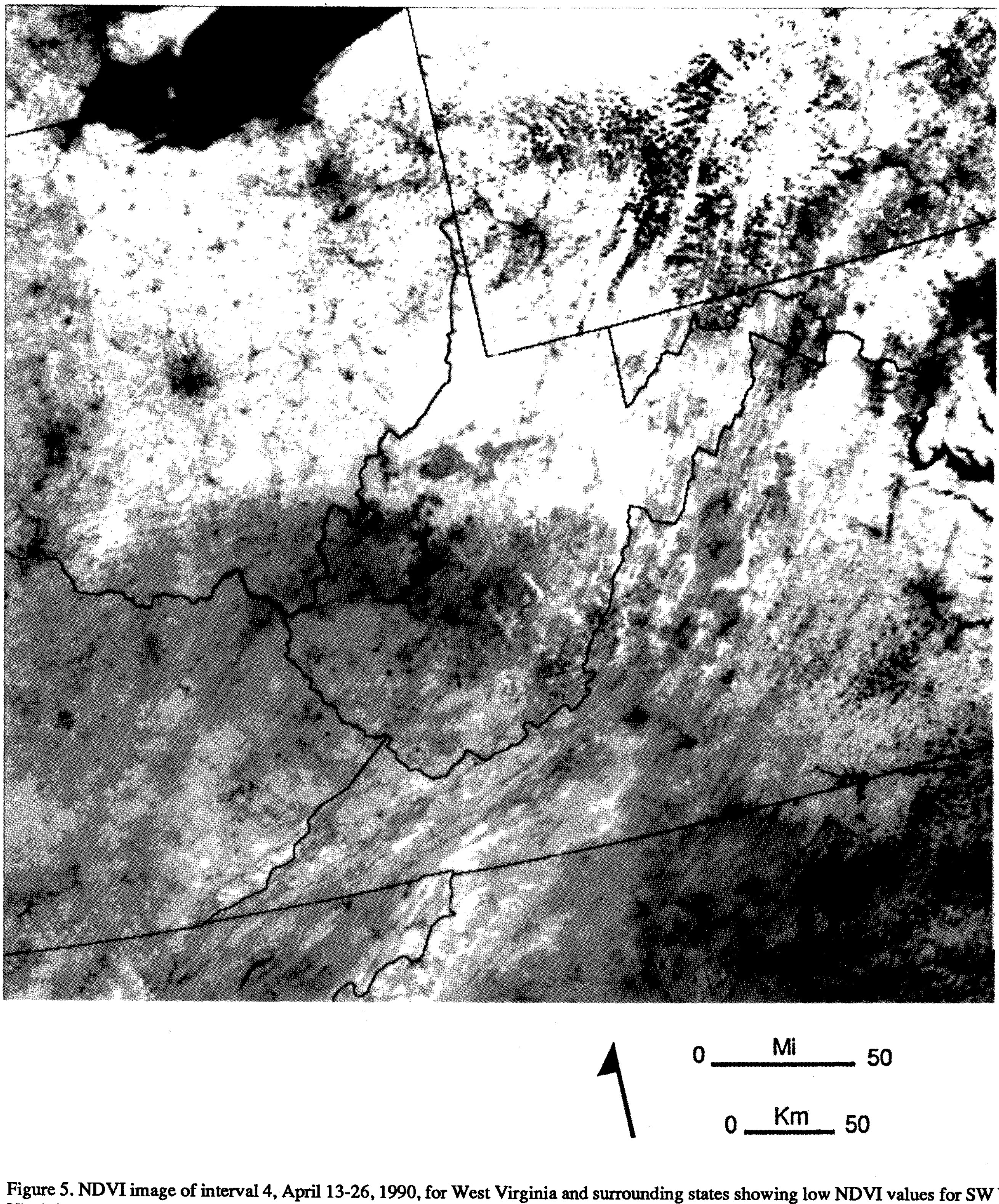

Figure 5. NDVI image of interval 4, April 13-26, 1990, for West Virginia and surrounding states showing low NDVI values for SW West Virginia.

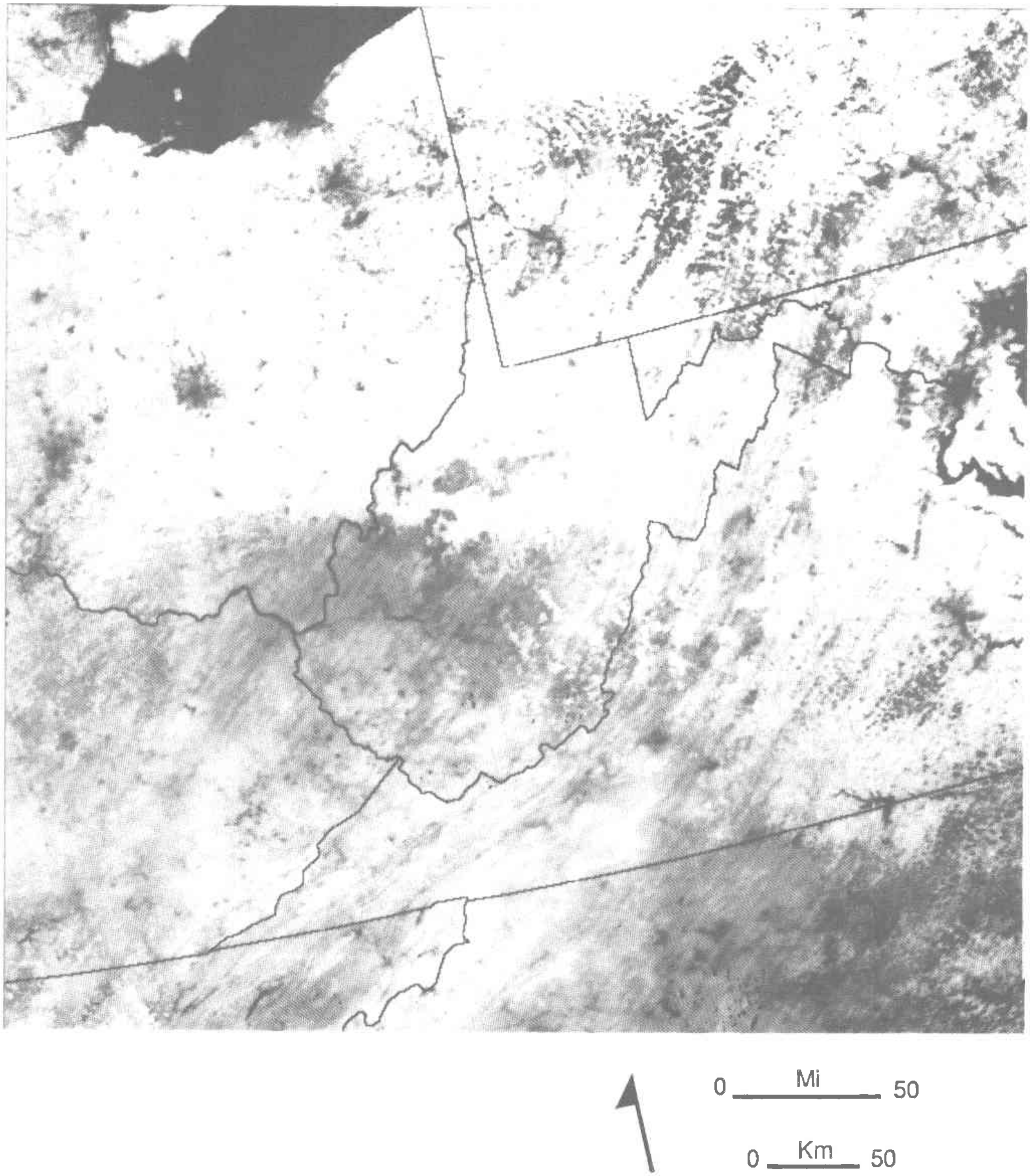

Figure 5. NDVI image of interval 4, April 13-26, 1990, for West Virginia and surrounding states showing low NDVI values for SW West Virginia.

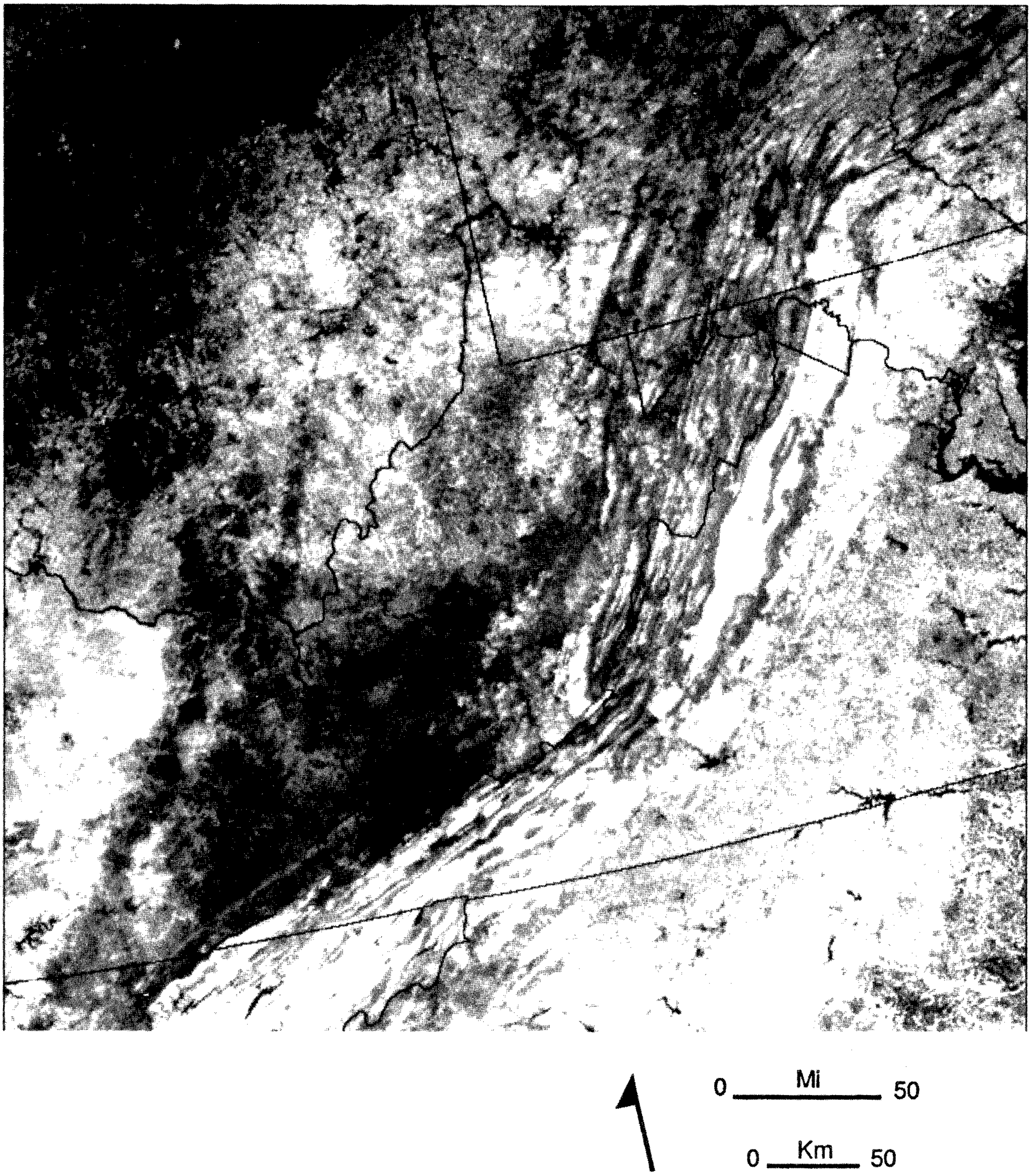

Figure 6. NDVI image of interval 13, August 17 - 30, 1990, for West Virginia showing swath of lower NDVI values across central West Virginia related to mosaicking of image composite.

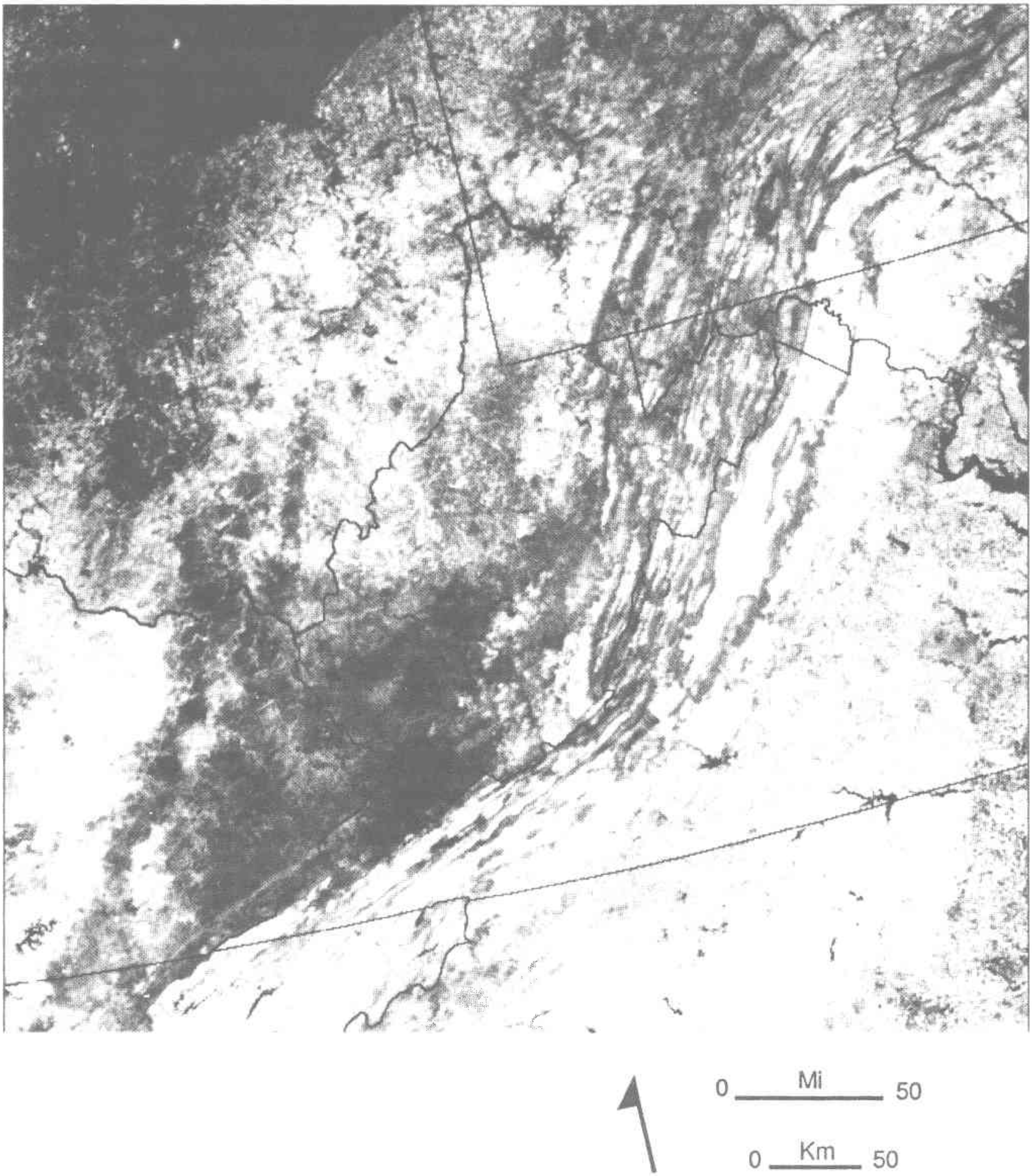

Figure 6. NDVI image of interval 13, August 17 - 30, 1990, for West Virginia showing swath of lower NDVI values across central West Virginia related to mosaicking of image composite.

RECOGNITION OF REEFS IN THE SUBSURFACE ROCK RECORD: AN EXPERIENCE IN FRUSTRATION

JOHN T. GALEY MEMORIAL ADDRESS

GERALD M. FRIEDMAN

Department of Geology, Brooklyn College and Graduate School of the City University of New York, Brooklyn, NY, 11210, and Northeastern Science Foundation affiliated with Brooklyn College, Rensselaer Center of Applied Geology, 15 Third Street, P.O. Box 746, Troy, NY 12181-0746

ABSTRACT

Reefs live in high-energy settings, where shallow-water waves surge relentlessly back and forth, and storms batter the reef. Yet reef samples as young as modern and as old as Paleozoic have been misinterpreted as low-energy facies. In a Ph.D. examination a candidate misidentified a modern reefrock as a lithified lime mud, known as micrite, and inferred its depositional environment as "low-energy as in a lagoon". Where does the problem lie?

Submarine finely-crystalline or cryptocrystalline cement precipitates in reefs within millimeters to centimeters of the reef's surface. This cement mimics micrite, and misidentification of this cement for micrite leads to misidentification of facies. Since micrite of matrix origin and finely-crystalline or cryptocrystalline cement are indistinguishable it is easy to confuse high-energy reef facies for low-energy lime-mud facies. Hence recognition of reefs in the subsurface rock record is an experience in frustration.

INTRODUCTION

John T. Galey to whose memory this address has been dedicated served as my mentor in the Eastern Section of AAPG. I recall first meeting John at an Advisory Council meeting of National AAPG. Later when I became president of the New York State Geological Association he recruited me for service on the Eastern Section's Executive Committee, where in turn I served as Treasurer, Secretary, Vice President, and President, and from there moved on to the AAPG National Vice Presidency. John was Chairman of the Committee that awarded me Honorary Membership in the Eastern Section. A long walk through downtown Houston served as John's recruitment vehicle to generate my enthusiasm for extra commitment to the Eastern Section. Since John was a third- generation oil finder, in fact an oil finder *par excellence*, thought that in honor of John I wish to speak on a subject that relates to traps that make oil giants. I have selected reefs.

Reef facies form the most prolific hydrocarbon reservoirs, in fact no other single facies holds as much oil as reefs. Production occurs in reefs as old as Silurian and as young as Quaternary. I was myself involved in research exploration which led to discovery of a reef field with cumulative reserves of 2.2 BBO. Even larger reef giants exist. More recently in the eastern United States reef facies have begun to serve as reservoirs for gas storage.

Since reefs form such important reservoirs it would seem logical to assume that identification of reefs in logs and cores would be a relatively simple matter, but unfortunately this is not so. Identification of reefs, even in good cores, is an experience in frustration.

CASE HISTORY OF REEF MISIDENTIFICATION

Using dynamite I blasted modern reefrock to determine the internal characteristics and porosity prospects of reefs in their natural settings (Friedman, 1973,1975,1985; Friedman et al, 1974). In a Ph.D. examination, I asked a candidate to examine the samples from the freshly blasted reefrock and (1) describe the samples and identify their lithology and (2) interpret their depositional environment. The candidate termed the modern reefrock a lithified lime mud or micrite and identified the depositional environment as "low-energy as in a lagoon," yet the samples had been collected from the reef front, where shallow water waves surge relentlessly back and forth and storms batter the reef, thus providing the highest energy possible in a marine setting.

THE PROBLEM

The search for potential reservoirs in carbonate rocks considers depositional processes and products. Primary porosity and hydrocarbon-reservoir characteristics are commonly related to the energy in the environment of deposition. In general carbonate sediments deposited in high-energy environments are prone to develop primary porosity and through diagenetic processes these same sediments may develop secondary porosity. With these energy-related concepts in mind, geologists in the 1950's developed classifications based on energy level. As Ham and Pray stated (1962, p. 10) "the concept of energy or water turbulence of the depositional environment provides a significant interpretive parameter for classification of carbonate rocks. 'High-energy' and 'low-energy' carbonate sediments are those which have been deposited respectively in turbulent or quiet waters. The energy concept is well recognized in most modern classifications, although indirectly, by the focus on the relative abundance of grains and matrix." According to Dunham (1962, p. 111) this distinction between sediment deposited in calm water and sediment deposited in agitated water is fundamental. "Inasmuch as calm water is characterized by (lime) mud being able to settle to the bottom and remain there, it seems that the muddy rocks (that is those in which lime mud accumulated between sand-size carbonate particles) deserve to be contrasted with (lime) mud-free rocks" (Dunham,1962, p.112-113).

In oral presentations and published papers geologists have used the term "micrite cement". To save embarrassment appropriate references will be omitted here. Clearly as micrite has come to be understood, no such usage as "micrite cement" should exist. The material is either micrite (= physically deposited matrix) or it is cement, it cannot be both. For micrite cement substitute cryptocrystalline or finely crystalline cement or else the depositional environment will be incorrectly inferred.

According to the concept of naming and classifying carbonate rocks three kinds of end members are considered: (1) gravel-,sand-, or silt-size particles, (2) cement, which binds these particles into a solid limestone and has been chemically or biochemically deposited, and (3) mechanically deposited lime mud, which formed as a sedimentary ooze in a low-energy setting. The mechanically deposited lime mud, following lithification, is known as micrite (Folk 1959). The distinction between micrite and cement is critical; it affords a valuable means for interpretation of the energy in the depositional environment. The presence of micrite relates to a low-energy, sluggish setting, whereas that of cement reflects turbulence. The distinction between sediment deposition in sluggish waters and sediment deposited in turbulent waters is fundamental. Reefs are composed of skeletal particles held together by finely crystalline or cryptocrystalline cement that looks like micrite (Figs.1,2). Unwary geologists have described such reefrock, which is a high-energy facies, as a mudstone, wackestone, biomicrite, or simply micrite and erroneously interpreted it as a low-energy product. A recent paper on modern reefs names the reefrocks, mudstones and wackestones cemented by finely crystalline or cryptocrystalline high-magnesian calcite cement (Brachert and Dullo, 1991). Yet according to Dunham (1962), "the distinction between sediment deposited in calm water and sediment deposited in agitated water is fundamental", and the terms mudstone and wackestone reflect a low-energy setting in which the presence of (lime) mud signifies calm waters. Reefrock can never be mudstone or wackestone. The finely crystalline or cryptocrystalline cement of reefs seductively suggests low-energy deposition, yet it is produced in the high-energy environments of current-, wave-, and surge-swept reef fronts.

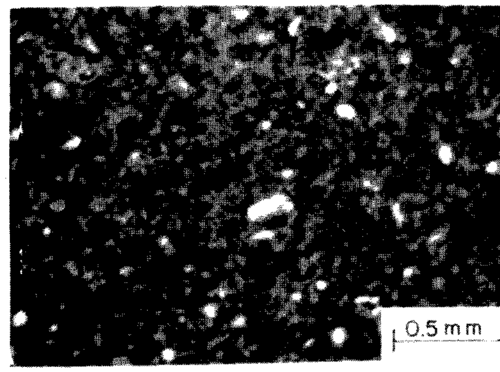

Figure 1.

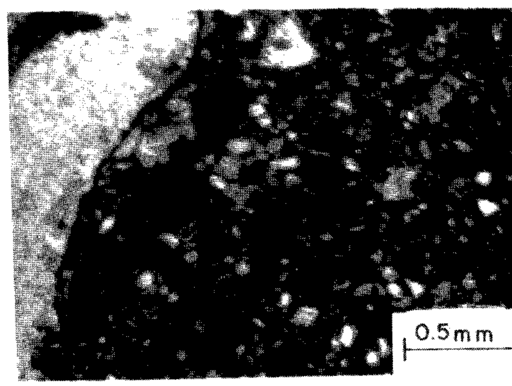

Figure 2.

Figures 1 and 2. Photomicrographs of thin sections of modern reefrock from the Red Sea in which various skeletal fragments are cemented by cryptocrystalline cement.

DILEMMA OF REEF IDENTIFICATION

Blasting open a modern coral reef or drilling through such a reef rarely displays framework-building organisms in growth positions. Biting and boring and rasping or mechanical breakdown convert solid colonies of calcium-carbonate skeletons secreted by the reef organisms into an ever-increasing supply of skeletal particles that accumulate within the reef or in the vicinity of the reef. Among this skeletal debris, coral fragments may be relatively uncommon. Most corals break down into sclerodermites and then further into aragonite needles (Hubbard, 1976). Thus, for instance contiguous to the Great Barrier Reef of Australia, coral fragments make up only 2 to 15% of the total debris (Bennett, 1971). Boreholes through modern reefs reveal mostly debris; framework builders in a position of growth are sporadic or even absent.

In borehole samples of modern reefs, skeletal debris of corals is under represented. The debris present is held together by cryptocrystalline cement which looks like micrite. No wonder reefrock has been described as wackestone, biomicrite, or simply micritic limestone, that has been erroneously referred to a low-energy setting.

In the Appalachian Basin Devonian Helderberg reefs have been termed biostrome rather than the more appropriate term bioherm, presumably because their geometry in outcrop is sheetlike rather than moundshaped. In my experience with reefs of all ages I have observed that most large reefs are flat on top and bottom. Close examination of the reef facies reveals a fine-grained matrix between the framework-building stromatoporoids. This matrix resembles micrite, a lithified former lime mud; hence this facies, like modern reefs,may be misinterpreted as representing a low-energy setting.

Cretaceous reefs which form the most prolific single reservoirs in the Middle East and in Mexico and to a lesser extent in the Gulf of Mexico (such as the Sligo Formation of Louisiana) are composed of reefrock particles cemented together. Framework-building rudistids usually occur as fragments. Almost never are framework builders in a growth position. In the Mishrif Formation of the Middle East, such a Iraq, whole rudistids in life position are nowhere found, and the coarsest debris present is only a few centimeters across. Descriptions of rudistid reef reservoirs from the Black Lake Field of Louisiana state the following: "the rudistid (reef-reservoir) facies is composed of micritic rudistid and micritic rudistid skeletal wackestones" (Reeckmann and Friedman, 1982). This quoted sentence expresses that the dilemma stays with us: micrite and wackestone translate as low-energy lime mud in the kind of setting in which the high-energy reef facies is unlikely to develop. Once again the matrix between skeletal particles formed as a cryptocrystalline or finely crystalline cement that mimics lithified lime mud or micrite.

Hence recognizing reefrock may be an experience in frustration: submarine cryptocrystalline or finely crystalline cement that is size carbonate particles) deserve to be contrasted with (lime) mud-free rocks" (Dunham,1962, p.112-113).

In oral presentations and published papers geologists have used the term "micrite cement". To save embarrassment appropriate references will be omitted here. Clearly as micrite has come to be understood, no such usage as "micrite cement" should exist. The material is either micrite (= physically deposited matrix) or it is cement, it cannot be both. For micrite cement substitute cryptocrystalline or finely crystalline cement or else the depositional environment will be incorrectly inferred.

According to the concept of naming and classifying carbonate rocks three kinds of end members are considered: (1) gravel-,sand-, or silt-size particles, (2) cement, which binds these particles into a solid limestone and has been chemically or biochemically deposited, and (3) mechanically deposited lime mud, which formed as a sedimentary ooze in a low-energy setting. The mechanically deposited lime mud, following lithification, is known as micrite (Folk 1959). The distinction between micrite and cement is critical; it affords a valuable means for interpretation of the energy in the depositional environment. The presence of micrite relates to a low-energy, sluggish setting, whereas that of cement reflects turbulence. The distinction between sediment deposition in sluggish waters and sediment deposited in turbulent waters is fundamental. Reefs are composed of skeletal particles held together by finely crystalline or cryptocrystalline cement that looks like micrite (Figs.1,2). Unwary geologists have described such reefrock, which is a high-energy facies, as a mudstone, wackestone, biomicrite, or simply micrite and erroneously interpreted it as a low-energy product. A recent paper on modern reefs names the reefrocks, mudstones and wackestones cemented by finely crystalline or cryptocrystalline high-magnesian calcite cement (Brachert and Dullo, 1991). Yet according to Dunham (1962), "the distinction between sediment deposited in calm water and sediment deposited in agitated water is fundamental", and the terms mudstone and wackestone reflect a low-energy setting in which the presence of (lime) mud signifies calm waters. Reefrock can never be mudstone or wackestone. The finely crystalline or cryptocrystalline cement of reefs seductively suggests low-energy deposition, yet it is produced in the high-energy environments of current-, wave-, and surge-swept reef fronts.

DILEMMA OF REEF IDENTIFICATION

Blasting open a modern coral reef or drilling through such a reef rarely displays framework-building organisms in growth positions. Biting and boring and rasping or mechanical breakdown convert solid colonies of calcium-carbonate skeletons secreted by the reef organisms into an ever-increasing supply of skeletal particles that accumulate within the reef or in the vicinity of the reef. Among this skeletal debris, coral fragments may be relatively uncommon. Most corals break down into sclerodermites and then further into aragonite needles (Hubbard, 1976). Thus, for instance contiguous to the Great Barrier Reef of Australia, coral fragments make up only 2 to 15% of the total debris (Bennett, 1971). Boreholes through modern reefs reveal mostly debris; framework builders in a position of growth are sporadic or even absent.

In borehole samples of modern reefs, skeletal debris of corals is under represented. The debris present is held together by cryptocrystalline cement which looks like micrite. No wonder reefrock has been described as wackestone, biomicrite, or simply micritic limestone, that has been erroneously referred to a low-energy setting.

In the Appalachian Basin Devonian Helderberg reefs have been termed biostrome rather than the more appropriate term bioherm, presumably because their geometry in outcrop is sheetlike rather than moundshaped. In my experience with reefs of all ages I have observed that most large reefs are flat on top and bottom. Close examination of the reef facies reveals a fine-grained matrix between the framework-building stromatoporoids. This matrix resembles micrite, a lithified former lime mud; hence this facies, like modern reefs,may be misinterpreted as representing a low-energy setting.

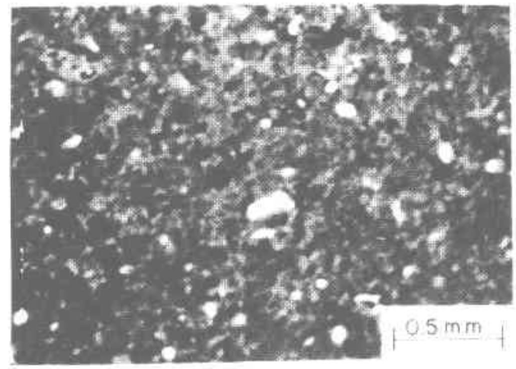

Figure 1.

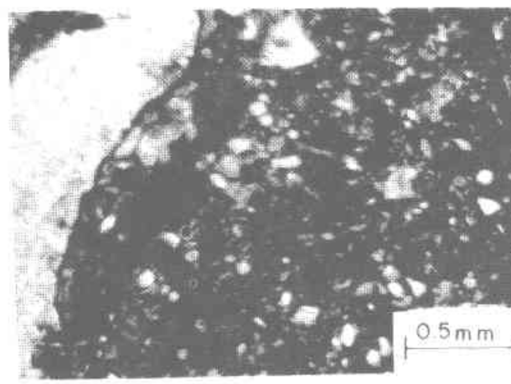

Figure 2.

Figures 1 and 2. Photomicrographs of thin sections of modern reefrock from the Red Sea in which various skeletal fragments are cemented by cryptocrystalline cement.

Cretaceous reefs which form the most prolific single reservoirs in the Middle East and in Mexico and to a lesser extent in the Gulf of Mexico (such as the Sligo Formation of Louisiana) are composed of reefrock particles cemented together. Framework-building rudistids usually occur as fragments. Almost never are framework builders in a growth position. In the Mishrif Formation of the Middle East, such a Iraq, whole rudistids in life position are nowhere found, and the coarsest debris present is only a few centimeters across. Descriptions of rudistid reef reservoirs from the Black Lake Field of Louisiana state the following: "the rudistid (reef-reservoir) facies is composed of micritic rudistid and micritic rudistid skeletal wackestones" (Reeckmann and Friedman, 1982). This quoted sentence expresses that the dilemma stays with us: micrite and wackestone translate as low-energy lime mud in the kind of setting in which the high-energy reef facies is unlikely to develop. Once again the matrix between skeletal particles formed as a cryptocrystalline or finely crystalline cement that mimics lithified lime mud or micrite.

Hence recognizing reefrock may be an experience in frustration: submarine cryptocrystalline or finely crystalline cement that is precipitated within millimeters to centimeters of the surfaces of reefrock is identical in appearance with micrite of supposed mechanical origin as matrix. Case histories abound in which unwary geologists have misidentified the reefrock for low-energy facies.

REFERENCES CITED

Benett, I, 1971, The Great Barrier Reef. Melbourne, Australia, Lansdowne, 183 p.

Brachert, T.C,and Dullo, W.C., 1991, Laminar micrite crusts and associated foreslope processes, Red Sea: Journal Sedimentary Petrology,v. 61, p. 354-363.

Dunham, R.J, 1962, Classification of carbonate rocks according to depositional texture, *in* W.E Ham (ed.), Classification of Carbonate Rocks: American Association Petroleum Geologists, Memoir 1, p. 108-121.

Folk, R. L, 1959, Practical petrographic classification of limestones: American Association Petroleum Geologists Bulletin, v. 43, p. 1-38.

Friedman, G.M,, 1973, Cementation in reefs: Centre de Recherches Exploration-Production, Pau-Société National Elf Aquitaine, Bulletin, v. 7, no. 1, p. 171-176.

Friedman, G.M., 1975, The making and unmaking of limestones or the downs and ups of porosity: Journal Sedimentary Petrology v. 45, p. 379-398.

Friedman, G.M., Amiel, A.J., and Schneidermann, N., 1974, Submarine cementation in reefs: example from the Red Sea: Journal Sedimentary Petrology, v. 44, p. 816-825.

Ham, W.E. and Pray, L.C.. 1962, Modern concepts and classifications of carbonate rocks, in W.E. Ham (ed.), Classification of Carbonate Rocks: American Association of Petroleum Geologists, Mem. 1, p. 2-19.

Hubbard, J.A.E.B., 1976, Sediment budgeting: A timed study of scleractinian necrology [abs.]: 25th International Geological Congress, Abstracts, v. 3, p. 845.

Reeckmann, A., and Friedman, G.M., 1982. Exploration for carbonate petroleum reservoirs. New York. John Wiley & Sons, 213 p.

EMD AND THE BALANCE OF ENERGY RESOURCES

John W. Gabelman

The Energy Minerals Division began about 1973 as an ad hoc committee of AAPG formed to address the entry of many oil companies and petroleum geologists into the budding uranium resource industry. The effort was successful immediately and the Committee was converted to a formal Division in July 1977 with 760 charter members.

Membership histories of professional groups dedicated to a commodity also illustrate the progress of that commodity. EMD membership (Figure 1) grew at a steep rate along with the uranium boom (actually the third of this century) to the boom peak in 1984, thereafter declining as the industry withered under attacks of environmentalists and those over-fearful of radiation. It rose again from an alltime low in 1984, as coal replaced uranium in responding to expanding power needs, but at a lower and more cyclic rate. We have experienced only three intervals of decline, but despite overall growth, the Division has not risen significantly above 2000 members.

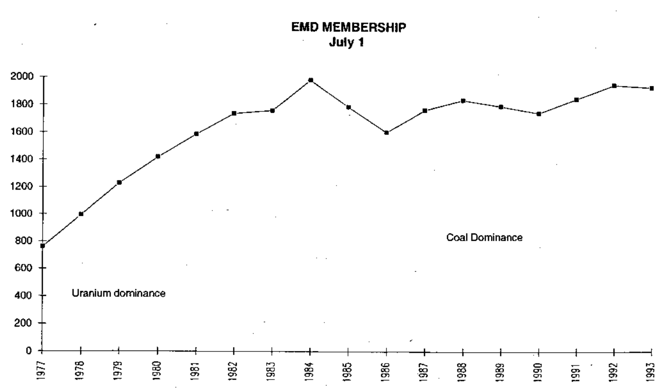

Figure 1.

Figure 2 compares the membership histories of EMD and AAPG for the EMD lifetime. EMD, despite its peaks and troughs, illustrates a flat curve compared to the broad AAPG peak correlative with America's response to the OPEC stimulated oil shortage of the mid 1970's. AAPG's subsequent decline corresponds with our worsening economy. The EMD 1984 trough nearly coincides with the AAPG peak.

Figure 3 shows EMD membership as a percentage of AAPG. After a steep rise to 5.8% in 1980 the percentage curve dropped to a low of 4% in 1986, then rose at about the same rate as its decline, to the current highest peak of nearly 6%. Since its first sharp rise, membership has fluctuated about a plateau averaging 4.9 % of AAPG. Outwardly this suggests a limit of about 5% of AAPG petroleum geologists who are interested in energy minerals. While this inference may be broadly accurate, it is countered by the independence of the individual membership curves on a minor scale. AAPG expanded across the EMD trough and has since shrunk while EMD expanded. Whereas AAPG represents petroleum geologists, EMD has shifted emphasis from uranium to coal. The possible reality of the 5% average limit is significant to EMD's ambition to expand.

The distribution of EMD members (Figure 4) does not reflect the distribution of the energy minerals (coal, coalbed methane, uranium, tar sands, oil shale, geothermal fluids, and hydroelectric water). The Gulf Coast region is proficient in oil and gas, but deficient in energy minerals, yet that Section boasts most members. These are inferredly petroleum geologists interested in energy minerals. The reverse resource abundance prevails in the region of the Eastern Section which has the second largest membership. There most are coal geologists. The Rocky Mt. region is about equally endowed with oil/gas and energy minerals, and is the third largest section with presumably a comparable mixture of geologists. The Pacific region and section membership resembles those of the Gulf Coast.

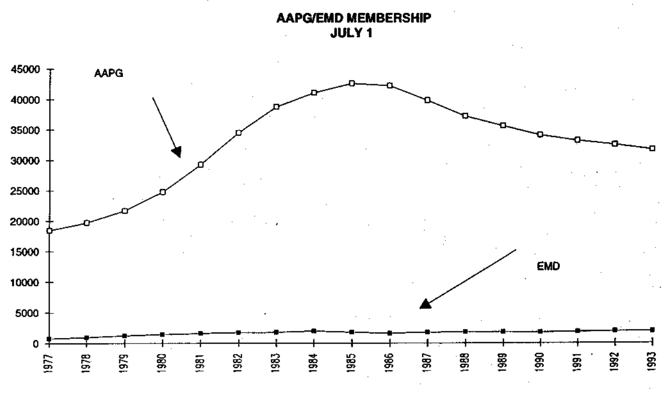

Figure 2.

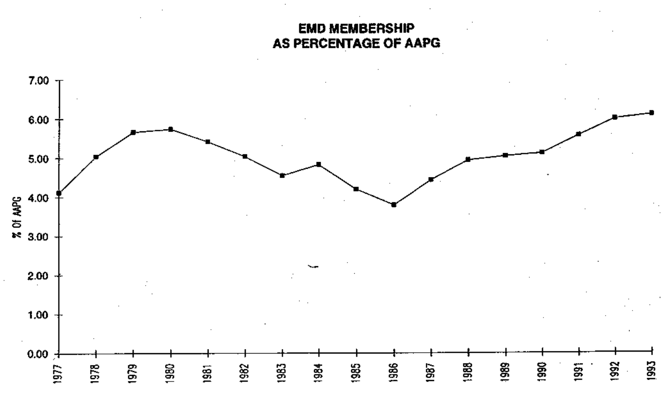

Figure 3.

The surprise is the large portion of foreign members. 310 members are supplied by 61 countries, listed in Figure 5. Figure 6 shows the distribution of foreign members. Canada understandingly leads, followed in decreasing order by Australia, England, Germany, Japan, and Argentina. Thereafter 20 countries have from 10 to 3 members each. Lastly 39 members are supplied by 35 countries. The number of countries is greatly disproportionate to the number of members in each. Memberships in countries such as Canada and Argentina expectably are dominated by petroleum geologists, but those in many countries obviously poor in known oil and gas, probably are oriented principally toward energy minerals. The disproportionate membership in these countries suggests they are fertile fields for membership expansion.

MEMBERSHIP DISTRIBUTION
ENERGY MINERALS DIVISION
4 JUNE 1993

	Eastern	Gulf Coast	Mid-Continent	Southwest	Rocky	Pacific	International
Membership	331	447	157	183	313	186	310

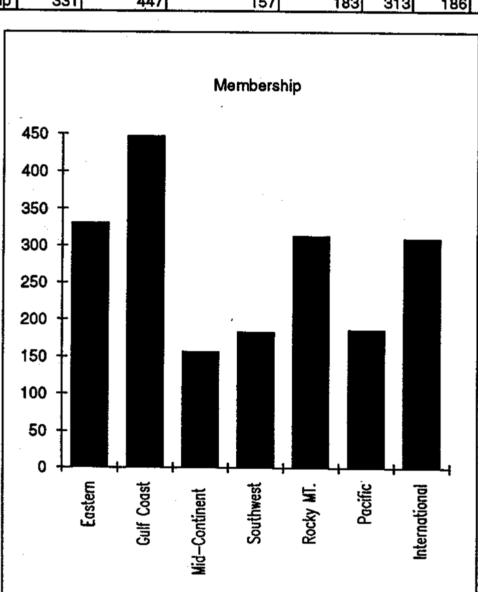

Figure 4.

COUNTRIES OF EMD FOREIGN MEMBERS

1993

AGUADILLA	FRANCE	NIGERIA
ALGERIA	GERMANY	NORTH IRELAND
ARGENTINA	GREECE	NORWAY
AUSTRIA	(HAWAII)	PAKISTAN
AUSTRALIA	HONG KONG	PERU
BARBADOS	HUNGARY	PHILIPPINES
BELGIUM	INDIA	POLAND
BOLIVIA	INDONESIA	REP. SINGAPORE
BRAZIL	ITALY	SAUDI ARABIA
B. I. DARUSSALAM	IRAN	SCOTLAND
CANADA	IRELAND	SLOVENIA
CANOVANAS	IVORY COAST	SPAIN
CHILE	JAPAN	SWEDEN
CHINA	KOREA	SWITZERLAND
COLUMBIA	KUWAIT	TAIWAN
COSTA RICA	MALTA	THAILAND
CYPRUS	MALAYSIA	TURKEY
DENMARK	MEXICO	U.A.EMIRATES
EGYPT	NETHERLANDS	VENEZUELA
ENGLAND	NEW ZEALAND	YUGOSLAVIA
		ZIMBABWE

Figure 5.

Expectations for EMD expansion are closely allied to the relative industrial significance of the several energy mineral commodities. Figure 7 presents the history of total domestic energy production in quadrillion BTUs from 1949 through 1992, differentiated by the major resource types. Data are from the DOE Annual Energy Review 1992 (DOE/EIA0384(92). Coal use cycled and shrank across the industrial strike years to its low in 1961 when it trailed oil. Since then it has expanded steadily (with insignificant cycles). Gas shows a dramatic expansion in the early 1960's, shrinking thereafter, then rising again. Oil has maintained the steadiest proportion of production, gradually shrinking to third place. The surprise is nuclear power which has expanded steadily since inception in 1969, despite the reduction of the domestic uranium resource industry to a token p roduction from in-situ leaching. This expansion, based on imported uranium, demonstrates forcefully how uranium, despite its environmemtal objections and the crippling experiences of reactor construction, is capturing the growth increment in power production. This growth foretells the return of uranium prominence, probably dominance, although the resource expansion will be international. Domestic known resources cannot compete with richer and larger foreign deposits, principally in Canada and Australia.

Figure 8 presents the same history of produced major energy resources as percentages of total energy used. These show more drammatically the welfare of each commodity. King Coal dropped across the John L. Lewis years to a deep trough, rising again to a lesser crown as coal assumed the role originally expected of uranium. Gas significantly illustrates a near-mirror-image curve with coal, showing that it was the commodity which most compensated for the coal depression. Oil, despite its cycles, gradually but steadily decreased across the years until presently it accounts for only slightly more than twice the nuclear power. Nuclear still lags 10% of the total. Only nuclear power has steadily grown across two hardly noticeably bumps. The growth rate of nuclear power about equals that of coal, the increased use of which was intended to compensate for the failure of nuclear power beginning in the late 1970's. That uranium has maintained this growth rate again emphasizes the quiet strength of nuclear power despite the efforts to kill it.

Coalbad methane is included in gas statistics as a major contributor to total energy. Of the remaining energy minerals only hydroelectric water and geothermal fluids have been economically exploited domestically. Hydroelectric water has not heretofore in EMD been considered an energy mineral (because only engineering geology is significantly involved), yet it is a mineral on the same basis as geothermal fluids. Tar sands are produced on a significant scale in Canada, and oil shales in Estonia, but our domstic extensive oil shales and minor tar sands are not presently competitive. The relative participation of minor energy minerals in domestic energy production, for the same period, is shown in Figure 9, with nuclear power as comparator. Hydroelectric power production has maintained the steadiest rate over the years, demonstrating the saturation of resource capacity, but has shrunk in terms of expanding total energy. The geothermal contribution would not even show on Figure 7. However, significantly geothermal energy production has expanded steadily since 1970. This expansion is more because of federal subsidy than intrinsic economic viability. It is well known that only natural steam is currently viable without subsidy, and steam constitutes only a minor portion of liquid-dominated geothermal resources. Our government promotes the development of liquid-dominated geothermal resources, along with wind and solar power, as alternate energy resources against times of need. Indeed such emphasis betrays a naive belief that these clean resources can someday replace the polluting resources such as coal, oil, and uranium. However, geothermal energy will remain a volumetrically insignificant energy source, and oil shale and tar sands will remain economically unviable for the near future.

Figure 10 expresses the division of domestic and imported produced energy resources since 1960. Time intervals are in five-year increments until 1980, and yearly thereafter. Domestic production grew at a steep rate until 1970, thereafter leveling off. This levelling reflects the saturation of domestic capacity in economic rather than geologic terms. Foreign resources simply are produced more cheaply. Domestic production is likely to expand only if foreign supplies are interrupted for any reason. Imports have expanded steadily, representing the difference between domestic capability and growing domestic demand, and will continue to do so.

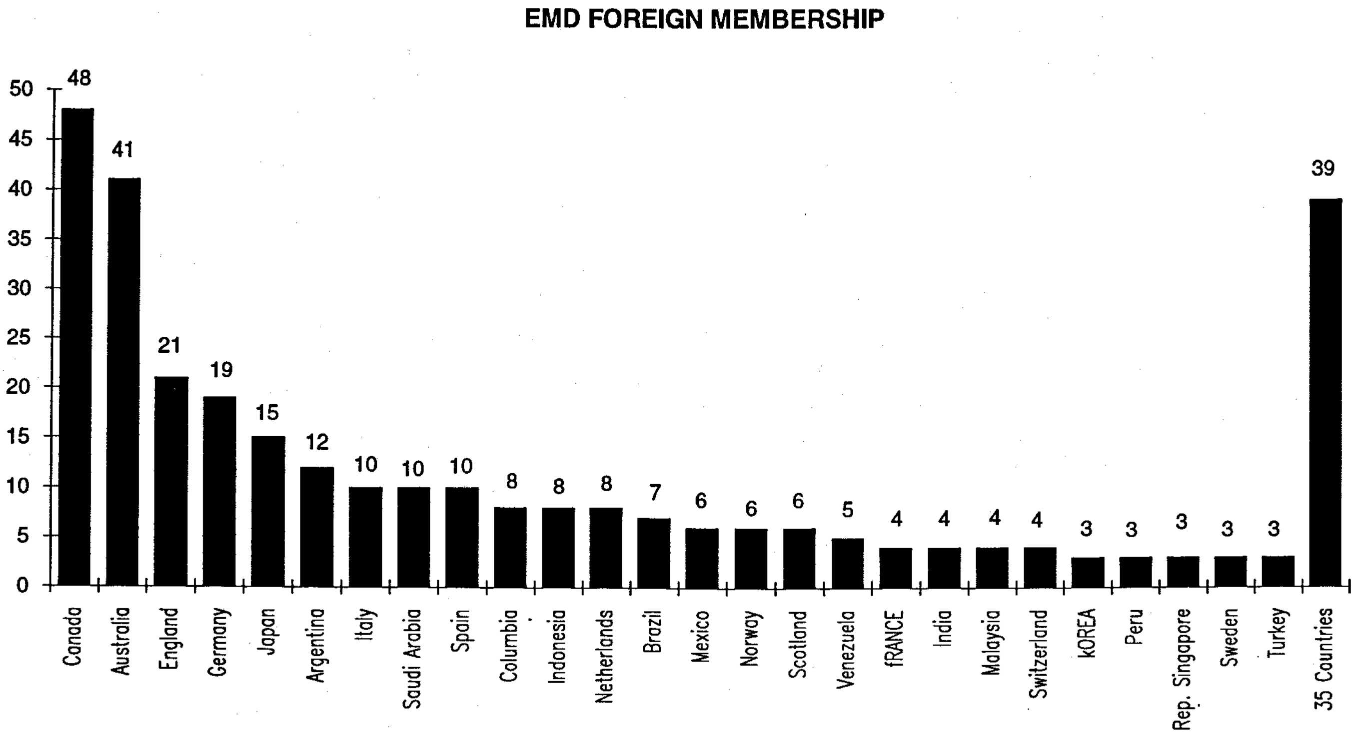

Figure 6.

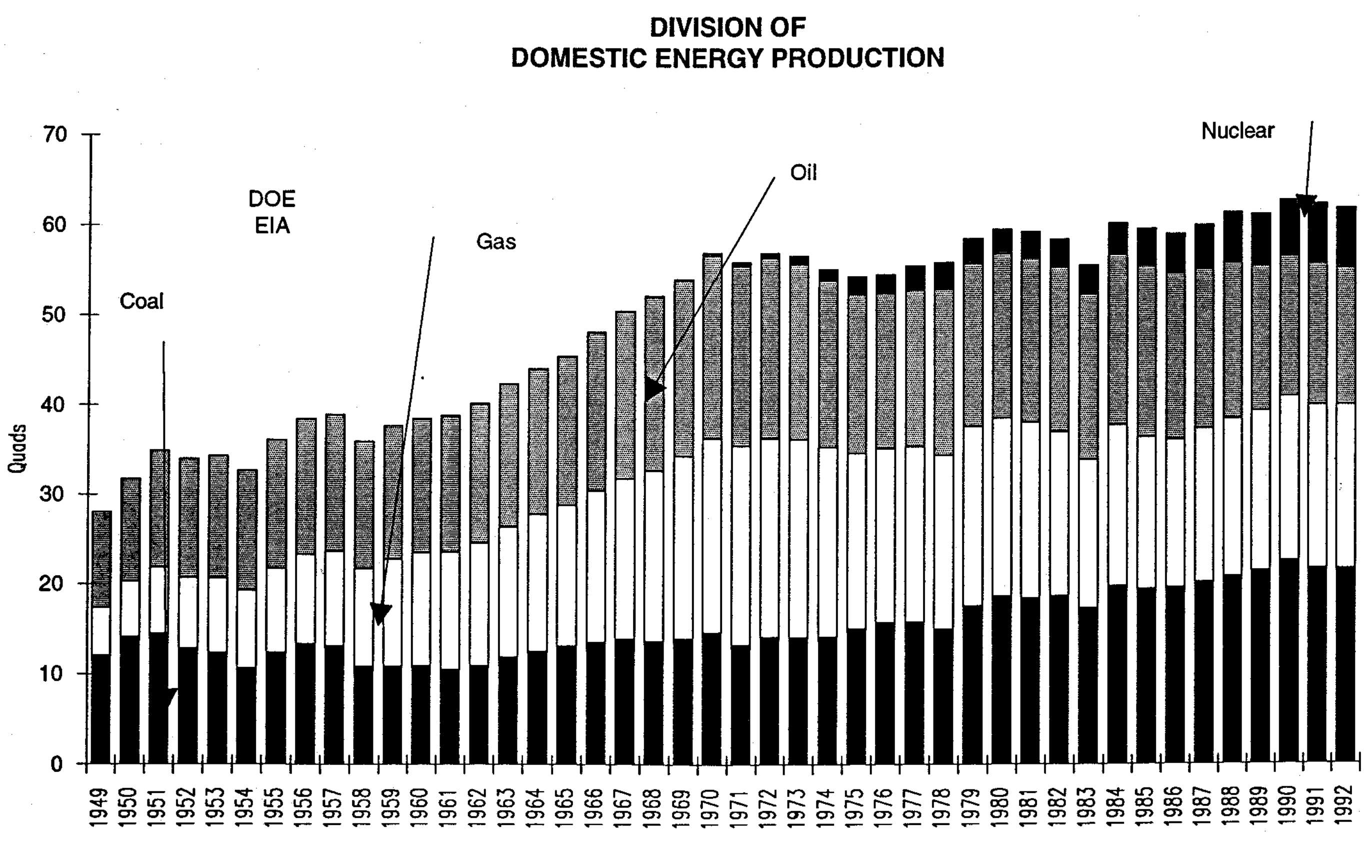

Figure 7.

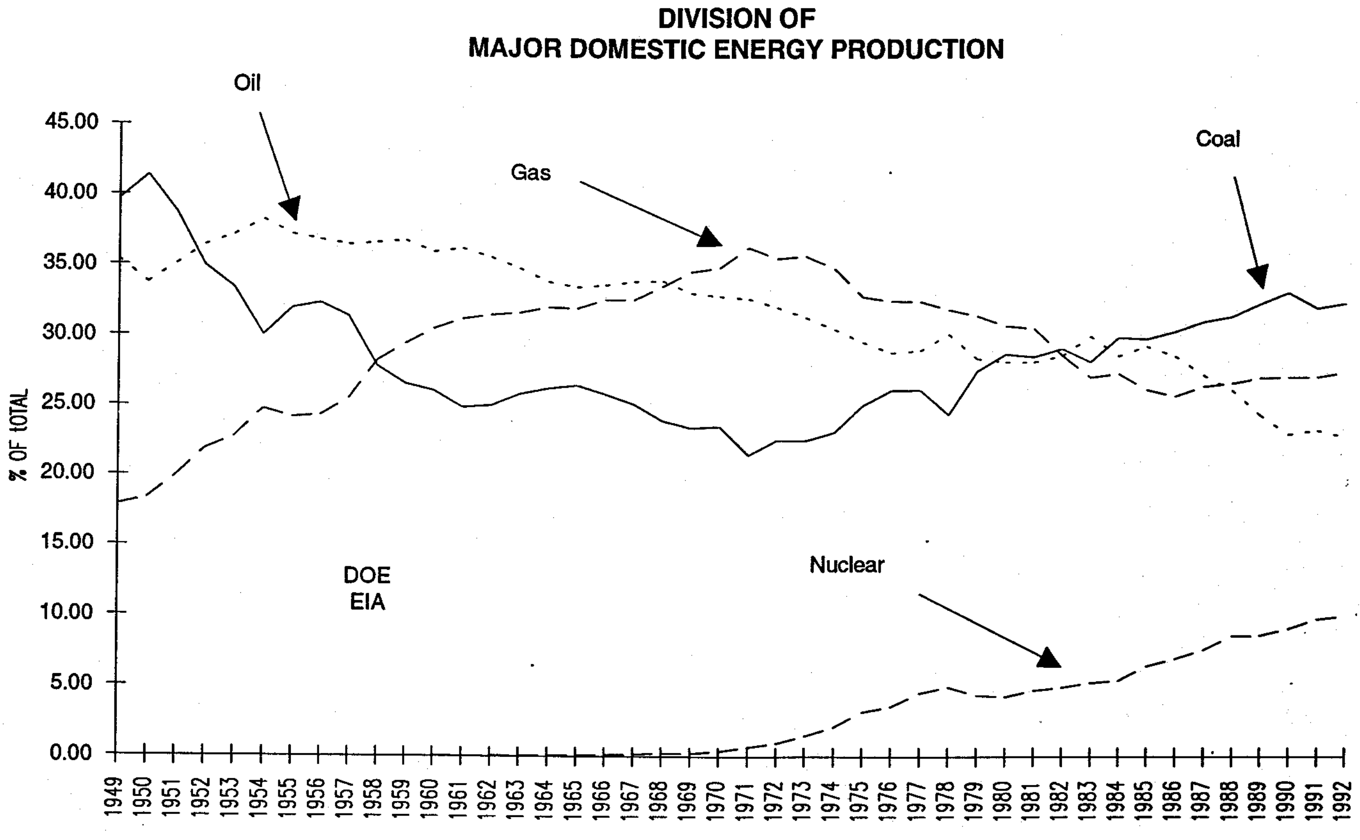

Figure 8.

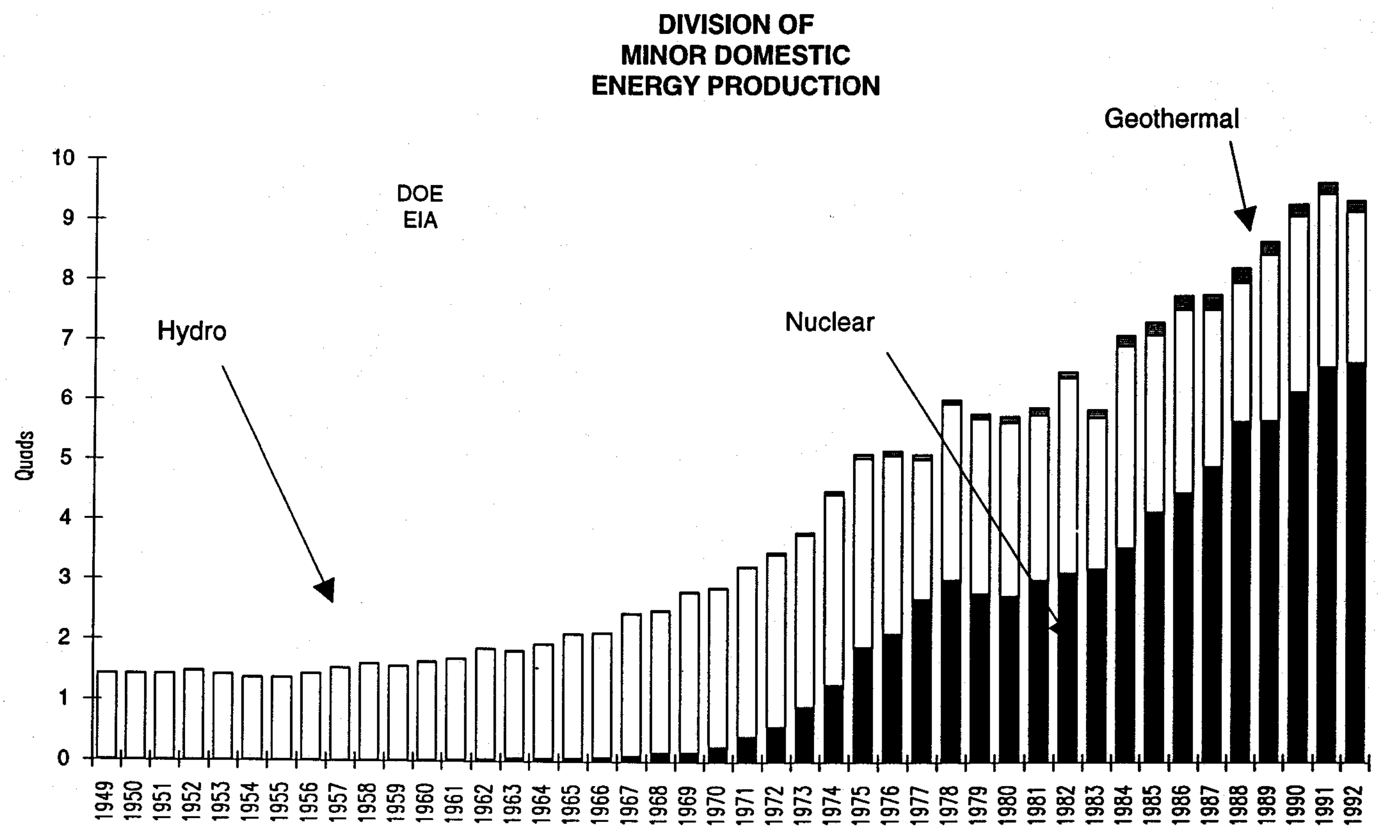

Figure 9.

The significance of this chart to EMD is the potential role of energy minerals under the various scenarios of future imported supply flow. The common assumptions which have governed the national investment in energy resource research and development is that the inability of the domestic production base to expand heralds the exhaustion of domestic oil and gas, and the interruption of imports should be compensated by the readiness of alternate resources to fill the gap. For America (including Canada) these have been uranium, tar sands, oil shale, geothermal, solar and wind. However, America responded to the latest and most severe interruption (that of the mid-1970's) by the successful concerted domestic oil exploration/development effort which eliminated the need to call on alternate resources (and also created the peak in AAPG membership). Planners had not failed to consider that the price increases which were expected to justify alternate resource development, also justified production of higher-cost petroleum. Remaining petroleum resources were considered inadequate. The surprise was that resources had been geologically underestimated. If any forecasting failure is to be levied, it should be that economics is a more critical determinant of reserves and resources than geology.

A more realistic scenario for anticipating the future of energy resources is that imports will remain uninterrupted and will increase. The saturation of domestic production capacity being economic rather than geological, centers of greatest geological and production activity will shift to less explored, underdeveloped, and more cheaply operated foreign fields. I believe that domestically, coal alone will remain dominantly and independently viable by virtue of technological inovations, if it can survive the onslaughts of environmentalism.

The strength of EMD has been its embrace of all the energy resources except hydrocarbons and its ability to shift emphasis among them. However, our statistics reveal a tendency toward stagnation. EMD membership has been dependent primarily on the interest of petroleum geologists (being a division of AAPG), secondarily on the commodities of dominance, and thirdly on the domestic scene. Because of its broad scope EMD perhaps is best positioned to define the realistic balance of energy resources, and having a membership composed from industry, government, academia, and "national laboratoria" is perhaps best able to do so with least prejudice. For its expansion EMD might well focus more on international resources and the foreign professionals responsible for their discovery and development. The future of EMD appears secure, and hopefully bright.

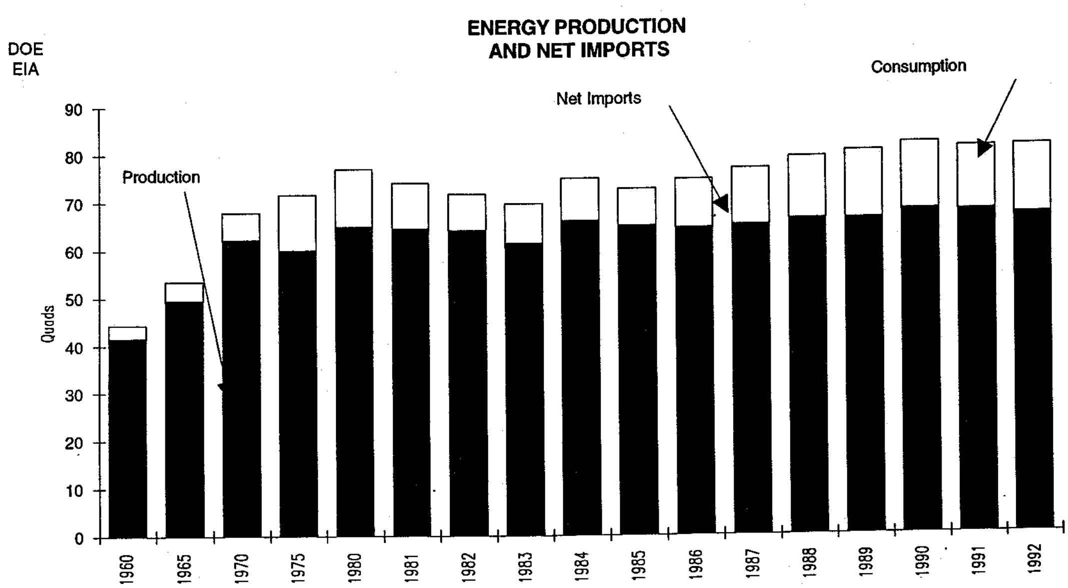

Figure 10.

Russia: Survival or Failure

Robert E. Ebel
Senior Associate
Center for Strategic & International Studies

When I have an opportunity to talk with a Western businessman, when I ask about his view of the future with regard to doing business in Russia, and when he responds that he is "cautiously optimistic," the following comes to mind.

Someone has observed that a Russian pessimist is one who believes that things cannot possibly get worse, while a Russian optimist would argue that yes, they certainly can.

What can I say about what is going on in the former Soviet Union? Only that these are very good times for historians, but very bad times for forecasters.

One day not long ago President Yeltsin was walking along the banks of the Moscow River, trying to collect his thoughts, trying to find a way out of all his problems. When he spotted an old lantern, partly buried in the mud. He picked up the lantern, knocked off as much mud as he could, and tried to polish it up with the sleeve of his coat. A genie suddenly appeared from inside the lantern and said that as your reward for setting me free, I will grant you one wish.

Yeltsin thought for a moment, then reached into his coat pocket and pulled out a map, studied the map intently and said, "I would like peace for the world."

The genie replied, no, he could not deliver that, it was much too difficult. Try again.

"Well", Yeltsin responded, "I would like to see my country move quickly and painlessly to a free market economy."

The genie stared at him, and then replied, "Could I see that world map again?"

Let me try to give you a snapshot of what life is like in Russia today. Large numbers of the population think they are worse off now, than they were under Communism. Yet I do not detect any particular nostalgia for the past. In May of this year the average wage in Russia was the equivalent of $37 per month; the minimum monthly wage was around $4.30. Per capita income in May was $21.73, while the cost of 19 basic food products was $10.50. Thus, half the income goes just to cover the cost of these 19 basic food products.

Russia is under great stress and strain. The stresses and strains of trying to cope with the monumental changes taking place in the country clearly are taking its toll. The birth rate has fallen by 14% during the first six months of this year, while the death rate has gone up by 20%. Abortion is an explosive issue in the US. But how many abortions do you think there were in Russia just in 1991? About 3.5 million, or almost 2 million more than the number of live births that year. For years now, abortion has been the preferred method of birth control, the other methods having been discredited.

There has been a noticeable increase in the number of deaths as a result of accidents. Alcoholic poisoning, up by 2.4 times; murder up by 1.6 times; suicide up by a third.

Inflation is running around 20% or more per month. Last year, 1992, the inflation rate was 2,500%. Most Russians have experienced little or no inflation in their entire lifetimes.

To date, the State has chosen inflation over unemployment. But that choice cannot hold forever. The authorities understand and recognize that. Eventually the decline in industrial output and the impact of economic reform will take it's toll in the form of bankruptcies. Factories will shut down, shops will close, hundreds of thousands will lose their jobs.

Russian economists compare what is happening to their country with the great American depression of '29-33, observing that the decline has been about the same. Perhaps so. Industrial output in Russia as of January 1, 1993 was 66% of January 1, 1990. And output has fallen by 18% in the first half of this year, compared with the first half of 1992.

But, these economists continue, their situation is really much worse, compared to our Depression. First, because of the accompanying high inflation rates and, second, because their collapse is continuing, with no turnaround likely, I would judge, before 1996.

I cannot leave this portion of my comments without some mention of the crime and corruption sweeping the country. Most of the violence has to do with extortion. Last July 19, at 2:10 in the afternoon, criminals with machine guns attacked the Alliance Car Dealership. The dealership had its own armed guard. When the air cleared, 4 were dead. Two days later the assistant manager of a cafe and 2 employees were killed. On July 30, late in the morning, the Russian manager of one of the most well-known restaurant in Moscow was found executed. The following day, thugs broke into an apartment and shot a Swedish businessman. The next day, a rep from United Telecom Marketing was found dead from stab wounds in a major, downtown Moscow hotel.

Nationwide, there have been 100-150 contract killings of businessmen this year, and 10 of bank officials, and multiple terrorists bombings of homes, offices and cars.

It is, as one observer noted, Chicago of the 1920s and 1930s.

You may have read recent newspaper accounts of widespread outbreaks in Russia and in the other former Soviet republics of dangerous diseases, epidemics of cholera, diphtheria, typhus and, even one case of the bubonic plague. Poor sanitation, and a lack of drugs have been cited as major causes, as well as a reluctance to be vaccinated. Also, low nutritional levels contribute: the average Russian receives 20% fewer calories and 40% fewer vitamins than they need.

What has been a particular legacy of Communist rule? A devastated environment, among other things: poisoned rivers, ruined forests, dried up lakes, and urban areas choked with pollution.

If you would like to pursue this subject, I can highly recommend "Ecocide in the USSR," by Murray Feshbach. The book will tell you about pollution fouling 75% of the surface water in the country, that 4 out of 5 rural hospitals lack hot water, of surgeons having to make do with razor blades in the place of scalpels.

The ecological mess that Russia finds itself in can be traced back, in large part, to the philosophy that any sacrifice was justified to turn the Soviet Union into a military superpower.

It would be difficult to compile a listing of the greatest environmental tragedies that have taken place in the former Soviet Union. But certainly the Chernobyl nuclear power accident of April, 1986 would stand at the top of any list. The list might also include: 1. The drainage and loss of the Aral Sea, 2. the poisoning of Uzbekistan by pesticides, 3. the release, by an explosion, of radioactive materials at Kyshtym, a secret site near Chelyabinsk, 4. the use of the Arctic Ocean as a dumping ground of nuclear wastes, and 5. nuclear weapons testing and fallout.

On a more personal basis, only about 1 in 6 Russians live in an area where pollution of the environment meets permissible norms. Half of the Russian citizenry use and drink water that does not meet sanitary-hygienic conditions.

Several years ago, before the breakup of the Soviet Union, the Institute of Geography of the Soviet Academy of Sciences had identified about 300 areas whose environment was unfavorable for human habitation. These territories occupied 16% of the Soviet Union. And if ruined reindeer pastures in the tundra were included, the unfavorable area rises to 20%.

What about the oil and gas industry? Each day there are two pipeline accidents in Russia. Oil pipeline spills in the 1st quarter, 1993 resulted in the loss of some 250,000 bbl of oil, and a massive contamination of the surrounding area. Last year there were 9 blowouts in the oil fields, and 6 already this year. Some 20% of the associated natural gas produced in Russia -- or 290 billion cubic feet -- is flared off every year.

The Astrakhan natural gas field, where the sulfur content is very high, continues to operate in an unstable manner, such that it has been recommended that people living within a defined health protection zone around the field, be moved elsewhere.

I made my first visit to the Soviet Union in August of 1960. as a member of the first oil delegation from the US to visit that country in the postwar years. We were not impressed with what we saw. We saw an industry lagging 15 years or so behind the West in terms of technology. We saw a labor force poorly paid, poorly housed and poorly fed. But we came away with an awareness of the obvious potential of this country to become a major oil producer and exporter. And, given the government control over natural resources, there was fear that the rich oil fields represented a very real threat to the world oil market and in turn to those multinational oil companies operating in that market.

That fear was never realized. While the Soviet Union did enter the world market, and eventually became a major player, it conducted itself in a fashion just like its competitors. It sought the greatest return on what it had for sale. Contractors were strictly honored; politics rarely intruded.

What if we visited those oil fields today? What would we find? Unfortunately, we would find a growing technological gap, a decaying infrastructure, a high labor turnover, and idle oil wells exceeding 30,000 in number, or 1 in 5.

During the 33-odd years separating my first visit to the Soviet Union, and my last, which came this past April, the former Soviet Union had made the most of its oil potential, becoming the world's leader in oil and gas production, a major player in oil exports and the world leader in gas exports.

In 1988 Russia hit its peak of some 11.4 million b/d, almost 50% more than what the US produces today. Then, a collapse set in, and by the end of this year, Russia will have lost some 4.2 million b/d of oil production.

Throughout the history of the world oil industry, there has been no other producer who has undergone such a transformation when the circumstances have been dictated not by war or by the workings of the market place, but rather as a result of mismanagement of a superior natural resource. Now made more dramatic by the political changes surrounding this transformation.

What has gone wrong with Russia's oil industry? Can we compare its collapse with our own decline in production?

Not at all. Reduced oil production in our country has come about because of the availability of cheaper foreign oil, and the willingness of the consumer and our government to place potential oil-bearing regions out-of-bounds. In the interim, our reliance on foreign oil approaching that magic 50% level, but we continue to ignore the perils of such dependence.

The collapse of oil production in Russian can be attributed to a variety of causes, but particularly to mismanagement and shortages of capital. The power struggle between Yeltsin and his Parliament over the economic future of the country has made the potential Western investor ever more mindful of the uncertainties to be faced. However, perhaps we should not come down too hard on Russia and political risk. After all, there is a good measure of political risk taken on by our oil industry as it attempts to do business within the border of the US. Is Kazakhstan any riskier than California? Ask Chevron.

Let me give you an appreciation of just what troubles the oil industry. Water is overwhelming the producing fields. Today, on average, every barrel of crude brought to the surface is accompanied by about four barrels of water. New discoveries are small in size and fall far short of replenishing produced oil.

Oil refineries are badly outmoded by Western standards, with light product yields averaging barely 63%. Only 14% of the production equipment in the oil industry meets world standards.

More than 70% of the equipment in the oil refining industry is obsolete and requires replacement. Only 10% of the productive assets of the gas industry can be said to meet world standards, and about 15% awaits replacement.

If your own means are limited, as they are for Russia, then the natural recourse is to look abroad for help. Thus the rationale for joint venture. But the political and economic uncertainties of Russia clearly have not been lost upon the Western businessman.

Political and economic stability are desirable elements for investment, whatever that investment might be made. Our companies and our government have worked hard to bring that message to Russia, but with uneven success.

The difficulties US companies have encountered in their negotiations in Russia reminds me of a story whose moral is that not all joint ventures treat partners equally.

A chicken and a pig are sitting around the table talking, as pigs and chickens often do. Now it seems that this chicken and this pig have not been friends for very long. Indeed, for a number of years, they had been enemies. But things do change, and they both realized they would be better off if they buried the hatchet. The pig spoke up: "You know, now that we are friends, perhaps we could do some business together. But what?"

There was silence for a while, then the chicken said, "Well, we might do a joint venture together."

"Not a bad idea, but what kind of joint venture?"

The chicken thought for a moment, and said, "How about ham and eggs?"

The pig was enthusiastic, but then reality set in. "Wait a minute now. That would be o.k. for you, but what about me? I would be dead."

The chicken smiled knowingly, and said, "Well, that's the way it is with some joint ventures."

In the energy industry in any country, reliable statistics are an essential to an understating of what is going on. There are plenty of statistics on Russia today, probably more than ever, but can we trust what we are being told?

The secretary of the local Communist Party -- when there was a Communist Party -- makes his annual visit to the nearby state farm, to meet with its manager.

"Tell me, Misha," he asks, "how are things going?"

"Comrade Secretary," Misha replies, "things are going very well. Why, if we were to pile our potatoes one on top of the other, they would reach all the way to God."

"Now, Misha," the secretary admonished, "you are a good Communist, and all good Communists know there is no God."

"Well, yes, I know that, I know there is no God," answered Misha. "And by the way, there are no potatoes either."

There is a reason why I have emphasized what is happening to the oil industry of Russia. Not only that any economic turnaround for the country will be led by a revitalized oil industry. It is more than that. And this reasoning would apply to any major oil consuming or oil producing country.

Oil fuels much more than automobiles are airplanes. It fuels military power, national treasuries and international politics. Because of this, it is no longer just a commodity to be bought and sold within the confines of supply and demand balances. Rather, it has been transformed into a determinant of well-being, of national security and international power for those who possess this vital resource, and the converse for those who do not.

While oil goes about attracting all the headlines, what is happening with regard to other forms of primary energy: coal, natural gas and nuclear power?

The decline and fall of the Russian coal industry has been overshadowed by the collapse in oil production, a much higher profile activity. Yet the collapse in coal has come close to mirroring the collapse in oil, for much the same reasons. Coal actually began to experience difficulties beginning in the 1970s, because of deteriorating geological conditions, a shortage of experienced workers, inadequate investment and the extreme distance of new mines from consumers.

The electric power industry of Russia faces an immense crisis. First, it has little or no spare generating capacity, other than that which may become idle, as generation declines, for whatever the reason. Most industrialized countries would feel uncomfortable with spare capacity under 15%. At the moment, the crisis is eased because of the decline in demand.

Second, lurking in the background, and threatening not just the nuclear power industry of the FSU, but of the West as well, are the 11 Chernobyl-type reactors still operating in Russia, along with 2 such reactors in Lithuania and 2 more in Ukraine.

Finally, to the only current success story in the energy sector. That, of course, is the natural gas industry. This, despite the fact that natural gas production in Russia declined, if only slightly in 1992, for the first time in its history. Production last year totalled 640 billion cubic meters, or 22.6 trillion cubic feet. For comparison, the US in 1992 produced about 17.8 trillion cubic feet. Moreover, while Russia was busily exporting the US had to import to cover its requirements.

Russia today is the world's leading exporter of natural gas and is not likely to relinquish that position any time soon. In 1992 a total of 205.6 billion cubic meters or about 7.3 trillion cubic feet of natural gas crossed Russian international borders enroute to buyers in the FSU and outside.

On occasion in the past I have referred to a joke making the rounds in Moscow, as a way of giving the audience an insight into the then current mood of the people. The joke went something like this.

A Russian optimist is one who still teaches his children how to read and write in their native language. A pessimist is one who teaches his children to read and write in English and Chinese. But a Russian realist is one who teaches his children to fire a Kalashnikov rifle for the coming civil war.

Unfortunately, civil war has arrived, although not in the broad context we might think of. There is fighting between Azerbaydzhan and Armenia, and within the republics of Georgia and Tadzhikstan. We should now add the republic of Moldova to the list, where there is fear that conflict between the ethnic Romanian majority and the Russian-speaking minority will escalate to full-scale war. And don't forget the growing tensions between the Ukraine and Russia.

Is there hope for Russia? Will matters eventually improve?

A Russian and a Pole met with God to discuss the affairs of state of the two countries. God asks the Pole if he felt life would ever improve in this country.

"Yes," the Pole replied, "but not in my lifetime."

God then turned to the Russian, and put the same question to him. Will life ever improve in his country?

The Russian listened thoughtfully, then answered, "Yes, but not in your lifetime."

SEDIMENTARY FACIES OF THE PLIOCENE YORKTOWN FORMATION AND RELATED STRATIGRAPHY, STRUCTURE, AND GEOMORPHOLOGY OF THE INNER COASTAL PLAIN, NORTHEASTERN VIRGINIA

Robert B. Mixon, David S. Powars, and J. Stephen Schindler
U.S.Geological Survey, 926 National Center, Reston, VA 22092

INTRODUCTION

The Inner Coastal Plain of Virginia and North Carolina includes extensive upland areas underlain by fine to coarse sand and gravel sheets of late Tertiary age. Although these deposits have been the subject of considerable study in recent years (Goodwin and Johnson, 1970; Newell and Rader, 1982; Johnson and others, 1987; Berquist and Goodwin, 1989; Carpenter and Carpenter, 1991), their stratigraphy, correlations, and ages are still the subject of much controversy. The nonfossiliferous to very sparsely fossiliferous character of these sand and gravel sheets has made age determinations difficult. And commonly, as in the Richmond area of Virginia and in the Potomac River basin of southern Maryland, erosion and truncation of upper Miocene and lower and middle Pliocene rock units by younger formations has disconnected the nonfossiliferous sands and gravels of updip areas from their downdip, fossiliferous equivalents. However, in our trip area in the uplands of northern Virginia, the downdip, fossiliferous, shallow-shelf sands of the Pliocene Yorktown Formation can be traced continuously in the updip direction into nonfossiliferous gravelly sands deposited in marginal-marine and fluvial-deltaic environments.

Our trip is intended to familiarize participants with the stratigraphy, depositional environments, structural setting, and geomorphology of upper Miocene and Pliocene deposits in the Inner Coastal Plain of northern Virginia. Thus, our field trip stops and discussions focus on the Yorktown Formation and, to a lesser extent, the underlying Eastover Formation. However, older formations are briefly described to facilitate discussion of Coastal Plain structures and the effect of structure on the distribution and thickness of Coastal Plain units. At our first stop (fig. 1), which is near the western margin of the Coastal Plain, we will examine the thin, truncated, updip remnants of six unconformity-bounded formations of late Paleocene, early Eocene, middle and late Miocene, and Pliocene age. At later stops, we will focus on the extensive sheets of sand and gravel that cap upland areas--using differences in lithology, primary sedimentary structures, and thickness to help interpret depositonal environments and stratigraphic and paleogeographic relationships (Table 1).

GEOLOGIC AND GEOMORPHIC SETTING

The field trip area in northeastern Virginia encompasses parts of two vastly different geologic terranes--the Appalachian Piedmont to the west and the Atlantic Coastal Plain to the east. The rolling, hilly Piedmont terrane consists of metamorphosed sedimentary, volcanic, and plutonic rocks of late Precambrian and Paleozoic age. These rocks are generally steeply dipping and exhibit a strong northeast-southwest structural grain. Fresh, unweathered rock exposed in the deeper stream valleys and on the steeper slopes is hard and resistant to erosion. The more gentle slopes and ridge tops are covered by a mantle of soft decomposed rock (saprolite) about 30 to 60 ft (10 to 18 m) in thickness, derived by prolonged weathering of the underlying crystalline rock. The surface of the Piedmont crystalline rock is irregular but dips generally eastward beneath the onlapping Coastal Plain strata.

The Coastal Plain deposits consist mainly of unlithified sand, silt, clay, and gravel that, except for compaction and dehydration, are little altered since deposition. The various formations range in age from late Early Cretaceous to Holocene. These strata commonly dip gently seaward, constituting an eastward-thickening clastic wedge overlying crystalline basement rock. Farther east and south, the thick sedimentary fill of the early Mesozoic Taylorsville basin intervenes between the Coastal Plain deposits and the crystalline basement.

Differential erosion along the contact between the hard Piedmont crystalline rocks and the much softer Coastal Plain strata commonly causes waterfalls or rapids to form in streams at, or slightly west of the contact between the two rock types. The Fall Line, a term applied to an imaginary line connecting the falls or rapids in successive streams crossing from the Piedmont into the Coastal Plain, is the upstream limit of navigability on major rivers and, consequently, the site of important colonial cities such as Richmond, Fredericksburg, and Washington. The Fall Line, or Fall Zone as it is sometimes called, trends northward from Richmond to Fredericksburg and northeastward from Fredericksburg to the District of Columbia.

THE THORNBURG SCARP

A low, highly dissected coastwise scarp near the inner edge of the Coastal Plain can be traced in the field and on topographic maps from the Richmond, Va., area northward through Henrico, Hanover, Caroline and Spotsylvania Counties to the city of Fredericksburg on the Rappahannock River (fig. 2). This feature was named the Thornburg scarp by Mixon (1978). At Fredericksburg, the scarp's northward trend changes fairly abruptly to the northeast. This segment of the scarp extends northeastward through Stafford and Prince William Counties into Fairfax County, Va., roughly parallelling on the northwest, the en echelon, high-angle reverse faults of the Stafford fault zone (fig. 2). The coastwise scarp's overall linear trend and its bounding relationship to the Pliocene Yorktown Formation to the east suggest that it is a marine shoreline cut by wave erosion during a period of high sea level associated with the maximum transgression during Yorktown deposition (see section on Yorktown Formation).

The north-trending segment of the scarp is well developed in the vicinity of Thornburg on U.S. Highway 1 in southeast Spotsylvania County. In this area and in northwestern Caroline County adjacent to the south, the altitude of the toe of the Thornburg scarp is typically about 265±5 ft (81±1.5 m) but ranges from about 255 to 270 ft (78-82 m). The scarp crest ranges from about 280 to 300 ft (86 to 92 m). The continuity of the scarp is interrupted at major transverse streams, such as the Motto, Matta, Po, Ni, and Rappahannock Rivers, where the scarp's break in topography turns up each stream and becomes gradually less distinguishable. This relationship indicates that major stream courses were well established by the middle Pliocene and that the streams were supplying much of the

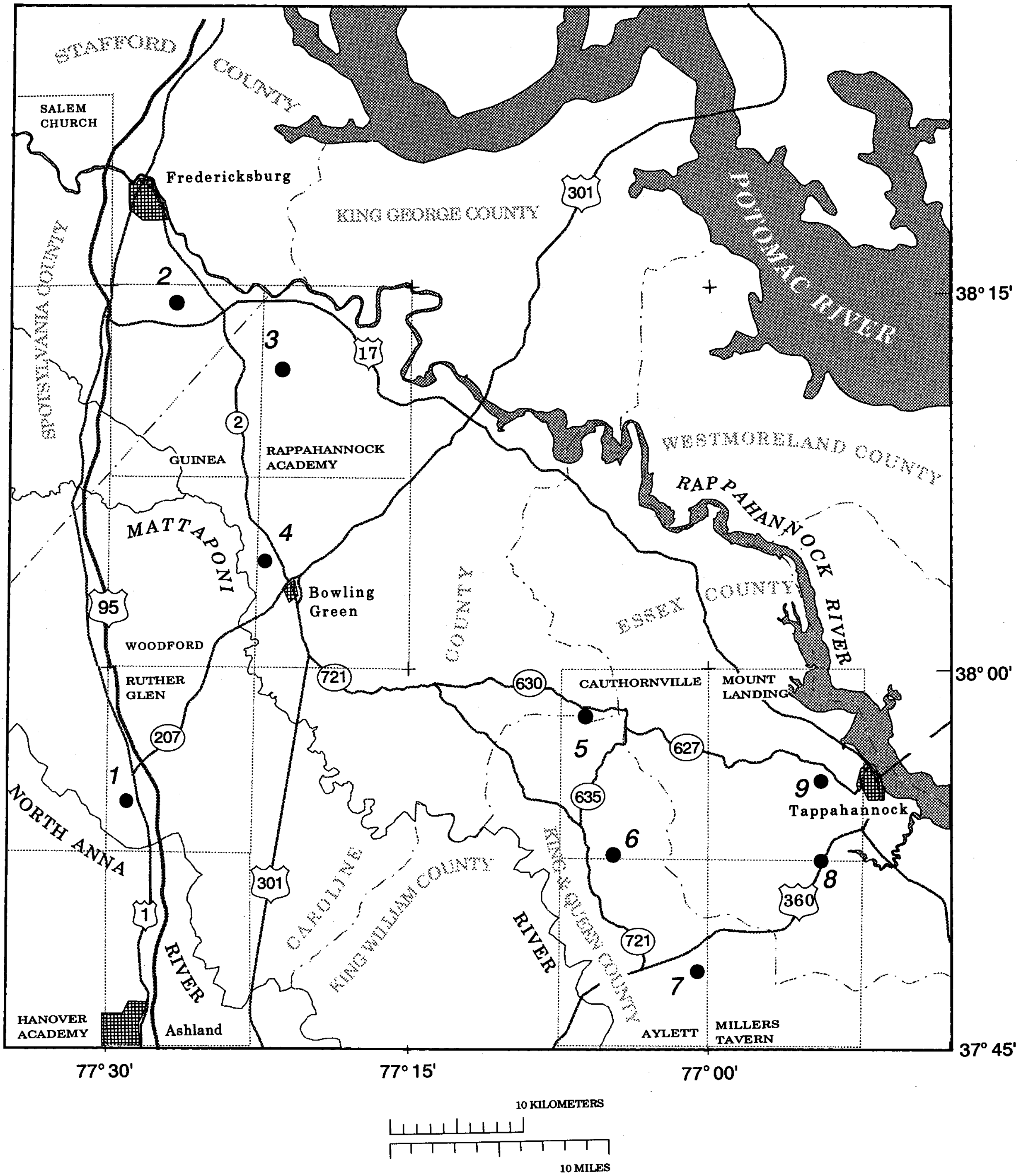

Figure 1.Map showing field trip area in northeastern Virginia and location of field trip stops. Dotted lines show areas of 7.5 minute quadrangles mentioned in text.

Table 1. Age, thickness, and generalized lithology of Cretaceous and Tertiary rock units in field trip area

Rock unit	Age	Thickness	Lithology
Bacons Castle Formation	Late Pliocene	0-45	Quartzose sand, gravel, clay, and silt, yellowish orange and reddish
Yorktown Formation	Early and early late Pliocene	0-85	Quartz and feldspar sand and gravel; shelly at base in downdip areas
Eastover Formation	Late Miocene	0-40	Fine shelly sand, silt, and clay; bluish gray
Bon Air gravel	Late middle to late Miocene	0-30	Fine to coarse sand, gravel; yellowish and reddish brown
St. Marys Formation	Late middle Miocene	0-30	Fine shelly sand; bluish and pinkish gray
Choptank and Calvert Formations	Early and middle Miocene	0-140	Fine sand, clay-silt; olive gray, diatomaceous
Nanjemoy Formation	Early Eocene	0-130	Shelly, glauconitic quartz sand; muddy, micaceous, greenish gray
Marlboro Clay	Paleocene	0-30	Kaolinitic clay-silt, red to gray
Aquia Formation	Paleocene	0-90	Shelly, glauconitic quartz sand; light to dark olive gray
Potomac Formation	Early Cretaceous	0->1400	Feldspathic sand, gravel, and illite-montmorillonite-kaolinite clay

sediment reworked by the transgressing Pliocene sea.

West of the Thornburg scarp is the very dissected Piedmont upland which has mostly V-shaped valleys and narrow interfluve areas ranging in altitude from about 290 ft (88 m) near the scarp to about 380 ft (116 m) along the higher Piedmont ridges to the west. The upland is underlain mainly by crystalline rocks and saprolite, but deeply weathered sand and gravel deposits of Miocene age are also present as thin caps on the higher interfluves. These capping sands and gravels of the Piedmont upland include a lower unit consisting of well-sorted fine sand of marine origin and an upper unit of coarse, poorly sorted, matrix-supported gravel and sand which we believe to be equivalent to the Bon Air gravel of Goodwin and Johnson (1970) in the Richmond area (Johnson and others, 1987; Berquist and Goodwin, 1989).

To the east of the Thornburg scarp, a topographically lower, somewhat less deeply dissected upland surface slopes gently seaward to its eastern edge at the Broad Rock scarp (fig. 2; Johnson and others, 1987). This upland's fairly flat, less eroded interfluve areas, ranging in altitude from 270 ft (82.3 m) at the toe of the Thornburg scarp to about 180 ft (55 m) at the Broad Rock scarp, are believed to closely approximate the original depositional surface of the Yorktown Formation (see discussion of the Yorktown in section on stratigraphy).

TERTIARY AND CRETACEOUS STRATIGRAPHY

BACONS CASTLE FORMATION (Tbc)

In that part of the field trip area lying east of the Broad Rock scarp (fig. 2), as much as 45 ft (14 m) of sand, gravel, silt, and clay of the Bacons Castle Formation caps the Coastal Plain uplands (Table 1). There, the Bacons Castle rests unconformably on middle Pliocene beds of the Yorktown Formation (fig. 3). The Bacons Castle thins westward to a feather edge at the Broad Rock scarp, which is believed to be the paleoshoreline formed during deposition of the formation. In our area, the Bacons Castle is very poorly exposed. Elsewhere, the lithology and sedimentary structures of the formation suggest deposition in braided-stream, tidal-flat, and tidal-channel environments (Ramsey, 1988). The Bacons Castle Formation has not yielded dateable fossils; however, its stratigraphic position above the Yorktown Formation suggests a late Pliocene age.

YORKTOWN FORMATION (Ty)

The Yorktown Formation was named by Clark and Miller (1906) for exposures of shelly sand and clay in cliffs along the York River near Yorktown in southeastern Virginia. There, the formation is 60 ft (18 m) thick and contains fossil assemblages indicating a shallow-shelf depositional environment. On the basis of well-exposed sections along the James, York, and Rappahannock Rivers in southeastern and central Virginia, Ward and Blackwelder (1980) redefined the Yorktown Formation and divided it into four members: a basal Sunken Meadow Member, and the overlying Rushmere, Mogarts Beach, and Moore House Members. Differences in the lithologies, fossil content, and geographic distributions of these members suggest deposition in three transgressive pulses. The Sunken Meadow Member, representing an early Pliocene transgression, is thin or absent in updip areas of the northern Virginia Coastal Plain. The Rushmere and Mogarts Beach Members, which represent the second (maximum) transgression during Yorktown deposition (Ward and Blackwelder, 1980; Ward and Strickland, 1985), extend westward to the Fall Line and, at least locally, lap onto crystalline rocks of the outermost Piedmont. The Moore House Member, representing a possible third transgressive pulse of minor extent overlies the Rushmere and Mogarts Beach Members but appears to be restricted to the outer Coastal Plain of southeastern Virginia and northern North Carolina. Except for the Rushmere (see Stop 7), the members have not been recognized in updip areas of northern Virginia where the Yorktown consists of poorly fossiliferous to nonfossiliferous, fine to coarse sand and sandy gravel deposited in various marginal-marine environments. In these areas, previous workers have extended usage of the Yorktown Formation to include both marginal-marine and fluvial-deltaic equivalents of the fossiliferous shallow-shelf deposits of central and southeast Virginia (see Stephenson and MacNeil, 1954; Newell and Rader, 1982; Johnson and others, 1987; Powars, 1987; Mixon and others, 1989; Pavich, Jacobson, and Newell, 1989). The Pliocene age of the Yorktown Formation is based on studies of planktonic foraminifers,

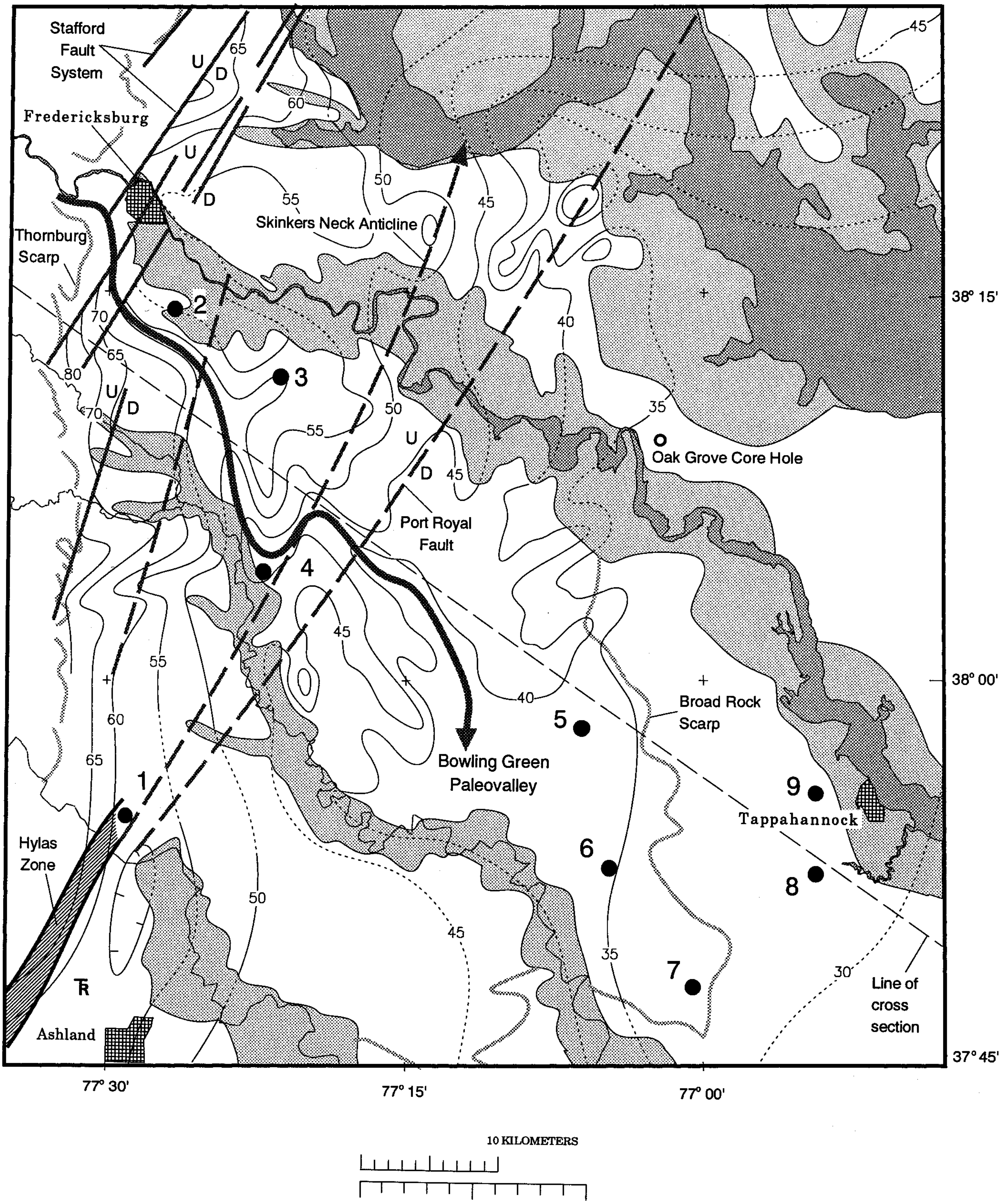

Figure 2.Map of trip area showing 5-m-contours on base of Yorktown Formation, trends of Thornburg and Broad Rock scarps, Stafford and Port Royal faults, and axis of Skinkers Neck anticline. Bowling Green paleovalley is an ancient course of Rappahannock River. Gray pattern along streams shows extent of Quaternary terrace deposits. TR locates area of early Mesozoic Taylorsville basin outcrop near Ashland, Va.

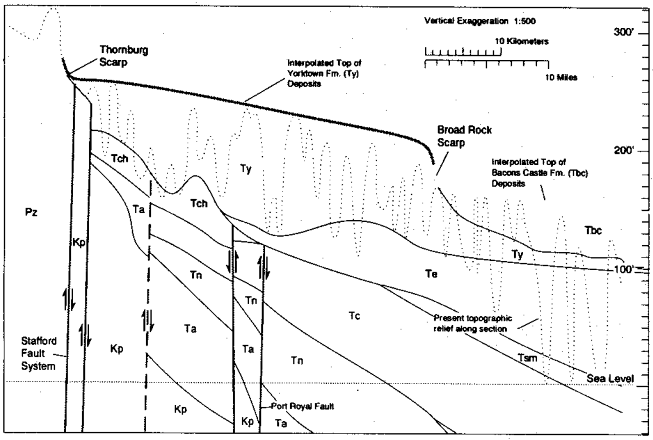

Figure 3.Generalized cross section of inner Coastal Plain showing distribution of Cretaceous and Tertiary rock units in relation to major faults and Thornburg and Broad Rock scarps. Line of section shown on figure 2. See text for unit symbols.

ostracodes, and nannofossils from shelf deposits in southeast Virginia and North Carolina (Akers, 1972; Gibson, 1983; Hazel, 1983; Cronin and others, 1984). These workers placed the Yorktown in foraminiferal zones N 18, N 19, and N 20 of early and early late Pliocene age. The most recent detailed study of the Virginia section (Dowsett and Wiggs, 1992) assigns the Yorktown to zones N 19-20.

Stratigraphic and geomorphic relationships

In the trip area, the Yorktown Formation is a sheet-like deposit of sand, gravel, silt, and clay that caps the uplands of the inner Coastal Plain. Our mapping shows that, from east to west across the trip area, these deposits unconformably overlie the Eastover Formation, the Choptank Formation, Bon Air gravel equivalents, and crystalline rocks of the Piedmont. Formation thickness ranges from about 80 ft (24 m) in the deeper lows on the pre-Yorktown erosion surface (fig. 2) to a feather edge at the north-trending Thornburg scarp (see also fig. 2 and Mixon, 1978). This coastwise scarp is believed to be a wave-cut paleoshoreline formed during a high stand of the sea associated with the maximum transgression during Yorktown deposition (Ward and Blackwelder, 1980; Dowsett and Cronin, 1990). Thus, the Thornburg scarp is the western, updip limit of marginal-marine and delta-plain deposits of the Yorktown Formation. Along the Broad Rock scarp in the eastern part of the map area (figs. 2, 3), the beds of the upper Yorktown are truncated by the Bacons Castle Formation of latest Pliocene age. East of the scarp, the Bacons Castle unconformably overlies the lower part of the Yorktown Formation.

Lithology

In our field trip area, the Yorktown Formation consists of thin- to very thick-bedded, fine to coarse quartz and feldspar sand and sandy gravel; minor amounts of clay and silt occur as thin- to thick beds interbedded with the coarser materials. Pebbles and cobbles are dominantly vein quartz and quartzite but include gneiss and schist derived from the Piedmont and basalt and red mudstone and sandstone from the early Mesozoic Culpeper basin. In the down-dip direction (eastern and southeastern parts of the trip area), sand of the Yorktown becomes more quartzose and is overall finer grained and better sorted. In these areas (Stops 6 and 7), the basal beds of the Yorktown contain some glauconite, sand- to pebble-sized phosphate and, locally, shell material. Because the Yorktown Formation consists of highly permeable materials, and because it caps the higher interfluve areas, the formation is commonly deeply oxidized to yellowish gray, yellowish orange, and reddish brown. Where fresh, the strata are light to dark gray or bluish gray.

Over much of the area, the base of the Yorktown Formation is marked by a pebbly lag ranging in thickness from less than a foot (0.3 m) to as much as 15 ft (4.6 m) in lows on the pre-Yorktown erosion surface (see Stops 3 and 5). These basal lag deposits commonly grade upward within a few feet into fine to coarse, massive to crossbedded sand characterized by sparse to very abundant *Ophiomorpha nodosa,* a clay-lined, noded burrow commonly filled with sand. These burrows are thought to be made by a marine crustacean similar to the present day mud shrimp, *Callianassa major*. The shrimp occurs in various marine environments--including barriers, backbarriers, and the nearshore sublittoral zone--wherever salinities and current energy are moderately high (Frey and others, 1978). In updip areas, crossbedded, pebbly sands containing *Ophiomorpha* commonly grade upward, or laterally, into alternating beds of fine sand, silt, and clay exhibiting flaser and lenticular bedding. These beds, believed to represent shoreface and intertidal deposits, form a distinctive, 5- to 15-ft-thick (2- to 5-m-thick) unit that can be mapped over wide areas of the northern Virginia Coastal Plain.

Bowling Green Paleovalley

Contours on the base of the Yorktown Formation in parts of six counties in northern Virginia show an irregular surface that dips generally eastward from altitudes of about 270 ft (82 m) at the toe of the Thornburg scarp to about 98 ft (30 m) near Tappahannock (fig. 2). In the western part of the trip area, the contours delineate a shallow, sinuous, 3.6-mi-wide (6-km-wide) paleotopographic low incised about 33 to 50 ft (10 to 15 m) below the general level of the pre-Yorktown erosion surface (see fig. 2). This feature, which intersects the present-day Rappahannock River valley at the edge of the Piedmont near Embrey Hill just west of Fredericksburg, is believed to be a Rappahannock River paleovalley of early(?) Pliocene age. From Embrey Hill, the paleovalley trends southeastward through the Guinea quadrangle to the vicinity of Bowling Green. Just northwest of Bowling Green, the paleovalley veers abruptly to the northeast before resuming a southeasterly course through the eastern Bowling Green and Supply quadrangle areas. The northeastward deflection of the paleovalley mimics the deflection of the present-day Rappahannock River at Skinkers Neck, suggesting that the abrupt change in direction of both the modern and ancient river courses may be influenced by the Skinkers Neck anticline (fig. 2).

Outcrops along the upper part of the paleovalley in the Salem Church, Spotsylvania, and Guinea quadrangle areas show that the valley fill is mainly medium to coarse gravelly sand and pebble and cobble gravel of fluvial origin (see Stop 2 description). Some of the better exposures of fluvial deposits are in the high cuts for the Richmond, Fredericksburg, and Potomac Railroad about one mile north of Summit (see Guinea quadrangle) where the railroad crosses the area of the paleovalley fill. There, the railroad cuts show large-scale trough crossbedding in coarse sand and gravels that fill a series of channels up to 65 ft (20 m) or more in width. These fluvial channel fills appear to grade upward and laterally into a large fluvial-deltaic complex that constitutes the surficial deposits of the inner Coastal Plain in a multi-county area east and south of Fredericksburg.

EASTOVER FORMATION (Te)

In the study area, the Eastover Formation is mainly very fine to fine sand that is variably silty and clayey and thick- to very thick-bedded or massive. Where fresh, the Eastover beds are dark gray to bluish gray and greenish gray; weathered outcrops are yellowish gray, greenish yellow, and yellowish brown. A fairly diverse molluscan assemblage is dominated by the gastropod *Turritella plebia* and large bivalves including *Isognomon, Dallarca, Ostrea compressirostra, Chesapecten middlesexensis, Placopecten principoides*, and *Mercenaria*. The bivalve *"Spisula" rappahannockensis* was dominant in environments characterized by quiet, shallow waters and muddy substrates (Ward, 1992).

In downdip areas (Essex County), where the Eastover is thicker and more typically developed, beds of medium-grained, crossbedded sand occur in the upper part of the Eastover, suggesting upward-shoaling waters. In central Essex County (Stops 8 and 9), the upper Eastover includes a 15- to 20-ft-thick (5- to 6-m-thick) unit consisting of alternating, thin to very thin beds of sand and clay. Bedding types include lenticular bedding exhibiting both connected and isolated sand lenses.

From east to west, the Eastover beds successively overlie the St. Marys, Calvert, and Choptank Formations and lap onto crystalline rocks of the outermost Piedmont and red beds of the early Mesozoic Taylorsville basin. In the updip direction in Caroline County, the Eastover is sharply truncated by the Yorktown beds along the crest of the Skinkers Neck structural high and is absent to the west of the high.

ST. MARYS FORMATION (Tsm)

The St. Marys Formation consists of bluish- to pinkish gray, muddy, very fine sand and sandy clay-silt that is locally abundantly shelly (Newell and Rader, 1982; Ward and Krafft, 1984; Mixon and others, 1989a). The formation is 31 ft (9.5 m) thick in a core hole at Essex Millpond on Mill Creek, about four miles (6.5 km) south-southeast of Tappahannock, Va. at the eastern edge of the trip area (W.L. Newell, USGS, unpublished data). At this locality, the diverse well-preserved molluscan assemblage indicates deposition in shallow-shelf waters of normal salinity and suggests warm-temperate to subtropical climatic conditions (Ward, 1992). The presence of the large bivalve *Chesapecten santamaria* in the mill-race exposures at Essex Millpond clearly indicates correlation with the upper part of the St. Marys Formation (Windmill Point beds of Blackwelder and Ward, 1976) in its type area along the St. Marys River in St. Marys County, Md. The St. Marys Formation has been considered to be late middle Miocene and (or) early late Miocene in age (Gibson, 1983). The beds at Essex Millpond have yielded a small planktonic foraminiferal assemblage indicative of foraminiferal zone N 16, supporting an early late Miocene age for the upper part of the St. Marys.

CALVERT AND CHOPTANK FORMATIONS (Tc, Tch)

These formations are lithically rather similar; thus, poorly exposed, isolated outcrops of these units are difficult to differentiate. Both formations consist of fine to very fine quartzose sand and diatomaceous clayey silt and silty clay. The sandy sediments are poorly sorted to well sorted and are commonly thick-bedded or massive. Locally, both formations contain abundant molds and casts of marine mollusks and poorly to well preserved diatom floras.

A single section of the diatomaceous beds commonly contains one to several sand-silt-clay sequences ranging in thickness from about 6 to 40 ft (2 to 12 m). The coarser, lower part of each sequence consists of very fine to fine sand containing scattered fine to medium pebbles of quartz and phosphate, bones and teeth of marine vertebrates, and rare shell fragments. The basal sands grade upward into sandy clay-silt containing diatoms and sparse sponge spicules; the clay-silt commonly grades upward into very fine, massive sand.

Diatom zonations by Abbott (1978) and Andrews (1988) indicate equivalence of the lower and middle parts of the diatomaceous section in the field trip area to the Plum Point Marl and Calvert Beach Members of the Calvert Formation in Maryland; in Virginia, these beds are as much as 100 ft (30.5 m) thick. The upper part of the section, as much as 40 ft (12 m) thick in the structural low between the Stafford and Skinkers Neck faults, is considered to be equivalent to the Choptank Formation.

The thick-bedded to massive, poorly sorted clay-silt and clayey and silty fine sand of the Calvert and Choptank Formations suggest deposition in low-energy, fairly deep water environments well below wave base. Cross-stratification is commonly absent, but a few cross-laminated beds indicate weak bottom currents. The Calvert and Choptank beds in the trip area are mainly of middle Miocene age (foraminiferal zones N 10-11).

AQUIA AND NANJEMOY FORMATIONS (PAMUNKEY GROUP) (Ta, Tn)

In their type areas along the Potomac River northeast of Fredericksburg, Va., the Aquia and Nanjemoy Formations consist of abundantly fossiliferous, dark-gray to greenish-gray, thick-bedded or massive glauconitic quartz sand interbedded with a few thin to thick beds of sandy and shelly limestone (Ward, 1985). There, the Aquia and Nanjemoy Formations are, respectively, as much as 90 ft (28 m) and 130 ft (40 m) thick. Thus, the 5- to 6-ft-thick sections of Aquia and Nanjemoy that crop out in the walls of the Caroline Stone Company quarry (fig. 6, Stop 1) in southwestern Caroline County are only very thin, truncated remnants of these formations. The successive westward onlap of the Aquia, Nanjemoy, Choptank, and Eastover beds onto the Hylas zone cataclastic rocks, as observed in exposures in the Caroline Stone Company quarry walls, and similar onlapping relationships indicated by USGS core holes in the Woodford quadrangle area (fig. 1) help define a crystalline basement high on the northwest side of the early Mesozoic Taylorsville basin (Weems, 1980).

POTOMAC FORMATION (Kp)

In much of the trip area, the crystalline basement is overlain by thick fluvial-deltaic deposits of the Lower Cretaceous Potomac Formation. Along the outcrop belt, which trends southward through Fredericksburg and eastern Spotsylvania County, the Potomac consists mainly of gray- to greenish-gray, medium- to very coarse-grained feldspathic sand, gravelly in part. The sand is generally trough crossbedded and is interbedded with smaller amounts of gray or grayish-green, sandy silt and clay, commonly mottled red. The uppermost part of the Potomac locally includes pale-gray to white, moderately well-sorted sand characterized by gently inclined crossbeds and laminae of black heavy minerals.

The Potomac Formation thickens from a feather edge in outcrop just west of the Fall Line to more than 1400 ft (426 m) in the subsurface in the vicinity of the Oak Grove core hole at the eastern edge of the field trip area (fig. 1). The unconformable surfaces at the base and top of the Potomac, easily recognized in boreholes and in outcrop, provide the extensive mapping horizons used to define the Stafford fault zone, the Skinkers Neck anticline, and the Port Royal fault (figs. 3, 4). Through much of this region, porous and permeable sandy units in the Potomac Formation are a major source of water for municipalities and institutional and industrial users.

Analyses of diverse palynomorph assemblages indicate that the Potomac Formation in northern Virginia is of Barremian, Aptian, and Albian age.

COASTAL PLAIN STRUCTURE

Our surface and subsurface mapping delineates three main structures, including faults and low-amplitude folds, that deform the Coastal Plain strata in northern Virginia. Early studies (Mixon and Newell, 1977, 1982) recognized and described the Stafford fault system, which is adjacent on the west and northwest of the field trip area (figs. 2, 3). The Stafford system is a series of en echelon, northeast-striking, northwest-dipping, high-angle reverse faults that displace both the Paleozoic crystalline rocks of the Piedmont and the overlying Coastal Plain formations of late Mesozoic and Cenozoic age. The fault zone is known to extend for more than 30 mi (50 km) along the Fall Line and the northeast-trending reach of the Potomac River; its position supports the belief that the long, northeastward-arcing segment of the Fall Line in northern Virginia and Maryland and major river deflections along it have been tectonically influenced (Mixon and Newell, 1977).

Our more recent investigations (Mixon and Powars, 1984; Powars, 1987; Mixon, Powars, and Daniels, 1992) have focused on mapping the eastern part of the Fredericksburg, Va.-Md., 30 x 60 minute quadrangle at 1:100,000-scale. This area is of great interest tectonically because it straddles the trace of the early Mesozoic Taylorsville basin border faults (Weems, 1980, 1981) as projected from the outermost Piedmont northeastward beneath the Coastal Plain cover rock. Additionally, the outcrop belt of the Hylas cataclastic rocks in the Piedmont (see Stop 1), which mark a major zone of late Paleozoic ductile shearing and thrusting along the west sides of the Richmond and Taylorsville basins, project northeastward in the subsurface along the western edge of the buried Taylorsville basin. Our surface and subsurface mapping along these old structural discontinuities shows that the regional eastward dip of the overlying Cretacoeus and Tertiary strata is interrupted at Skinker's Neck on the Rappahannock River by a long, linear, northeast-trending anticlinal fold (figs. 4, 5).

The fold, named the Skinkers Neck anticline by Mixon, Powars, and Daniels (1992), extends from the Bowling Green area north-northeastward for about 25 mi (40 km) to the vicinity of Fairview Beach on the Potomac River (fig. 4). Our structure contour and isopach maps for Cretaceous and Tertiary mapping horizons define a 3- to 5-mi-wide (5- to 8-km-wide), low-amplitude, anticlinal fold that appears to be faulted along its northwest side (fig. 5). The axis of the gently northeast-plunging fold crosses the Rappahannock River at Skinkers Neck, a land area bounded on three sides by a large, northward-projecting meander bend of the river (see fig. 4). The anticlinal axis closely parallels the western edge of the buried Taylorsville basin; this relationship strongly suggests reactivation of the Taylorsville basin border faults and (or) the zone of westward thrusting represented by the Hylas cataclastic rocks.

A northwest-southeast cross section east of Stop 4 at Bowling Green shows stratigraphic and structural relationships across the Skinkers Neck anticline and the Port Royal fault, a zone of low-displacement faulting and monoclinal folding farther downdip (figs. 4, 5). Control for the cross section consists of continuous cores and geophysical logs from four USGS coreholes and two water wells. The fault along the northwest side of the Skinkers Neck anticline is interpreted as a southeast-dipping, high-angle reverse fault (Mixon, Powars, and Daniels, 1992). Across the fault, vertical separation of the unconformable contact between the Lower Cretaceous Potomac Formation and the overlying upper Paleocene Aquia Formation is about 50 ft (15 m), whereas vertical separation of the basal beds of the lower Eocene Nanjemoy Formation is only about half as much. These relations and the absence of the Marlboro Clay (fig. 5) on the upthrown side of the fault suggest an episode of faulting, uplift, and erosion after deposition of the Aquia and prior to deposition of the Nanjemoy. Post-Nanjemoy faulting and uplift are also indicated but the amount of deformation is partly obscured by extensive erosion of the Nanjemoy prior to deposition of the Miocene Calvert Formation. Slight uplift and minor fault offset of the Calvert and Choptank Formations are inferred because of dip reversals (west dip) mapped in these units in King George County (Powars, 1987). Available drill data are not sufficient to show presence or absence of small-scale faulting that may affect the upper Miocene Eastover Formation and the Pliocene Yorktown Formation. The cross section and isopach map (figs. 4, 5) show marked thinning of the Aquia and Nanjemoy beds from southeast to northwest over the crest of the anticline. Thicker sections of these units and of the Calvert and Choptank Formations are preserved in the structural low to the northwest of the anticline. To the southeast, the relative down-to-the-coast displacement of Cretaceous and Tertiary beds along the Port Royal fault causes abrupt thickening of the Coastal Plain section.

In contrast, the overlying Eastover Formation thins to the northwest and appears to be absent west of the Skinkers Neck anticline. The rapid thinning of the Eastover and its absence in updip areas in northern Virginia is partly because of relative uplift of the Coast Plain strata to the northwest of the Port Royal fault and, in part, because of strong truncation by the Yorktown Formation.

STOP DESCRIPTIONS

STOP 1. CAROLINE STONE COMPANY QUARRY ON LONG CREEK, SOUTHWESTERN CAROLINE COUNTY, RUTHER GLEN 7.5-MIN. QUADRANGLE

Hylas mylonite zone and Taylorsville basin

The Caroline Stone Company quarry is near the edge of the Coastal Plain in southwestern Caroline County about 1.1 mi (2 km) northwest of the U.S. Route 1 bridge over the North Anna River. There, cataclastic rocks of the Hylas mylonite zone are being quarried to produce crushed stone. The northeast-trending Hylas zone, which is about 2 mi (3.2 km) wide in this area, borders the northwest side of the early Mesozoic Taylorsville and Richmond basins. This belt of highly sheared and jointed rocks, including mylonite, ultramylonite, protomylonite, and mylonite gneiss, is believed to mark a major, east-dipping thrust fault in the basement rocks. The zone of late Paleozoic thrusting and the early Mesozoic border fault of the Taylorsville basin (Weems, 1980, 1981) project northeastward beneath Coastal Plain deposits in the Ruther Glen, Bowling Green, and Rappahannock Academy quadrangle areas. Our mapping of the Coastal Plain formations (Mixon and Powars, 1984, and Mixon, Powars, and Daniels, 1992) in these areas has identified Cretaceous and Tertiary structures, including the Skinkers Neck anticline and related faults (fig. 5) that are superposed on the western border fault of the Taylorsville basin and the projection of the Hylas zone. These relationships indicate continued release of compressional stress along the Hylas zone and (or) reactivation and reversal of movement on the extensional faults of the early Mesozoic basins.

Coastal Plain stratigraphic section

The more than 40 ft of Coastal Plain strata that are exposed in

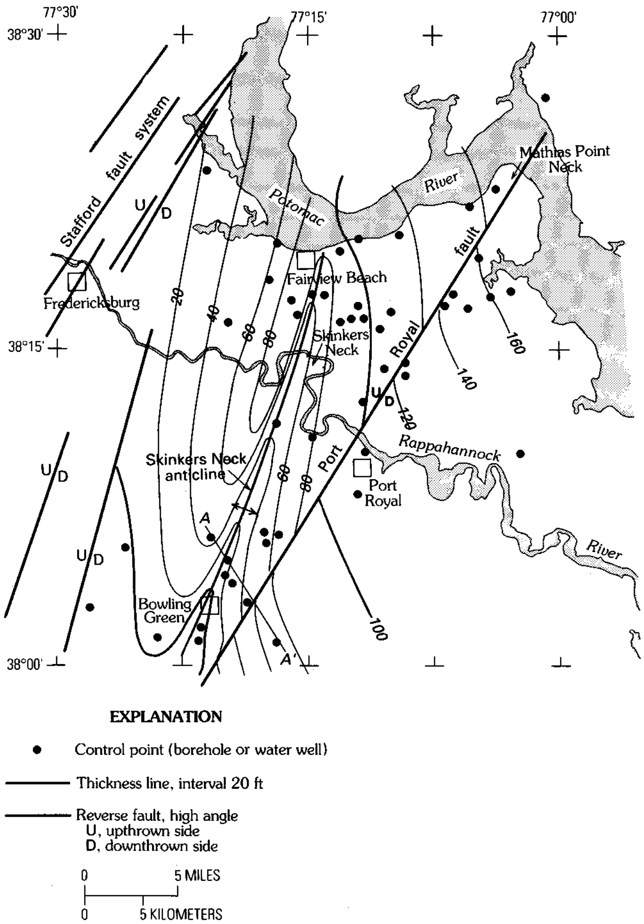

Figure 4. Isopachs of lower Eocene Nanjemoy Formation showing thinning of unit across Skinkers Neck anticline and abrupt thickening on east side of Port Royal fault. After Mixon, Powars, and Daniels (1992).

the quarry walls above the crystalline Piedmont rocks include the thin, truncated remnants of five marine formations and the lowermost, marginal-marine part of the Yorktown Formation (fig. 6). Both marginal-marine and fluvial-deltaic components of the Yorktown are present in the quarry area and constitute the surficial formation. The marine formations, consisting of the lower part of the Aquia Formation, the upper member of the Nanjemoy Formation, a 3-ft-thick (1-m-thick) remnant of the Calvert Formation, and the Choptank and Eastover Formations have been described by Marr and Ward (1987, 1993). A small, gullied embankment at the west end of the quarry exposes the Eastover Formation and the overlying *Ophiomorpha* beds of the Yorktown.

In the quarry the upper surface of the crystalline rock is very uneven. Thus, locally in the quarry, the erosional highs on the crystalline rock are directly overlain, successively, by the Aquia, Nanjemoy, Calvert and Choptank, and Eastover Formations. Altitudes of formational contacts obtained by levelling indicate that in the quarry area the Coastal Plain formations dip gently westward (G.H. Johnson, oral communication, 1993). This suggests uplift and tilting of the relatively upthrown block adjacent on the northwest of the Fork Church fault, which has been mapped along the northwest side of the Taylorsville basin by Rob Weems (1980).

STOP 2. FLUVIAL-DELTAIC SAND AND GRAVEL DEPOSITS, YORKTOWN FORMATION, K.R. BEVERLY OFFICE PARK, GUINEA 7.5 MIN. QUADRANGLE

At the K.R. Beverly Company office park, silty clay and clayey fine sand of the Choptank Formation of middle Miocene age constitute the lower 20 ft (6 m) of section exposed in the long, steep embankment at the east side of the park (fig. 6, Stop 2). These strata are assigned to the Choptank on the basis of marine diatom assemblages in samples from nearby outcrops and core holes (George Andrews, written communications, 1983-1985). The upper 26 ft (8 m) of the exposed section are fine to very coarse gravelly sand of the lower part of the Yorktown Formation, which overlies the Choptank beds with marked erosional unconformity. The upper Miocene Eastover Formation is absent by truncation at this locality and elsewhere on the northwest side of the Skinkers Neck anticline (figs. 4, 5).

Our map showing the configuration of the base of the Yorktown Formation (fig. 2) indicates that the Yorktown section at Stop 2 is on the northeast flank of the Rappahannock River paleovalley. Laterally, the coarse, poorly sorted sediments constituting the paleovalley fill disconformably underlie or intertongue with better sorted and generally finer grained sand, silt, and clay deposited in very nearshore shelf and intertidal environments. These marginal-marine deposits are well exposed at Stops 3 and 4.

STOP 3. MARGINAL-MARINE DEPOSITS OF THE LOWER PART OF THE YORKTOWN FORMATION, WARE CREEK BORROW PIT, FORT A.P. HILL, RAPPAHANNOCK ACADEMY 7.5-MIN. QUADRANGLE

The Ware Creek borrow pit is 5.4 mi (9 km) southeast of Stop 2 and about 1.2 mi (2 km) northeast of the Bowling Green paleovalley (fig. 2). As at Stop 2, the Yorktown beds unconformably overlie fine to very fine marine shelf sand of the Choptank Formation (fig. 6). Here, however, a greater thickness of the Choptank is preserved because the locality is in a broad structural low bordered on the west by northeast-trending, high-angle reverse faults and on the east by the Skinkers Neck anticline (fig. 2).

In the Stop 3 area, the lowermost Yorktown beds are overall finer grained and better sorted than at Stop 2. A lag of fine to coarse pebbly sand marks the base of the Yorktown; maximum pebble size is about 1.5 in (4 cm) in long dimension. Sand-filled burrows extend downward from the basal Yorktown, penetrating the Choptank to a depth of 1.5 ft (0.5 m). The burrowed basal contact, clay drapes and clay-filled ripple troughs, heavy-mineral laminae, and large, clay-lined *Ophiomorpha* (exposed when the pit was active) suggest deposition in a shallow-water, marginal-marine environment. The overlying coarse sand and sandy cobble gravel exposed in the upper part of the pit are part of the sheet of fluvial-deltaic deposits that prograded eastward over the shelf during the regressive phase of the Yorktown.

STOP 4. INTERTIDAL TO SUBTIDAL DEPOSITS OF THE LOWER PART OF THE YORKTOWN FORMATION, ROUTE 605 ROAD CUT, NORTHWEST BOWLING GREEN

The 20 ft (6 m) of sand and gravel exposed in the roadcut probably represent the upper beds of the lower part of the Yorktown in this area (fig. 6). Near the base of the cut is a poorly exposed gravel bed consisting mainly of pebbles of vein quartz and quartzite

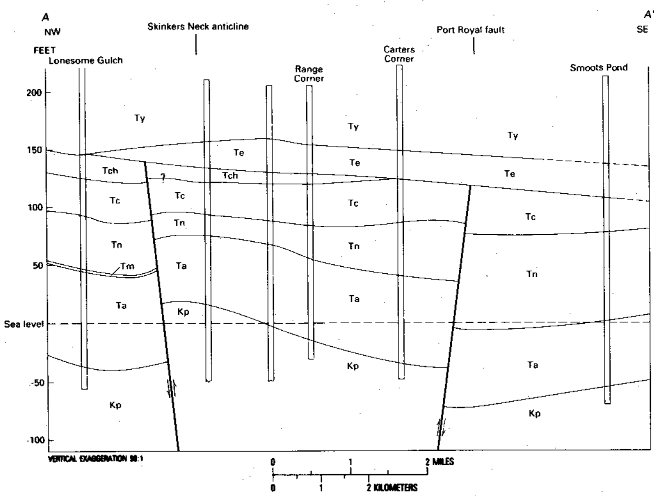

Figure 5.Geologic cross section of the Skinker's Neck anticline and Port Royal fault, Bowling Green area, Caroline County, Virginia. Location of section is shown in figure 4. See text for unit symbols.

and cobble-sized clasts of silty clay that weather to dark red. Above the gravel bed are about 10 ft (3 m) of planar- and trough-crossbedded, fine to medium sand containing abundant, large, clay-lined, sand-filled *Ophiomorpha nodosa*. Minor amounts of clay-silt are present as clay drapes on crossbeds and as isolated, clay-filled ripple troughs (simple flaser bedding). These sedimentary structures, in combination with *Ophiomorpha*, suggest deposition in shallow, tidally influenced waters. Rhythmic sand/mud bedding typical of tidal flats (including lenticular and flaser bedding of several types) is better developed at this horizon at nearby localities. For many years, the landfill at Taylor's Corner on the Fort A.P. Hill Military Reservation, which is now covered and sealed, provided exceptionally good exposures of intertidal deposits (Rappahannock Academy 7.5 min. quadrangle).

A 5-ft-thick (1.5-m-thick) section of gravelly sand at the top of the highway cut exhibits very long (15 ft (4.6 m)) and very gently inclined crossbeds emphasized by white quartz pebbles and small cobbles strung out along bedding planes. Clasts include a few pebbles and cobbles of silty clay. The gravelly sand unit appears to fill a very shallow channel and suggests higher energy currents than do the underlying *Ophiomorpha* beds.

STOP 5. LOWER AND MIDDLE PARTS OF THE YORKTOWN FORMATION AT TIGNOR, SOUTHEASTERNCAROLINE COUNTY, CAUTHORNVILLE 7.5-MIN. QUADRANGLE

Stop 5 is at low roadcuts along Route 624 just south of the community of Tignor and about 15 mi (24 km) east-southeast and downdip from Stop 4 at Bowling Green. This long, continuous section (fig. 6) provides a useful tie point between the largely nonfossiliferous marginal-marine and fluvial-deltaic deposits of updip areas and the fossiliferous shelf sands of the Yorktown that crop out in King and Queen County, Va., several miles to the southeast of Tignor (see Stop 7, this guidebook). In contrast with the generally upward-coarsening sequences of updip areas (Stafford, King George, and Spotsylvania Counties, and northwestern Caroline County), the Yorktown at Tignor includes three upward-fining sequences; each of the upper two sequences appears to be overall finer grained than the one below.

Near the bottom of the long hill on Route 624 just south of Tignor, road cuts expose a few feet of well sorted, fine to very fine, micaceous sand of the upper part of the Eastover Formation. The unconformable contact between the Eastover and the Yorktown is not well exposed. The lower 24 feet of the Yorktown consists mostly of poorly sorted, fine to very coarse, gravelly sand that grades upward to somewhat better sorted, fine- to medium sand containing abundant *Ophiomorpha*. This basal, upward-fining unit (alt. 132-156 ft) appears to be equivalent to glauconitic sands of the lower part of the Yorktown that were encountered by augering during the mapping of the Supply 7.5-min. quadrangle (R.E. Weems, USGS, personal communication, 1991). (The Supply quadrangle is adjacent to the east of the Bowling Green quadrangle and diagonally northwest of the Cauthornville quadrangle).

At Tignor, the gravelly sands and *Ophiomorpha* beds of the lower part of the Yorktown are abruptly overlain by a second, thinner, upward-fining sequence (alt. 156-164 ft). The 3-ft-thick (1-m-thick) basal lag is mostly medium- to very-coarse sand with abundant very fine to fine pebbles of quartz; chert is present but uncommon. This pebbly coarse sand grades upward into about 5 ft (1.5 m) of clayey and silty, very fine sand.

The highest upward-fining sequence (alt. 164-180 ft) is similar to the underlying unit, but it also includes a small channel filled with alternating, thin- to very thin beds of fine sand and clay-silt. The left side of the channel is cut into ripple-bedded, fine-grained, quartz and black heavy mineral sands that include a few clay flasers at the top. The lithology and sedimentary structures in these beds suggest deposition in a tidally influenced, marginal-marine environment.

STOP 6. LOWER PART OF THE YORKTOWN FORMATION, BORROW PIT ON ROUTE 660 KING AND QUEEN COUNTY, CAUTHORNVILLE 7.5-MIN. QUADRANGLE

The Yorktown outcrops at Stop 6 are 6.4 mi (10.2 km) south-southeast and downdip from the Tignor, Va., section (Stop 5). Here, as at Tignor and Bowling Green (Stop 4), the lower part of the Yorktown includes sandy strata containing abundant large, clay-lined *Ophiomorpha nodosa* (fig. 6). These strata, exposed for a few feet above the pit floor at altitudes of about 130-135 ft (39.6-41.1 m), are believed to be roughly equivalent to the *Ophiomorpha* beds at Tignor at altitudes of 147-156 ft (44.8-47.5 m). Here and at Tignor, the *Ophiomorpha* beds are overlain by thin, gravelly sands at the base of an overlying upward-fining sequence. At this locality, however, a few "ghosts" of convex-upward and concave-upward, disarticulated valves of large mollusks occur in the lower part of the gravelly sand.

The most conspicuous feature of the Yorktown section at this locality are the numerous hard ledges of sand and gravel cemented with hydrated iron oxides (limonite-goethite). The degree and extent of cementation suggests that the unaltered Yorktown sediments contained appreciable amounts of iron minerals such as ilmenite and magnetite.

STOP 7. EASTOVER AND YORKTOWN FORMATIONS, FLEETS MILLPOND, KING AND QUEEN COUNTY, AYLETT 7.5-MIN. QUADRANGLE

Outcrops along the steep wall of the old millrace at Fleets Millpond show about 5 ft (1.5 m) of very shelly sand of the lowermost Yorktown unconformably overlying about 10 ft (3 m) of bluish-gray, clayey and silty fine sand of the Eastover Formation (fig. 7). The Eastover beds contain molds of the small bivalve *Spisula rappahannockensis*, an Eastover guide fossil. The Yorktown molluscan assemblage includes at least 15 species; some of the more common taxa are *Mercenaria* sp., *Chesapecten madisonius*, *Chesapecten jeffersonius* ("transitional" form), *Crassatella* sp., and a large high-spired gastropod, *Turritella pillsburyi*. *Chama congregata* has also been reported from this locality and from two nearby localities in the Millers Tavern quadrangle (fig. 1; see also Stephenson and MacNeil, 1954). The fossil assemblage in the lower part of the Yorktown at this locality suggests deposition in shallow, nearshore-shelf waters of normal salinity. The molluscan taxa suggest correlation with the Rushmere Member of the Yorktown Formation (L.W. Ward, oral communication, 1993).

STOP 8. UPPER PART OF THE EASTOVER AND LOWERMOST YORKTOWN FORMATIONS, U.S. ROUTE 360 ROADCUT, ESSEX COUNTY, MILLERS TAVERN QUADRANGLE

Three distinctive lithic units are present in the 30-ft-thick (9-m-thick) roadcut section exposed at Stop 8. The lower unit, which consists of ten feet (3 m) of clayey and silty, very fine gray sand containing sparse molds of small mollusks, is only the uppermost part of a fairly thick sequence of shallow-shelf deposits constituting the lower and middle part of the Eastover Formation in this area (see Stop 9 for a more complete Eastover section).

The middle lithic unit consists of about 14 ft (4 m) of rhythmically bedded clay, silt, and fine to medium sand characterized by wavy and lenticular bedding. Sands at the irregular base of the unit fill large, conspicuous burrows to a depth of four to five feet (1-2 m) into the underlying fine shelf sands of the Eastover, suggesting the possibility of a break in deposition between the two units. Crossbedded sand forming a small sandbar or sand wave 3-4 ft (1 m) in thickness suggests relatively high-energy currents. The middle unit is commonly believed to be a regressive phase of the Eastover Formation (Ward and Blackwelder, 1980, fig. 11; Newell and Rader, 1982, Stop 6). As an alternative, the rhythmically bedded muds and sands of the middle unit might be interpreted as a back-barrier facies of the Rushmere Member of the Yorktown, which represents the maximum transgression during Yorktown deposition. The unconformity at the base of the upper lithic unit would then be interpreted as a ravinement surface separating backbarrier deposits from the overlying basal gravel of shelf sands of the Rushmere. Another, much less likely possibility is that the alternating sands and muds of the middle unit represent an updip, backbarrier or restricted shelf facies of the basal Sunken Meadow Member of the Yorktown.

The upper lithic unit is the basal part of the Yorktown Formation. It consists of 6 to 8 ft (2-2.5 m) of very poorly sorted pebbly sand above the irregular erosion surface at the top of the middle unit. Pebbles of phosphate, fish teeth, and scattered molds of *Chesapecten* sp. and other mollusks indicate a marine lag deposit.

STOP 9. EASTOVER FORMATION, ROUTE 618 ROAD CUTS AT HOSKINS CREEK, WEST OF TAPPAHANNOCK, VA, MOUNT LANDING 7.5 MIN. QUADRANGLE

The long roadcut along Route 618 on the southwest side of Hoskins Creek exposes most of the Eastover Formation and the uppermost part of the underlying St. Marys Formation (Newell and Rader, 1982). At this locality, the lower and middle part of the Eastover includes a basal fine silty sand and, above a concealed interval, a thick unit of medium- to dark gray silty clay and clayey silt that coarsens upward to clayey and silty very fine sand (fig. 7). Some beds are intensely bioturbated. These muddy shelf deposits contain scattered molds and casts of mollusks, including the high-spired gastropod *Turritella* sp. and the small bivalve *"Spisula" rappahannockensis*, an Eastover Formation guide fossil. The upper part of the Eastover section consists of alternating thin beds and laminae of fine sand and clay-silt.

The predominance of horizontally bedded, fine-grained sediment (clay, silt, very fine sand) in the lower part of the Eastover and the low species diversity of the molluscan assemblage suggest deposition in a fairly low energy, restricted basin on the inner shelf. The rhythmic sand/clay bedding in the upper part of the Eastover suggests upward-shoaling waters affected by tidal currents.

A low roadcut near the foot of the hill, now partially overgrown with small trees and bushes, exposes the basal silty sand of the Eastover Formation and the unconformable contact with pinkish weathering, very clayey fine sand of the underlying St. Marys Formation. The unconformity is marked by a thin pebble lag of quartz, chert, and phosphate. Maximum pebble size is as much as 2 in (5 cm) in long dimension.

TRIP ROUTE

Mileage

0.0 Trip begins in Williamsburg, Va., at 7:30 a.m. at front entrance of Fort Magruder Inn. From Williamsburg, drive westward on Interstate 64 (I-64) about 35 mi to junction with I-295 Bypass around Richmond. Bear right at exit ramp onto I-295 and continue northwest for 20 mi to junction with I-95 north.

55.5 Bear right onto I-95 north. Continue northward about 14.5 mi and take exit to Va. Route 30 at Kings Dominion amusement park.

70.0 Turn left onto Va. 30 and go west a short distance to intersection with U.S. 1. Turn right onto U.S. 1 and go northward past Doswell, crossing the North Anna River.

74.0 At 0.5 mi north of U.S. 1 bridge over North Anna River, turn left onto gravel access road to Caroline Stone Company quarry. To enter the quarry, visitors must stop at the office and obtain permission from the manager.
STOP 1, Caroline Stone quarry. We will examine outcrops in an embankment on right-hand side of road at western end of quarry. Area on left-hand side of road (quarry side) is extremely dangerous because extensive fracturing of quarry walls makes large slumps likely. **Please do not go into area between road and quarry.**
Road log resumes at junction of quarry access road and U.S. 1. Proceed north on U.S. 1 about 26 mi to traffic signal at intersection with U.S. 17 Bypass on the south side of Fredericksburg.

100.0 Turn right onto U.S. 17 Bypass and go east for 3.0 mi to intersection with Va. 608, turn left onto Va. 608 for 0.1 mi, turn left onto Va. 635 and go 0.4 mi to right-hand turn into small office park.

103.5 **STOP 2, K.R. Beverly office park.** Fluvial sands and gravels are exposed in the high embankment along east side of office park. At end of discussion, we retrace our route for 0.5 mi to U.S. 17 Bypass.

104.0 At intersection of Va. 608 and U.S. 17 Bypass, turn left onto U.S. 17 Bypass and continue eastward 2.7 mi to traffic signal at intersection at New Post. Turn right onto Va. Route 2 and go 2.5 mi to small community of Corbin, turn left onto Va. 610 and go 0.6 mi to intersection with Burma Road. Continue straight on Burma Road for

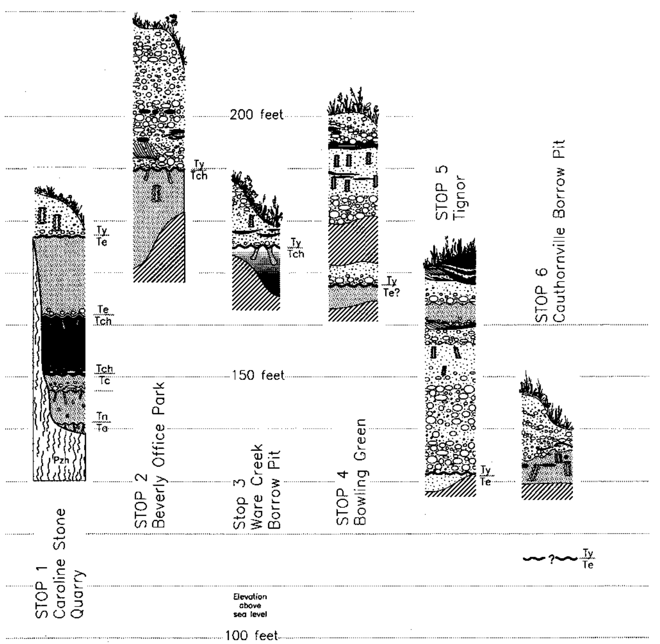

Figure 6.Stratigraphic sections exposed at Stops 1-6 in western part of field trip area.

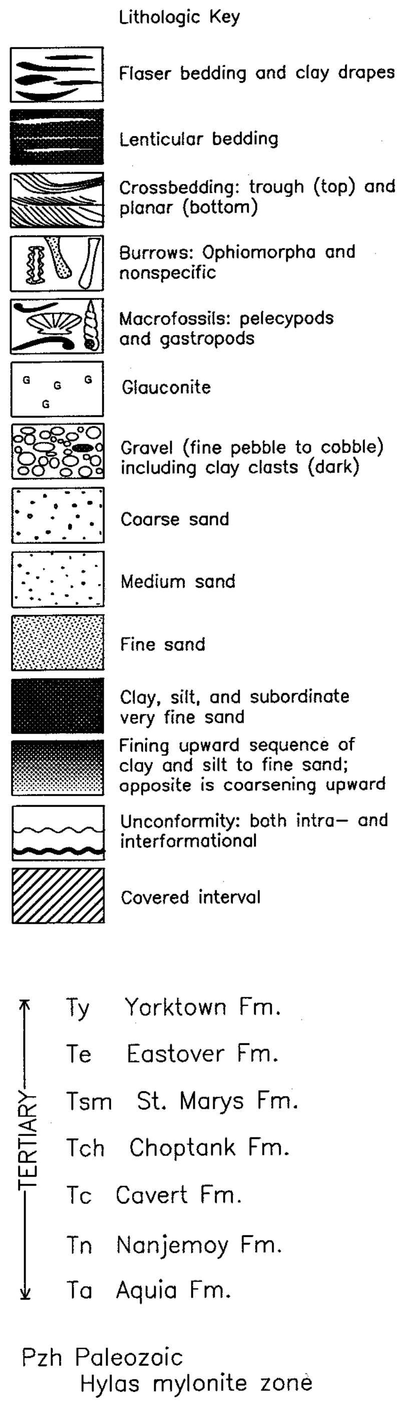

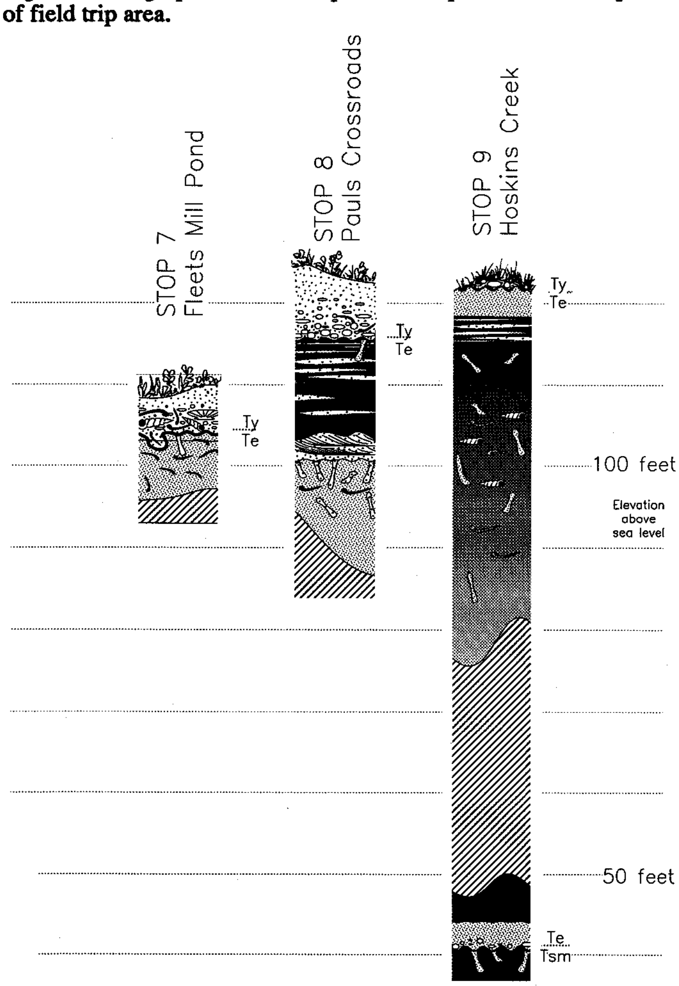

Figure 7.Stratigraphic sections exposed at Stops 7-9 in eastern part of field trip area. Refer to figure 6 for lithologic key.

0.4 mi to Fredericksburg Geomagnetic Center and another 0.4 mi to gate to Fort A.P. Hill Military Reservation. A military policeman will meet us at the gate and open it for us. Continue eastward 0.3 mi on Burma Road to intersection with gravel road. Turn right (south) for 0.1 mi to trail on left that leads to Stop 3.

110.9 **STOP 3, Ware Creek borrow pit.** This stop is an old, partially overgrown sand and gravel pit on the hillside above Ware Creek. Steep-walled gullies at the downhill side of pit provide good outcrops of the lower part of the Yorktown Formation. Retrace route 1.7 mi to Corbin.

112.6 At intersection of Va. 610 and Va. 2 turn left (south) onto Va. 2 for 9.6 mi to junction with Va. 605 in northwest Bowling Green. Turn right on Va. 605 (Paige Road) and go west 0.3 mi to the deep roadcut on right-hand side of highway which exposes sand and gravel of the Yorktown Formation.

122.5 **STOP 4, Bowling Green.** Park on the wide, flat road shoulder on the left side of highway just uphill from the Yorktown outcrops.
Retrace route for 0.3 mi to Va. Route 2.

122.8 Turn right onto Va. 2. Continue southward on Va. 2 for 3.8 mi, passing through downtown Bowling Green, to intersection with Va. 721. Turn left onto Va. 721 and continue eastward for 6.6 mi to Sparta. At Sparta take Va. 630 for 7.2 mi almost due east to the small community of Tignor.

136.6 **STOP 5, Tignor.** Park at wide gravelly area at intersection of Va. 630 and Va. 624, across the road from the Tignor general store. The Yorktown section is exposed in shallow road cuts along Va. 624, which leads southward from Tignor into King and Queen County.
Continue southward on Va. 624 for 3.3 mi to intersection with Va. 635.

139.9 Turn right onto Va. 635 and continue south 3.0 mi to junction with Va. 721. Continue southward on Va. 721 for 1.2 mi to the community of Owenton.

144.1 At Owenton, take Va. 660 eastward toward Cauthornville for 0.9 mi, passing Garnetts Millpond on the left.

145.0 **STOP 6, Cauthornville borrow pit.** The entrance road to the borrow pit is on the left (north) side of Va. 660 and part way up the hill on the east side of Garnett Millpond. Commonly, the entrance is closed by a steel cable. Visitors to the pit should ask permission from Mr. Raymond Robinson who lives at the top of the hill.

145.9 At Owenton, turn left on Va. 721 and continue south 8.6 mi to intersection with U.S. 360 at St. Stephens Church. Turn left on U.S. 360 and go northeast 1.8 mi to intersection with Va. 631 South at Shepherds Church. Turn right onto Va. 631 and go 1.2 mi southeast to Fleets Creek and Fleets Millpond.

161.5 **STOP 7, Fleets Millpond.** The millpond is on private property. Permission to visit the area **must** be obtained from the owner, Mr. Nicholas Stolfi, P.O. Box 8, St. Stephens, Va. 23148. Mr. Stolfi lives in the house overlooking the millpond. Visitors should park on the southeast side of Fleets Creek. Follow a narrow footpath upstream through the woods to a steep-walled millrace. At low water levels, it is possible to descend to the floor of the millrace to examine relatively fresh outcrops of the upper part of the Eastover Formations lower part of the Yorktown.
Retrace route to U.S. 360 at Shepherds Church.

162.7 Turn right onto U.S. 360 and continue northeast 8.6 mi (0.6 mi northeast of Pauls Crossroads) to deep cuts along the highway where the upper part of the Eastover and lowermost Yorktown strata are well exposed.
STOP 8, Pauls Crossroads. As outcrops are in cuts for southbound lanes of the four-lane highway, continue downhill to the first turnaround. Return uphill in southbound lanes and park on road shoulder next to outcrops. For the stratigraphic section at this locality, see figure 7 and stop description.

We plan to end the field trip at Stop 8. Stop 9 is described as an alternate stop for those interested in seeing a more complete section of the Eastover Formation.

We will return to Williamsburg via West Point, Va., following U.S. 360, Va. 30, and I-64.

REFERENCES CITED

Abbott, W.H., 1978, Correlation and zonation of Miocene strata along the Atlantic margin of North America using diatoms and silicoflagellates: Marine Micropaleontology, v. 3, p. 15-34.

Akers, W.H., 1972, Planktonic foraminifera and biostratigraphy of some Neogene formations, northern Florida and Altantic Coastal Plain: Tulane Studies in Geology and Paleontology, v. 9, no. 1-4, 139 p.

Andrews, G.W., 1988, A revised marine diatom zonation for Miocene strata in the Southeastern United States: U.S. Geological Survey Professional Paper 1481, 29 p.

Berquist, C.R., Jr., and Goodwin, B.K., 1989, Terrace gravels, heavy mineral deposits and faulted basement along and near the Fall Zone in southeastern Virginia, 21st Annual Meeting Virginia Geological Field Conference, 29 p.

Blackwelder, B., and Ward, L.W., 1976, Stratigraphy of the Chesapeake Group of Maryland and Virginia: Guidebook for Field Trip 7b, Geological Society of America 1976 joint meeting NE-SE Section.

Carpenter, R.H., and Carpenter, S.F., 1991, Heavy mineral deposits in the upper Coastal Plain of North Carolina and Virginia: Economic Geology, v. 86, p. 1657-1671.

Clark, W.B., and Miller, B.L., 1906, A brief summary of the geology of the Virginia Coastal Plain: Virginia Geological Survey Bulletin 2, p. 11-24.

Cronin, T.M., Bybell, L.M., Poore, R.Z., Blackwelder, B.W., Liddicoat, J.C., and Hazel, J.E., 1984, Age and correlation of emerged Pliocene and Pleistocene deposits, U.S. Atlantic Coastal Plain: Palaeogeography, Palaeoclimatology, Palaeoecology, v. 47, p. 21-51.

Dowsett, H.J., and Cronin, T.M., 1990, High eustatic sea level during the middle Pliocene: Evidence from the southeastern U.S. Atlantic Coastal Plain, Geology, 18(5): 435-438.

Dowsett, H.J., and Wiggs, L.B., 1992, Planktonic foraminiferal assemblage of the Yorktown Formation, Virginia, USA: Micropaleontology, v. 38, no. 1, p. 75-86.

Frey, R.W., Howard, J.D., and Pryor, W.A., 1978, Ophiomorpha: its morphologic, taxonomic, and environmental significance: Palaeogeography, Palaeoclimatology, and Palaeoeconology, v. 23, p. 199-229.

Gibson, T.G., 1983, Stratigraphy of Miocene through Pliocene strata of the United States Central Atlantic Coastal Plain, Smithsonian Contributions to Paleobiology, 53: 35-80.

Goodwin, B.K., and Johnson, G.H., 1970, Guidebook to the geology of the upland gravels near Midlothian, Virginia: 11th Annual Field Conference, Atlantic Coastal Plain Geological Association Guidebook, pt. 2, 35 p.

Hazel, J.E., 1983, Age and correlation of the Yorktown (Pliocene) and Croatan (Pliocene and Pleistocene) Formations at the Lee Creek Mine, *in* Ray, C.E., ed., Geology and paleontology of the Lee Creek Mine, North Carolina, I.: Smithsonian Contributions to Paleobiology, no. 53, p. 81-199.

Johnson, G.H., Goodwin, B.K., Ward, L.W., and Ramsey, K.W., 1987, Tertiary and Quaternary stratigraphy across the Fall Zone and western Coastal Plain Southwestern Virginia, in Geological Excursions in Virginia and North Carolina: Guidebook, Field Trips no. 1-7, Geological Society of America, Southeastern Section, p. 87-144.

Marr, J.D., Jr., and Ward, L.W., 1987, Geology of the Caroline Stone Quarry: Virginia Division of Mineral Resources, Virginia Minerals, v. 33, p. 29-33.

Marr, J.D., Jr., and Ward, L.W., 1993, Geology of the Caroline Stone Quarry: Virginia Explorer, v. 9, no. 1, p. 7-11.

Mixon, R.B., 1978, The Thornburg, Scarp: a late Tertiary marine shoreline across the Stafford fault system, in Mixon, R.B., Newell, Wayne L., 1978, The faulted Coastal Plain margin at Frederickbsurg, Virginia -- Tenth Annual Virginia Geology Field Conference, October 13-14, 1978: Reston, Va., p. 41-47.

Mixon, R.B., Berquist, C.R., Newell, W.L., Johnson, G.H., Powars, D.S., Schindler, J.S., and Rader, E.K., 1989, Geologic map and generalized cross sections of the Coastal Plain and adjacent parts of the Piedmont, Virginia: U.S. Geological Survey Miscellaneous Investigations Series Map I-2033, 2 sheets, scale 1:250,000.

Mixon, R.B., and Newell, W.L., 1977, The Stafford fault system: Structures documenting Cretaceous and Tertiary deformation along the Fall Line in northeastern Virginia: Geology, v. 5, p. 437-440.

Mixon, R.B., and Newell, W.L., 1982, Mesozoic and Cenozoic compressional faulting along the Atlantic Coastal Plain margin, Virginia, *in* Lyttle, P.T., ed., Central Appalachian geology: NE-SE GSA meeting, 1982 Field Trip Guidebooks, American Geological Institute, Falls Church, Va.

Mixon, R.B., and Powars, D.S., 1984, Folds and faults in the Inner Coastal Plain of Virginia and Maryland--Their effect on distribution and thickness of Tertiary rock units and local geomorphic history, *in* Frederiksen, N.O., and Krafft, Kathleen, eds., Cretaceous and Tertiary stratigraphy, paleontology, and structure, southwestern Maryland and northeastern Virginia; Field Trip volume and guidebook (for field trip held Oct. 17, 1984): Reston, Va., American Association for Stratigraphic Palynologists, p. 112-122.

Mixon, R.B., and Powars, D.S, and Daniels, D.L., 1992, Nature and timing of deformation of upper Mesozoic and Cenozoic deposits in the Inner Atlantic Coastal Plain, Virginia and Maryland, *in* Gohn, G.S., ed., Proceedings of the 1988 U.S. Geological Survey Workshop on the Geology and Geohydrology of the Atlantic Coastal Plain: U.S. Geological Survey Circular 1059, p. 65-73.

Mixon, R.B., Powars, D.S., Ward, L.W., Andrews, G.W., 1989 (1990), Lithostratigraphy and molluscan and diatom biostratigraphy of the Haynesville cores, northeastern Virginia Coastal Plain, Chapter A, *in* Mixon, R.B., ed., 1989, Geology and paleontology of the Haynesville cores, Richmond County, northeastern Virginia Coastal Plain: U.S. Geological Survey Professional Paper 1489, p. A1-A48.

Newell, W.L., 1985, Architecture of the Rappahannock estuary-neotectonics in Virginia, *in* Morisawa, M., and Hack, J.T., eds., Tectonic Geomorphology: Proceedings of the 15th Annual Binghamton Geomorphology Symposium, Sept. 1984, p. 321-344.

Newell, W.L., and Rader, E.K., 1982, Tectonic control of cyclic sedimentation in the Chesapeake Group of Virginia and Maryland, *in* Lyttle, P.T., Central Appalachian geology, northeast-southeast GSA meeting, 1982 Field Trip Guidebooks: Falls Church, Va., American Geological Institute, 26 p.

Pavich, M.J., Jacobson, R.B., and Newell, W.L., 1989, Geomorphology, neotectonics, and process studies in the Rappahannock River basin: 28th International Geological Congress Field Trip Guidebook T218, American Geophysical Union, 22 p.

Powars, D.S., 1987, Geology of the King George Quadrangle, King George County, Virginia, and a brief discussion of the regional stratigraphy and structure: Unpublished Masters thesis, George Washington University, 194 p.

Ramsey, K.W., 1988, Stratigraphy and sedimentology of a Late Pliocene intertidal to fluvial transgressive deposit, Bacons Castle Formation, upper York-James Peninsula, Virginia: University of Delaware Ph.D. dissertation, Newark, Delaware, 321 p.

Stephenson, L.W., and MacNeil, F.S., 1954, Extension of Yorktown Formation (Miocene) of Virginia into Maryland: Geological Society of America Bulletin, v. 65, p. 733-738.

Ward, L.W., 1985, Stratigraphy and characteristic mollusks of the Pamunkey Group (lower Tertiary) and the Old Church Formation of the Chesapeake Group-Virginia Coastal Plain: U.S. Geological Survey Professional Paper 1346, 78 p.

Ward, L.W., 1992, Molluscan biostratigraphy of the Miocene, Middle Atlantic Coastal Plain of North America: Virginia Museum of Natural History, Memoir Number 2, 159 p., 26 plates.

Ward, L.W., and Blackwelder, B.W., 1980, Stratigraphic revision of upper Miocene and lower Pliocene beds of the Chesapeake Group, Middle Atlantic Coastal Plain: U.S. Geological Survey Bulletin 1482-D, 61 p.

Ward, L.W., and Krafft, Kathleen, 1984, eds., Stratigraphy and paleontology of the outcropping Tertiary beds in the Pamunkey River region, central Virginia Coastal Plain: Atlantic Coastal Plain Geological Association 1984 Field Trip Guidebook, 280 p.

Ward, L.W., and Strickland, G.L., 1985, Outline of Tertiary stratigraphy and depositional history of the U.S. Atlantic Coastal Plain, *in* Poag, C.W., ed., Geologic Evolution of the United States Atlantic Margin, New York: Van Nostrand Reinhold Company, p. 87-123.

Weems, R.E., 1980, Geology of the Taylorsville Basin, Hanover County, Virginia, in Contributions to Virginia Geology IV: Virginia Division of Mineral Resources Publication 27, p. 23-38.

Weems, R.E., 1981, Geology of the Hanover Academy quadrangle, Virginia: Virginia Division of Mineral Resources Publication 30, text and 1:24,000 scale map.

ENVIRONMENTAL GEOLOGY AND CARBON BASED RESOURCES FROM THE FIELD TO THE CLASSROOM A SHORT COURSE FOR SECONDARY TEACHERS

Laure G. Wallace
U.S. Geological Survey

James V. O'Connor
University of the District of Columbia

For the first time, the Eastern Section of AAPG sponsored a secondary teacher program in conjunction with the regional meeting. With seed funds from the AAPG Foundation and time and materials support from the U.S. Geological Survey (USGS), the University of the District of Columbia and the College of William and Mary, 25 teachers and 12 presenters participated in an intensive two day short course.

Titled, "Environmental Geology and Carbon Based Resources - From the Field to the Classroom", the full field guide is available as Open-File Report 94-19, by O'Conner and others, from the U.S. Geological Survey, Earth Science Information Center (ESIC), Mail Stop 306, Box 25286, Denver Federal Center, Denver, CO 80225. A single copy can be purchased and copies can be made for distribution.

The course was broken into two parts - a full day field trip and a hands-on workshop. The program began on the Saturday before the meeting in the metropolitan Richmond area. Teachers visited a wetland area to learn about environments of deposition for carbon resources, extract and evaluate wetland samples and discuss the latest technological advances with employees from Hatcher and Thayer, a local environmental research firm. This was followed with a visit to a local quarry for a mapping activity and to abandoned coal fields in the Richmond Basin for coal sample collecting. A number of stops dealt with environmental issues in resource development, transportation and petroleum storage. This was complemented with information on the newest research tools and information on assessing water quality and quantity in the James River and ideas for using local cemeteries as a teaching resource. At each stop earth science professionals shared information on the latest research and technology and this was followed by an activity which teachers would be able to use with their students.

Sunday, the teacher participants spent the day building on the information from the field program. A USGS palynologist talked about sedimentary environments worldwide. This was coupled with an activity where the teachers had to design and fill their own graben model. The West Virginia Geological Survey presented an excellent set of activities for classroom use, on depositional environments, and strip logs, cross section and isopach map development. A coal geologist from the USGS had teachers ranking samples of bituminous, anthracite and lignite, and a field researcher from the Virginia Division of Mineral Resources took participants on a trip through time, from the coal mining processes and hazards of early mining operation to current day equipment, technology and mining practices. Teachers had fun examining some of the legal and fiscal issues that impact mining activity by using an activity in which they mined chocolate chip cookies and reclaimed their developed area. (Some found unique ways to dispose of the mining debris!) The short course was wrapped up with an excellent presentation on "Global Change - the Human Perspective," by a visiting colleague from Canada.

The concept of the program was simple. We wanted the teachers to accomplish five things:

1) Develop a good solid foundation for understanding the environment of deposition for carbon based resources.

2) Learn about methodologies for assessing the amount and extent of carbon-based resources.

3) Understand the necessity for balance between societal need for energy resources and the environmental impact of developing these resources.

4) Develop connections with local organizations and resources that will support them in their teaching.

5) Try out and take back to their students, well tested field and classroom activities so that they could immediately begin to use what they learned in the short course back in the classroom.

Earth science teachers, those who hold the key to engaging bright new minds in our field of study or who simply need to impart scientific literacy for the good of our society, are hampered by multiple societal, bureaucratic and educational problems. Teachers do not identify a lack of materials as a problem, but finding them and adapting them for classroom use is. Mostly, teachers identify a need for partnerships with local scientists who can teach them about the newest research and technology and help them reach into the diverse community of scientists that represent the multiple fields represented in Earth Science.

We are pleased that the Eastern Section and the AAPG Foundation supported this program for the 1993 Williamsburg, VA, meeting. Even with a relatively small meeting, it was not difficult to find members interested in sharing their knowledge with local teachers. Even those who had never tried this before, found that it was an exciting and fun way to educate on their work. Very seldom are we showered with such immediate praise and appreciation for our time and efforts. Evaluations by the teachers, who included national award winning teachers to teachers with minimal background in the earth sciences, were overwhelmingly positive. Some noted that this was the best teacher enhancement program that they have attended in their career as an earth science teacher, for seldom do they have the opportunity to spend time with a group of scientific experts expanding their knowledge and understanding of the earth sciences. Perhaps this program will begin a history of teacher outreach programs at Eastern Section meetings.

MILANKOVITCH CYCLES, SEQUENCES AND EARLY DIAGENESIS ON CARBONATE PLATFORMS FORMED UNDER GREENHOUSE VS ICEHOUSE CONDITIONS: IMPLICATIONS FOR RESERVOIRS IN CARBONATE ROCKS

J. FRED READ
DEPT OF GEOLOGICAL SCIENCES
VIRGINIA TECH
BLACKSBURG VA 24061 USA

INTRODUCTION

This short course will focus on showing the relationship between Milankovitch driven sea level changes, carbonate cycles and depositional sequences, and their diagenesis. We will examine:

1. the controls on carbonate platform deposition,
2. types of platforms,
3. fundamentals of carbonate sequence stratigraphy
4. types of small scale cycles that make up depositional sequences, and their relationship to low, moderate and high amplitude Milankovitch sea level changes and global greenhouse vs icehouse conditions, and
5. the diagenetic modification of these cycles resulting from sea level fluctuations involved in their deposition under the prevailing climate (in part modified from Read and Horbury, in press).

Hopefully, the course will provide you with a better understanding of why many carbonate platforms that formed under greenhouse conditions (e.g. Early Ordovician Knox Group in the Appalachians or Late Permian of Texas) are dolomitized and how this affects porosity, why Mississippian ramps in the Appalachians have only a few tidal flat facies, many disconformities and little early spar cementation, why Pennsylvanian carbonate platforms formed under ice-house conditions have many disconformities and dissolution enhanced porosity, and shale aquitards if land attached, why some depositional sequences contain regional early sparry cements associated with paleoaquifers, and how karst development during long term emergence of platforms generates porous reservoir zones.

CONTROLS ON CARBONATE DEPOSITION

Excellent reviews are given in Vail et al. (1991) and Schlager (1992).

Subsidence: Thermal and tectonic subsidence (driving subsidence) related to stretching or cooling of the lithosphere is the fundamental process that creates the initial space for sedimentation in cratonic basins and passive margins (Fig. 1B). In foreland basins, loading due to thrust emplacement is a major cause of subsidence (Fig. 1A). The isostatic loading associated with newly emplaced water and sediment in sedimentary basins creates additional space due to isostatic flexural subsidence. Assuming local isostasy and neglecting flexure, a widespread transgression of an emergent shelf could cause roughly an additional 40% subsidence just due to water load. Similarly, transgressing a previously emergent shelf and filling this with sediment could cause a total sediment pile that is 2 to 3 times the thickness of the initial depth on flooding. Conversely, eroding sediment results in uplift due to unloading. Isostatic response times appear less than a few thousand years. To find the amount of driving subsidence involved in deposition of a basin fill, one needs to remove the subsidence due to loading by progressive backstripping the sediment using a geohistory plot or burial history curve (total subsidence vs time) (Van Hinte, 1978) (Fig. 1A). In general, long-term subsidence rates are less than sedimentation rates in most settings and will not cause drowning by themselves.

Sea-Level Change: Global sea level changes with time due to 1. changes in the volume of the ocean basins, in part due to heat flow through mid-ocean ridges and 2. due to global ice volume. The dominant sea level cycles forming the fundamental unit of sequence stratigraphy, the 3rd order depositional sequence are roughly from 0.5 to 5 m.y. duration. These are bundled into longer term (2nd order) sea level cycles typically tens of millions of years long, and then into 1st order cycles 200 to 300 m.y. long (Vail et al., 1977) (Fig. 2).

It is of fundamental importance to the petroleum or coal geologist to realize that high frequency sea level cycles are superimposed on these longer term cycles (Fig. 2B), and it is these that cause rapid flooding of platforms to form the parasequences. For flooding, rates of high frequency sea level rise (plus subsidence) have to be faster than sedimentation rates which is helped by the apparent asymmetric form of these sea level cycles, with a rapid rise (deglaciation) and gradual fall (glaciation). These sea level cycles have quasi-periods in much of the Mesozoic-Cenozoic of roughly 19 to 23 k.y. (precession), 41 k.y. (obliquity or tilt), 95 to 130 k.y. and 400 k.y. (short and long term eccentricity) (Fischer, 1964; 1982; Goldhammer et al., 1990; Mitchum and Van Wagoner, 1991). Precessional and obliquity cycles in the Early Paleozoic may be shorter (roughly 17 and 30 k.y. respectively) (Berger et al., 1989). The stratigraphic record appears to show a dominance of one or more of these quasi periods at different geological times. For example the late Pleistocene shows dominantly 100 k.y. sea level fluctuations, whereas pre-700 k.y., 40 k.y. cycles appear to dominate the Pleistocene record (Ruddiman et al., 1986). Pennsylvanian cycles commonly show a strong 100 and/or 400 k.y. signal (Fischer, 1986). Mid-Triassic sea levels appear to show a dominance of roughly 20 k.y. fluctuations with only small 100 k.y. oscillations (Goldhammer et al., 1990). Extracting these high frequency signals from the stratigraphic record will be a major challenge but will provide an extremely powerful tool for interpreting the cyclic record at the reservoir scale.

During global ice-house conditions (Fig. 2A), Milankovitch sea level fluctuations generally were large (up to 100 m or more). At the other extreme during global greenhouse conditions, sea level fluctuations generally were small and probably less than ten meters (Koerschner and Read, 1989; Goldhammer et al., 1990, Wright, 1992). However, even during predominantly global green house times, 3rd order low stand or transgressions might have higher

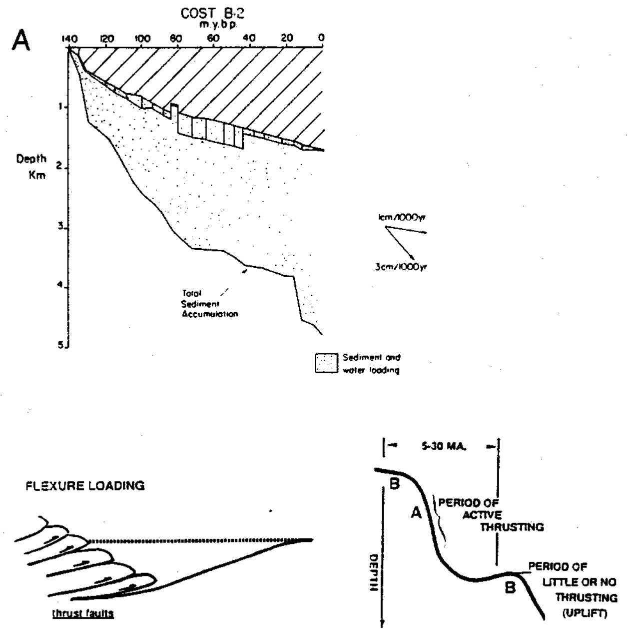

Figure 1. Subsidence history plots. A. Example of subsidence history plot from a passive margin (COST B-2 WELL). Lower curve is total subsidence whereas upper curve (vertical hachuring) is backstripped subsidence or thermo-tectonic subsidence after sediment and water loading have been removed given the estimates of paleobathymetry (from Watts, 1981).
B. Schematic diagrams illustrating subsidence due to flexural loading by thrust sheets (left) and subsidence history plot on the right (from Vail et al., 1991).

amplitude, high frequency sea level changes reflecting waxing and waning of small ice sheets. Conversely, during global ice house times (Fig. 2A), 3rd order high stands might show decreased high frequency sea level amplitudes due to overall waning of ice sheets (Ferry , 1991 pers. comm; Elrick and Read, 1991). Thus during deposition of part of a single depositional sequence, there may be a marked change in amplitude of the Milankovitch sea level signals.

Rate of Sediment Accumulation: Rates of carbonate sedimentation in tropical settings tend to be strongly dependent on light, and hence water depth because of the biotas (corals, green algae, sea grasses, termed chlorozoan association). Thus there is a rapid drop off in growth rate below 10 m (Fig. 3A) hence these tend to form rimmed platforms (Schlager, 1992). These reef builders also tend to be limited to near normal salinities, and to waters warmer than 20°C winter temperature (roughly between 30 degrees latitude). Tropical carbonate sedimentation rates generally easily exceed subsidence rates (Fig. 3B), however, only reef assemblages are able to keep pace with high amplitude sea level rises of several meters/k.y.

In contrast, temperate water carbonates do not show such a light dependence because assemblages are dominated by bryozoans, mollusks and forams (termed bryomol or foramol association); consequently, although temperate water carbonates do not show high shallow water production rates, they show little decrease in sedimentation rates into deeper water, thus these tend to form gently sloping ramps (Schlager, 1992; Lees, 1975).

Clastic poisoning due to turbidity reducing light or suffocating filter feeders is important in reducing carbonate production rates toward sites of fine clastic influx and is a major cause of intrashelf basid formation. Lowered salinities in these areas also likely reduce production rates. On interiors of huge shallow water Paleozoic platforms, distance from the ocean and its source of calcium ions also may keep production rates low resulting in cratonic deeper water carbonate blankets and intrashelf basins.

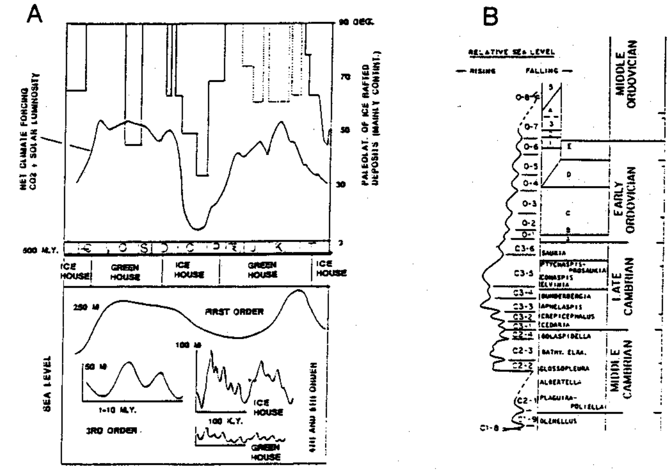

Figure 2 A. Relationship between ice house and green house conditions, eustasy and global CO2. Upper part of graph shows paleolatitudes of ice-rafted glacial deposits in continental regimes (cross-hatched) and those of possible marine origin (stippled), modified from Frakes and Francis (1988), plotted against geological time, as well graph showing net forcing of climate due to changes in CO2, their effect on radiative forcing, and long term increase in solar luminosity (modified from Crowley and Baum, 1992 and Berner, 1991). Times of generalized ice house vs. green house conditions are shown on the time axis, and are modified from Fischer (1982). Lower part of diagram shows first order Vail sea level curve for the Phanerozoic. Bottom of diagram shows a 3rd order sea level curve with 1 to 10 m.y. periods, and schematic 4th and 5th order sea level curves which would be superimposed on the longer term curves.
B. Example of relative sea level curve for Middle Cambrian to Early Ordovician passive margin carbonate platform in the Appalachians, showing a roughly 50 m.y. rise-fall, and superimposed 1 to 5 m.y. sea level fluctuations (3rd order). Higher frequency sea level fluctuations would be superimposed on this longer term curve. After Read (1989).

BASIC TYPES OF CARBONATE PLATFORMS

Standard Facies Belts of Carbonate Platforms

Tidal Flat Facies: Facies arranged in cyclic, upward shallowing units 1-10 m thick. In humid zones facies are subtidal-intertidal burrowed limestone with supratidal cryptalgal laminites, and inland freshwater algal marsh deposits, coal, or siliciclastics. In arid zones facies are burrowed to non-burrowed pellet muds and cryptalgal heads, overlain by abundant intertidal cryptalgal laminite sheets, supratidal evaporites, or eolian-fluvial clastics.
Lagoonal Facies: Mainly bedded pellet limestone or lime mudstone, or cherty, burrowed skeletal packstone to mudstone, with local biostromes of colonial metazoans. Minor, thin interbeds of peritidal fenestral or cryptalgal carbonates reflecting periods of shallowing of lagoon to tide levels.
Shoal-water complex of banks, reefs, and ooid/pellet shoals: Occur as shallow-ramp skeletal banks or lime-sand shoals, or shelf-edge

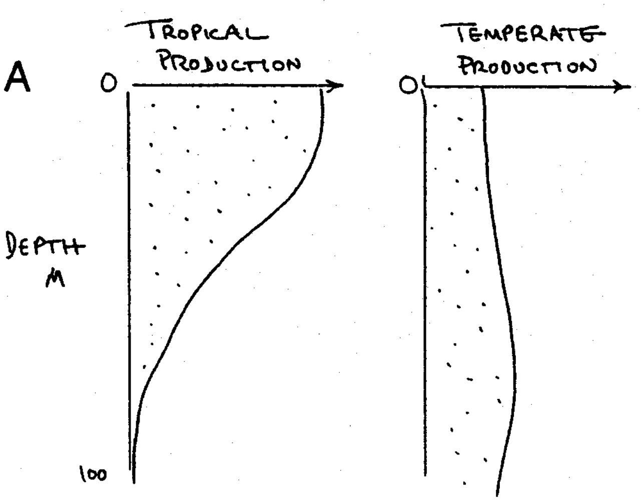

Figure 3. Sediment production/accumulation rates. A. Left: Production vs depth curve for tropical area, showing maximum production in shallow water decreasing rapidly (below 10 to 40 m) to low values, because of the light dependance of the biota. Right: Production vs depth curve for temperate water carbonates showing the much slower decrease in production into deeper water, reflecting the dominance of organisms (e.g. bryozoans, crinoids) that are not light dependant.

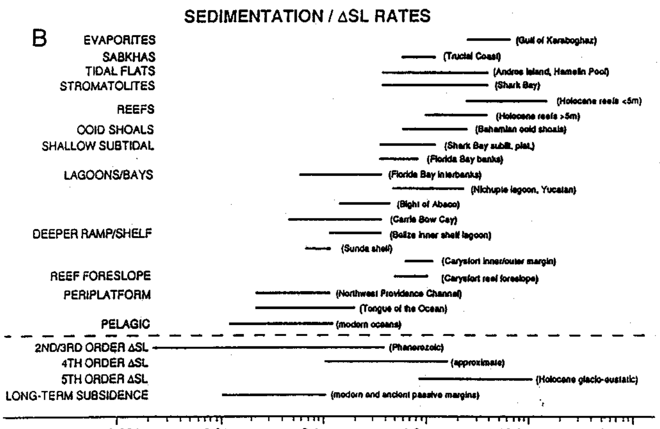

Figure 3 B. Table showing plot of sedimentation rates (horizontal axis, log scale) against various environments, as well as the ranges for various eustatic changes and long term subsidence. Based on a table in Schlager (1981).

skeletal reefs and skeletal or oolitic sands. On ramps, they pass gradually downslope into deep-ramp facies. On steeply sloping rimmed shelves, they pass downslope into foreslope and slope deposits .

Deep shelf and ramp facies: Cherty, modular bedded, skeletal packstone or wackestone, with abundant whole fossils, diverse open-marine biotas, and upward-fining, storm-generated beds. Water depths 10 to 40 m and largely below fair-weather wave base, but commonly above storm wave base.

Slope and basin facies: Adjacent to steeply sloping platforms, foreslope and slope deposits have abundant breccias and turbidites interbedded with periplatform lime and terrigenous muds. Adjacent to ramps, slope and basin deposits are thin-bedded, periplatform lime and terrigenous muds that generally have few sediment-gravity flow deposits. Basinal deposits in Paleozoic rocks commonly are shale, with carbonate-content increasing toward the platform. Basinal deposits in Mesozoic and Cenozoic rocks may be shale or pelagic limestone. Slope and basin floor may be anoxic and lacking benthic organisms; thus, deposits will be laminated and nonburrowed. Where slope and basin waters are oxic, deposits may be burrowed and fossiliferous.

Platform Types:

Rimmed carbonate shelves (Ginsburg and James, 1974) are shallow platforms whose outer wave-agitated edge is marked by a pronounced increase in slope (commonly a few degrees to 60_ or more) into deep water (Figs. 4A). They have a semicontinuous to continuous rim or barrier along the shallow shelf margin. Depositional or accretionary rimmed shelves show both up-building and out-building; they generally lack high marginal escarpments; and shelf edge and foreslope/slope facies may intertongue (rather than abut). Bypass margins of rimmed shelves occur in areas of rapid upbuilding where shallow water sedimentation deeps pace with sea-level rise. Bypassing may be associated with a marginal escarpment and/or a gullied bypass slope. Erosional margins commonly are characterized by high, steep erosional escarpments up to 4 km relief. Reefal carbonates rim the platform, and are exposed on the upper few hundred meters of the upper escarpment. Downslope, due to erosional retreat of the escarpment by mechanical defacement, the escarpment exposed bedded, cyclic lagoonal, and peritidal beds.

Many rimmed shelves have inshore or intrashelf basins lying behind the shallow carbonate rim. The basins commonly pass landward into coastal siliciclastics and to seaward into the shallow carbonate rim by way of a gently sloping ramp. Intrashelf basins have water depths of a few tens of meters, and lie below fair-weather wave base but parts may be above storm wave base. Sediment fills are shale with thin beds of quartz- and lime silt, intraformational conglomerate, glauconite, and radial-ooid packstone in storm-generated, upward-coarsening, and upward-fining units. Sub-wave base fills may be euxinic to dysaerobic organic rich limestone and shale.

Carbonate ramps (Figs. 4B,C) have gentle slopes (generally less than 1_) on which shallow wave-agitated facies of the nearshore zone pass downslope (without marked break in slope) into deeper water, low-energy deposits. They differ from rimmed shelves in that continuous reef trends generally are absent, high-energy lime sands are located near the shoreline, and deeper water breccias (if present) generally lack clasts of shallow shelf-edge facies. Homoclinal ramps have relatively uniform, gentle slopes (1 to a few meters/km or a fraction of a degree) into the basin. Distally steepened ramps have the shoal-water complex well back on platform separated from the slope by a broad deep ramp; the slope facies contain abundant slumps, breccias, and allochthonous lime sands but deep-water breccias lack clasts of shallow-platform sands or reefs, and only contain clasts of deep-ramp or slope facies. Low-energy, distally steepened ramps have widespread deep-ramp mud blankets seaward of the shoal-water complex, whereas high-energy, distally steepened ramps have broad lime-sand blankets over much of the deep ramp, with muds (and slope breccias and turbidites) being restricted to the slope and basin margin. Shoal-water complexes on homoclinal and low-energy, distally steepened ramps include skeletal banks or ooid-pellet sand shoals; these may be either fringing or barrier complexes. High-energy, distally steepened ramps have wide beach-dune complexes, and extensive thin shelf sand blankets extending to depths of over 100 m.

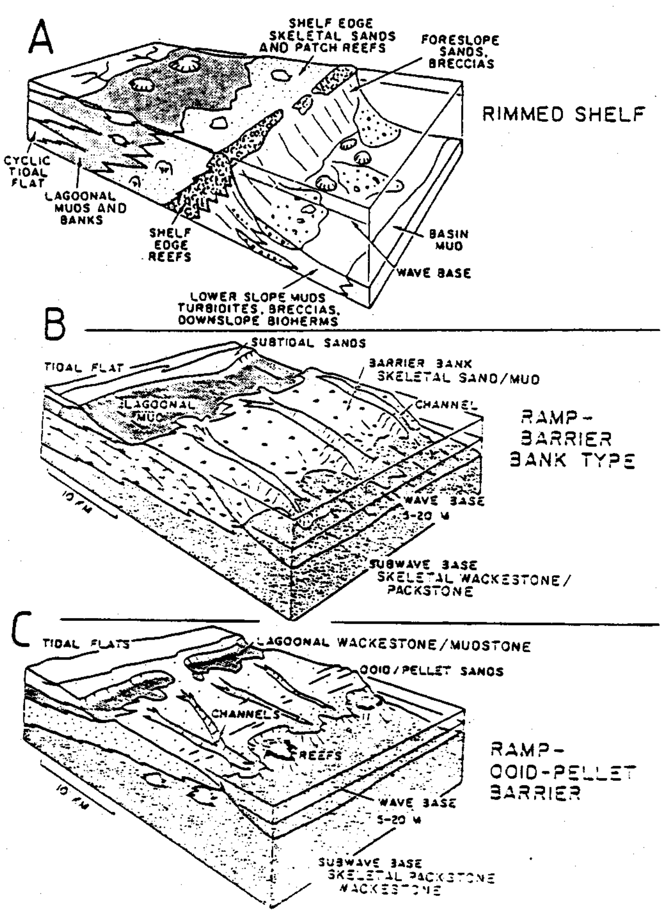

Figure 4. Types of Carbonate Platforms A. Rimmed carbonate shelf showing steep slopes at shelf edge. B. Carbonate ramp with skeletal bank and C. carbonate ramp with oolitic shoal complex (from Read, 1985). Note the low slopes on the ramps compared with the rimmed shelves.

Isolated platforms are platforms separated from continental shelves by deep water, and commonly are tens to hundreds of kilometers wide, located above rifted continental or transitional crust or on volcanic sea mounts. Interiors of reef-rimmed platforms may be dominated by skeletal limestone, where interiors are relatively deep (up to 20 m). In contrast, where platforms are shallow and flat-topped, interior facies may be dominated by cyclic nonskeletal peloidal sands and muds, and platform margins are shoals and eolian islands of ooid grainstone with subordinate reefs. One of the major differences between isolated platforms and other types is that margins may be windward, leeward or tide-dominated.

Drowning of Carbonate Platforms: Where subsidence or sea-level rise exceeds upbuilding, platforms may undergo drowning (Kendall and Schlager, 1981; Schlager, 1981). Incipient drowning (Kendall and Schlager, 1981) occurs where relative sea level rise exceeds rate of carbonate upbuilding, but the platform surface stays within the euphotic zone. Consequently, the system is able to recover because rate of sea-level rise decreases relative to rate of sediment deposition. In some incipiently drowned sequences, deepening may push the platform below the euphotic zone, but deeper water benthonic assemblages are able to build up into the photic zone, assisted by accumulation of lime and siliciclastic muds carried in from shallow platform areas. Facies typical of incipiently drowned platforms are nodular and thin-bedded argillaceous limestones (whole fossil wackestone/mudstone with some lime-sand layers) tens to hundreds of meters thick that overlie shallow platform facies from which rise scattered large buildups. Storm-generated, upward-fining beds may be common in the deeper water facies, along with hardgrounds. Terminal drowning of platforms occurs where rate of relative sea-level rise exceeds vertical accumulation rate and the platform is submerged below the euphotic zone, terminating rapid production and accumulation of carbonate by photosynthetic organisms (Kendall and Schlager, 1981). The euphotic zone in the open ocean may extend down to 100 m, but may be as little as 30 m in basins where fine-grained carbonate or clastics are abundant. Following drowning, platforms may become surfaced by hardground, by deep-water, nodular, argillaceous limestone, by pelagic carbonates, or by periplatform talus shed from adjacent shallow parts of platforms. Condensed sequences with numerous hardgrounds may develop, or in areas of nondeposition, submarine unconformities or chemical sediments (iron, manganese, phosphorite, or sulfide crusts) may develop.

SMALL SCALE CYCLES OR PARASEQUENCES OF CARBONATE PLATFORMS

Parasequences: Large scale depositional sequences (0.5 to 5 m.y.) on carbonate platforms are themselves composed of small scale carbonate cycles or parasequences, in a similar manner to siliciclastic shelves and ramps. These parasequences are the building blocks of depositional sequences and commonly are 1 to 10 meters thick, typically asymmetric, shallowing upward units, containing a marine flooding surface at the base. In updip areas, the cycles consist of shallow subtidal facies that can be overlain by tidal flat facies and a capping disconformity; downdip they consist of deeper water-facies shallowing up to shallower water facies and tend to have more conformable tops with overlying cycles. Parasequences that formed under low amplitude fluctuations of sea level will have only limited disconformity development at cycle tops, but those formed under high amplitude fluctuations, as in the Pleistocene, have well developed disconformities and karstic surfaces bounding them.

Parasequences and Composite Eustasy: Most ancient meter- to decameter-scale carbonate cycles or parasequences relate in part to high frequency, Milankovitch-driven climate changes and their associated sea level fluctuations (Fig. 5A). This is indicated by
1. estimates of cycle durations that lie in the 20 to 400 k.y. band (Heckel, 1980, 1985; Koerschner and Read, 1989; Goldhammer et al., 1990, 1993),
2. by bundling of some meter scale (20 k.y. precessional) carbonate cycles into sets of 5 (eccentricity bundles) due to precessional sea level cycles riding on eccentricity cycles (Goldhammer et al., 1990),
3. by spectral analysis of time series constructed from cyclic stratigraphic sections, using the cycle facies as a proxy for relative water depth, and stratigraphic thickness as a proxy for time, which yields periodicities suggestive of Milankovitch forcing, given the problems associated with incomplete cyclic stratigraphic records and missed beats (Bond et al., 1991; Goldhammer et al., 1990, 1993), and
4. by evidence of high frequency sea level drops off the platform forming disconformities, breccias, soils, and vadose fabrics on tops of parasequences (Goldhammer et al., 1990; Koerschner and Read, 1989).

Autocyclic Parasequences: In contrast, static sea level (autocyclic) models of carbonate cycle formation have been proposed by Ginsburg

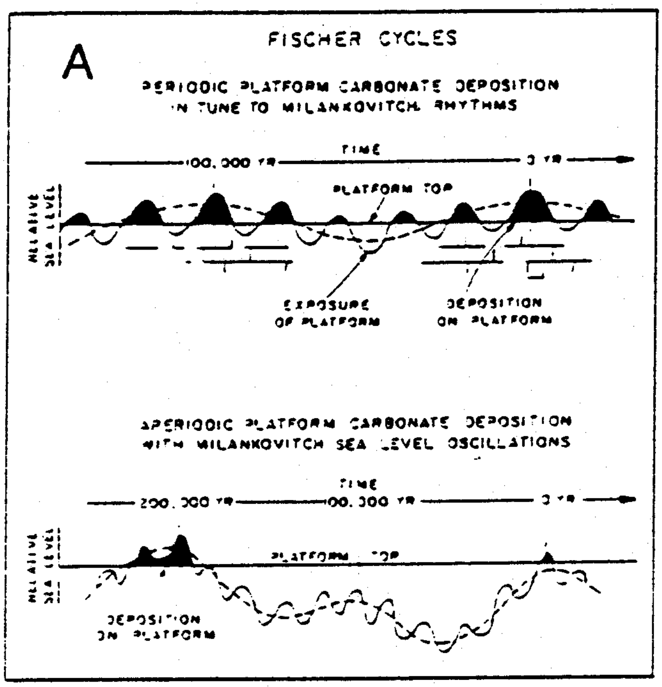

Figure 5. End member scenarios for formation of meter scale carbonate cycles.
A. Formation of carbonate cycles by fluctuations in sea level caused by Milankovitch orbital forcing of climate and sea level.

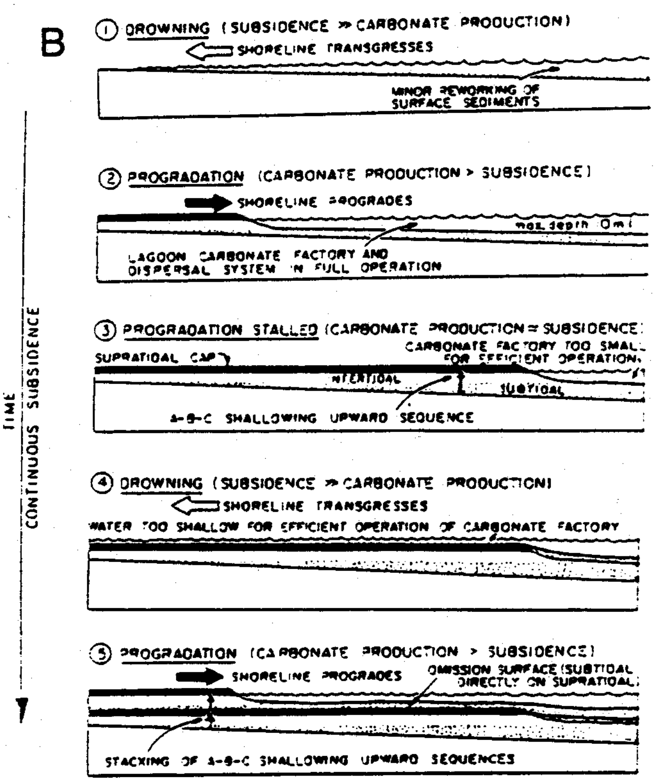

B. Diagram illustrating the formation of autocycles under static sea level using Ginsburg's 1971 model. From Hardie and Shinn, 1986).

(1971), Goldhammer et al. (1990), Kozar et al. (1990) and Hardie et al. (1991) (Fig. 5B). They postulate that flooding of the carbonate platform is caused by long-term gradual subsidence during periods of non-deposition, caused by shrinkage of the subtidal carbonate factory due to progradation of tidal flats. Deposition resumes after a lag time or depth is reached and the carbonate factory restarts. Note however, that autocycles likely will lack the diagenesis associated with sea level drop off the platform, since the autocycles will shallow to the position of static sea level. Furthermore, given typical passive margin subsidence rates, it would require tens of thousands of years of non deposition following inception of marine flooding for the platform to subside to depths of a few meters to initiate deposition of each cycle.

STACKING OF PARASEQUENCES INTO DEPOSITIONAL SEQUENCES AND SYSTEMS TRACTS

These small scale carbonate cycles or parasequences are stacked into larger scale packages or depositional sequences that are resolvable at the seismic scale. Good recent summaries of fundamental definitions are given in Vail (1987), Van Wagoner et al. (1988), Sarg (1988), Schlager, 1992, and Handford and Loucks (in press). Sequence stratigraphic units result from the interaction of rates of subsidence, eustatic sea level change and sedimentation and thus are process-based sedimentary units. The direction of long-term movement of the shoreline (transgression or regression) is a function of sedimentation rate vs. rate of creation of space on the shelf (related to rate of subsidence and eustatic sea level change and termed accommodation rate). Although eustatic sea level fluctuations are important in formation of depositional sequences, tectonics also are important and may be difficult to separate without high resolution biostratigraphic data on a global scale. Consequently, relative sea level curves, which are the sum of tectonic subsidence and eustatic sea level change can be employed.

The sequence stratigraphic approach was developed mainly from seismic sections in which sequences and systems tracts were defined largely on stratal geometries (e.g. onlap, offlap, downlap) (Fig. 6A). In contrast, much depositional sequence stratigraphy at the reservoir scale is done using well logs, cores or outcrop sections, and thus depends on a totally different type of data set (Fig. 6B). Integrating these two approaches is the challenge facing today's explorationist.

Why Use Sequence Stratigraphy?: The sequence stratigraphic approach should be applied because it allows us to break up a basin's stratigraphy into genetically related packages defined by bounding surfaces (sequence bounding unconformities, transgressive surfaces, maximum flooding surfaces). Sequences and systems tracts are physically mappable entities at a scale greater than lithologically (and locally) defined formations. Thus sequence stratigraphy helps greatly simplify formation-based stratigraphy with its myriad of local names and commonly arbitrary boundaries and groupings of lithologies. From a practical standpoint, the much cited criticism against sequence stratigraphy (whether or not depositional sequences and inferred sea level cycles are able to be correlated interbasinally or globally) is of little importance to most of us, especially in terms of reservoir development in mature basins.

Sequence Boundaries:

Depositional sequences are bounded updip by unconformities and characterized by onlap of younger units onto the sequence boundary (Sarg, 1988). In eustatic cycles, the unconformities or sequence boundaries correlate with the time of maximum sea level fall rate which exceeds subsidence rate on that part of the platform. In outcrop or core as opposed to seismic sections, many sequence boundaries on the outer platform are difficult to define as a single surface, and commonly are developed as a zone of disconformity-bounded parasequences (6B). Downdip, sequence boundaries become conformable and pass underneath the low stand deposits. Note that sequence boundaries (especially in downdip areas) differ from classic transgressive-regressive cycle boundaries which are placed at the top of the regressive package, beneath the overlying transgressive unit. Type 1 sequence boundaries are characterized by emergence of the platform out beyond the shelf edge and can be caused by eustatic sea level falling faster than the shelf edge is subsiding. Clearly these boundaries are going to be more common on rimmed shelves than ramps. Type 2 sequence boundaries may have erosional disconformities updip, but sea level does not significantly expose the margin; such sequence boundaries may result from eustatic sea level fall being less than subsidence, and such type 2 boundaries are typical of ramps (Fig. 6C).

Parasequences that make up depositional sequences are bundled into 3 basic systems tracts traceable from the inner shelf out into the basin and deposited during low stand, transgression and high stand.

Low Stand Systems Tract (LST):

These are the first deposits of a depositional sequence, and generally conformably overlie the sequence boundary in the basin and slope. Unconformity-related karsting and soil formation may develop updip on the platform during the low stand.

With Type 1 sequence boundaries where sea level falls off the shelf edge on steep margins, a low stand wedge of allochthonous (resedimented) debris from the margin may be deposited during falling sea level, due to failure by oversteepening or slope front erosion (Fig. 6B). Note that this wedge of debris flows and turbidites may be indistinguishable from debris flows resulting from tectonically induced slope failure. On the outer shelf or slope immediately updip from the talus wedge, several stranded parasequences may be deposited at this time related to forced regression (Posamentier et al., 1993). As sea level fall slows and the low stand position of sea level is approached, deposition of a ramp/shelf margin wedge of shallow water carbonate produced in place may occur in the shallowed slope areas, and the slow relative rise in sea level (static sea level plus continued subsidence) will cause onlap of these shallow water facies up the slope and onto the outer platform.

Autochthonous low stand ramp margin wedges associated with type 2 boundaries occur commonly on ramps where sea level does not fall below the bank- or shelf margin (Fig. 6C). This shelf or ramp margin wedge typically consists of several shallow water parasequences localized near the basin margin. They show limited onlap onto the platform and limited seaward progradation and downlap onto the basin floor because during the low stand, sea level is either slowly falling, static or slowly rising, thus background subsidence results in some relative sea level rise.

In arid settings, basins both on the shelf, and downslope from the shelf may become sites of low stand evaporites or evaporitic dolomites. Given sufficient seawater influx, these basins can have high evaporite sedimentation rates of several meters to tens of meters/k.y. In both arid and humid settings, siliciclastics can bypass the top of the platform, and be deposited on the basin floor as deep water fans.

Transgressive Systems Tract (TST):

The TST is separated from the underlying LST along the platform margin by a marine flooding surface (the transgressive surface) across which facies go from shallow water to relatively deeper water facies, and is the first significant marine flooding surface across the outer shelf or ramp (Figs. 6B,C). Parasequences of the TST show onlap onto the sequence boundary (or zone), and they may show the retrogradational (sedimentation rate less than accommodation rate) or aggradational stacking patterns (sedimentation rate equals accommodation rate). Shallow water facies capping cycles will show progressive backstepping upward in the section, and at the same time there will be backstepping of deep ramp or foreslope facies beneath basin facies. Individual parasequences of the TST are the thickest of all the systems tracts and will contain many with very open marine subtidal bases. This is because accommodation rate is high, resulting in maximum water depths during short term sea level rises. TST parasequences have tidal flat facies either absent or restricted to the inner platform, and show the least development of disconformities/soil formation due to the high accommodation rate, which decreases the amount of time cycles remain emergent during short term sea level falls.

Highstand Systems Tract: This is separated from the TST by maximum flooding surface onto which parasequences may downlap if there is a significant decrease in sedimentation rate downdip, as with rimmed shelves (Fig. 6B). On many ramps, there is little decrease in sedimentation rate with water depth, thus stratal units show little if any downlapping onto this surface (Fig. 6C). The maximum flooding surface typically occurs relatively high on the sea level curve, but prior to the actual sea level high stand. This largely reflects the effects of high rate of sea level rise, coupled with maximum load induced subsidence due to widespread sedimentary loading over the platform due to widespread marine flooding. However, on flat topped isolated platforms, the maximum flooding surface may occur during the time of maximum sea level rise rate.

Parasequences of the HST show marked progradational geometries; upward in the section parasequences become dominated by shallower water and peritidal facies, and become thinner upward (due to progressive decrease in accommodation which in eustatic cycles is due to slowing of sea level rise and then onset of sea level fall). Individual parasequences are relatively thin and restricted compared to the TST and LST. In arid settings, progradational HST evaporitic cycles interfingering updip with siliciclastics may be common.

Sequence Boundaries, Systems Tracts in Foreland Basins: Foreland basins may develop stratigraphies that are different from passive margins or cratonic basins (Posamentier and Allen, 1993; Flemings and Jordan, 1991). This is because craton-attached carbonate platforms extending into foreland basins are receiving most of the siliciclastic sediment from the side with the highest subsidence rate and there may be periodic upwarping associated with a peripheral bulge. Ponding of coarse siliciclastics may occur on the tectonically active margin during thrusting, causing maximum deepening in the basin and apparent offlap along the cratonic margin synchronous with uplift on the peripheral bulge. Thus the regressive-transgressive events forming the sequence boundary are out of phase on the distal vs proximal margins. With cessation of thrusting, erosion of the tectonic highlands coupled with decreased load induced subsidence causes rapid progradation of coarse clastics out across the basin and onlap onto the cratonic margin.

Foreland basins also will show a proximal zone adjacent to the tectonically active basin margin in which subsidence always exceeds eustatic sea level fall, and hence will contain only conformable sections. In contrast, further out from the tectonically active margin, subsidence rates will sometimes be exceeded by eustatic sea level fall, and so will develop unconformities in the section. During sinusoidal sea level change and constant thrust rate, shore-

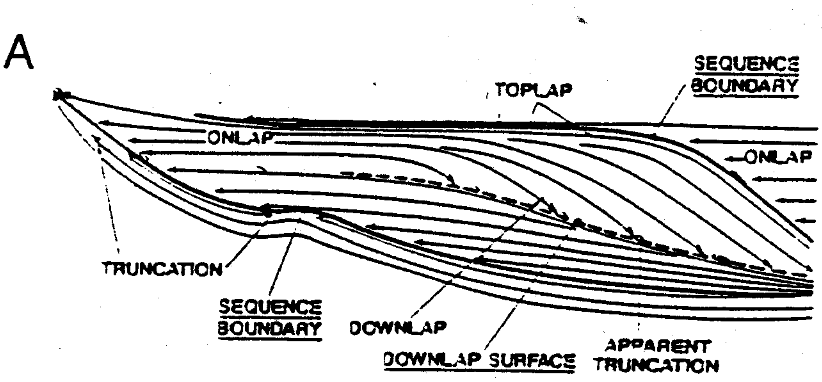

Figure 6 A. Stratal geometries used in defining sequences and systems tracts using seismic stratigraphic methods.

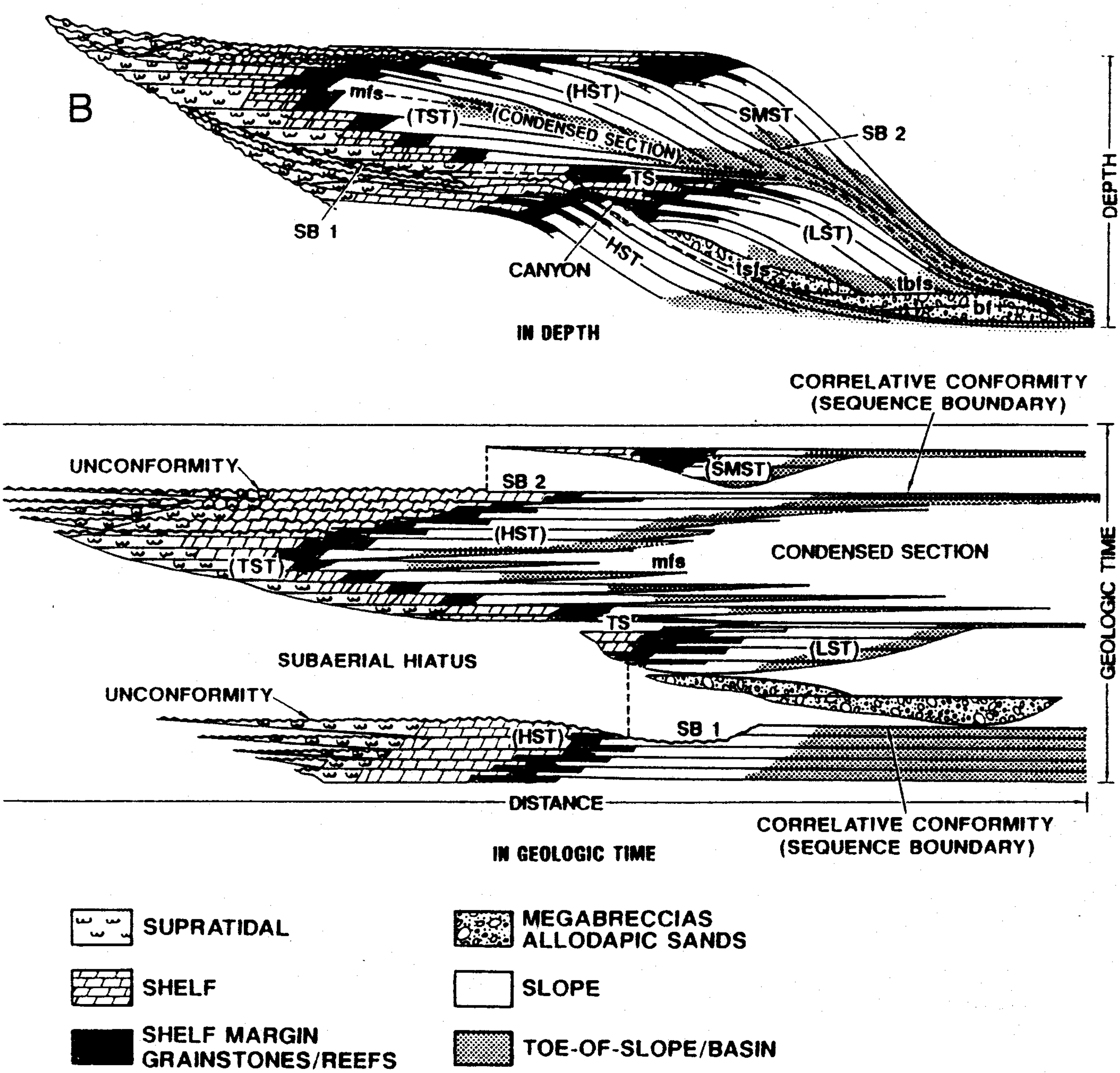

Figure 6B. Rock-based sequence stratigraphy and facies of a rimmed shelf with a relatively steeply sloping margin plotted in terms of depth (top) and time (bottom). Modified slightly from Vail (1987).

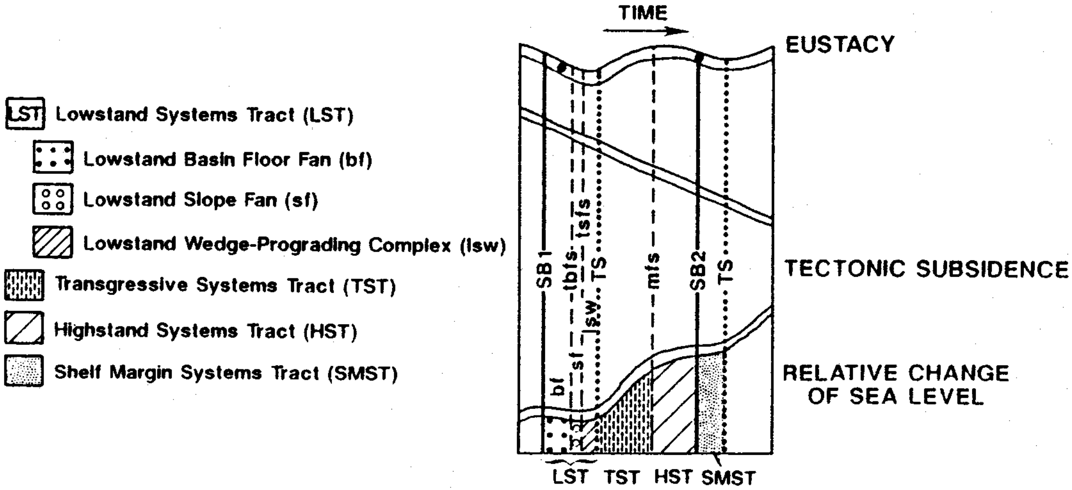

Figure 6 B continued. Interpreted relationship of systems tracts to eustatic sea level curve and relative sea level (After Vail, 1987).

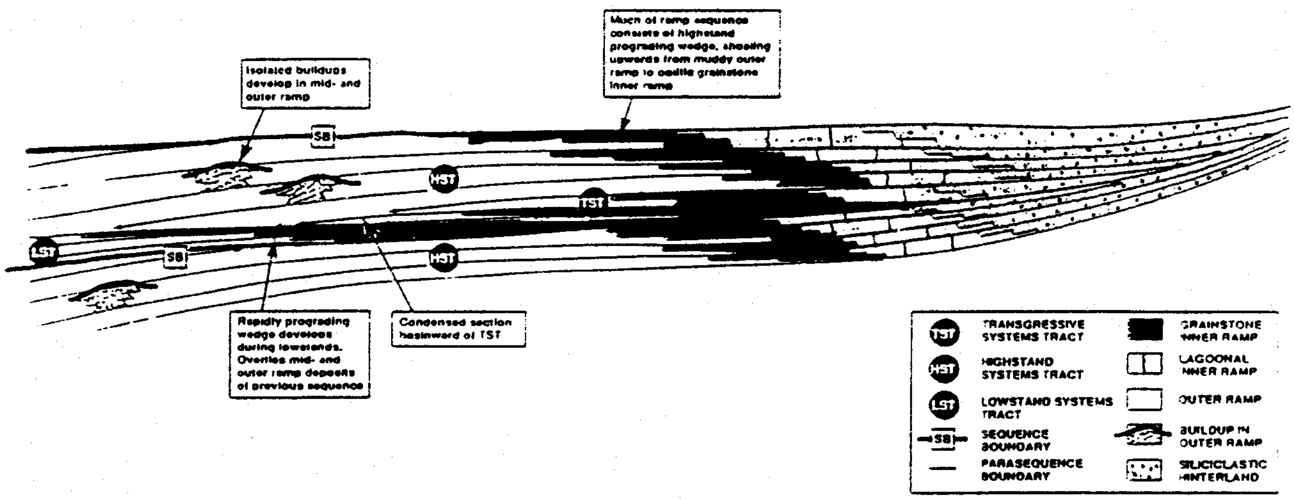

Figure 6C. Sequence stratigraphy and systems tracts of a carbonate ramp. Note that there is relatively little thinning downdip and that slopes are relatively gentle. Consequently, systems tracts merely move up or down the ramp rather than being influenced by sea level dropping of the edge of the platform as in rimmed shelves. From Burchette and W

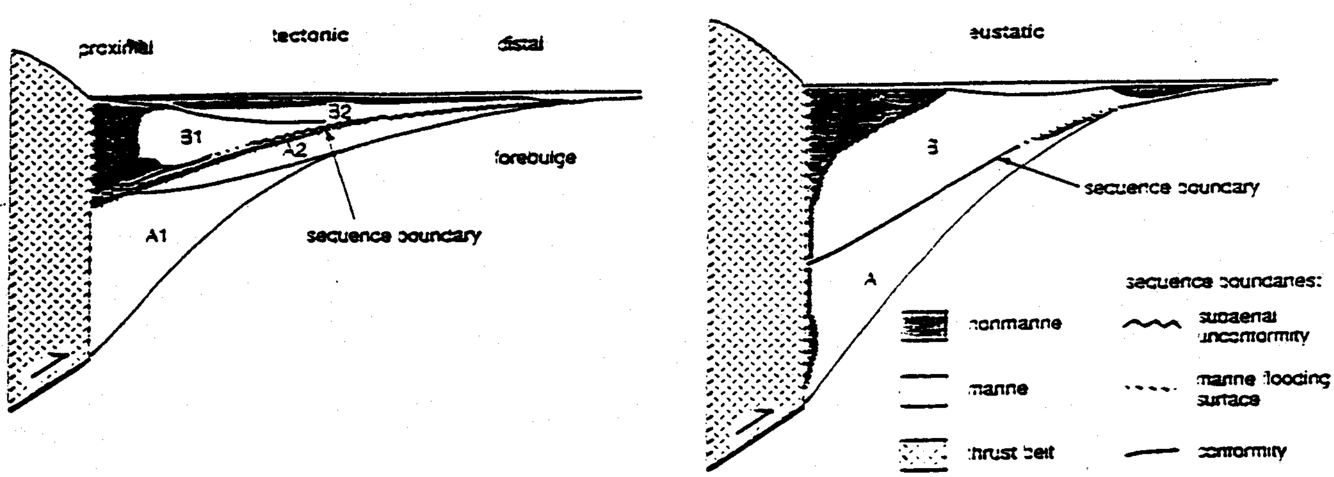

Figure 6 D. Cartoon showing differences in sequence stratigraphy in foreland basin with only episodic thrusting (top) vs a foreland basin affected only by eustasy (bottom). Labels A and B indicate depositional sequences. With episodic thrusting only (top), sweeping progradations occur during times of tectonic quiescence and proximal transgressive-regressive cycles are out of phase with the distal margin. With eustatic sea level change only, and steady thrusting (lower diagram) proximal shoreline movements are in-phase with distal transgressions and regressions. From Jordan and Flemings (1991).

line movements are in phase on the proximal vs distal margins. Actual basins probably reflect a combination of both of the above scenarios.

CYCLIC PLATFORMS AND DIAGENESIS ASSOCIATED WITH GREENHOUSE SMALL, HIGH FREQUENCY SEA LEVEL OSCILLATIONS

Key Features

During greenhouse times when there is little ice, high frequency 20 to 100 k.y. (and perhaps 3rd order) sea level fluctuations will be small. Carbonate platforms that formed under these small (perhaps less than 10 m) sea level fluctuations typically are aggraded and flat-topped to gently sloping. On rimmed shelves, isolated platforms and the inner parts of ramps, sections commonly have very shallow water to peritidal meter scale cycles or parasequences with regionally extensive tidal flat caps (Fig. 7A) because the tidal flats are able to prograde as fast as sea level falls off the platform. High relief buildups such as pinnacle reefs are absent from the shallow platform top (Koerschner and Read, 1989; Wright, 1992). The parasequences tend to have "layer cake" stacking patterns, arranged into large scale transgressive onlap and regressive offlap patterns within 3rd order depositional sequences (Read and Goldhammer, 1988; Koerschner and Read, 1989; Read, Osleger and Elrick, 1991). Fewer cycles develop on the slowly subsiding inner platform compared to the outer platform.

Disconformities are relatively poorly developed even though cycle tops may remain emergent for tens of thousands of years, because sea level only falls a short distance below the platform surface. Maximum emergence of individual cycle tops occurs during 3rd order sea level fall when regolith, siliciclastic- or tepee-capped cycles can develop (Goldhammer et al., 1990; Koerschner and Read, 1989). Tidal flat facies do not develop on many small carbonate platforms a few kilometers wide because of the high energy conditions; instead cycle tops can have dolomitic soils developed on subtidal beds (Goldhammer et al., 1990). The cycles are sub-seismic scale, and are typical of the Cambro-Ordovician of the U.S. Appalachians (Koerschner and Read, 1989; Demicco, 1985), Late Silurian and Early Devonian of New York (Goodwin and Anderson, 1985), many Mid to early Late Devonian platforms in Australia and North America (Read, 1973; Wendte and Stoakes, 1982; Elrick, pers. comm., 1992), and the Late Permian of the Permian Basin, U.S.A. (Borer and Harris, 1991).

Arid zone cycles have highly restricted, commonly oolitic and cryptalgal mound facies and intertidal laminite caps; cycles are partly to completely dolomitized by brines sourced from the tidal/supratidal surface (Fig. 7A). Reservoir facies can occur in fine laminated dolomite caps where intercrystal porosity is preserved, in cycle capping siliciclastics, or in interparticle and intercrystal porosity in variably dolomitized, subtidal grainstones; plugging of grainstone porosity by sulfate minerals can leave only the fine dolomites permeable. Reservoir thickness is rarely more than 2 to 3 m, and sabkha evaporites can provide extensive seals. This results in strongly stratified, layered reservoirs. The cycles are evident even in highly dolomitized core, and wireline logs are useful in identifying and correlating the cycles by picking out the evaporite cap.

Humid zone cycles commonly have very fossiliferous subtidal facies, and fossiliferous subtidal facies, and fenestral to rare supratidal laminite caps (Fig. 7B). Tops are planar to microkarsted, and can have be associated with shale. Aragonite fossils commonly are leached and fenestral porosity can be occluded by fibrous marine and vadose/phreatic sparry calcite cement. These cycles will be most porous in their lower part but cycle tops will have more primary porosity than their arid counterparts, such that internal seals will be poorly developed. Reservoirs will be layered and have permeability baffles. More homogeneous and better reservoirs will

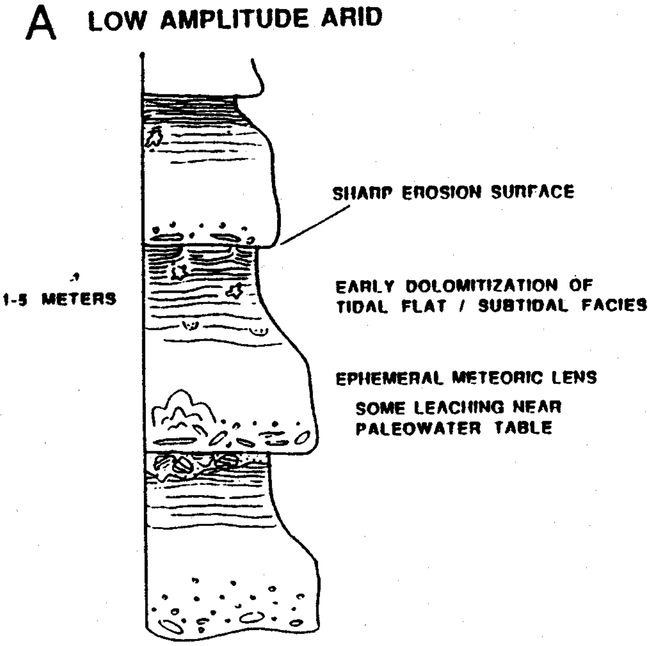

Figure 7 A. Idealized stratigraphic columns showing carbonate cycles generated under arid climate and low amplitude sea level fluctuations. Initially, only the tidal flat laminites are dolomitized, but with repeated progradation, cycles become completely dolomitized and there may be local leaching of aragonite beneath the flats.

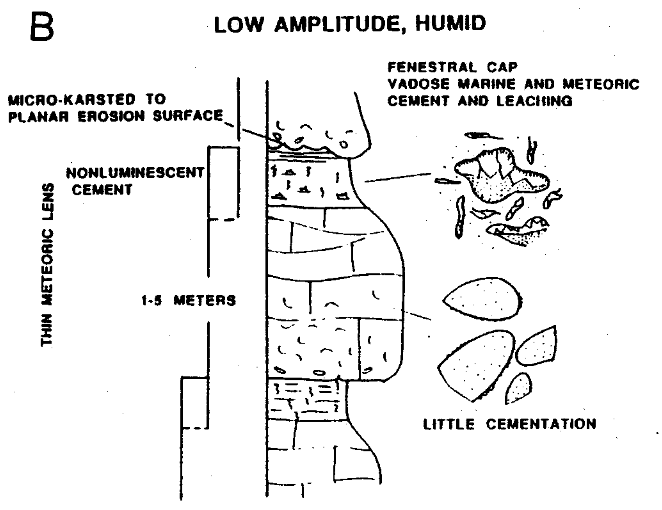

Figure 7 B. Idealized stratigraphic column of carbonate cycles generated during low amplitude sea level fluctuations in a humid climate. Marine vadose, meteoric vadose and possibly shallow phreatic cements are typically confined to the fenestral tidal flat cap which may show some micro-karsting. Laminites relatively scarce.

occur downdip in subtidal grainstone complexes. Cycles are subseismic scale and should be identifiable by modern wireline logs particularly if cycle boundaries have a clastic component.

Cambrian-Early Ordovician Cycles, Eastern U.S.A.: Examples of Greenhouse Cycles formed under Semi arid Climate: Extensive tidal-flat capped cycles of the Appalachian Late Cambrian-Early Ordovician passive margin (Knox-Beekmantown Group) (Fig. 7A) probably were formed under low amplitude Milankovitch sea level oscillations (Fig. 7C, D) with the cyclic record perhaps modified by autocyclic processes (Koerschner and Read, 1989; Osleger and Read,1991; Montanez and Read ,1992a,b; Goldhammer et al., 1993). These cycles host major petroleum and lead-zinc deposits whose localization is controlled mainly by the overlying unconformity, discussed later. Cycles are 1 to 5 m thick with lower parts of restricted subtidal thin bedded muddy carbonates, algal mounds, oolite, and regionally extensive caps of laminated dolomite with local, silicified evaporite nodules reflecting semi-arid climate (Mazullo and Friedman, 1975; Friedman, 1980).

Third order sequences are not easily defined on the basis of sequence bounding unconformities in the Knox Group, because the sequences are mainly conformable over much of the shelf (Fig. 7E). Thus sequence boundaries are actually zones of meter scale cycles. Third order sequences are evident on the outer platform by thick, shallowing upward, limestone rich TST cycles overlain by restricted, thin dolomite cycles of the HST and LST, some of which contain quartz sand and shale in the caps or reworked into the bases of overlying cycles; also, some of the late HST and LST cycles have brecciated tops (Hardie, 1986; Read and Goldhammer, 1988; Koerschner and Read, 1989) (Figs. 7 F, G and H). In the subsurface Rome Trough, some low stand systems tracts have evaporite rich dolomite cycles (Ryder et al., 1992).

Fischer plots (Fischer, 1964) in which cumulative cycle thickness corrected for linear subsidence, is plotted against time, provide a relatively objective way of defining the 3rd order sequences and the inferred 1 to 5 m.y. sea level cycles in the Knox Group because of the large number of meter scale cycles developed (Read and Goldhammer, 1988; Goldhammer et al., 1993) (Figs. 7G, H). The plots may be visualized as plotting departure from mean cycle thickness vs. cycle number (proxy for time) (Saddler et al., in press). Thus thick cycles form during times of increased accommodation rate (e.g. 3rd order rise) whereas thin cycles form during times of decreased accommodation rate (e.g. 3rd order falls). The Fischer plots are traceable interbasinally, suggesting that they are defining eustatic 3rd order cycles (Goldhammer et al., 1993).

Most of the dolomitization in the Knox Group was early and synsedimentary, which is indicated by dolomite clasts locally reworked across meter scale cycle boundaries into overlying subtidal limestones and under semi-arid climate (Mazullo and Friedman, 1975; Montanez and Read, 1992a). The dolomitization is virtually complete on the inner platform affecting both tidal flat caps, and subtidal facies. On the outer platform, only HST/LST are highly dolomitized; dolomite in the TST is restricted to laminite caps of cycles. Undolomitized subtidal parts of some cycles preserve minor evidence of meteoric diagenesis (aragonitic cements, meniscus cement, minor crystal silt, and some leaching of ooids). The laminated caps of cycles were dolomitized by brines beneath extensive tidal-supratidal flats (Fig. 7I). The dolomites initially appeared to have had heavy oxygen isotope values and low Fe and Mn and moderate intercrystal porosity. These dolomites were subsequently reset to varying degrees by replacement and overgrowth by burial dolomite resulting in non porous dolomites that geochemically resemble burial dolomites (Montanez and Read, 1992b).

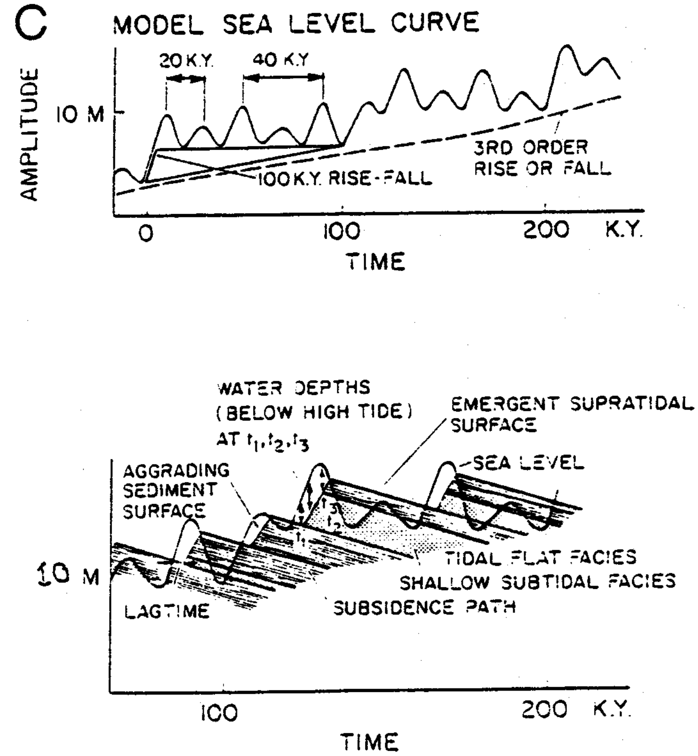

Figure 7 C. Computer model illustrating how carbonate cycles may form under small Milankovitch oscillations in sea level. Top: sea level curve and bottom, track of sediment surface and facies developed plotted on a time vs distance/stratigraphic thickness plot (Koerschner and Read, 1989).

Late Permian San Andres-Grayburg Cycles and Arid Zone Diagenesis, Permian Basin, U.S.A.: Late Permian (Lower Guadalupian) San Andres and overlying Grayburg dolomites are major oil reservoirs in the Permian Basin of West Texas (Major, Bebout and Lucia, 1988). The San Andres and Grayburg formations (Longacre, 1980; Harris and Stoudt, 1988; Chuber and Pusey, 1985; Hovorka et al., 1993) form two or three depositional sequences which are composed of many 1 to 10 m thick parasequences that are thoroughly dolomitized (Fig. 8). The parasequences were formed by small, high frequency fluctuations in sea level in relatively arid settings. Lower parts of depositional sequences are non-cyclic, open marine carbonates, or poorly cyclic, muddy carbonates with grainstone caps. These are overlain by thick successions of cyclic restricted shelf, mollusk-peloid dolopackstone/wackestone and local tidal flat dolomites, or toward the ramp margin by dolomitized grainstone dominated cycles (oolitic, peloidal or skeletal), some of which coarsen upwards and developed low relief over the crestal shoal. These parasequences are capped by erosion surfaces or local tidal flat facies. The upper parts of depositional sequences contain early dolomitized cyclic peritidal facies which form the superposed and marginal seals for the reservoirs. These peritidal facies are fenestral laminated, pisolitic and commonly have tepee structures, interbedded anhydrite, and may be capped by regional eolian siliciclastics.

The San Andres-Grayburg Formations underwent early dolomitization probably from hypersaline brines from tidal flats (Major et al., 1988). The high frequency cyclicity has generated porous reservoir zones up to 15 m thick, separated by relatively impermeable seals. Some reservoirs occur in dolomitized grainstone with interparticle and intercrystal porosity (Major et al., 1988; Hovorka et al., 1993). These grainstones appear to have undergone diagenesis in meteoric lenses beneath local tidal flats or bar crests; these meteoric lenses probably were related to high frequency sea level

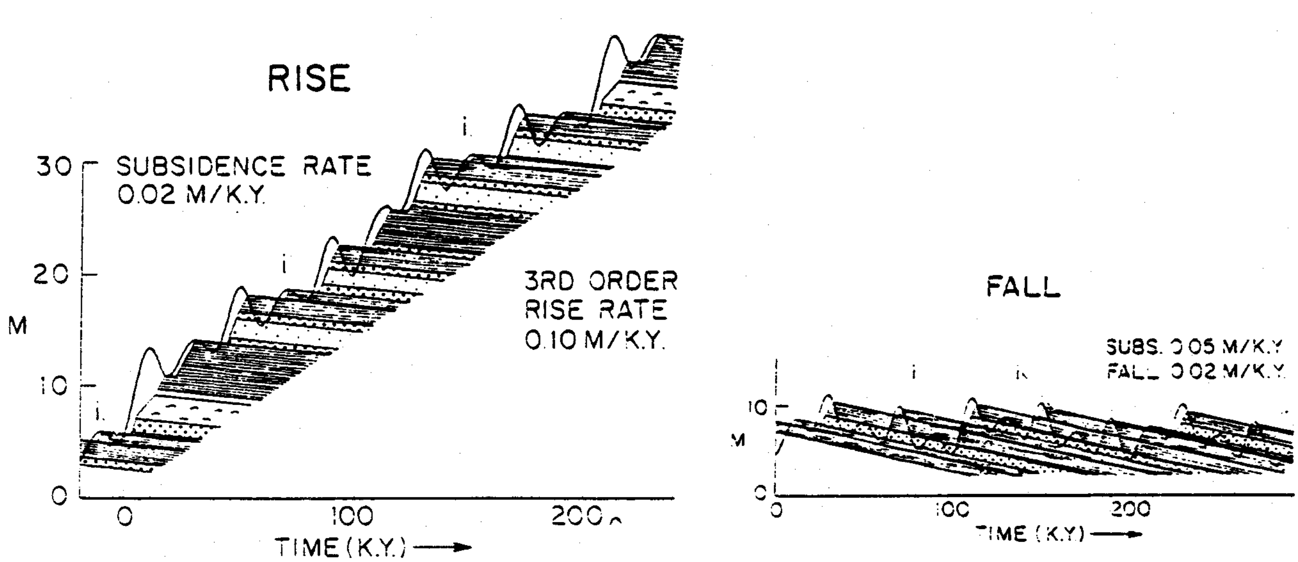

Figure 7 D. Computer model space-time plots showing how carbonate cycles are formed during long term sea level rise and superimposed Milankovitch sea level changes (left) and long term fall with superimposed Milankovitch sea level changes (right). The increased accommodation space on the rise allows more cycles to be formed (fewer missed beats) compared with the long term fall.

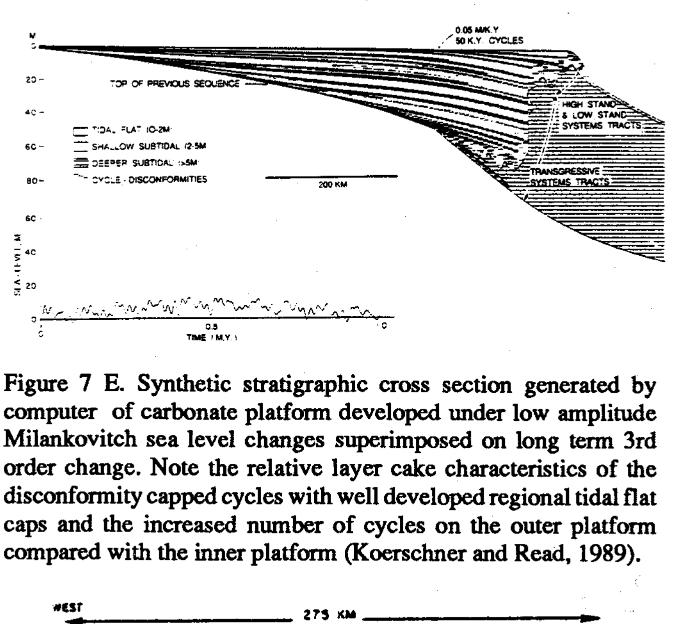

Figure 7 E. Synthetic stratigraphic cross section generated by computer of carbonate platform developed under low amplitude Milankovitch sea level changes superimposed on long term 3rd order change. Note the relative layer cake characteristics of the disconformity capped cycles with well developed regional tidal flat caps and the increased number of cycles on the outer platform compared with the inner platform (Koerschner and Read, 1989).

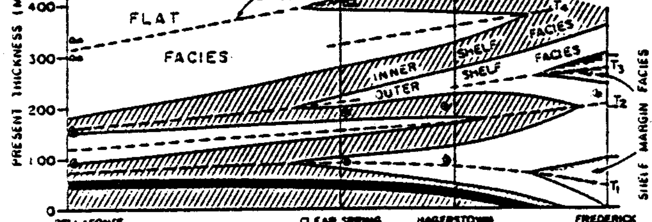

Fig. 7 F. Regional stratigraphic cross-section of the Early Ordovician Beekmantown Group showing depositional sequences in Pennsylvania and Maryland (Hardie, 1989). The transgressive-regressive cycles correspond to the portions of the Fischer plot in 7G labelled O-3 to O-6.

fluctuations that formed the parasequences (Hovorka et al., 1993). This caused leaching of the metastable grains, mineralogic stabilization, and partial intergranular cementation which helped preserve porosity against compaction. However, many grainstones became tight due to plugging by sulfate cement (Longacre, 1980; Chuber and Pusey, 1984). Many reservoirs also commonly occur in muddy skeletal carbonates that were dolomitized and leached; porosity in these is typically in fine grained dolomite with skel-moldic and intercrystalline porosity (Longacre, 1980; Harris and Stoudt, 1988).

<u>Late Permian Yates Carbonate-Siliciclastic Cycles and Arid Zone Diagenesis, Permian Basin, U.S.A.</u>: Regressive siliciclastic units capping peritidal cycles in the Late Permian (Late Guadalupian) Yates Formation, Permian Basin, form significant hydrocarbon reservoirs (Fig. 9). Carbonate-siliciclastic cycles interpreted to have formed under 4th order (100 to 400 k.y.) low amplitude eustasy occur in the Late Permian Yates Formation, Permian Basin, U.S.A. (Borer and Harris, 1991). On the inner shelf, the cycles are dominated by anhydrite, halite and red argillaceous siltstones. These pass into middle and outer shelf dolomite-siltstone-sandstone cycles. The carbonate parts of cycles are lagoon/tidal flat facies on the middle shelf to pisolite shoal facies on the outer shelf. The Permian carbonates were pervasively dolomitized by downward and seaward migration of brines generated from the evaporitic shelf (Adams and Rhodes, 1960). The siliciclastics relate to 4th order sea level falls, and are the major hydrocarbon reservoirs in the subsurface

<u>Diagenesis, Humid Climate and Low Amplitude Sea Levels, Middle Ordovician Peritidal Cycles, Virginia-Maryland</u>: The Middle Ordovician Limestones in Virginia (Knox unconformity to base of Bays-Moccasin formations) contains a large scale, 10 to 15 m.y. 2nd order depositional sequence, and three internal 3rd order sequences (Fig. 10A) but has been broken into many formations, many of which change names at county lines and artificially hinder the understanding of the regional stratigraphy and facies relations.

The peritidal parts of sequences contain many meter scale cycles that formed under humid climate and low amplitude sea level fluctuations, perhaps with an autocyclic component (Read, 1980; Read and Grover, 1977; Grover and Read, 1978; Mitchell, 1985)..

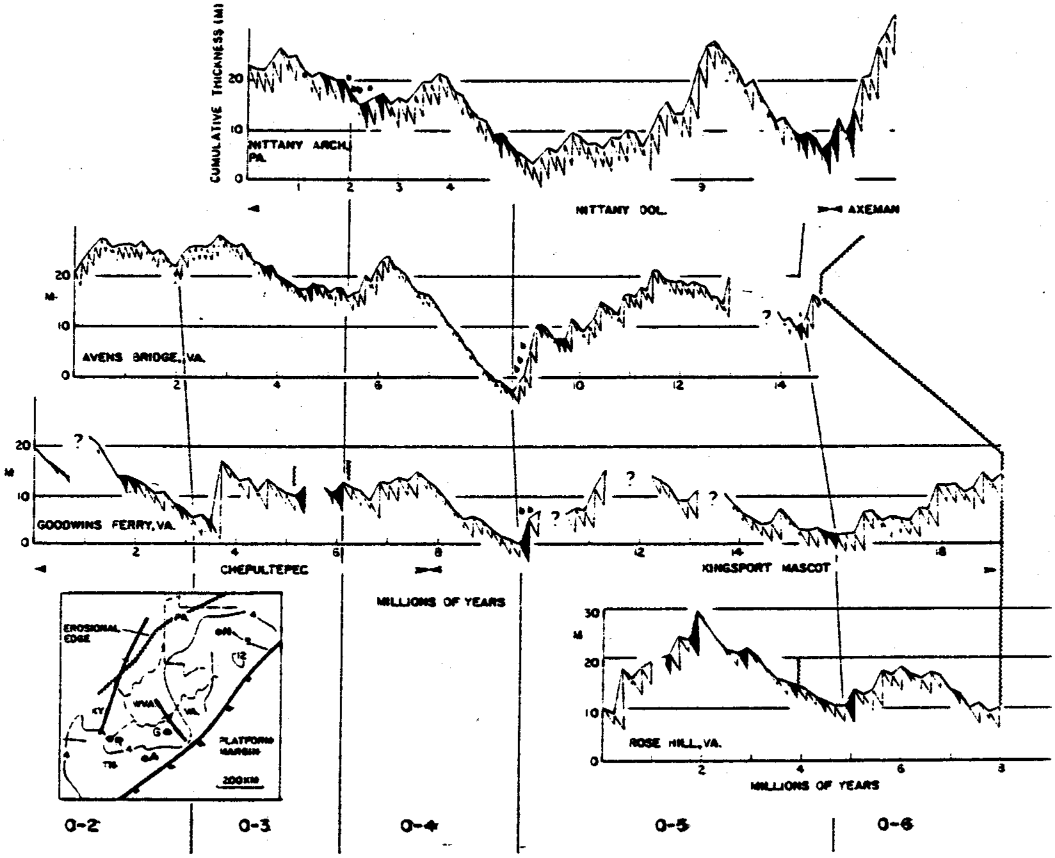

Figure 7 G. Fischer plots which graph changes in accommodation space for the Early Ordovician rocks, Pennsylvania to Virginia. Inset shows location of measured sections - N is Nittany Arch, PA., A is Avens Bridge, VA., G is Goodwins Ferry, VA and R is Rose Hill, VA. On the Fischer plots, small vertical lines are cycle thicknesses, and short inclined lines sloping down to right are linear subsidence paths for each cycle. Increases in accommodation are shown by wavy line sloping up to the right, whereas decreases in accommodation are shown by lines sloping down to right. Note the relatively good correlation between the plots, and the tendency for quartz-rich cycles (black) to occur on the long term falls. The plots probably reflect eustatically driven accommation changes, because they can be correlated over very large regions. From Read and Goldhammer, 1988).

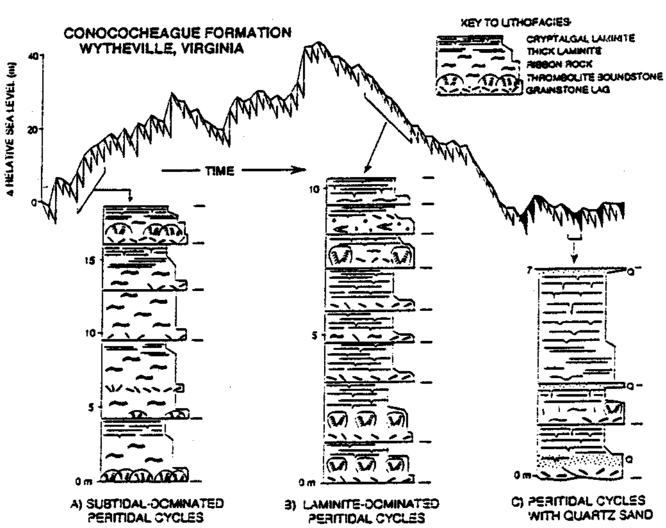

Figure 7 H. Fischer plot of Late Cambrian cycles in the Virginia Appalachians, Wytheville, measured by Koerschner and Read (1989), from Osleger and Read (1991). Plot shows well defined 3rd order rise-fall, with quartz sandy cycles on the low stand. Stacking patterns of representative cycles are shown below their position on the plot. Note the difference in scales on the 3 columns, and the thick open marine cycles that developed on the rise, vs the thin peritidal cycles that formed on the fall.

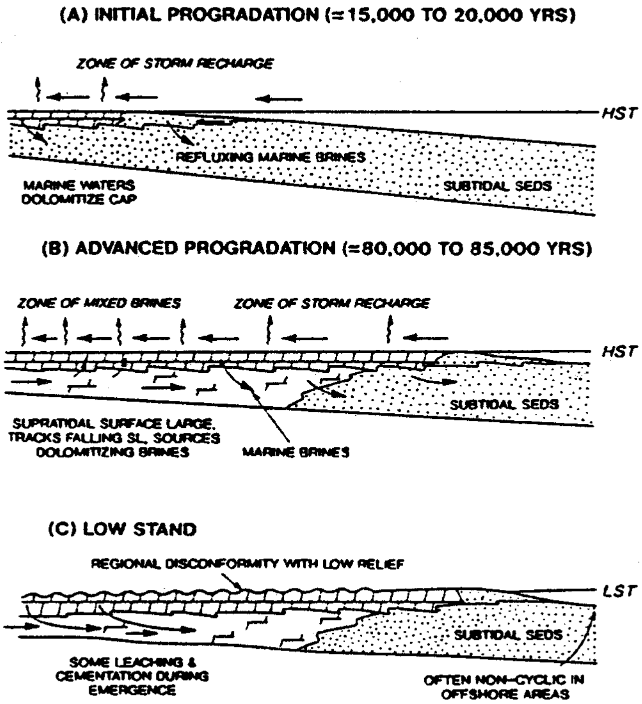

Figure 7 I. Schematic diagram of the hydrology of an arid tidal flat, modified from McKenzie, Hsu and Schneider (1980) and Montanez and Read (1992b). The carbonate cycle consists of a lower, subtidal unit and a capping unit of tidal flat laminite. Undolomitized limestone shown by stippled pattern; dolomite is shown by standard dolomite "brick" pattern. HST and LST are highstand sea level and lowstand sea level. A) Highstand situation during intial progradation when dolomitizing brines are generated by evaporation of tidal and storm flooding of flats. B) Situation during fallina sea level after considerable progradation of flats. Updip, the supratidal surface becomes a disconformity, and continental waters may mix with marine brines generated by storm recharge. Much of the inner platform section becomes dolomitized by refluxing brines. C) At the low stand of sea level, much of the supratidal surface becomes a regional disconformity, and minor leaching of subtidal facies beneath the laminite cap may occur.

Cycles are restricted to inner ramp settings, and cannot be traced downdip into marine units. Supratidal cyclic facies are best developed in Maryland (Row Park-New Market of the St Pauls Group), and consist of meter-scale cycles of filament-rich but otherwise unfossiliferous LLH stromatolites (coastal fresh water lake/marsh) to thin bedded, filament-rich micrites (marsh) or supralittoral mudcracked laminites (Mitchell, 1985; Hardie, 1986) (Fig. 10B). The more open marine Virginia cycles (Blackford-Elway-Five Oaks formations) are 1 to 10 m thick, and consist of open marine skeletal limestone, up into pellet limestones and then into tidal flat caps of fenestral and rarely laminated limestone topped with planar to scalloped, microkarstic surfaces.

Dolomite is rare and restricted to rare beds of supratidal intraclastic packstone. The cycles show much vadose to shallow phreatic meteoric diagenesis which is limited to upper parts of cycles reflecting development of a shallow meteoric ground water system during emergence and a wet climate (Grover and Read, 1978; Read and Grover, 1977; Grover and Read, 1983) (Fig. 10C and D). Some cycle tops are microkarsted and several of these surfaces are regional. Microkarstic surfaces have mud-filled solution enlarged fissures and the subjacent beds have leached aragonite shells and fenestral and moldic pores with pendant and pore-rimming early fibrous- and sparry calcite cement linings (zoned nonluminescent) and crystal- and pellet silt fills, typical of vadose meteoric diagenesis (Grover and Read, 1978; Dunham, 1969) (Fig. 7B).

CARBONATE SEQUENCES, CYCLES AND DIAGENESIS ASSOCIATED WITH MODERATE AMPLITUDE, 4TH /5th ORDER SEA LEVEL FLUCTUATIONS

Moderate fluctuations (perhaps 20 to 50 m range) in high frequency sea level should typify times when the globe is transitional between ice house and green house conditions. Such times might include the Early to Late Ordovician, Early to Late Carboniferous, Early to Late Permian and the early Tertiary (Fig. 2A).

Key Features

Parasequences that formed under moderate fluctuations in sea level (20 to 50 m magnitudes) tend to be less layer cake than low amplitude cycles. Instead the cycles have a moderately shingled arrangement on the platform, reflecting moderately large 100 to 400 k.y. sea level fluctuations which cause large scale horizontal migration of peritidal deposystems during 20 to 40 k.y. sea level fluctuations (Read, Osleger and Elrick, 1991)(Fig. 11A). Outer ramp cycles can have deeper subtidal argillaceous limestone in lower parts, beneath grain-rich shallow water caps, due to rapid deepening during high frequency transgressions. These deeper water tongues die out onto the inner platform, where cycles commonly are grainstone-dominated. Tidal flat facies cap only a few cycles generally, which instead have karstic erosional tops developed on shallow subtidal facies (Figs. 11B,C) (Horbury, 1987; Horbury and Adams, 1989; Wright, 1992). Tidal flat facies can form linear belts on some platform cycles during 4th and 5th order high- and low stands of sea level (Fig. 11A), but regional tidal flat capped peritidal facies appear to be best developed during 3rd order (1 to 10 m.y.) high stands (Elrick and Read, 1991)(Fig. 11D). It is not clear whether this just is due to decreased accommodation or due to lowered 5th order amplitudes during 3rd order highstand deposition, compared with the transgressive systems tract.

Depositional porosities are highest in grainy upper parts of cycles, and porosity zones tend to be thicker (up to 10 m or more) than the lower amplitude cycles. Also, argillaceous, muddy lower parts of cycles tend to act as partial internal seals resulting in subseismic stratified reservoirs. Arid zone carbonate cycles (Fig. 11B) can have porosity in tops of cycles plugged by caliche formation and vadose fibrous cements. Subtidal grainy parts of cycles lack early sparry cements and retain much primary porosity. Regionally prograding peritidal dolomites and evaporites can form seals to 3rd order sequences. Humid zone cycles (Fig. 11C) may show some karsting and soil formation at cycle tops, while upper parts of cycles undergo some moldic and vuggy dissolution, along with plugging of primary and secondary porosity by vadose and upper phreatic sparry calcite cements. Middle or lower parts of cycles, if grainy, may be less well cemented and retain more primary porosity. Muddy cycle bases undergo stabilization of carbonate muds in meteoric waters and some moldic porosity formation. Because of development of thick ground water zones, meteoric diagenesis may extend down into underlying older cycles, if seals are poorly developed. Sub-seismic pre-burial reservoirs will be stratified, with relatively homogeneousporosity and some permeability baffles, and should be identifiable from cores and electric logs.

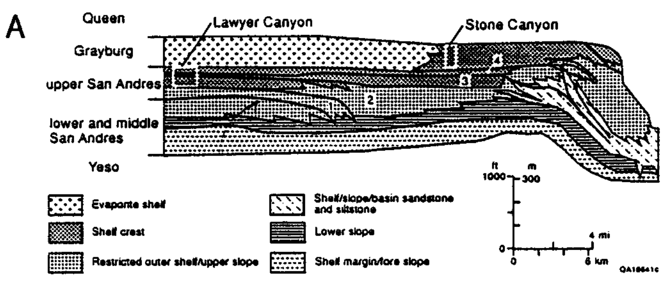

Figure 8A. Low amplitude Permian cycles of the San Andres-Grayburg formations, Guadalupe Mountains, New Mexico (from Hovorka et al., in press). Regional cross section.

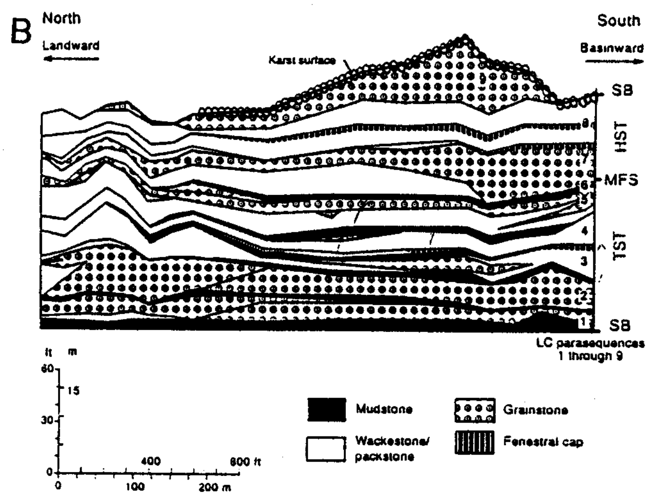

Figure 8B. Detailed cross section of basal upper San Andres depositional sequence, Lawyer Canyon, showing mudstone to wackstone/packstone to grainstone to fenestral capped cycles, and regional karstic surface at the sequence boundary.

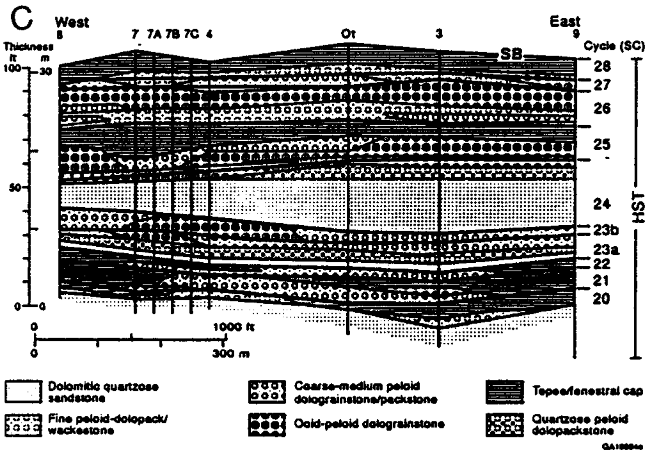

Figure 8 C. Detailed cross section of Grayburg Formation showing tepee/fenestral or dolomitic sandstone capped grainstone cycles of the HST and the sequence boundary. Note that in both the cross sections, diagenesis associated with paleo-groundwaters during high frequency sea level drops modified and helped to preserve the porosity and in some cases caused enhanced permeability.

Diagenesis, Humid Climate, Moderate Amplitude Sea Levels British Dinantian (Mississippian) Cycles (modified from A.Horbury): Northern British Mississippian cycles were formed on isolated- and land-attached rimmed shelves (Somerville, 1979a,b; Walkden, 1987; Horbury, 1989). Cycles are capped by 30 or more well developed paleokarstic surfaces (Fig. 11C) and have periodicities of 100 to 200 k.y. and are related to onset of Permo-Carboniferous Gondwana glaciation. Cycles are made up of skeletal and peloidal packstone and grainstone (and rare oolite and fenestral mudstones) in upwards shoaling units. Regression was rapid as indicated by subaerial exposure surfaces and paleosols directly on subtidal facies (Horbury, 1989; Walkden and Walkden, 1990). Paleosol fabrics are complex (Davies, 1991), and reflect a dry-wet-dry cycle (S. Vanstone, pers. comm. 1992), which is probably related to 5th order climatic cyclicity superimposed on 4th order climate cycles (Gray, 1981, quoted by Tucker, 1985). They comprise a thin, rooted rhizoconcretionary interval up to 1 m thick (semi-arid phase), cut by a clay-covered, mammilated paleokarst with up to 2 m relief (wet phase) (Walkden, 1987; Horbury, 1989). Superimposed later fabrics such as laminated caliche and breccia (semi-arid phase) are rare.

In cycles on the isolated rimmed platforms, the shallowest subsurface meteoric cements are rare pendant and ponded vadose brown fibrous cements, and brown equant cements which are very dull luminescent and related to calcrete mottle formation in soil zones. These are the dry climatic phase and were short-lived rapid precipitation events in localized diagenetic environments (Horbury, 1987; Horbury and Adams, 1989). There also are shallow (5 to 15m depth) meteoric cements, which formed by reprecipitation of the bulk of the calcite dissolved beneath the paleokarst, probably during the wet climatic phase. These cements are volumetrically abundant and are clear nonluminescent calcites with very fine bright subzones which cannot be correlated for more than a few millimeters. They develop on all substrates but are thicker as syntaxial cements and are best developed close (5 to 15m) beneath the paleokarst from which they are sourced (Horbury and Adams, 1989). In contrast, deeper in the phreatic lenses, well developed correlatable zoned clear calcite cements occur (Fig. 11C). These are a volumetrically insignificant but important cement type that formed by slow precipitation of calcite in deeper (15 to 120 m subpaleokarst) parts of meteoric lenses of successively younger paleoaquifers. These cements only occur where rimmed shelves are relatively isolated from probable laterally-sourced meteoric water, e.g. areas of permanent emergence such as onlap margins onto basement. Each emergent event was recorded by growth of a couplet of bright to non-luminescent cement. Hence there are roughly the same number of cement couplets as there are eustatic cycles containing these cements (Fig. 11C). Where meteoric lenses rested on a shale aquitard, the cement couplets are most abundant low in the section, and decrease upward into younger cycles. They extend over a limited vertical range beneath the parent paleokarst surface, with younger couplets progressively appearing upsection (Horbury and Adams, 1989).

Each isolated rimmed platform developed different cement stratigraphies because the response of each structural unit to subsidence, the facing direction, connectivity to larger oceanic water masses and input of clastics from nearby basement terrains all influenced the detailed vertical and lateral facies mosaic on each platform. Because on an isolated platform, the availability of metastable carbonate from karst dissolution is a function of facies thicknesses deposited prior to emergence, differences between platform cements and trace elements precipitated from meteoric systems reflect the individual subsidence history of each platform, even though the mechanism that triggers cementation is eustatic. Horbury and Adams (1989), found much small scale internal variation and correlation problems with this morphology of cement where local

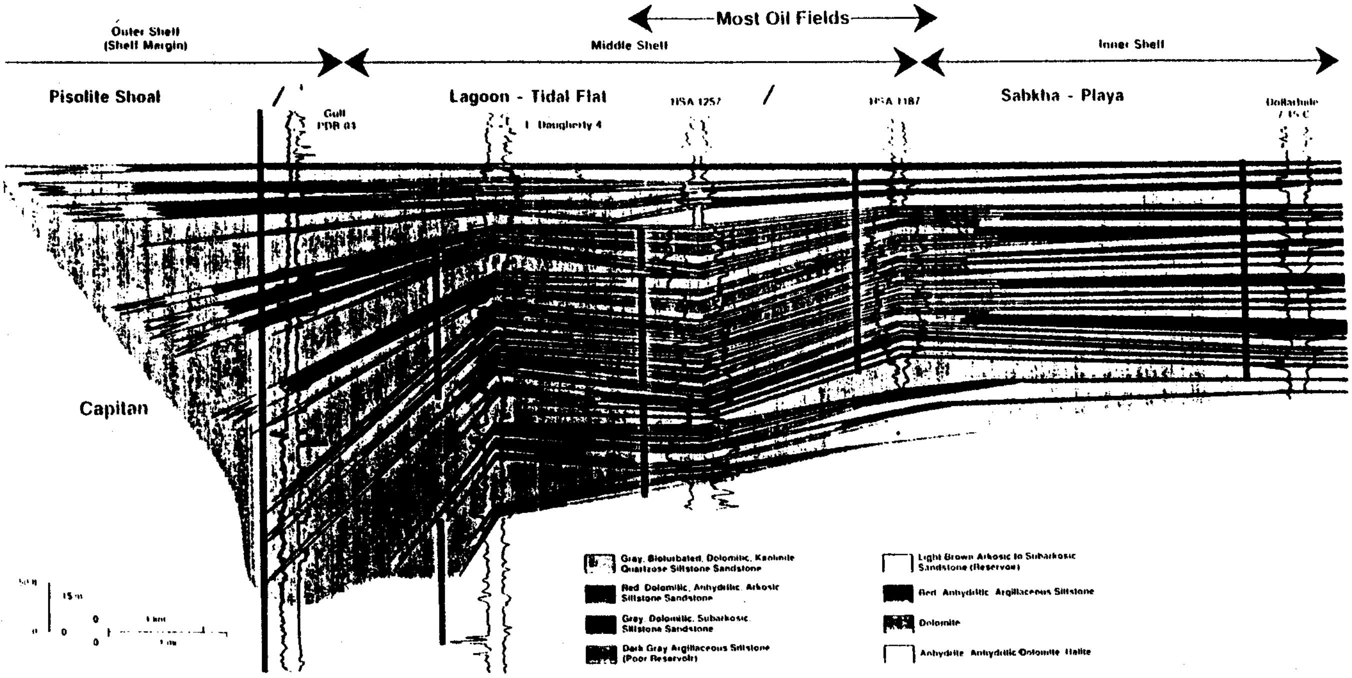

Figure 9 Composite dip oriented cross section showing distribution of siliciclastics lithofacies, in Late Permian Yates Formation, Central Basin platform, Texas. For each well gamma ray log is on right and density log is on left. From Borer and Harris, 1991.

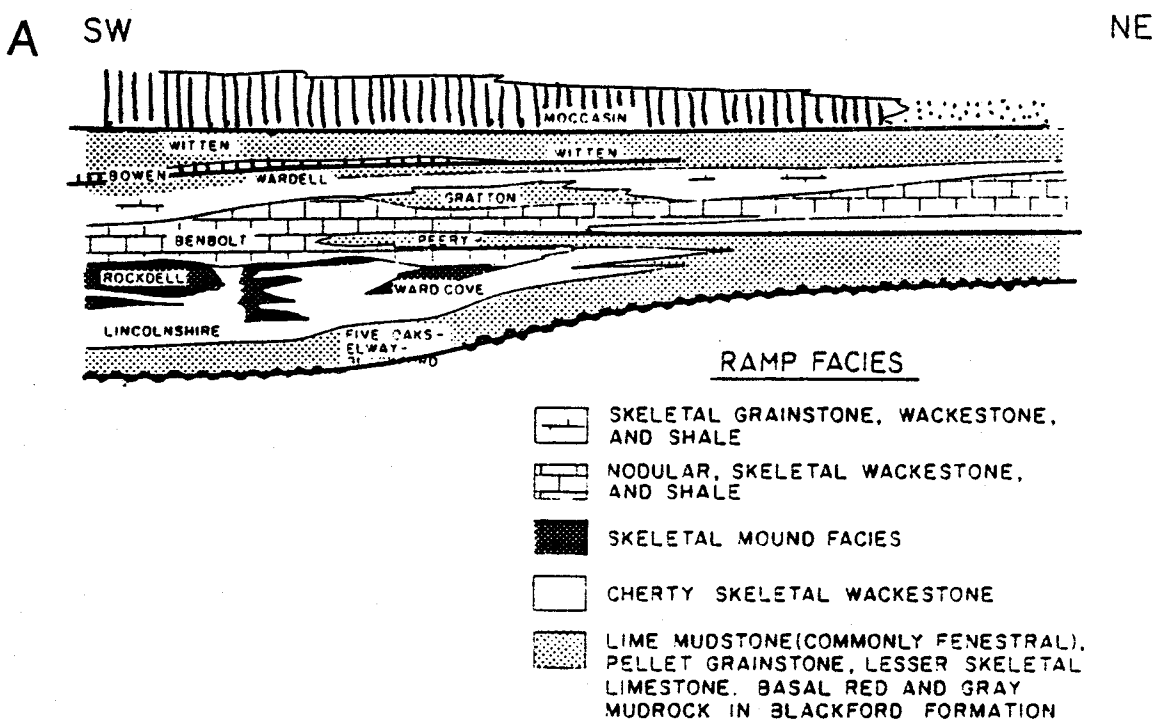

Figure 10 A. Stratigraphic cross section of the Middle Ordovician Limestones, Virginia (mainly Chazy-Blackriveran). Well developed humid zone cycles that formed under low amplitude fluctuations of sea levelf occur in the peritidal Blackford-Elway-Five Oaks succession; in the Wardell to Witten interval the cycles appear to reflect a slightly more arid setting.

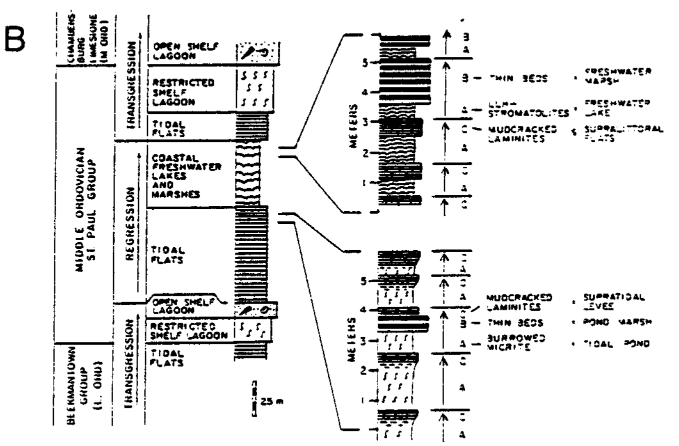

Figure 10 B. Facies succession and shallowing upward tidal flat cycles in the Middle Ordovician St. Paul Group, Maryland (Hardie and Shinn, 1986). These represent the updip equivalents of the lower part of the Middle Ordovician sequence in 10A.

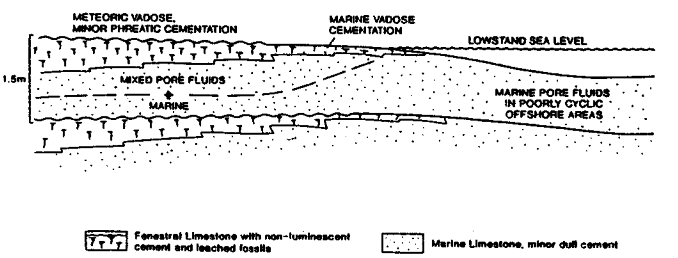

Figure 10C. Schematic diagram illustrating tidal flat diagenesis in non-channelled tidal flats under humid climate. A shallow meteoric vadose and phreatic zone of freshwater (less than 2 m) is generated on the inner parts of tidal flat, beneath a microkarstic surface. To seaward, tidal flats are subjected to marine vadose diagenesis.

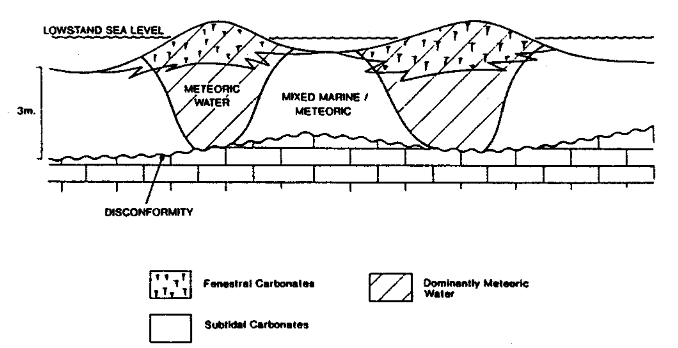

Figure 10 D. Schematic diagram showing lenses of meteoric water beneath local highs ("levees and palm hummocks") of channelled tidal flats under humid climate (modified from Gebelein et al., 1980).

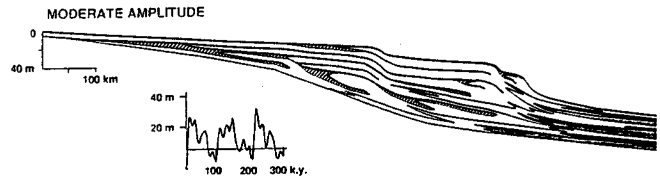

Figure 11 A. Synthetic stratigraphic cross section generated under moderate amplitude Milankovitch sea level fluctuations. Under these conditions the tidal flats are not regional but are restricted to still stands of sea level, thus they commonly occur in downdip positions and pass updip into disconformities (Read et al., 1991). The small carbonate cycles are much less regional when compared to those formed under lower amplitude fluctuations of sea level.

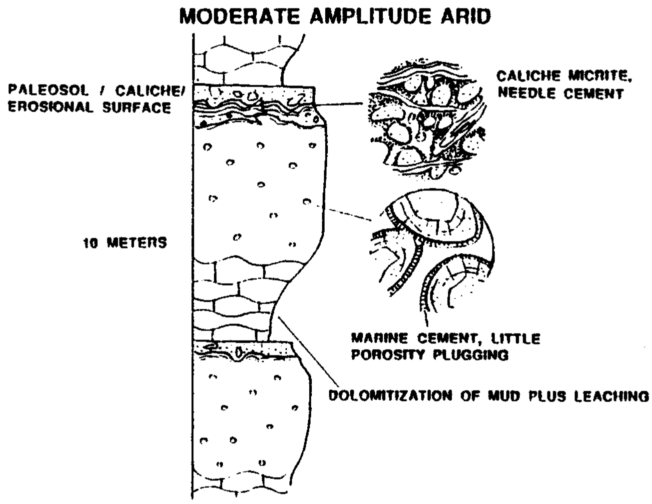

Figure 11 B. Oolitic carbonate cycles formed under moderate amplitude Milankovitch sea level fluctuations and arid climate.

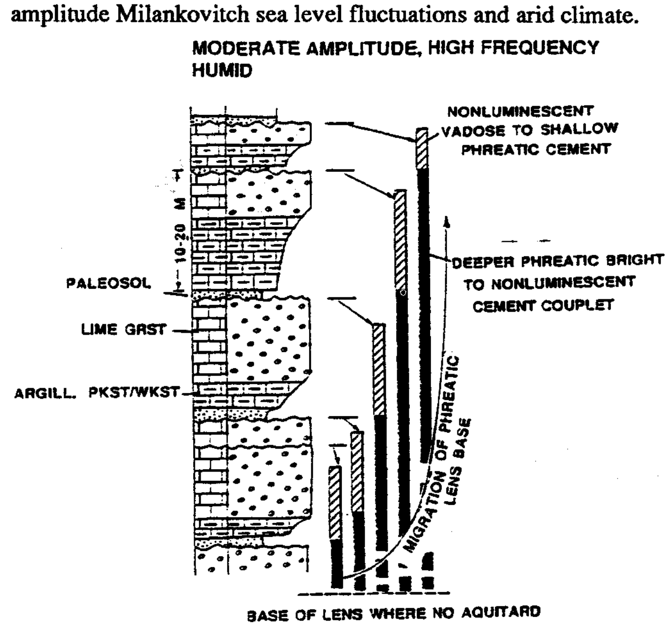

Figure 11 C. Typically skeletal carbonate cycles formed under moderate amplitude Milankovitch sea level fluctuations and humid climate (modified from Horbury and Adams, 1989). Repeated sea level fluctuations causes establishment of successive, thick meteoric lenses and their distinctive cement zones that are superimposed on earlier cements, especially in lower parts of lenses.

topography influenced flow patterns in the meteoric lens, for example close to the emergent platform and low stand margin where surface water runoff was into 30 m paleovallies.

Cyclically exposed land attached-platforms possess many of the diagenetic features noted above, but phreatic cement zones are not correlative, possibly because they formed in locally developed meteoric lenses fed by lateral flow from permanently emergent areas (Horbury, 1987; Horbury and Adams, 1989).

Diagenesis Under Arid Conditions and Moderate Amplitude Sea Levels Late Mississippian, Eastern U.S.A.: These cycles formed on a broad ramp and are dominated by oolitic and skeletal grainstone cycles up to 6 m thick, capped by microkarsted surfaces, local caliches and detrital chert; caliches are best developed at the 3rd order sequence boundaries (Niemann and Read, 1988; Nelson and Read, 1989; Al-Tawil, pers. comm., 1992). Lagoonal and tidal flat facies are relatively rare capping cycles. The semi-arid climate inhibited diagenetic alteration during the moderate amplitude fluctuations because meteoric ground waters were poorly developed. Subaerial diagenesis was mainly restricted to upper parts of cycles where caliche crusts and detrital carbonate- and chert-veneered erosion surfaces formed (Niemann and Read, 1988; Harrison and Steinen, 1978). The main cements within the caliche profiles are fibrous turbid cements (needle fiber calcites), micrite coatings on grains and rhizocretions formed by carbonate precipitation on roots and rootlets (Fig. 11B); sparry calcite cementation and leaching was relatively minor until the Late Mississippian-Early Pennsylvanian when the climate became humid (discussed later). Because there was little early sparry calcite cementation of oolitic grainstone facies during 4th/5th order sea level falls, the distribution of the hydrocarbon reservoirs is tied to the lateral and vertical distribution of grainstone bodies. Intergranular porosity was decreased in more deeply buried downdip sections by over-compaction during burial. Chalky microporosity is important in some of the gas reservoirs in the oolite units, although it is not clear whether this relates simply to later emergence and sequence-bounding unconformity development or is due to burial fluids.

Mississippian of Wyoming-Montana: The Early Mississippian Madison Group in the U.S. Rocky Mountains predominantly formed under moderate amplitude sea level fluctuations (Elrick and Read, 1991), perhaps interspersed with times of lower amplitude fluctuations during 3rd order highstand. The Madison Group consists of a supersequence, composed of basin/deep ramp to shallow ramp to tidal flat/sabkha facies and solution collapse breccia (Lodgepole-Mission Canyon-Charles Evaporites). The supersequence has several 3rd order sequences with well developed 1 to 10 m thick parasequences or cycles (Dorobek, pers. comm., 1991); Elrick and Read, 1991) (Fig. 11D). Transgressive systems tract cycles in the Lodgepole Formation consist of commonly dolomitized skeletal wackestone/mudstone passing up into ooid grainstone with erosional tops; downslope, the cycles are deeper water, laminated or burrowed dark muds that grade up into storm-deposited skeletal/oolitic packstone-grainstone caps. Tidal flat facies are generally absent. In contrast, high stand systems tract cycles are dominated by dolomitized thin peritidal cycles of subtidal oolitic/pelletal carbonates overlain by tidal flat laminated caps. Modelling of the cycles suggested that the parasequences were formed by moderate (40 m) fluctuations in sea level, in order to generate transgressive systems tract, oolitic cycles free from tidal flat facies on the shallow ramp while at the same time deeper water mud up into storm-deposited grainstone cycles were forming on the deep ramp/slope. However, the high frequency sea level fluctuations needed to be reduced in magnitude in order to generate the well developed tidal flat capped cycles of the high stand systems tract. This raises the likelihood of the high frequency sea level fluctuations being highest in transgressive systems tracts, and decreasing into the high stand systems tracts.

The Whitney Canyon-Carter Field, Wyoming is in the Madison Group and is volumetrically the largest gas producer in the U.S. Rocky Mountains (Harris, Flynn and Sieverding, 1988). Most production is from over 100 m of porous fine dolomite interbedded with fine calcitic dolomite and tight lime grainstone. This porosity zone is underlain by fine grained, deeper water basinal limestone and overlain by a fractured and brecciated section of sabkha limestone and dolomite. In the main porosity zone, the best reservoirs occur in cycles of porous fine grained, dolomitized subtidal wackestone/mudstone overlain by tight crinoidal grainstone. The fine to very fine grained dolomite forms the reservoir facies and has intercrystal porosity along with skel-moldic porosity. The dolomites likely were generated from brines from the overlying, thick prograding evaporitic sabkha facies in the upper Madison Group. These brines refluxed downsection to dolomitize permeable subtidal wackestone/mudstone but not the cemented (?) grainstone units which now form tight limestone units. The Mission Canyon dolomites were subsequently modified in meteoric or mixed water environments recharged from the overlying unconformity (Dorobek et al., in press). The tight lime grainstones may have escaped dolomitization because they were already cemented (Harris, Flynn and Sieverding, 1988), although Dorobek et al. (in press) considered the much of the Mission Canyon calcite cements post-date the early dolomite.

Limestones in the Frobisher-Alida zone of the Upper Mission Canyon, Glenburn field, produce from stacked porosity zones. Some of this porosity occurs in carbonates previously described as marine algal and oolitic facies, and reinterpreted as subaerial carbonates (Gerhard, 1985). These facies include vadose pisolite and carbonate crusts, with much vuggy interparticle and fenestral porosity. Porosity development was in part coeval with anhydrite deposition in pans and sabkas suggesting that the waters involved in forming the vadose fabrics were periodically hypersaline. These anhydrites form the updip and overlying seals.

Mid-to-Late Ordovician Red River Group, Williston Basin of Montana and North Dakota: The predominantly Late Ordovician Red River Group in Montana likely formed under moderate amplitude, high frequency oscillations under arid conditions since at this time there was an important Gondwana glaciation during a "greenhouse" time of high CO2 (Fischer, 1982; Crowley and Baum, 1991). The Red River Group contains at least 2 to 3 upward shallowing cycles 10 to 20 meters thick, which are stacked in a thinning upward package. Cycles are composed of subtidal burrowed carbonate passing up into laminated dolomite and basin wide anhydrite caps (Longman, et al., 1983). The laminated dolomite and evaporite facies in the various fields have been interpreted on the basis of presence or absence of structures indicating emergence, as subtidal shallow basinal caps of "brining-upward" cycles (Longman et al., 1983) or tidal flat/sabka facies with solution-collapse features (Derby and Kilpatrick, 1985).

In the Cabin Creek Field, cycles have disconformable, solution brecciated tops and evaporites are poorly preserved (Derby and Kilpatrick, 1985). The fine to microcrystalline dolomites are stratiform and are considered to have formed in and beneath sabkas and the sulfate minerals leached by meteoric waters to form the dominant vuggy reservoir porosity of the dolomites along with the intercrystal porosity. In contrast, fields described by Longman et al. (1983) have numerous pods of porous dolomite up to 60 m thick and 1.6 km diameter, which form the petroleum reservoirs below the

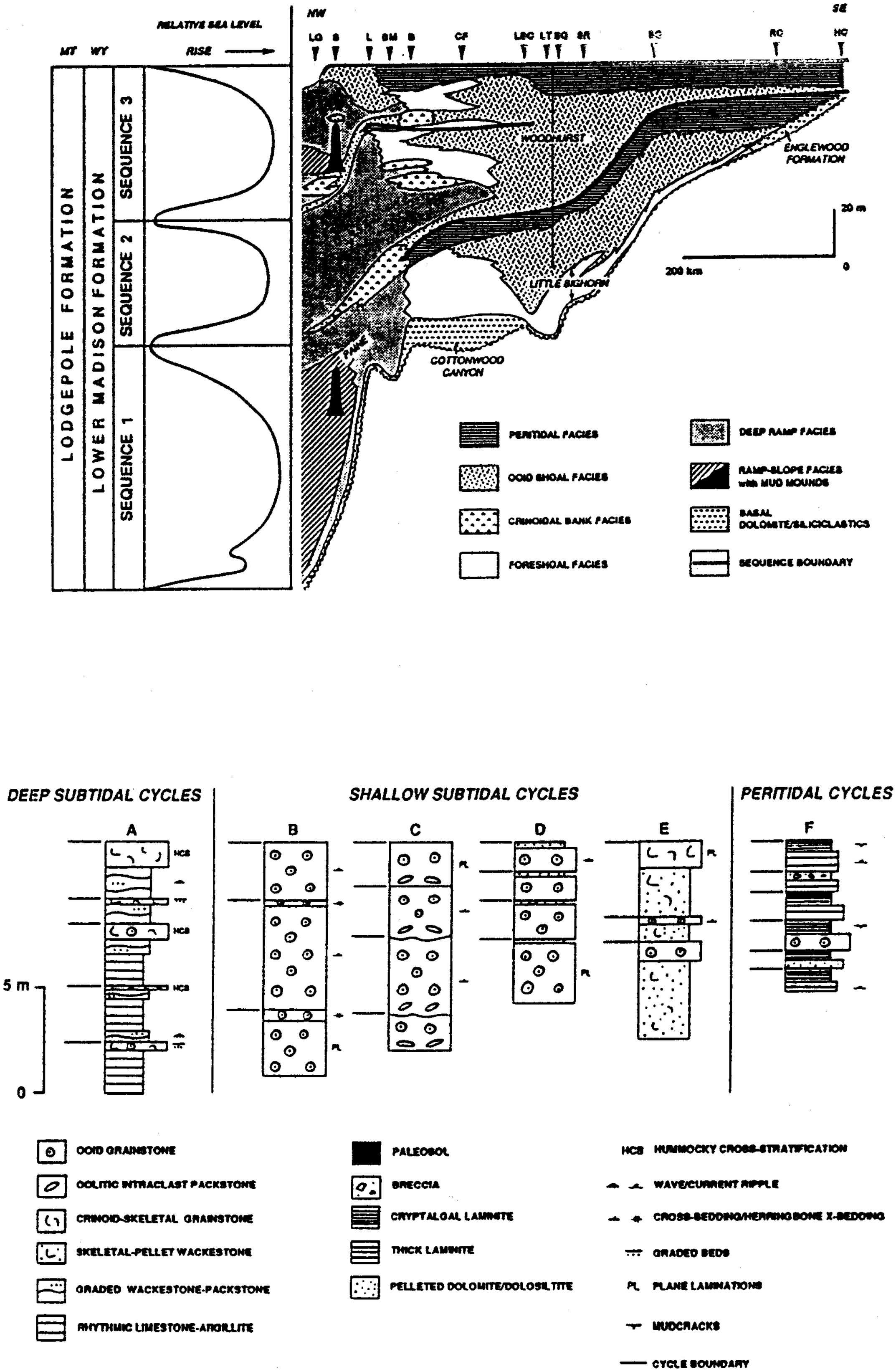

Figure 11D. Top: regional cross section approx. 700 km long, showing depositional sequences in the Mississippian Lodgepole Formation, believed to have developed under high frequency, moderate amplitude eustasy (Elrick and Read, 1991). Bottom: examples of cyclic carbonates from the inner ramp, outer ramp and slope. Note the relative scarcity of tidal flat facies except within the HST (Elrick and Read, 1991).

lowest ('C') anhydrite. The regional distribution of the dolomite pods marked by concentric distribution of cryptocrystalline dolomite passing out and downward into porous fine and medium grained reservoir dolomite, and then into tight partly dolomitized burrowed limestone, suggest a model of reservoir dolomitization by brine seepage through holes in the anhydrite during or immediately after anhydrite deposition (Longman et al., 1983). This dolomite porosity probably was significantly enhanced by burial leaching (R. Perkins, pers. comm., 1992).

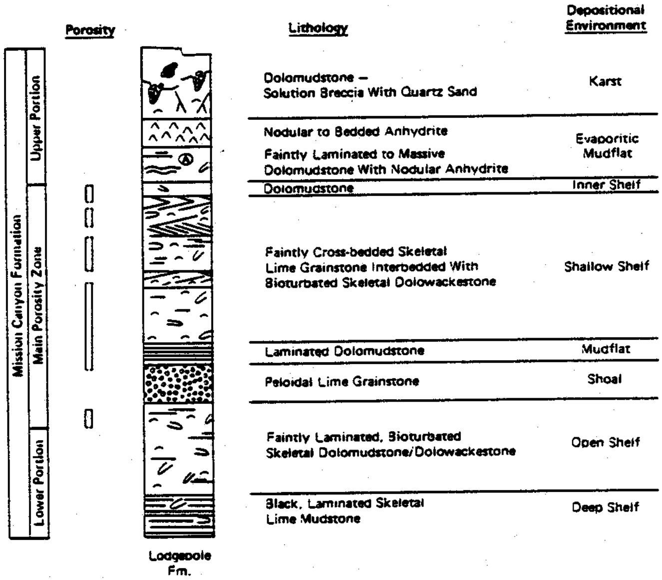

Figure 11E. Idealized composite section of Mississippian Mission Canyon in Whitney Canyon-Carter field, Wyoming (Harris, Flynn and Sieverding, 1988).

CARBONATE SEQUENCES, CYCLES AND DIAGENESIS ASSOCIATED WITH HIGH AMPLITUDE 4TH/5TH ORDER SEA LEVEL OSCILLATIONS

Large, high frequency fluctuations in sea level (60 to over 100 m oscillations) appear to have characterized global icehouse times of the Pleistocene, the Pennsylvanian-Early Permian and the Late Precambrian (Fischer, 1982)(Fig. 2A). Parasequences or cycles appear to have been dominated by eccentricity (100 to 400 k.y.) rhythms (Wright, 1992).

On relatively flat-topped platforms, the carbonate cycles form layer cake successions of 1 to 10 m thick, dominantly subtidal 4th order cycles punctuated by subaerial, karstic disconformities (Perkins, 1977; Beach, 1982)(Fig. 12A). Reef crest facies may trace out the path of relative sea level fluctuations.

On ramps, cycles are erosionally bounded, and have highly shingled lateral and vertical stacking pattern, due to 20 and 40 k.y. fluctuations riding on larger amplitude 100 to 400 k.y. sea level fluctuations (Read, Osleger and Elrick, 1991)(Fig. 12B). One hundred k.y. and 400 k.y. lowstand cycles are confined to the outer ramp and have no updip equivalents. Cycles are extremely difficult to correlate without highly distinctive, continuous marker beds.

Pinnacle reefs and banks are common on tropical platforms that formed under these high amplitude sea levels due to rapid flooding of the platform, and cycles vary greatly in thickness. Cycles lack tidal flat facies because sea level falls off the platform faster than tidal flats can prograde. Thus any high-stand tidal flat facies and associated dolomites are likely to be in narrow bands adjacent to cratonic shorelines or in the lee of cemented islands. Cycles updip are dominated by shallow water facies capped by clastics or major disconformities. Mid-ramp or mid-shelf cycles may preserve a transgressive succession overlain by deep water shale/pelagite (maximum flooding) which shallow up into shallow water buildups or grainstone shoals, and then into clastics, or a capping disconformity. Deep-shelf/ramp margin cycles can have deep water pelagics that are burrow-mixed with low-stand shallow water sediments such as ooids (Logan et al., 1969).

High amplitude sea level fluctuations in the 20 k.y. to 400 k.y. range are likely to leave diagenetic signatures reflecting the large scale vertical and lateral migration of diagenetic zones. These large scale sea level fluctuations can cause the rocks to be subjected repeatedly to meteoric vadose, meteoric phreatic, mixing zone and sea water diagenetic environments (Fig. 12C). Any meteoric diagenesis during 4th or 5th order highstands would be restricted to eolian islands or newly emergent shoals where sediments can undergo cementation and leaching of aragonite associated with island water tables that may be ephemeral (Budd and Land, 1990). However the bulk of the diagenesis is likely to occur during regional platform emergence, associated with lowered sea levels during 20, 40, 100 or 400 k.y. still-stands.

Humid zone carbonate cycles can have single to multiple caliche horizons capping cycles if there is wet-dry seasonality and numerous karstic caverns and sinkholes can extend downward through several cycles. Cycles that contain internal seals of deep water shale/carbonate can have primary porosity preserved in early cemented and leached, regressive upper parts of cycles that resist compaction (Heckel, 1983) to form highly stratified reservoirs. Coarser grained cyclic successions such as high energy reefs may lack internal seals and can form poorly stratified reservoirs. In successions of high amplitude carbonate cycles with poorly developed internal seals, uppermost cycles can have primary intergranular porosity, while lower ones will show increasing moldic, vuggy and cavernous porosity due to superimposed meteoric diagenetic events caused by large scale sea level fluctuations. It may be difficult to identify these subseismic scale cycles in core or wireline logs because of the extensive diagenetic overprint.

In arid zone cycles formed under large, high frequency sea level fluctuations, porosity may be plugged at cycle tops by caliche, but below this zone will be mainly primary intergranular in non-dolomitized buildup and shoal-grainstone units. In dolomitized cycles related to high stand sabkas on the inner platform, or late high stand to low stand evaporite basins whose refluxing brines dolomitize underlying facies, the porosity will be secondary intercrystal and remnant primary intergranular porosity in the dolomites along with primary intergranular porosity in limestone.

High Amplitude Cycles, Late Miocene Reefs, Spain: The detailed geometries along an exposed rimmed shelf margin that formed under high amplitude sea level oscillations (Fig 12D) have been described by Pomar (1991 and in press). The platform consists of bedded lagoonal facies, reef core, reef slope and open shelf facies. The facies together make up sigmoidal units, whose tops are erosionally bounded updip and pass downdip into conformities. These are bundled into sets of sigmoids, composed of a lower prograding unit, an aggrading unit, an upper prograding unit that downlaps onto a condensed interval, and an offlapping/downstepping unit. The set of sigmoids has an erosional top that correlates downdip with a conformable contact; perhaps each set of sigmoids

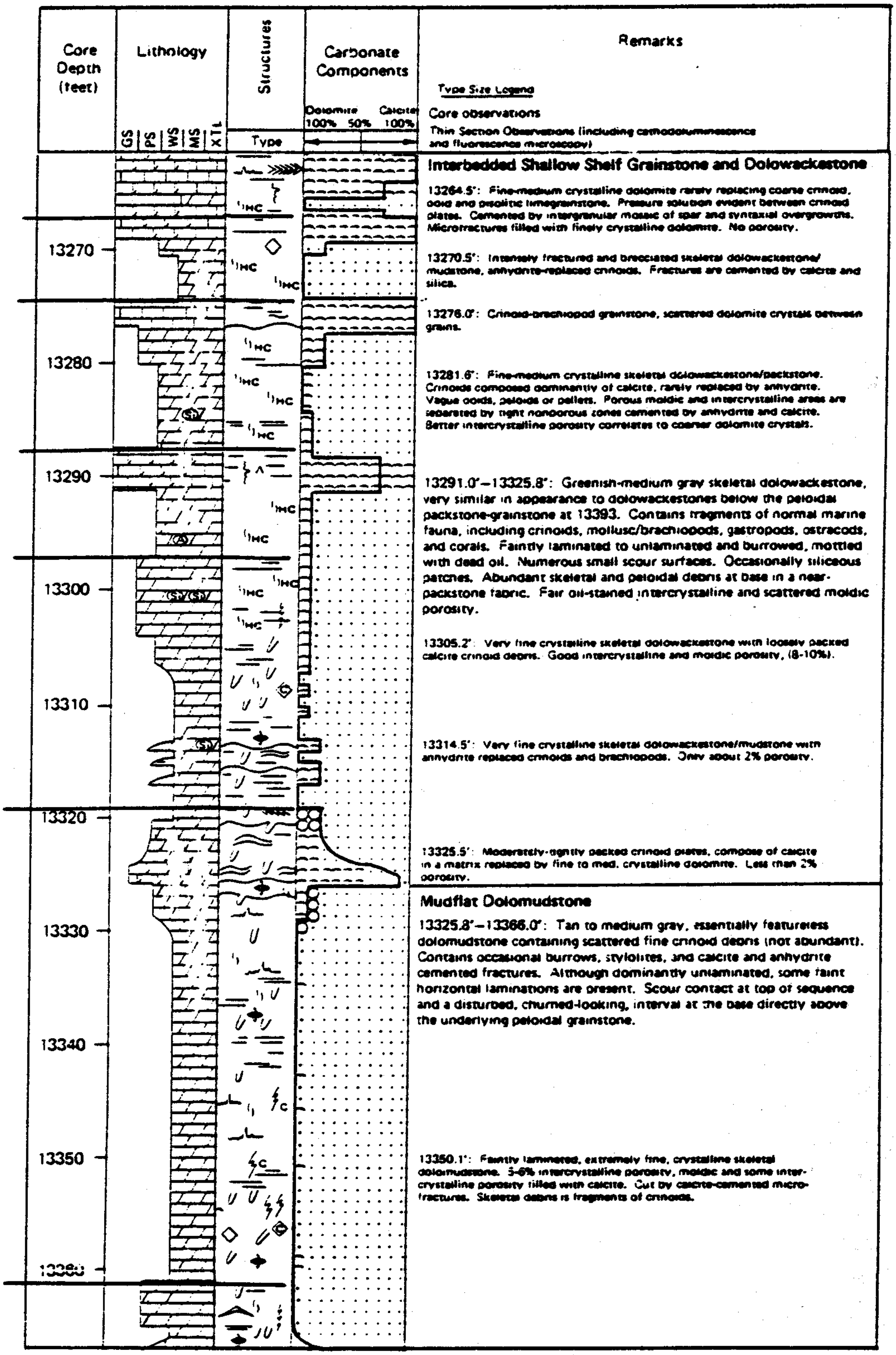

Figure 11 F. Example of core description of Mississippian rocks from Whitney Canyon-Carter field, Wyoming, showing inferred shallowing upward cycles in the dolostones (from Harris, Flynn and Sieverding, 1988).

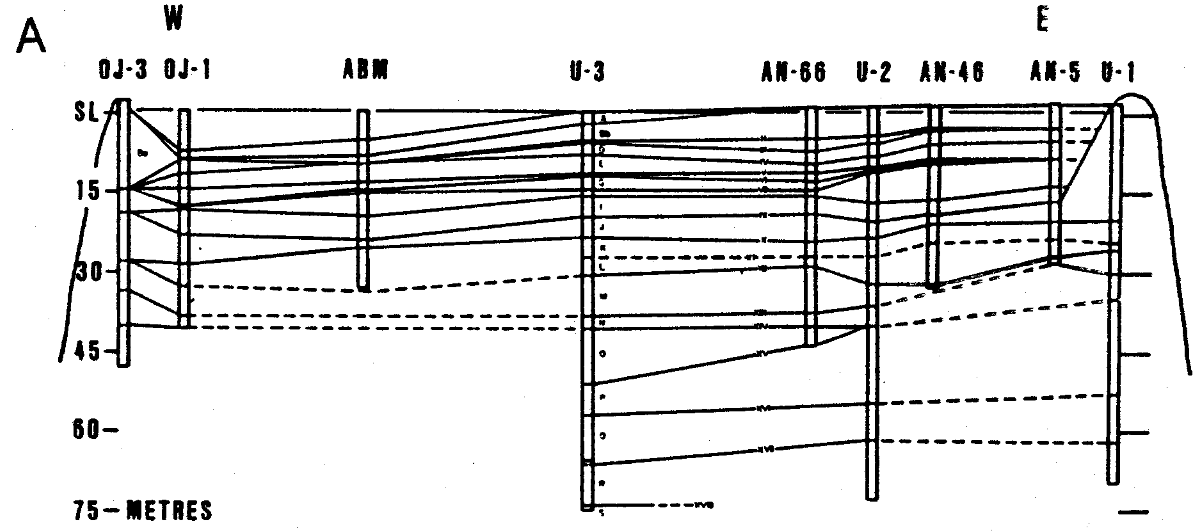

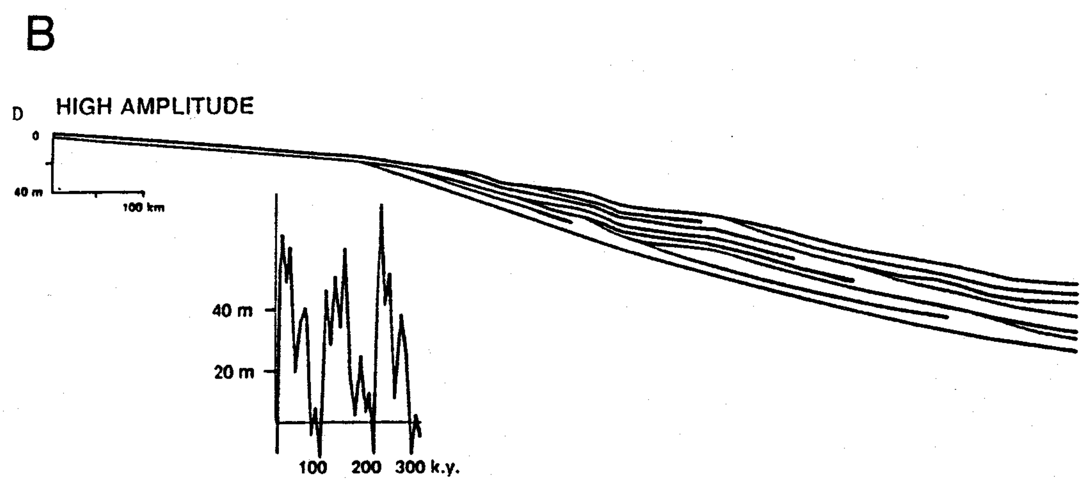

Figure 12 A. Correlation of subaerial discontinuity zones across northeastern Great. Bahama Bank (Beach 1982).
B. Synthetic stratigraphy on a ramp that developed under high amplitude Milankovitch sea level fluctuations. Cycles lack tidal flat caps, and are difficult to correlate with updip or downdip counterparts, based on individual sections or wells, due to limited continuity in the dip direction.

represents a precessional cycle although this is not clear. These sets of sigmoids are in turn bundled into cosets, each containing a lower progradational, an aggradational, upper progradational and a downstepping/offlapping package and an upper major erosional surface; each coset is considered by Pomar (1991) to be a 100 k.y. cycle. These probable 100 k.y. cosets are in turn bundled into possible 400 k.y. packages themselves characterized by progradation to aggradation to progradational and downstepping geometries. Finally, the prograding reefs form the HST of one of the Late Miocene 3rd order sea level cycles. The reef-rimmed platform was prograding into over 100 m of water, and the 100 k.y. sea level changes likely were 60 to 70 m whereas the higher frequency ones were about 10 to 30 m.

Pleistocene Cycles and Humid Zone Diagenesis, Bahamas: Bahamian Pleistocene platform cycles are 1 to 10 m thick, disconformity bounded units (Beach, 1982) (Fig. 12A). Karst features, caverns, vugs, leached zones occur at many levels (Beach, 1982; Dill, 1977; Ginsburg et al., 1990) (Fig. 9). Such karst features include large sea water-filled sinkholes over 100 m deep, extensive solution-enlarged joints (hundreds of meters to kilometers long) parallel and perpendicular to the bank margin, and vertical and horizontal passages commonly many meters wide (Dill, 1977; Smart et al., 1988). These are enlarged by meteoric dissolution at the surface, and in the shallow subsurface by waters in the mixing zone which is up to 10 m thick. They may have partial to complete fills of blocks and finer sediment of marine and terrestrial origin. These cavernous zones honeycomb the platform (Dill, 1977; Beach, 1982; Ginsburg et al., 1990).

In Bahamian platform cores (Beach, 1982), the complex interlayering of diagenetic phases as predicted by the sea level history (Fig. 12C) is rarely able to be deciphered. Within each cycle, the amount of induration is greatest just beneath the disconformity surface, where primary and secondary pore space may be almost totally occluded; this induration decreases markedly downward. Also, younger cycles show little cementation overall, but induration increases into lower, older cycles, reaching a maximum a few cycles (at 10 to 15 m subsurface depth) below the present platform top, where rocks are moderately well cemented and large vugs and channels are pervasive. The amount of leaching of aragonite and formation of secondary porosity appears to offset the amount of precipitated calcite cement resulting in little net loss of pore space (Beach, 1982, Harrison et al., 1984). The porosity of the nonskeletal (originally aragonitic) sediments averages 35%, whereas porosity of the skeletal (initially calcitic) sediments at depth averages 10 to 15%. Primary porosity passes downward into secondary porosity below about 10 m below the platform top (cf. Halley and Schmoker, 1983 for Florida). In the Bahamian cores, two and perhaps 3 stages of cementation tied to Quaternary sea level falls were recognized by Beach (1982). The first cements in cycles are recrystallized marine cements. Sea level fall causes deposition of meteoric, intergranular sparry cements and overgrowths, with inclusion-rich rinds on cements near the disconformity, and common rhizocretions. The cements subsequently may be overlain by infiltrated marine sediment following deposition of the next marine unit. Karstic vugs and channels lined with second generation cements are ascribed to the resultant sea level fall. With the next sea level rise and fall, a third generation of meteoric cements may develop (Beach, 1982). Much of the cementation could be vadose even though diagenesis is more rapid in the phreatic zone (Matthews and Frohlich, 1987; Budd, 1988), but vadose calcites (except for caliche) can rarely be distinguished from the phreatic calcites (Beach, 1982; Harrison et al., 1984), although vugs and channels lined with spar and silts likely are vadose.

In some beds, leaching and calcite cementation was followed by mixing-zone(?) dolomitization, while in younger units this pre-dolomite leaching phase is absent. Even with conservative dolomite production rates, modelling suggests that substantial amounts of mixing zone dolomites in these platforms may occur below subsurface depths of about 50 m to 100 m (Matthews and Frohlich, 1987; Humphrey and Quinn, 1989). It is unclear whether the bulk of dolomites in these platforms is mixing-zone (Ward and Halley, 1985; Humphrey, 1988), or related to marine water circulation through the platform (Whitaker and Smart, 1990 and this volume), or due to reflux of brines generated by evaporation during more arid phases (Berner, 1965; Goldstein et al., 1991b) or due to thermal convection of cool, deeper marine waters (Saller, 1984).

<u>Pennsylvanian Holder Formation, Humid Zone Diagenesis, New Mexico</u>: Goldstein (1988) describes probable humid zone diagenesis associated with Late Pennsylvanian eustatic sea level fluctuations in the cyclic Holder Formation, New Mexico. There are up to 20 cycles from 6 to 30 m thick, which consist of shale/siltstone/sandstone with limestone conglomerate pebbles, overlain by wackestone, then by lime sands or bioherms, and cycle-capping paleosols. The sea level fluctuations were over 30 to 50 m in magnitude based on paleorelief of a shelf edge subaerial exposure surface (Goldstein, 1988), and likely were up to 100 m based on continent-wide facies analysis (Heckel, 1980).

Paleosol fabrics (Goldstein et al., 1991a) dominate the upper meter of cycles and apparently formed under fresh-water, water-logged conditions. Most common pores are molds after aragonite fossils and few aragonite fossils were neomorphosed. The sediments show little distinguishable vadose cementation. The bulk of the calcite cementation occurred on the shelf-edge and shelf-crest associated with successive phreatic lenses fed by cycle capping disconformities. Some lenses may have been associated with perched water tables due to interlayered shale or cemented limestone aquitards. The aquitards limited the thickness of the lenses from a few meters to 36 m. Some lenses show maximum early cementation just beneath the subaerial disconformity, whereas in others, maximum cementation was lower in the lens. In contrast to shelf margin facies, basin or lagoonal rocks show little early cementation. The poor correlation between fine cement zones probably is due to the numerous fine shaly aquitards in the Holder Formation, which affected downward flow of water, and tended to make the penetrating waters suboxic.

<u>Pennsylvanian Cycles and Diagenesis of the U.S. Mid-continent</u>: Heckel (1983) described a diagenetic model for U.S. Mid-continent cyclothems of Mid-Pennsylvanian age (Fig. 12E). The diagenetic signature has characteristics of humid conditions with widespread sparry cements, and abundant leaching, to semi-arid conditions with caliche, local evaporites. Cycles are a few meters to over ten meters thick and consist of basal near-shore shales, transgressive limestone, a core black shale (marking maximum marine flooding), regressive, coarsening upward, open marine limestones, bank- and shoal water facies, and a caliche or paleosol mudstone cap (Heckel, 1980; Watney et al., 1989).

Caliches, red paleosols, rhizoliths and leach fabrics were developed on cycles that formed under more arid paleoclimates in western Kansas, whereas karstification was more prevalent in the wetter paleoclimates of southeastern Kansas (Heckel, 1980; Watney et al., 1989, Goldstein et al., 1991a). The transgressive limestones below the core black shales show little early diagenesis and retained their aragonite mineralogy into early burial when they underwent pervasive overcompaction and neomorphism of aragonite to calcite (Fig. 12E). The core shale apparently acted as an aquiclude, shielding the underlying transgressive limestone from downward penetration of meteoric water. In contrast, the upper, regressive limestones show much early marine cement, paleocaliche and soil formation, abundant leaching of aragonitic grains and pervasive blocky calcite cementation prior to much compaction (Fig. 12E). This moldic and vuggy porosity is important in the Pennsylvanian reservoirs whereas calcite cementation and mud infiltration has occluded porosity in non-reservoir rocks (Ebanks and Watney, 1985). Similar leached reservoirs due to large scale migration of fresh-water lenses during high amplitude 4th order glacio-eustasy occur in regressive bryozoan and foram limestone portions of cyclothems above deeper water clayey facies in the Mid-Pennsylvanian Goen Limestone, Central Texas (Maquis and Laury, 1989). These facies have better porosity than the associated algal mound facies and early phreatic calcite cementation locally acted to partly occlude porosity (Marquis and Laury, 1989).

<u>Pennsylvanian Horseshoe Atoll and Meteoric Diagenesis, Texas</u>: The raised rim buildups on the southern and eastern margin of the Horseshoe Atoll are host to billion barrel fields that developed as a result of large, high frequency sea level fluctuations and attendant fresh water diagenesis (Schatzinger, 1983; Reid and Tomlinson-Reid, 1991). The buildups contain numerous erosionally bounded parasequences. Tidal flat, fenestral dolomitic mudstone were restricted to local shoals in the interior of the buildups on the elevated rim. Oolitic grainstones developed belt-like shoals over the buildups along the northern margin of the rim and are major reservoir facies. The buildup facies are phylloid algal wackestone mounds bordered downslope by sponge-algal-bryozoan mounds (in water depths up to 20 m), which passed downslope into deeper shelf and slope muds. These muds form seals within and lateral to the buildups. During the repeated sea level falls, islands developed

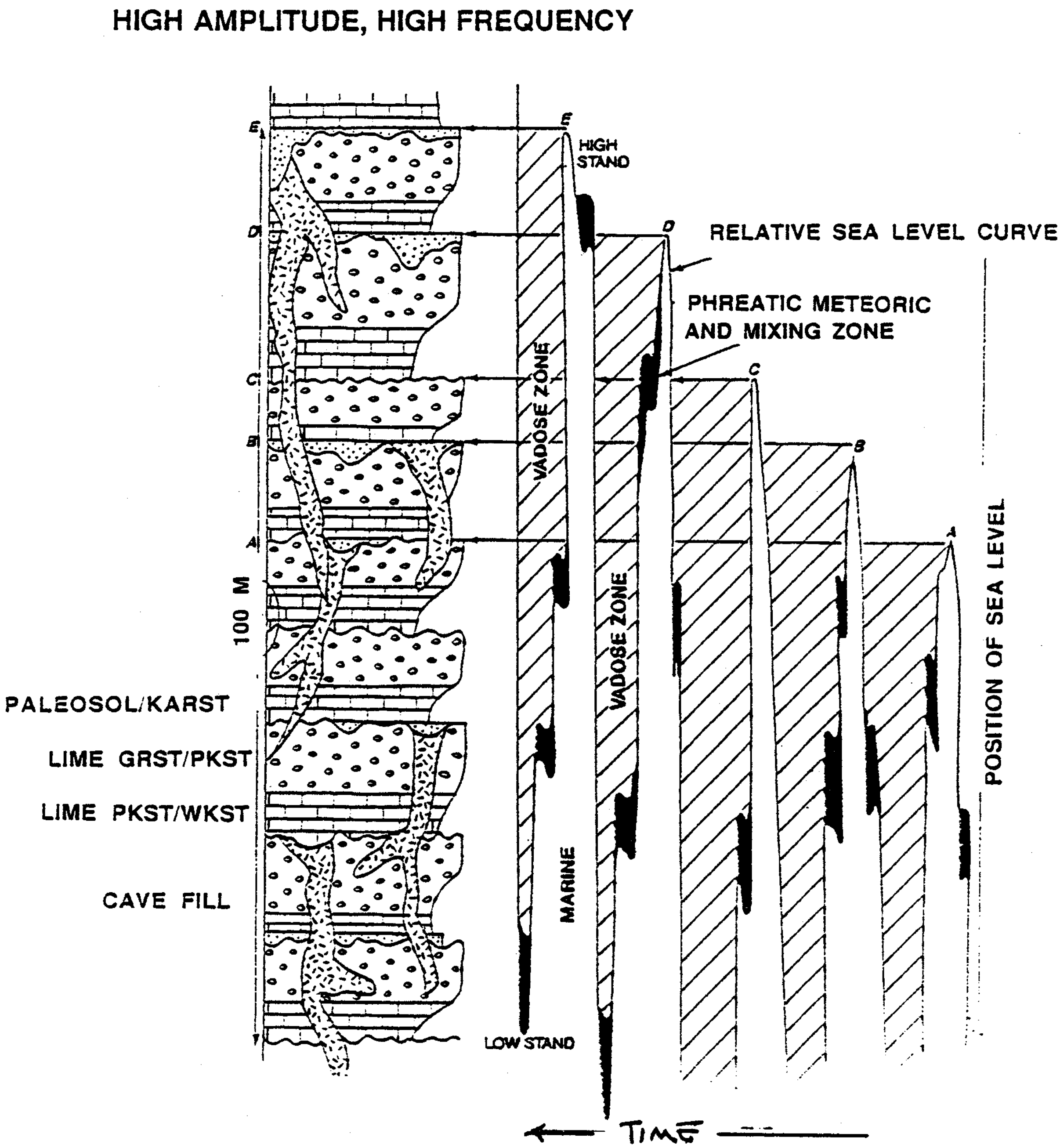

Figure 12 C. Diagenetic model of carbonate cycles that formed under high frequency, high amplitude sea level fluctuations. Cycles are disconformity-bounded, may be karsted with cavern systems extending down through several cycles, and sediments are subjected to a complex sequence of diagenetic fluids and events, due to the large scale sea level fluctuations. Modified from Matthews and Frohlich (1987).

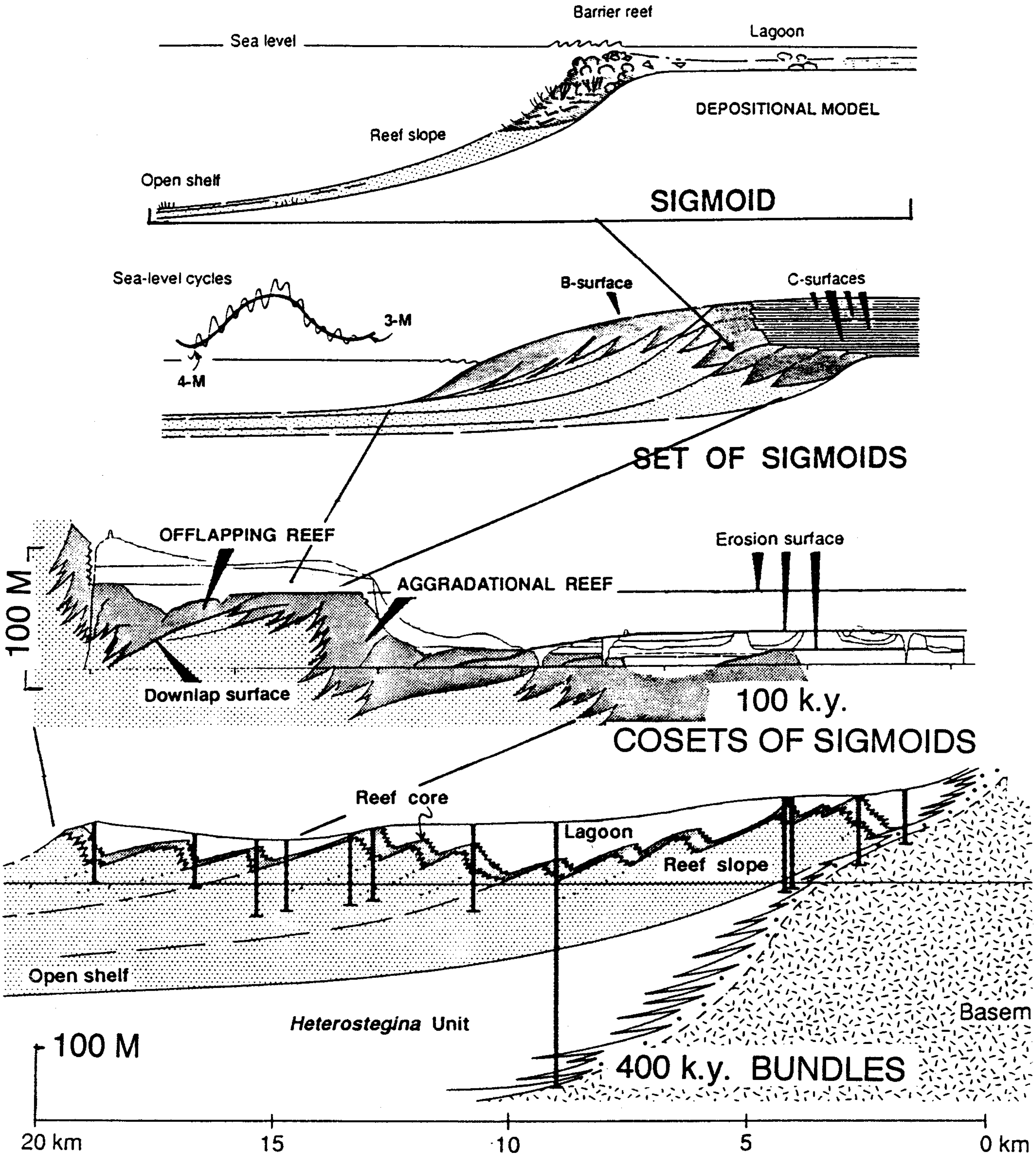

Figure 12 D. Response of reef rimmed shelf margin to high frequency high amplitude sea level fluctuations, Miocene of Spain (from Pomar, 1991 and in press). Basic unit of the shelf margin is the sigmoid (top). These sigmoids are arranged into sets (next diagram) and then into cosets of sigmoids, considered to be 100 k.y. cycles (2nd diagram from bottom). Finally, these are bundled into larger scale packages equated with 400 k.y. cycles (bottom).

weathered zones, paleosols and eolianites, and meteoric lenses caused leaching to form oomoldic and skelmoldic porosity, some dissolution of calcite cement, recrystallization of mud and grains to microcrystalline calcite, and secondary vug- and small cave development. Repeated exposure of the mounds even occurred during final drowning of the complex, attesting to the large fluctuations in sea level. The leached oolite grainstones have up to 30% porosity and up to 100 md permeability. Porosity and permeability is slightly lower in skeletal grainstones and low in the leached mound facies, even though these may have high porosity.

Arid Zone Diagenesis, Middle Pennsylvanian, Paradox Basin Cycles, U.S.A.: Middle Pennsylvanian shelf cycles (Fig. 12F) in the Paradox Basin form major reservoirs (Choquette and Traut, 1963; Pray and Wray, 1963; Wilson, 1975). The shelf carbonates contain large scale, regionally correlative cycles up to thirty m thick and possibly 100 to 400 k.y. duration, that contain higher frequency (ave. 6m thick) cycles possibly 20 to 40 k.y. duration (Goldhammer et al., 1991). Cycle facies include basal reworked sandstone, deep water black laminated dolomitic shale and argillaceous mudstone, spiculitic muds with packstone lenses, and small phylloid algal, mud-rich mounds 6 to 12 m thick, with non-skeletal and skeletal packstone/grainstone caps. Most caliches are only developed on cycles associated with regionally correlatable 4th order 'sequence' boundaries. Most cycle-boundaries are marked by subaerial exposure surfaces or in downslope positions, by algal laminites and evaporites. Basin sections contain 29 correlative shale-evaporite, 4th order cycles.

Meteoric diagenesis caused by major sea level falls is evident in upper parts of shelf cycles, which show much leaching of aragonite in algal bank facies, skeletal packstone/wackestone and non-skeletal grainstone/packstone caps (Wilson, 1975), and much non-luminescent, non-ferroan sparry cement (Dawson, 1988). The restriction of the meteoric diagenesis to upper parts of cycles even though 4th order eustatic sea level falls of 50 to 60 m were involved, probably relates to gradual subsidence diminishing the relative sea level fall to 20 m or so (Goldhammer, et al., 1991). Shale and muddy carbonates low in the cycles also acted as aquitards, preventing deep penetration of meteoric waters. The evidence for meteoric diagenesis in these cycles is interesting in view of the arid conditions of deposition of time-equivalent evaporites in the Paradox Basin.

In contrast, Middle Pennsylvanian subsurface algal mounds of the Bug and Papoose Canyon fields of the Paradox basin, Utah and Colorado show evidence of more typical arid zone diagenesis (Roylance, 1990). The mounds underwent marine aragonite cementation, followed by some leaching of capping facies above mounds, brecciation and dolomitization; there was little sparry calcite cementation, in spite of substantial sea level fluctuations but there was considerable porosity reduction by anhydrite and less common halite cements.

DIAGENESIS ASSOCIATED WITH LONG TERM SEA LEVEL CHANGE

Regional uplift or 3rd order (1 to 10 m.y.) sea level falls form widespread regional unconformities. Given sufficient rainfall, the unconformity surface acts as a recharge area for regional aquifers, which strongly controls early diagenesis in the sequence (Fig. 13). In newly deposited sediments, the water movement is via intergranular pores by diffuse flow. However, with increasing time and increasing cementation and leaching, water movement becomes dominated by conduit flow along widening joints and caves undergoing dissolution beneath the karst surface. Pleistocene mature karstic terrains include those documented by Purdy (1974a, b), Smart et al. (1987), Xie-Pei and Qi (1979) from British Honduras and China and there are many examples in the humid climates of SE Asia (Horbury, pers. obs.). Detailed discussions of geological aspects of paleokarst are given in James and Choquette (1988) and Wright, Estaban, and Smart (1991).

Key Features

Diagenesis related to major unconformities can extend tens to some hundreds of meters downsection. In newly emergent terrains, intergranular porosity in diffuse flow aquifers can be plugged by early meteoric phreatic cements, whose abundance decreases downsection and downflow. However, development of chalky and moldic porosity may offset this porosity decrease. Beneath unconformities that are emergent for millions of years, karstic relief, breccia filled cave systems with both marine and non-marine fills, and burial induced fracturing of cave-roofs may form extremely compartmentalized reservoirs. In the subsurface in non-cored well data, it is easier to identify the products of karstification such as porosity development/occlusion, rather than the surface itself (Estaban and Klappa, 1983). Where clastic or basinal facies overlie the unconformity, a high gamma log count due to glauconite or uranium may mark the flooding surface. The unconformity may be evident in a marked biostratigraphic break. In seismic reflection profiles, unconformity relief will be difficult to distinguish from relief associated with pinnacle reefs or other high relief buildups.

Unconformity-Related Diagenesis Associated with Diffuse Flow Aquifers Late Mississippian carbonates of the Appalachians: Late Mississippian carbonates of the Appalachians were cemented in diffuse flow aquifers during 2 major phases of unconformity development (Niemann and Read, 1988; Nelson and Read, 1989). These ramp carbonates contain regionally traceable shallow burial calcite cements that are early non-ferroan, CL-banded zones extending down into the carbonates from a few meters to over 60 m (Fig. 14). The cements can be traced over thousands of square kms and from tens to over 200 kms downdip. The cement zones are 1. nonluminescent 2. luminescent and 3. nonluminescent cement. These "zones" commonly contain thin CL-defined cement laminae which are not regionally correlative. In the Appalachians, the nonluminescent cements pass downdip into dull luminescent cements (Fig. 14). The cement stratigraphy can still be recognized in these dull CL cements using Dickson's stains sensitive to Fe content of the calcites (Nelson and Read, 1989). The nonluminescent-dull-nonluminescent zonation of updip areas is equivalent to pink-purple-pink staining, dull CL zones downdip. In the Appalachians, the early nonferroan zoned cements fill up to 80% of the pore space updip, decreasing to less than 40%, 80 kms to the south away from the postulated recharge area.

The nonluminescent-luminescent-nonluminescent cement zones all are low in iron, and could have formed from oxidizing pore waters sourced from the Late Mississippian and Mississippian-Pennsylvanian unconformities capping the sections (Niemann and Read, 1988). At this time the climate in the Appalachians was becoming wet and tropical, and deltas were prograding out over the carbonate ramp. The lower of these two unconformities sourced the waters for the zone 1 nonluminescent cements. The succeeding nonferroan luminescent cement formed during the subsequent Late Mississippian transgression which caused stagnation of the aquifer. The later nonluminescent zone formed during development of the Mississippian-Pennsylvanian unconformity. The updip nonluminescent cements (zones 1 and 3) are interpreted to have time-equivalent dull CL cements downdip where waters were more

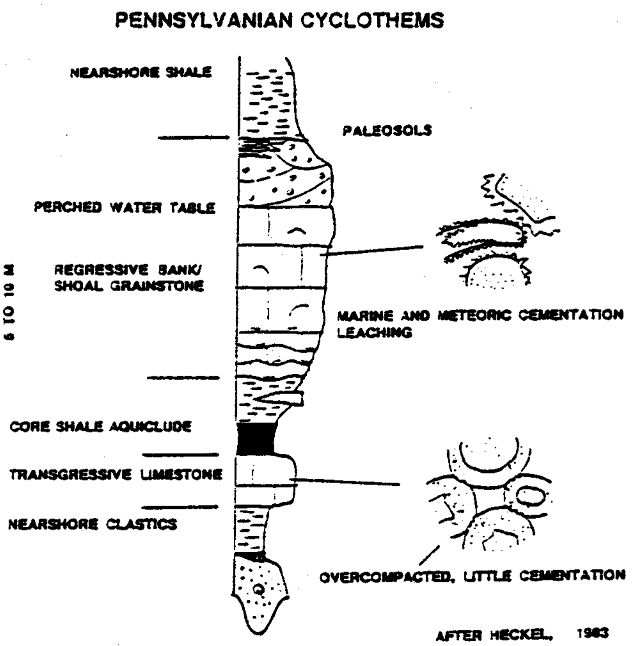

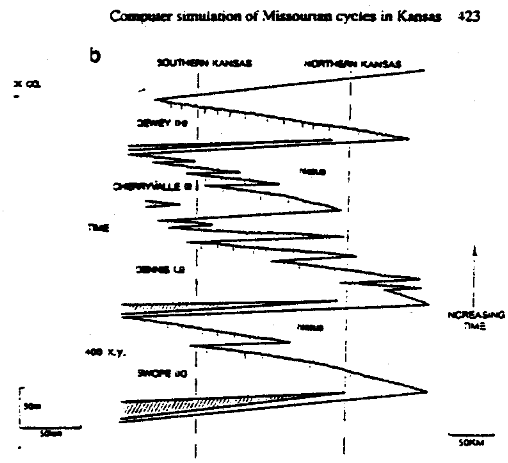

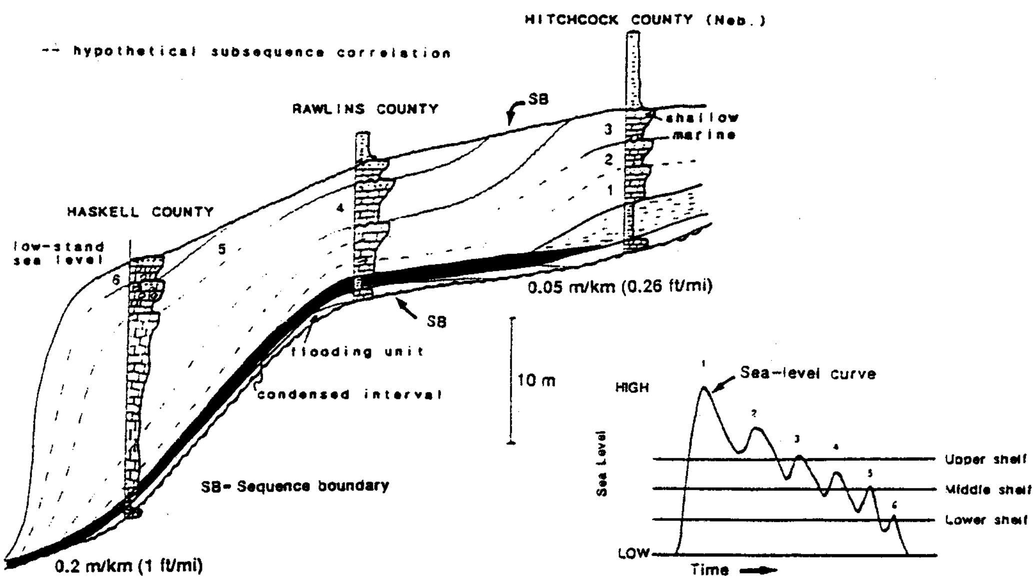

Figure 12 E. Pennsylvanian cyclothems of the mid-continent. Top left: Schematic cycle of Pennsylvanian cyclothem showing vertical stacking of facies, and diagenetic overprint. After Heckel, 1983. Top right: Time-distance cross section showing relative sea level inundation associated with major cycles of the Kansas City Group, western Kansas. Condensed sections shaded; wavy lines at tops of packages are subaerially exposed bounding surfaces. (Watney et al., 1991).
Bottom: Conceptual model of Upper Pennsylvanian (Missourian) carbonate shelf cycle from ramp in western Kansas. Flooding unit (thin carbonate), condensed section (black shale) and shallowing upward (highstand) carbonates typify major cycles; minor cycles punctuate the major cycles (from Watney et al., 1991).

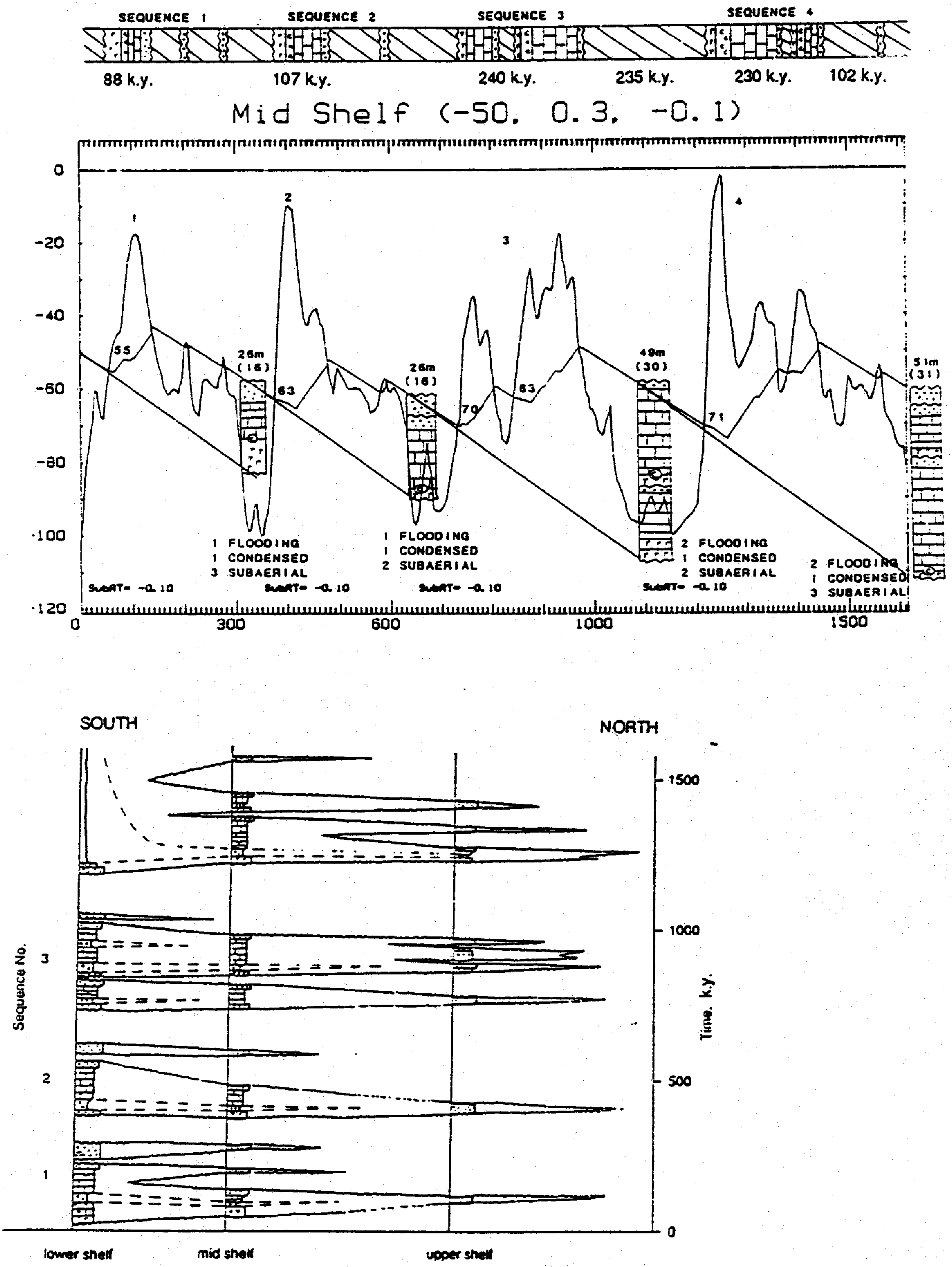

Figure 12 E continued. Top: Computer simulation for a mid-shelf setting for Pennsylvanian (Missourian) cycles, western Kansas. Initial sediment elevation is -50 m, sedimentation rate is 0.3 m / k.y., subsidence rate is 0.1 m / k.y.
Bottom: Time-stratigraphic diagram for upper, middle and lower shelf settings generated by computer model. Note similarity to time-distance cross-section shown previously. Watney et al. (1991).

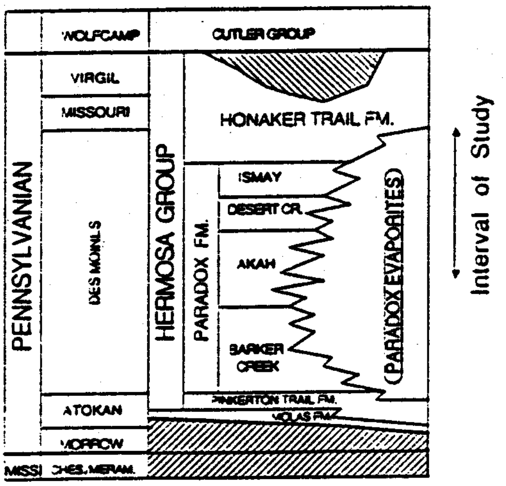

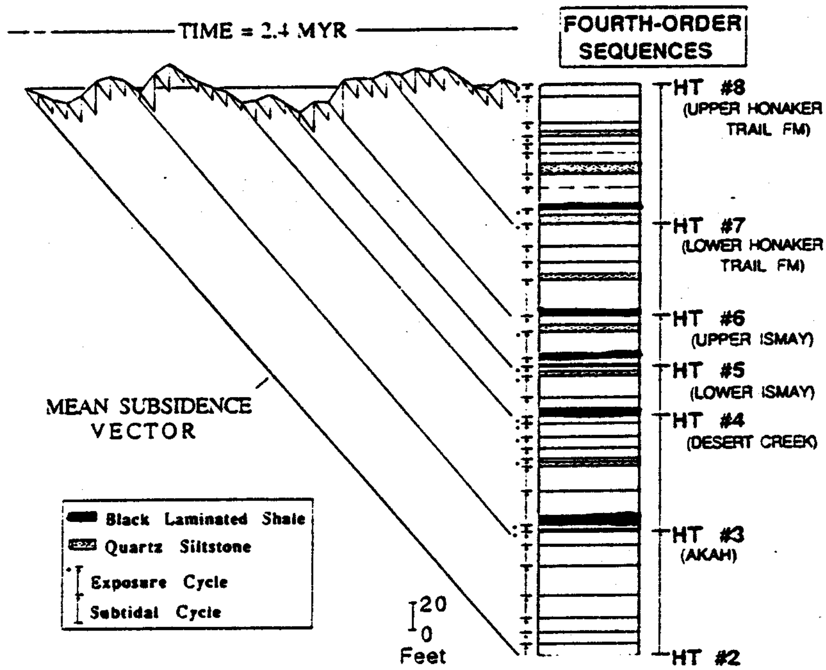

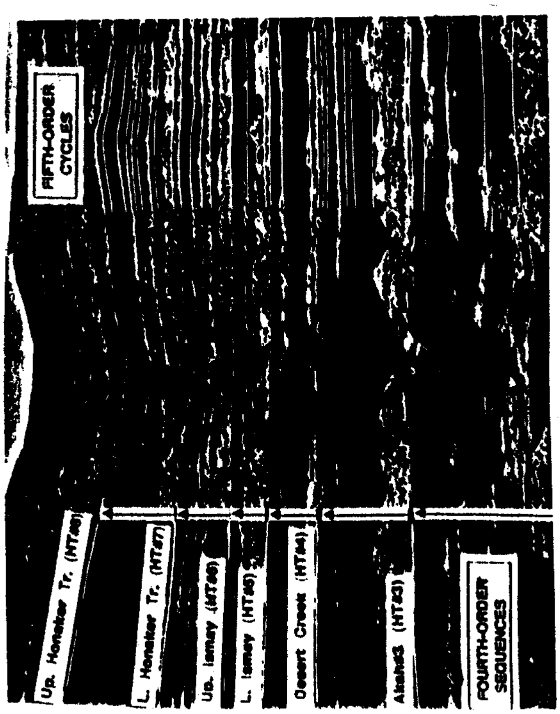

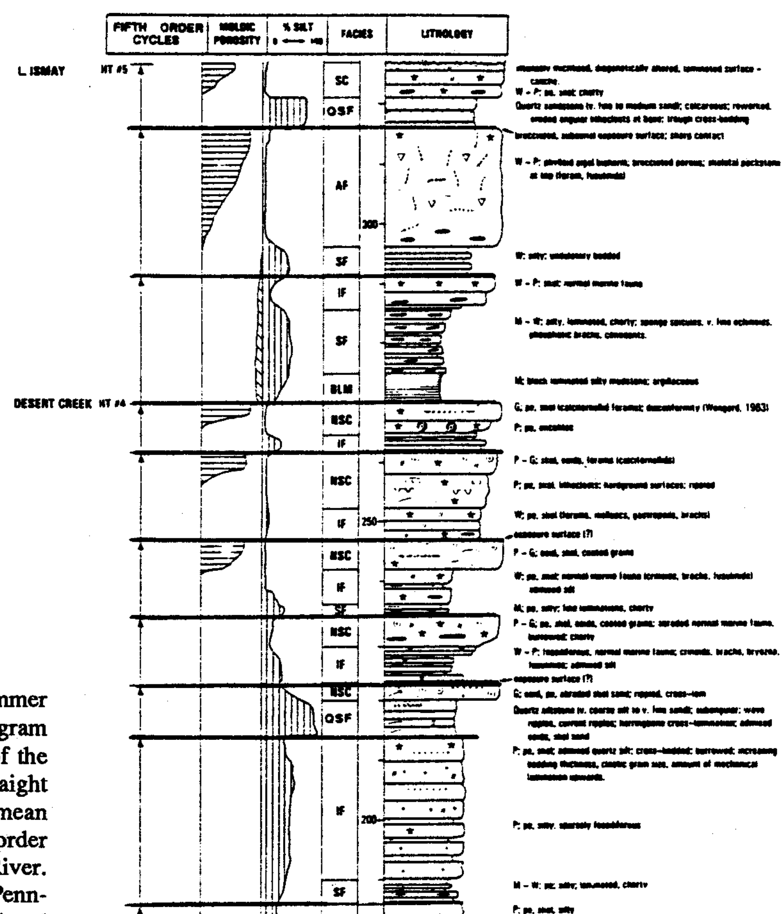

Figure 12 F. Pennsylvanian Paradox Basin cycles (from Goldhammer et al., 1991): Top left: Pennsylvanian chronostratigraphic diagram for the Paradox Basin. Top right: simplified stratigraphy of the Pennsylvanian Honaker Trail section, and its Fischer plot; straight line connecting base of Fischer plot to base of section is mean subsidence vector. Bottom left: 4 order sequences and 5th order cycles, opposite Honaker Trail area on west side of San Juan River. Bottom right: portion of measured section of Honaker Trail Pennsylvanian, southeast Utah, spanning 4th order sequences HT 4 and 5 (Desert Ck. and L. Ismay). These cycles are regionally correlatable.

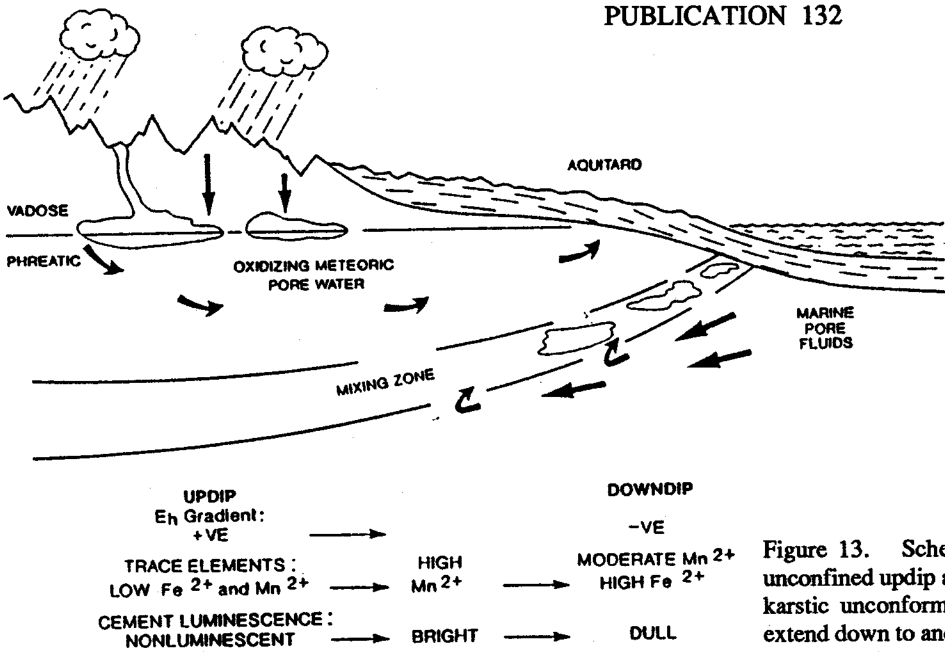

Figure 13. Schematic diagram of a carbonate aquifer that is unconfined updip and confined by aquitard downdip. The regional karstic unconformity acts as a recharge area. Numerous caves extend down to and are localized by groundwater table, and by the coastal mixing zone. Regional gradients in Eh, reduced Fe and Mn, and cathodoluminescence of clear calcite cements are shown.

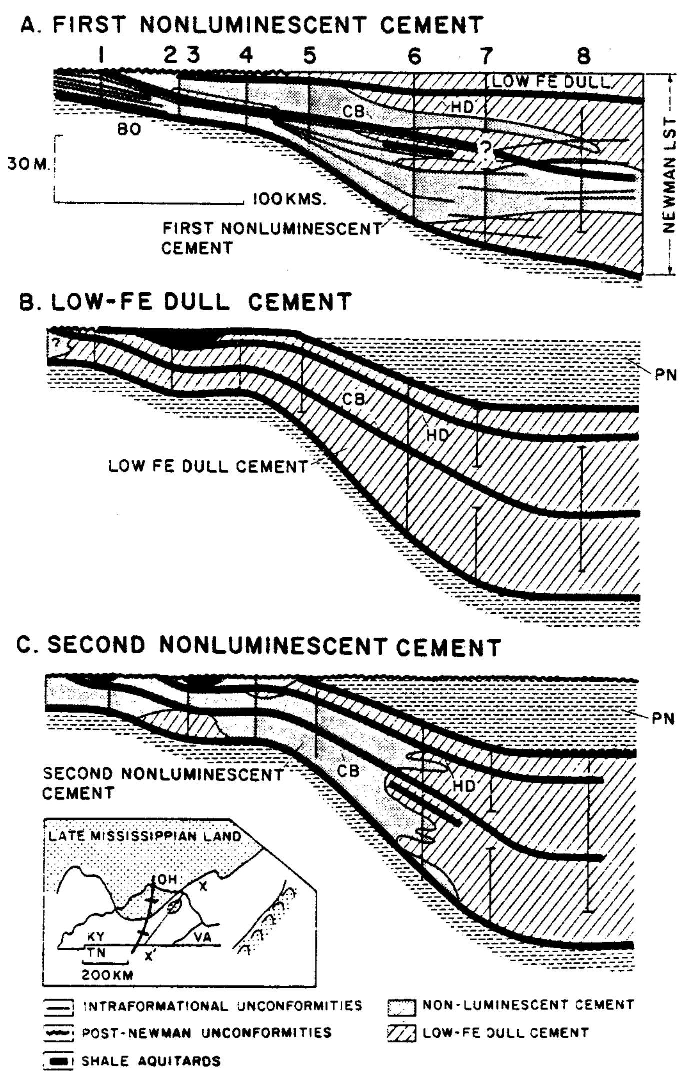

Figure 14. Schematic model showing the depositional history of meteoric cements in the diffuse flow paleoaquifer in the Mississippian Newman Limestone, Kentucky (Niemann and Read, 1988). The first generation of cements (A) formed from an aquifer sourced from above the Glen Dean Limestone in the Late Mississippian; this aquifer had oxidizing waters updip (shaded areas) and more reducing waters downdip (cross hatched areas). Following Late Mississippian Pennington transgression, this aquifer shifted updip, resulting in more reducing waters in the carbonates, and Fe rich cements (B). With the Mississippian-Pennsylvanian unconformity development, a major regional aquifer generated the next generation of cements from oxidizing groundwaters that passed downdip into more reducing waters.

reducing. Although there are unconformities lower in the Mississippian carbonates in the Appalachians, these had little effect on cementation because they developed during arid conditions (Niemann and Read, 1988). These unconformity-sourced cements tended to plug primary porosity updip, but appear to have caused only limited plugging of pore space downdip where much of the Mississippian produces. The aquifer waters also caused metastable mineralogies to be converted to low Mg calcite updip, and could have formed chalky porosity in some of the updip ooid shoals in the Appalachians.

Note that not all shallow burial calcites are deposited from meteoric waters sourced from unconformities, but may in some cases be sourced from refluxing brines associated with evaporites higher in the section (Goldstein et al., 1991) or from waters sourced from tectonic highlands peripheral to foreland basins, with flow via aquifers (karstic zones, quartz sands, or carbonate sands) (Grover and Read, 1983; Dorobek, 1987).

Diagenesis Associated with Mature Karstic Terrains, Knox-Ellenburger Unconformity, U.S.A.: The Knox-Ellenburger unconformity that caps the Cambro-Ordovician sequence throughout much of North America (Mussman et al., 1988; Kerans, 1988; Knight, James and Lane, 1991) has localized important hydrocarbon and Pb-Zn deposits. It is up to 10 m.y. duration, and is the boundary to the "Sauk Sequence" of Sloss (1963), one of the fundamental 2nd order cycles of North America (Vail et al., 1977). The unconformity formed during a global sea level fall and in the Appalachians, during uplift associated with a subduction -related peripheral bulge. The unconformity developed during a time of increasingly humid climate, in contrast to the semi-arid conditions that typified Knox cyclic deposition. The unconformity surface locally has over 130 m of erosional relief. There are well developed cavern- and -sinkhole fills (both subaerial and margin, and intraformational breccias due to dissolution of limestone and collapse of the overlying dolomite (Mussman et al., 1988). Extensive collapse breccias tens to 250 m beneath the unconformity formed in the meteoric phreatic and mixing zone associated with a thick zone (up to 100 m) of meteoric ground water.

Nonluminescent cements occur down to 200 m below the unconformity surface (Mussman et al., 1988). Down section, the nonluminescent cements are absent, and the limestones are cemented by dully luminescent cement. These cements tended to plug porosity in the upper 200 m of section, so that the main porosity was karst-related vug, fissure and cavernous porosity. The initial nonluminescent cement sequence probably relates to development of a paleoaquifer whose waters were oxidizing to depths of 100 to 200 m below the unconformity reflecting the humid setting and the highly permeable character of the carbonates. The meandering networks of caves and intraformational breccias probably carried large volumes of meteoric water into the subsurface. With stagnation of the aquifer, possibly during Middle Ordovician transgression, bright cements were deposited as the waters became more reducing. A second non-luminescent cement in the upper Knox carbonates was due to regeneration of the paleoaquifer system by upland sourced meteoric waters which caused cementation in the overlying Middle Ordovician carbonates (Grover and Read, 1983).

Paleokarstic reservoirs occur in the Early Ordovician Ellenburger Group, Texas. These reservoirs have cumulative production of 1.4 billion barrels of oil through 1985 with low recovery efficiencies due to extreme horizontal and vertical compartmentalization of reservoirs. They have been described in detail by Kerans (1988). Most reservoirs occur in the upper 60 to 150 m of the unit regardless of the original peritidal depositional facies and occupy laterally extensive breccia zones (Fig. 15A). They contain a lower collapse zone of chaotic dolostone clast-support breccias of highly variable thickness, averaging 15 to 30 m, with zones of unbrecciated dolomite in the lower part (Figs. 15A,B). Porosity is from 1 to 15%. These are overlain by a middle zone of cave fill, siliciclastic-matrix supported chaotic breccias of Ellenburger dolomite and clasts of shale and sandstone (from the overlying Simpson Group), and intervals of crudely bedded sandstone and shale with local soft-sediment folds and faults (Figs. 15A,B). This siliciclastic middle zone has a distinctive log signature and also forms a low permeability barrier. The upper zone, the cave roof, is highly fractured dolomite with fitted- to rotated clast fabrics. Porosity is from 2 to 20% and the zone is the major pay interval (Figs. 15A,B).

The karstic cave systems developed at a stable paleogroundwater table 30 to 60 m below the top of the Ellenburger. The lower breccias are cave-collapse, stope-deposits whereas the middle matrix rich zone is a Middle Ordovician marine cave fill, analogous to present day blue holes. The cave-roof fracture breccias were formed during later burial compaction and fracturing of the cave roof. The breccia distribution and muddy cave fills cause the high degree of compartmentalization of these reservoirs.

SUMMARY

Frequency and magnitude of sea level fluctuations, in association with climate and tectonics, influence the type of diagenetic modification on cyclic carbonate platforms.

1. On carbonate platforms formed under small, high frequency sea level fluctuations, diagenesis is mainly intracyclic. Under relatively dry climate, diagenesis is dominated by early dolomitization and shallow leaching associated with prograding, regional tidal flat/evaporite facies capping parasequences. Depositional porosity commonly is intergranular in grainy parts of cycles or in cycle-capping siliciclastics, and intercrystal in the dolomites. Porosity inversion may result from sulfate cementation of grainstones and dolomitization and leaching of muddy skeletal carbonates. Anhydrites form internal seals resulting in multiple pay zones but will highly stratify these sub-seismic scale reservoirs. Under more humid conditions there is little dolomitization, and limestone caps of cycles may undergo some microkarsting, leaching and sparry calcite cementation associated with thin fresh-water lenses. Low amplitude parasequences might be recognizable using electric logs, gamma and density-type tools recording the dense anhydrites, tight dolomites, or cycle capping siliciclastics or felspar rich dolomite caps, or in downdip areas, the basal, possibly organic rich mudstones or argillaceous limestones.

2. Platforms that formed under moderate (few tens of meters), high frequency sea level fluctuations have more limited development of regional tidal flats and cycles are dominantly of subtidal facies that coarsen upward. Paleokarstic erosion surfaces marking 4th order emergence events cap parasequences and should be continuous over much of the shelf. Major flooding surfaces at bases of cycles should help separate these parasequences from low amplitude types. Under wet climatic conditions, cycles are capped by karstic disconformities and diagenesis can be intercyclic, with calcite cements extending down through several cycles because of repeated establishment of successive, relatively thick groundwater bodies during lowstands. This results in stabilized, lithified limestone cycles with most porosity occlusion near cemented cycle tops. Because the basal facies of cycles are low-porosity muddy carbonates, the best depositional porosity will be in grainy midparts of cycles. Under drier climates, there is little sparry calcite cementa-

tion or leaching, cycles have caliche at tops and metastable sediments can be preserved into the burial environment. Porosity is best developed in grainy cycles, but also can occur in dolomitized and leached muddy skeletal facies beneath prograding, evaporitic highstand systems, and in subaerial pisolitic carbonates. Reservoirs typically are 4th order, sub-seismic scale and stratified.

3. With large (tens to over 100 m), high frequency sea level fluctuations, diagenesis is markedly inter-cyclic, and sediments are subjected to rapid, large scale vertical migration of diagenetic environments through many cycles. Thus cycles are subjected to large scale (typically 4th order) alternation of diagenetic environments that include marine pore waters, mixing zone, meteoric phreatic and meteoric vadose, but they only retain a partial record of the sea level fluctuations. Sediments high on the platform remain in the vadose zone for much of the time. Under humid climates, leaching of metastable carbonate in grainstones forms excellent reservoirs containing much cavernous, vuggy and moldic porosity at many levels in the section and extending through many cycles. In highly permeable sections, cements and leach fabrics are difficult to tie to individual disconformities and reservoirs are sub-seismic scale and weakly stratified. On the other hand, aquitards (shale or muddy carbonates) in cycles can perch ground waters, limiting meteoric diagenesis to regressive, grainy facies of cycles to form sub-seismic scale, highly stratified reservoirs. In arid settings, sediments undergo caliche formation and some karsting, but most retain their original metastable mineralogies and are relatively poorly cemented except at cycle tops and deeper in the section. These sediments may be dolomitized by refluxing brines from high stand evaporite basins.

4. Long-term sea level changes of 1 to 10 m.y. or more, which commonly form seismic-scale supersequence- and sequence-bounding unconformities, when coupled with humid climates may generate long-standing, regional aquifers many tens to hundreds of kilometers wide, fed from the regional unconformity surface or prograding deltaic systems. Aquifers in newly deposited sediments are characterized by diffuse flow and deposit cements showing a regional cement stratigraphy. Sediments in updip areas become leached to form moldic porosity, metastable carbonates are stabilized to calcite and can form chalky porosity, and cements are precipitated from oxidizing meteoric phreatic groundwaters. Further downdip or low in the section, cements decrease in abundance and are formed from more reducing phreatic groundwaters. Downdip sediments may remain as metastable mineralogies until they are stabilized or leached in the burial environment and can form reservoirs which are prone to over-compaction.

With time (a million to tens of millions of years), mature karst develops over the unconformity surface, and diffuse flow aquifers develop into conduit flow types as cementation plugs intergranular and moldic porosity. The karst is characterized by erosional topography, sinkholes, caves and underground passages and most meteoric fluids move by conduit flow. Major reservoirs occur in breccias that surface the unconformity and fill caves, or are localized in compaction-fractured cave roofs. These permeable zones can be separated by muddy cave fills which partition these high compartmentalized reservoirs.

BIBLIOGRAPHY

Adams, J.E. and M.L. Rhodes, 1960, Dolomitization by seepage refluxion: A.A.P.G. Bull. 44, p. 1912-1920.

Beach, D.K., 1982, Depositional and diagenetic history of Pliocene-Pleistocene carbonates of northwestern Great Bahama Bank; Evolution of a carbonate platform: Ph.D. Dissertation, University of Miami, Fischer Island Station, 447 pp.

Berger, A., Loutre, M. F., and Dehant, V., 1989, Influence of the changing lunar orbit on the astronomical frequencies of pre Quaternary insolation patterns: Paleoceanography, v. 4 , p. 555-564

Berner, R.A., 1965, Dolomitization of Mid-Pacific atolls: Science, v. 147, p. 1297-1299.

Berner, R.A., 1991, A model for atmospheric CO_2 over Phanerozoic time: American Journal of Science, v. 291, p. 339-376.

Borer, J.M. and P.M. Harris, 1991, Lithofacies and cyclicity of the Yates Formation, Permian Basin: Implications for reservoirheterogeneity: A.A.P.G. Bull. v. 75, p. 726-779.

Bond , G. C., Kominz, M.A., Beavan, J., 1991, Evidence for orbital forcing of Middle Cambrian peritidal cycles: Wah Wah range, south-central Utah.

Budd, D.A., 1988, Aragonite-to-calcite transformation during fresh-water diagenesis of carbonates: insights from pore-water chemistry: Geol. Soc. America Bull., v. 100, p. 1260-1270.

Budd, D.A. and L.S. Land, 1990, Geochemical imprint of meteoric diagenesis in Holocene ooid sands, Schooner Cays, Bahamas: Correlation of calcite cement geochemistry with extant groundwaters: Jour. Sedimentary Petrology, v. 60, p. 361-378.

Burchette, T.P. and Wright, V.P., 1992, Carbonate ramp depositional systems: Sedimentary Geology, v. 79, p. 3-57.

Choquette, P.W. and J.D. Traut., 1963, Pennsylvanian carbonate reservoirs, Ismay field, Utah and Colorado, *in* R.O. Bass, ed., Shelf Carbonates of the Paradox Basin, Four Corners Geological Society, 4th Field Conference Gdbk., p. 157-184.

Chuber, S. and W.C. Pusey, 1985, Productive Permian carbonate cycles, San Andres Formation, Reeves Field, West Texas: *in* P.O. Roehl and P.W. Choquette, Carbonate Petroleum Reservoirs, Springer-Verlag, New York, p. 289-308.

Crowley, T.J. and S.K. Baum, 1991, Toward reconciliation of Late Ordovician glacieation with very high CO_2 levels: Journal of Geophysical Researtch, v. 96, p. 22,597-22,610.

Davies, J.R., 1991, Karstification and pedogenesis on a Late Dinantian carbonate platform, Anglesey, North Wales: Proc. Yorkshire Geol. Soc., v. 48, p. 297-322.

Dawson, W.C., 1988, Ismay reservoirs, Paradox Basin diagenesis and porosity development: Rocky Mountain Association of Geologists, 1988 Carbonate Symposium, p. 163-174.

Demicco, R.V., 1985, Patterns of platform and off-platform carbonates of the Upper Cambrian of western Maryland: Sedimentology, v. 32, p. 1-22.

Derby, J.R. and J.T. Kilpatrick, 1985, Ordovician Red River Dolomite reservoirs, Killdeer Field, North Dakota; *in* P.O. Roehl and P.W. Choquette, eds., Carbonate Petroleum Reservoirs, Springer-Verlag, New York, p. 59-70.

Dill, R.F., 1977,Blue holes - Geologically significant submerged sinkholes and caves off British Honduras and Andros, Bahama Islands, *in* Proceedings, Third International Coral Reef Symposium, Rosenstiel School of Marine and Atmospheric Science, University of Miami, Florida, p. 237-242.

Dorobek, S.L., 1987, Petrography, geochemistry and origin of burial diagenetic facies, Siluro-Devonian Helderberg Group (carbonate rocks), Central Appalachians (abs.): AAPG Bull., v. 71, p. 492-514.

Dorobek, S.L., T.M. Smith and P.M. Whitsitt, in press, Microfabrics and

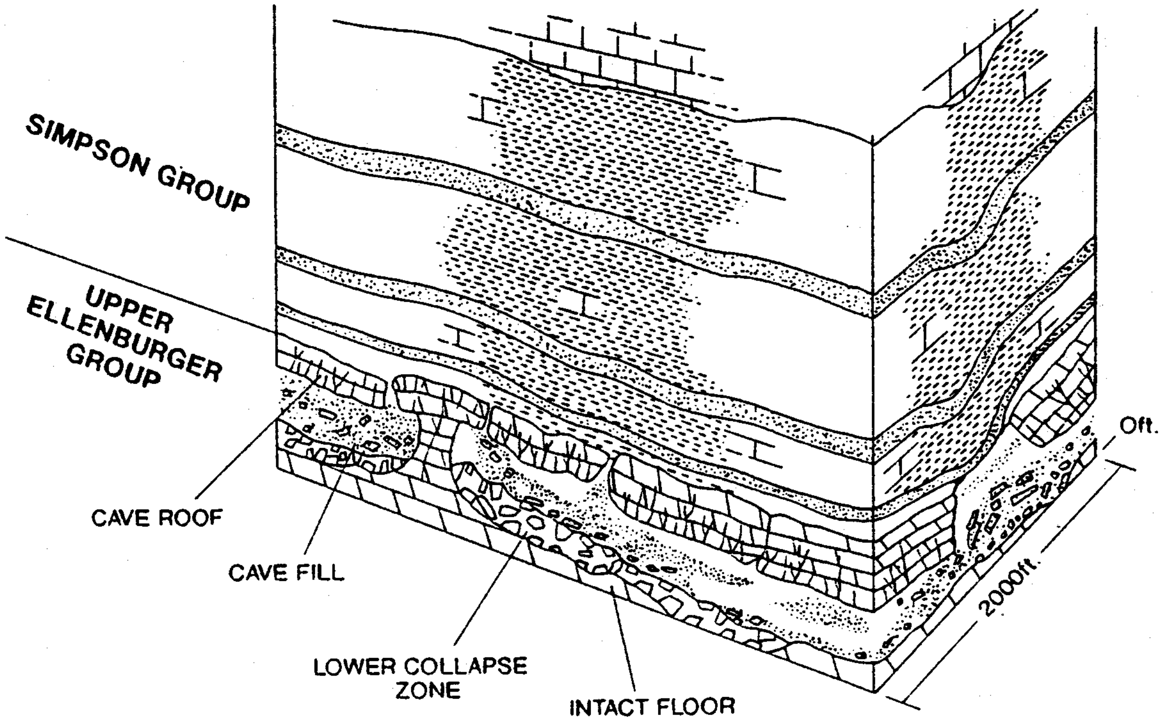

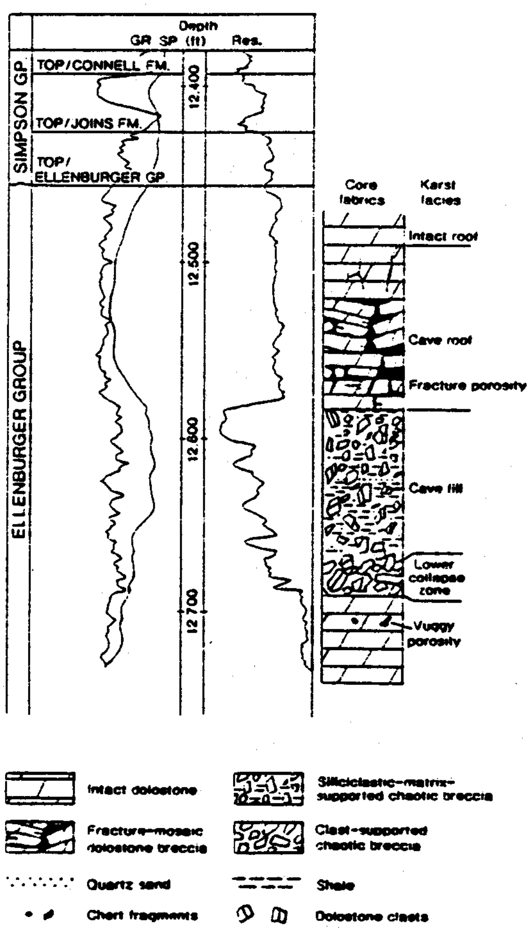

Figure 15. Karst generated during long term lowered sea level which exposed the Cambro-Ordovician platform, U.S.A. (from Kerans, 1988).

A) Block diagram showing sub-unconformity cave system.

B) Comparison of log signature and karst facies in Gulf 000-1 TXL well, Emma Ellenburger reservoir. Much of the porosity is in the fractured cave roof.

geochemical signatures associated with meteorically altered dolomite: examples from Devonian and Mississippian carbonates of Montana and Idaho: *in* R. Rezak and D. Lavoie, eds., Carbonate Microfabrics: Frontiers in Sedimentary Geology Series, Springer-Verlag, New York, p. ___.

Dunham, R.J., 1969, Early vadose silt in Townsend Mound (Reef), New Mexico, *in* G.M. Friedman, ed., Depositional Environments in Carbonate Rocks, Soc. Econ. Paleontologists and Mineralogists Spec. Publ. No. 14, p. 139-181.

Ebanks, W.J. Jr. and W.L. Watney, 1985, Geology of Upper Pennsylvanian carbonate oil reservoirs, Happy and Seberger fields, northwestern Kansas: *in* P.R. Roehl and P.W. Choquette, eds., Carbonate Petroleum Reservoirs, Springer-Verlag, New York, p. 239-250.

Elrick, M.E. and J.F. Read, 1991, Development of cyclic ramp-to-basin carbonate deposits, Lower Mississippian, Wyoming and Montana: unpub. Ph.D. dissertation, Virginia Polytechnic Institute and State University, Blacksburg, Virginia, 169 p.

Estaban, M. and C.F. Klappa, 1983, Subaerial exposure environment: in P.A. Scholle, D.G. Bebout and C.H. Moore, Carbonate Depositional Environments, AAPG Memoir 33, p. 1-54.

Fischer, A.G., 1964, The Lofer cyclothems of the Alpine Triassic: Kansas State Geological Surv. Bull. 169, v. 1, p. 107-150.

Fischer, A.G., 1982, Long-term climatic oscillations recorded in stratigraphy, in Climate in Earth History, National Academy Press, Washington D.C., p. 97-104.

Frakes, L.A. and J.E. Francis, 1988, A guide to Phanerozoic cold polar climates from high-latitude ice-rafting in the Cretaceous: Nature, v. 333, p. 547-549.

Friedman, G.M., 1965, Dolomite is an evaporative mineral: Evidence from the rock record and from sea-marginal ponds of the Red Sea: *in* D.H. Zenger, J.B. Dunham and R.L. Ethington, eds., Concepts of Dolomitization: SEPM Spec. Publ. 28, p. 69-80.

Gebelein, C.D., R.P. Steinen, P. Garrett, E.J. Hoffman, J.M. Queen and L.N. Plummer, 1980, Subsurface dolomitization beneath the tidal flats of West Andros Island, Bahamas, *in* D.H. Zenger, J.B. Dunham and R.L. Ethington, Eds., Concepts and Models of Dolomitization, S.E.P.M. Special Publication, No. 28, p. 31-49.

Gerhard, L.C., 1985, Porosity development in the Mississippian pisolitic limestones of the Mission Canyon Formation, Glenburn field, Williston Basin, North Dakota: in P.O. Roehl and P.W. Choquette, eds., Carbonate Petroleum Reservoirs, Springer-Verlag, New York, p. 193-205.

Ginsburg, R.N., 1971, Landward movement of carbonate mud: new model for regressive cycles in carbonates (abst.): AAPG Bull., v. 55, p. 340.

Ginsburg, R.N., P.K. Swart, G.P. Eberli, D.F. NcNeill and J.A.M. Kenter, 1990, Bahamas Drilling Project Phase 1, Appendix 1 and 2, Comparative Sedimentology Laboratory, Rosenstiel School of Marine and Atmospheric Science, University of Miami, 32 p.

Goldhammer, R.K., P.A. Dunn and L.A. Hardie, 1990, Depositional cycles, composite sea-level changes, cycles stacking patterns, and the hierarchy of stratigraphic forcing: Examples from Alpine Triassic carbonates: Geol. Soc. America Bulletin, v. 102, p. 535-562.

Goldhammer, R.K., E.J. Oswald and P.A. Dunn, 1991, Heirarchy of stratigraphic forcing: Example from Middle Pennsylvanian shelf carbonates of the Paradox Basin: *in* E.K. Franseen et al., Sedimentary Modelling: Computer simulations and methods for improved parameter definition: Kansas Geological Survey Bull. 233, p. 361-413.

Goldhammer, R.K., Lehmann, P.J. and Dunn, P.A., 1993, The origin of high frequency platform carbonate cycles and third order sequences (Lower Ordovician El Paso Group, West Texas): Constraints from outcrop data and modelling: Jour. Sediment. Petrology, v. 63, p. 318-359.

Goldstein, R.H., 1988, Cement stratigraphy of Pennsylvanian Holder Formation, Sacramento Mountains, New Mexico: AAPG Bull., 72, p. 425-438.

Goldstein, R.H., J.E. Anderson, and M.W. Bowman, 1991a, Diagenetic responses to sea-level change: Integration of field, stable-isotope, paleosol, paleokarst, fluid inclusion, and cement stratigraphy research to determine history and magnitude of sea-level fluctuation: *in* E.K. Franseen et al., Sedimentary Modelling: computer simulations and methods for improved parameter definition: Kansas Geological Survey Bull. 233, p. 139-162.

Goldstein, R.H., B.P. Stephens, and D.J. Lehrmann, 1991b, Fluid inclusions elucidate conditions of dolomitization in Eocene of Enewetak atoll and mid-Cretaceous Valles Platform of Mexico (Abstract): *in* A. Bosellini et al., eds., Dolomieu Conference on Carbonate Platforms and Dolomitization, Ortisei/St. Ulrich, Val Gardena/Grodental, The Dolomites, Italy, p. 93.

Goodwin, P.W. and E.J. Anderson, 1985, Punctuated aggradational cycles: A general hypothesis of episodic stratigraphic accumulation: Journal of Geology, v. 93, p. 515-533.

Gray, D.I., 1981, Lower Carboniferous shelf paleoenvironments in North Wales. Unpubl. Ph.D. Thesis, University of Newcastle-upon-Tyne, p. ___.

Grover, G.A. Jr. and J.F. Read, 1978, Fenestral and associated diagenetic fabrics of tidal flat carbonates, Middle Ordovician New Market Limestone, southwestern Virginia: Jour. Sedimentary Petrology, v. 48, p. 453-473.

Grover, G.A. Jr. and J.F. Read, 1983, Paleoaquifer and deep burial cements defined by cathodoluminescent patterns, Middle Ordovician carbonates, Virginia: AAPG Bull., v. 78, p. 1275-1303.

Halley, R.B. and J.W. Schmoker, 1983, High-porosity carbonate rocks of South Florida: progressive loss of porosity with depth: A.A.P.G. Bull. v. 67, p. 191-200.

Hardie, L.A., A. Bosellini and R.K. Goldhammer, 1986, Repeated subaerial exposure of subtidal carbonate platforms, Triassic, Northern Italy: evidence for high-frequency sea level oscilations on a 10 year scale, Paleoceanography, 1:447-457.

Hardie, L.A., P.A. Dunn and R.K. Goldhammer, 1991, Field and modelling studies of Cambrian carbonate cycles, Virginia Appalachians - discussion: Journal of Sedimentary Petrology, v. 61, p. 636-646.

Harris, P.M., P.E. Flynn and J.L. Sieverding, 1988, Mission Canyon (Mississippian) reservoir study, Whitney Canyon-Carter Creek field, southwestern Montana, *in* A.J. Lomando and P.M. Harris, Giant Oil and Gas Fields - A _ore Workshop: SEPM Core Workshop 12, v. 2, p. 695-740.

Harris, P.M. and E.L. Stoudt, 1988, Stratigraphy and lithofacies of the San Andres Formation, C.S.Dean "A", XIT, and SW Levelland units of Levelland-Slaughter field, Permian Basin: *in* A.J. Lomando and P.M. Harris, Giant Oil and Gas Fields, A Core Workshop, SEPM Core Workshop No. 12, p. 649-694.

Harrison, R.S., L.D. Cooper and M. Coniglio, 1984, Late Pleistocene carbonates of the Florida Keys: *in* Carbonates in Subsurface and Outcrop, 1984 CSPG Core Conference, Canadian Society of Petroleum Geologists, Calgary, Alberta, Canada, p. 291-306.

Harrison, R.S. and R.P. Steinen, 1978, Subaerial crusts, caliche profiles and breccia horizons: comparison of some Holocene and Mississippian exposure surfaces, Barbados and Kentucky: Geol. Soc. America Bull., v. 89, p. 389-396.

Heckel, P.H., 1980, Paleogeography of eustatic model for deposition of midcontinent Upper Pennsylvanian cyclothems: *in* T.D. Fouch and E.R.

Magathan, eds., Paleozoic Paleogeography of west-central United States, West-Central United States Paleogeography Symposium 1, Rocky Mountain Section SEPM, p. 197-215.

Heckel, P.H., 1983, Diagenetic model for carbonate rocks in Mid-continent Pennsylvanian eustatic cyclothems: Jour. Sedimentary Petrology, v. 53, p. 733-759.

Heckel, P., 1985, Recent interpretations of Late Paleozoic cyclothems: in Proceedings of the Third Annual Field Conference, Mid-Continent Section, SEPM, Lawrence, Kansas, p. 1-22.

Horbury, A.D., 1987, Sedimentology of the Urswick Limestone Formation in South Cumbria and North Lancashire. Unpublished Ph.D. Thesis, University of Manchester, 668 p.

Horbury, A.D., 1989, The relative roles of tectonism and eustacy in the deposition of the Urswick Limestone Formation in South Cumbria and north Lancashire, *in* R.S. Arthurton, P. Gutteridge and S.C. Nolan, eds., The Role of Tectonics in Devonian and Carboniferous Sedimentation in the British Isles. Yorkshire Geol. Soc. Occasional Publ. no. 6, p. 153-169.

Horbury, A.D. and A.E. Adams, 1989, Meteoric phreatic diagenesis in cyclic late Dinantian carbonates, northwest England: Sedimentary Geology, v. 65, p. 319-344.

Hovorka, S.D., H.S. Nance and C. Kerans, 1993, Parasequence geometry as a control on permeability evolution: examples from the San Andres and Grayburg Formations in the Guadalupe Mountains, New Mexico: The University of Texas at Austin, Bureau of Economic Geology Report, in press.

Humphrey, J.D., 1988, Late Pleistocene mixing zone dolomitization, southeastern Barbados, West Indies: Sedimentology, v. 35, 327-348.

Humphrey, J.D. and T.M. Quinn, 1989, Coastal mixing zone dolomite, forward modelling, and massive dolomitization of platform-margin carbonates: Jour. Sedimentary Petrology, v. 59, 438-454.

Hsu, K.J. and J. Schneider, 1973, Progress report on dolomitization - hydrology of Abu Dhabi sabkhas, Arabian Gulf, in B.H. Purser, eds., The Persian Gulf; Holocene Carbonate Sedimentation and Diagenesis in a Shallow Epicontinental Sea: New York, Springer-Verlag, p. 409-422.

Jordan, T.E. and Flemings, P.B., Large-scale stratigraphic architecture, eustatic variation and unsteady tectonism: A theoretical evaluation: Journal of geophysical Research, v. 96, p. 6681-6699.

Kendall, G. St. C., and Schlager, W., 1981, Carbonates and relative changes in sea level: Marine Geology ,v. 44, p. 181-212

Kerans, C., 1988, Karst-controlled reservoir heterogeneity in Ellenburger Group carbonates of West Texas: A.A.P.G. Bull., v. 72, p. 1160-1173.

Knight, I., N.P. James and T.E. Lane, 1991, The Ordovician St. George unconformity, northern Appalachians: The relationship of plate convergence at the St. Lawrence Promontory to the Sauk/Tippecanoe sequence boundary: Geological Society of America Bull., v. 103, p. 1200- 1225.

Koerschner, W.F. and J.F. Read, J.F., 1989, Field and modelling studies of Cambrian carbonate cycles, Virginia Appalachians: Jour. Sed. Petrology, v. 59, p. 654-687.

Kozar, M.G., L.J. Weber and K.R. Walker, 1990, Field and modelling studies of Cambrian carbonate cycles, Virginia Appalachians - Discussion: Jour. Sedimentary Petrology, v. 60, p. 790-794.

Kupecz, J.A., 1989, Petrographic and geochemical characterization of the Lower Ordovician Ellenburger Group, west Texas: Ph.D. Dissertation, University of Texas, Austin, 157 p.

Lees, A., 1975, Possible influence of salinity and temperature on modern shelf carbonate sedimentationL Marine Geology, v. 19, p. 159-198.

Logan, B.W., 1974, Inventory of diagenesis in Holocene-Recent carbonate sediments, Shark Bay, Western Australia, *in* B.W. Logan et al., Evolution and diagenesis of Quaternary carbonate sediments, Shark Bay, Western Australia: A.A.P.G. Memoir 22, p. 195-250.

Longacre, S.A., 1980, Dolomite reservoirs from Permian biomicrites: in R.B. Halley and R.G. Loucks, eds., Carbonate Reservoir Rocks, SEPM Core Workshop No. 1, p. 105-117.

Longman, M.W., T.G. Fertal and J.S. Glennie, 1983, Origin and geometry of Red River Dolomite reservoirs, western Williston Basin: A.A.P.G. Bull. 67, p. 744-771.

Major, R.P., D.G. Bebout, and F.J. Lucia, 1988, Depositional facies and porosity distribution, Permian (Guadalupian) San Andres and Grayburg Formations, P.J.W.D.M. field complex, Central Basin Platform, West Texas: *in* A.J. Lomando and P.M. Harris, eds., Giant Oil and Gas Fields, A Core Workshop, SEPM Core Workshop 12, v. 2, p. 615-648.

Marquis, S.A. Jr., and R.L. Laury, 1989, Glacio-eustasy, depositional environments, and reservoir character of Goen Limestone cyclothem (Desmoinesian), Concho Platform, Central Texas: A.A.P.G. Bull. 73, p. 166-181.

Matthews, R.K. and C. Frohlich, 1987, Forward modelling of bank-margin carbonate diagenesis: Geology, v. 15, p. 673-676.

Mazzullo, A.J. and Friedman, G.M., 1975, Conceptual model of tidal influenced deposition on margins of epeiric seasL Lower Ordovician (Canadian) of eastern New York and southwestern Vermont: AAPG Bull., v. 59, p. 2123-2141.

McKenzie, J.A., K.J. Hsu and J.F. Schneider, 1980, Movement of subsrface waters under the sabkha, Abu Dhabi, U.A.E., and its relation to evaporative dolomite genesis: SEPM Spec. Publ. No. 28, p. 11-30.

Mitchell, J.C., P.J. Lehmann, D.L. Cantrell, I.A. Al-Jallal and M.A.R. Al-Thagafy, 1988, Lithofacies, diagenesis and depositional sequence; Arab-D Member, Ghawar Field, Saudi Arabia, in SEPM Core Workshop No. 12, p. 459-514.

Mitchell, R.W., 1985, Comparative sedimentology of shelf carbonates of the Middle Ordovician St. Paul Group, Central Appalachians: Sedimentary Geology, v. 43, p. 1-41.

Mitchum, R.M., Jr. and J.C. Van Wagoner, 1991, High frequency sequences and their stacking patterns: sequence-stratigraphic evidence of high-frequency eustatic cycles: Sedimentary Geology, v. 70, p. 131- 160.

Montanez, I.P. and J.F. Read, 1992a, Fluid-rock interaction history during stabilization of early dolomites, Upper Knox Group (Lower Ordovician), U.S. Appalachians: Jour. Sedimentary Petrology, in press.

Montanez, I.P. and J.F. Read, 1992b, Eustatic control on dolomitization of cyclic peritidal carbonates: Evidence from the Early Ordovician Knox Group, Appalachians: Geological Society of America Bull., in press.

Mussman, W.J., I.P. Montanez and J.F. Read, 1988, Ordovician Knox paleokarst unconformity, Appalachians: *in* N.P. James and P.W. Choquette, eds., Paleokarst, Springer-Verlag, New York, p. 211-228.

Niemann, J.C. and J.F. Read, 1988, Regional cementation from unconformity-recharged aquifer and burial fluids, Mississippian Newman Limestone, Kentucky: Jour. Sediment. Petrology, v. 58, p. 688- 705.

Nelson, W.A. and J.F. Read, 1989, Updip to downdip cementation and dolomitization patterns in a Mississippian aquifer, Appalachians: Jour. Sedimentary Petrology, v. 60, p. 379-396.

Perkins, R.D., 1977, Depositional framework of Pleistocene rocks in South Florida: *in* P. Enos and R. Perkins, Quaternary Sedimentation in South Florida, The Geological Society of America Memoir 147, p. 131-198.

Pomar, L., 1991, Reef geometries, erosion surfaces and high-frequency sea-level changes, Upper Miocene Reef Complex, Mallorca, Spain, Sedimentology, v. 38, p. 243-269.

Pomar, L. N., in press, High-resolution Sequence Stratigraphy in Prograding Miocene Carbonates: Application to Seismic Interpretation, AAPG Memoir on "Carbonate Sequence Stratigraphy".

Posamentier, H.W. and Allen G.P., Siliciclastic sequence stratigraphic patterns in foreland ramp-type basins: Geology, v. 21, p. 455-458.

Posamenteir, H.W., Summerhayes, C.P., Hag, B.U. and Allen, G.P. (Editors), 1993. Sequence stratigraphy and facies Int. Assoc. Sedimentol., Spec. Publ., 18 (in press).

Pray, L.C. and J.L. Wray, 1963, Porous algal facies (Pennsylvanian) Honaker Trail, San Juan Canyon, in R.O. Bass, ed., Four Corners Geological Society, 4th Field Conf. Gdbk., p. 204-234.

Purdy, E.G., 1974a, Karst-determined facies patterns in British Honduras: Holocene carbonate sedimentation model, Bull. Amer. Assoc. Petrol. Geol., 58:825-855.

Purdy, E.G., 1974b, Reef configurations: cause and effect, *in* Laporte, L.E. (editor), Special Publication of the Society of Economic Paleontologists and Mineralogists, 18:9-76.

Qi, F. and W. Xie-Pei, 1984, Significant role of structural fractures in Rengiu Buried - Hill Oil Field in eastern China, Amer. Assoc. Petrol. Geol. Bull., 68:971-982.

Ramsay, A.T.S., 1990, The sedimentology and sequence stratigraphy of the Asbian platform carbonates in South Wales (abs): Abstracts of Papers, 13th International Sedimentological Congress, Nottingham, England, p.448.

Read, J.F., 1973, Paleo-environments and paleogeography, Pillara Formation (Devonian), Western Australia: Bull. Canadian Petroleum Geology, v. 21, p. 344-394.

Read, J.F., 1980, Carbonate ramp-to-basin transitions and foreland basin evolution, Middle Ordovician, Virginia Appalchians: Amer. Assoc. Petroleum Geol. Bull.,v. 64, p. 1575-1612.

Read, J.F. and R.K. Goldhammer, 1988, Use of Fischer plots to define 3rd order sea-level curves in peritidal cyclic carbonates, Early Ordovician, Appalchians: Geology, v. 6, p. 895-899.

Read, J.F. and G.A. Grover, Jr., 1977, Scalloped and planar erosion surfaces, Middle Ordovician limestones, Virginia: analogues of Holocene exposed karst or tidal rock platforms: Jour. Sedimentary Petrology, v. 47, p. 956-972.

Read, J.F., D.A. Osleger and M.E. Elrick, 1991, Two-dimensional modelling of carbonate ramp sequences and component cycles: *in* E.K. Franseen et al., eds., Sedimentary Modelling: Computer simulations and methods for improved parameter definition: Kansas Geological Survey Bull. 233, p. 473-488.

Reid, A.M. and S.A. Tomlinson-Reid, 1991, The Cogdell field study, Kent and Scurry Counties, Texas: A post-mortem, *in* M.P. Candelaria, ed., Permian Basin Plays - Tomorrow's Technology Today, West Texas Geological Society Publ. No. 91-89, p. 39-66.

Roylance, M.H., 1990, Depositional and diagenetic history of a Pennsylvanian algal-mound complex: Bug and Papoose Canyon fields, Paradox Basin, Utah and Colorada: A.A.P.G. Bull. 74, p. 1087-1099.

Ruddiman, W.F., Raymo, M., McIntyre, A., 1989, Matuyama 41,000-year cycles: North Atlantic Ocean and northern hemisphere ice sheets, Earth and Planetary Science Letters, v. 80, p. 117-129

Ryder, R., Harris, A.G. and Repetski, J.E., 1992, Stratigraphic framework of Cambrian and Ordovician rocks in the Central Appalachian Basin from Medina County, Ohio, through Southwestern and South-Central Pennsylvania to Hampshire County, West Virginia: U.S. Geol. Survey Bull. 1839, Ch. K, 32 p.

Sadler, P.M., Osleger, D.A. and Montanez, I.P., in press, On labelling, interpretation , and the length of Fischer plots: AAPG Bull.

Saller, A.H., 1984, Petrologic and geochemical constraints on the origin of subsurface dolomite, Enewetak Atoll: an example of dolomitization by normal seawater: Geology, v. 12, p. 217-220.

Sarg, J.F., 1988, Carbonate Sequence Stratigraphy: *in* C.K. Wilgus and others, eds., Sea-Level Changes: An Integrated Approach: SEPM Spec. Publ. 42, p. 156-181.

Schatzinger, R.A., 1983, Phylloid algal and sponge-bryozoan moudn-to-basin transition: A Late Paleozoic facies tract from the Kelly-Snyder field, West Texas: *in* P.M. Harris, ed., Carbonate Buildups - A Core Workshop, SEPM Core Workshop No. 4, p. 244-303.

Schlager, W., 1981, The paradox of drowned reefs and carbonate platforms: Geological Society of American Bulletin, v.92, p. 197-211

Schlager, W., 1992, Sedimentology and sequence stratigraphy of reefs and carbonate platforms: AAPG Continuing Education Course Note Series #34, 71 p.

Sloss, L.L., 1963, Sequences in the cratonic interior of North America: Geol. Soc. America Bull., v. 74, p. 93-113.

Smart, P.L., R.J. Palmer, F. Whitaker and V. P. Wright, 1988, Netunian dikes and fissure fills: an overview and account of some modern examples: *in* N.P. James and P.W. Choquette, eds., Paleokarst, Springer-Verlag, New York, p. 149-163.

Somerville, I.D., 1979a, Minor sedimentary cyclicity in late Asbian (upper D1) limestones in the Llangollen district of North Wales: Proc. Yorkshire Geol. Soc., v. 42, p. 317-341.

Somerville, I.D., 1979b, A cyclicity in early Brigantian (D2) limestones east of the Clwydian Range, North Wales, and itsuse in correlation: Geological Journal, v. 14, p. 69-86.

Tucker, M.E., 1985, Shallow-marine carbonate and facies models, *in* P.J. Benchley and B.P.J. Williams, Sedimentology: recent developements and applied aspects, Geol. Soc. London Spec. Publication 18, p. ___.

Vail, P.R., 1987, Seismic stratigraphic interpretatation using sequence stratigraphy. Part 1: Seismic stratigraphy interpretation procedure, *in* Bally, A.W. (ed), AAPG Atlas of Seismic Stratigraphy, v. 1, AAPG Studies in Geology, no. 27, p. 1-10

Vail, P. R., et al., 1991, The stratigraphic signatures of tectonics, eustasy and sedimentology - an overview: *in* G. Einsele, W. Ricken and A. Seilacher, eds., Cycles and Events in Stratigraphy, Springer-Verlag, p. 617-659.

Vail, P.R., R.M. Mitchum, and S. Thompson, III, 1977, Seismic stratigraphy and global changes of sea level, Part 4: Global Cycles of relative changes of sea level, *in* C.A. Payton, Seismic Stratigraphy - Applications to hydrocarbon exploration: A.A.P.G. Memoir 26, p. 83-97.

Van Hinte, J.E., 1978, Geohistory analysis - application of micro-paleontology in exploration geology: AAPG Bull v. 62, p. 201-222.

Van Wagoner, J.C., H.W. Posamentier, R.M. Mitchum, P.R. Vail, J.F. Sarg, T.S. Loutit and J. Hardenbol, 1988, An overview of the fundamentals of sequence stratigraphy and key definitions; *in* C.K. Wilgus et al., eds., Sea-Level Changes - An Integrated Approach, SEPM Spec. Publ. 42, p. 39-46.

Walkden, G.M., 1987, Sedimentary and diagenetic styles in late Dinantian carbonates of Britain, *in* J. Miller, A.E. Adams and V.P. Wright, eds., European Dinantian Environments. Wiley, Chichester, p.131-155.

Walkden, G.M. and G.D. Walkden , 1990, Cyclic sedimentation in carbonate and mixed carbonate-clastic environments: four simulation programs for a desktop computer: *in* M.E. Tucker et al., eds., Carbonate Platforms, Facies Sequences and Evolution, Spec. Publ. No. 9, International Assoc. of Sedimentologists, p. 55-78.

Ward, W.C. and R.B. Halley, 1985, Dolomitization in a mixing zone of near-seawater composition, Late Pleistocene, northeastern Yucatan Peninsula: Jour. Sedimentary Petrology, v. 55, p. 407-420.

Watney, W.L., J. French and E.K. Franseen, 1989, Sequence stratigraphic interpretations and modelling of cyclothems in the Upper Pennsylvanian (Missourian) Lansing and Kansas City groups in eastern Kansas, Kansas Geological Society 41st Annual Field Trip Guidebook, Lawrence, Kansas, 211 p.

Watts, A.B., 1981, The U.S. Atlantic continental margin: subsidence history, crustal structure and thermal evolution: *in* A.W. Bally et al., eds., Geology of Passive Continental Margins, AAPG Education Course Note Series #19, p. 2-1 - 2-75.

Wendte, J.C. and F.A. Stoakes, 1982, Evolution and porosity devlopment of the Judy Creek reef complex, Upper Devonian, Central Alberta: *in* W.G. Cutler, Canadas Giant Hydrocarbon Reservoirs, Canadian Society of Petroleum Geologists, Calgary, Alberta, p. 63-81.

Whitataker, F.F. and P.L. Smart, 1990, Active circulation of saline ground waters in carbonate platforms: Evidence from the Great Bahama Bank: Geology, v. 18, p. 200-203.

Wilson, J.L., 1975, Carbonate facies in geologic history: Springer-Verlag, New York, 471 p.

Wright, V.P., 1992, Speculations on the controls on cyclic peritidal carbonates: ice-house versus greenhouse erustatic controls: Sedimentary Geology, v. 76, p. 1-5.

Wright, V.P., M. Estaban and P. Smart, 1991, Palaeokarst and palaeokarstic reservoirs: Uiversity of Reading, ___ p.

Wright, V.P. and T.J. Faulkner, 1990, Sediment dynamics of early Carboniferous ramps: Geol. Jour., v. 25, p. 139-144.

ABSTRACTS

ABINOLFI, FREDERICK, MAHER IBRAHIM, FRED GRAY, and ANDREW RADFORD, U.S. Department of the Interior, Minerals Management Service, Herndon, VA.

Environmental and Regulatory Costs in Oil and Gas Resource Evaluation

Fair-market value of tracts offered for lease on the outer continental shelf is determined by competitive bidding. When the Minerals Management Service (MMS) determines that competition is insufficient, it evaluates a tract's value before accepting a bid. Development delays and costs associated with environmental and other government requirements affect economic resource estimates.

The petroleum industry, aware of environmental needs, has aimed exploration at large, natural gas prospects. Also, MMS focuses leasing on areas where development would have the least impact on the environment.

Three prospects in the Mid-Atlantic Planning Area that differ greatly in size and water depth were selected to illustrate how costs and delays affect resource estimates. A discounted cash-flow model, which incorporates the statistical principles of multiple trials, random sampling, range of values, and marginal probability, attempts to simulate the offshore exploration and development process. However, the model is just a model; it only simulates the predictable. Sensitivity analysis of the cash-flow model to cost and delay variables provides information on a prospects resources and present worth.

Lead time before development affects development and operating costs, especially in deep water. These costs affect estimates of economic field life and potential reserves. In assessing oil and gas resources, one must consider environmental and regulatory costs and the possibility of long delays in offshore development. This study describes how to predict these costs and their effect on resource estimates.

BARANOSKI, MARK T., AND MARK E. WOLFE, Ohio Department of Natural Resources, Columbus, OH.

Natural Gas Plays of the Knox Group in the Appalachian Basin: A Significant Element of the U.S. Department of Energy Atlas of Major Appalachian Gas Plays

Oil and gas have been produced from the Knox Group in the Appalachian basin since the early 1900s. However, only since the 1960s have significant volumes of hydrocarbons been produced. Porosity development along the Knox unconformity is the dominant geologic control for hydrocarbon migration and entrapment. Other important controls include stratigraphy, diagenesis, paleokarst, structure, and fractures. Cumulative production is ultimately controlled by the reservoir conditions characteristic to each play. The two most significant Knox plays in terms of total cumulative gas production are (1) the Lower Ordovician-Upper Cambrian eroded shelf sandstones known as the Rose Run sandstone in Kentucky, Ohio, and Pennsylvania, and the Theresa sandstone in New York, and (2) the Lower Ordovician-Upper Cambrian paleokarstic carbonates known as the Beekmantown dolomite in Kentucky, Ohio, and Tennessee, and the Copper Ridge (Trempealeau) dolomite in Ohio. Minor, volumes of gas have been produced from fracture and paleokarstic carbonate plays in the Knox dolomite of Kentucky, Tennessee, and Virginia, and from localized sandstones of the Copper Ridge (Trempealeau) in Ohio. Some individual wells in Ohio have produced more than 1 billion ft^3 of gas from the Beekmantown, Rose Run, or Copper Ridge (Trempealeau). Cumulative gas production from all the Knox plays in the Appalachian basin has been in excess of 60 billion ft3 of gas. The Knox Group plays are currently the most active exploration targets in the basin.

BAUERT, CARMEN, Institute of Geology, Tallinn, Estonia, and HEIKKI BAUERT, University of North Carolina, Chapel Hill, NC.

Chitinozoan Biostratigraphy-A Good Correlation Tool for Ordovician Rocks: Case Study of Baltoscandian oil Shale Interval

Chitinozoans are organic-walled microfossils known from marine sedimentary rocks of Ordovician to Devonian age. In Baltoscandia, chitinozoans have been extensively studied since the 1930s and chitinozoan biostratigraphy of Ordovician-Silurian succession is quite well established. Because the Ordovician-Silurian carbonate sequence contains only a scarce graptolite fauna, chitinozoans and conodonts are considered the most valuable faunal groups for stratigraphic correlation, with the chitinozoans offering even better temporal resolution due to their widespread occurrence, planktonic origin, and relatively easy taxonomy. Also, small samples (100-300 g) can yield several hundreds of chitinozoans.

In this study, chitinozoan distribution is compared in two Middle Ordovician (Llanvirn to Caradoc) core sections: Tamsalu-565 (central Estonia) and Bliudziai-150 (southern Lithuania). The distance between studied sections is about 470 km. The studied intervals are 51 and 27 m thick in the Tamsalu-565 and Bliudziai-150 cores, respectively. Both sections are highly condensed with numerous hardgrounds, but without major hiatuses. The Tamsalu-565 boreholes was drilled in the Tapa oil shale deposit and contains 17 kukersite-type oil shale beds up to 2.3 m thick.

Both sections yielded a numerous and diverse chitinozoan fauna. Altogether, 14 genera and 55 species were recorded. Although many chitinozoan species are long ranging, several with limited vertical range are useful biostratigraphically and suggest a good correlation between the studied sections.

Chitinozoans can be regarded as a perspective faunal group in the United States for correlating subtidal to basin carbonate sediments, particularly when small sample size is a critical factor.

BRANNOCK, MICHAEL C., Quaker State Corporation, Belpre, OH.

The Starr Fault System of Southeastern Ohio

The Starr fault system is a series of east-west-trending faults located in southeastern Ohio. This fault system was discovered by mapping the anomalous sedimentary sequence of the "Big Lime." The Big Lime is a driller's term for the stratigraphic section that includes the Lower Devonian Onondaga through Middle Silurian Lockport formations. The use of trend-surface analysis identified the probable fault orientation, which was then verified by seismic.

The system is a series of high-angle faults, originating in the Precambrian, that occur along a narrow corridor traversing several townships. Analysis of the sedimentary section preserved by faulting indicates fault movement after the deposition of the Bass Islands Formation, which was followed by a regional unconformity that removed the Bass Islands and a part of the upper Salina Formation. The Onondago subsequently was deposited, masking fault movement evidence in the shallower formations. Some minor movement occurred later, as is evidenced by expansion in the Devonian shale sequence. The geometry of the fault system and other data suggest a pattern similar to the Albio-Scipio field of southern Michigan.

A group of wells were drilled to test the Ordovician Trenton and Black River formations to determine the existence of secondary dolomite, which could be a potential reservoir. Secondary dolomite was encountered, but no commercial hydrocarbons were found in either the Trenton or Black River. Other formations produced hydrocarbons and water from fractured zones that were not known for this behavior. Other probable fault systems in southern Ohio, identified by using the same mapping techniques, may provide deeper targets for future drilling.

BROCKMAN, ALLEN R., and GEORGE E. HARLOW, JR., * U.S. Geological Survey, Richmond, VA.

The Shallow Aquifer System at the Naval Surface Warfare Center, Dahlgren Laboratory, Dahlgren, Virginia

In 1992, the U.S. Geological Survey began a 3-yr study of the hydrogeology at the Naval Surface Warfare Center Dahlgren Laboratory (NSWCDL) at Dahlgren, Virginia. The purpose of the study was to determine the altitude of the top, thickness, extent, water level, and hydraulic conductivity of the aquifers and confining units within 220 ft of land surface.

A literature review indicated that one unconfined aquifer (the Columbia aquifer) and one confined aquifer (the Aquia aquifer) were up to 200 ft deep at the NSWCDL, but a preliminary analysis of electric and natural-gamma geophysical logs collected during the study identified another confined aquifer (the Chickahominy-Piney Point aquifer, between the Columbia and Aquia aquifers) not indicated in the literature. The presence of this aquifer at the NSWCDL was confirmed by analysis of split-spoon core samples.

The shallow aquifer system at the NSWCDL includes three aquifers and two confining units; they are: from the upper most downward, the Columbia aquifer (10 to 28 ft thick), the Calvert confining unit (20 to 45 ft thick), the Chickahominy-Piney Point aquifer (16 to 31 ft thick), and the Aquia aquifer (thickness exceeds 23 ft). None of the wells penetrated to the base of the Aquia aquifer.

COHEN, ARTHUR D., University of South Carolina, Columbia, SC, THOMAS D. DAVIES, Exxon Exploration Company, Houston, TX, and WILLIAM SPACKMAN, Pennsylvania State University, University Park, PA.

Sulfur Conents of Peats at the Confluence of Carbonate and Peat-Forming Depositional Systems, Southeastern Florida.

Complex stratigraphic and compositional relationships have been reported by others at sites where coal beds are laterally in contact with marine carbonates (such as in the southern portion of the Illinois basin). These basin edges are important in that they may (1) represent sites of active coal mining, (2) contain important clues as to the development of the basin, and (3) be sources of the dispersed terrestrial organics encountered in nearby marine rocks. This study was undertaken to investigate peat/carbonate relationships in a modern setting, with initial research on sulfur contents relative to stratigraphic/petrographic conditions. Thirty-eight cores were taken along northwest-southeast transects from the mainland to Florida Bay. The most inland cores consist entirely of peat, representing transgression of marine types (mangrove) over freshwater types. Toward the carbonate-rich bay, a more complex stratigraphy exists. Marine carbonates and peats interfinger, with erosional contacts indicating that parts of the peat sequence are missing. AT the coastline, most of the peat is replaced by marine carbonate except for thin (1-10 cm) basal erosional remnants. Florida Bay cores also contain basal parts (usually overlain by marine carbonates), with the best preserved peat sequences tending to occur beneath bay islands. Total sulfur ranges from 0.6 to 5.0% (dry) at the most inland sites, 2.5 to 7.8% near the coastline, and 1.5 to 5.9% in bay sediments. Total sulfur is higher in marine than freshwater peats, but freshwater peats overlain by marine peats are enriched in sulfur. Freshwater peats beneath marine carbonates are relatively low in sulfur, but are higher if the peat is overlain by a marine peat being overlain by the carbonate.

COLLINS, STEVEN L., University of North Carolina, Chapel Hill, NC

Relative Trace-Element Concern Indexes for Eastern Kentucky Coals

Coal trace elements that could affect environmental quality were studied in 372 samples (collected and analyzed by the Kentucky Geological Survey and the United States Geological Survey) from 36 coal beds in eastern Kentucky.

Relative trace-element concern indexes are defined as the weighted sum of standardized (subtract mean; divide by standard deviation concentrations. Index R is calculated from uranium and thorium, index 1 from elements of minor concern (antimony, barium, bromine, chlorine, cobalt, lithium, manganese, sodium, and strontium), index 2 from elements of moderate concern (chromium, copper, fluorine, nickel, vanadium, and zinc), and index 4 from elements of greatest concern (arsenic, boron, cadmium, lead, mercury, molybdenum, and selenium). Numerals indicate weights, except that index R is weighted by 1, and index 124 is the unweighted sum of indexes 1, 2, and 4.

Contour mapping indexes is valid because all indexes nonnugget effect variograms. Index 124 is low west of Lee and Bell counties, and in Pike County. Index 124 is high in the area bounded by Boyd, Menifee, Knott, and Martin counties and in Owsley, Clay, and Leslie counties. Coal from some areas of eastern Kentucky is less likely to cause environmental problems than that from other areas.

Positive correlations of all indexes with the centered log ratios of ash, and negative correlations with centered log ratios of carbon, hydrogen, nitrogen, oxygen, and sulfur indicate that trace elements of concern are predominantly associated with ash. Beneficiation probably would reduce indexes significantly.

COMER, JOHN B., and NANCY R. HASENMUELLER, Indiana Geological Survey, Bloomington, IN, WAYNE T. FRANKIE, Illinois State Geological Survey, Champaign, IL, and TERRENCE HAMILTON-SMITH, Kentucky Geological Survey, Lexington, KY.

Gas Potential of New Albany Shale (Devonian-Mississippian) in the Illinois Basin

A study to update and evaluate publicly available data relating to present and potential gas production from New Albany Shale in the Illinois basin was conducted cooperatively by the Indiana, Illinois, and Kentucky geological surveys (Illinois Basin Consortium), and was partially funded by the Gas Research Institute. Deliverables included a plate of stratigraphic cross sections and six basin-wide maps at a scale of 1:1,000,000 showing (1) major structural features, (2) core locations, (3) structural elevation of the top of the formation, (4) total thickness, (5) average initial production/initial open-flow from producing gas fields, and (6) vitrinite reflectance (R_o).

The New Albany Shale is an organic-rich brownish black shale present throughout the Illinois basin. Gas potential of the New Albany Shale may be great because it contains an estimated 86 tcf of natural gas and has produced modest volumes since 1858 from more than 60 fields, mostly in the southeastern part of the basin. Reservoir beds include organic-rich shales of the Grassy Creek (Shale), Clegg Creek, and Blocher (Shale) members. Limited geologic and carbon isotope data indicate that the gas is indigenous and thermogenic. T_{max} data suggest that, statistically, gas generation begins at R_o values of 0.53% and may begin at R_o values as low as 0.41% in some beds.

New Albany Shale reservoirs contain both free gas in open-pore space and gas absorbed on clay and kerogen surfaces. Natural fracturing is essential for effective reservoir permeability. Fractures are most common near structures such as faults, flexures, and buried carbonate banks. Based on limited data, fractures and joints have preferred orientations of 45-225° and 135-315°. Commercial production requires well stimulation to connect the well bore with the natural fracture system and to prop open pressure-sensitive near-borehole fractures. Current stimulations employ hydraulic fracture treatments using nitrogen and foam with sand as a propping agent.

EDSON, GARY, FREDERICK ADINOLFI, FREDERICK GRAY, MAHER IBRAHIM, JACK KIENZIE, FRED LISHMAN, and KUNG HUANT, U.S. Minerals Management Service, Herndon, VA.

Petroleum Exploration and the Atlantic OCS

The largest Atlantic outer continental shelf (OCS) lease sales was the first one, Sale 40 in 1976. Ninety-three Baltimore Canyon Trough petroleum leases were issued, and industry's winning bids totaled $1.1 billion. The highest bonus bids were for leases overlying the Schlee Dome, then called Great Stone Dome, a large structure with a very large fetch area. By 1981, seven dry wells on the dome moderated this initial flush of optimism. However, subeconomic quantities of gas and light oil were discovered on the nearby Hudson Canyon Block 598-642 structure.

Now after 9 lease sales, 410 lease awards, and 46 exploration wells, United States Atlantic petroleum exploration activity is in a hiatus. Fifty-three leases remain active under suspensions of operation. Twenty-one lease blocks, about 50 mi offshore from Cape Hatteras, have been combined as the Manteo Exploration Unit. Mobil and partners submitted an exploration plan for the unit in 1989.

The Atlantic OCS has petroleum potential, especially for gas. With only 46 exploration wells, entire basins and plays remain untested. During the present exploration inactivity, some petroleum evaluation of the Atlantic OCS continues by the Minerals Mangagement Service and others. Similarities and differences are being documented between United States basins and the Canadian Scotian Basin, which contains oil and gas in commercial quantities. Other initiatives include geochemical, thermal history, seismic stratigraphic, and petroleum system modeling studies. The gas-prone Atlantic OCS eventually may make an energy contribution, especially to nearby East Coast markets.

FRANTZ, JOSEPH H. JR., S. A. Holditch & Associates, Inc., Pittsburgh, PA, KENT GUIDRY and DON LUFFEL,
ResTech Houston, Inc., Houston, TX, and WEST KUBIK, K & A Energy Consultants, Tulsa, OK.

Evaluation of the Berea Sandstone Formation in Eastern Pike County, Kentucky

Geologic, reservoir, and stimulation descriptions for the Berea sandstone formation in eastern Pike County, Kentucky, were obtained by integrating geologic, core, log, well test, and hydraulic fracture analyses. Our results indicate the Berea in this area is a very low-permeability (0.1 md), naturally fractured, multilayer reservoir with porosities ranging from 5 to 9%, water saturations from 30 to 70%, net pays from 30 to 70 ft, and reservoir pressures from 700 to 800 psia. Clays, mica, cement, and very fine quartz grains account for the low permeability. We identified two independent, noncommunicating Berea and packages, each with its own system of short, near-vertical, natural fractures. Natural fractures were observed in the core, on the formation microscanner log, and on the borehole television in both the upper and lower sands. In both sand packages, an anisotropic fracture network exists consisting of a dominant northeast-southwest-trending set, and a less abundant intersecting set. We determined the hydraulic fracture propagated northeast-southwest, and thus parallel the most closely spaced natural fractures, limiting the impact of the hydraulic fracture treatment in the Berea. In addition, the natural fracture frequency is inferred to be highly variable between wells based on long-term production from older, Berea-only completions in this area ranging from 40 million scf to 2.5 Bdcf.

The Gas Research Institute (GRI) has been sponsoring a cooperative well program with Ashland Exploration, Inc. (AEI) during the past two years targeting the Devonian Shale and Berea sandstone formations in Pike County of eastern Kentucky. Operators typically complete both the shales and Berea in one well bore in this area. This presentation summarizes the research results of the Berea cooperative well, the COOP 2 (Ashland FMC 80). The specific objectives of the Berea evaluation in the COOP 2 were to develop an integrated reservoir description for stimulation design and predicting long-term well performance, identify geologic production controls, determine the in-situ stress profile, and develop Berea log interpretation models for gas porosity and stress. To satisfy these objectives, data were collected and analyzed from 146 ft of whole core, open-hole geophysical logs, including formation microscanner and digital sonic, in-situ stress measurements, and prefracture production and pressure transient tests. In addition, data from a minifracture, a fracture stimulation treatment, and postfracture performance tests were analyzed.

We determined the integrated reservoir/hydraulic fracture descriptions from analyzing the data collected in the open- and cased-hole, in addition to the log interpretation models developed to accurately predict gas porosity and stress profiles. Results can be applied by operators to better understand the Berea reservoir in the study area, predicts well performance, and design completion procedures and stimulation treatments. The methodology can also be applied to other tight-gas sand formations.

HAMILTON, PIXIE A., U.S. Geological Survey, Richmond, VA, and JUDITH M. DENVER, U.S. Geological Survey, Dover, DE.

Effects of Agriculture Chemicals on Natural Geochemistry of Shallow Groundwater, Delmarva Peninsula, Delaware, Maryland, and Virginia

Agriculture practices affect water chemistry in the water-table aquifer throughout the Delmarva Peninsula. The Delmarva Peninsula, located in the Atlantic coastal plain physiographic province, includes most of Delaware and the entire eastern shore of Maryland and Virginia. Land area is 6050 mi^2, of which about 48% is agricultural. Groundwater in the water-table aquifer is susceptible to nonpoint sources of contamination because of (1) the prevalent use of inorganic fertilizers, manure, and lime, (2) the shallow depths to the water table (generally less than 20 ft), and (3) the high permeability of the soil.

Groundwater unaffected by agriculture practices generally is characterized by low specific conductance (median value of 63 microsiemens/cm at 25°C) because the aquifer is composed mainly of insoluble quartz sand with minor amounts of feldspar and clay minerals. Most of the major dissolved constituents are derived from rainfall and weathering of feldspars. Regional geochemical patterns are evident and relate to lithology and groundwater-flow patterns. Calcium bicarbonate- and sodium bicarbonate-type waters are common in the interior of the peninsula, sodium chloride type-water is common in coastal and tidal areas, and calcium sulfate chloride-type water is common in areas underlain by estuarine deposits along the margins of the peninsula and in forested wetlands.

Groundwater affected by agricultural practices generally is a calcium magnesium nitrate type, with a median specific conductance of 183 μs/cm at 25°C. Calcium and magnesium are from agricultural lime and the nitrate is from fertilizer and poultry manure. Agriculture affects groundwater composition throughout the peninsula, except in areas of poorly drained and relatively impermeable clay-silt sediments that characterized by high exchange capacities and limited zones of oxidation.

KNIGHT, IAN, and DAVID HAWKINS, Department of Mines and Energy, St. John's, Newfoundland, Canada.

Western Newfoundland, Canada, a Lower Paleozoic Basin with Hydrocarbon Potential

Western Newfoundland hosts an early Paleozoic passive margin that was destroyed by later convergence and is now preserved in a foreland fold and thrust belt. Autochthonous Cambrian-Ordovician carbonate and siliciclastic rift, shelf, and foreland basin cover sequences are structurally overlain by allochthonous comprising of coeval deep-water periplatform and oceanic sedimentary, volcanic, and ophiolitic rocks. Geologic relationships indicate that allochthonous deep-water sediments were partly emplaced above the autochton by late Ordovician Taconian orogenesis. Recent mapping of a post-Silurian, pre-Mississippian triangle zone in the offshore, and of an imbricated thrust stack involving basement, cover, and allochthons above shelf carbonates in the onshore indicates that the present disposition of lower Paleozoic rocks is the product of Acadian foreshortening of at least 100 km.

The stratigraphy, geologic setting, and history of the lower Paleozoic rocks and the presence of oil shows in wells, seeps, and bitumin throughout the area mark western Newfoundland as a potential hydrocarbon basin similar to other lower Paleozoic examples within the Appalachian system. Strata-bound and structural dolomite reservoirs are common in the autochthon and occur locally in the allochton. Source rocks occur in both the deep-water and foreland basin sequences. Allochthonous deep-water shales have total organic carbon values of up to 8.37%, whereas foreland basin black graptolitic shales range up to 2%. Pyrolysis data and conodont color alteration indices document immature to mature thermal maturation in the southern part of the area and mature to overmature maturation in the northern part of the area.

KUBIK, WEST, K & A Energy Consultants, Tulsa, OK.

Styles of Natural Fracturing and Their Controls on Reservoir Development, Devonian Shale, Eastern Kentucky

The Devonian shales have a long established production history throughout a large portion of the Appalachian basin. Within the GRI experimental development research area (EDRA) of eastern Pike County, Kentucky, these reservoirs commonly have very low matrix permeabilities (10^{-9} to 10^{-7} md.), and a well-developed natural fracture system is critical to reservoir deliverability and economic production. An accurate characterization of these natural fractures is an important part of reservoir exploration in the Devonian shale.

Detailed subsurface mapping and the description of 440 ft of oriented core have resulted in the identification of three major components to the natural fracture system in this reservoir: (1) a regional joint system present throughout the pay interval and study area, overprinted locally by either (2) a flexure-related region of apparent large-scale joints or joint swarms, or (3) locally developed, small-scale, low-angle reverse faults. Each of these components exerts specific controls on reservoir behavior and productive capacity.

The regional joint system provides the basic background permeability for the Devonian shale within the study area, and results in a baseline of production for the majority of the wells in the area. These joints are developed predominantly within the lower Huron black shales and are characterized by multiple orientations and limited vertical extents. An east-west set appears to be the dominant set within the reservoir. The presence of this dominant set along with other intersecting sets is believed to provide the best reservoir quality.

Within the northwestern part of the study area, significant washout response commonly is observed on the density log and is believed to represent the presence of narrow, but vertically extensive, joint swarms. These features are isolated primarily along, and are believed to be genetically related to, the trend of the D'Invilliers flexure, a reactivated basement structure. The presence of these features is occasionally associated with significantly enhanced production (on the order of 300%) over baseline levels.

Within the central part of the area, small-scale, reverse faults have been identified in a large number of wells. These faults generally are developed only within the lower Huron and immediately overlying sections, and are believed to be relatively low-angle features, likely associated genetically with the Pine Mountain and related large-scale thrust systems of the Alleghenian front immediately south and southeast of the area. Virtually, all these features are associated with substantial production increases (50-100%) over baseline.

The presence of these production-enhancing features is critical to the economics of Devonian shale development within areas such as the EDRA. Exploration/development planning, and completion-zone selection should focus strongly on identifying these distinctive features.

LYONS, P. C.., U.S. Geological Survey, Reston, VA, A. T. CROSS, Michigan State University, East Lansing, MI, Z. GAO, University College of Cape Breton, Sydney, Nóva Scotia, Canada, K. GILLIS, Nova Scotia Department of Natural Resources, Stellarton, Nova Scotia, Canada, J. H. CALDER, Nova Scotia Department of Natural Resources, Halifax, Nova Scotia, Canada, E. L. ZODROW, University College of Cape Berton, Sydney, Nova Scotia, Canada, and R. D. CONGDON, U. S. Geological Survey, Reston, VA.

Discovery of In-Situ Carbonate Petrifactions (Coal Balls) in the Foord Seam (Westphalian C., Upper Carboniferous), Stellarton, Nova Scotia, Canada: Implications for Origin of Sulfur in the Foord Seam

Carbonate petrifactions (coal balls) were discovered in situ in the 13-m-thick Foord Seam (Westphalian C) at the Westray open-pit mine at Stellarton, Nova Scotia, Canada. These are the first in-situ coal balls discovered in Nova Scotia. This bed, the thickest and oldest coal mined in the Carboniferous coal basins of the Maritime Provinces of Canada, is the uppermost seam of the Albio Member of the Stellarton Formation and is known for its low sulfur content (mean = 0.5% total sulfur), the lowest of all Maritime Canada coals.

The coal balls are up to 60 cm in length and are scattered abundantly from the bottom to the top of the seam, including the shale parting. The principal minerals contained in the coal balls (n = 6), as determined by semiquantitative x-ray diffraction (XRD) analysis, are siderite (70-100%), dolomite (0-20%), quartz (0-5%), and traces of a clay mineral (illite?). Calcite and pyrite were detected in trace amounts by SEM-EDAX and by single-crystal XRD analysis. As determined by whole-rock and coulometric methods, the coal balls are composed of Fe_20_3 (4443.6-60.0%), MgO (1.5-3.8%), Ca0 (1.8-7.2%), Mn0 (0.13-35%), SiO_2 (0.9-11.7%), Al_20_3 (0.3-6.2%), TiO_2 (0.03-0.23%), K_20 (<0.01-0.8%), Na_20 (0.09-0.16%), P_2O_5 (0.09-0.27%), CO_2 (29.5-36.4%), and organic carbon (1.1-3.4%). The following genera were tentatively identified in the coal balls; *Sigillaria*, *Lepidodendron*, and an unidentified fern(?).

The almost complete absence of pyrite in the coal balls suggests a chemical link with the pyrite-poor Foord Seam. We hypothesize that sulfate-rich marine water or recycled marine sulfate from evaporites from the Lower Carboniferous Windsor Group were unavailable in the peat-forming mire, and, therefore, siderite was favored over pyrite. A nonmarine origin of the siderite also is suggested by the nearly pure end-member nature of the siderite ($Fe_{0.94\pm10.03}Mg_{0.02\pm10.02}Ca_{0.04\pm0.01}Mn_{<0.01}Sr_{<0.01}Ba_{<0.01}$; n = 48), a composition consistent with siderite of freshwater origin. Because of the lack of sulfate or H_2S to form pyrite, sulfur combined almost exclusively with the organic molecules of the lycopod-rich peat, and this lack of sulfate or H_2S favored the low-sulfur content of the Foord Seam.

MESKO, THOMAS O., U.S. Geological Survey, Richmond, VA.
Delineation of Hydrogeologic Terranes in the Piedmont and Blue Ridge Physiographic Provinces-Southeastern and Mid-Atlantic United States

In 1988, the U.S. Geological Survey began an appraisal of the regional groundwater and surface-water resources in the southeastern and mid-Atlantic areas of the United States as part of the Appalachian Valleys-Piedmont Regional Aquifer Systems Analysis (APRASA) study. The regional study was divided into two study units on the basis of physiographic province: (1) the Valley and Ridge province, (2) and the Piedmont and Blue Ridge provinces on the basis of hydraulic properties of crystalline and sedimentary rock. A geographic information system (GIS), digitized from state geologic maps, was used as a basis to relate regional geology and lithology to discharge from more than 25,000 wells in the two provinces.

The approach included (1) assignment of rock lithology to each geologic formation in the GIS; (2) aggregation of all polygons containing the same rock lithology into lithologic groups; (3) the relation of specific well information, such as well discharge, to each lithologic group; (4) aggregation of all values of well discharge for each lithologic group; (5) determination of a median value of well discharge for each lithologic group; (6) the ranking of each lithologic group according to the median value of well discharge; and (7) assignment of each lithologic group to a hydrogeologic terrane on the basis of the rank of the median value of well discharge. Each terrane was delineated according to median well discharge categories, which ranged from 0 to 10 gal/min, >10 to 20 gal/min, >20 to 30 gas/min, ?30 to 50 gal/min. All five categories of median well discharge were identified in the Piedmont province in 33 lithologic groups. In the Blue Ridge province, only two ranges-0 to 10 and >10 to 20 gal/min were identified in 18 lithologic groups.

NOLDE, JACK E., Virginia Division of Mineral Resources, Charlottesville, VA, and ROBERT C. MILICI, U.S. Geological Survey, Denver, CO.
Stratigraphic and Structural Controls of Natural Gas Production from the Berea Sandstone (Mississippian), Southwestern Virginia

The Berea Sandstone, a major reservoir 5000 ft beneath the Virginia plateau, produces nonassociated gas, from west to east, from the Roaring Fork, Nora, Glick, and Berwind trends. Production generally in stratigraphically controlled, but may be structurally enhanced in the Berwind trend on the southwest-plunging Dry Fork anticline.

The Berea is within a shale sequence and grades generally from sandstone to siltstone westward. Production in Roaring Fork coincides approximately with relatively small areas of slightly greater siltstone thickness. The Nora and Glick trends, major northeast-extending zones as much as 150 and 60 ft thick, respectively, are 14 mi apart, 10 mi across, and up to 30 mi long. These trends are parallel to the Mississippian paleoshoreline and contain prodelta sediments that accumulated at or below wave base.

In the Nora trend, the Berea produces where it is greater than 60 ft thick. Initial well-head pressures generally range from 500 to 800 lb/in^2, and final open flows commonly range up to 1400 MDFD, with the maximum reported as 4992 MCFD. Eastward toward the source of sediment, as little as 40 ft of Berea produce gas in the Glick and Berwind fields. Initial open flows increase eastward, reflecting increases in grain size, porosity, permeability, and perhaps in fractures. In the Nora trend, natural open flows for 10% of the wells exceed 150 MCFD; in the Glick and Berwin fields, open flows for 30 to 60% of the wells, exceed 150 MCFD.

OLDHAM, ANNE V., THOMAS E. REPINE, BASCOMBE, M. BLAKE, and KIMBERLY J. TIMBERLAKE, West Virginia Geological and Economic Survey, Morgantown, WV
Coal-Bed Methane Resources and Subsurface Definition of the Middle Pennsylvanian Alleghany Formation in Northern West Virginia

Traditional correlation methods have not proven effective in the subsurface definition of the Alleghany Formation. Sandstones are discontinuous, of channel fill origin, and have log signatures that are not uniquely traceable on a regional basis. Erosion and/or nondeposition associated with fluvial-deltaic channels were responsible for observed coal-bed discontinuities and resulted in preservation of incomplete depositional sequences. Lowermost Alleghany Formation and underlying Pottsville Group sandstones often coalesce and/or split. The regional unconformity between Mississippian and Pennsylvanian systems effectively prohibits correlation of sandstones above the middle Mississippian Greenbrier Limestone due to gross variations in sediment thickness and lithology.

In the overlying Conemaugh Group, core descriptions are helpful in locating marine zones and red beds, which may then be located on geophysical logs and used in correlations. The combined use of data from coal exploration core holes, gamma-ray and density logs, oil and gas well drillers' logs, and interval thicknesses derived from outcrop studies has allowed tentative subsurface definition of the Allegheny Formation. The number and thicknesses of Allegheny coal beds, associated sandstones, and reported gas shows have been mapped for use in future coal-bed methane development.

The West Virginia Geological and Economic Survey developed this integrated approach to correlation while studying the coal-bed methane potential of the Alleghany Formation in northern West Virginia under contract to the Texas Bureau of Economic Geology and funded by the Gas Research Institute.

ORTIZ, ISAIAS, THOMAS F. WELLER, and ROBIN V. ANTHONY,* United Energy Development Consultants, Pittsburgh, PA, D. DZIEWULSKI, BioIndustrial Technologies, Pittsburgh, PA, J. LORENZEN, ResTech, Pittsburgh, PA, and J. H. FRANTZ, JR., S. A. Holditch & Associates, Inc., Pittsburgh, PA.
Disposal of Produced Waters: Underground Injection Option in the Black Warrior Basin

The disposal of large volumes of water produced simultaneously with coal-bed methane is a costly, environmentally sensitive problem. Underground injection into deeper, naturally fractured, low-porosity formations is feasible provided that the total dissolved solids level of these formation waters comply with Environmental Protectional Agency guidelines. Greater fracture density in proximity to structures formed by Appalachian and Ouachita tectonism, along with a higher total dissolved solids level in both the production and injection formation waters, occurs in the eastern, southern, and northern margins of the coal-bed methane (CBM) area of the Black Warrior basin in Alabama.

Injection permeability is developed where fractures intersect formations with suitable lithologies and thickness. Initial results indicate that the lower Pottsville sands, which thicken to the south, have the highest initial injection potential, although these sands appear dirty and tight on the logs. Normal faulting and matrix porosity, in addition to fracturing, may increase permeability in this formation. In the shallower, northern edge of the CBM area, thin-bedded Mississippian sands with high porosity, such as the Hartzelle, may be present. Injection potential also occurs in the fractured Devonian chert and siliceous carbonate lithologies in the Upper Silurian where they thicken to the southwest, and in sandy carbonate lithologies in the undifferentiated Silurian and Ordovician at the eastern margin of the overthrust. The Cambrian-Ordovician Knox Formation has injection potential in a 6-mi-wide zone at the eastern margin of the basin, where the upper Knox is dolomitized below the unconformity.

PRECHT, W. F., Reef Resources & Associates, Miami, FL, R. B. ARONSON, Smithsonian Institution, Washington, DC, P. J. EDMUNDS, California State University, Northridge, CA, and D. R. LEVITAN, University of California, Davis, CA.

Hurricane Andrew's Effect on the Florida Reef Tract

On August 24, 1992, Hurricane Andrew, a small and powerful category IV hurricane passed over southern Florida leaving behind an unmatched path of destruction and devastation, with the storm's eye moved rapidly (16 MPH) over the northern portion of the Florida reef tract. Sustained winds measured within the eyewall of the hurricane were measured in excess of 145 MPH. The damage to the reefs, however, was not commensurate with the extensive damage observed on land. The reefs that were most affected are located in Biscayne National Park, between the Carysfort Light to the south and the Fowey Rocks Light to the north. In fact, the major portion of the reef tract from the Key Largo Marine Sanctuary, south to the Dry Tortugas, sustained little or no damage.

Investigations of reefs within the Key Largo National Marine Sanctuary have revealed the following: (1) most physical damage to the reefs occurred in waters of less than 10 m depth; (2) branching coral, especially the acroporids sustained the most damage; (3) many head corals were displaced and overturned; and (4) large amounts of sediments were shifted both onto and off reef buttresses.

In conclusion, major reef damage was localized within a relatively narrow band, less than 30 mi in width. The actual damage sustained was minimal due to the path of Hurricane Andrew being located on the northern fringe of the reef tract, which put most of the major reefs on the favorable, south side of the storm.

PRECHT, WILLIAM F., Reef Resources & Associates, Miami, FL.

Stratigraphic Evidence from Reef Studies for a Double-High Sea Stand During the Last Interglacial Maximum

Exposures of reefal limestones from the Pleistocene allow for an excellent opportunity to evaluate carbonate platform history relative to glacio-eustatic changes in sea level. Detailed studies from the Falmouth Formation, Jamaica (Sangamon-Isotope Stage 5E) reveal a distinct relationship between internal facies mosaics, subsequent diagenetic alteration, and variations in relative sea level.

Temporally, the reefs are composed of two parasequence-scale, shallowing-upward packages. The absolute water depths for reef facies have been calculated using reef crest materials that accurately express the position of a low-tide datum. As such, a representation of the sediment accommodation space for the platform has been reconstructed and the progressive filling of this space can be evaluated with respect to the internal anatomy of reef facies.

The base of the Falmouth Formation is characterized by a transgressive surface. This surface onlaps the karsted Hopegate Formation and indicates the start-up phase of reef development. Within the lower parasequence, the reef is composed of a well-zoned fringing reef complex. Vertical (temporal) changes reveal an initial rapid deepening, related to flooding of the platform, followed by a progressive shallowing of reef facies, characteristic of a catch-up style of reef development. As the reef continues to shallow, the accommodation space across the narrow platform becomes more restricted and the community structure changes accordingly. This facies change signifies the termination of aggradational reef growth and also marks the uppermost limit of the lower parasequence.

Renewed sea level rise over the platform is characterized by a flooding surface overlain by a shallow-water parasequence, comprised of a keep-up style reefal community with coarse bioturbated, coralgal sediments. The upper limit of this parasequence is concomitant with the Sangamon sea level maximum. A wave cut north developed in the Hopegate Formation some 5 m above present sea level clearly delineates the maximum flooding of the platform. Subsequent sea level fall subaerially exposed the platform and has resulted in localized extensive facies and fabric specific diagenetic modification and alteration.

Development of a relative sea level curve based on the reconstruction of reef facies in time-slices strongly suggests the development of a double-high sea stand during the last major interglacial maximum. Calibration of this curve based upon uranium-series dating of well-preserved aragonitic corals from these parasequences also argues in favor of a double-peak in sea level, the lower peak developing between 134 and 127 Ka and the upper peak developing about 124 to 199 ka. In addition, this study area is compared to other exposed, coeval reefal sequences from the Caribbean and western Atlantic. These reefs, almost without exception, detail a similar development history, a testament to a eustatic sea level signal corresponding to the two parasequences.

REED, BENJAMIN, C., Ohio University, Athens, OH.

Late Carboniferous and Early Mesozoic Deformation in the Western Cumberland Basin, Nova Scotia

Late Carboniferous transpressional deformation related to docking of the Meguma and Avalon terranes produced a series of rapidly subsiding subbasins within the Cumberland basin. In the western Cumberland basin, the Athol syncline contains the Joggins and Springhill coal seams and represents a local depocenter of Westphalian B-C conglomerates, lithic arenites, and siltstones that thicken toward the synclinal axis. The absence of Westphalian B-C strata elsewhere in the Maritimes indicates regional Late Carboniferous uplift and erosion, and suggests that development of the Athol syncline was contemporaneous with deposition.

Late Carboniferous strike-slip faults adjacent to the Athol syncline record dextral motion south of the Cumberland basin (Cobequid fault) sinistral motion along the basin's northwestern margin (Havery-Hopewell fault). These faults are interpreted to be synthetic and antithetic structures related to a dextral shear regime in which the Athol syncline and adjacent subparallel folds record the direction of regional compression during basin development. Early Mesozoic deformation of the Athol syncline occurs along a zone of east-west-trending faults, the Athol-Sand fault zone (ASFZ), that truncates the syncline's southern limb. To the east, the ASFZ splays north to deform coal measures in the Spring-hill area. To the west, along the coast of Chignecto Bay, the ASFZ comprises numerous normal, reverse, and oblique-slip faults that suggest changes in the direction of strike-slip. Kinematic analysis indicate motion was predominantly sinistral. The development of the Athol syncline therefore is interpreted to have been controlled by syndepositional, dextral transpression during the Late Carboniferous, followed by sinistral transtension related to the Fundy rift.

ROSE, PETER, R., Consultant, Austin, TX, JOHN C. JONES, Mika, Myers, Beckett & Jones, Grand Rapids, MI, and LEW P. MURRAY, Miller Oil Corporation, Traverse City, MI.

Energy in the Balance: Exploration and the Environment

In September 1991, a Michigan court ruled that the State of Michigan owed Miller Brothers $42 million. The award was given as compensation for a 1987 taking of their property in which drilling permits were illegally denied.

Miller Brothers was able to present a convincing case by establishing a sound basis for the evaluation of the property in question. This was achieved by constructing an objective, well-documented, convincing analysis by integrating: (1) a detailed understanding of the geology of the subject area; (2) a production database of analog producing fields, projecting ultimate recoveries; (3) detailed cash flow models establishing present monetary value of reasonable production cases; (4) risk analysis forecasting the numbers and size of expected new field discoveries and their associated probabilities; and (5) the fair market value of the property based upon the determination of expected monetary bids for a free market acquisition of such properties.

To preserve a domestic energy supply, our industry needs to be willing to confront opposition and when necessary to undertake and prosecute similar lawsuits. To do so successfully, a company must be determined to stand on principle and committed to the full use of technical expertise. As geologists, we need to be willing to develop accurate and highly detailed analyses of the geologic environments within which we are working.

RYDER, ROBERT T., JOHN J. MILLER, JOHN A. GROW, and NICHOLAS M. RATCLIFFE, U.S. Geological Survey, Reston, VA, and Denver, CO.

In 1985, North Central Oil Corporation drilled a 10,500-ft well in Bucks County, Pennsylvania, to test for oil and gas in Triassic-Jurassic strata of the Newark Group in the Newark basin. The hole was located about 5 mi southeast of the border fault on the crest of the Revere anticline, a transverse structure that plunges northwestward toward the border fault. This drill hole, No. 1 Cabot-KBI, penetrated in descending order 2900 ft of lacustrine red and gray shale (Passaic Formation of Jurassic and Triassic age), 3600 ft of lacustrine gray and black shale (Lockatong Formation of Triassic age), and 4000 ft of fluvial sandstone and red shale (Stockton Formation of Triassic age). Although the drill hole abandoned, it revealed excellent gas shows throughout the Lockatong Formation and parts of the Stockton Formation.

Acoustic and density logs from the well were converted to a synthetic seismogram that ties stratigraphic intervals in the borehole with seismic events on the nearby, 33-mi-long Seitel NB-1 seismic line. Formation contacts, probable intraformational unconformites, and lithologic units, such as 50-ft-thick fluvial sandstones in the Stockton Formation, are identified and traced for tens of miles away from the well. Moreover, beneath the drill site in the Stockton Formation, the 48-fold seismic line shows a large anticline that is subparallel to the border fault. This anticline has no surface expression, but, in combination with the intersecting Revere anticline, provides an obvious exploration target. Our interpretation suggests that the No. 1 Cabot-KBI drill hole ends about 1500 ft above the border fault and the underlying middle Proterozoic basement. As recognized in other interpretations of the line, the border fault dips southeastward at approximately 30° beneath the basin to a depth in the upper crust that exceeds 25,000 ft. The maximum thickness of the lower Mesozoic sequence along the line is located several miles southeast of the drill site, where it is estimated to be about 17,000 ft. High-amplitude seismic events from the Stockton Formation on the southeastern flank of the large anticline may indicate undiscovered gas accumulations.

SEGALL, M. P., D. J. COLQUHOUN, and C. WICKER, University of South Carolina, Columbia, SC.

Clay-Size Mineralogy of Selected Samples from the Upper Eocene Barnwell Group (Upland Unit, Tobacco Road Sands, Dry Branch Formation) and Middle Eocene Santee Formation, South Carolina

Surficial and near-surface soils reflect a variety of lithologies and depositional environments that are difficult to differential because of intense leaching and rapid or laterally inconsistent facies changes. Binocular microscopic examination, SEM/EDX observations, and XRD analysis indicate that Barnwell Group sediments are transitional. Fluvially-derived upland sediments contain poorly crystallized detrital kaolinite with a swirl-pattern microtexture. Hydroxy-interlayered vermiculite is prevalent throughout the unit. Tobacco Road Sands are characterized by well-crystallized authigenic kaolinite with a "fanned" macrostructure, and well-formed hexagonal plates that inherited their directional information from a precursor muscovite. Sediments of the Dry Branch Formation contain high concentrations of smectite and flocculated, relatively poorly crystallized kaolinite flakes reflective of marine depositional conditions. Interfingering of the units is suggested based on alternation of mineralogic signatures. This type of environmental control is expected for a low-gradient fluvial/transitional/marine depositional system. The marine Santee Formation contains authigenic Ca-minerals (Ca-zeolites and authigenic calcite). Unique mineralogic and morphologic signatures are useful for determining environmental constraints among the cores and understanding the movement and formation of these smallest particles within the groundwater system.

SHAFFER, BRIAN N., Cyprus Emerald Resources, Waynesburg, PA.

Structural Implications on the Deposition of the Upper Freeport Coal Bed in Eastern Greene County, Pennsylvania

The orientation, geometry, thickness, and quality of the Upper Freeport coal bed suggests that syndepositional tectonic activity influenced the accumulation of peat and its laterally equivalent sediments. Both strike-parallel and strike-normal structures appear to influence the deposition of the Upper Freeport coal bed. Strike-parallel structures are faults that were active during the Carboniferous, but do not penetrate into the Carboniferous section. The Carboniferous rocks at the surface within the study area reflect deeper structures as a series of gentle synclines and anticlines. The Upper Freeport coal bed was deposited as a domed peat across the Belle Vernon anticline, which represents the upthrown side of a syndepositionally active deep fault. Laterally equivalent fluvial channel sediments were deposited on the downthrown side of the structure, represented at the surface by the Waynesburg syncline. The influence of syndepositionally active faults on the distribution, thickness, and quality of the Upper Freeport coal bed is similar to the previously reported influence of contemporaneous growth faults on the distribution and thickness of Carboniferous coal beds in Kentucky and Alabama.

Strike-normal features also influence the position, geometry, and thickness of the Upper Freeport coal bed. The strike-normal features appear to be produced by deep strike-slip faulting. A major no-coal zone within the Upper Freeport coal bed lies within and parallel to the trend of a cross-strike discontinuity within the study area.

SIRON, D. L., and D. J. COLQUHOUN, University of South Carolina, Columbia, SC.

Textural Distribution of Barnwell Group Sediments, Northwest South Carolina Coastal Plain

Drill-log data, core descriptions, and grain size analyses were combined to clarify stratigraphic relationships of the Upland unit, Tobacco Road Sand, and Dry Branch Formation. Geologic cross sections produced from 34 power auger holes on the South Carolina coastal plan reveal unique textural characteristics indicative of variable depositional conditions. The Upland Unit consists of a high variability of grain sizes with high clay/sand ratios reflective of irregular deposition within a fluvial environment. Interlaminated fine-grained sand/clay layers suggest an overbank depositional setting. Cobbles up to 3 in. in diameter are common with pebble lag channel deposits generally occurring at the base of the unit. These well-rounded "potato" cobbles are surrounded by a matrix of medium- to coarse-grained angular quartz sand. Tobacco Road sands show characteristics of a transition between Upland fluvial and underlying marine Dry Branch sediments. These sands are moderately well sorted, medium to coarse grained, and have a subangular to subrounded morphology.

Tobacco Road sands are more uniform in size then sediments found in the Upland unit and include a higher percentage of finer grain sizes with variable clay contents. The Dry Branch Formation is composed of well-sorted, fine-grained sands with low clay/sand ratios characteristic of uniform deposition in a shallow-marine environment. These results indicate textural variability among sediments in the upper Eocene Barnwell group can be used to infer depositional conditions.

SITES, ROY S., and KAREN K. HOSTETTLER, Division of Mineral Resources, Charlottesville, VA.

Southwest Virginia Underground Coal Mine Map Database and Base Maps-Synopsis of an Ongoing Coalfield Project

In September 1991, the Department of Mines, Minerals, and Energy of the Commonwealth of Virginia entered into an agreement with the Office of Surface Mining to prepare a coal mine map database and to produce 1:24,000 scale individual coal-bed base maps showing documented underground mined areas throughout the Southwest Virginia coal field. The project results are to provide public, industry, and all levels of government a much-needed means of initial evaluation of many coalfield related concerns. The completed maps will be incorporated into an integrated geographic information system (GIS).

Evaluating the entire coalfield involved a preliminary review of 48 quadrangles. Ongoing detailed, accurate information gathering of extensive underground mine map files was necessary to provide a needed organized map database. Construction of coalfield index maps of information gathered to date provide insight into coalfield-wide outcrop patterns, mine distributions, and coal-bed trends. A completed set of individual maps, referenced to the underground mine map database, showing the types of mining applicable per coal bed per quadrangle is the designated project output.

SPEIRAN, GARY K., U.S. Geological Survey, Richmond, VA

Flow and Quality of Groundwater in Coastal Discharge Areas of the Eastern Shore, Virginia

Variations in shallow geology, topography, and land cover affect the flow and quality of groundwater near coastal discharge areas on the eastern shore of Virginia. Groundwater discharges from the water-table aquifer to streams, estuaries, and saltwater and freshwater wetlands. Sediments in many discharge areas have variable, lithology, mineral content, and organic content because previously deposited sediments were eroded and redeposited in differing nearshore environments. Sediment changes coincide with changes in land-surface elevations because original sediments were eroded and redeposited at different sea level elevations. Where land-surface elevations decrease, the water table approaches land surface.

These variations in sediments coincide with changes in land cover from upland fields to lowland forests and wetlands. Evapotranspiration becomes a major pathway for groundwater discharge in lowlands during the growing season. The effects of evapotranspiration result in low lateral hydraulic gradients, upward hydraulic gradients that can equal the magnitude of lateral hydraulic gradients, and diurnal fluctuations in the water table as great as 1 ft. Where water-table altitudes decrease, groundwater discharges from underlying confined aquifers.

Groundwater quality reflects sources of water and geochemical changes. Distinctly different water-quality types result from the effects of agricultural practices, water discharged from underlying confined aquifers, and brackish water probably from the combined effects of recharge caused by tidal flooding and lateral inflow caused by evapotranspiration. Organic matter in sediments decreases dissolved oxygen concentrations in groundwater and can cause a shift from oxidizing to reducing reactions.

SPIKER, E. C. and A. L. BATES, U.S. Geological Survey, Reston, VA.

Sulfur Isotopic Evidence for Controls on Sulfur Incorporation in Peat and Coal

Pyritic sulfur isotope $d^{34}s$ values were used as a measure of two principal controls on sulfur incorporation in peat and coal, the availability of sulfate, and the activity of sulfate-reducing bacteria in the peat-forming mire. Relatively low $d^{34}S$ values indicated an open system with a relatively abundant supply of sulfate that exceeded the rate of sulfate reduction to sulfide, whereas relatively high $d^{34}S$ values indicated a closed system with a more limited supply of sulfate. For example, in the high-sulfur (>3% S), Holocene deposits of Mud Lake, Florida, pyritic sulfur $d^{34}S$ values decrease sharply across the transition from peat to the overlying lacustrine sapropel, which corresponds to an increased supply of sulfate from the lake waters. Likewise, syngenetic pyrite in the high-sulfur Minto coal bed (Pictou Group, Westphalian C) in New Brunswick, Canada, show up to 10% negative shifts in $d^{34}S$ in attrital layers containing detrital quartz and illite, consistent with an increased supply of sulfate from streams entering the peat-forming mire. In contrast, positive pyritic sulfur $d^{34}S$ values in high-sulfur, channel-fill coal beds (lower Breathitt Formation, Middle Pennsylvanian) in eastern Kentucky indicate that a steady supply of sulfate was exhausted by very active microbial sulfate reduction in the channel-fill peat.

SWAIN, LINDSAY, A., U.S. Geological Survey, Richmond, VA.

Hydrogeological Characteristics of the Bedrock Aquifers in the Appalachian Valley and Ridge, Piedmont, and Blue Ridge Physiographic Provinces of the Eastern and Southeastern United States

In 1988, the U.S. Geological Survey began a regional study of the aquifer systems within the Appalachian Valley and Ridge, Piedmont, and Blue Ridge physiographic provinces. The project area covers more than 142,00 mi^2 of the eastern and southeastern United States from the northern border of New Jersey to Birmingham, Alabama.

The principal study objectives were to delineate, describe, and quantify the hydrogeologic terranes, and the significant characteristics of the groundwater flow systems within the bedrock aquifers. In the regional approach to accomplish these objectives, the hydrogeologic framework and groundwater conditions in each province were evaluated. In the localized approach, representative basins were intensively studied and their hydrogeologic characteristics were quantified by means of groundwater modeling.

Preliminary findings indicate that maximum discharge of wells in the Valley and Ridge, Piedmont, and Blue Ridge provinces are 8000, 2200, and 830 gal/min, respectively. Median nondomestic discharges of wells in each of these provinces are 37 (4287 wells), 30 (8100 wells), and 20 (668 wells) gal/min, respectively. In the crystalline rocks of the Piedmont and Blue Ridge provinces, the median well discharge is greater in the southern half of the study area than in the northern half. However, in the sedimentary rocks of the Mesozoic rift zones within the Piedmont province, well discharge generally decreases from north to south. At some locations in crystalline rocks in the Piedmont, zones of high yield have been identified between depths of 350 and 650 ft.

THOMAS, ROBERT B., and PATRICK J. BURNS, Eastern Mountain Fuel, Inc., Parkersburg, WV.

Porosity Trends of the Lower Ordovicians Rose Run Sandstone in Holmes, Tuscarawas, and Coshocton Counties, Ohio

Density, porosity, and thickness were calculated for the Rose Run Sandstone in over 300 electric logs from Holmes, Tuscarawas, and Coshocton counties, Ohio, to determine depositional and reservoir patterns. Complete, uneroded sections of the Rose Run were encountered in approximately 200 wells. Average gross thickness of the main sand body of the Rose Run in the study area is 70 ft, with a maximum of 94 ft and a minimum of 51 ft. Average porosity for the main sand body is 9.8%. Porosity-feet (porosity ¥ height) values were calculated from the logs. The porosity-feet values range from 0.89 to 8.95 with an average of 4.35. Within the study area, the main sand body of the Rose Run is composed of three distinct sandstone lenses.

Regional mapping of the Rose Run Sandstone in a 1600 mi2 area of Holmes, Tuscarawas, and Coshocton counties indicates a northwest-southeast thick trend of the main sand body of the Rose Run. Generally, higher porosity-feet and average porosities are observed along the thick trend when compared to the thin areas of the Rose Run. The northwest-southeast thick trend also is coincident with a regional northwest-southeast structural low on the base of the Rose Run. This thick, porous, structurally low area is interpreted to be a tidal channel. Detailed mapping of the individual sand lenses of the Rose Run also indicates the existence of a system of meandering tidal channels within the boundaries of the larger tidal channel.

WEAVER, DOUGLAS R., Texaco Exploration and Production Inc., New Orleans, LA.

An Environmentally Correct Drilling Effort-Texaco's Taylorsville Basin Exploration Program

Through the early and mid-1980s, Texaco conducted geophysical, geochemical, and stratigraphic test programs along the Mid-Atlantic Coast of the United States. A drilling program was ultimately focused at the Triassic sediments of the Taylorsville basin straddling the Virginia-Maryland border. Three wildcat wells were drilled between 1989 and 1992. All were dry holes.

Although the prospect was a geological disappointment to Texaco, the environmental concern and precaution exhibited throughout the effort stand as testament to a major oil company's ability to conduct operations in an environmentally prudent manner. Although the operations involved only inland drill sites, all locations were extremely close to the Chesapeake Bay, one of the world's most fragile estuarial ecosystems. Protective techniques employed included the use of closed freshwater mud systems, protective levee and drainage containment, comprehensive backup and emergency plans, and heightened safety awareness.

Texaco also embraced an open policy regarding public education and input. By means of town meetings, public hearings, and thousands of rig visits, Texaco believes it has enhanced the public perception and enthusiasm for exploratory drilling in the Tidewater region.

WILSON, B. R., Virginia Division of Gas and Oil, Abingdon, VA

The Virginia Gas and Oil Act of 1990-A Regulatory Perspective

The Virginia Gas and Oil Act states that its provisions are to be "...liberally construed to effectuate..." certain specific purposes. The focus of these purposes is promoting and encouraging exploration and development, conserving gas and oil resources, using environmentally sound exploration and exploitation practices, coordinating coal mining and hydrocarbon exploration, and showing concern for the rights of mineral and surface owners. The act, through and along with the Gas and Oil Regulation promulgated under the act and adopted August 1, 1991, addressed these objectives in many ways. Some examples are requirements that permit applications, including drilling water analyses, fluid and solid disposal plans, and site-specific operations plans detailing erosion and sediment control measures; provisions requiring notification of all affected mineral and surface owners prior to permit issuance; simultaneous permitting of boreholes to be alternately used as coalbed methane producers or deep-mine ventilation holes, depending on the proximity of mining activity. A perspective of the 2 yr since the adoption of the regulation allows consideration of how well the purposes of the act are being met, and how it has affected the industry it regulates.

WOMACK, D. GENE, Halliburton Geophysical Services, Inc., Houston, TX.

Seismic Operations in Environmentally Sensitive Areas IAGC Initiatives

As environmental concerns continue to expand on a global basis, the petroleum industry can expect a continuing stream of new legislation, regulations, and permitting conditions addressing this critical subject. Exploration programs involving seismic surveys will likely be a focal point for these governmental actions and public initiatives.

Because of the diversity of circumstances faced by geophysical field crews and the potential adverse impact from such activities, our industry must develop heightened sensitivity and operating practices that demonstrate that such work can be done in an environmentally compatible manner. The International Association of Geophysical Contractors (IAGC) has taken a proactive approach to this issue by producing a comprehensive set of recommended worldwide operating guidelines to assist its member companies and others in planning and carrying out geophysical data acquisition activities in an environmentally responsible manner.

These IAGC guidelines are designed to address key environmental issues present in six specific operating environments: arctic areas, coastal areas (including wetlands and marshes), level and semilevel forested areas, and marine areas. Careful planning, proper communication with both the public and government agencies, and knowledge of specific local issues can help to bring about a cooperative and positive approach to future petroleum exploration and development in environmentally sensitive areas.

Furthermore, recognition, acceptance, and adoption to these IAGC guidelines by both the petroleum industry and regulatory agencies can help promote access to explore-without unreasonable or unnecessary restrictions-in environmentally sensitive areas. This can help reduce oil company client and geophysical contractor liability and, at the same time, provide a much needed boost to our industry's public image.

Development of these guidelines has been a truly international effort incorporating input from all regions of the world as to content, format, and localized semantics. In trying to achieve worldwide functionality, IAGC has attempted to establish a balance environmental diligence, reasonable practices, and economic considerations.

ZHENG, LI, THOMAS H. WILSON, and ROBERT C. SHUMAKER, West Virginia University, Morgantown, WV

Small-Scale Structural Heterogeneity and Well-Communication Problems in the Granny Creek Oil Field of West Virginia

Seismic interpretations of the Granny Creek oil field in West Virginia suggest the presence of numerous small-scale fracture zones and faults. Seismic disruptions interpreted as faults and/or fracture zones are represented by abrupt reflection offsets, local amplitude reductions, and waveform changes. These features are enhanced through reprocessing, and the majority of the improvements to the data result from the surface consistent application of zero-phase deconvolution. Reprocessing yields a 20% improvement of resolution. Seismic interpretations of these features as small faults and fracture zones are supported by nearby offset vertical seismic profiles and by their proximity and fracture zones are supported by nearby offset vertical seismic profiles and by their proximity to wells between which direct communication occurs during waterflooding.

Four sets of faults are interpreted based on subsurface and seismic data. Direct interwell communication is interpreted to be associated only with a northeast-trending set of faults, which are believed to have detached structural origins. Subsequent reactivation of deeper basement faults may have opened fractures along this trend. These faults have a limited effect on primary production, but cause many well-communication problems and reduce secondary production.

Seismic detection of these zones is important to the economic and effective design of secondary recovery operations, because direct well communication often results in significant reduction of sweep efficiency during waterflooding. Prior information about the location of these zones would allow secondary recovery operations to avoid potential problem areas and increase oil recovery.

1993 HONORS AND AWARDS SESSION

Eastern Section American Association of Petroleum Geologists

John T. Galey Memorial Award -
Gerald M. Friedman

Honorary Membership -
G. Warfield Hobbs, IV

Honorary Membership -
Philip L. Martin

Distinguished Service Award -
Gayle H. McColloch, Jr.

Distinguished Service Award -
Robert A. Trevail

George V. Cohee Public Service Award -
Katharine Lee Avary

Outstanding Educator Award -
Donald E. Hattin

Gordon H. Wood, Jr. Memorial Award -
Aureal T. Cross

I.C. White Memorial Award -
John Manley Dennison

DEG
Meritorious Contributions Award -
William G. Murray

Certificate of Merit
Thomas R. Jake
Robert A. Trevail
Joan E. Crockett
Dale K. Helpingstine
Stephen T. Whitaker
Donald F. Oltz
Laure G. Wallace
Arthur P. Schultz
Brenda Pierce
Thomas A. Fitzgerald
Jane R. Eggleston
Kenneth C. Ashton

1992 RECOGNITION

A.I. Levorsen Memorial Award -
Lisa K. Goetz,
J. Gary Tyler,
Roger L. Macarevich,
David L. Brewster, and
Jagadeesh R. Sonnad

Vincent E. Nelson Memorial Award -
Colin G. Treworgy

Margaret Hawn Mirabile Memorial Award -
Todd Hendricks and
Stephen O. Moshier

EMD Best Paper -
Donald C. Haney and
James C. Cobb

EMD Best Poster -
Colin G. Treworgy

1993 RECOGNITION

Margaret Hawn Mirabile Memorial Award
(Best Oral Paper by a student)-
Kurt A. Donaldson

Vincent E. Nelson Memorial Award
(Best Poster Paper) -
Carmen Bauert

A.I. Levorsen Memorial Award
(Best Oral Paper) -
Robert E. Davis

Ralph L. Miller Memorial Award
(Best Energy Minerals Division Oral Paper) -
James C. Hower

Best Energy Minerals Division Poster Paper -
Carmen Bauert

Best Division of Environmental Geosciences Poster Paper -
Harry J. Hansen

The following two winners tied for **Best Division of Environmental Geosciences Oral Papers** -
Lew P. Murray and
Pixie A. Hamilton

Volunteer Judges at 1993 Eastern Section AAPG Meeting

Robert Byrne
James Cobb
Judith Denver
Albert Dikas
Joseph Frantz
Patricia Fulton
Rick Goings
Mary Ann Gross
Robyn Hannigan
David Harris
Kenneth Hollett
Keneth Johnson
Philip Martin
Jane McColloch
Joseph Megler
James Noel
Samuel Pees
Brenda Pierce
Thomas Repine, Jr.
Bonnie Robinson
John Roen
John Rupp
Arthur Schultz
Cathlene Williams
John Wirth